Comprehensive proteomic profiling of clinically relevant strains of *Mycobacterium tuberculosis*

Julian S Peters

This thesis is submitted in fulfilment of the academic requirements

for the degree of

Doctor of Philosophy in Medical Biochemistry

in the Faculty of Health Sciences

University of Cape Town

April 2014

Declaration

I hereby declare that: (1) the above thesis is my own unaided work, both in conception and execution, and that apart from the normal guidance of my supervisor, I have received no assistance apart from that stated below; (2) except as stated below, neither the substance or any part of the thesis has been submitted in the past, or is being, or is to be submitted for a degree in the University or any other University. I am now presenting the thesis for examination for the Degree of Doctor of Philosophy in Medical Biochemistry.

Signature: _____

Name: Julian Sithembekile Peters

Date: /04/2014

Abstract

Tuberculosis is an airborne infectious disease caused by the bacillus known as *Mycobacterium tuberculosis*. Despite limited genetic variability, *Mycobacterium tuberculosis* strains exhibit vast discrepancies in phenotypic presentation in terms of virulence, elicited immune response and transmissibility. This study aims to use Mass Spectrometry (MS) tools to quantitatively and qualitatively investigate the total proteome expressed by various epidemiologically significant strains within the *Mycobacterium tuberculosis* complex (MTBC) as well as a clinically relevant non-tuberculous Mycobacteria (NTM) strain when cultured *in vitro*. We aim to use the experimental data obtained using discovery mass spectrometry to identify candidate proteins to use in the design of multiple reaction monitoring (MRM) MS experiments for targeted biomarker validation in patient derived biological samples such as sputum. Liquid chromatography mass spectrometry (LC MS/MS) and data capture were carried out using the LTQ Orbitrap Velos. 1D LC was carried out on gel fractionated samples to increase proteome coverage. This allowed a significant increase in the number of protein identifications of up to 80% proteome coverage per strain. Comparative analysis of the datasets was carried out to identify and define the core-proteome expressed across all strains as well as to identify differentially expressed proteins amongst the strains.

Extensive bioinformatics analysis on the data to identify candidate proteins that differ between the pathogenic and non-pathogenic strains with diverse clinical phenotypes which may act as markers of differential pathogenicity and virulence. MS1 based label free quantification was used in the discovery experiments to assess quantitative differences in the proteomes. In order to validate these candidate markers, targeted MS experiments were carried out using a more sensitive and specific MS/MS platform known as selected reaction monitoring (SRM) was carried out across the strains. SRM assays were designed and optimized for a total of 43 proteins. 23 of these proteins were shortlisted as possible biomarkers of differential phenotype from the discovery experiment. Assays for the remaining 20 were designed without prior observation in any strain in the discovery experiment. Targeted assays were run across the 7 strains to verify the results of the discovery experiment. In line with the hypothesis, differential expression of key proteins that are involved in various aspects that affect the phenotype such as drug resistance, evasion of the immune system and dormancy were observed in a semi-quantitative manner across the strains in study. The assays developed in this study will enable the verification of the presence or absence of the specific *M. tuberculosis* proteins in any sample type.

Acknowledgements

- Firstly, to my Creator, for wisdom and knowledge comes from Him, through him all things are possible.
- In no particular order, I would like to thank everybody who has contributed to me being able to complete this work:
- To Prof Jonathan Blackburn: You have supported me in more ways than just supervision. I would have never completed this work without you and I will always be thankful for that!
- Members of the Blackburn Lab group especially the proteomics group including Brandy Young-Gqamana, Putuma Gqamana, Nelson Soares, Andrew Nel, Brandon Murugan, Shaun Garnett, Liam Bell, Ryan Goosen, Tariq Ganief, Katie Viljoen, Alex Giddey and Zandi Mlamla for all the brilliant ideas and just being there to chat or to troubleshoot. You all are awesome.
- To Prof Lennart Martens and the Ghent university collaborators, Thilo Muth, Sven Degroeve and Giulia Gionelli for assisting with the bioinformatics work.
- To Prof Nicky Mulder and members of the CBIO group especially Gerrit Botha and Fara for the bioinformatics input.
- To Prof Ruedi Aebersold and all members of his group in ETH Zurich, thank you for allowing me to carry out the SWATH-MS work in your lab. Much thanks especially to Olga Schubert for babysitting me in and out of the lab in ETH.
- To Prof Mark Nicol and Rajesh Sarkar from Medical Microbiology unit for providing me with strains and also for training, trouble-shooting and valuable discussions that shaped this work
- To Prof Rob Warren from Stellenbosch thank you for providing me with some of the strains that I used in this study.
- A special thanks to Cashifa Karriem for making my life easier with all the admin which would have had me pulling off my hair strand by strand. Cash you are awesome!!!!!!
- And to my family: My parents and siblings who have forever encouraged me, pushing me to be the best, believing in me more than l believed in myself. For supporting me and being patient with me even if you didn't understand what l was doing.
- Last but not least thanks to my husband Mukendi Mpoyi for being there to listen and support me through my work. I would never have had finished this without your love

and support. Thank you for being patient with me and encouraging me to complete this.

Table of Contents

Glossary/Abbreviations

2D-DIGE - Two dimensional in difference gel electrophoresis

2DE - Two dimensional gel electrophoresis

ADC – Albumin dextrose catalase

ANOVA- Analysis of variance

ATP - Adenosine triphosphate

BBB- Blood brain barrier

BCG- Bacille deCalmette Gèurin

BP - Base pair

CAS - Central Asian

CF- Culture filtrate

CID- Collision induced dissociation

CNS - Central nervous system

CNS- Central nervous system

CV- Coefficient of variation

Da- Daltons

DAVID- Database for annotation and visualisation

DDM- di-dehydroxy-mycobactins

DNA- Deoxy-ribonucleic aid

DOTS - Direct Observed treatment strategies

DTT -Dithiothreitol

EAI - East African Indian

ECD- Electron capture dissociation

EDTA - Ethylenediaminetetraacetic acid

ELISA - Enzyme-linked immunosorbent assay

EMPAI- Empirical modified protein abundance index

ESI- Electron spray ionisation

ETD- Electron transfer dissociation

FASP- Filter aided sample preparation

FDA - Food and drug administration

FDR- False discovery rate

GO- Gene ontology

H- Haarlem

HGT - Horizontal gene transfer

HIV- Human immunodeficiency virus

HPLC - High performance liquid chromatography

iBAQ- Intensity based absolute quantitation

ICAT - Isotope-coded affinity tag

ID- Identifications

IHC - immunohistochemistry

IRPMD- Infrared multi-photon dissociation

IS - Insertion Sequence

iTRAQ - isobaric tag for relative and absolute quantitation

KCl - Potassium chloride

KDa- Kilodalton

kV – Kilo Volts

LAM- Latin American

LC - liquid chromotography

LSP - Large sequence polymorphs

iRT- indexed Retention time

m/z - mass to charge ratio

ms- milli-seconds

MAC- Mycobacterium avium complex

MALDI-MS - Matrix-assisted laser desorption/ionization mass spectrometry

MIRU-VNTR - Mycobacterial Interspersed Unit Variable Number Tandem Repeats

MEV- Multi-experiment viewer

MMTS- Methyl methane-thiosulfonate

MRM- Multiple reaction monitoring

MS - Mass spectrometry

MS/MS- Tandem MS

MTBC - Mycobacterium tuberculosis complex

MuDPIT - Multidimensional protein identification technology

MW - Molecular weight

MWCO- Molecular weight cut-off

MWM - Molecular weight marker

Mycobacterium tuberculosis- M. tuberculosis

NHLS- National Health Laboratory Service

NSAF- Normalised spectral abundance factor

OD- Optical density

OADC- Oleic acid albumin dextrose catalase

ORF - Open reading frames

PCR - Polymerase chain reaction

PPM- Parts per million

PPE - Proline-Proline-Glutamine

PSM- Peptide spectral match

QqQ- Triple quadrupole

RD - Region of deletion

RFLP - Restriction fragment length polymorphism

RPLC- Reverse phase liquid chromatography

RNA - ribonucleic acid

ROS - reactive oxygen species

RT - room temperature

SA - South Africa

SDS - PAGE - sodium dodecyl sulphate polyacrylamide gel electrophoresis

SDS - sodium dodecyl sulphate

SILAC - Stable Isotope labeling with amino acids in cell culture

SIn- Spectral index

SNP - Single nucleotide polymorphs

SRM-Selected reaction monitoring

TA- Toxin anti toxin

TB – Tuberculosis

TBDB- Tuberculosis database

TCEP- Tris-2-carboxyethyl-phosphine

TEMED-Tetramethylethylenediamine

TIC- Total ion count

TFA- Trifluoro acetic acid

TOF - time of flight

TPP- Trans proteomic pipeline

TP-Total protein

WHO - World health organisation

Chapter 1: Tuberculosis phylogeny review

1.1 Introduction

Tuberculosis (TB) is a chronic infectious disease caused by the tubercle bacillus known as *Mycobacterium tuberculosis*. Although it is one of the oldest diseases known to mankind, *M. tuberculosis* still continues to be a global public health challenge, infecting and killing millions of people annually. Over the last century, a vaccine and drugs together with active treatment strategies such as the direct observed treatment strategy (DOTS) have been developed and successfully used to reduce the global TB burden. However a steady increase in the global disease burden has been observed since the early 1990's with the world health organisation (WHO) declaring it a state of emergency in 1993 [1].

1.2 Current distribution and burden of the disease

Socio-economic factors as well as HIV associated co-mortality and morbidity are among the chief factors that have led to the resurgence of TB. [2–4]. The World Health Organization (WHO) reported an incidence of 8.7 million cases and a total of 1.42 million deaths in 2011 [5]. Although the burden of the disease is highest in Asia and the Pacific regions (60%), the African continent exhibits the highest incidence rates of the disease relative to the population as seen in Figure 1 below. In parts of South Africa today, the incidence rates are as high as 1 600 per 100 000, attributable in part to co-incidence of the TB and HIV epidemics and in part to the failure to control TB.

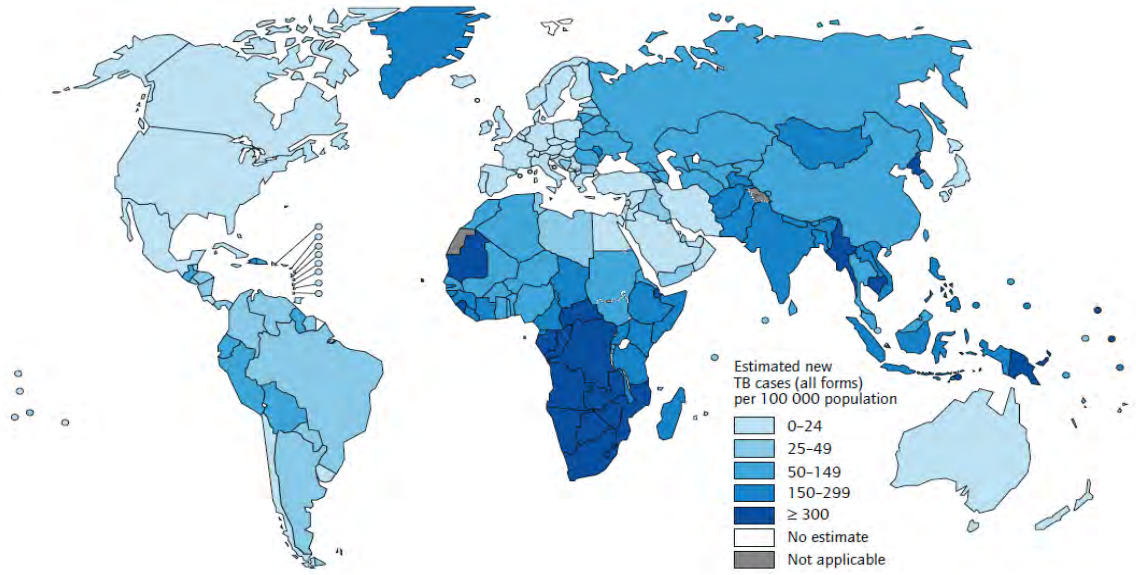

Figure 1.1: Current global incidence rates of tuberculosis infection: Adapted from WHO Global Tuberculosis Report 2012 [5].

1.3 Life cycle of *Mycobacterium tuberculosis*

Infection with *Mycobacterium tuberculosis* presents a major challenge in predicting prognosis. Most infectious diseases proceed through the pipeline shown in Fig 1.2a below showing a predictable flow from exposure to outcome of disease. However, *M. tuberculosis* infection deviates from this normal expected sequence of events due to complex dynamic interactions between host and pathogen that make the outcome of infection unpredictable thus rendering the infection challenging to control as shown in Fig 1.2b. The outcome of the disease is a direct consequence of the nature of the immune response that the bacterium is exposed to upon entry into the host as shown in Figure 1.2c. A TH1 response has been shown to be protective to the bacterium resulting in latent infection whilst a TH2 response results in the impaired protection to the bacterium hence active disease [6].

Mycobacterium tuberculosis bacilli enter a new host through the aerosol route. They are initially taken up by macrophages in the upper respiratory tract which then transport the infecting bacilli into macrophages of the lower lung environment. The organism then multiplies in activated macrophages then it ruptures the macrophage and infects more macrophages. Cell mediated immunity (CMI) is the chief immune response employed to control *M. tuberculosis* infection [7,8]. Despite the utility of CMI in controlling *M. tuberculosis* infection, it is also responsible for the observed pathology associated with TB such as necrosis of lung tissue, formation of granuloma's and inflammation via release of tumour necrosis factor alpha (TNF-α), IFN-γ [9].

The success of *Mycobacterium tuberculosis* as a pathogen lies in its ability to deviate from the above described sequence of stages from exposure to outcome. *Mycobacterium tuberculosis* has the ability to reach a state of compromise with the immune system where it can persist in the macrophage without being killed. This is known as latent TB infection (LTBI). In this state, the organism can live indefinitely within the host nonetheless growing at a rate that does not promote active disease. As a result, the host is smear negative, shows no symptoms and exhibits normal chest x-rays whilst the microbe undergoes little or no cell division and basal metabolism (http://www.cdc.gov/tb/).

However in 10% of the population, under certain conditions, predominantly immuno-suppression, the organism is capable of causing active disease [10]. The latent state of the bacillus is not well understood but it is known that in this state, the bacillus enters a quiescent

state of metabolic slow down [11]. LTBI poses an unseen threat to the control of TB as it creates a pathogenic reservoir and may promote the emergence of drug resistant forms of TB.

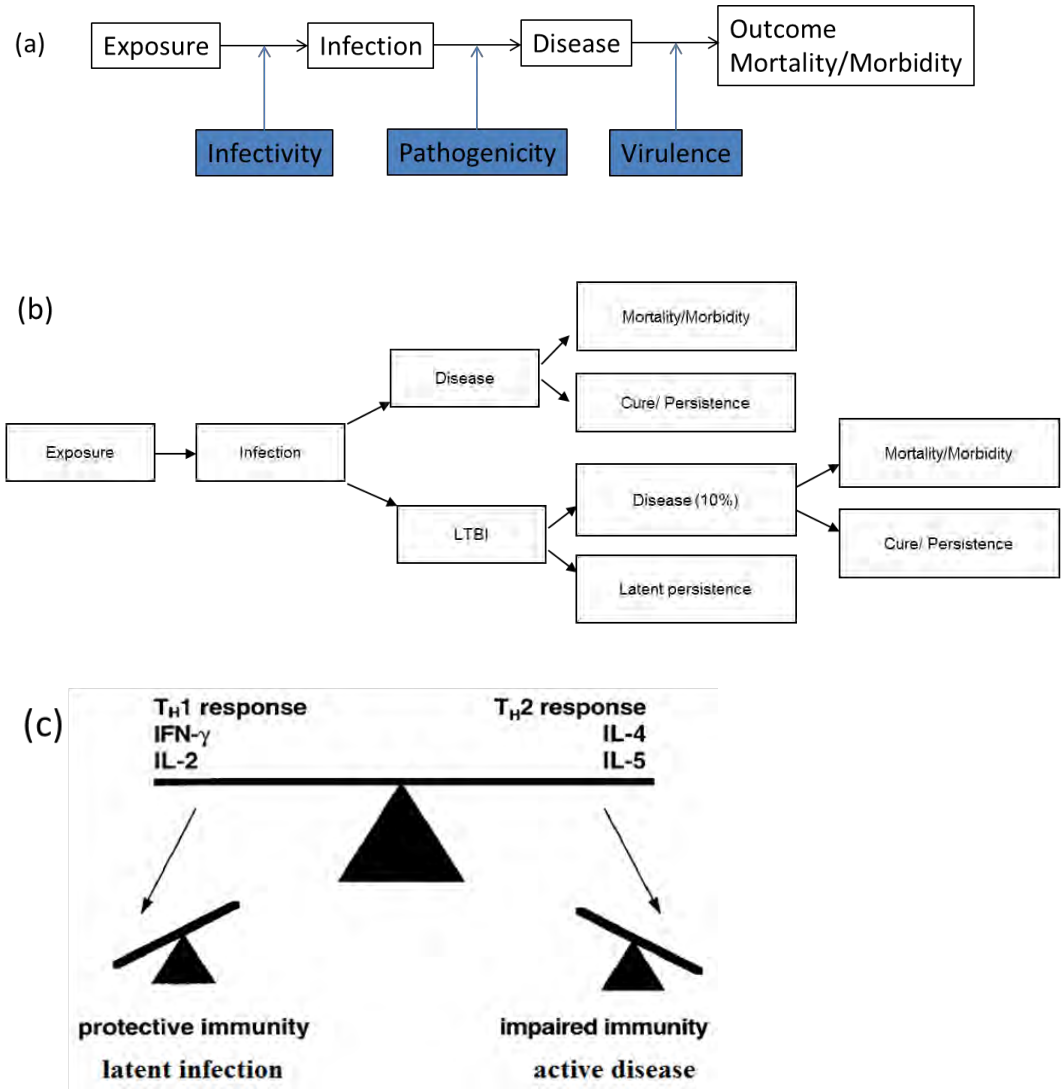

Figure 1.2: Tuberculosis infection exposure to outcome. (a) shows the normal pipeline of infectious diseases from exposure to outcome. (b) shows the deviation of tuberculosis infection from the normal pipeline of infection. (c) shows the balance between the types of immune response elicited and the outcome of infection (adapted from Schluger *et al* [6].

Members of the *Mycobacterium tuberculosis* complex (MTBC) comprise a variety of human and animal pathogens including *M. cannetii*, *M. pinnipedii*, *M. bovis*, *M. caprae*, *M. africanum* and *M. microti*. These exhibit immense genetic homogeneity with genetic conservation of 99.9% amongst strains. This strict level of genetic homogeneity led to the assumption that genetic variety amongst different strains would not be of any clinical significance [12]. However, despite the observed limited genetic variability of *Mycobacterium tuberculosis* isolates, they have been observed to exhibit vast discrepancies in phenotypic presentation especially in clinical outcome and epidemiological behaviour [13–17].

The aspects of clinical presentation that have been found to be diverse amongst different strains in the development of the disease can cumulatively be termed virulence traits. These encompass severity of disease, propensity to launch into active disease instead of latent infection, transmissibility, inclination towards extra-pulmonary infection (bone, blood, CNS) immunopathology, drug resistance and ultimately mortality rate [17–21]. This has led to the suggestion that the diversity of *Mycobacterium tuberculosis* strains may be an important determinant in the development of the disease and outcome of infection [22,23].

Experimental studies using various models of infection have accumulated evidence that a number of traits manifested by members of the MTBC may be influenced by the genetic and evolutionary background of *Mycobacterium tuberculosis* strains [24–28]. It remains to be determined though whether the genetic differences between different strains translate to proteomic differences which can further facilitate the understanding and characterisation of differential virulence. This review describes the molecular diversity found within the MTBC and further correlates it with differential virulence characteristics observed amongst strains in various studies.

1.4 The genome of *Mycobacterium tuberculosis*

The genome of *Mycobacterium tuberculosis* has been extensively studied since the isolation of the H37Rv strain in 1905. The complete genome sequence of the bacillus has been sequenced and characterised [11]. The combination of genomics and bioinformatics has seen an increase in the annotated sequences linking what could be otherwise unknown genetic sequences to possible functions. The genome is predicted to carry about 4047 open reading frames (ORF), each averaging about 1114bp and containing only 6 pseudogenes [11,29]. Analysis of *M. tuberculosis* transcripts and protein products using bioinformatics has enabled of practical function to approximately 40% of the genome. To 44% of the genome, predicted function has been assigned based on identified similarities to known genes of other organisms. The remaining 16% resemble no known proteins and hence are predicted to be novel proteins whose functions are explicit to *M. tuberculosis* [11]. A summary of the *M. tuberculosis* genome functionalities is shown in Figure 1.3 below.

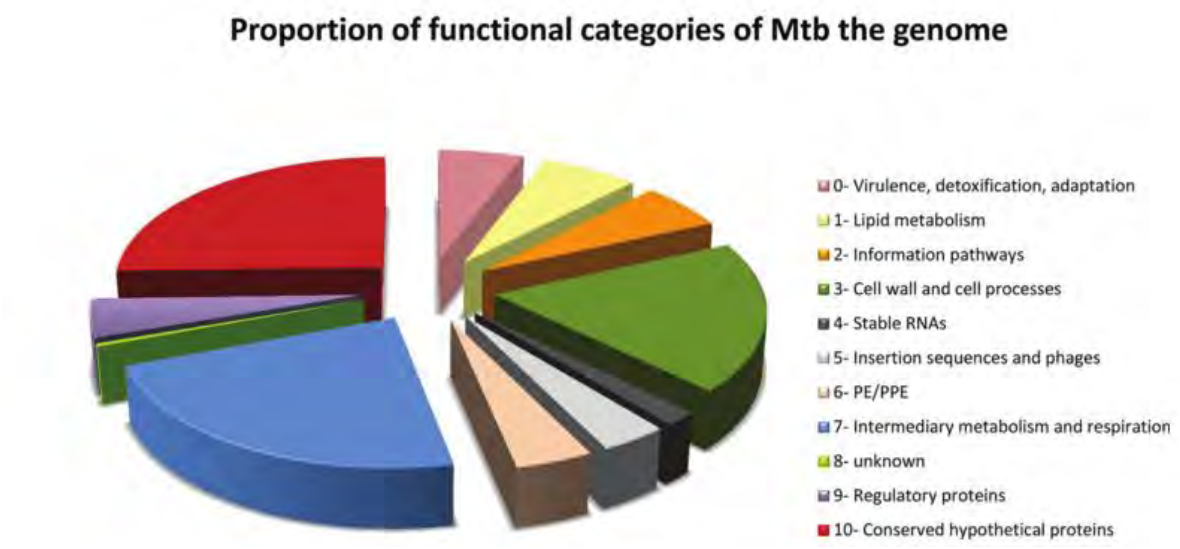

Figure 1.3: The distribution of functional categories in the *Mycobacterium tuberculosis* genome. Conserved hypotheticals, unknown, intermediary metabolism and respiration classes dominate and constitute approximately $^{2}/_{3}$ of the functional repertoire of *M. tuberculosis* whilst leaving the rest of the classes to fill in the remaining $^{1}/_{3}$. (Obtained from Tuberculist version 2.3 release 22, (http://tuberculist.epfl.ch/)

Phylogenetically, *Mycobacterium tuberculosis* is flanked by closely related Mycobacterial species collectively known as non-tuberculous Mycobacteria (NTM) shown in Fig 1.4 below. NTMs are acid fast mycobacteria other than *Mycobacterium leprae* that fall short of the MTBC group. These organisms are generally dubbed environmental bacteria residing normally in soil and water [30]. Previously, NTM infections were not given much attention and clinical implications of NTM infection were not considered critical. However with an increase in immunosuppression driven by HIV, misuse of immunosuppressive drugs and steroids they are now considered potentially pathogenic [31,32]. They are the most common opportunistic infections causing tuberculosis like symptoms in HIV positive individuals. The most common NTM's are members of the *Mycobacterium avium* complex in the USA closely followed by *Mycobacterium kansasii* and *Mycobacterium ulcerans* [31,33,34]. Although some of these organisms cause disease, 16S RNA phylogenetic analysis clearly sets the MTBC apart meaning that although there may be similarities, well-defined distinctions still exist between disease caused by the MTBC and NTMs.

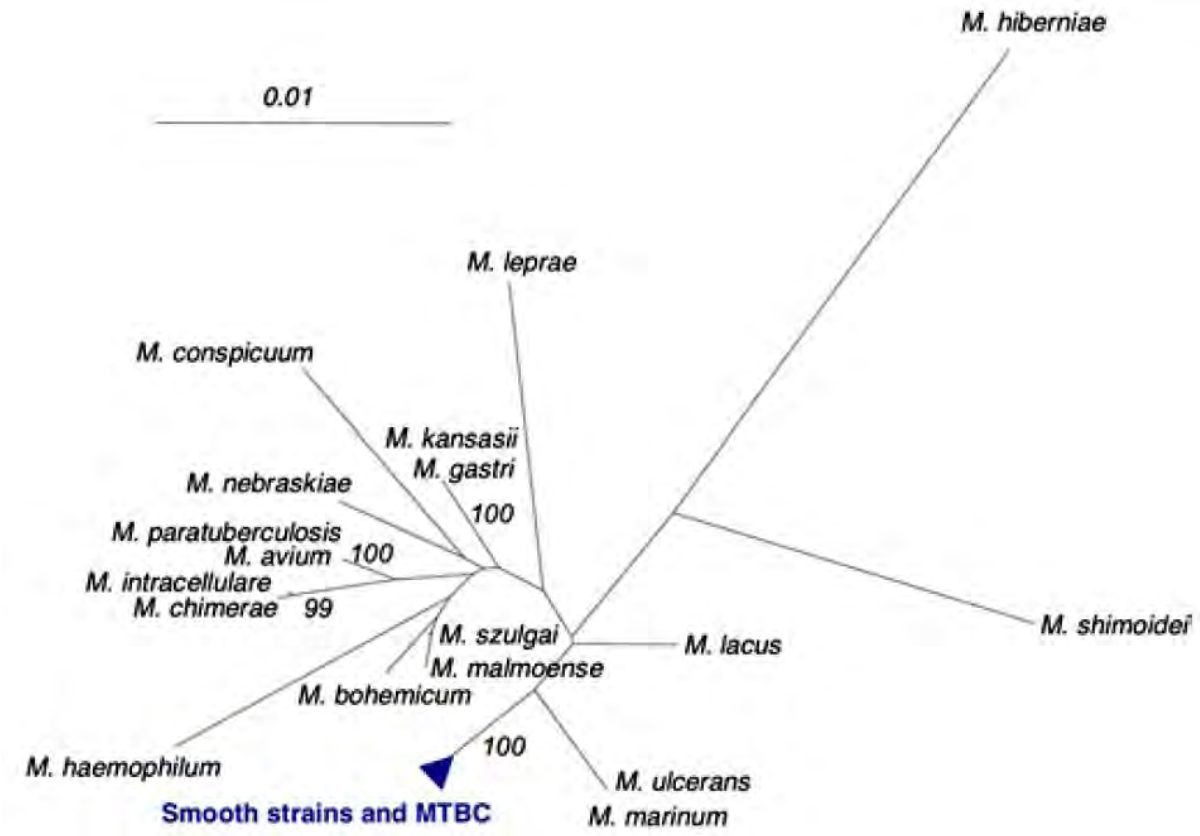

Figure 1.4: Phylogenetic position of *Mycobacterium tuberculosis* among other major species of the *Mycobacterium* genus based on 16S rRNA comparison. Adapted from Gutierrez *et al*, 2005 [35].

1.5 Sources of genetic variation in *Mycobacterium tuberculosis*

Genetic variation within the MTBC genome is minimal due to the restricted niche, hence the genome of *Mycobacterium tuberculosis* is considered a closed pan genome. This automatically limits horizontal gene transfer (HGT) as a source of genetic variation [36,37]. Consequently, the sources of variation in the MTBC genome mainly come from deletion, duplication, rearrangement and polymorphisms which include single nucleotide polymorphs (SNPS) and large sequence polymorphs (LSP) [14,38]. Studies have shown that variations in the genome are mostly localised to certain areas of the genome [39–41] suggesting that *Mycobacterium tuberculosis* has an intrinsic ability to constrain mutations to certain regions of its chromosome [38]. It is these variations in the genome that are used to separate *M. tuberculosis* strains into different lineages.

1.6 Strain typing of *Mycobacterium tuberculosis*

Genetic analysis based methods of strain typing *Mycobacterium tuberculosis* have proven to be an essential tool in differentiating strains of the MTBC. These methods have replaced biochemical methods that were previously used [42] which tended to be laborious and lacked

depth in terms of elucidating phylogenetic relationships. The first standard method of genetic strain typing was *IS6110* restriction fragment length polymorphism (RFLP). Subsequently, more powerful techniques have been developed including spoligotyping, Mycobacterial Interspersed Unit Variable Number Tandem Repeats (MIRU-VNTR) and direct genome sequencing platforms which enable the profiling of whole genome sequences for polymorphs [43].

1.6.1 RFLP (*IS6110*)

Restriction fragment length polymorphism (RFLP) for *Mycobacterium tuberculosis* typing is based on the existence of multiple copies of identical sections of an insertion DNA sequence that contains a distinct restriction endonuclease site [44]. The repetitive insertion sequence (IS) in *Mycobacterium tuberculosis* is a 1355bp DNA sequence known as the IS6110 element and contains a PvuII restriction site [45–48]. Analysis of these sequences and their copy numbers in the chromosome provides strain specific epidemiological information that is highly reproducible [44].

A detailed description of RFLP using the *IS6110* element has been described by van Embden *et al* [49]. Briefly the genome is digested with PvuII enzyme and the fragments are run on a gel before hybridization with an *IS6110* probe to produce a distinct banding pattern. This method was found to be reproducible and reliable in displaying Mycobacterial diversity due to the stability of the *IS6110* element [47,50]. However, the ability to differentiate strains using the *IS6110* element is dependent on the copy number of the *IS* element. It has been shown to be more effective in strains with copy numbers above 5 hence it is not comprehensive enough to cover strains that have low copy numbers [51].

1.6.2 Spoligotyping (Spacer oligotyping)

This method is based on the presence of direct repeat loci containing 36bp tandem repeats separated by varying lengths of up to 43 unique spacer sequences between 35 to 41 bp in the *Mycobacterium tuberculosis* genome [47,52]. The standard spoligotyping method is described by Groenen *et al* [53]. Briefly, polymerase chain reaction (PCR) is used to amplify the spacer sequences between the direct repeat elements and hybridizes them to an array of membrane bound probes corresponding to a selection of given spacer sequences. Strains differ in the number of direct repeats and in the presence or absence of particular spacer sequences [43,46]. The utility of spoligotyping is extensive and the results are reproducible. This method has been

used to describe 32 295 strains from 122 countries in the spolD4 database [54]. However, the discriminatory power is low when distinguishing between very closely related strains. For example various strains of the W-Beijing family have been shown to have identical spoligotypes [47,55,56].

1.6.3 Mycobacterial Interspersed Repetitive Units-Variable Number Tandem Repeats (MIRU-VNTR)

This method is based on the presence of short repetitive nucleotide sequences that are found in the genome of *Mycobacterium tuberculosis* as tandem repeats of variable length and number known as variable number tandem repeats (VNTR) [57]. The presence of repetitive human-like mini-satellite sequences of between 40 to 100bp known as Mycobacterial Interspersed Repetitive Units (MIRU) are found in 41 loci in the genome of *Mycobacterium tuberculosis* H37Rv [58,59]. The polymorphic nature of 12 of these MIRU was found to be useful for phylogenetic characterisation hence, utilising the 12 MIRU and the VNTR, a PCR based method was developed that amplifies either 15 or 24 of these loci [60]. The result of a MIRU-VNTR experiment is a unique 12 digit number per strain denoting the number of repeats at each locus.

The main advantage to this method is the adaptability to high throughput automation as well as the digitalization of the MIRU-VNTR patterns which make it suitable for global study of Mycobacterial molecular epidemiology [58,61]. Furthermore, its discriminatory power has shown to be higher than spoligotyping [61–64], however it has been found to be less discriminatory than *IS6100* RFLP typing for strains with high copy number *IS6110* [65]. In some cases therefore all three methods are used together to either complement or clarify the result. Hence although each method has its merits, using a combination of all 3 methods gives the highest discriminatory power [12].

1.6.4 Large sequence polymorphisms

Large sequence polymorphs also known as regions of deletion (RD) [29] in the *Mycobacterium tuberculosis* genome have been shown to represent unique irreversible changes in the genome [22,66]. Compared to previously described micro-satellite and repeat sequences, their stability allows them to define long-standing phylogenetic relationships between species of the MTBC. LSP are assessed by PCR thus making LSP-typing a robust and high-throughput method of

defining phylogenies of the MTBC that has been used in various classification studies [22,41,66–68].

1.6.5 Single nucleotide polymorphisms

Automated genome sequencing platforms have identified SNP, scattered through the *Mycobacterium tuberculosis* genomes as key indicators of genetic drift within the MTBC. These polymorphisms are broadly grouped into 2 categories including synonymous SNP and non-synonymous SNP. In the latter, the SNP results in a tangible change in phenotype such as alterations in drug resistance, whilst in the former, there are no observable changes in phenotype. Both types of SNP have been used to phylogenetically classify *Mycobacterium tuberculosis* strains [13,69,70]. All the above methods of *M. tuberculosis* strain typing are compared and contrasted in Table 1.1 below.

Table 1 Comparison of techniques for molecular typing or evaluating genetic diversity within *Mycobacterium tuberculosis*

	IS*6110* RFLP	Spoligotyping	MIRU-VNTR	LSP analysis	SNP analysis
Discriminatory power	Excellent	Fair to poor	Good to excellent (newer protocols)	Poor	Poor, likely to improve with increased SNP identification
Ease of use	Time consuming and technically demanding; requires extracted chromosomal DNA	Rapid and simple; can be performed directly on specimens or heat-killed cultures	Rapid and fairly simple; automation requires access to sophisticated equipment; can be performed on heat-killed cultures	Simple and robust	Rapid and fairly simple; high-throughput analysis requires access to sophisticated equipment
Interpretation	Simple, but not easily standardised	Simple visual interpretation	Simple visual interpretation	Straightforward	Straightforward
Data sharing	Complex, lack of standardised nomenclature	Straightforward, standardised binary or octal coding	Straightforward, standardised numerical coding	Straightforward, standardised nomenclature	Straightforward, standardised nomenclature
Utility for epidemiological investigations	Excellent due to high discriminatory power	Useful for rapid cluster identification but requires secondary confirmation	Excellent and rapid with newer protocols	Poor due to low discriminatory power	Poor at present due to low discriminatory power
Utility for phylogenetic analysis	May be limited by irregular rates of transposition and favoured sites	Fairly good correlation with SNP-based phylogeny; large deletions may bias analysis	Relatively poor correlation with SNP-based phylogeny	Useful for evolutionary history (sequential deletions) and for identifying major lineages	Gold-standard; low rate of SNPs in *M. tuberculosis* necessitates large-scale sequencing to identify informative SNPs

Table 1.1: Comparison of strain typing methods that have been used to classify *Mycobacterium tuberculosis* strains. Adapted from Nicol *et al* 2008 [17].

1.7 Phylogeny and Classification of Mycobacterium tuberculosis

Early classification techniques using non-synonymous SNPs classified *Mycobacterium tuberculosis* into 2 broad categories, the ancient and modern lineages. For example, combinations of SNPs in the *katG* and *gyrA* genes that are associated with drug resistance were assessed across 850 patient samples, revealing that strains of *M. tuberculosis* fell into 3 principal genetic groups whilst *Mycobacterium bovis* formed a separate group, as shown in Figure 1.4 below [71].

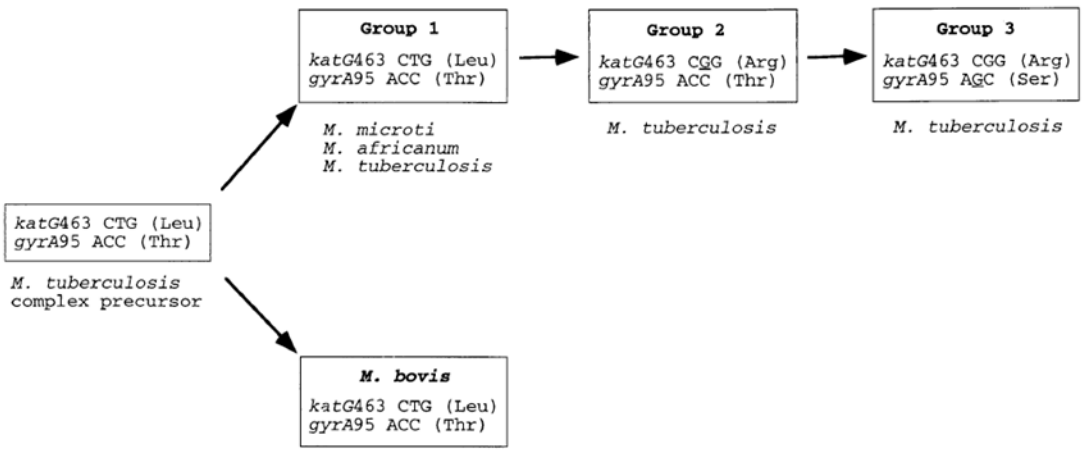

Figure 1.4: The classification of MTBC into principal genetic groups based on two nsSNPs. Adapted from Sreevatsan *et al* 1997 [71]

Classification resolution was further increased in a study by Brosch *et al* [41] who assessed LSP across 20 variable regions in the *Mycobacterium tuberculosis* genome, including RD1-14, RvD and the TbD1 region, which was the basis for the initial classification by Sreevatsan *et al* [71]. It was observed in this study that *Mycobacterium tuberculosis* lineages still grouped into ancient and modern lineages as before, but that a clearer resolution was observed for the evolution of the animal strains including *Mycobacterium canettii*, *Mycobacterium microti* and the various strains of *Mycobacterium bovis,* as shown in Figure 1.5 below.

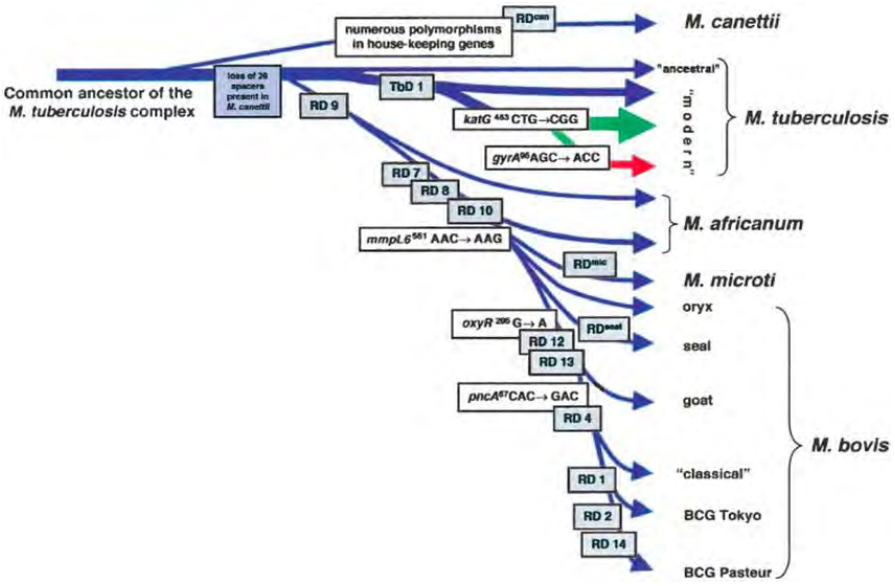

Figure 1.5: The scheme of evolutionary pathway representing the region of deletion in *Mycobacterium tuberculosis* lineages. Adapted from Brosch *et al* 2002 [41].

The utility of large sequence polymorphs for describing deep phylogenetic relationships in the MTBC was then demonstrated by Gagneux *et al* [22] in a study carried out over 11 years in San Francisco. In this study, comparative whole genome hybridization assays were carried out on 19 lineage specific LSP's across 111 strains revealing six main lineages within the MTBC. Furthermore there was a strong correlation between the host and the geographic origin of the strains as seen in Figure 1.6 [22] suggesting co-evolution of *Mycobacterium tuberculosis* strains with their host populations.

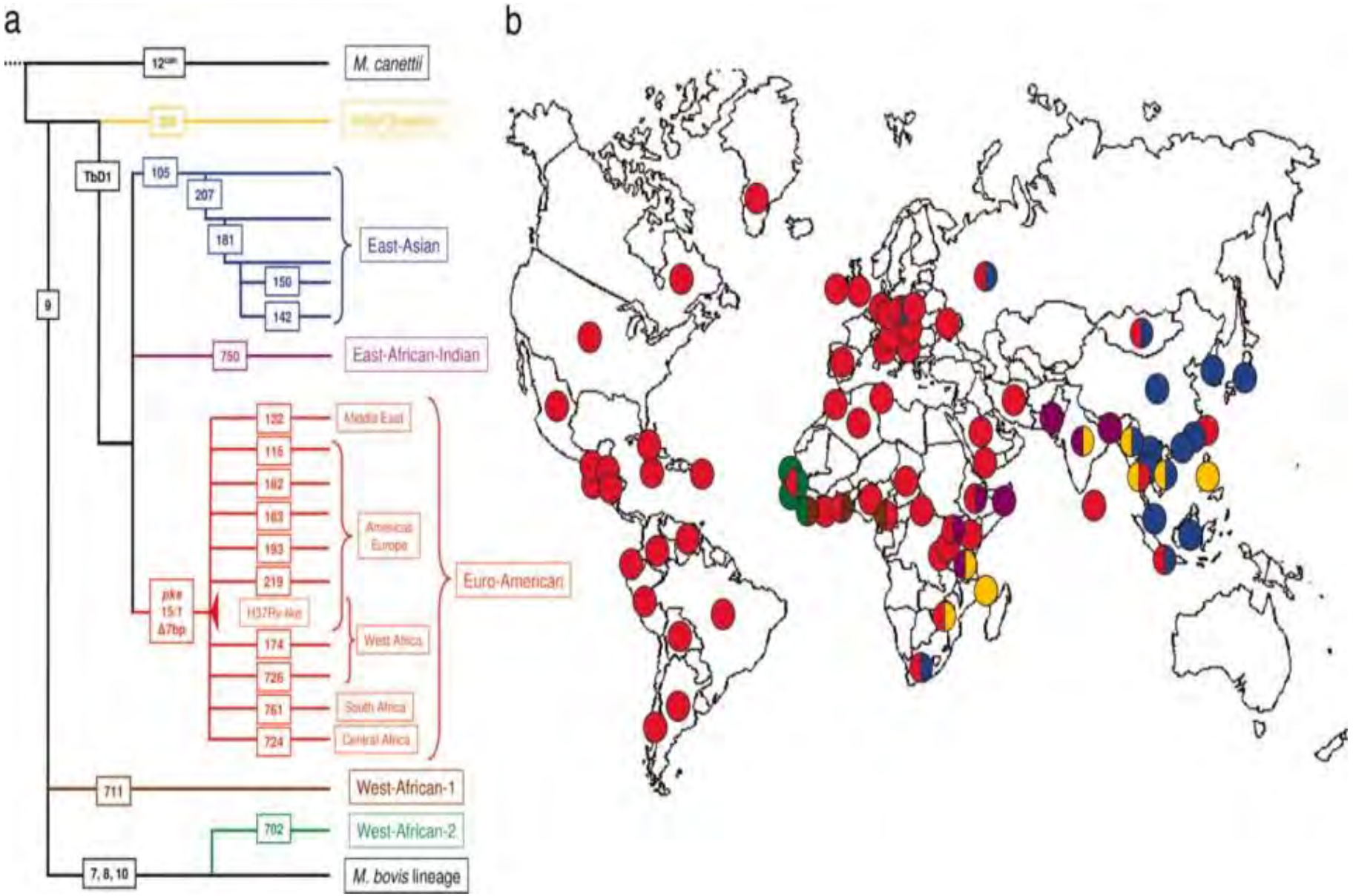
a
b
M. canettii
TbD1
105
207
181
150
142
East-Asian
9
750
East-African-Indian
122
115
182
183
193
219
Euro-American
174
726
761
724
711
West-African-1
702
West-African-2
7, 8, 10
M. bovis lineage

Figure 1.6: Global distribution of Mycobacterium tuberculosis strains. (*a*) LSPs define a global phylogeny for *Mycobacterium tuberculosis*. The names of the lineage-defining LSPs or regions of difference are shown in rectangles. The geographic regions associated with specific lineages are indicated. (*b*) The six main lineages of *Mycobacterium tuberculosis* are geographically structured. Each dot corresponds to 1 of 80 countries represented in the global strain collection. The colours of the dots relate to the six main lineages defined in Figure. 1*a* and indicate the dominant lineage(s) in the respective countries. Adapted from Gagneux *et al* 2006 [22].

The 4th spoligotype database describes 9 main spoligotype defined *Mycobacterium tuberculosis* genotype families also with fine geographic genetic predisposition, again suggesting a fine correlation with human demography [54]. Using the MIRU-VNTR strains, Wirth *et al*, also revealed insights into the origin and demography of the MTBC and its dynamic association with the human host. This study revealed 2 distinct clades using the neighbour joining algorithm. In one clade, all human *Mycobacterium tuberculosis* isolates were grouped and a separate clade encompassed all animal MTBC strains (*Mycobacterium microti, Mycobacterium bovis, Mycobacterium caprae* and *Mycobacterium pinipedii*) together with the human isolates from West-Africa (*Mycobacterium africanum* West African 1 and 2) [72].

The grouping in this study appears to be broadly congruent with that were carried out previously using large sequence polymorphs (LSP) and spoligotyping [62]. A further study by Hershberg *et al* 2008 used synonymous as well as non-synonymous SNP's on multi-locus sequencing of 89 genes across 108 strains to study the genetic drift between strains and the associated evolutionary consequence [70]. This recent global phylogenetic classification identified a total of 488 SNP's and also separated *Mycobacterium tuberculosis* to ancient and modern lineages. The study further established a phylogenetic correlation between genetic variability in *Mycobacterium tuberculosis* strains and the geographical distance travelled by these strains from the ancestral progenitor with evidence that the MTBC in Africa and subsequent spread throughout the world following human migration patterns [70] as shown in Figure 1.7 below.

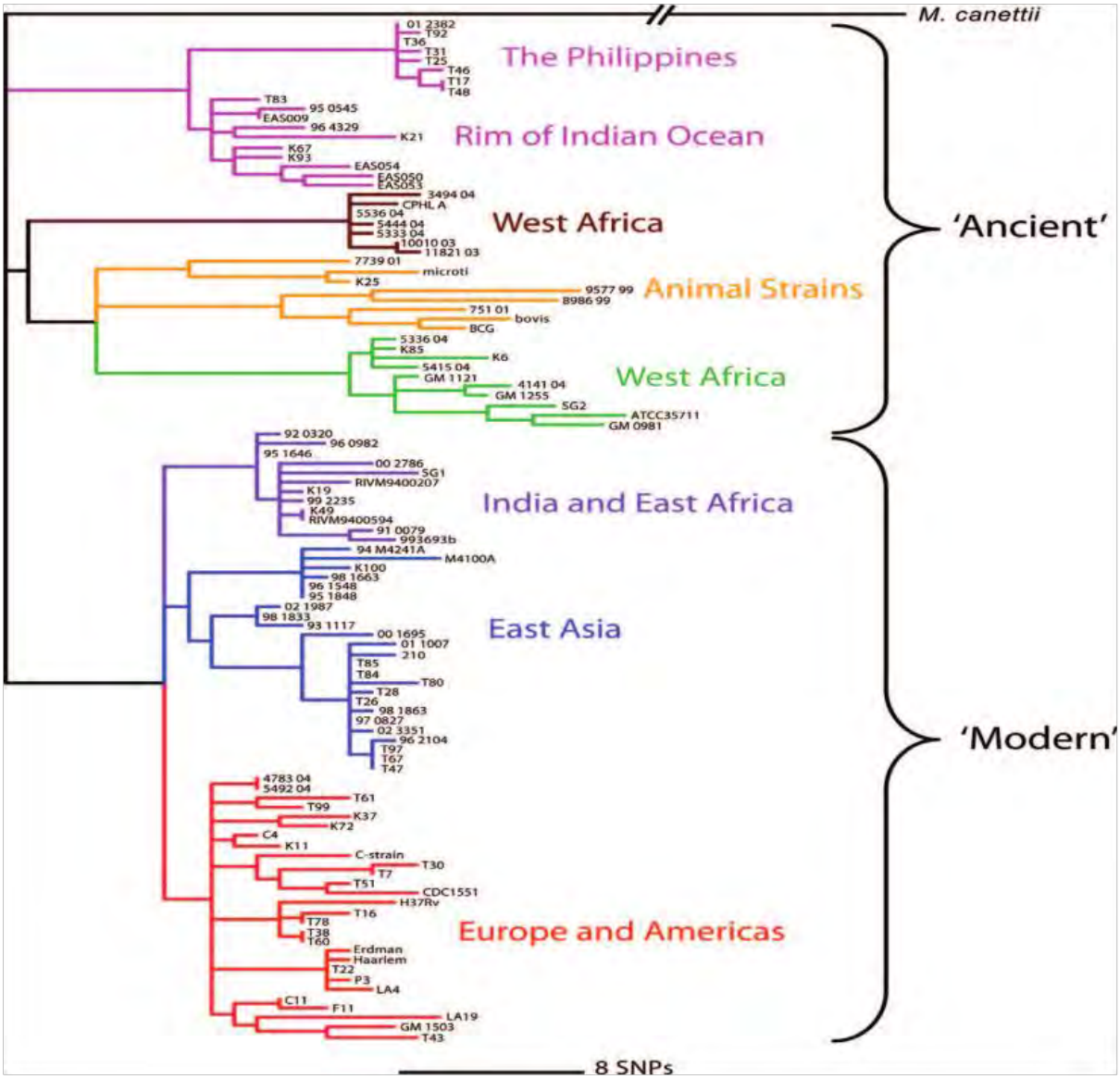

Figure 1.7: Global phylogeny of *M. tuberculosis* based on multi-locus sequencing of 89 genes from 108 strains. Adapted from Hershberg *et al* 2008 [70]. Each node denotes individual representative strains.

Furthermore, Comas *et al* 2010 used whole-genome sequencing on 22 strains and obtained classification similar to that previously produced using LSP's and SNP's [73]. Based on this method of classification, a change in the nomenclature of the MTBC was suggested by the authors to that shown in Table 1.2 below. Due to confusion surrounding previous nomenclatures, this nomenclature will be used further in this thesis.

Comas et al lineage classification	Name	Strains
Lineage 1	Indo-oceanic	EAI
Lineage 2	East Asian	Beijing
Lineage 3	CAS/Delhi	CAS
Lineage 4	Euro-American	LAM, H, X, T, S & others
Lineage 5	West- African 1	*M. africanum* (Afri 2)
Lineage 6	West-African 2	*M. africanum* (Afri 1)

Table 1.2: Lineages and strains represented by the lineage. EAI- East African Indian, CAS- Central Asian, H- Haarlem, LAM-Latin American Mediterranean, AFRI- *M. africanum*.

From such analyses, it becomes clear that numerous external selective forces have driven the evolution *of Mycobacterium tuberculosis,* including human demography, migratory flows, passed tuberculosis epidemiology, and history of livestock domestication [1]. Evidence also suggests that evolutionary characteristics of *Mycobacterium tuberculosis* with the human host could have a combined effect in the spread of phenotypes such as drug resistance, hence linking genetic phylogeny to observed phenotype.

1.8 Transcriptomic analysis on *M. tuberculosis*

It has been shown that genomic variation is in part responsible for some of the variation observed among strains of tuberculosis. However, variations in gene expression also play a role in differential phenotype. The transcriptome of *M. tuberculosis* has been studied in different strains under various conditions. The tuberculosis database (TBDB) contains a composite of all transcriptomic experiments that have been carried out on various strains of *M. tuberculosis* and some major NTMs under a myriad of conditions, treatments and in various disease models (http://www.tbdb.org). Transcriptomic profiling of differentially virulent strains revealed that clear differences exist between strains of different virulence and shed light on the broad basis of differential phenotypes.

A noteworthy transcriptomic study was done comparing the human laboratory strain H37Rv and the bovine tuberculosis strain *M. bovis*. This study revealed that there are no differences in the genes between the strains, however there are significant differences in gene expression which may possibly be responsible for differences in the pathogenicity and host preference. A total of ninety two genes were found to be significantly differentially expressed including lipid metabolism, regulatory proteins, PE/PPE and toxin-antitoxin systems [74]. Approximately half

of the differentially expressed genes observed in this study are in agreement with previous studies also comparing the H37Rv and *M. bovis* suggesting that these genes are possibly tied to differential phenotype by more than chance [75].

In another study, analysis of the laboratory strain H37Rv and a mutant of H37Rv with a RD1 deletion similar to that of *M. bovis* BCG [76]. Analysis of this pair of strains links a known change in the genome to a known change in phenotype. This analysis revealed that deletion of the RD1 region significantly affected the expression of 15 other genes outside the RD1 locus including Rv0824c, Rv2391, Rv2392 and Rv2590 among others. This suggests that defined alterations in the genome are capable of affecting gene expression outside the specific loci hence making it challenging to define phenotype simply from looking at the genotype.

In another study, comparison between clinical strains Beijing strain (H8N8) and CDC1551 showed that after 6 hours of infection, the CDC1551 strain up-regulated more stress response genes than the Beijing strain. In contrast, after 24 hours of infection of macrophages, the more virulent Beijing strain had up-regulated genes involved in lipid synthesis and cholesterol metabolism genes compared to CDC1551. This immediately suggests that different strains have different approaches to process of infection. Whilst the CDC1551 strain may act by counteracting stress response due to activation of macrophages, the Beijing strain sub-optimally activates macrophages hence preventing the associated stress cascade induced by activated macrophages [77].

Global transcriptomic analysis carried out by Homolka *et al* 2010 revealed that genetic variation between strains has a significant impact on global gene expression. In this study, they defined a core transcriptome of *M. tuberculosis* that is expressed by many strains during infection [78]. This core transcriptome was defined as the common set of genes that *M. tuberculosis* needs to express in order to remain a successful intracellular pathogen. Their study revealed a total of 364 genes with significant differential expression between at least one pairwise comparison as well as genotype specific signatures. For example they show that the virS-mym operon (Rv3082c-3089) is deregulated in all EAI strains and the dosR two-component regulator (Rv3132c-3133c) is overexpressed in all Beijing strains [78].

Transcriptome analysis carried out by Rose *et al* 2013 compared lineages 1 and 2 and observed clear relationships between the genotype and transcriptional phenotype. In this study it was

observed that the difference arose from 3 mechanisms. Firstly amino acid changes in transcriptional regulators resulted in the loss of control of the associated genes [79]. Secondly, alterations in nucleotide sequences resulted changes in promoter activity and the creation of start sites within intergenic regions. The result of this was observed to be the formation of functionally active but truncated proteins which have altered effect on immune recognition hence phenotype. The third category was that of genes whose difference in expression was not caused by mutations *per se* but rather specific patterns of inherent changes in gene expression. For examples some lineages were observed to express toxin-antitoxin systems more than others[79] This study shows in-depth the effects of mutations on gene expression as well as lineage specific inherent mechanisms influence phenotype.

1.9 The role of proteins in tuberculosis phenotype

Determination of the global proteome at individual strain level is a vital complementary procedure to whole genome studies because the repertoire and abundance of proteins expressed in different cells is influenced by transcription and translation which are themselves complex dynamically regulated processes that depend on both genotype and environmental factors. Since proteins govern all basic processes in the cell and since the correlation between gene and protein expression levels is generally poor, it becomes necessary to carry out a proteomic investigation to complement the picture that the genome paints, in order to understand the different observed clinical phenotypes exhibited by different strains of this otherwise genetically homogenous organism.

Clinical implications of strain diversity can be described by the phenotypic presentations of the strain or organism, including aspects such as mortality, morbidity, bacterial load, transmissibility, drug resistance, tendency to enter into latency and virulence. Some of these traits have been widely described at the genomic level using various models [71,80–87] however, only a few studies exist to relate phenotype directly to proteomic differences between strains.

The ideal way to associate certain phenotypes with a specific protein or groups of proteins is to knockout the gene encoding that protein and to observe the characteristic changes that the absence of that protein confers on the phenotype in *in vitro* and in *in vivo* models. The most classic example of proteins linked to phenotype is the RD1 region deletion in BCG strains which results in the attenuation of BCG strains such that they are routinely used as live

attenuated global vaccine strains. The RD1 region contains structural genes encoding 9 proteins (including ESAT-6 and CFP-10) that are known to be all present and functional in virulent strains of *Mycobacterium tuberculosis*. Knockout of the RD1 region from *Mycobacterium tuberculosis* H37Rv has resulted in a similar attenuation to that of *Mycobacterium bovis* BCG whilst a RD1 knock-in experiment on *Mycobacterium bovis* BCG has resulted in the replacement of a virulent phenotype similar to *Mycobacterium tuberculosis* [88,89]. Other examples of studies that have been carried out using single knockout studies to determine the effect of single proteins on virulence are summarised in Table 1.3 below.

Rv Locus	Gene Name	Protein name	Function	Type of experiment	Phenotype	Reference
Rv3763	lpqH	19 kDa protein	Host signalling	Gene disruption and complementation	Strain rapidly cleared from the lungs and spleen	[90,91]
Rv3874 & Rv3875		ESAT-6 & CFP-10	Immuno-modulation	Knock-out and knock-in	Attenuation in macrophages, Mouse models and human models	[41,88,89,92]
Rv2220	glnA1	Glutamine synthase	Synthesis of cell wall component of pathogenic strains	Enzyme inhibitor	Inhibited growth in macrophage and guinea pig models	[93,94]
Rv3810	erp	erp		Inactivation using 2 step plasmid approach	Attenuation in murine macrophage models, Lungs and spleen of mouse models	[95]
Rv2940	mas	mas	Synthesis of long chain fatty acids (PDIM's)	Gene disruption and complementation	Attenuation in macrophages & mice	[96,97]
Rv2930	fadD26	fadD26	Acyl-co-A fatty acid metabolism (PMID's)	Transposon mutagenesis	Reduced bacterial load in mouse lungs	[96,98,99]
Rv2941	fadD28	fadD28	Acyl-co-A fatty acid metabolism (PDIM's)	Transposon mutagenesis	Reduced bacterial load in mouse lungs	[100]
Rv2942	mmpl7	mmpl7	Possible substance export molecule	Transposon mutagenesis	Failure to transport PMID's resulting in attenuated growth in mice	[98,101]
Rv3804c	fbpA	antigen 85 complex	Transport of long chain fatty acids	Mutant using linear DNA construct	Severe attenuation in human ad mouse macrophages	[102,103]
Rv0642c	mmaA4	mmaA5	Methyl-transferase for the formation of mero-mycolic acids	Inactivation using 2 step plasmid approach	Normal growth *in-vitro* however does not make methoxy-mycolates, Marked cell wall alteration which becomes less permeable, Resistance to ROS	[104–106]
Rv0470	pcaA	pcaA	Methyl-transferase that forms cyclo-propane residues on mycolic acids	Transposon mutagenesis	Abnormal colony morphology, Less virulent as judged by a mortality assay using mice, Cleared more rapidly from the lungs	[107]
Rv0899	ompA	ompA	Porin for substance transport	Inactivation using 2 step plasmid approach	Delayed growth in acid conditions, Attenuation in both human and mouse macrophage models	[108]
Rv0475	hbhA	hbhA		Inactivation using 2 step plasmid approach	Longer generation time and low bacterial load in the spleen compared to wild type	[109]
Rv0467	icl/aceA	isocitrate lyase	Energy production	Allelic replacement using plasmid system	Killed more rapidly in macrophages, Severely affected by CMI	[110]
Rv1345	fadD33	fadD33	Acyl-co-A synthase fatty acid oxidation	Inactivation using 2 step plasmid approach	Decreased virulence in liver similar to H37Ra	
Rv1755c, Rv2349c-Rv2351c	pclA,B,C, D	pcl proteins	Phospholipases	Transposon mutagenesis	Attenuation in mice	[111]
Rv3601c-Rv3602c	panC & panD	panC & pan D	Pantothenate biosynthesis	Transposon mutagenesis	Attenuated virulence as measured by survival time and bacterial load, Protection phenotype similar to BCG	[112]
Rv2987c	leuD	isopropylmalate isomerase	Biosynthesis of leucine	Inactivation using 2 step plasmid approach	Mutant could not grow in murine macrophages or kill SCID mice, Attenuation protection similar to that of BCG	[113,114]
Rv2192c	trpD	anthranilate phosphoribosyl transferase	Tryptophan biosynthesis	Inactivation using 2 step plasmid approach	Severely attenuated in macrophages, Difficulty growing in mice, could not kill mice	[95,115,116]
Rv0500	proC	pyroline carboxylate reductase	Proline biosynthesis	Inactivation using 2 step plasmid approach	Mutant attenuated in murine models	[116]
Rv0780	purC	phosphoribosylamino-imidazole-succino-carboxamide synthase	Purine biosynthesis	Inactivation using 2 step plasmid approach	Mutant attenuated in macrophage models and reduced (*M. bovis*) to completely absent (*M. tuberculosis*) growth phenotype thus severe attenuation of *M tuberculosis*	[117]
Rv1811c	mgtC	mgtC	Magnesium uptake	Inactivation using linear DNA construct	Mutant shows poor growth in human macrophages and mouse models	[118,119]
Rv2383c	mbtB	mbtB	Mycobactin biosynthesis	Inactivation using 2 step plasmid approach	Poor growth in low Fe^{3+} conditions *in-vitro*, Grows slower in human macrophages	[120–123]
Rv2711	ideR	ideR	Regulator of iron uptake and storage	Site directed mutagenesis with second site suppressor	Deregulated siderophore production, Reduced response to oxidative stress, Poor growth in macrophage models, Attenuation in mouse models, Reduced bacterial load in mouse models by up to 4 log units	[123–125]
Rv1161	narG	Nitrate reductase	Anaerobic respiration	Inactivation using 2 step plasmid approach	No replication in *M. bovis* BCG mutant in SCID mouse models but was not cleared from the lungs but growth and cleared in wild type mice	[126,127]
Rv1908c	katG	Catalase peroxidase	Degrades H_2O_2 and organic peroxides and ROI	Spontaneous mutations	Mutations result in in attenuation in guinea pig models in terms of morbidity assays, Attenuation in the lungs and spleen of infected mice and rapidly cleared by the immune system after normal growth	[128–130]

Rv2428	ahpC	Alkyl hydroperoxide reductase	Detoxify organic hypdroperoxides	Antisense method	More sensitive to hydrogen peroxide attack, Decreased virulence in guinea pig model showing 3 log units less bacterial load	[128,130,131]
Rv3846	sodA	Superoxide dismutase	Degradation of superoxides	Antisense method	Severely attenuated in mouse models showing 5 log units less CFUs in the lungs and spleen, Rapid clearance from organs	[132,133]
Rv0342	sodC	Superoxide dismutase	Degradation of superoxides	Inactivation using linear DNA construct & 2 step plasmid procedure	Mutant killed more efficiently in activated murine macrophage models	[132,134]
Rv2703c	sigA	Principal sigma factor	Transcription of housekeeping and virulence genes	Complementation of an avirulent *M bovis* strain with a mutation that caused partial loss of sigA	Attenuated M bovis strain returned to wild type using morbidity assay in guinea pig	[89,135–137]
Rv3286c	sigF	Sigma factor F	Transcription of stress response signatures	Inactivated by allelic replacement	No macrophage phenotype however virulence is attenuated in mouse models using mortality assays	[138,139]
Rv1221	sigE	Sigma factor E	Transcription of stress response signatures	Inactivated by allelic replacement & 2 step plasmid procedure	Mutant more sensitive to temperature changes, detergent exposure, oxidative stress, poor growth/attenuation in murine macrophages and reduced virulence as judged by killing assays	[140–142]
Rv3223c	sigH	Sigma factor H	Transcription of stress response signatures	Inactivation using linear DNA construct & 2 step plasmid procedure	Mutant is sensitive to SDS, heat shock, growth in mice and macrophages unaffected however fewer granulomas and delayed pulmonary inflammation	[143,144]
Rv0757	phoP	Response regulator	Sensor for Magnesium starvation	Inactivation using 2 step plasmid approach	Mutant grows poorly in mouse macrophages and organs, Attenuated in human macrophages	[145,146]
Rv0903c	prrA	Response regulator		Transposon mutagenesis	Growth of the mutant is stunted in primary macrophages, Decreased bacterial load in the spleen of mice	[139,147]
Rv0981	mprA	2 component response regulator		Inactivation using 2 step plasmid approach	Mutant grew faster in wild type human macrophages however it did not persist in the lungs and livers of mice as it was cleared faster than wild type	[148]
Rv2031	hspX	Alpha chrystallin	Heat shock protein	Transposon mutagenesis	Attenuation in macrophage models	[149–152]
Rv0353	hspR		Repressor of heat shock proteins	Inactivation using 2 step plasmid approach	Mutant is attenuated in mouse models	[153]
Rv3416	whiB3		Transcriptional regulator	Inactivation using 2 step plasmid approach	M bovis mutant was severely attenuated in guinea pigs but M tuberculosis mutants survived longer in mouse models	[154]
	pks1-15	polyketide synthesis	Formation of phenolic glycolipids	Inactivation of pks gene cluster	Mutant has lower bacillary load in CSF and brain, lower leukocytosis, decreased dissemination to other organs, lower levels of TNF in rabbit models of tuberculosis meningitis	[82,130,155,156]
Rv2770	PPE44	ppe44	Possible antigen	Naturally occurring SNP's found in certain strains of the w-beijing genotype	Strains with the SNP's had increased expression of the protein, Higher antibody titres, Differential host immuno-pathogenesis	[157]

Table 1.3: Proteins of known relevance to phenotype based on various phenotype assessment models.

In order to associate particular characteristics to clinical outcome of strains, it is important that comprehensive studies be carried out across strains. To this end, whole proteomes can now in principle be compared between strains that are known to exhibit different phenotypes and proteins that are differentially expressed between these strains can be pinpointed. In such an approach, phenotype is most likely to be attributed to a group of proteins rather than a single protein.

Various studies to this end have been undertaken, with most comparing two strains. A classic example here is the study by de Souza *et al*, comparing a hyper-virulent and hypo-virulent strain of *M. tuberculosis* [158]. This study discovered that from a total of 1668 proteins, 101 had significant differential expression between the 2 strains of the same lineage but with different phenotype. The list of differentially expressed proteins included regulatory proteins, lipid metabolism proteins and immunogenic proteins amongst others [158]. A number of similar studies have been done comparing two to four strains at most [159–162].

For example de Souza et al compared a hyper virulent strain of the W-Beijing genotype to a hypo virulent strain of the same lineage using label free proteomics. They observed that a total

of 53 proteins were over-expressed in the hyper virulent strain and these fell into the cell wall organisation and regulatory protein category. Furthermore, their study revealed that key immunogenic proteins are under expressed in the hyper virulent phenotype leading to the suggestion that hyper virulent strains modulate the expression of key virulence proteins as a mechanism to evade the immune system [163].

In a study by Pheiffer *et al*, gel based proteomics was used to compare three strains *of M. tuberculosis* including a Beijing strain, a family 23 (F23) strain and the laboratory strain H37Rv. They observed that key proteins associated with virulence are differentially expressed including α-chrystallin, antigen 85, ESAT-6, Hsp65 and Pst1 among others [159]. Comparison of four strains including the K-strain, H37Rv, H37Ra and BCG showed that a probable glycogen phosphorylase (*GlgP*) and a haloalkane dehalogenase (*LinB*) were up-regulated in the clinical strain K –strain compared to the other strains after phagocytosis indicating critical proteins that possibly define current human infection pathways [160].

Alternatively, a group of proteins can be selected to be studied in a targeted manner across strains, for example, Dheenadayalan *et al*, focused on the expression of 16 proteins of the PPE family under different conditions in different strains [164]. Differential expression of the entire set of proteins was observed in different growth conditions and states as well as different strains. This differential expression can then be loosely tied to the known observed differential phenotypes, prompting the further validation of those proteins for the phenotype observed. The robust nature of such studies mentioned above makes them hypothesis generators that highlight subsets of proteins for further study.

1.10 Aims of thesis

Tangible clinical differences have been observed amongst patients infected with different strains of *M. tuberculosis*. But genomic approaches have yet to explain the observed phenotypic differences. This thesis therefore describes a proteomic approach aimed towards unravelling bacterial factors that could contribute to the observed phenotypic differences amongst strains. Using *in vitro* cultures, I aim to:

1. Carry out a comparative liquid chromatography mass spectrometry (LC MS/MS) study across seven strains of the genus *Mycobacterium*, six of which belong to the MTBC group, where 5 are known to be pathogenic and one (BCG) being non-pathogenic. The remaining strain is an outlier belonging to the NTM group which is widely non-

pathogenic like BCG, however both are known to cause disease in HIV-infected individuals. This study aims to assess the total repertoire of proteins produced and their relative quantities in each sample.

2. Based on data obtained from the *in vitro* investigation, identify proteomic correlates of pathogenicity, virulence and latency that could shed light on the molecular origin basis of differential clinical phenotypes of these strains.
3. Devise criteria to select a group of candidate proteins from the data generated from the *in vitro* study and to develop multiple reaction monitoring (MRM) assays for each candidate using *in vitro* cultures.
4. Quantify the selected candidate proteins for which MRM assays have been developed in a panel of clinical samples such as sputum samples and determine clinically viable biomarkers that are either strain specific or that are applicable across multiple different strains for use in a clinical setting.

It is entirely plausible that the mechanisms that result in differential phenotype observed amongst different strains are due to complex interactions between host and pathogen genetics, which have been shown to co-evolve together through the centuries [22] but that is beyond the scope of this thesis which is largely restricted to *in vitro* studies.

To date, differential phenotype studies that have been carried out are more genetic in nature. Proteomics is a broad term that refers to the study of the proteome of biological systems such as cells, organelles or whole organisms [165,166]. Proteomic studies have been used to discover disease associated biomarkers which some of which have been used as diagnostic targets. Modern tandem mass spectrometry based proteomics allows the comparison of expression levels of thousands of discrete proteins in many different biological systems.

Chapter 2: Proteomics technologies and applications literature review

2.1 Proteomics Introduction

The proteome is the entire complement of proteins produced by a cell at any point in time under the given conditions. This follows the central dogma of molecular biology that states that the genome is expressed into mRNA (the transcriptome) which is then translated to proteins [167]. Whilst the genome acts as a static template to provide constant memory for the cell, the proteome is very dynamic and acts as the molecular machinery for almost all functions of the cell. As a result, DNA remains constant in different cells of the same organism and even under different conditions whilst the proteome varies widely according to cell type and conditions of the biological system, which is crucial to the survival of the cell under those specific conditions.

Proteomics is a broad term that refers to the study of the proteome of biological systems such As cells, organelles or whole organisms. It includes identification, visualization, separation, characterization and quantitation of the proteins [165,166]. The methodologies used in proteomics were initially mainly gel and antibody based but they have since shifted to more modern non-gel based and high-throughput mass spectrometry approaches. At the extremes, proteomics coupled to mass spectrometry (MS) allows the measurement of expression levels or changes in expression levels of either a single protein amongst thousands, or of the entire set of discrete proteins in the given system. However, there are more isoforms of proteins than the corresponding genomes and all possible isoforms have eluded the proteomics field to date. In a study by Coromina *et al*, 422 splice variants were obtained from 163 gene sequences [168]. In a separate study, proteomic evidence of splice variants was demonstrated for over a 100 drosophila genes [169]. On the other hand, alternative transcription and translation initiation sites may be used to allow for the expression of different genes over and above the gene sequence template [170,171]. Thus MS has had a massive impact on making (transforming, developing) the field of proteomics into a dynamic and rapidly evolving field of science.

2.2 Mass spectrometry based proteomics

Mass spectrometry is a technique that is used to elucidate elemental composition of a sample, chemical structure of molecules as well as determining the mass of molecules by measuring the mass to charge ratio of charged particles. In mass spectrometry, a device known as a mass spectrometer ion source is used to vaporize then ionize a sample before it is accelerated in an

electric field. A mass analyzer then sorts ions according to their masses in the electric field using the applied electromagnetic field. And finally, a detector records the intensities of each ion of a given mass to charge ratio (*m/z*), producing a mass spectrum which can then be used to determine the molecular composition or structure of each ion as well as relative abundances [172]. To accomplish this, every mass spectrometer has 3 basic components; include an ion source for ionization; a mass analyzer; and a detector.

2.3 Ionization techniques

The technique used for ionization determines which molecules can be analyzed by the mass spectrometer. For biological samples of solid and liquid nature such as those used in this study, the most commonly used methods are matrix assisted laser desorption ionization (MALDI) and electrospray ionization (ESI) [173,174]. In MALDI, the sample is mixed together with the 'matrix' and then it is spotted onto a metal plate to dry and co-crystallize. The matrix is a small organic compound that has absorbance at the same wavelength as the laser that will be used for ionization. Typically, ultra-violet laser light is used to vaporize the matrix and, as it vaporizes, it does so together with the mixed analyte in a manner similar to a volcanic eruption, bringing the analyte to a gaseous protonated state [175].

In ESI, the analyte, typically a chromatographic eluent in an acidic solution is pumped at micro or nano flow rates through a very thin tapered hypodermic needle at high voltage (kV). This electrostatically disperses small micrometer sized droplets which rapidly vaporize and ionize the analyte as it exits the thin outlet [173,175]. One advantage that ESI holds over MALDI is that it can be carried out in direct and continuous combination with liquid chromatography (LC) which MALDI is not directly compatible with, thereby giving greater resolution [175,176]. By comparison, MALDI must be carried out offline with respect to any prior LC fractionation with each fraction spotted individually onto the target plate for subsequent analysis.

2.4 Mass analyzers

2.4.1 TOF

This mass analyzer measures the time of flight of an ion from the source to the detection point, propelled by an electric field of known strength through a field free evacuated flight tube of known length. The m/z is then calculated based on the TOF and the initial charge of the ion [174,177] and according to the formula $m/z = 2eVt/L^2$ [178] for a time of flight mass

spectrometer where *V* is the velocity of the ion, *L* is the length of the flight path and *t* is the flight time. A schematic of the TOF analyzer is shown in Figure 2.1 below.

2.4.2 Ion trap

Ion trap mass analyzers use various mechanisms to trap and store ions. This allows the user to manipulate the ions by using direct current (DC) and radio frequency (RF) electric fields in a series of carefully timed events. The biggest advantage with ion traps is that extended ion storage and m/z analysis MS/MS can take place with less sample loss compared to TOF [179]. The trap acts as a storage mechanism for ions hence allowing an ion or groups of ions to be analyzed and released in controlled intervals [180]. This allows for longer scan times, increased resolution and higher sensitivity [175].

The Orbitrap is a derivative of the ion trap instruments. In this setup, ions are electrostatically trapped around a central spindle shaped electrode to which current is applied to keep ions oscillating along its axis. As the ions oscillate around the spindle they emit current that can be directly measured as the ions pass nearby two detectors within the mass analyzer region [181]. Peptide ions oscillate inside the orbitrap to generate a very good image current that is characteristic of the m/z value of the particular ion and, which can be further mathematically processed using Fourier transform methods to produce high-quality mass spectra that are characterized by high accuracy, sharp peaks and little to no overlap between neighbouring peaks. As a result, the orbitrap is used in experiments that require high resolution for a large number of ions from complex samples such as discovery experiments.

2.4.3 Quadrupole mass analyzers

Quadrupole analyzers are a distinct set of mass analyzers that consist of 4 parallel metal electrodes. Oscillating electrical fields are created by applying direct and alternating current to the rods. When such an electric field is applied, only ions of a certain *m/z* have a stable trajectory and hence can pass through the rods to reach the detector and the rest are expelled between the rods due to their unstable trajectory [179]. Different *m/z* ranges can be selected for by changing the potentials applied to the rods. This can be done as discrete steps between different *m/z* ranges or in a continuous manner [178]. A schematic of a triple quad is shown in Figure 2.1 below.

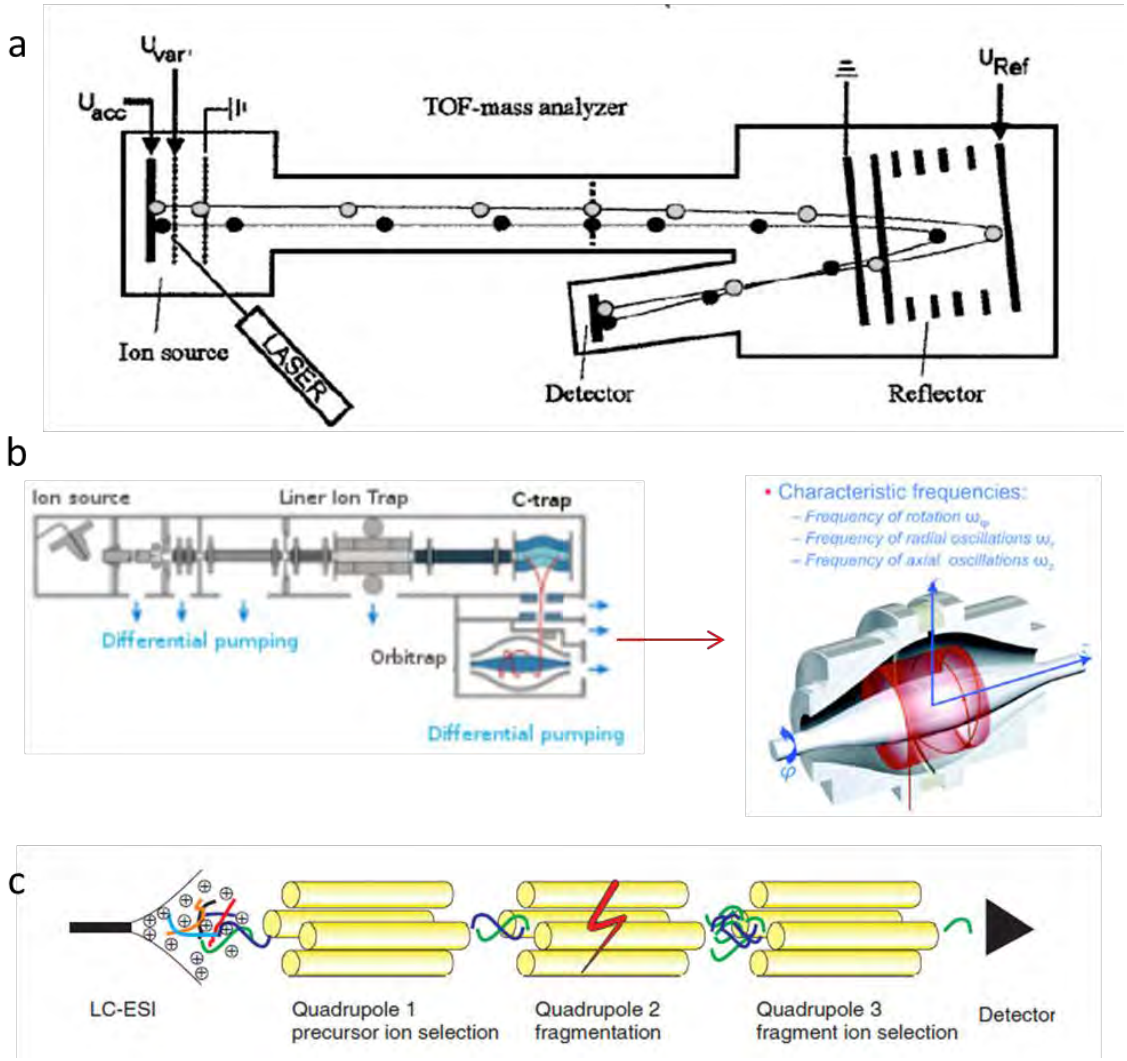

Figure 2.1: Schematic of mass analyzers. (a) shows a MALDI mass analyzer set up. A sample co-crystallized with the matrix is irradiated by a laser beam, leading to sublimation and ionization of peptides. A laser acts as a source of energy to create a strong acceleration field which imparts a fixed kinetic energy to the ions produced by the MALDI process. These ions travel down a flight tube and are turned around in an ion mirror, or reflector, to correct for initial energy differences. The mass-to-charge ratio is related to the time it takes an ion to reach the detector; the lighter ions arrive first. Adapted from Mann *et al* 2001 [175]. (b) shows an orbitrap instrument which has two traps that perform an initial scan of the m/z ratio of the ions before they undergo collision and their fragments analysed by the orbitrap mass analyser which identifies ions based on their cyclical trajectory in an electric field that is applied between two electrodes Figure adapted from Perry *et al*, 2008 [182]. In a triple quadrupole (c), the first and third quadrupoles Q1 and Q3 are mass analyzers and the second Q2 is a collision cell. In the first quadrupole, the specific m/z are selected thus filtering out most co-eluting ions. However, owing to identical mass, one interfering ion (blue) remains. In quadrupole 2, the analytes are fragmented. The m/z selection in the third quadrupole filters out all the fragments of the blue analyte and leaves only a particular fragment of the green analyte for specific detection (adapted from Lange *et al* 2008 [183]).

The choice of mass analyzer depends on what the researcher wants to achieve in the experiment. For example if a researcher requires specificity and high sensitivity for a specific peptide, then the quadrupole mass analyzer would be useful. However if a researcher wants to

identify as much peptides as possible without a specific target, then TOF or orbitrap mass analyzers can be used. Mass analyzers can be summarized in Table 2.1 below.

Analyzer	Implementation	Type	Resolving power	Mass accuracy	Limit of detection	Dynamic range
Quadrupole	TQ-QTOF	In-beam	1,000–2,000	Low	Very low	4–5
Ion trap	IT	Trapping	1,000–2,000	Low	Very low	2–3
TOF	Q-TOF	In-beam	>25,000	High	Low	3
OT/ICR	Hybrid	Trapping	>50,000	Very high	Low	3

Table 2.1: Summary of mass analyzers; Comparison of relative characteristics of mass analyzers including dynamic range, resolving power, mass accuracy, limit of detection and type and implementation.

2.5 Detector

Detectors are the most ubiquitous part of the MS instrument technology platform as they are generally the same among different type of mass spectrometers. Whilst ion detectors can either be analogue or digital, most instruments currently use analogue detectors that record the ion current.

2.6 Chromatographic techniques coupled to MS

Major restrictions in large scale protein identification arise from large number of proteins and the huge differences in abundance, covering several orders of magnitude in dynamic range and often exceed the dynamic range of the mass spectrometer itself. For example, the human serum proteome covers about 10 orders of magnitude as shown in Figure 2.2 below. However, mass spec instruments have dynamic range coverage of about 10^5 to 10^6. Such restrictions mean that low abundance proteins are often masked and are therefore difficult to identify.

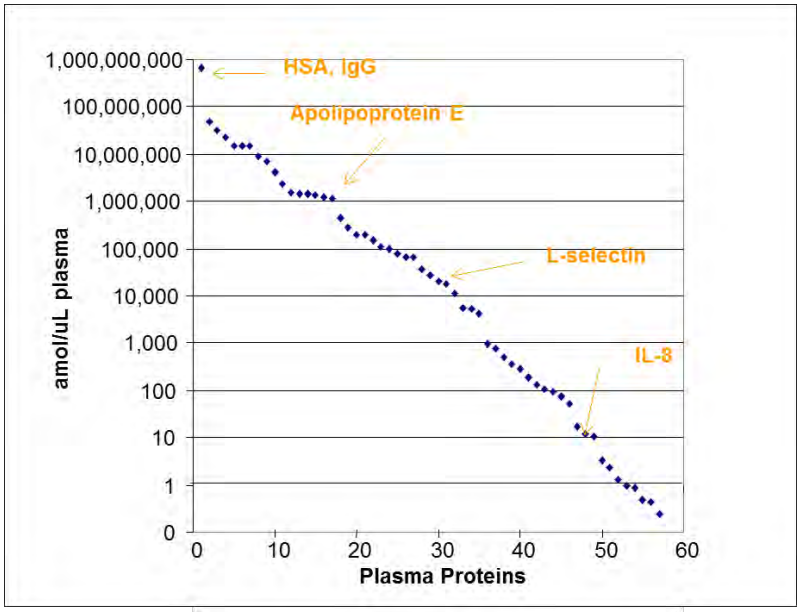

Figure 2.2: Dynamic range of protein concentrations in human plasma. Graph shows that the human plasma proteome spans about 10 orders of magnitude. Adapted from Anderson et al 2003 [184].

As the complexity of biological systems being studied by MS increases, there is an increase in the need for more powerful and highly resolving separation techniques. Thus the key to comprehensive analysis by MS depends on separating the sample into several less complex fractions of the original sample prior to MS or MS/MS. This need has driven the development and use of chromatographic techniques coupled to mass spectrometry. The general idea of chromatography is to bring a mixture into a mobile phase and pass it through a stationary phase. In the stationary phase, the analytes bind to a resin, with some analytes binding much stronger than others; analytes are then released from the stationary phase at specific intervals when conditions that favor their dissociation [185].

Liquid chromatography is an attractive approach to the analysis of complex mixtures of polar and non-polar substances such as proteins or peptides. During liquid chromatography, peptides or proteins are adsorbed to the column which is the stationary phase [186]. When the stationary phase is more polar than the mobile phase then the LC is termed normal phase LC. When the mobile phase is more polar than the stationary phase, then the LC is termed reverse phase chromatography (RPLC). As conditions within the column can are altered, the degree of association between the protein/peptide and the resin can be altered [187], enabling the fractionation of initially complex biological samples prior to MS spectral acquisition.

2.7 Alternative pre-fractionation techniques

Alternative pre-fractionation methods that do not involve chromatography can also be used in conjunction with chromatographic separation when increased resolution is needed for more complex samples. Such pre-fractionations can be carried out off-column. The method of choice for fractionation depends on what an individual experiment aims to achieve. For example in a study of a eukaryotic cell, fractionation can be done at organelle level by separating each organelle and analyzing its proteome separately. By comparison, when analyzing specific groups of proteins e.g. glyco-proteins or phospho-proteins, they can be enriched using various affinity chromatographic techniques such as phospho-protein columns and glycoprotein enrichment platforms.

For samples where the target proteins are not known as is the case in so-called shotgun experiments, fractionation can be carried out on the entire sample using methods that separate the entire sample into smaller fractions whilst retaining coverage of all proteins. For such experiments, fractionation may be done for example in-gel using polyacrylamide gel electrophoresis (PAGE) to separate the proteins based on molecular weight. Alternatively, it may be done off-gel by means of molecular weight cut-off filters or semi-permeable membranes such as dialysis and ultra-filtration. These separated protein fractions can then be digested with trypsin and run separately on the LC column [166].

2.8 Tandem mass spectrometry

Tandem mass spectrometry is considered the mass spectrum, of the mass spectrum in that it elucidates more accurate information on the peptide sequence. During tandem mass spectrometry on peptide mixtures, the initially identified ions are further fragmented by high energy collision with an inert gas to generate a set of nested fragments that are one amino acid shorter than the previous fragment whose mass is then further analyzed to identify the amino acid sequence. This allows the resolution of any ambiguities that arise from using peptide mass alone for the identification of peptides. A schematic of MS/MS is shown in Figure 2.3 below. Tandem mass spectrometry gives a level of information above the identification of the peptide as it can elucidate amino acid modifications and substitutions if the expected sequence was already known. It is now chiefly used in high throughput proteomic mass spectrometry studies in which current MS instruments are coupled to LC platforms for direct peptide analysis separated from reverse phase columns [165].

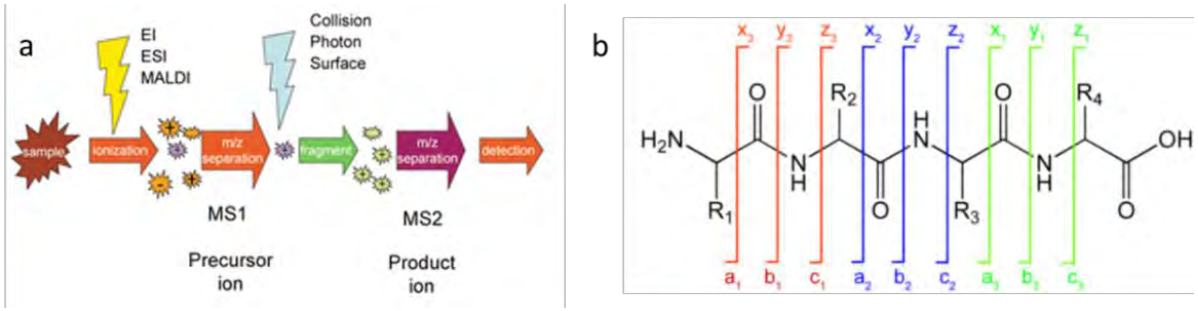

Figure 2.3: (a) Representation of MS and subsequent MS/MS: In the first round of MS, samples are ionized and the m/z of the precursor ion is determined. Peptides can be separated by m/z at this point. In the second round of MS, the ionized precursor ion is partially fragmented to its constituent product ions which are then determined by the detector. (b) Nomenclature of peptide ions: An illustration of typical ions formed by peptide fragmentation during MS/MS, when the peptide fragments at the peptide bond, from the N to the C terminus, b ions are formed with the charge at the N terminus. When the peptide fragments from the C to the N terminus, y ions are formed with the charge at the C terminus. Peptides chains can however fragment at other points other than the peptide bond. When this happens, alternative ions are formed (a, c, x, z).

2.9 MS based proteomics strategies

2.9.1 Shotgun proteomics

Protein mixtures are usually derived from a variety of experiments, including organelle enrichments, secreted proteins, enrichment experiments and whole-cell lysates. Such complexity means that the protein chemistry is diverse,, hence defining a single set of conditions compatible with all proteins in one LC run is challenging [188]. For this main reason, peptide centered proteomics is typically preferred over protein centered proteomics.

Shotgun proteomics uses protease enzymes to cleave each protein in a mixture to its constituent proteolytic peptides and then attempts to determine which protein each peptide is derived from. Each cleaved protein gives rise to a multiple tryptic fragments, by so doing, further increasing sample complexity, hence the need for prior sample fractionation. Peptides generated through protease digestion are then identified by either peptide mass fingerprinting or direct sequencing of the peptides. In peptide mass fingerprinting, the masses of the collection of peptides are used as a fingerprint to identify the protein from which they are derived. Consequently, peptide mass fingerprinting can only be used for organisms whose genome has been sequenced and the entire list of all actual protein sequences available as it relies on prior knowledge of peptide masses [189]. Furthermore, since the mass of any one peptide is related to its amino acid composition, but not to its sequence, the *m/z* values of individual peptides cannot be used to unambiguously identify the parent protein or the amino acid sequence. [190,191]. Moreover, where there are multiple splice variants of a single protein, the identification of shared peptides

cannot be used to identify the specific splice variant that has been produced. Peptide mass fingerprinting is therefore only really useful when all the peptides are derived from a single protein, as is the case for example in a 2D gel based proteomic experiment.

The alternative approach to fingerprinting is fragmenting the whole peptide to its constituent amino acids to determine the amino acid sequence which can then be matched to a database of known peptide sequences. Theoretically, peptide chains fragment along the backbone at peptide bonds from the N to the C terminus as shown in Figure 2.3 above to produce the ions from which the amino acid sequence can be determined. Peptide fragmentation can be done by a number of methods including collision-induced dissociation (CID), electron capture dissociation (ECD), electron transfer dissociation (ETD) and infrared multi-photon dissociation (IRMPD) amongst others [190,192–194].

The shotgun approach in proteomics is predominantly used as a discovery platform [165]. It is a robust platform that when used with appropriate instrumentation is capable of identifying thousands of proteins in complex samples. It is normally applied to whole cell lysates where the composition of the sample is unknown and the researcher wants to identify as many of the proteins in the sample. A typical "bottom up" shotgun workflow is contrasted to a "top down" workflow in Figure 2.4 below.

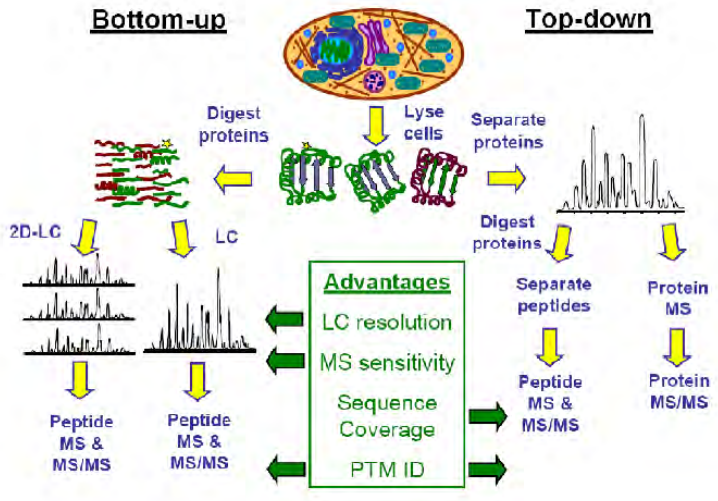

Figure 2.4: Bottom up vs Top down proteomic strategies. Similarities and differences between the peptide centric and protein centric approach are depicted. The fundamental difference is that MS/MS can be done directly on the protein in the top down strategy whereas the bottom up only works with peptides.

Peptide centred rather than protein centred proteomics is normally the method of choice in unravelling the proteomic complement of a sample because the nature of liquid chromatography that is coupled to MS separates peptides better than proteins. As a result, mass spectrometers identify intact proteins with less sensitivity compared to peptides. Secondly peptides are generally easier to fragment in MS/MS (MS2) compared to whole proteins and finally peptides are more soluble under conditions compatible with ionization [187]. With good resolution, peptide centric proteomics can identify between up to 10 000 proteins in a sample and if coupled with a fractionation technique, the number increases substantially [195–197].

2.9.2 Shotgun data analysis

Analysis of shotgun MS data presents a bottleneck in the workflow of high throughput proteomics as more efficient and accurate methods are still being sought out that are able to correctly assign as many of the MS spectra as possible [198]. Spectra from MS experiments can be interpreted using 3 general methods. Peptide sequences can be interpreted *de novo* without the use of a theoretical database for cross comparison [199–201]. Sequence tag based searching is another method that uses unambiguous sequence tags derived from spectra and attempts to match them to a theoretical database, by so doing joining a *de-novo* based and a database based search [175]. The third method is a correlation based method which uses correlation scores to determine the accuracy of a match between experimental spectra and theoretical spectra from a database [202].

Currently, the interpretation of spectra from shotgun proteomics experiments is predominantly based on database spectral matching due to the complexity of interpreting *de novo* search results. Data analysis is heavily dependent upon the availability of protein sequence databases and their present annotation. Amongst the most commonly used search algorithms for spectral matching today are Paragon (within Protein Pilot), Mascot, Sequest, X!Tandem, Crux, Peaks and MaxQuant [195,198,203–207].

2.9.2.1 Sequest/Crux

Sequest was one of the first database search algorithms developed for interpreting MS/MS spectra as well as scoring peptide identifications thereof [202]. Sequest works by creating a theoretical digest of the target protein fasta file through an *in silico* digest of the proteins in the target fasta file. The *in silico* digest is created using trypsin or the protease that will be used in the experiment, hence producing theoretical peptide fragments which an ideal experiment

should produce. The theoretical peptide fragments are then used to create theoretical spectra. Sequest then measures the correlation between experimentally obtained spectra and the expected theoretical spectra obtained from the *in silico* digest of the target fasta. It then determines the best peptide match to the database using a correlation score known as the X-Corr score algorithm. This scoring algorithm picks the top 500 matching preliminary scoring peptides and then carries out a correlation analysis for each by correlating theoretical, reconstructed spectra against the experimental spectrum.

Crux, an improvement of Sequest is an open source software tool that incorporates a number of statistical methods to analyse, interpret and validate MS/MS spectra [198]. Like Sequest, it matches each spectrum with a theoretical database spectrum and retrieves candidate peptides for a given spectrum. Additionally, for each protein in the target fasta file, Crux generates tryptic digests of reversed or shuffled proteins to create a database of decoy peptides. The decoy database is used to provide a good null model and thus enable the estimation of accurate false discovery rates. For spectrum searching and interpretation, Crux uses either Sequest search or Search-for-matches [190]. The output from these spectrum matching algorithms then goes through a number of multiple testing and machine learning validation tools which incorporate decoy database spectra to assign statistical confidence values to each peptide spectrum match, by so doing, further distinguishing between correct and incorrect peptide matches.

Algorithms for estimating statistical confidence include Barista, Percolator and q-ranker [198,208]. A schematic of how Crux works is shown in Figure 2.5 below. Peptides identified within the acceptable confidence threshold are then used to identify the parent protein. In cases where a peptide can be mapped to multiple proteins, Crux contains the Barista verification algorithm that can be set to prevent ambiguous peptides from being used as the sole identifier for a protein. Other database search based algorithms also function in a similar manner although they may exhibit some differences especially in the algorithms used for validation of spectra and estimation of statistical confidence.

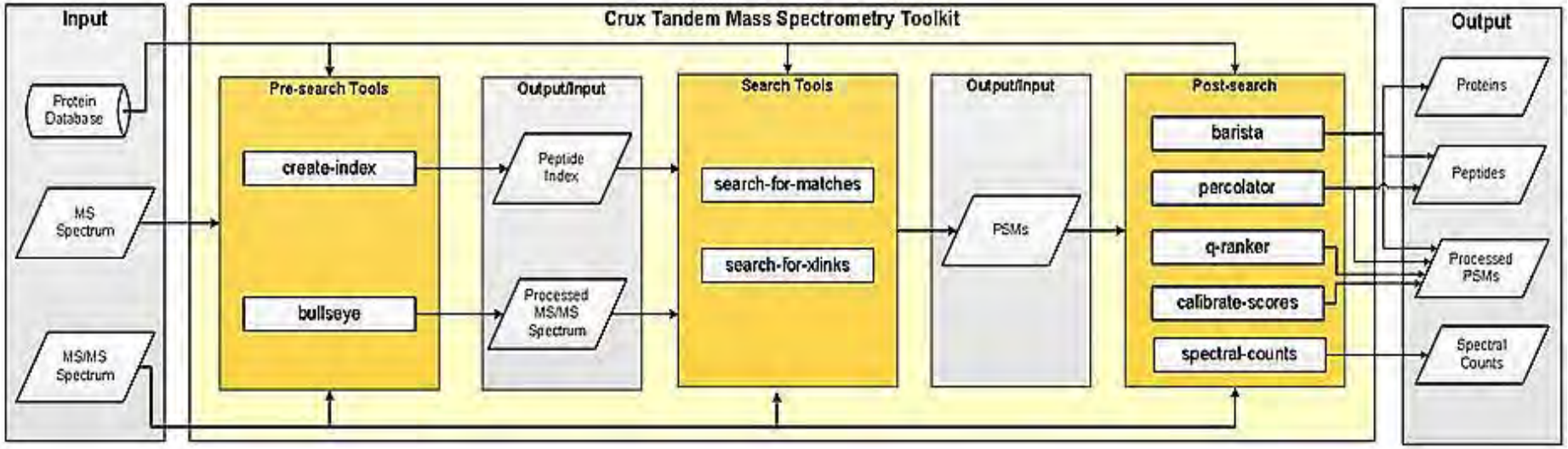
Input
Protein Database
MS Spectrum
MS/MS Spectrum
Crux Tandem Mass Spectrometry Toolkit
Pre-search Tools
create-index
bullseye
Output/Input
Peptide Index
Processed MS/MS Spectrum
Search Tools
search-for-matches
search-for-xlinks
Output/Input
PSMs
Post-search
barista
percolator
q-ranker
calibrate-scores
spectral-counts
Output
Proteins
Peptides
Processed PSMs
Spectral Counts

Figure 2.5: Workflow using Crux search algorithm: A package containing various spectral matching algorithms (search-for-matches, sequest search, search-for-links) coupled to various validation tools (q-ranker, q-values, percolator). Various combinations of pathways can be used to search then best data can be extracted [198].

2.9.3 Validation of results from search engines

Despite subtle differences in how each search engine comes to a confident assignment of a subset of peptides, they all employ an analogous set of procedures to achieving the final goal. In general, experimental and theoretical spectra are matched to produce a list of the best matching spectra known as peptide spectral matches (PSM's). Due to the fact that overlap exists between correct and incorrect decoy PSMs, each database then aims to remove erroneous matches from the PSMs, hence setting apart true positives from false positives which are matches by chance with some definable probability such as the p-value [209].

Most search engines use decoy database searching to correct for false positives, thus ensuring that matches are strictly not by chance using the false discovery rate (FDR) assignment. False positives are PSM's that are found with high statistical significance but are in fact not real findings. FDR calculations are multiple statistical tests that are carried out together in which it is expected that many of the tests should remain positive for true positives, hence it is sometimes called multiple testing correction. Where only a few null hypothesis are expected to be false, family wise error rate (FWER) is used to determine statistical significance level of individual hypothesis to ensure that the probability of any single false positives among all tests is controlled at the nominal significance level (Bonferroni correction) [210]. However when analysing high-dimensional data such as micro-array or high-throughput proteomic data, using such an approach results in an increase in type II errors hence FDR is used instead of FWER. The FDR associated with a particular p-value score is the expected percentage of false positives within that dataset of scores above the threshold [211,212]. It is the proportion of null hypothesis that are rejected erroneously. FDR can be set at the global level of the whole protein output or it can be set at the local level of each individual PSM. A maximum of 5% FDR is normally considered acceptable.

Apart from the FDR, multiple scores are used by database search engines to verify PSM results. These include P-values[213], E-values [211], Q-values and q-ranker [208] amongst other scores. Furthermore, whole algorithms such as TPP can be used to further verify PSM and protein assignments from multiple database search engines such as Crux, X!Tandem or

mascot at peptide and protein level using Peptide Prophet [214], Protein Prophet [215,216] and iProphet [203,217,218].

2.9.4 Shotgun quantitation:

MS driven proteomics has developed methods to quantify proteins so as to determine protein abundance or changes thereof in disease states compared to normal. Methods of quantitation are generally divided to 2 categories; label based and label free which can either provide absolute or relative quantification [219,220]. Label based quantitation in proteomics studies is grounded on the ability to label samples with one or more stable isotopes. Quantitation is then deduced out by comparing the ratio of the MS signal of the tryptic peptide with that of the isotopically labelled analog [221]. Labelling can be carried out using heavy isotopes such as carbon (^{13}C) or nitrogen (^{15}N), for example SILAC labelling uses amino acids with ^{13}C or ^{15}N. Experiments are carried out in duplicate except that one supplied with media containing amino acids labelled with heavy isotopes whilst the other is labelled with light isotopes. Spectra obtained from the heavy labelled isotope are distinct from those of the light isotope due to the mass shift that results from mass differences in the carbon and nitrogen atoms in each experiment [222].Tandem mass tags (TMT) is another relatively new method of tag based relative quantitation which can label up to 10 experimental sample groups at a time [223,224]. Using these tags allows for the determination of variations in peptide quantities between experiments based on the differences of the intensities of each tag in each sample relative to those in other samples [225].

Alternative label based quantitation methods can be used such as isobaric tags for relative and absolute quantitation (iTRAQ). The peptides are quantified based on the signals of the different *m/z* of the fragment reporter ions after the peptide has been analyzed by MS/MS [176,226,227]. Although label based methods are more powerful since they give more accurate quantitation value, label free methods are more popular as they are simpler and cheaper to perform and can be carried out without extra steps in the preparation of samples.

Label free methods of quantitation can depend directly on the spectra obtained in the initial MS run in which case they are termed ion counting methods. When they depend of information extracted from the MS/MS run, they are termed spectral counting. 3 main algorithms are routinely used for spectral counting including spectral index (Sin), normalized spectral abundance factor (NSAF) and exponentially modified protein abundance index (emPAI) [228–

230]. These algorithms are all found within Crux, however they are also used in other search engines.

2.9.4.1 Label free quantitation

Exponentially modified protein abundance index (emPAI)

emPAI is a modified version of protein abundance index (PAI) that calculates the total number of observed modified peptides and divides these by the total number of observable peptides as a measure of abundance. Observable peptides are those in the database that have a mass that falls within the range of identified peptides. The PAI value is exponentially modified to derive the emPAI score. Each and every protein in the dataset is then normalized by dividing its emPAI score by the sum of the emPAI scores of all the identified proteins giving it the final value which is used as a quantitative value [230].

$PAI = {}^{\text{Total observed}}/_{\text{Total observable}}$

$EmPAI = 10^{PAI} - 1$

$\text{Protein content} = {}^{\text{emPAI}}/_{\sum (\text{emPAI})}$

2.9.4.2 Normalized spectral abundance factor (NSAF)

NSAF relies on the number of spectra identified rather than the number of peptides. The number of spectra obtained is the divided by the length of the protein to obtain a protein abundance which is then normalized by dividing by the total sum of protein abundances in the dataset [229].

$\text{Score} = {}^{\text{number of spectra}} / {}_{\text{protein length}}$

$\text{Abundance} = {}^{\text{score}} / {}_{\sum \text{of scores}}$

2.9.4.3 Spectral Index (SIn)

Spectral index obtains the relative quantitation value by taking the sum of matched fragment ion intensities from all spectra identifying that protein and divides this by the sum of all matched fragment ion intensities identified across all spectra. This is the divided by the length of the protein to correct for protein size [231].

$\text{Score} = {}^{\text{matched fragment ion intensities for protein}} / {}_{\sum \text{of all matched fragment ion intensities of all proteins}}$

$\text{Sin} = {}^{\text{score}} / {}_{\text{protein length}}$

Careful analysis of a yeast digest dataset using the 3 spectral counting methods revealed that NSAF analysis was the closest to label based quantitation than emPAI and Sin. Sin is relatively

good in using spectral intensities; it suffers from increased noise due to the inclusion of signals from noise spectra. emPAI is less sensitive as it uses the highest level information (peptide). NSAF combines spectral level and peptide level information hence it occupies the middle ground between emPAI and SIn [232].

2.9.5 Protein sequence databases

As mentioned earlier, most search algorithms are database dependent meaning they require already known compiled protein sequence information. A number of repositories for such information are available to the scientific community. This includes universal protein databases that contain protein and genomic information from all organisms such as UniProt, Swissprot and Ensembl. These databases contain protein sequences from whole genome projects either from electronic annotation or experimentally backed proteins. They also go a step further in annotating by linking to gene ontologies and pathway analysis (http://www.UniProt.org).

Alternatively organism specific sequence databases also exist that not only combine genomic and protein sequences but also act as a repository for all organism centric information including SNP's, splice variants, experimental information and gene ontologies etc. Two such databases relevant to this project are the tuberculosis database (http://www.tbdb.org) that covers the genus *Mycobacterium* and tuberculist (http://www.tuberculist.org) which is specific for *Mycobacterium tuberculosis*. In these databases one can find the most information on *Mycobacterium tuberculosis* whether at DNA, mRNA, protein level including pathways and expression levels of individual proteins under various conditions. These databases are also a good platform to return to post protein assignment of spectra to make an informed choice of which proteins might be relevant to follow up in future experiments.

2.10 Targeted proteomics

Quantitation of specific proteins from the site of disease is basically obstructed by two problems. The first is the amount of the target protein, which for the purposes of biomarkers, it is usually the less abundant proteins [233]. The second issue is obfuscation by orthologous proteins derived from other microbes, which makes probing for unknown or undefined biomarkers in such samples complex quite challenging. A better strategy would be to identify and quantify pre-determined proteins by developing a peptide-specific MS assay. This targeted approach of finding proteins is known as selected or multiple reaction monitoring (SRM/MRM).

MRM is a highly sensitive, selective and robust method which has been used routinely in the pharmaceutical industry to detect the presence and abundance of biomolecules such as drugs in body fluids[165,234]. MRM experiments take advantage of the triple quad (QqQ) instrument (described above in section 2.4.3) to selectively isolate and monitor precursor ions corresponding to the mass of the specified peptide [183]. The QqQ machine is then programmed to repeatedly sweep through a list of precursor, product ion m/z pairs called transitions and then record the intensity of the fragments that pass through both isolation windows [235].

Assuming that each chosen transition identifies a specific peptide which in turn identifies a specific protein, this allows the instrument to monitor a specific set of target proteins rather than blindly sequencing the most intense peaks which is the strategy of shotgun proteomics. Added advantages of MRM are its broad dynamic range (up to 5 orders of magnitude) [236], ability to quantitate and multiplex with reproducibility as well as high sensitivity at attomolar range which is the typical range of many unique proteins that have biomarker potential [183,237].

Despite the favourable attributes of this technology, it is still not as widely used in the proteomic community because it requires much time to develop a high quality MRM assay and only a few transitions can be candidly monitored in a single run. Assay validation typically requires the acquisition of full scan MS/MS spectra for the target peptide on the same MS platform (instrument) that will be used to run the assay (usually the QqQ). Developing an MRM assay can be summarised in four major steps as follows: target protein selection, target peptide selection, SRM transition selection and finally obtaining protein quantification.

2.10.1 Target protein and peptide selection

The target proteins are chosen usually from the output of a discovery experimental dataset. If the peptide is found in experimental data with strong peak and ion intensity then it is chosen as a good MRM target. From the list of target proteins, specific peptides are chosen for the assays. Special attention must be taken in choosing target peptides because some peptides are present in multiple proteins hence they cannot be used as conclusive evidence for the presence of a specific protein. As a result it is recommended to cross check peptide specificity using programs such as BlastP or Skyline [237,238]. Furthermore, as this type of mass spectrometry

is heavily dependent on pre-calculated m/z and retention time, it is important that all aspects of the chosen peptides are stable to enable targeting and reproducibility.

Some peptides are not easily observable by MS due to the presence of MS incompatible peptide-centric properties [235]. Basically the best flying peptides are usually chosen for MRM analysis and these include and these peptides normally have MS favourable attributes such as the absence of chemically modifiable residues which result in unpredictability and consequently irreproducibility [183]. For example peptides containing methionine and tryptophan residues as these are prone to oxidation. Furthermore, peptides containing glutamine or asparagine are generally avoided as these residues easily convert to glutamate and aspartate hence their predictability and reproducibility is compromised [183]. Peptides containing more than one cysteine residue were avoided due to the fact that these residues easily tend to form disulphide bonds hence altering their chemical properties and subsequently their elution properties. Also peptides along protein sequences that have multiple strings of Lysine and arginine are avoided as the chances of missed cleavage or differential cleavage are high approach [183]. Such unpredictability is not ideal for this type of MS. This re-iterates the need for prior shotgun MS or some prior experimental evidence from which a researcher can determine which peptides are in fact observable in a MS experiment. Ideal target peptides should thus preferably be a combination of prior experimental MS observation and unique protein mapping [239]

An alternative to running a shotgun MS experiment *a priori* to use for peptide selection is the use of a peptide library repository. Peptide Atlas is the most commonly used peptide library repository. It is a broad collection of validated spectral libraries of various experiments, carried out independently by different groups. It contains MS/MS observations together with the associated annotations of the peptides obtained from different experimental conditions and different study instruments which have all been reprocessed using a single processing pipeline.

As an alternative to full on discovery experiments, researchers may create synthetic peptide libraries from the proteins of interest and observe these directly in the MS instrument used for MRM experiments (QqQ). This approach eliminates the need for the discovery experiment as it gives only the specific information on the peptide of interest directly on the platform on which it will be assessed. These peptides can also be used as reference standards for validating the peptides from the complex lysates and their transitions on the MRM specific instrument [240].

2.10.2 Transition selection

The next step is the selection of appropriate transitions of the target peptides. In MRM assays, a suitable set of precursor and fragment ion masses for a given peptide called MRM transitions are used to infer the presence of that peptide in the particular sample in question [237]. The appropriate retention time for the transitions can also be obtained from previous experiments if they have been run on the same instrument. The importance of knowing the retention time beforehand in MRM experiments is that the instrument can then be programmed *a priori* to limit the time frame in which to monitor for a specific transition by so doing, freeing the instrument promptly to detect other transitions [240]. This increases the number of transitions that can be scanned by the instrument per given time.

2.10.3 Quantitation in targeted proteomics

The final step is obtaining quantitation information of the target peptide population. Quantitation can be relative or absolute. Absolute quantitation involves the use of labelled peptides whilst relative quantitation uses the signal intensity of native unlabelled peptides to extrapolate relative abundances of the peptides in question [241–244]. MRM experimental development tools are available that assist the researcher to design and run MRM experiments. These include platforms such as Peptide atlas, PeptideSieve, MRMPilot, Cytoscape and targets identification for quantitative analysis MRM (TIQAM) among others [183]. These tools have been used as starting points in reproducibly identifying small amounts of specific peptides from complex tryptic digests using MRM MS. A basic MRM workflow is depicted in Figure 2.6 below.

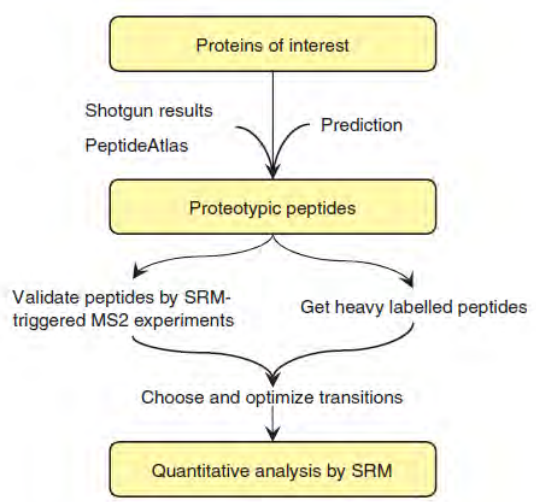

Figure 2.6: Workflow of SRM based proteomic assays. Intergrating data from multiple sources including electronic prediction and experimental evidence to select strong candidate peptides which are then validated by SRM triggered MS/MS. From there the best transitions can be chosen which will be used in the final quantitative MRM assay Adapted from Lange et al 2008 [183].

2.11 Recent developments in MS approaches

2.11.1 MS^E

Recent and more rapid analysis of complex multicomponent samples such as biological fluids that enable the elucidation of elemental composition and fragmentation information is constantly under development. Such analysis can now be carried out using fairly new and modern state-of-the-art MS which allows simultaneous acquisition of exact mass at high and low collision energy known as UPLC/MSE [245]. This new method of LC/MS uses a shrewd approach where parallel alternating scans are acquired at either low collision in the collision cell to obtain precursor ion information, or using high collision energy to obtain full-scan accurate mass fragment, precursor ion and neutral loss information.

This type of MS maximizes the instrument duty cycle and collects both precursor and fragment ion information in exact mass mode in a single analytical run. Because it generates both precursor and product ions are easily linked using retention times, mass defect or a combination of both in a single analytical run, it eliminates the need to rerun the samples to obtain further MS/MS spectra. This approach is faster than traditional MS followed by MS/MS analysis and also provides data that was previously not readily obtained as both MS and MS/MS data for all of the ions in the data set are generated [245]. This approach promises to provide excellent chromatographic and MS efficiencies for the task of structural elucidation in complex mixture analysis problems.

2.11.2 MSX

A different and more recent MS approach that uses a multiplexing strategy that analyses 5 separate m/z isolation windows per spectrum has been described by Egertson *et al* 2013 [246]. Spectra are demultiplexed into five separate 4 m/z isolation windows using a strategy analogous to Hadamand multiplexing. This results in high data sampling frequency such as that observed for data independent acquisition with higher selectivity. The demultiplexing strategy was used to improve precursor selectivity by narrowing down the range of potential precursors for an MS/MS spectrum from a 20 to a 4 m/z window. Furthermore, the fragment ions obtained are unmixed as they are obtained from a narrow window of precursors of 4 m/z. This technique

was applied to a *S. cerevisiae* lysate run on a Q-Exactive (Thermo-Fischer Scientific) and was shown to provide structural selectivity information as well as quantification [246].

2.11.3 SWATH-MS

Another new and sophisticated MS approach has been developed that allows MRM-like sensitivity on shotgun-range protein numbers. The SWATH-MS principle differs to current methods of shotgun MS in that it is data independent acquisition of spectra [247]. In shotgun MS, data is acquired in a data dependant manner depending on which ions are most intense in the mixture. Generally, the most intense ions are picked first for fragmentation by so doing under-sampling the less intense ions which are mostly from the under-expressed proteins. This becomes a problem because disease biomarkers are usually under-expressed in the cell.

SWATH-MS is data independent acquisition mixed with targeted extraction of ions for analysis in the first quadrupole. This type of MS makes use of a quadrupole (QqTOF) mass analyser coupled to a TOF. In the first quadrupole (Q1), ions are picked in a range of 25Da (which are referred to as the SWATH windows (SWATH's) [247]. Then the ions picked here are fragmented in the second quadrupole (Q2) using CID, then they are analyzed by a TOF analyzer. This starts from a m/z window of 400 to a maximum of 1200. The ions are picked in sequential 25Da windows to cover the entire m/z window beginning from 400 to 1200. There is 100ms per isolation window which means the cycle time to the next sampling point in the retention time is 3.2 seconds. A typical SWATH-MS run is 2 hours and it basically maps the entire sample regardless of ion intensity (Figure 2.7).

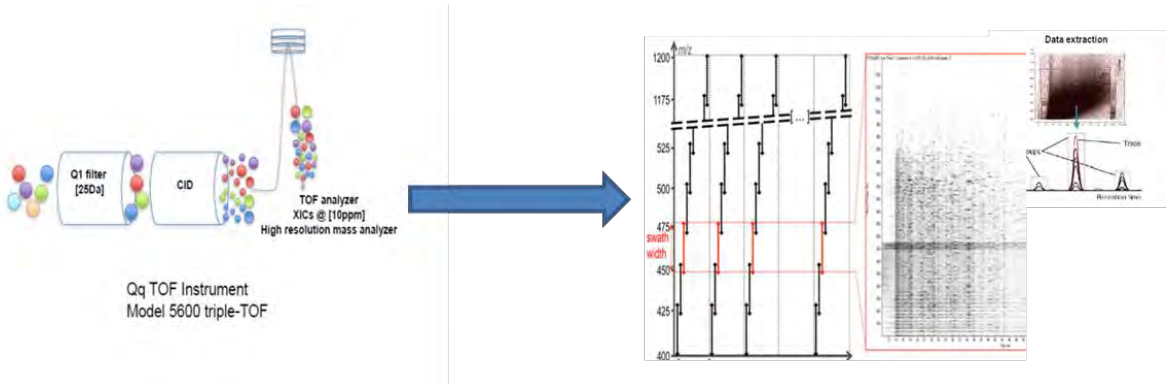

Figure 2.7: Peptide ion sampling used in SWATH-MS. 25Da ion window is isolated in the first quadrupole and fragmented by CID the second quadrupole and the fragments are analysed using a high resolution TOF analyser. The overall result is a series of fragment ion spectra obtained during the entire chromatographic elution (retention time) range by repeatedly sampling stepwise through 32 discrete precursor isolation windows of 25-Da width (black double arrows) across the 400–1200 m/z range. The series of isolation windows acquired for a given precursor mass range and across the LC is referred to

as a “swath” (e.g., series of the red double arrows). The cycle time is defined as the time required to return to the acquisition of the same precursor isolation window. Note that the dotted line before the beginning of each cycle depicts the optional acquisition of a high resolution, accurate mass survey (MS1) scan Adapted from Gillet *et al* [247]. The bigger heat map depicts the complexity of the spectra obtained within the single SWATH window depicted by the red arrows. The denser heat-map is the sample map of the entire SWATH experiment inclusive of all SWATH windows from the beginning to the end of the gradient. A single spot represents a single peptide ion as shown.

Data obtained from SWATH-MS experiments is searched using actual validated experimental spectra rather than theoretical spectra as is usually the case with shotgun proteomics. Whilst this is also a spectral matching platform like Sequest, it allows direct comparison of spectra in the context of actual experiments including tangible aspects such as retention time and peak intensity. Experimental spectra are compared to a composite spectra standard file containing multiple peptide ion result peaks from different instruments and experimental settings to cover a wide possibility of spectra output from the same peptide [248]. Because of multiple sampling of each peptide at different time points, results from SWATH-MS are searched using a more specialised algorithm known as openSWATH [249]. The results are then rigorously validated using various filters and scores based on the match of the experimental spectra to the experimental spectral library.

This method can be reproducibly used to identify and quantify thousands of proteins from acquisition of all possible spectral data from a shotgun experiment. Sampling and protein quantification provided by SWATH-MS is similar to that provided by SRM experiments. Protein standards spanning a range of protein concentrations are used spiked into the sample and used to calculate protein abundance based on the observation that protein concentration is directly proportional to the signal intensity observed in MS experiments [250]. The MS instrumentation technology and sampling technique in SWATH-MS it is similar to that used in SRM as shown in Figure 2.8 below. The main difference is that in SWATH-MS, the precursor selection window is wider and the repeated sampling of the same peptides in different SWATH windows gives multiple spectra for the same peptide. On the other hand SRM samples a single peptide across the gradient to give a single spectra as shown in Figure 2.8.

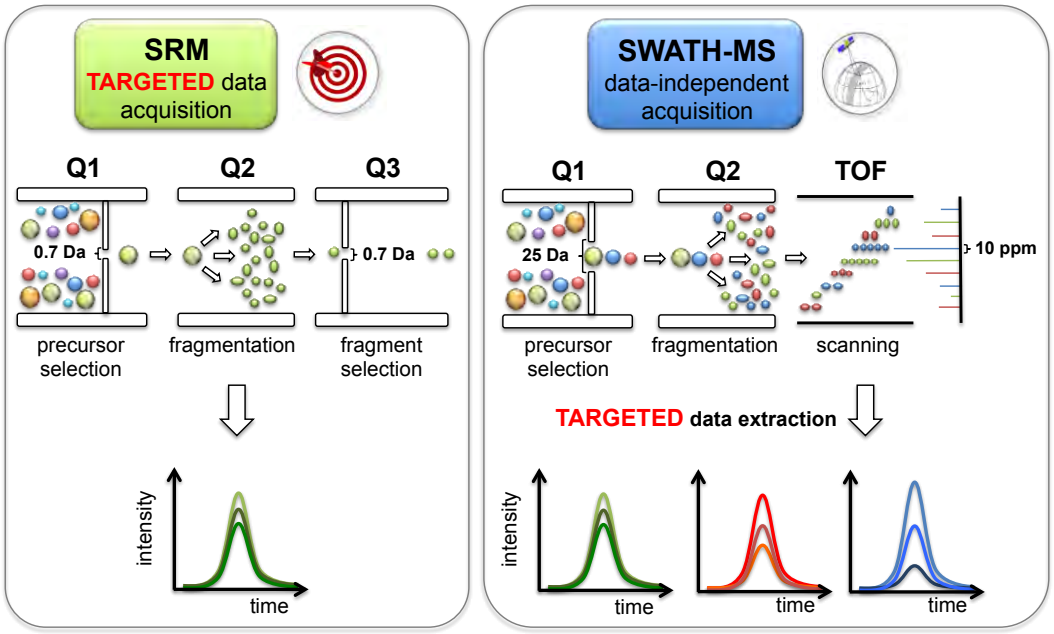

Figure 2.8: Comparison of SRM and SWATH-MS techniques. In the first quadrupole, a smaller isolation window of 0.7 Da is used for selection of specific ions in the SRM experiments whereas a larger isolation window of 25Da is used for the selection of all peptide ions within that *m/z* window. Note that unlike SRM, this sampling is not specific to any peptide but instead all peptides that fall within that broad *m/z* window. Adapted from Gillet *et al* [247]

2.12 Conclusion

Proteomics has vast applications in industry especially in health where new drugs and diagnostics are required for many diseases. The 3 major types of proteomic approaches discussed in this thesis are summarised in Figure 2.9 below.

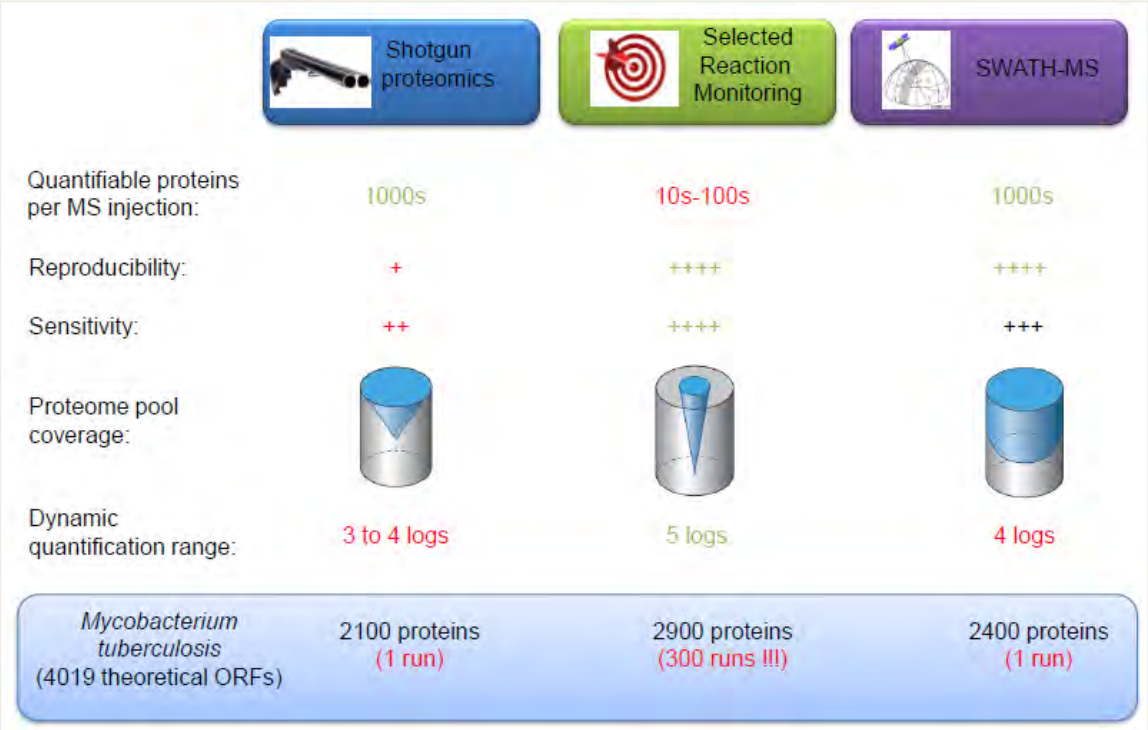

Figure 2.9: Comparison of performance of 3 MS techniques including reproducibility, sensitivity, coverage and dynamic range. Adapted from Schubert et al [248].

The robustness of the proteomic field requires the researcher to know the exact question they need to answer and subsequently choose an experimental and analysis pipeline that will answer the question at hand. Every research question falls into a specific category of the clinical proteomics pipeline (Figure 2.10) and the category in which it falls determines the experimental approach. Mass spectrometry proteomics can be used at every point in the pipeline of diagnostic marker discovery as seen in Figure 2.10 below.

Clinical proteomics workflow
Body fluid/ Tissue samples
Sample preparation
Defining proteomes, qualitative differences
Defining proteomes, quantitative differences
Validation , qualitative and quantitative
MS Approach
Shotgun MS
SWATH-MS Label based and label free quantitation
SRM-MS
MS-Instrumentation
High resolution low sensitivity trap instrumente.g. Orbitrap
High resolution high sensitivity trap/TOF instrumente.g. Q-TOF
Low resolution high sensitivity trap instrumente.g. triple quad

Figure 2.10: Clinical proteomics pipeline and contribution by MS the bottom row describes the current pipeline from discovery to validation of biomarkers that has been implemented in big pharma companies to date. The middle row depicts the type of MS approaches that can be used for each stage of the biomarker discovery pipeline. The top row depicts the type of instrumentation required for each stage of the biomarker discovery pipeline.

For discovery experiments, shotgun approach is mostly used whereas a targeted approach is used for verification before validation in clinical samples. The high throughput nature of MS based proteomics as well as lower cost per data point makes it an attractive choice for many protein-centred studies compared to non-MS technologies. In this thesis we aim to use the varied proteomic applications that MS technologies offer to define whole proteomes of members of the genus Mycobacterium including members of the MTBC and NTM.

Chapter 3: Methods development for obtaining maximum proteome coverage

3.1 Introduction

Since the isolation of the laboratory strain H37Rv in 1905, the genome of *Mycobacterium tuberculosis* has been sequenced and extensively studied [11]. As previously mentioned the Mycobacterial genome exhibits immense homogeneity and is one of the most well conserved microbial genomes, however this fact is seemingly a fast changing dogma. It is considered a "closed pan genome" due to the bacterium's restricted niche and subsequent limited access to the rest of the microbial gene pool [251]. Despite the observed limited genetic variability, they exhibit vast discrepancies in phenotypic presentation in terms of virulence, elicited immune response and transmissibility [12,15,17,252].

Members of the *Mycobacterium tuberculosis* complex (MTBC) are characterised by slow growth, genetic homogeneity, latency, resistance to physical and chemical challenges and a complex extracellular lipid wall [253]. The lipid cell wall is the most distinctive feature of the Mycobacterial cell wall and it represents at least half of the dry weight of the organism. It plays a variety of roles including serving as structural components, energy reserves, permeability barrier, antigenic presentation as well as conferring protective properties [1]. It is this exclusive lipid wall that sets mycobacteria apart from other gram positive bacilli by offering a level of protection over and above the usual peptidoglycan cell wall exhibited by other gram positive bacteria (Figure 3.1). The rigid complex nature of the lipid cell wall makes it impenetrable to many chemicals which make it impossible to disrupt the cells by chemical means. The rigidity of the cell wall also means that extreme measures have to be taken to break open the cells whilst subtle enough to allow the extraction of undamaged proteome from within the cell and the membrane.

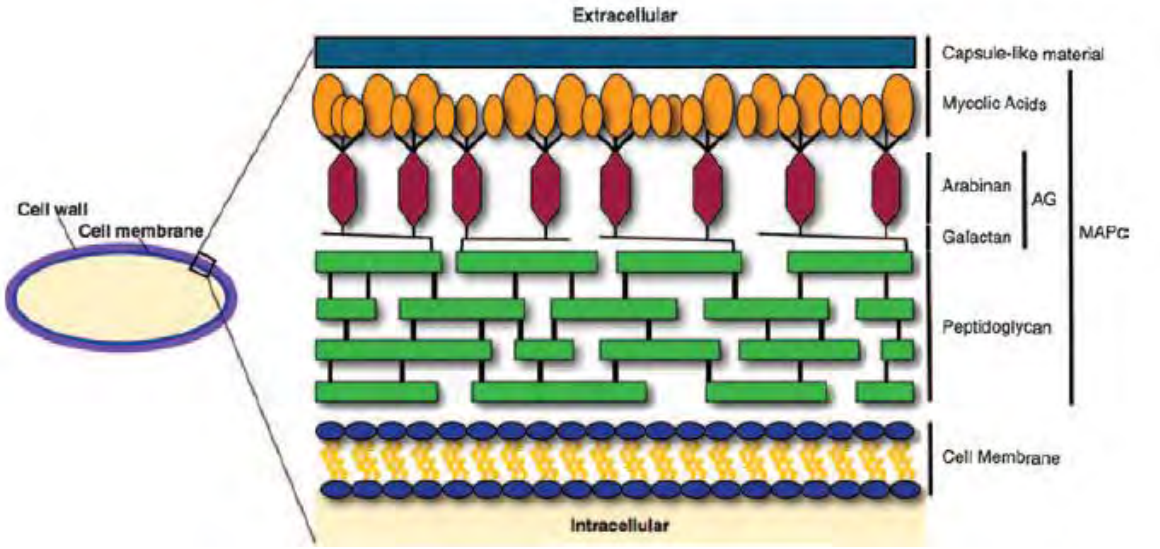

Figure 3.1: Structure of Mycobacterial cell wall. The Figure shows the components that make up the cell wall of members of the genus *Mycobacterium*. The cell bi-lipid layer of the cell membrane is shown at the bottom in direct contact with the intracellular matrix. This is followed by the peptidoglycan cell wall which is characteristic of every gram positive bacterium. Complex sugars including galactans and arabinans (arabino-galactans; AG) connect the peptidoglycan wall to a unique complex fatty acid layer known as the mycolic acids (mycolic acids peptidoglycan: MAPG). These are further covered by an external capsule made of complex carbohydrates. Adapted from Hett and Rubin [253].

The general hypothesis of this study is that members of the MTBC and the NTM *M. avium* will have measurable differences in their proteomes and that in depth proteomic profiling of the several strains could provide clues relating to differential phenotype and the clinical manifestations that they present. The overall aim of this thesis is to use shotgun mass spectrometry tools to quantitatively and qualitatively investigate the total proteomic complement expressed by various epidemiologically significant strains within the MTBC as well as clinically relevant NTM strains. However, to enable efficient cross-strain and cross-species comparison it is necessary to first obtain a high coverage of the proteome as possible.

This chapter therefore describes the method development process to obtain comprehensive proteome coverage from *M. tuberculosis* cell lysates grown *in vitro*. The study aims is to establish appropriate mass spectrometry (MS) compatible cell culture system and cell lysis protocols to maximize protein extraction from *M. tuberculosis* strains. Furthermore, we aim to harness MS tools and bioinformatics strategies to improve total proteome coverage expressed by various epidemiologically significant strains within the *Mycobacterium tuberculosis* complex (MTBC) as well as a clinically relevant non-tuberculous Mycobacteria (NTM) strain when cultured *in vitro*.

3.2 Materials and Methods

3.2.1 Strain Selection

Seven strains were selected for investigation in this study including six members of the MTBC and a member of the NTM group. Members of the MTBC differed in virulence ranging from the attenuated *M. bovis* BCG to highly virulent *M. tuberculosis* W-Beijing whilst the NTM *M. avium* is the chief cause of pulmonary tuberculosis in HIV positive individuals. The strains can be summarised as follows in Table 3.1.

Organism	Grouping	Lineage	Spoligo-number	Phenotype
M. tuberculosis H37Rv	MTBC	Lineage 4 (Laboratory strain)	777777477760771	Limited virulence
M. bovis BCG	MTBC	Vaccine strain	676773777777600	Limited virulence
M. bovis	MTBC	Bovine strain		Hypo-virulent (typically bovine)
M. tuberculosis W-Beijing	MTBC	Lineage 2 (clinical strain)	000000000003771	Hyper-virulent, hyper-transmissible, by-passes latent stage, considerable drug resistance, worldwide
M. tuberculosis LAM	MTBC	Lineage 4 (clinical strain)	774377007760771	Ranges between Hypo and Hyper-virulent, widespread
M. tuberculosis CAS	MTBC	Lineage 3 (clinical strain)	702777740003771	Hypo-virulent, clustered in the central Asian region
M. avium	NTM			Wide spread pulmonary TB-like symptoms only in HIV+

Table 3.1: Strains chosen for the study. The table defines which strains were used in this study, the phenotype and which group each of organism's fall into.

3.2.2 Cell culture

3.2.2.1 Method 1

The above mentioned bacterial strains (Table 3.1) were plated on Middlebrook 7H11 (Sigma) agar base supplemented with OADC (Sigma) and incubated at 37˚C for an average of fourteen to twenty one days. A single colony was picked from each plate and subsequently cultured in 10ml of Middlebrook 7H9 (Sigma) broth supplemented with Albumin dextrose until OD reached values consistent with log phase growth (OD_{600} 0.6-0.9; approximately 7 days). This starter culture was used to seed a larger culture of 190ml of middlebrook 7H9 broth with albumin, dextrose and catalase (ADC) supplement as at 37˚C until OD reached between log phase averagely OD_{600} 0.6-0.9 (approximately fourteen days). Cells were grown under constant agitation and tween 80 was added to the media to avoid clumping. Furthermore, before the OD was taken, the cultures were further agitated in order to break any visible clumps. As this was taken as a general rule of thumb across the strains, any bias would have been equal across the strains. These Mycobacterial cultures were all prepared and stored in a category 3 biological safety containment facility according to health and safety guidelines.

3.2.2.2 Method 2

Bacterial strains (Table 3.1) were plated on Middlebrook 7H11 (Sigma) agar base supplemented with OADC (Sigma) and incubated at 37˚C for an average of fourteen to twenty one days. A single colony was picked from each plate and subsequently cultured in 10ml of wholly synthetic Sautons media (2% glycerol, 0.4% L-asparagine, 0.2% glucose, 0.2% citric acid, 0.05% mono-potassium phosphate, 0.05% magnesium sulphate, 0.015% Tween 80, 0.005% ferric citrate, 0.00001% zinc sulphate; pH 7.4) until the culture reached early log phase (OD 0.6). The 10ml early log phase culture was used to seed 190ml of fresh Sautons medium in roller bottles. These were sealed and incubated at 37°C at 5% CO_2 until OD reached 0.9 (approximately 6 weeks). These Mycobacterial cultures were all prepared and stored in a category 3 containment facility according to health and safety guidelines.

3.2.3 Protein extraction and preparation for MS/MS

3.2.3.1 Method 1

Due to the nature and complexity of the Mycobacterial cell wall, it was necessary to develop a novel protein extraction process harsh enough to break open the cells whilst subtle enough to maintain protein integrity and yield maximum coverage of the proteome and being compatible with use in a category 3 facility, given the infectious nature of the organism. Furthermore, the protein extraction method needed to be compatible with downstream processing by mass spectrometry, hence the procedure was separated into two parts: The first part allowed the release of protein from the cell in sodium dodecyl sulphate (SDS) whilst the second part prepared the extracted protein for mass spectrometry.

The cell pellet was separated from the culture filtrate proteins by centrifuging at 4,000g for 15 minutes. The culture filtrate was filtered through a 0.2 Micron filter (Millipore) and then stored at -20˚C for further processing. Cell lysis was carried out using both physical and chemical methods by boiling the cell pellet in 1% SDS buffer (1% SDS, 100 mM Tris-Cl pH 7.6, 0.1 mM dithiothreitol (DTT), 1 mM PMSF) for 30 minutes with vortexing every 10 minutes. This was done to solubilise the lipid cell wall and burst the cells open. Cell debris was separated from the protein containing supernatant by centrifugation at 10,000g for 15 minutes and the supernatant containing the protein was collected in a separate tube. This was carried out in a biological safety category 3 containment facility according to health and safety guidelines.

To prepare the total cellular protein (TP) sample for mass spectrometry, the protein had to be stripped of excess SDS and a method developed by Sandri *et al* 1993 was adapted in this study [254]. In brief, the sample was diluted in 25 mM Tris, 192 mM glycine, pH 8.3 to a final concentration of 0.1% SDS. 1N NaOH was added to a final concentration of 0.15N to raise pH to 12, after which potassium chloride was then added from a 2M stock solution to a final concentration of 180 mM. The mixture was incubated at room temperature for 10 minutes, after which the precipitate was removed by centrifugation at 650g for 15 minutes. Literature suggested that this would reduce free (unbound) SDS concentration by up to 90% to a final concentration of 0.01%.

The supernatant containing protein-bound SDS was incubated on ice for 30 minutes. Ice cold TCA was then added to a final concentration of 10% to drop the pH to 2. The sample was kept on ice for 10 minutes before adding one tenth volume of 2M KCl to precipitate protein-bound SDS. The sample was left to stand at room temperature for 5 minutes before centrifugation at 650g for 15 minutes at 4˚C to pellet the protein. The pellet was resuspended in 2M urea and quantified using a BCA assay.

Culture filtrate (CF) proteins were precipitated by addition of 4 volumes of ice cold 100% acetone and collected by centrifugation at 4000g. The pellet was washed in 20% acetone and resuspended in 2M urea after which protein concentration was determined using BCA quantitation. Protein concentration in each TP or CF sample ranged from 2.5µg/µl to 40µg/µl. In preparation for mass spectrometry, 100µg of each TP and CF sample was reduced using tris-2-carboxyethyl-phosphine (TCEP) at 60˚C for an hour then alkylated to block cysteine residues using methyl methane-thiosulfonate (MMTS) for 30 minutes at room temperature in the dark. Trypsin (Promega) was added at 1:20 (w/w) trypsin to protein ratio and the mixture was incubated at 37˚C overnight for protein digestion. Peptides were desalted using C18 ziptips (Thermo Scientific). 5µg of each peptide sample was loaded onto C18 ziptips and washed through using 10µl of 0.1% tri-fluoro acetic acid (TFA). Washes with 0.1% TFA were repeated twice and the peptides were eluted into a new eppendorf tube using 70% acetonitrile (ACN) in water.

3.2.3.2 Method 2

Proteins were extracted in a biosafety level 3 facility in line with health and safety guidelines. Briefly, the cell pellet was separated from the culture filtrate by centrifugation at 4,000g for 15

minutes on a bench-top centrifuge. Cell lysis was carried out by boiling the cell pellet in 1% SDS buffer (1% SDS, 100 mM Tris-Cl pH 7.6, 0.1 mM dithiothreitol (DTT), 1 mM PMSF) for 30 minutes. Cell debris was separated from the protein containing supernatant by centrifugation at 10,000g for 15 minutes on a bench top centrifuge and the supernatant containing the protein was retained in a clean tube. Protein extracts from cell lysates were concentrated and buffer exchanged to 2M urea buffer using 3kDa MWCO filters (Millipore). Culture filtrate proteins were concentrated and buffer exchanged into 2M urea using 15ml 10kDa MWCO filters. Protein concentration was determined using the BCA assay kit (Thermo Scientific).

Proteins were separated according to molecular weight using an SDS PAGE gel system. The separating gels were made from 12% of acrylamide: bis-acrylamide, 0.375M Tris-Cl (pH 8.8), 7.5% SDS, 0.5% ammonium persulphate and 0.1% TEMED. The stacking gels consisted of 4% acrylamide: bis-acrylamide, 0.125M Tris-Cl (pH 6.8), 0.1% SDS, 0.5% ammonium persulphate and 0.1% TEMED. 40µg of each sample (CF or TP) was mixed with an equal volume of 5x sample buffer (31.25ml of 1M Tris-Cl (pH8), 10g SDS, 25ml glycerol, 5µl β-mercaptoethanol, 7µl of 2% bromo-phenol blue and 41.9ml distilled water) and heated at 65ºC for 5 minutes. Electrophoresis was performed from anode to cathode at 100V using a BioRad mini-Protean II gel system until the bromophenol blue dye reached the bottom of the gel. Visualization of the proteins on the gel was performed by staining with the coomasie brilliant blue R250 for 1 hour (50% methanol, 10% acetic acid and 0.1% coomasie brilliant blue R250). Destaining of the gels was carried out by incubating on a shaker overnight at room temperature in destaining solution (10% methanol, 10% acetic acid).

Each gel lane for each strain sample was cut into 5 pieces (5 culture filtrate fractions and 5 intracellular protein fractions, hence a total of 10 fractions per strain). All gel pieces were cut into smaller cubes and washed twice with water followed by 50% (v/v) acetonitrile for 10 minutes. The acetonitrile was replaced with 50 mM ammonium bicarbonate and incubated for 10 minutes. Washing with 50mM ammonium bicarbonate was repeated twice to remove acetonitrile. All the gel pieces were then incubated in 100% acetonitrile until they turned white, after which the gel pieces were dried *in vacuo*. Proteins were reduced with 10 mM DTT for 1 h at 57°C. This was followed by brief washing steps of ammonium bicarbonate followed by 50% acetonitrile before proteins were alkylated with 55 mM iodoacetamide for 1 h in the dark.

Following alkylation the gel pieces were washed with ammonium bicarbonate for 10 minutes followed by 50% acetonitrile for 20 minutes and the dried *in vacuo*. The proteins in the gel pieces were digested with trypsin (Promega) at 37^0C overnight in a 1:50 trypsin: protein ratio. The resulting peptides were extracted twice with 70% acetonitrile in 0.1% formic acid for 30 min, and then dried and stored at -20^0C. Dried peptides were dissolved in 5% acetonitrile in 0.1% formic acid and in preparation for nano-LC chromatography and mass spectrometry analysis.

3.2.4 LC MS/MS and data capture

3.2.4.1 Method 1

To assess the efficiency of each tryptic digest, 2µg per sample was loaded onto a C18-reverse phase Eksigent nano-fluidic HPLC column (15 cm length 75µm diameter: AB Sciex) and peptides were eluted using an increasing amount of acetonitrile up to 80% acetonitrile and 0.2% TFA at a flow rate of 300 nl/min over 90 minutes. Following this, 20µg of each digested protein sample was vacuum dried and sent to ThermoFisher (Hemel Hempsted, UK) for 1 Dimensional Liquid Chromatography Mass Spectrometry (1D LC MS/MS) analysis.

The sample was first diluted to 250 ng/µl and 1µg of each sample was injected into a C18 reverse phase LC (Easy nLC; Thermo Scientific) coupled to an LTQ Orbitrap Velos mass spectrometer (Thermo Scientific). Peptides were separated on a 15 cm x 100 µm C18 column containing 5µm C18 Reprosil particles (Nikkyo Technos; Japan) using increasing amounts of acetonitrile up to 80% and 0.1% formic acid as the mobile phase. The Orbitrap was used in a 'Top 20' data-dependent mode, with a full-scan run at a 50 nL/min flow-rate for 120 minutes to select and fragment precursor ions for identification. Peptides were fragmented using collision induced dissociation (CID) method and the Orbitrap analyzer was programmed to choose the 20 most intense precursor ions from each MS1 scan, where each precursor ion represents a specific peptide. Each peptide was then fragmented in MS/MS using CID to produce the b and y fragment ions from which the sequence of the peptide was determined by spectral matching.

Two sequential injections of un-fractionated TP of each sample were analysed on the LTQ Orbitrap Velos, whilst a single injection of each CF sample was similarly analysed. During the second injection of the TP samples, the Mass Spectrometer was programmed with an exclusion list to ignore all the peptides it encountered in the first injection so as to generate larger peptide coverage. The high sensitivity instrumentation of the Orbitrap Velos, equipped with a collision

cell for improved isolation and fragmentation with a high scan speed and resolving power, allowed for high resolution MS and low resolution MS/MS data acquisition in the mass analyzer. Each injection of every TP or CF sample resulted in acquisition of approximately 29,000 high quality spectra.

3.2.4.2 Method 2

Machine based-fractionation of peptides was carried out using the Thermo Scientific LTQ Orbitrap Velos Mass Spectrometer. 2µg of each peptide sample (prepared using method 1) was injected onto an LC column and a full-scan run was carried out at a 50nL/min flow-rate for 90 minutes to select and fragment precursor ions for identification as described in the previous section (Section 3.2.4.1). The Top 20 CID method, was used as before to choose the 20 most intense precursor ions from each MS1 trace within four pre-determined *m/z* ranges (450-550, 550-700, 700-950, 950-1600), however with a shorter gradient of 90 minutes. Each peptide was then fragmented using CID to produce the b and y fragment ions from which the sequence of the peptide was determined by spectral matching. In total, four separate injections of each sample were analyzed to produce four raw spectra files which were then analysed using data analysis programs.

3.2.4.3 Method 3

All experiments were performed on a Thermo Scientific EASY-nLC II connected to a LTQ Orbitrap Velos mass spectrometer (Thermo Scientific, Bremen, Germany) equipped with a nano-electrospray source. For liquid chromatography, separation was performed on a EASY-Column (2 cm, ID 100µm, 5 µm, C18) pre-column followed by a EASY-column (10 cm, ID 75 µm, 3 µm, C18) column with a flow rate of 300 nl/min. Solvent A was 100% water in 0.1 % formic acid, and solvent B was 100 % acetonitrile in 0.1% formic acid. The gradient used was from 5-15 % B in 5 min, 15-35% B in 90 min, 35-60% B in 10 min, 60-80% B in 5 min and kept at 80% B for 10 min. MS/MS data was acquired from the Orbitrap Velos in Top 20 CID mode by Dr Salome Smit (University of Stellenbosch).

3.2.5 Data analysis

3.2.5.1 Method 1

RAW files were converted into ms2 and mascot generic format (MGF) files using ReAdW (Thermo-Foundation) software. In the first instance, MS/MS peptide fragmentation data was analysed using Protein Pilot (AB-Sciex; v.3.0) [255] and Sequest (within Proteome discoverer

v1.3) (http://www.thermo.com) in order to compare the different search engines and to determine which one was the best to use for analysis of all the data. Following the preliminary analysis, the use of Sequest was chosen in the first instance.

Each individual MS/MS spectra was searched against a database of theoretical spectra produced from an *in silico* trypsin digestion of all theoretical protein sequences in the relevant proteome. The protein sequences were all taken from a complete, non-redundant proteome Fasta file of the relevant individual strain (available in UniProt; shown in Table 3.2 below). Carbamidomethylation was set as a fixed modification whilst oxidation of methionine residues was set as a variable modification.

Strain	UniProt fasta
M. tuberculosis H37Rv	*M. tuberculosis* H37Rv ATCC 25618
M. tuberculosis LAM3	*M. tuberculosis* F11
M. tuberculosis W-Beijing	*M. tuberculosis* H37Rv ATCC 25618
M. tuberculosis CAS	*M. tuberculosis* H37Rv ATCC 25618
M. bovis	*M. bovis* AF2122-97
M. bovis BCG	*M. bovis* Pasteur_1173P2
M. avium	*M. avium* 104

Table 3.2: UniProt fasta files used for database searching per strain; the *M. tuberculosis* H37Rv ATCC 25618 was used for those that did not have UniProt fasta files.

Two missed cleavages were allowed and initial peptide mass tolerance was set at 10 ppm whilst fragment mass tolerance was set to 0.5 Da. The peptide and protein false discovery rates (FDR) were set to a minimum of 1% and a maximum of 5%. False discovery rate analyses were calculated using a decoy database (which contained reversed protein sequences of the relevant Fasta file) to ensure that the results only used matches of high confidence peptides. At least two peptides were required for high confidence protein identifications.

3.2.5.2 Method 2

Multiple database search engines were used to assess the utility of bioinformatics approaches in the improvement of spectra assignment. A cloud computing platform termed ProteoCloud, developed and described in-depth by Muth 2011 [185], was used to characterize unidentified spectra from MS data that was obtained from cell culture and protein extraction method 1 and MS method 1. Cloud computing was developed in an effort to overcome the challenges that

come with the demand of high computational power when processing large quantities of spectra. Cloud computing allows the use of high performance virtual servers to rapidly assign high quality unidentified spectra. The work-flow for this approach is clearly described by Muth *et al*, 2012 [256].

Briefly, ProteoCloud employs an amalgamation of existing MS searching methods including de novo, database and tag based approaches including Crux, X!Tandem, OMSSA, Inspect and Pepnovo to perform a nearly exhaustive analyses on large proteomic mass spectrometry output. Each algorithm scores and validates the spectrum assignments differently however; a unifying q-value calculated using the Q-Vality software [257] is incorporated into the Cloud computing system. This allows the detection of a strong consensus (agreement between search engines), unique identification by a single search engine and strong contradictions in peptide assignments.

This bioinformatics platform amalgamates the results from all these search engines together using a voting system. In this system, each algorithm puts in a vote when it identifies a spectrum within the q-value specified by Q-Vality. It is taken in account that different algorithms identify different spectra, hence the voting system aggregates the vote of each algorithm and any confident identification by any algorithm is considered correct unless other algorithms assign the spectra to a different peptide with greater confidence. ProteoCloud using the X!Tandem parser [258] and OMSSA parser [259] to extract the output from the search engines into MySQL database where the output is analysed and prepared for presentation. The output from ProteoCloud is in the form of a user friendly graphic user interface (GUI) that shows the spectrum itself and its annotation corresponding to the matched peptide, protein identification, sequence coverage, NSAF value, peptide count, spectral count and the individual q-value scores per search engine that identified the peptide as show in Figure 3.2 below.

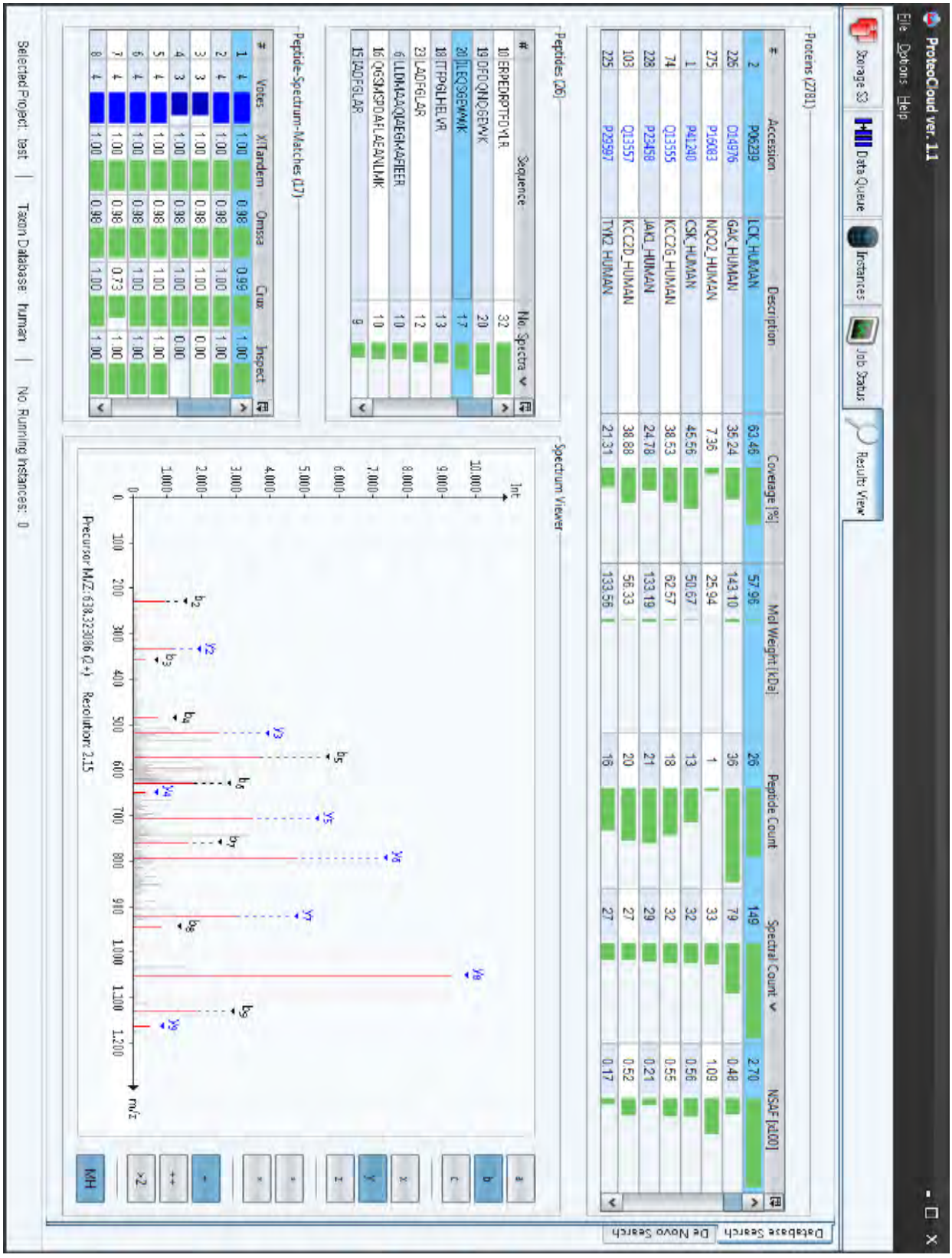

Figure 3.2: Sample GUI output from ProteoCloud depicting in the top panel from left to right the protein accession number, description, percentage sequence coverage, molecular weight, peptide count, spectra counted and NSAF value calculation; middle left panel depicts the identified peptide sequence; bottom left panel depicting the votes per search engine as well as their scores; the middle panel shows the spectra and how it matched to the peptide in question.

3.2.5.3 Method 3

A novel search algorithm called Rescore was developed and described by the group of Professor Lennart Martens (U-Ghent, Belgium). Briefly, this algorithm is a two-stage machine-learning based peptide to spectrum match (PSM) re-scoring engine. The first stage consists of a random forest predictor of fragment ion intensity that takes as input a peptide sequence and that produces a theoretical fragmentation spectrum with singly and doubly charged fragment ions, all with their own, predicted absolute intensity [260].

The second stage then provides a new score for PSMs provided by a classical search engine such as Mascot, by employing a Percolator-like re-analysis (again, using Random Forest) of features calculated for target and decoy hits. Differently from current algorithms, including Percolator, Rescore takes into account deviations between the measured and predicted peak intensities (as obtained from the first stage of Rescore). Due to the inclusion of this second dimension of information from the spectrum, Rescore provides more discriminative scores and better overall reproducibility across runs, due to the much better separation between correct and incorrect PSMs, and the ability of Rescore to clearly separate scores coming from closely homologous sequences. The entire methodology section is summarized in Figure 3.3 below.

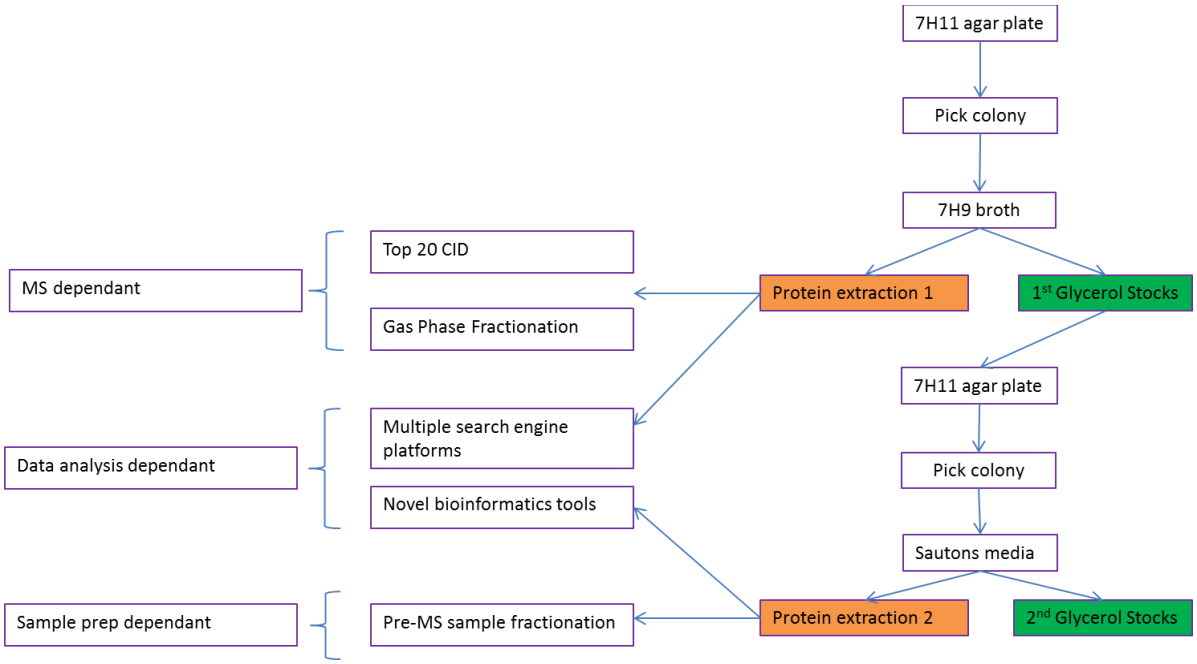

Figure 3.3: Workflow used in the method development process to maximize protein identification from in-vitro *M. tuberculosis* lysates.

3.3 Results and Discussion

3.3.1 Work-flow 1

Initial protein extraction and data described in this section was obtained from the workflow described in Figure 3.4 below.

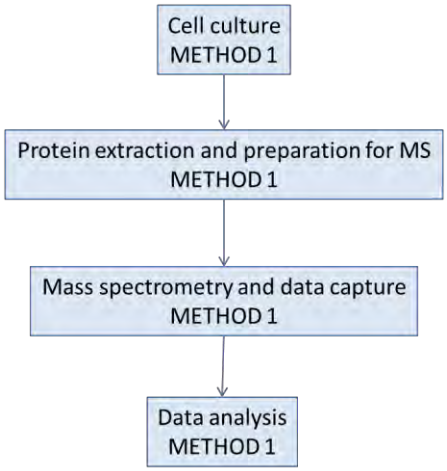

Figure 3.4: Work-flow approach used for initial analysis of *M. tuberculosis* to determine depth of proteome coverage.

3.3.1.1 Protein extraction

Following initial protein extraction using methodology workflow 1 (Figure 3.4), BCA quantitation of the initial protein indicated that large concentrations of protein were extracted for each sample with concentrations ranging between 2.5 µg/µl to 15 µg/µl for total cellular proteins and 10 µg/µl to 40 µg/µl for culture filtrate proteins. The proteins were analysed on a 1D SDS-PAGE gel to assess sample diversity and success of protein extraction. The 1D gel of both culture filtrate and cellular protein shown in Figure 3.5 below demonstrates that the method was successful in extracting a wide variety of proteins across each of the strains.

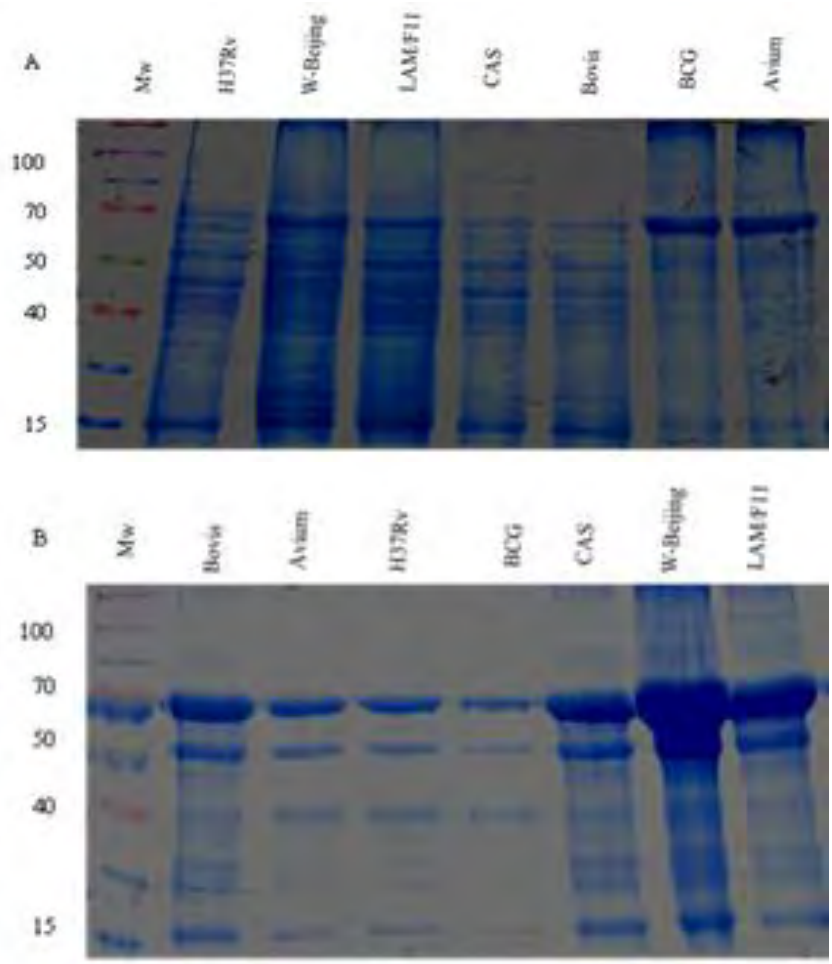

Figure 3.5: 1D gels of (a) total cellular protein and (b) culture filtrate protein extracted from the 7 strains. The 1D gel chromatograms show a clear separation of proteins according to molecular weight. Wide protein diversity is observed in both culture filtrate as well as total cellular proteomes suggesting that our method did not introduce a bias for either high or low molecular weight proteins.

3.3.1.2 Tryptic digest efficiency

To assess the efficiency of tryptic digest prior to MS/MS, 2µg of each digested sample was pooled and peptides were separated on a C18 column. The 1D LC trace that was obtained shown in Figure 3.6 below was used to evaluate the extent to which the protein sample was digested using trypsin.

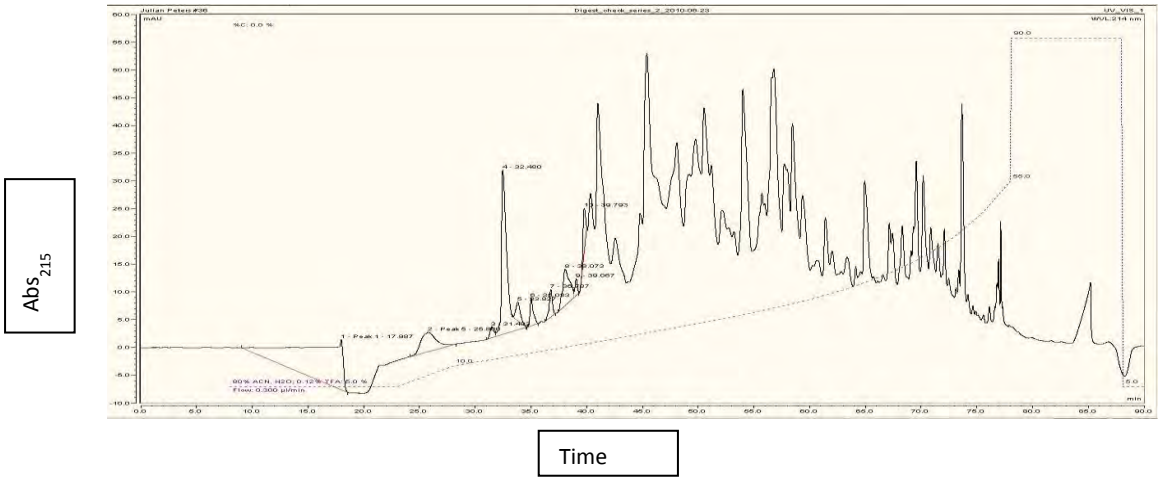

Figure 3.6: LC trace of the pooled tryptic digests. The LC trace shows that peptides elute across the time range between 20 minutes to 85 minutes and are distributed along the LC gradient with a maximum at approximately 60 minutes.

The LC trace was obtained and shown in Figure 3.6 above. Success of the tryptic digest obtained from the workflow depicted in Figure 3.3 was confirmed using a descriptive analysis software package in Protein Pilot, whose results are summarized in Table 3.3 below.

Missed Cleavages	Spectra in selected set	% of selected set
0	3695	80.4%
1	865	17.5%
2	84	1.7%
3	6	0.1%
4	7	0.1%
5	2	0.01%

Table 3.3: The table shows protein pilot descriptive statistics summary showing MS/MS breakdown of the tryptic digest of H37Rv. The table shows that the majority of spectra (80.4%) contained no missed cleavages. Overall, 99.6% of the spectra had a maximum of two missed cleavages whilst 0.2% had more than 3 missed cleavages. Note: The tryptic digests of all other strains showed a similar trend.

3.3.1.3 Orbitrap data analysis and protein yields

Each TP and CF sample was analysed on the Orbitrap Velos and an each produced its own LC-MS and MS/MS datasets. As shown below, the MS1 scan of H37Rv again confirms a successful tryptic digest with the total ion chromatogram in Figure 3.7a showing a steady elution of peptides across the LC gradient. The 2D MS chromatogram demonstrates the complexity of the sample, showing a significant number of discrete tryptic peptides eluting at the marked time point indicated on the 1D chromatogram (~2,600sec).

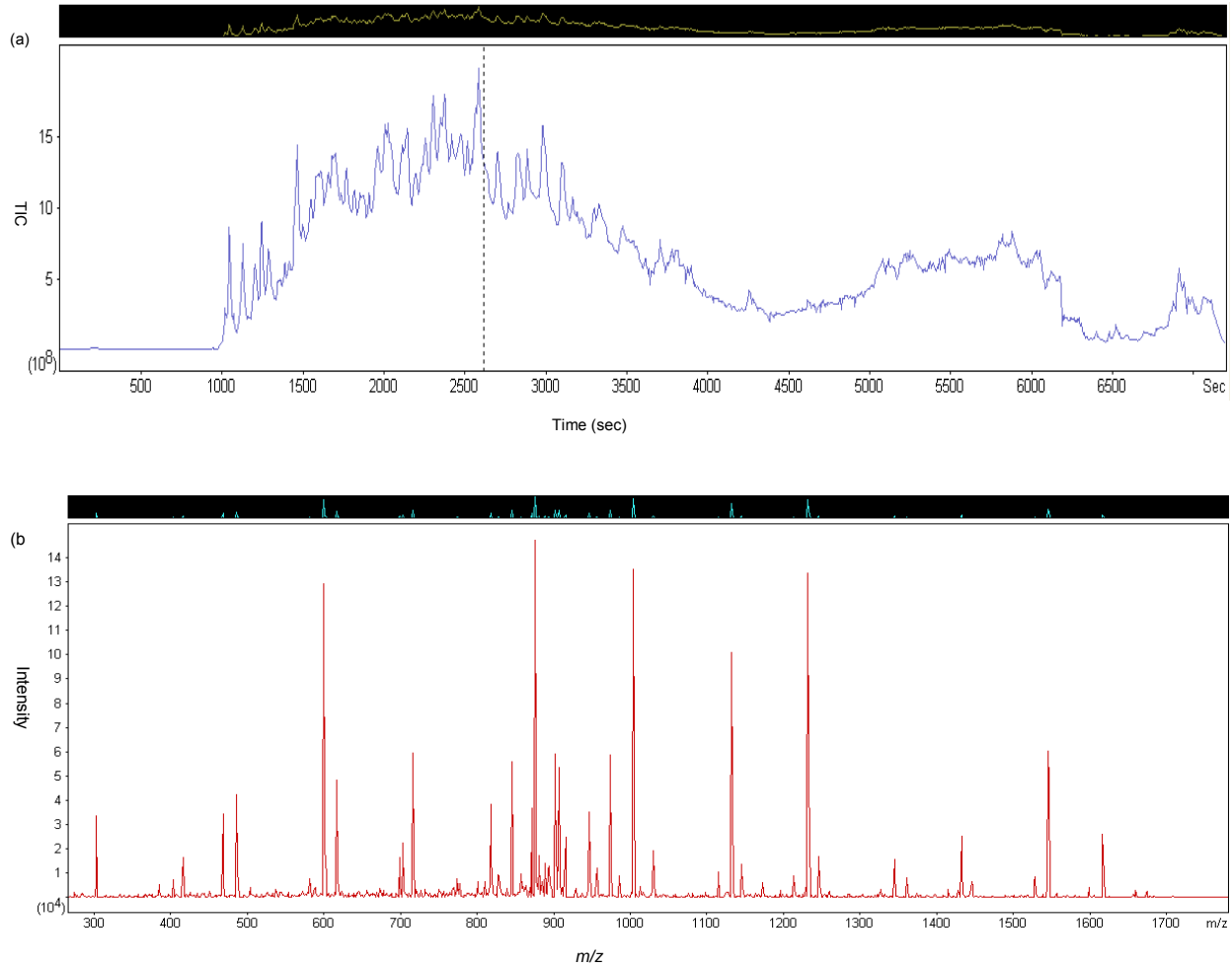

Figure 3.7: LC MS/MS raw data for H37Rv TP injection 1 (a) The elution profile of peptides showing the total ion count across the timeframe with a peak elution between 2,000 and 3,000 seconds; (b) An expanded 2D view of all the peptides eluted at the selected time point of 2,600 sec in the 1D chromatogram.

Following sequential CID-based MS/MS fragmentation of each of the Top 20 peptides in each sequential 2D chromatogram, b and y ions were produced for each peptide and recorded in individual MS/MS spectra. This provided the peptide sequence information from which protein identifications were subsequently made. Using the Top 20 CID data for H37Rv, the Sequest database search algorithm identified 3 000 high confidence peptides that were used to identify a total of 1 023 proteins when the MS/MS spectra were searched against the UniProt H37Rv Fasta file. Figure 3.8 below shows the b and y ion fragmentation ions obtained for a single high confidence peptide used to identify the highest scoring protein the 60kDa chaperonin groEL2.

(a)

Spectrum List

Spectrum	Time	Prec MW	Prec m/z	Prec z	Prot N	Best Sequence	Modifications	Conf	Theor MW	z
1.1.1.4324.1		1266.5837	634.2991	2	7	SQQSFEEVSAR		99	1266.5840	2
1.1.1.6747.1		1272.6693	637.3419	2	27	SEEAQLVVVGSR		99	1272.6674	2
1.1.1.9271.1		1272.7288	637.3716	2	1	AVEKVTETLLK	Carbamyl(K)@4	99	1272.7289	2
1.1.1.11666.1		1290.6946	646.3546	2	31	FLLDQAITSAGR		99	1290.6932	2
1.1.1.7691.1		1297.6895	649.8520	2	3	VTSIHSLLDEGK		99	1297.6877	2
1.1.1.7695.1		1297.6904	433.5708	3	3	VTSIHSLLDEGK		99	1297.6877	3
1.1.1.10689.1		1299.6302	650.8224	2	4	QELDEISTNIR	Gln->pyro-Glu@N-term	99	1299.6306	2
1.1.1.10579.1		1299.6315	650.8230	2	4	QELDEISTNIR	Gln->pyro-Glu@N-term	99	1299.6306	2
1.1.1.6048.1		1301.6575	651.8360	2	5	GSLVEGGIGGTEAR		99	1301.6576	2
1.1.1.16745.1		1341.7662	671.8904	2	1	VALEAPLKQIAF	Carbamyl(K)@8	99	1341.7656	2

(b)

Peptide ID Hypotheses - 1.1.1.6048.1

Conf	Sc	Prot N	Sequence	Modifications	Theor MW	Theor m/z	z	ΔMass
99	21	5	GSLVEGGIGGTEAR		1301.6576	651.8361	2	-0.0001
< 1	8		ASTPNADPRFAR		1301.6477	651.8311	2	0.0098
< 1	8		QAGTIVAGAAADTR	Deamidated(Q)@1	1301.6576	651.8361	2	-0.0001

(c)

Fragmentation Evidence for Peptide

GSLVEGGIGGTEAR

Residue	b	b+2	y	y+2
G	58.0287	29.5180	1302.6648	651.8360
S	145.0608	73.0340	1245.6434	**623.3253**
L	**258.1448**	129.5761	**1158.6113**	**579.8093**
V	**357.2132**	179.1103	**1045.5273**	**523.2673**
E	**486.2558**	**243.6316**	**946.4588**	**473.7331**
G	**543.2773**	272.1423	**817.4163**	409.2118
G	**600.2988**	**300.6530**	**760.3948**	380.7010
I	**713.3828**	**357.1951**	**703.3733**	352.1903
G	**770.4043**	**385.7058**	**590.2893**	295.6483
G	**827.4258**	**414.2165**	**533.2678**	**267.1375**
T	**928.4734**	**464.7404**	**476.2463**	238.6268
E	**1057.5160**	529.2617	**375.1987**	188.1030
A	**1128.5531**	**564.7802**	**246.1561**	123.5817
R	1284.6543	**642.8308**	175.1190	88.0631

(d)

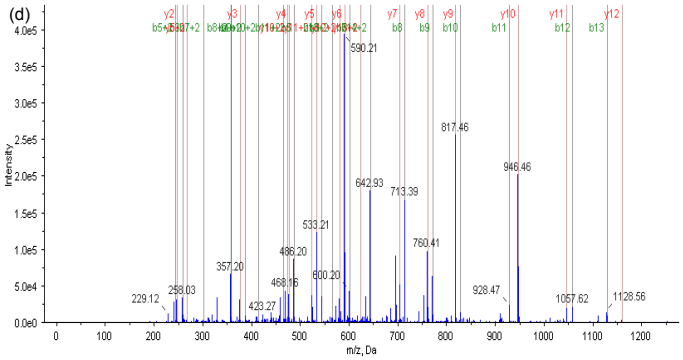

Figure 3.8: The b and y ions obtained following the fragmentation of one of the highest scoring peptides of the highest scoring protein (60kDa chaperonin) from the second injection of the H37Rv TP sample. (a) In green is shown the spectrum that identifies the specific peptide and shows the confidence of assignment for that peptide to be 99%; (b) The list of possible candidate peptides matching that spectrum (Peptide Hypothesis) as well as the best matching peptide within that list highlighted in green; (c) The fragmentation evidence, which is the list of which b and y ions corresponding to each depicted amino acid residue observed in the fragmentation of that peptide; (d) Each obtained b and y fragment ion of the peptide, its intensity and m/z fragments.

Table 3.4 below shows the total number of proteins identified per strain with Sequest inclusive of both culture filtrate and cellular proteins. Protein Pilot descriptive statistics software was used to analyse and arrange the data to give a comprehensive summary of the experiment as well as the results.

Strain	Total # Spectra	Total # PSM's	Total protein ID
M. tuberculosis H37Rv	28 273	5 185	1023
M. tuberculosis CAS	18 352	4 021	775
M. tuberculosis F11	24 586	4 214	866
M. tuberculosis W-Beijing	22 879	3 085	682
M. bovis	19 264	3 726	616
M. bovis BCG	23 455	2 034	305
M. avium	29 014	3 312	777

Table 3.4: Summary of total proteins identified per strain. The total number of proteins identified ranged from 305 in *M. bovis* BCG to 1,023 in *M. tuberculosis* H37Rv. The difference between H37Rv and other strains could be because *M. tuberculosis* H37Rv is the most extensively studied strain of *M. tuberculosis* and hence its sequence has been fully annotated whilst discrepancies in other strains are still being studied.

In order to get a picture of the global analysis of the identified protein set, gene ontology (GO) annotation was used. Gene ontology is an ongoing bioinformatics process that is used to standardize gene annotation across databases by the use of controlled species neutral vocabulary terms that are maintainable across the databases (http://www.geneontology.org). Gene ontology provides a concise summary of the gene in terms of molecular function, biological process and localisation in the cell. It also includes information on binding domains, catalytic processes as well the cellular events that the gene product is involved in for example cell cycle or transcription. This allows researchers to query datasets at multiple levels using keywords that define the attributes of interest. For example, using gene ontology, a researcher can determine the proportion of proteins in a query dataset that are involved in redox catalytic processes and narrow this down to cell wall associated redox catalytic processes. Gene ontology therefore makes it easier to understand datasets obtained from high throughput experimental approaches such as shotgun mass spectrometry.

Due to the fact that H37Rv is fully gene ontology (GO) annotated, we chose to use it as a template to assess the level of protein coverage and possible enrichment of certain proteins. This was done in order to evaluate the utility of our extraction method for a global proteomic analysis. GO analysis revealed that every class of protein was represented in our experimental sample, with the bulk being of proteins annotated as those of unknown function (approximately 33%) and enzymes (approximately 33%). Other classes of proteins represented include transport proteins, regulatory, virulence, lipoproteins, membrane, cellular processes and regulatory proteins. Under-representation was seen in the Proline-Glutamine and Proline-Proline-Glutamine (PE/PPE) family of proteins as see in Figure 3.9 below.

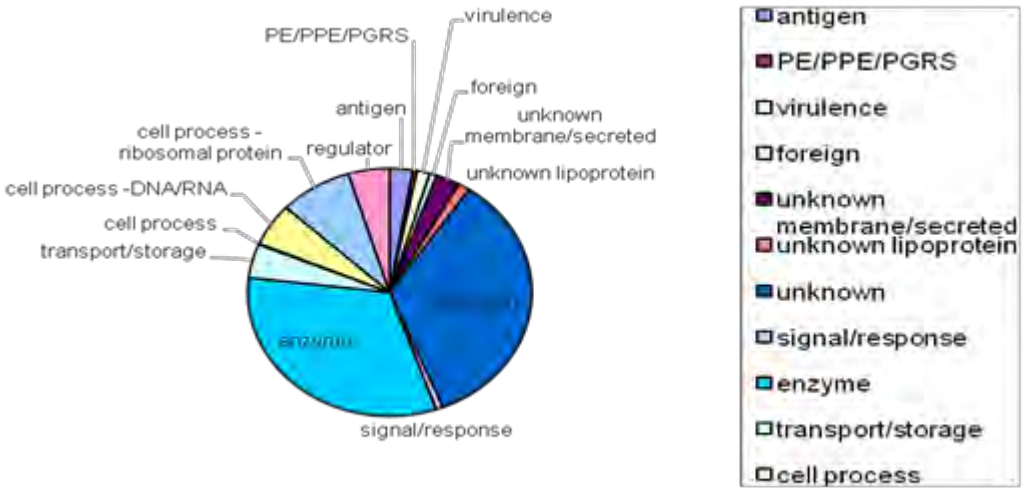

Figure 3.9: Distribution of biological function for *M. tuberculosis* H37Rv protein found. The pie chart is colour coded to defined groups of proteins and shows that every group of protein was represented to some extent in the experimental sample, although some groups dominated over others

The representation of most classes of protein suggests that although the simple MS-compatible rapid SDS based lysis method may have widespread utility in extraction of multiple classes of protein from organisms that require harsh methods of cell lysis. Whilst the protein extraction method is successful as seen by the SDS PAGE gel in Figure 3.4 above, the number of proteins obtained using this approach may not be the best for maximizing proteome coverage from *M. tuberculosis* for efficient cross strain/species comparison. The complete Mycobacterial genome encodes 4 023 proteins hence this initial dataset represents approximately 27% of the complete theoretical protein hence this prompted us to attempt to expand protein identification.

3.4 Work-flow 2: Machine based approach

Due to the fact that the initial protein extraction and peptide digestion method seemed to be successful (Figure 3.5, 3.6 and Table 3.3), a machine (mass spectrometer) based approach was explored as a means to increase protein identification. This gas phase fractionation method was chosen as it potentially allowed us improvement of raw data quality from peptide extracts that had already been pre-prepared, hence eliminating the need for repeated bacterial growths, protein extraction and preparation steps. Peptides that were extracted and used in the initial MS run (workflow 1: Figure 3.4) were re-run using MS analysis and data capturing method 2 described in Section 3.2.4.2 above. The work-flow for this approach is described in Figure 3.10 below.

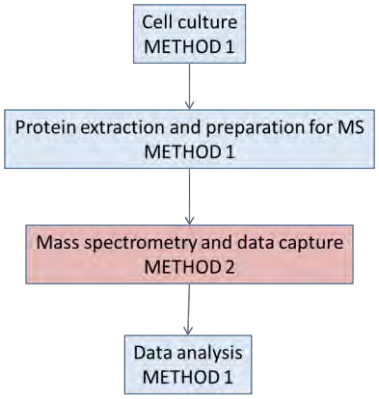

Figure 3.10: Work-flow approach used for machine based approach to increase proteome coverage of *M. tuberculosis* lysate.

Machine based fractionation is an alternative way to create an exclusion list. During machine based fractionation, the same sample is injected multiple times (in this case 4 times), and each time the machine is programmed to pick precursor ions within a specified mass window. Then as before, MS is run in the Top 20 data dependant mode, which picks the 20 most intense ions for analysis within each defined *m/z* window. In theory, this allows more ions to be sampled because different ions may emerge as more intense in smaller subgroups than in the undivided sample. However, this assumes that in every, MS1 spectrum there is an even distribution of precursor ions across the full specified mass range, however, this is not the case.

A heat-map of the overall machine based fractionation (Figure 3.11) indicated that identified peptides were distributed through-out the *m/z* ranges although most peptides were between the ranges 550-700 and 700-950. This is consistent with the LC trace in Figure 3.6 and 3.7 above. Using the top 20 CID method, 20 of the most intense peptide ions in each *m/z* range were fragmented and analyzed across the 90 minute run. Spectra obtained were analysed using data analysis method 1 described in Section 3.2.5.1 above. The four fractions were analysed individually and the results of all fractions were analysed then integrated to give a non-redundant total list of proteins.

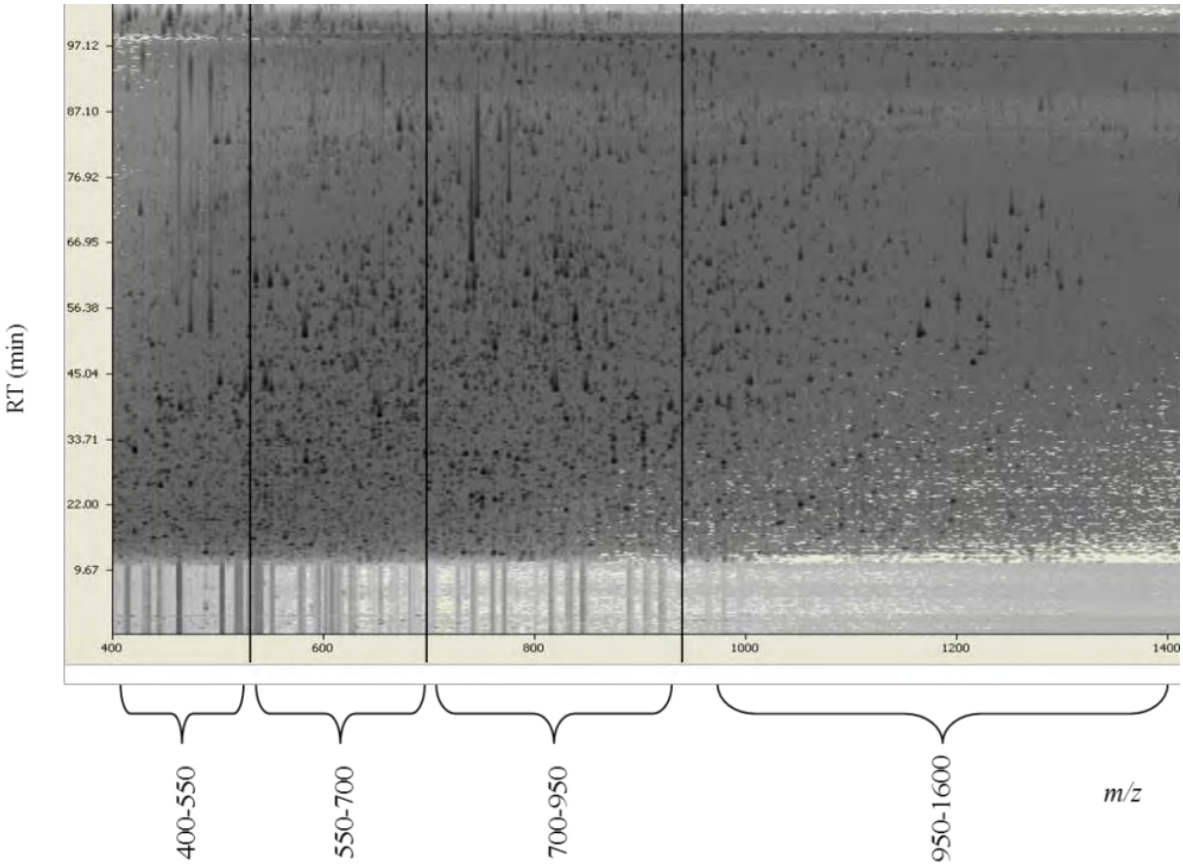

Figure 3.11: Machine based fractionation heat-map showing individual spots representing peptides eluted at various retention times from across the four defined *m/z* ranges for *M. tuberculosis* H37Rv. Intensity of the spots represents the concentration of the peptide.

It was expected that the numbers of proteins would increase from the initial method due to the gas phase fractionation approach, however although the number of spectra increased, the percentage of spectra assigned did not increase and subsequently the numbers of proteins identified actually decreased, as seen in Table 3.5 below. This could be due to peptide degradation between the initial run and the second run. Alternatively, the top 20 most intense ions that were sampled in each of the 4 separate *m/z* ranges could have been derived from the same abundant proteins in *M. tuberculosis*. The *M. tuberculosis* lysate is predicted to have a dynamic range of 10^4 [248] hence using this method, it is conceivable that the mass spectrometer repeatedly sampled peptides from the most abundant proteins hence resulting in no particular increase in the number of proteins.

The number of spectra obtained was compared between the first MS run and second gas phase fractionation MS run were compared to determine if there was an increase in the number of spectra during fractionation. An increase in the number of spectra would allow us to conclude that the there was repeated sampling of peptides from the same proteins. Comparison of tables

3.4 and 3.5 shows that there was an increase in the number of spectra when gas phase fractionation was carried out. The increase in the number of spectra without an increase in the number of proteins identified suggests that it is likely that the same peptides from an abundant protein or a set of abundant proteins were repeatedly sampled hence there was no increase in protein identification. Furthermore, since these samples were analysed by MS a considerable time apart, it is likely that peptides were degraded during that time. Purely from a stoichiometric perspective, more peptides from an abundant protein or set of proteins (albumin, GroEL) would be left behind compared to non-abundant proteins which would lead to the decrease in protein identifications.

Species	Number of spectra	Total # of PSMs	Total # of proteins
M. avium	32 145	6 918	690
M. bovis	35 586	5 043	540
M. bovis BCG	47 533	6 982	299
M. tuberculosis CAS	42 031	4 357	240
M. tuberculosis Beijing	48 624	5 084	678
M. tuberculosis LAM	50 197	7 241	920
M. tuberculosis H37Rv	52 780	12 458	1 018

Table 3.5: Comparison of number of spectra, PSMs and proteins obtained from H37Rv lysate processed using work-flow in Figure 2.2 versus workflow in Figure 2.7.

3.5 Work-flow 3: Data analysis based approach

This prompted us to challenge the exploitation of bioinformatics tools in an attempt to expand protein identification rates. Spectra that were obtained from the initial analysis using work-flow1 (Figure 3.4) were therefore re-analysed using data analysis method 2 described in Section 3.2.5.2 above. This approach allowed us to use pre-existing MS spectra obtained using work-flow 1 (Figure 3.4) and attempt to increase protein coverage without the need to re-extract proteins or re-run the MS. The workflow for this work is summarised in Figure 3.12 below.

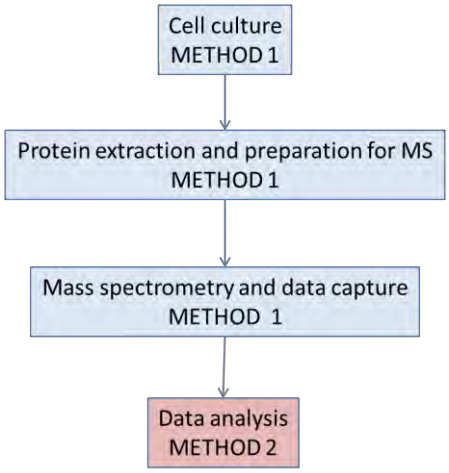

Figure 3.12: Work-flow approach used for bioinformatics based approach to increase proteome coverage of *M. tuberculosis* lysate.

Using the MS/MS spectra files of *M tuberculosis* H37Rv, the results show that each discrete search engine matches a unique number of spectra with varying degree of overlap among the search engines. The reason for this is that each search engine has different strengths and hence will only identify those within its algorithm boundaries. Using each individual search engine, the average number of peptide spectral matches observed was 2000. However the overall PSM's identified increased to 4500 at 5% FDR as shown in Figure 3.13 below The difference between 1% and 5% is approximately 1 200 PSMs hence indicating an increase of 1200 PSMs with 60 possible false identifications.

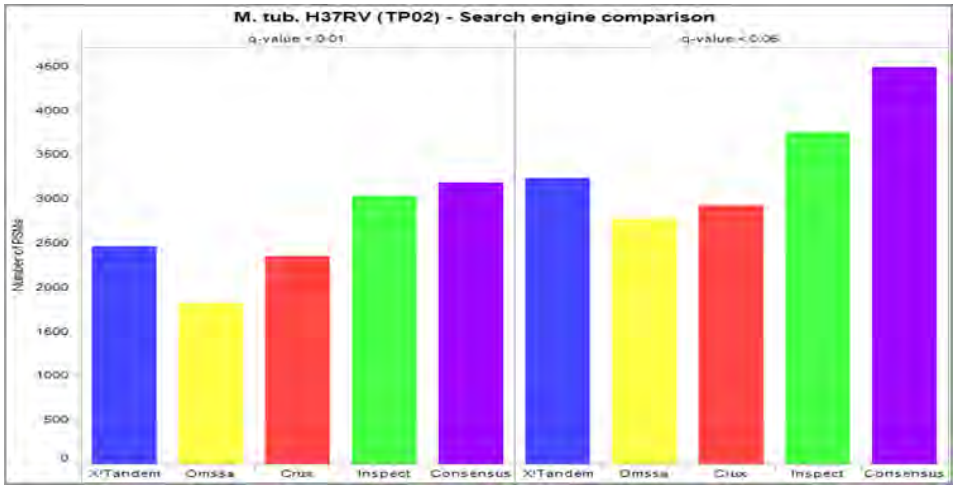

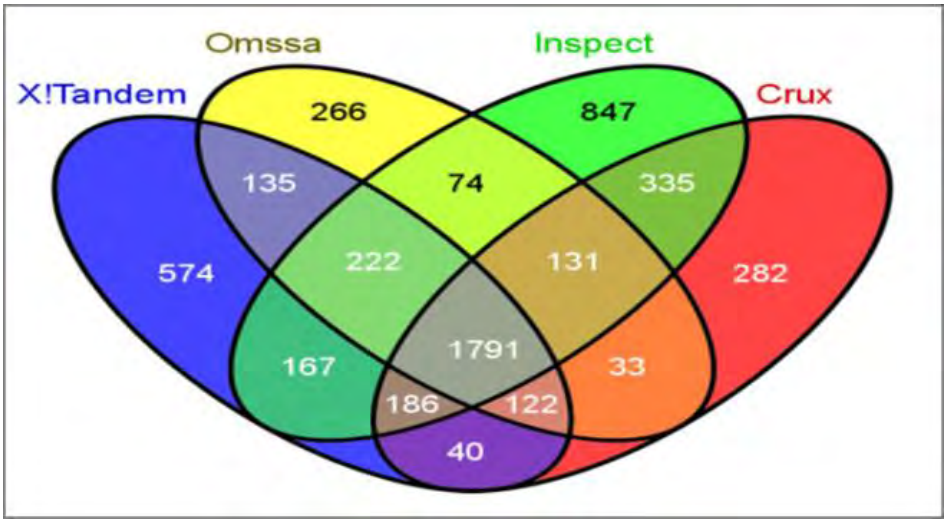

Figure 3.13: Bar graph showing the peptide coverage for *M. tuberculosis* H37Rv TP02 peptide sample injection obtained by 4 of the database search engines in ProteoCloud: The bar graph shows a representation of the peptides in the sample by each search engine at 1% and 5% FDR. It also shows the consensus which represents the total number of PSMs identified by all search engines. The venn diagram then shows the contribution of each search engine to the total number of peptides identified. Adapted from Muth 2011 [185].

It was observed in this analysis that using any individual search engine alone means that a number of legitimate peptide identifications are missed. Using multiple search engines allows peptides that are missed by one algorithm to be found by other algorithms without adding too many false positives, since each individual engine ensures minimal false positive during its individual search. Hence adding all peptides that are obtained from different search engines makes it is possible to attain peptide information that could have otherwise been unavailable by the use of only one or two search engines as shown in Table 3.6 below.

Search engine	Number of proteins
Mascot	699
OMSSA	780
Crux	824
Inspect	916
X!Tandem	895
Proteocloud	1 088

Table 3.6: Comparison of the non-redundant number of proteins identified by each single search engine compared to the non-redundant number found cumulatively by all search engines, using the example of the MS spectra obtained from the second injection of the *M. tuberculosis* H37Rv TP.

Analysis of this dataset in ProteoCloud shows that evaluation of complex tryptic digests by multiple search engines significantly increases the number of assigned PSMs hence it has the

potential to improve the protein coverage in any given dataset. However in this specific instance the increase in the number of PSM identifications did not equate to a significant increase in the number of proteins identified as protein identification only increased to 1 088 proteins in Table 3.7 below. The reason for this is because although more spectra were assigned, it was observed that more than half of the spectra per strain were from the contaminant BSA which is added to Middlebrook 7H9 media as a supplement. Due to their amount in the ADC supplement (5g/L), BSA peptides tend to dominate the spectra in terms of number and intensity, thus although total number of PSM's increased, the total number of proteins identified did not increase.

This is consistent with the data obtained from machine based fractionation where an increase in the number of spectra obtained did not necessarily equate to an increase in the number of PSMs assigned. While the number of spectra increased, the number of peptides and proteins identified from each search increased by a small margin further suggesting that there was either repeated sampling from the same abundant proteins or that PSMs to contaminants (such as BSA) were the major contribution to the increase in the number of spectra and PSMs assigned. This phenomenon is known as sample inherent ion suppression whereby dominant peptides from an abundant protein that are easily ionisable and are MS compatible are preferentially sampled and by so doing reducing the chance to sample peptides from other proteins. This leads to the suppression of peptide signals from other non-abundant proteins. This prompted us to consider a complete change in the entire method beginning from the cell culture, protein extraction and preparation method, MS analysis and data capture as well as data analysis.

Species	Number of spectra	Total # of PSMs	Total # of proteins
M. avium	58 013	6 654	780
M. bovis	80 538	5 615	791
M. bovis BCG	57 533	6 919	599
M. tuberculosis CAS	26 110	3 247	420
M. tuberculosis Beijing	81 914	4 241	678
M. tuberculosis LAM	80 904	7 696	920
M. tuberculosis H37Rv	84 930	18 059	1 088

Table 3.7: Total number of spectra, PSMs (below FDR 0.05) and proteins obtained using the bioinformatics approach to increase protein identifications.

3.6 Work-flow 4: Cell culture and protein preparation based approach

Protein extraction was repeated according to the workflow depicted in Figure 3.14 below. The overhaul in the approach to cell culture, protein extraction and data analysis saw a significant

improvement in the protein numbers by up to 3 fold with protein numbers above 3 000 (Figure 3.16c). The improvement in protein identifications was owed to a number of features of the new method. Firstly the cell culture media lacked the ADC supplement which is known to suppress the signal of many proteins in mass spectrometry. This may have been the initial compounding issue with the use of the peptide extract from Middlebrook 7H9 for whole cell protein analysis. Thus whilst Middlebrook 7H9 may be useful for DNA or RNA extractions, it is not ideal for protein extractions, especially for culture filtrate proteins where albumin is most concentrated.

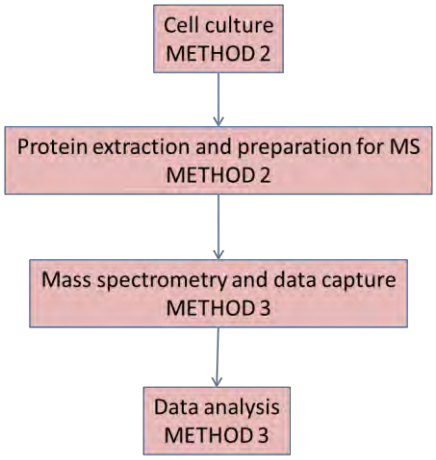

Figure 3.14: Work-flow approach used for bioinformatics based approach to increase proteome coverage of *M. tuberculosis* lysate.

Pre-fractionation of the peptide sample prior to MS has previously been proven in other experiments to be invaluable in simplifying the peptide mixture prior to MS analysis [166,187,248,261]. The problem with bulk sampling in MS is that a few proteins in biological samples such as bodily fluids and lysates are highly abundant resulting in large dynamic ranges between protein concentrations [262]. This results in a scenario where peptides from low abundance proteins are often masked by peptides from highly abundant proteins which then supresses their signal from the mass spectrometer or dominate the MS1 spectrum, meaning that the low abundance peptides are not selected for MS/MS analysis [263]. This essentially prevents comprehensive proteomic coverage and it has been repeatedly observed that separation of proteins or peptides prior to MS decreases complexity of the mixture increases the sensitivity of detection in each of the less complex generated fractions [264].

Following mass spectrometry, the new data analysis Rescore was used to assign peptide identities to the spectra. It was observed that the number of spectra significantly increased by

approximately two-fold for each strain. The increase in spectra per experiment resulted in an increase in the number of PSM's being assigned by more than three-fold as seen in Table 3.8 below. Furthermore, the spectra obtained in this study contained no contaminant spectra from BSA since Sautons media does not contain the ADC supplement, meaning that more peptides from each strain could be sampled due to unmasking by removal of the highly abundant albumin protein. This resulted in an increase in the proteins identified per strain (Table 3.8). It is noteworthy to mention that it could have been worth a try to evaluate the use of 7H9 with Dextrose and Catalase without albumin. It is speculated that this would have the growth stimulatory benefits of 7H9 without the MS-incompatible effects of BSA. This was however not done as Sautons media was equally satisfactory.

It has previously been assumed that MS2 peaks for the most important fragment ions have a high intensity, and that fragment ions of different types have the same high intensity (Craig and Beavis 2004). However, without an accurate model of the relationship between the amino acid composition of the peptide and the peak intensities in the corresponding MS2 spectrum, these *ad hoc* approaches fail to match fragment ions for which low intensity peaks are expected to be observed [260]. It has been shown that incorporating knowledge about this relationship between peak intensity and amino acid composition significantly improves peptide identification rates. This is the new addition in the Rescore algorithm and the probable source of its advantage over other algorithms.

This novel tool added a superior dimension to spectral assignment as it takes into account deviations between the measured and predicted peak intensities. Scores for PSMs provided by a classical search engine (Mascot), are reassessed by employing a Percolator-like re-analysis using random forest scores of features calculated for target and decoy hits as shown in Figure 3.15 below using an example of *M. bovis* BCG PSMs to show the expanse of the data collected per strain [260]. This algorithm allows more extensive but stringent peptide coverage from spectra that other classical search engines are unable to assign.

This novel search tool is based on a recently published MS/MS peak intensity prediction tool called MS^2 PIP [260]. This algorithm is capable of predicting the intensity of fragment ion signal peaks from a peptide sequence. MS^2PIP is capable of pre-processing large MS/MS datasets with confident PSM's to facilitate data-driven model induction using a random forest regression learning algorithm. The intensity predictions of MS2PIP have been evaluated on

several independent evaluation sets and found to correlate significantly better with the observed fragment-ion intensities as compared with the current state-of-the-art competing tools

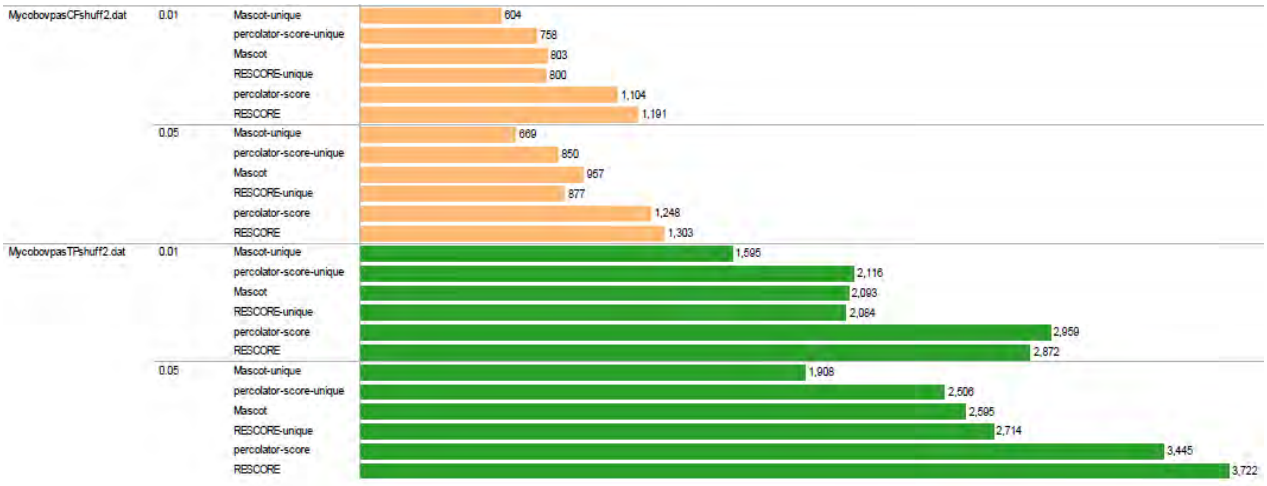

Figure 3.15: PSM data obtained for the 10 fractions of CF (orange) and TP (green) by each search engine platform with Rescore including Mascot, Percolator and Rescore at 1% and 5% FDR. The PSMs are separated into those unique to Mascot (Mascot-unique); unique to Percolator (Percolator-score-unique); unique to Rescore (Rescore-unique); present but not unique to Mascot (Mascot); present but not unique to Percolator (Percolator-score); present but not unique to Rescore (Rescore).

Following the prior realisation that using multiple search engines could improve PSM assignment, protein identifications using Mascot (which was further re-assessed using Percolator), Rescore and an independent Crux analysis were compared and contrasted. Using the example of H37Rv in Figure 3.16b, it was observed that although Rescore was superior in protein assignment, cumulative results from the 3 algorithms significantly increased the number of proteins.

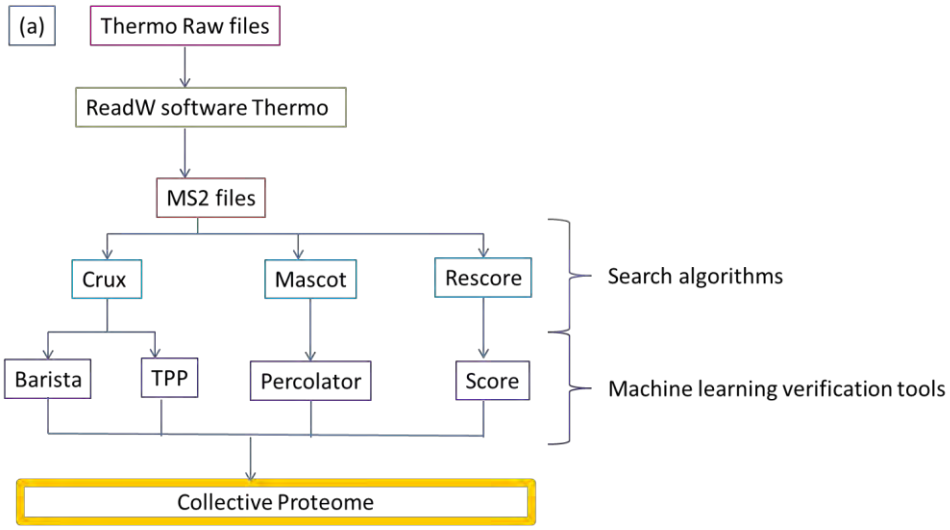

(b) H37Rv protein identifications using Rescore, Crux and Mascot

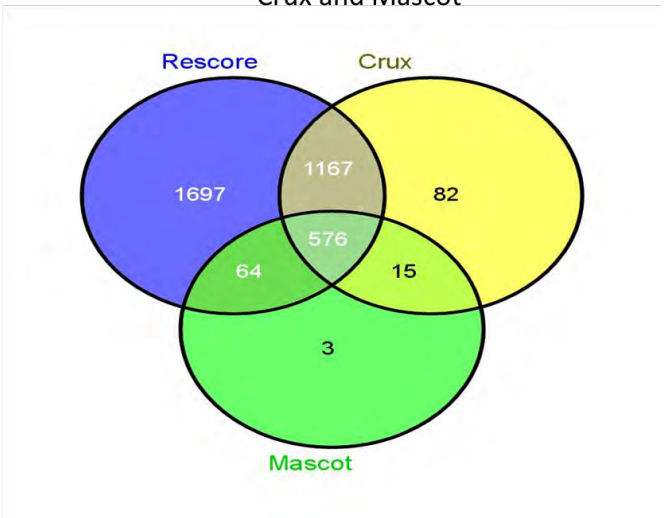

(c) Percentage proteome coverage per search engine (H37Rv)

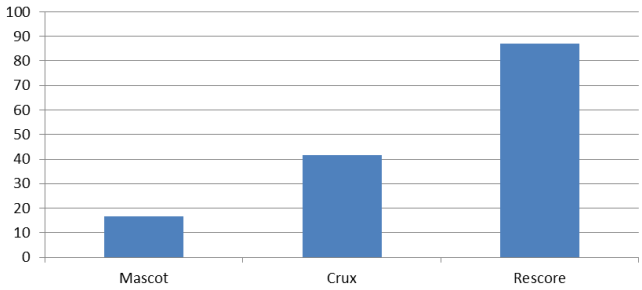

Figure 3.16: (a) Shows the bioinformatics analysis approach for protein analysis using work-flow 4 described in Figure 3.12 above. 3.13(b) Shows the comparison of non-redundant protein identifications between Mascot, Crux and Rescore database search engines. (c) Shows the percentage coverage of the experimental proteome compared to the theoretical proteome of *Mycobacterium tuberculosis* H37Rv at an FDR of 0.05.

Species	Number of spectra	Total # of PSMs	Total # of proteins
M. avium	103 379	18 674	4 250
M. bovis	128 874	19 394	3 461
M. bovis BCG	131 646	22 794	3 272
M. tuberculosis CAS	67 847	11 677	2 746
M. tuberculosis Beijing	107 887	23 674	3 224
M. tuberculosis LAM	103 826	24 013	3 500
M. tuberculosis H37Rv	100 604	24 712	3 604

Table 3.8: Total number of spectra, PSMs (below FDR 0.05) and proteins obtained using work-flow 4 to increase protein identifications.

Rescore shared half of the proteins identified with Crux whilst Mascot algorithm significantly trailed behind in the number of proteins identified. This may be because Mascot has been

previously been shown to be relatively ineffective in identifying high resolution MS2 spectra. From a total of 84 930 spectra, all search engines collectively identified 3 604 proteins in H37Rv meaning that roughly 90% of the theoretical *Mycobacterium tuberculosis* has been discovered using this approach. A comparison of all the methods discussed in this chapter for H37Rv as the representative strain is shown in figure 3.17 below.

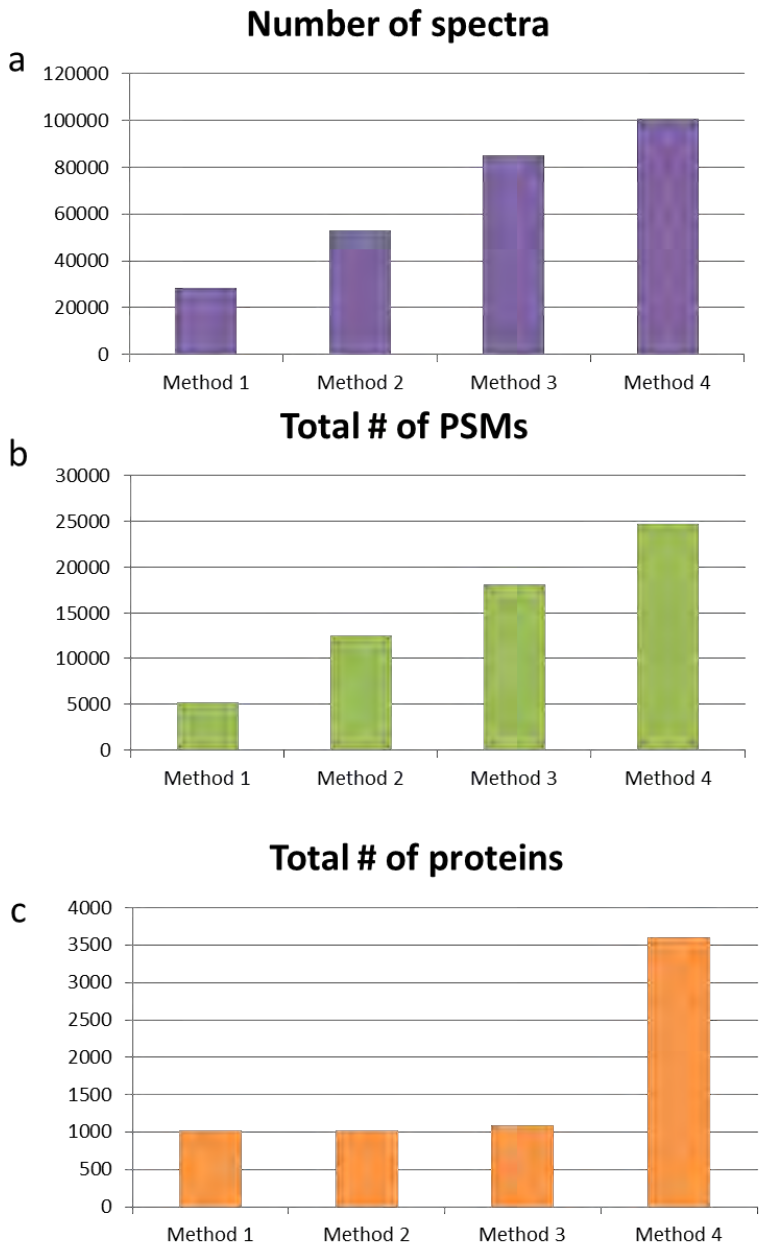

Figure 3.17: Histogram showing total number of spectra (a), PSM's (b) and proteins (c) obtained using each method described in this chapter using M. tuberculosis H37Rv results as a representative organism.

3.7 Conclusion

Analysis of denatured proteins of *Mycobacterium tuberculosis* by mass spectrometry requires simple conventional approaches to cell culture, protein extraction and peptide preparation. The simple rapid method of boiling the cell pellet in SDS based lysis buffer was sufficient to break open and release the entire complement of proteins from *M. tuberculosis* cells. It was observed that the cell culture system plays a role in the amount of protein yield obtained using mass spectrometry.

The use of commercial Middlebrook 7H9 broth supplemented with Albumin Dextrose Catalase (ADC) supplement resulted in fewer *M. tuberculosis* proteins being sampled and identified by mass spectrometry. This is due to the fact that there is a large amount of albumin in this media (5%) which results in the masking of the signal of low abundance proteins. The decreased identification of *M. tuberculosis* proteins is due to the data dependant sampling nature of discovery MS where peptide ions are picked based on intensity. The most intense ions are thus repeatedly picked for sampling which means that addition of large amounts of albumin over several orders of magnitude higher than the low abundance proteins of *M. tuberculosis* results in under-sampling of *M. tuberculosis* peptides. This method of protein extraction was not compared to mechanical shearing by glass beads for example which has been shown to be effective for the harvesting proteins. This is especially the case if intact proteins are required as it can break open the cells without having to denature the proteins. This was however not evaluated in this study as it was not necessary to obtain intact proteins since the proteins were subsequently going to be denatured and digested.

Apart from cell culture methods it was concluded that downstream processing of the protein post extraction determines the protein yield. It was observed that there is saturation in the number of proteins that can be found when analysing crude lysates regardless of MS instrument optimization or shrewd data analysis strategies. Pre-fractionation of proteins pre-MS was found to be expedient for increasing proteome coverage. Pre-fractionation divides the crude lysate into smaller groups of proteins with lower differences in concentration dynamic ranges. This results in the unmasking of more peptide ions to be sampled in each smaller group compared to when the sampling from one large undivided sample.

Sophisticated tools for MS spectral data interpretation also make a significant difference in the numbers of proteins identified. New improved algorithms are still being developed to interpret spectra form MS/MS experiments. The use of the newly developed Rescore database search

algorithm allowed the confident spectral assignment of over half of the proteins with PSM p-values below 0.05 that could not be assigned by other current algorithms within an acceptable threshold. Furthermore, combining results from multiple search engines increased the number of spectra interpreted and proteins identified in a dataset. This increases protein identifications by allowing protein identifications beyond the algorithm specifications of a single algorithm hence combining the power of multiple algorithms to interpret a single dataset.

For effective cross strain/species analysis, we consider proteome coverage of 90% to be adequate to identify authentic qualitative and quantitative differences rather than coincidental dissimilarities in the proteomes. The work described in this chapter has therefore established a variable approach to cell culture, protein extraction and preparation, tryptic digest, MS data analysis and capture as well as data interpretation that yields sufficient proteome coverage to carry out efficient cross species comparison, as required in subsequent chapters in this thesis.

Chapter 4: Defining core-proteomes of the *Mycobacterium tuberculosis* complex

4.1 Introduction

The genus *Mycobacterium* can be broadly divided into 2 groups. The first group, coined the *Mycobacterium tuberculosis* complex (MTBC), comprises of the classical human and animal pathogens namely *M. tuberculosis, M. africanum, M. microti, M. bovis, M. caprae* and *M. pinnipedii*. Although divided into over a thousand strains, members of the MTBC exhibit 99.9% identity at the genetic level [265]. The second group comprises of Mycobacterial species that are common in the environment and which are normally termed non tuberculous mycobacteria (NTM). Although they are generally dubbed "friendly bacteria", some NTMs have been implicated in human and animal disease [266–270].

Tuberculosis, caused by the bacterium *Mycobacterium tuberculosis*, remains one of the leading causes of death by a single pathogen worldwide. Despite the presence of a vaccine and a number of antibiotics for the disease, it continues to cause about 2 million deaths worldwide and 8 million new cases per year [271]. The emergence of multiple and extensively drug resistant strains, together with co-infection with HIV, are fuelling the pandemic, especially in developing countries.

HIV infection plays a pivotal role in the development of tuberculosis-like infection from individuals infected with NTM. The most common opportunistic infections causing tuberculosis like symptoms in HIV positive individuals are from the *Mycobacterium avium* complex, closely followed by *Mycobacterium kansasii* [31,33,34]. Out of all the NTM's, these two groups raise major concern because the tuberculosis-like infection caused by these organisms is not distinguishable from that caused by *M. tuberculosis* in HIV positive individuals using standard smear microscopy as the method of diagnosis [269,272]. In some countries infection with NTM automatically warrants treatment in immunocompromised individuals with 3 drugs which must include rifampicin [273,274]. Importantly, these clinical observations demonstrate *M. avium* is also pathogenic, suggesting that a comparative "omics" study might shed light on the molecular basis of Mycobacterial pathogenesis.

Genome sequencing projects have been completed for a number of species within the *Mycobacterium* genus including several strains of the MTBC as well as NTM such as *M.*

avium. However, many of the attributes contributing to the success of pathogens of the genus *Mycobacterium* remain a mystery.

Whilst genetic variation has been immensely studied, the clinical and epidemiological consequences of infection remain poorly understood [239]. These aspects are most likely driven by other molecular markers apart from the genome, such as the expressed proteome. It has also been observed that there is a poor correlation between the transcriptome and the proteome [275–278]. Furthermore, the transcriptome does not tell anything about post translational modifications (PTM) which play an important role in determining whether or not certain proteins are functional [279–281]. Thus while the genome and transcriptome have been studied, it is necessary to carry out a study on the proteome as it is the final product of the genome. The proteome is the entire complement of proteins produced by a cell from the translation of the protein coding region of the genome under the specific conditions that it inhabits. The biological significance of the proteome is paramount since it drives all processes from replication transcription to translation. A snapshot of exactly what a cell is undertaking can in principle be inferred directly from the expressed proteome, which makes it a useful map to study when attempting to determine phenotypic differences amongst closely related genomes.

Here, shotgun proteomic approaches were used to compare and contrast the total proteomic complements of 6 members of the MTBC and *M. avium*. The overall objective of the study was to define the core proteome expressed by different members of the MTBC under optimal conditions and to subsequently determine how the core-proteome changes when *M. avium,* a major pathogenic NTM that is genetically distant from the MTBC is added to the comparison.

The clinical parallels that exist between HIV infected individuals who are co-infected with either members of the *M. avium* complex (MAC) or MTBC suggest that molecular similarities at the expressed proteome level exist between these two groups that may define at least in part general mycobacteria-centric pathogenesis. Furthermore, the difference between the core proteomes expressed by these organisms may identify the *in vitro* expressed proteome that is exclusive to MTBC pathogenesis and could therefore possibly uncover new biomarkers for strictly *M. tuberculosis* infection. Their expression may however be host-pathogen dependant hence it would be ideal to assess these proteins at the site of disease.

4.2 Materials and methods

4.2.1 Bacterial Strains

Mycobacterium tuberculosis isolates H37Rv, W-Beijing, CAS and LAM3 were obtained from the Medical Microbiology Division of the University of Cape Town. The clinical strains representing lineages 2 (Beijing), 3(CAS) and 4(LAM3/F11) were isolated from paediatric patients from across Cape Town in Red Cross war memorial hospital. *Mycobacterium tuberculosis* H37Rv was used in all assays as a reference strain. Phylogeny of the isolates was determined using spoligotyping and MIRU-VNTR described in Sarkar *et al*, 2012 and determined as follows:

	Spoligotype	MIRU-VNTR	Lineage
H37Rv	777777477760771	243132253233552	Lineage 4 (Laboratory strain)
W-Beijing	000000000003771	442335464485372	Lineage 2 (clinical strain)
CAS 1	702777740003771	4423664??285373	Lineage 3 (clinical strain)
LAM3/F11	774377007760771	442365542253173	Lineage 4 (clinical strain)

Table 4.1: Genotype of selected *Mycobacterium tuberculosis* strains. Spoligotyping octal codes and MIRU-VNTR numbers for the strains under investigation in the study adapted from Sarkar et al [282].

The Danish strain of *Mycobacterium bovis* BCG was used in this study. The *M. avium* strain was obtained from the National Health Laboratory Services (NHLS) laboratory and was verified using line probe assays. *M. bovis* was obtained from Stellenbosch University Biomedical Sciences Department in Tygerberg Hospital, Cape Town.

4.2.2 Cell culture

Cells were maintained in wholly synthetic Sautons media (2% glycerol, 0.4% L-asparagine, 0.2% glucose, 0.2% citric acid, 0.05% mono-potassium phosphate, 0.05% magnesium sulphate, 0.015% Tween 80, 0.005% ferric citrate, 0.00001% zinc sulphate at pH 7.4). Briefly, 190 ml of Sautons medium was inoculated with a 10ml starter culture (approximately 10^8 bacteria/ml). The flasks were sealed and incubated at 37°C and 5% CO_2 with gentle agitation until OD_{600} reached 0.9 (approximately 6 weeks).

4.2.3 Protein extraction

Proteins were extracted in a Biosafety level 3 facilities in line with health and safety guidelines. Briefly, the cell pellet was separated from the culture filtrate by centrifugation at 4 000 g for 15

minutes in a bench-top centrifuge. After partition, both culture filtrate and cell pellet were kept for further analyses. Cell lysis was carried out by boiling the cell pellet in 1% SDS buffer (1% SDS, 100 mM Tris-Cl pH 7.6, 0.1 mM dithiothreitol (DTT), 1 mM PMSF) for 30 minutes. Cell debris was separated from the protein containing supernatant by centrifugation at 10,000 g for 15 minutes in a bench top centrifuge and the supernatant containing the protein was transferred into a clean tube. Protein extracts from cell lysates were concentrated and buffer exchanged to 2 M urea buffer using 3kDa MWCO filters (Millipore). Culture filtrate proteins were concentrated and buffer exchanged into 2 M urea using 15 ml 10 kDa MWCO filters. A 10 kDA filter was used for the filtrate because at the time, this was the smallest cut-off filter that was available for filtering large volumes. The 3 kDa cut-off filter was only available for volumes up to 500µl which was not quite possible for the large volumes of culture filtrate. However, according to manufacturer's product specifications (Millipore), proteins as low as 3 kDa are still retained on 10 kDa MWCO filters. Protein concentration was determined using the BCA assay kit (Thermo Scientific).

4.2.4 Protein separation (1D SDS PAGE)

Proteins were separated according to molecular weight using an SDS PAGE gel system. The separating gels were made from 40% of acrylamide: bis-acrylamide, 0.375 M Tris-Cl (pH 8.8), 7.5% SDS, 0.5% ammonium persulphate and 0.1% TEMED. The stacking gels consisted of 4% acrylamide: bis-acrylamide, 0.125M Tris-Cl (pH 6.8), 0.1% SDS, 0.5% ammonium persulphate and 0.1% TEMED. 40 µg of each sample (culture filtrate and intracellular protein) was mixed with an equal volume of 2x sample buffer and heated at 65ºC for 5 minutes. Electrophoresis was performed from anode to cathode at 100 V using a BioRad mini-Protean II gel system until the bromophenol blue dye reached the bottom of the gel.

4.2.5 Visualization of the protein

Visualization of the proteins on the gel was performed using Coomasie brilliant blue R250 for 1 hour (50% methanol, 10% acetic acid and 0.1% Coomasie brilliant blue R250). Destaining of the gels was carried out by incubating on a shaker overnight at room temperature in destaining solution (10% methanol, 10% acetic acid).

4.2.6 In gel trypsin digestion

Each gel lane for each strain sample was divided into 5 pieces (i.e. 5 culture filtrate fractions and 5 intracellular protein fractions hence a total of 10 fractions per strain). Each gel piece was

cut into smaller cubes and washed twice with water followed by 50% (v/v) acetonitrile for 10 minutes. The acetonitrile was replaced with 50 mM ammonium bicarbonate and incubated for 10 minutes. Washing with 50 mM ammonium bicarbonate was repeated twice to remove acetonitrile. All the gel pieces were then incubated in 100% acetonitrile until they turned white, after which the gel pieces were dried *in vacuo*. Proteins were reduced with 10 mM DTT for 1 h at 57 °C. This was followed by brief washing steps of ammonium bicarbonate followed by 50% acetonitrile before proteins were alkylated with 55 mM iodoacetamide for 1 h in the dark.

Following alkylation, the gel slices were washed with ammonium bicarbonate for 10 min followed by 50% acetonitrile for 20 minutes, before being dried *in vacuo*. The proteins in the gel cubes were digested with trypsin (Promega) at 37^0C overnight in a 1:50 trypsin: protein ratio. The resulting peptides were extracted twice with 70% acetonitrile in 0.1% formic acid for 30 minutes and then dried and stored at -20^0C. Dried peptides were dissolved in 5% acetonitrile in 0.1% formic acid and 10 µl injections were made for nano-LC chromatography.

4.2.7 Mass spectrometry

All experiments were performed on a Thermo Scientific EASY-nLC II connected to a LTQ Orbitrap Velos mass spectrometer (Thermo Scientific, Bremen, Germany) equipped with a nano-electrospray source. For liquid chromatography, separation was performed on a EASY-Column (2 cm, ID 100 µm, 5 µm, C18) pre-column followed by a EASY-column (10 cm, ID 75 µm, 3 µm, C18) column with a flow rate of 300 nl/min. The gradient used was from 5-15 % B in 5 minutes, 15-35% B in 90 minutes, 35-60% B in 10 minutes, 60-80% B in 5 minutes and kept at 80% B for 10 minutes. Solvent A was 100% water in 0.1 % formic acid; solvent B was 100 % acetonitrile in 0.1% formic acid. MS/MS data was acquired from the Orbitrap Velos in Top 20 CID mode by Dr Salome Smit (University of Stellenbosch).

4.2.8 Post MS Data analysis

Raw data was captured from the mass spectrometer and converted to MS2 files using MakeMS2 software (Thermo Scientific). The data was then analysed using multiple search engines as shown in Figure 3.16a (Chapter 3). Spectra were obtained from each fraction of the gel (a total of 10 fractions per strain) and were viewed using Peaks v5.3 [200]. Representative MS and MS/MS spectra obtained from H37Rv CF fraction 1 as shown in Figure 4.1a below indicating that tryptic digest was efficient with peptides eluting across the 120 minutes gradient with high intensity. Representative detailed MS/MS spectra identifying the peptide sequences

of GroEL2 and KatG per clinical strain showing the best scoring peptide per strain, the sequence of the peptide, the b and y ions that were observed and the charge state of each peptide as shown in Figure 4.1b below.

a (i)

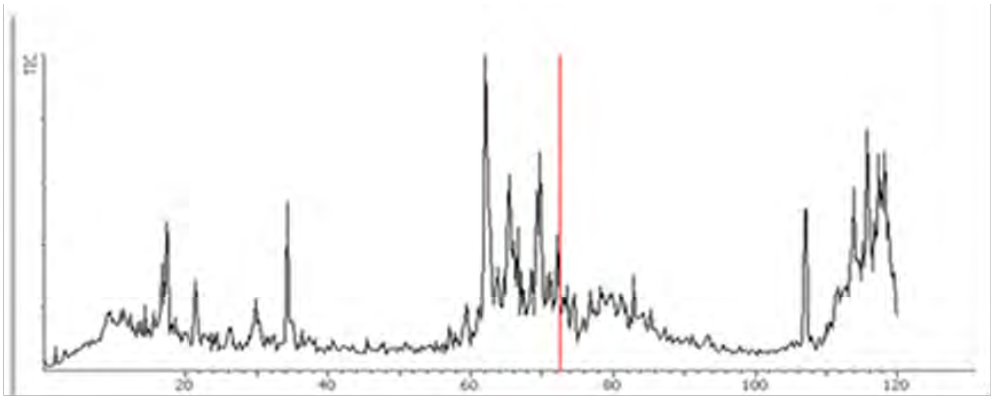

a (ii)

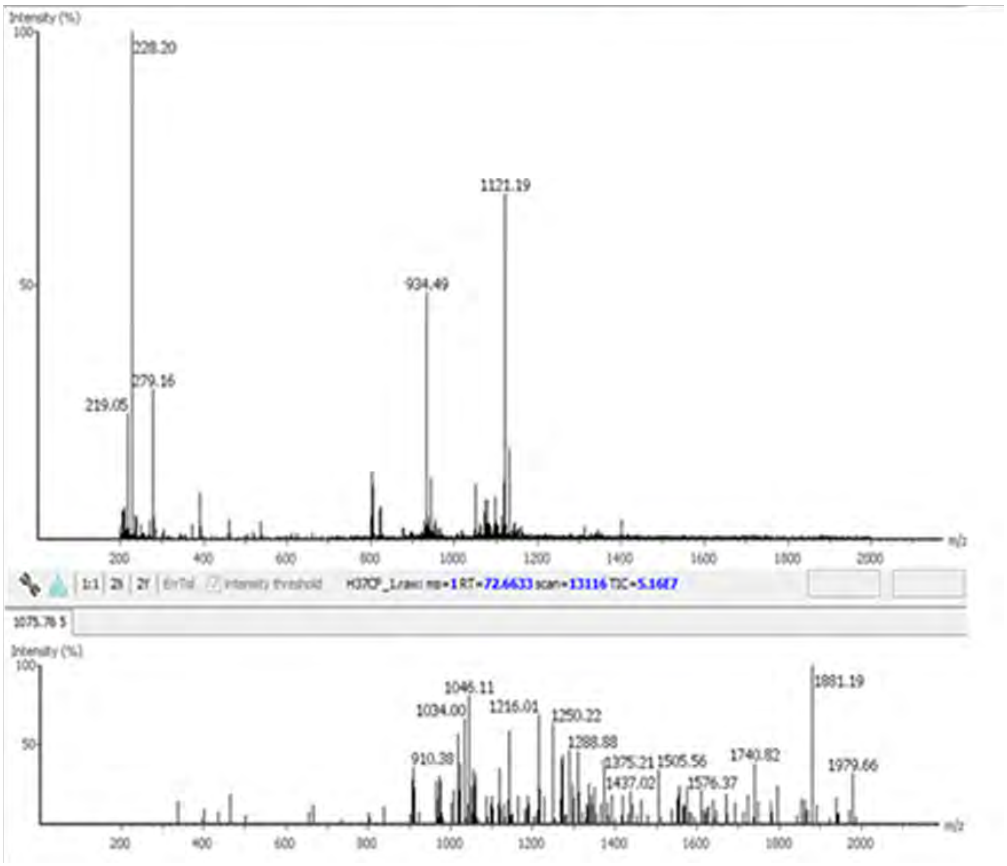

Figure 4.1: (a) Shows the TIC for H37Rv CF fraction 1. The red line on the MS1 marks the elution time point which is inflated in the stacked panels on the left show the complexity of the sample at that specific time point.

b (i)

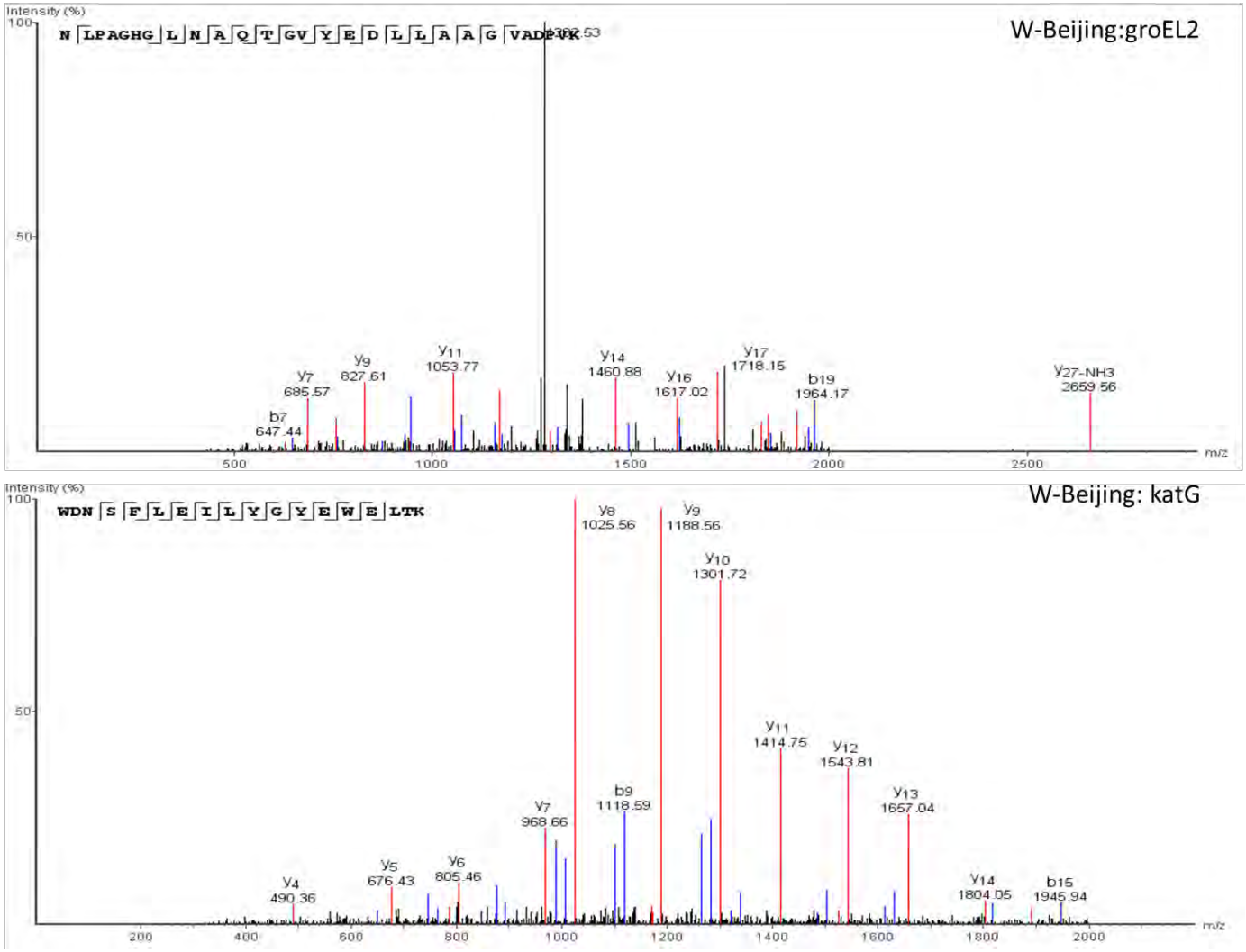
Intensity (%)
100
50
N L P A G H G L N A Q T G V Y E D L L A A G V A D P V K
W-Beijing:groEL2
y9 827.61
y11 1053.77
y14 1460.88
y16 1617.02
y17 1718.15
b19 1964.17
y27-NH3 2659.56
y7 685.57
b7 647.44
500
1000
1500
2000
2500
m/z
Intensity (%)
100
50
W D N S F L E I L Y G Y E W E L T K
W-Beijing: katG
y8 1025.56
y9 1188.56
y10 1301.72
y11 1414.75
y12 1543.81
y13 1657.04
b9 1118.59
y7 968.66
y5 676.43
y6 805.46
y4 490.36
y14 1804.05
b15 1945.94
200
400
600
800
1000
1200
1400
1600
1800
2000
m/z

b (ii)

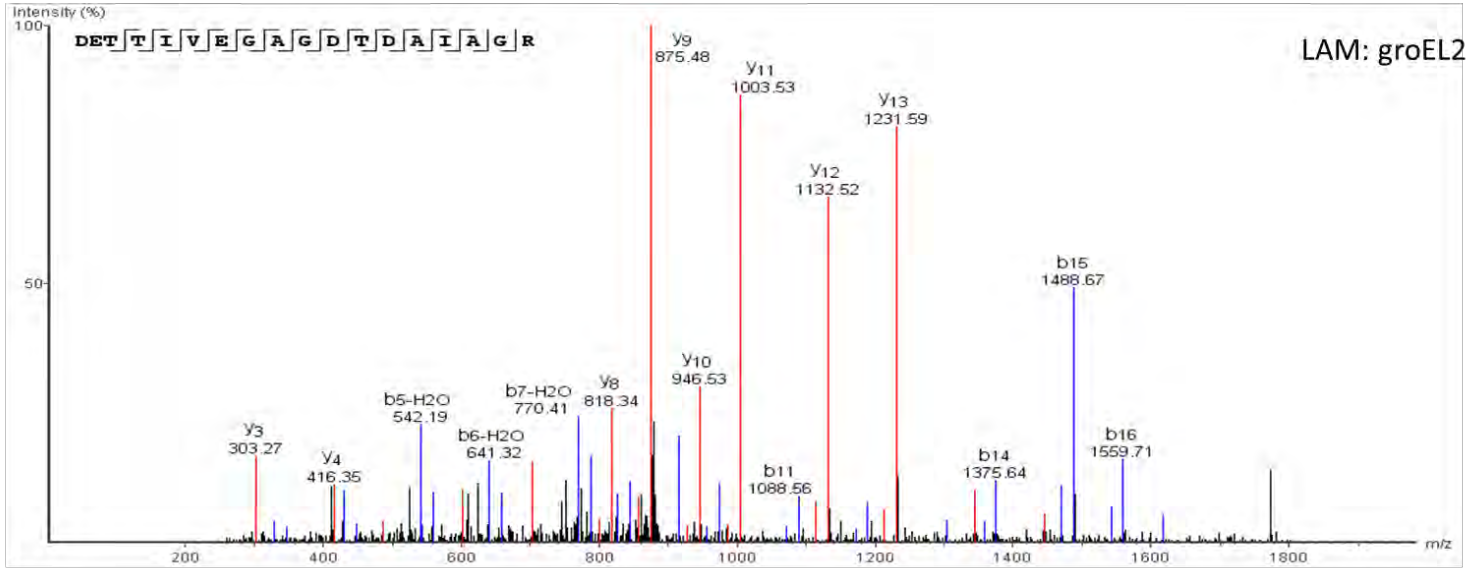
Intensity (%)
DETTIVEGAGDTDAIAGR
LAM: groEL2
y9 875.48
y11 1003.53
y13 1231.59
y12 1132.52
b15 1488.67
y10 946.53
b5-H2O 542.19
b7-H2O 770.41
y8 818.34
y3 303.27
b6-H2O 641.32
y4 416.35
b11 1088.56
b14 1375.64
b16 1559.71
m/z

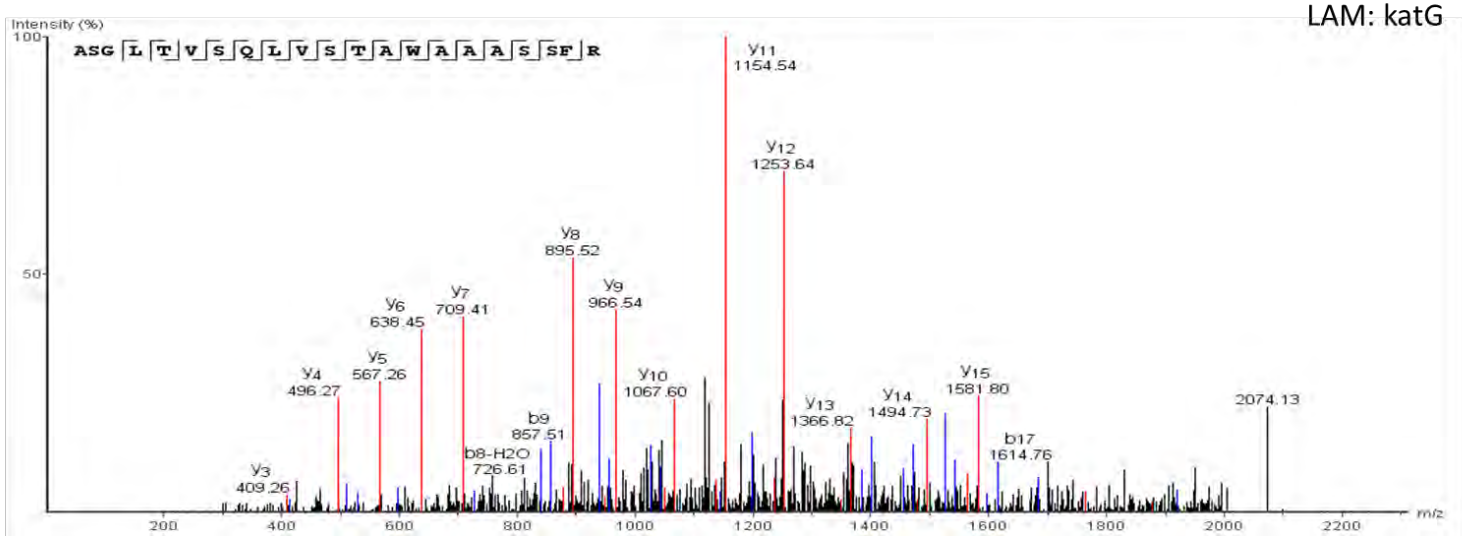
Intensity (%)
ASGLTVSQLVSTAWAAASSFR
LAM: katG
y11 1154.54
y12 1253.64
y8 895.52
y9 966.54
y7 709.41
y6 638.45
y5 567.26
y4 496.27
y10 1067.60
y15 1581.80
y13 1366.82
y14 1494.73
2074.13
b9 857.51
b17 1614.76
b8-H2O 726.61
y3 409.26
m/z

b (iii)

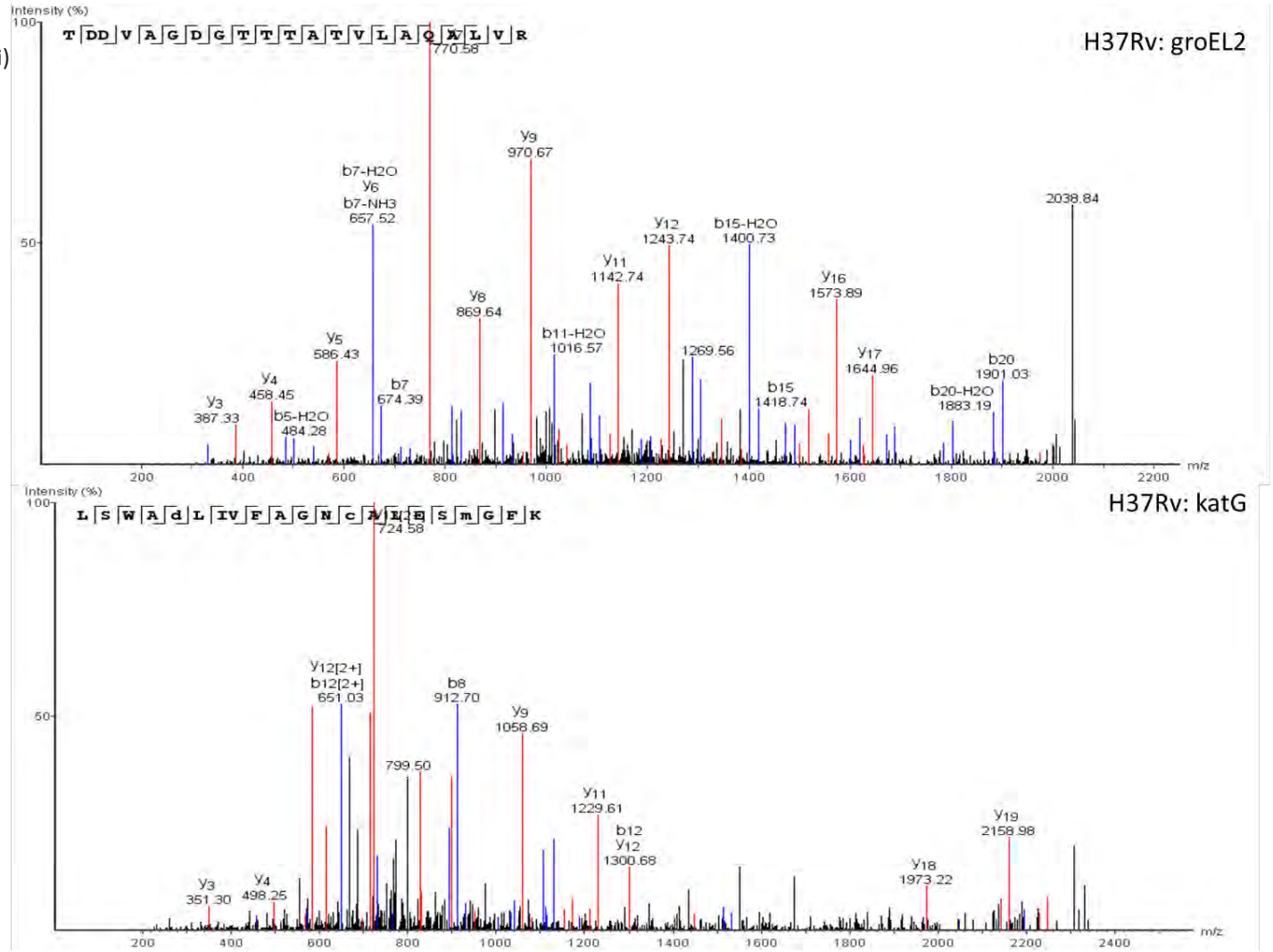
Intensity (%)
T DD V A G D G T T T A T V L A Q K L V R
H37Rv: groEL2
770.58
y9 970.67
b7-H2O y6
b7-NH3 657.52
y12 1243.74
b15-H2O 1400.73
2038.84
y11 1142.74
y16 1573.89
y8 869.64
y5 586.43
b11-H2O 1016.57
1269.56
y17 1644.96
b20 1901.03
y4 458.45
b7 674.39
b15 1418.74
y3 387.33
b5-H2O 484.28
b20-H2O 1883.19
m/z
Intensity (%)
L S W A d L IV F A G N C A IL E S m G F K
H37Rv: katG
724.58
y12[2+] b12[2+] 651.03
b8 912.70
y9 1058.69
799.50
y11 1229.61
y19 2158.98
b12 y12 1300.68
y18 1973.22
y3 351.30
y4 498.25
m/z

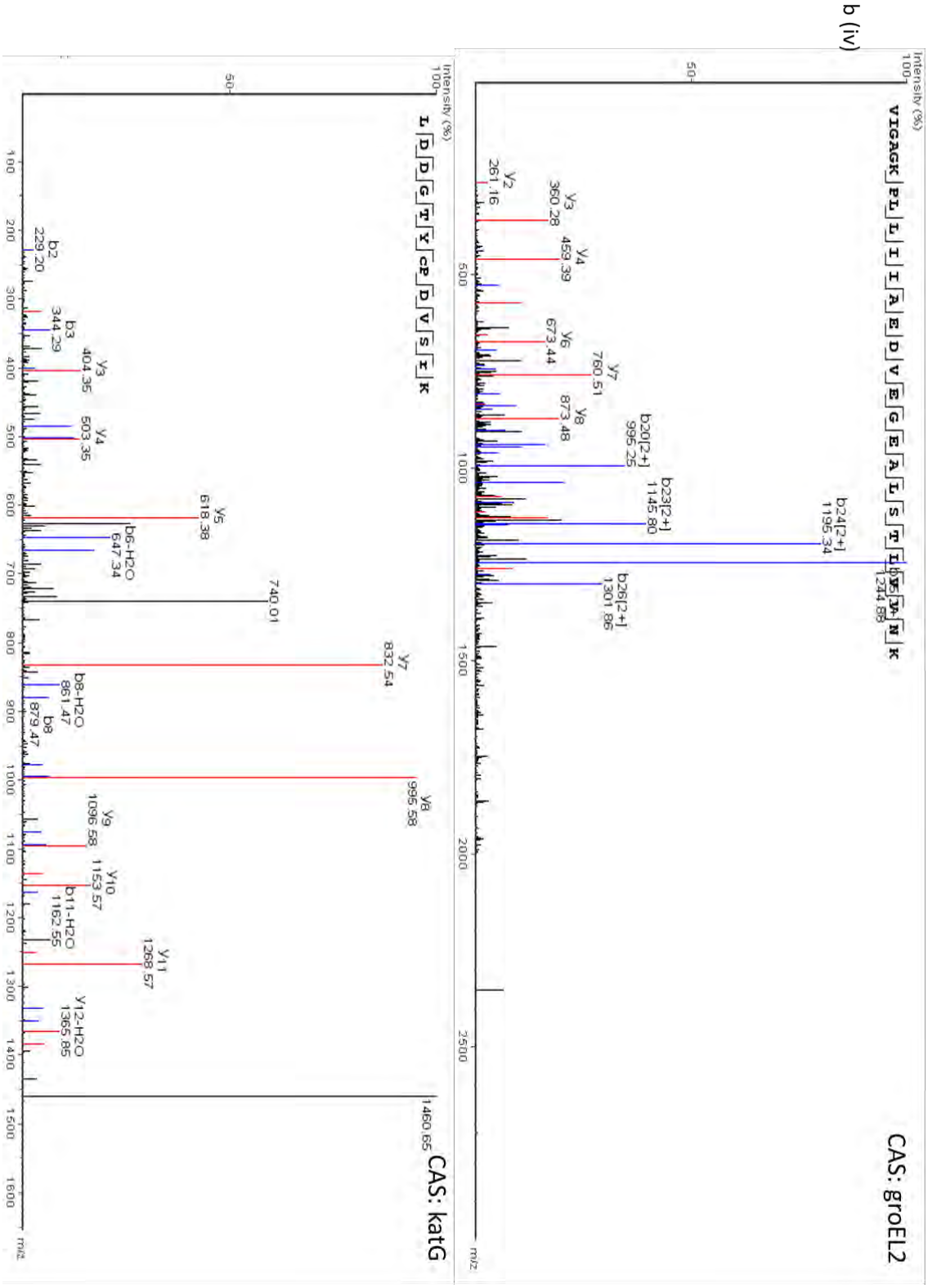

Figure 4 (b): The chromatogram shows the fragmentation MS/MS spectra of GroEL2 and KatG from *M. tuberculosis* W-Beijing; b (i), LAM; b (ii), H37Rv; b (iii) and CAS; b (iv) showing the best scoring peptide of each protein for each strain.

Raw MS/MS spectra were converted to MS2 format prior to analysis using ReadW software (Thermo Scientific). Initially Crux database [198] search engine was used as the computational

program to interpret the MS/MS spectra. Crux basically utilizes similar algorithms to Sequest [202] for peptide matching and scoring, but has decreased peptide candidate retrieval time and better back-end statistics to estimate the false discovery rates. Crux uses on-the-fly decoy databases to evaluate the statistical significance of a Peptide Spectral Match (PSM). The decoy databases of each fasta file are created by shuffling the target peptides, ensuring that each decoy peptide has the same amino acid composition and total mass as the corresponding target peptide.

The False Discovery Rate (FDR) is then estimated based on the decoy PSMs and the q-value that is reported for each PSM. Q-value is a statistical confidence measure that is analogous to p-value but incorporates an element of multiple testing. Unlike p-value, q-values uses decoy datasets to incorporate FDR [208]. Q-value is the minimum FDR at which a score is deemed significant. The FDR is defined as the expected value of the number of false positive features over the number of all expected features associated with a particular q-value. Crux database search engine results were further refined using Barista within Crux and using Trans-Proteomic Pipeline's (TPP) Peptide Prophet, Protein Prophet and iProphet algorithm [214].

The data was also independently searched using a novel search engine Rescore. Rescore is a two-stage machine-learning based peptide to spectrum match (PSM) re-scoring engine. The first stage of Rescore consists of a Random Forest predictor of fragment ion intensity that takes as input a peptide sequence and which produces a theoretical fragmentation spectrum with singly and doubly charged fragment ions, all with their own predicted absolute intensity. The second stage of Rescore then provides a new score for PSMs provided by a classical search engine such as Mascot, by employing a Percolator-like re-analysis (again, using Random Forest) of features calculated for target and decoy hits.

Differently from current algorithms, including Percolator, Rescore takes into account deviations between the measured and predicted peak intensities (as obtained from the first stage of Rescore). Hence Rescore searches come with internal mascot and percolator searches. Due to the inclusion of this second dimension of predicted peak intensity information from the spectrum, Rescore provides more discriminative scores and better overall reproducibility across runs. Rescore uses a double decoy strategy to assess its FDR. It uses one decoy to train the score on, and another independent decoy to assess the score. By so doing, it ensures that true hits are truly separated from false positives.

The protein databases used to generate theoretical spectra were strain specific individual non-redundant fasta files from Ensembl (www.ensembl.org), with the exception of LAM for which there is no Ensembl annotation, and W-Beijing whose annotated file is not sufficient for downstream cross strain comparison. For LAM, the UniProt fasta file was used (www.uniprot.org) and for W-Beijing, the H37Rv Ensembl fasta file was used. The parameters were standard across both searches and included carbamidomethylation of cysteine residues as a fixed modification whilst oxidation of methionine residues was set as a variable modification. Two missed cleavages were allowed and peptide mass tolerance was set at 10 ppm whilst fragment mass tolerance was set to 0.5 Da. Decoy databases were used for FDR analysis and a cut-off was set at 5% for protein identifications.

4.3 Results and Discussion

Effective analysis of MS data still presents a significant bottleneck in the workflow of high throughput proteomics data ad more efficient and accurate methods are still being sought out that are able to correctly map as many of the MS spectra as possible [198,209]. Various search engines are available for assignment of MS/MS spectra to the theoretical proteome. Each search algorithm is equipped with different statistical analysis tools that allow different statistical models to be applied to MS/MS data searching [198,203,204,208]

Due to differences in statistical model approaches, search algorithms are bound to give variable results for the same MS/MS query dataset. Each search engine will only identify a subset of the MS/MS dataset that lies within the confines of its statistical model. Overlap in PSMs and or proteins identified will exist between different search algorithms, yet some PSMs will only be identified by one search engine not another. Since search engines have different capacities, a researcher may ask the question how to utilize this to maximize PSM assignment in a MS/MS dataset.

In this study, tens of thousands of peptide obtained after trypsin digestion were processed by MS to produce unique spectra. Experimental and theoretical spectra generated *in silico* from the non-redundant Ensembl proteome fasta files were matched using the database search algorithm pipeline shown in Figure 4.1 to produce a list of the best matching spectra, referred to as peptide spectral matches (PSMs). The spectral matches were verified by using machine learning algorithms, as depicted in Figure 3.16a.

4.3.1 Protein inference

The PSMs obtained from the search were used to predict the expressed protein repertoire of each sample. Briefly, the MS/MS spectra from the ten fractions per strain were searched with each individual search engine. Performance of the search engines at the protein level was compared (Figure 4.2a) and the assessment showed that Rescore was capable of identifying more proteins than Mascot or Crux by a factor of 2. Having previously established that combining results from multiple search engines yields higher protein identifications [256], all the proteins identified from each individual search engine were combined and redundancy was removed to give one complete non-redundant dataset per study organism (Figure 4.2c).

Comparison of protein numbers obtained at 1% and 5% FDR showed that the use of 5% FDR allows a substantial increase in the number of true positives with an insignificant increase in the number of false positives, hence providing a favourable trade-off in true positives/matches over false positives/matches (Figure 4.2b). The final proteome obtained from each strain using all algorithms represented approximately $^{3}/_{4}$ of each of the theoretical protein fasta files, as seen in Figure 4.2c below and Table 4.2.

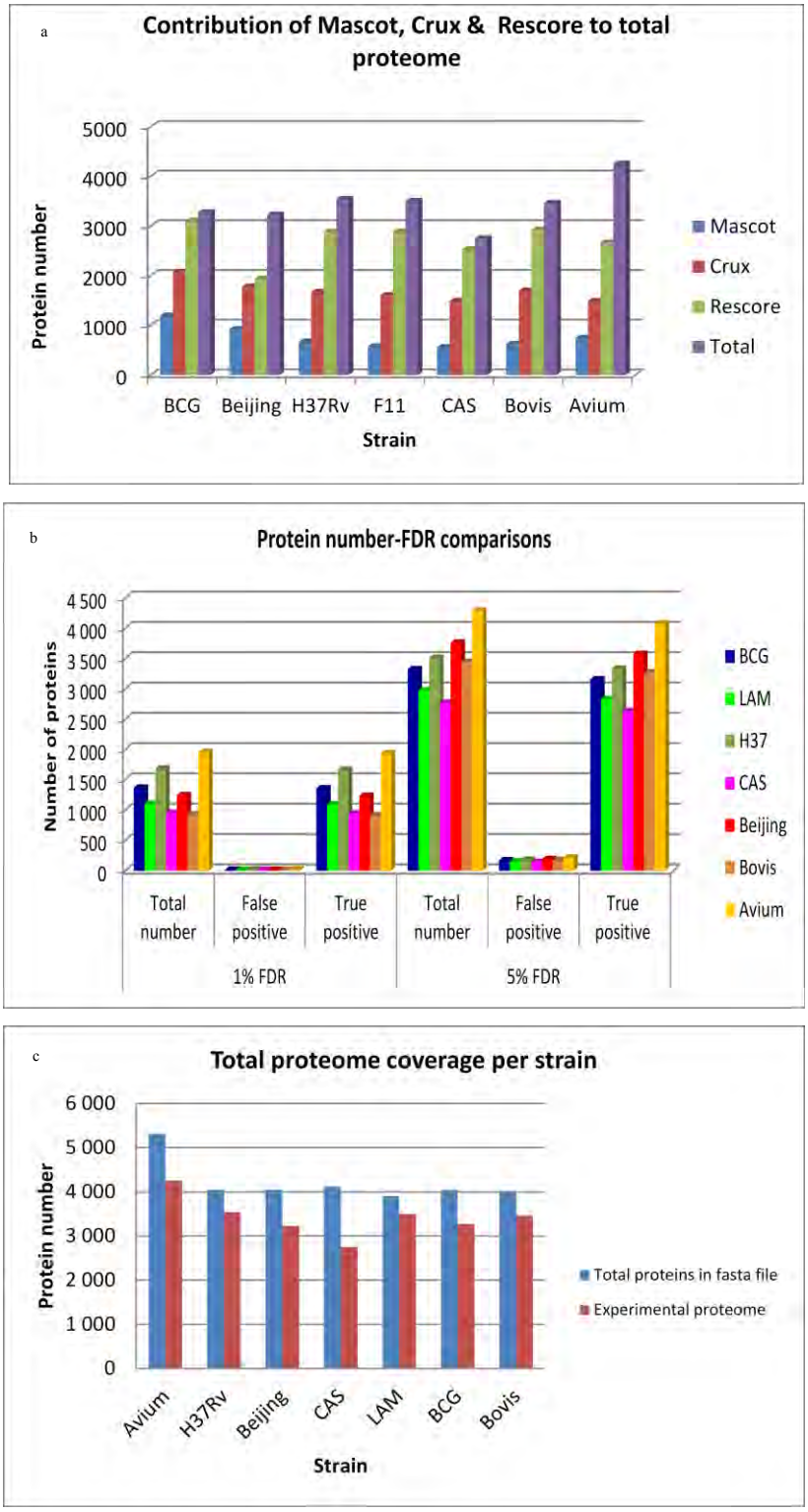

Figure 4.2: (a) shows the contribution of each of the search engines to the total number of non-redundant proteins obtained per strain at 5% FDR. Mascot is shown in blue bars, Crux is shown in red bars, Rescore is shown in green bars and the total no-redundant is shown in purple bars. (b) shows the comparison of 1% and 5% FDR across all strains, illustrating that the total number of proteins obtained for each strain at 1% FDR and the proportion of true and false positives in that FDR bracket and contrasting it to those obtained at 5% FDR bracket for each strain. (c) shows the experimental proteome (red bars) coverage per strain in comparison to the theoretical proteome (blue bars) for each strain.

Strain	Total # proteins in fasta file	Total # found in experiment	Percent coverage
M. avium	5 314	4 250	80
M. tuberculosis H37Rv	4 049	3 539	87
M. tuberculosis Beijing	4 049	3 224	80
M. tuberculosis CAS	4 049	2 746	68
M. tuberculosis LAM	3 904	3 500	89
M. bovis BCG	4 041	3 272	81
M bovis	4 001	3 461	86

Table 4.2: Total non-redundant number of proteins obtained in the experiment compared to the total number of proteins in the theoretical fasta file

4.3.2 Data alignment for downstream processing

To carry out an effective cross strain comparison, it was crucial to ensure that as much of the theoretical proteome as possible was covered in order to ensure that observed differences between the proteome are real rather than being artefacts of differential sampling or analysis in the discovery experiment. After obtaining a non-redundant dataset for each strain using strain specific databases, it became necessary to convert all the protein IDs into a standard protein ID by orthology mapping to allow comparison to take place effectively.

To do this, the total non-redundant IDs from each strain obtained by searching against its individual Ensembl fasta file was mapped back to the Ensembl H37Rv IDs. These were all in turn mapped to UniProt accession numbers and Tuberculist 'Rv' loci numbers as most downstream analysis tools such as GO analysis and pathway mapping use UniProt or Rv identifiers. It was observed that there is a slight deficiency in ortholog mapping data between databases (Ensembl and UniProt) as well as shortcomings in ortholog mapping between strains. These discrepancies lead to a slight loss of information as seen in Figure 4.3 below.

It was observed that the discrepancy in ortholog mapping was much more pronounced when mapping protein IDs to H37Rv from *M. avium,* which lies outside the MTBC group, with approximately 50% of the biological information lost in ortholog mapping *M. avium* as seen in Figure 4.3 below. This data is consistent with a concurrent bioinformatics analysis that shows that whilst *M. tuberculosis* isolates share 99% peptide identity amongst each other, *M. avium* shares only approximately 11% of its peptide repertoire identically with *M. tuberculosis,* with only approximately half its proteome being ortholog mapped to H37Rv (Table 4.3).

The observation immediately implies challenges in the comparison of experimental proteomes of MTBC strains and any other mycobacteria regardless of clinical similarities, and also sets an upper limit to the number of proteins that can be directly compared between members of the MTBC and *M. avium*, as seen in the Table 4.3 below where a maximum of approximately 2700 *M. avium* proteins have known orthologs in members of the MTBC. In contrast MTBC members share more than 3800 orthologous proteins amongst each other. This also suggests that cross species database searching as might be required in the absence of an annotated genome sequence can be used to search spectra within the MTBC with minimal loss of information, but that does not apply outside the MTBC boundary.

Species	Peptides	Other species	Orth Prot	Shared Pep	FP	FFP
M. avium	95 956	M. bovis	2 677	11 172	942	101
		M. bovis BCG	2 671	11 163	965	90
		M. tb H37Rv	2 701	11 256	952	101
		M. tb KZN	2 709	11 240	965	99
		M. leprae	1 381	5 938	423	66
		M. marinum	3 354	13 132	1 207	102
		M. smegmatis	3 184	8 166	1 632	50
		M. ulcerans	2 897	10 947	918	108
		M. paratuberculosis	4 005	67 748	791	35
M. bovis	75 469	M. bovis BCG	3 837	73 952	114	13
		M. tb H37Rv	3 825	72 864	201	44
		M. tb KZN	3 776	71 738	251	49
		M. leprae	1 419	6 638	333	73
		M. marinum	3 127	22 644	879	81
		M. smegmatis	2 576	6 691	1 375	107
		M. ulcerans	2 755	19 873	671	113
M. bovis BCG	75 307	M. tb H37Rv	3 774	72 547	2 760	273
		M. tb KZN	3 750	71 521	327	68
		M. leprae	1 413	6 638	330	163
		M. marinum	3 103	24 082	868	223
		M. smegmatis	2 568	6 684	1 373	160
		M. ulcerans	2 747	19 877	660	199
M. tb H37Rv	76 514	M. tb KZN	3 847	74 238	62	6
		M. leprae	1 419	6 647	345	73
		M. marinum	3 158	25 110	887	81
		M. smegmatis	2 600	6 728	1 392	99
		M. ulcerans	2 771	19 266	675	16

Table 4.3: Theoretical analysis of complete proteome fasts files comparing shared peptides and orthologous proteins. Number of identical peptides (Shared Pep) and orthologous proteins (Orth Prot) shared for each pairwise comparison is shown. The analysis takes into account the false positive (FP) which is the number of shared peptides between non-orthologous proteins and the false false positive,

(FFP) which is the number of identical peptides shared between two proteins are not annotated as orthologues but possibly are [283].

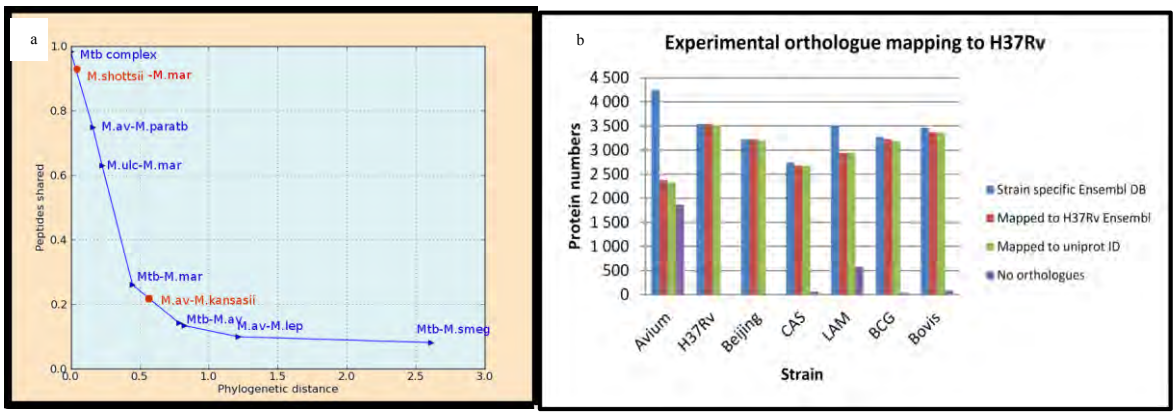

Figure 4.3: (a) The line graph depicts the phylogenetic distance of the stated pairwise comparisons as a function of shared peptides. An inverse relationship exists between the phylogenetic distance and the number of shared peptides per any pairwise comparison. [283] (b) The bar graph shows data mapping of the experimentally obtained proteins to *M. tuberculosis* H37Rv ID's for downstream analysis. The blue bars represent the strain specific IDs that were obtained using database searching with Ensembl fasta files. The red bars represent the strain specific Ensembl IDs that were orthologue mapped to Ensembl H37Rv IDs. The green bars represent the H37Rv Ensembl IDs that were mapped to UniProt ID's for downstream analysis. The purple bars indicate those with no annotated orthologues between the original strain specific Ensembl fasta file and the H37Rv Ensembl fasta.

4.3.3 Qualitative cross species comparison

With congruent IDs, strains could now be cross-compared to give a comprehensive qualitative comparison as summarised in Figure 4.4 below using Venny [284]. Protein IDs from the 4 strictly *Mycobacterium tuberculosis* strains were compared and, as expected, the majority of proteins were found to be shared amongst all strains, with less than 5% being strain specific (Figure 4.4). A total of 1938 proteins comprise the shared proteins among the 4 *M. tuberculosis* strains which will be further referred to as the *M. tuberculosis* core proteome. The 1938 proteins were mapped into 1 272 H37Rv identifiers (Annexure Table 4.1). This data was obtained using a cut-off of at least 2 peptides per protein with at least one of the peptides being identified with a FDR of 0.01. The remainder of the peptides could have been identified with a higher FDR, however, at least one had to be identified with high confidence. Increasing the number of peptides required to identify a protein would decrease the number of proteins identified.

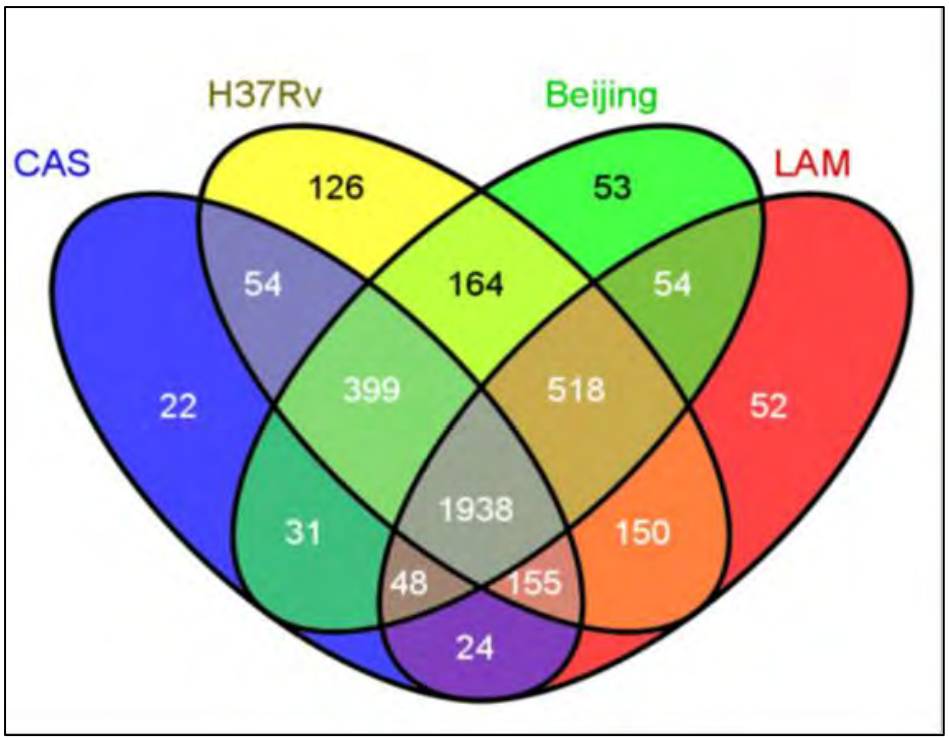

Figure 4.4: Qualitative cross strain/species data analysis. The analysis shows the overlap in the numbers of protein identifications between the 4 strictly *Mycobacterium tuberculosis* strains CAS, LAM, W-Beijing and H37Rv.

4.3.4 Functional annotation and pathway mapping of the *Mycobacterium tuberculosis* core-proteome

In order to understand the functional repertoire of the obtained experimental core proteome, a gene ontology analysis was carried out. Proteins were grouped into annotation clusters that have analogous themes (biological processes, molecular functions or cellular components) using a GOSLIM analysis to assess GO representation and GO coverage in comparison to the total theoretical *Mycobacterium tuberculosis* proteome.

Analysis of the individual strain proteomes revealed that all major protein classes were roughly equivalently represented across all strains. Furthermore, comparison of the experimental proteomes to the theoretical proteome revealed that the experimental proteomes mirrored that of the theoretical proteome, as shown below in Figure 4.5, hence confirming that the protein extraction and analysis approach used in this study did not discriminate any protein classes.

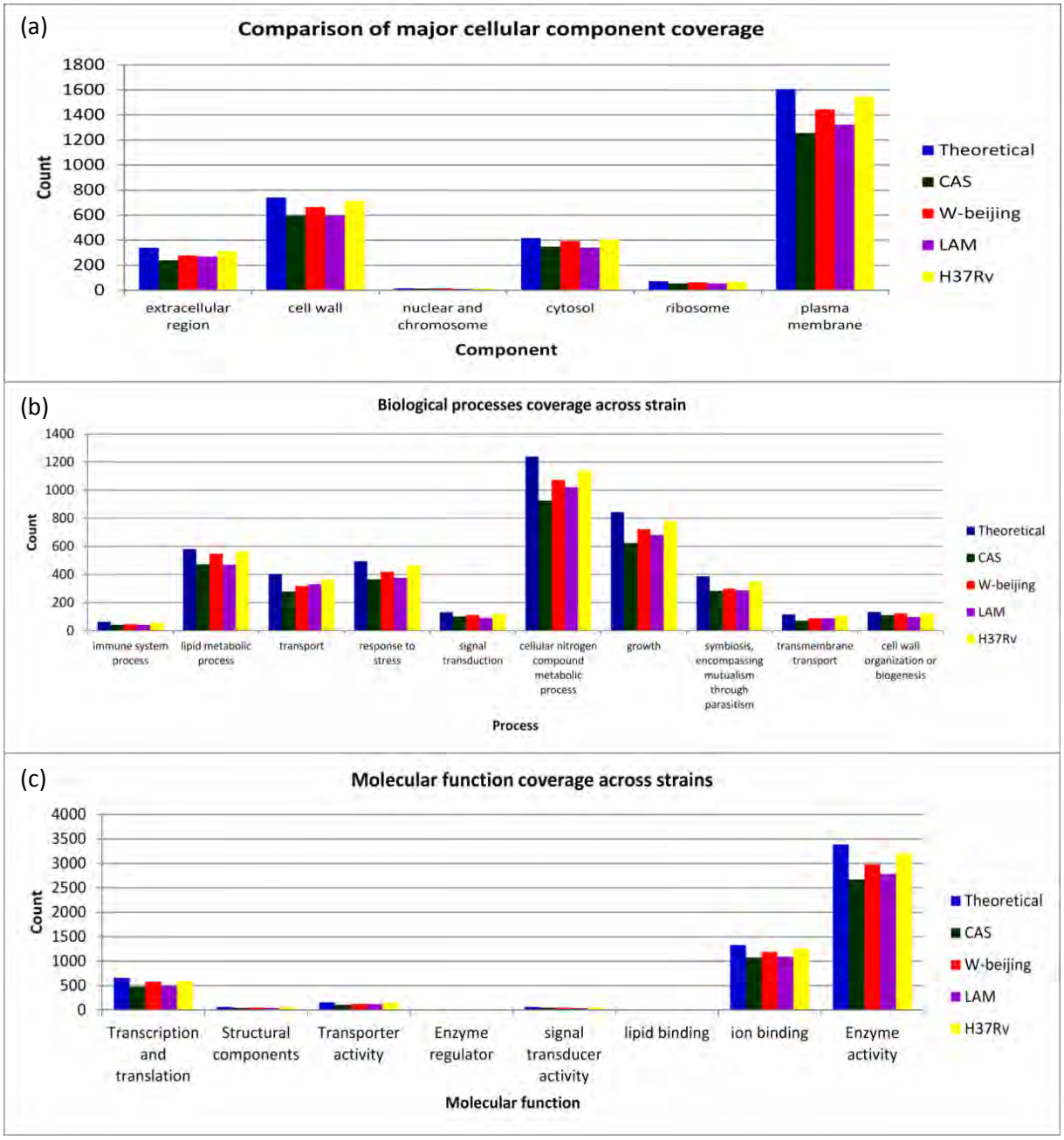

Figure 4.5: GO representation and GO coverage of across strains. The Figure shows the experimental representation and coverage of major gene ontology classes per strain in (a) biological processes (b) molecular function (c) cellular component. This is shown in comparison to the complete theoretical H37Rv GO classification using GO SLIM annotation.

Enrichment analysis of the 1938 shared *M. tuberculosis* core proteome was then carried out using DAVID [285,286] to decipher predominant themes in different groupings of the dataset. Protein clusters whose themes were enriched in the proteins shared by all strains were those required for overall growth of the microbe. This echoes the fact that most of the basic functions of the pathogenic organism are identical across strains and suggest that small qualitative differences could be responsible for the differences in clinical phenotype. The top 10 enriched

clusters are shown in Table 4.4 below. The enrichment score represents the summary of the biological theme or annotation cluster in relation to other clusters. The enrichment score is directly proportional to the GO count in the specific annotation cluster, hence a higher enrichment score means that there is a larger number of genes in the query dataset that fall into that annotation cluster. This function basically ranks overall importance of gene groups and a higher score indicates that there are more gene members of this group and that the process that they are involved in is likely important to the cell at that moment. An enrichment score of 1.3 is equivalent to a p-value of 0.05 therefore, all genes scoring above this score are deemed potentially noteworthy.

Annotation cluster	Enrichment score
Respiration processes	13.13
Transition metal binding	11.76
Ribosomal RNA processes	9.34
Lipid metabolism	6.96
Membrane and transmembrane	6.22
Stress response	5.22
Amino acid biosynthesis	4.79
Carbohydrate metabolism	4.59
FAD cofactor binding	3.85
Iron and sulphur binding	3.72
Secondary metabolism, catabolism and detoxification	3.62

Table 4.4: Top 10 enriched clusters amongst proteins common to all strains.

Because proteins are dynamic molecules that typically work as groups or in conjunction with a network of other classes of molecules to accomplish specific tasks, the shared proteins were also analysed in the context of represented pathways to get a better picture of the common processes that the core proteome underpins. Pathway mapping for the *Mycobacterium tuberculosis* core proteome was done within DAVID annotation using KEGG and Reactome. Further pathway analysis was carried out using iTUBY pathway mapping tool.

The dominating pathways amongst the core proteome are represented in Figure 4.6 below. Although KEGG database was superior in mapping pathways, it mapped only 47% of the

shared proteins to pathways. Over half of the data remained unmapped to pathways partly due to the fact that approximately $^{1}/_{3}$ of the *M. tuberculosis* proteome is only annotated as conserved hypothetical and unknown proteins whose functions and associated pathways are unknown. As a result, it becomes challenging to predict exactly what processes or pathways that such proteins are involved in.

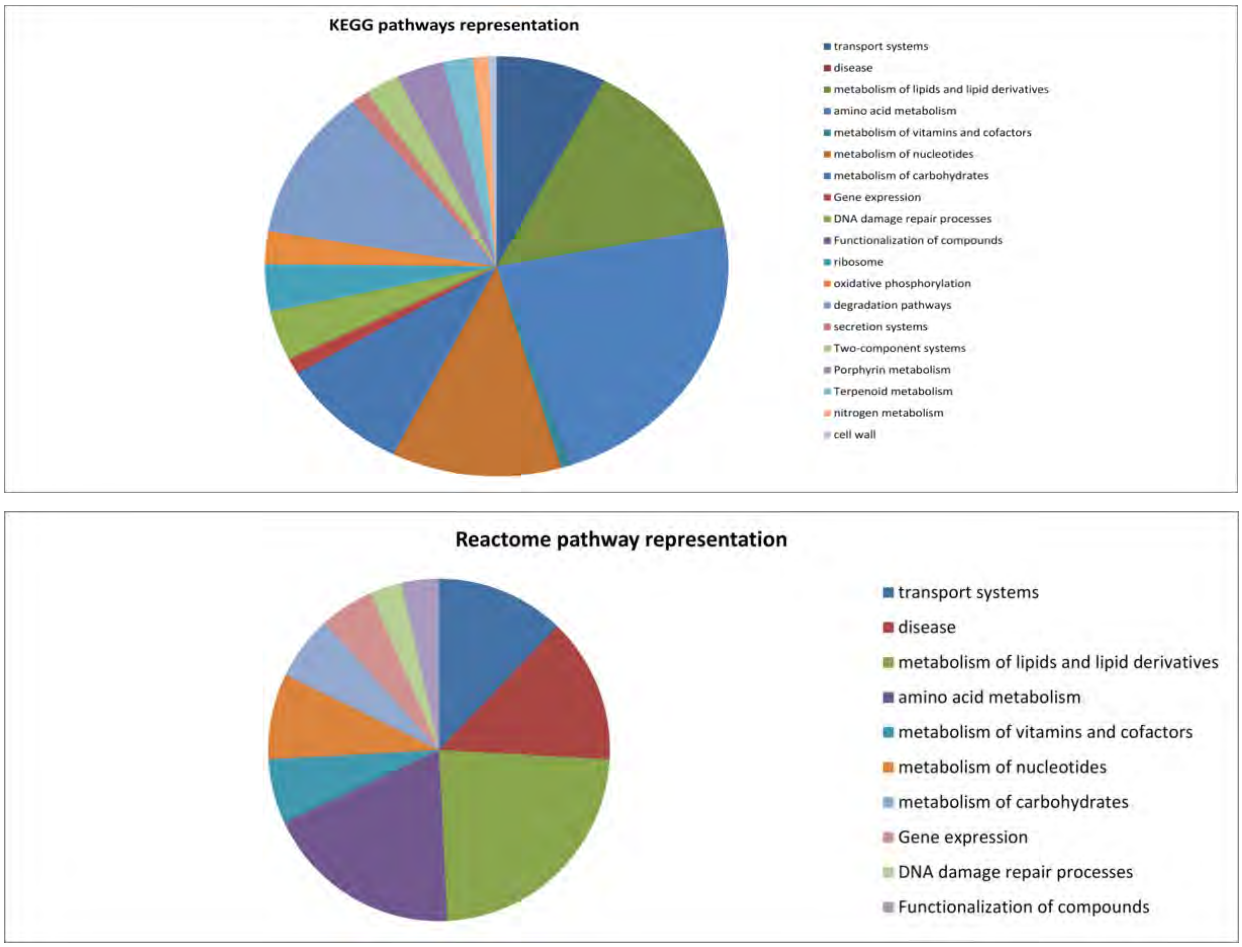

Figure 4.6: Pathway mapping of the *M. tuberculosis* core proteome. The pie charts show the distribution of the proteins common to all strains in major biological pathways using KEGG, and Reactome pathway mapping tools.

The iTUBY tool was used to place each protein into its context in the cell with regards to function and pathway and interacting proteins (http://www.ituby.org). This tool enabled visualisation of the proteins that are present for each pathway in the context of the entire pathway as well as those that are absent (Figure 4.7). Pathway analysis revealed that all major *M. tuberculosis* pathways were represented in the shared proteome along with a number of proteins that have not yet been assigned to specific pathways.

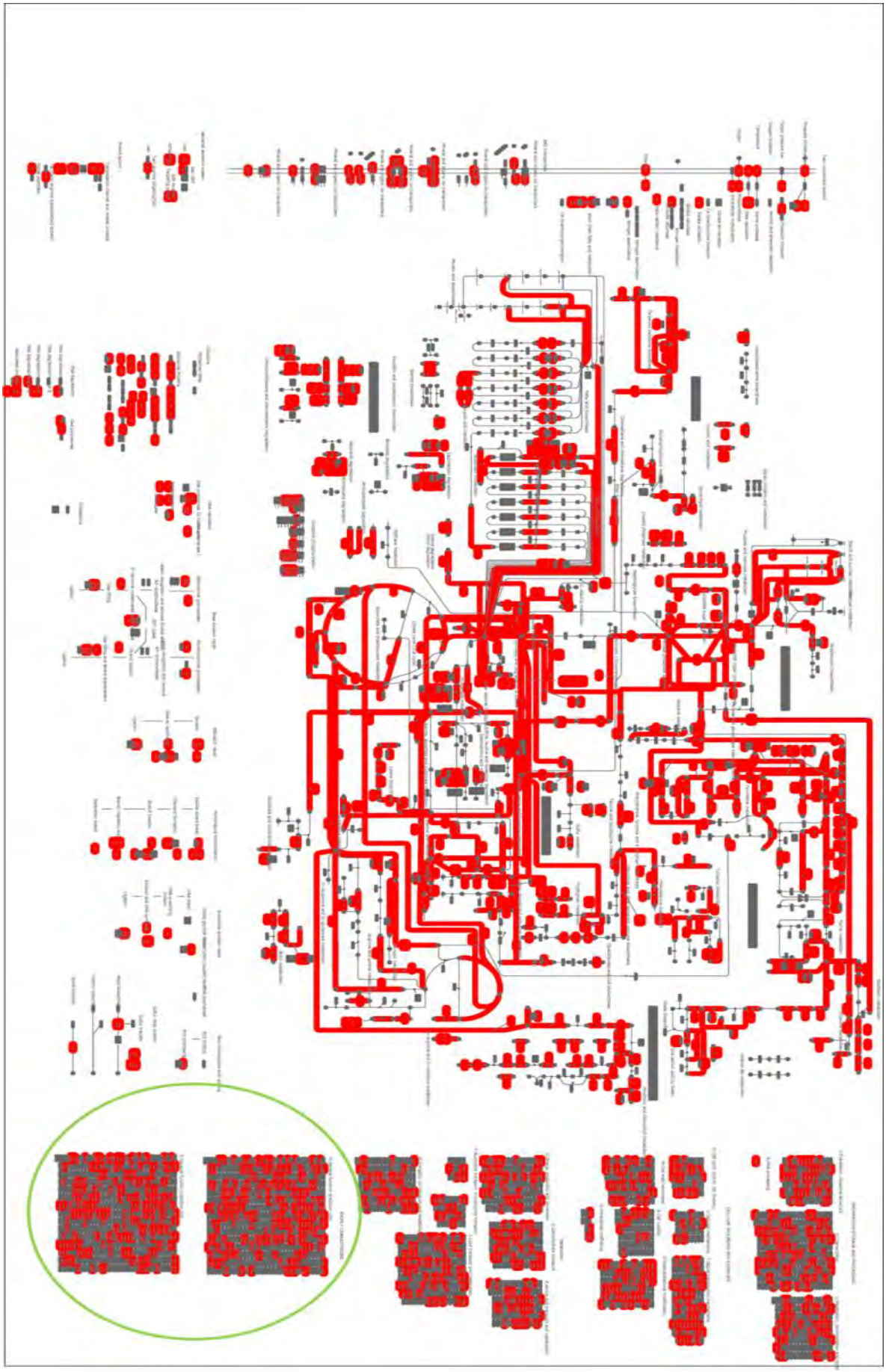

Figure 4.7: Pathway mapping for proteins shared by all *Mycobacterium tuberculosis* strains using the iTUBY mapping tool. The iTUBY mapping tool maps the obtained proteins to *M. tuberculosis* pathways in the context of the cell, including all pathways and interacting proteins in each pathway/functional category. All categories are accounted for in KEGG mapping whilst some but not all are present in Reactome. Proteins that have not been mapped to any pathways are circled in green.

4.3.5 Qualitative and functional assessment of the MTBC core-proteome

Perturbation of the 1938 *M. tuberculosis* core proteome was assessed when adding in *M. bovis* and *M. bovis* BCG to the analyses. It was observed that the shared proteome decreases from 1938 to 1734 as seen in Figure 4.8 which mapped into 1128 Rv identifiers (Annexure Table 4.2). Henceforth, this is referred to as the MTBC core proteome. This immediately suggests that whilst the MTBC is genetically a closed pan group, certain aspects of the proteome still exhibit species specific aggregation. A total of 204 proteins from the MTB core-proteome were not observed in the MTBC core-proteome. Whilst some of the 204 proteins are shared with either BCG or *M. bovis*, 45 of these were apparently unique to the *M. tuberculosis* strains in this study. 39 of these 45 proteins were mapped to Rv identifiers (Annexure Table 4.4), which revealed that about 50% of these as originated from insertion sequences and phage DNA and the remaining half is dominated by intermediary respiration, unknown proteins and conserved hypotheticals.

These 45 proteins are placed by iTUBY into categories as seen in Figure 4.9 and include mineral and organic ion transporters of the inositol phosphate metabolism, amino acid metabolism (histidine), caprolactam degradation, propinoate metabolism and post-translational modification. Proteins in this group may drive human tuberculosis specific characteristics of infection. Only a single PE/PPE protein (Rv3426) and a single virulence protein (Rv1966) are in this group.

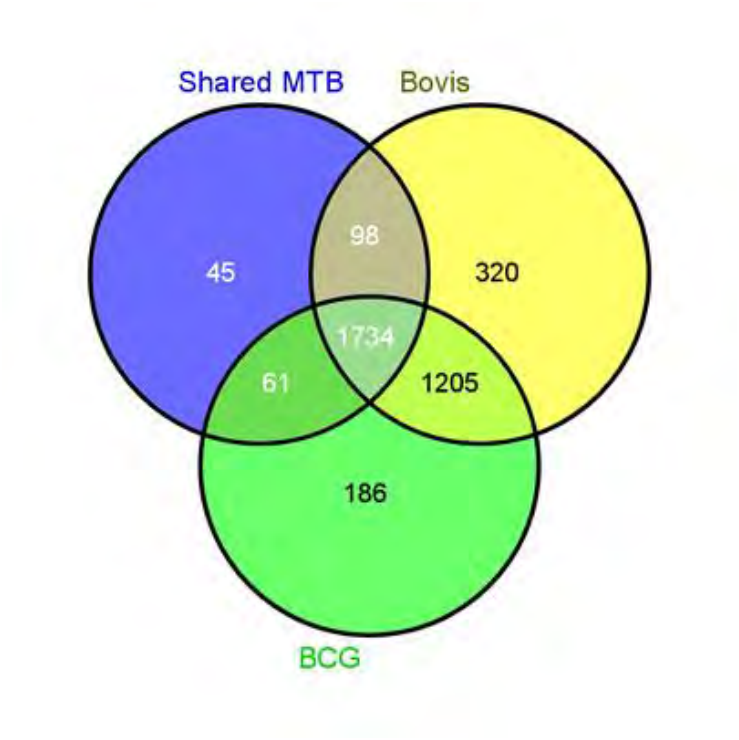

Figure 4.8: Qualitative cross species protein comparison across the 6 members of the MTBC. The venn diagram shows the overlap in the numbers of protein identifications between the 1938 MTB core proteome (blue circle) and the total protein identifications of *M. bovis* BCG (green circle) and *M. bovis* (yellow circle).

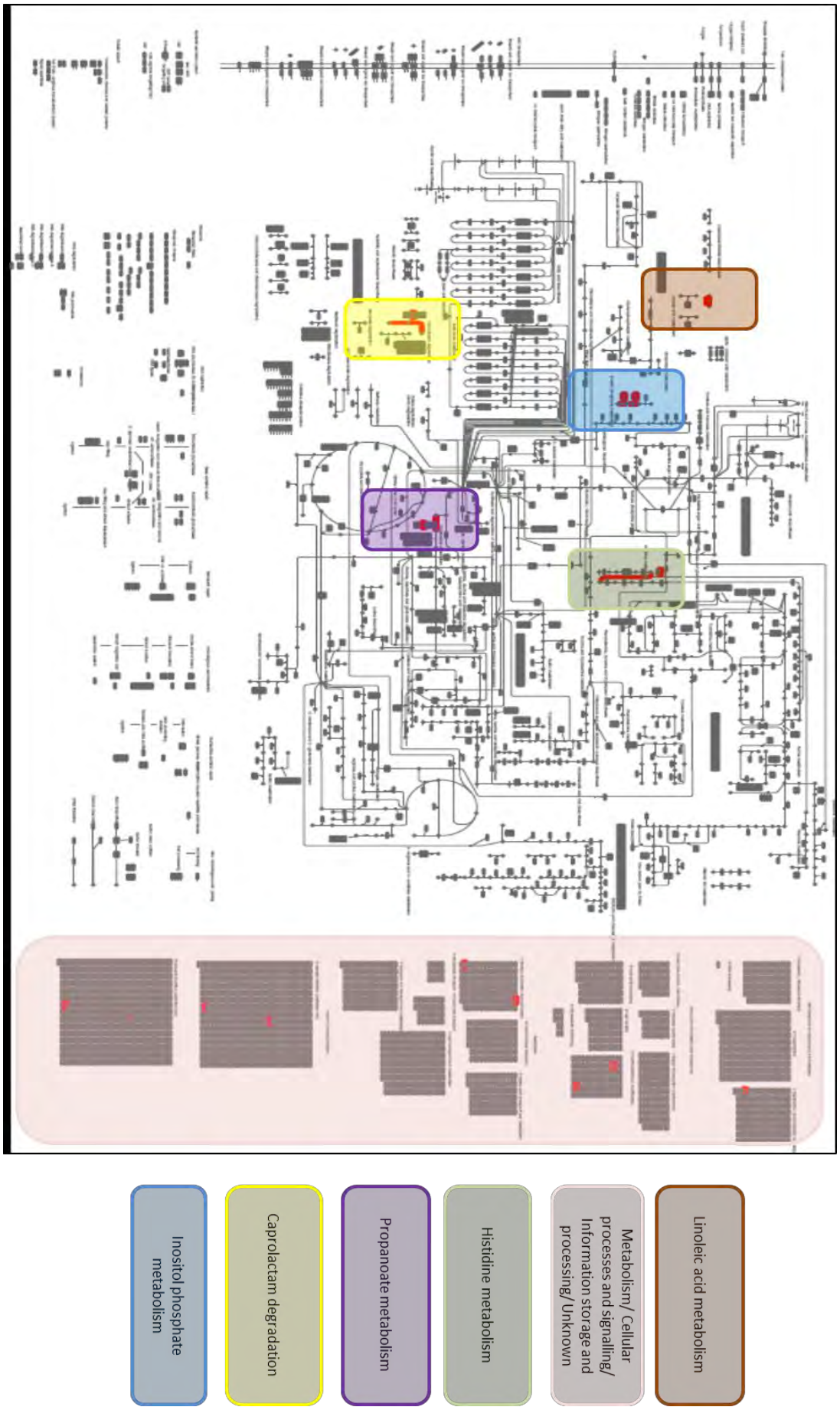
Linoleic acid metabolism
Metabolism/ Cellular processes and signalling/ Information storage and processing/ Unknown
Histidine metabolism
Propanoate metabolism
Caprolactam degradation
Inositol phosphate metabolism

Figure 4.9: iTUBY pathway mapping of proteins that remain specific to all shared *M. tuberculosis* strains when including proteins produced by *M. bovis* and BCG in the comparison.

4.3.6 Qualitative and functional assessment of the Mycobacterial core-proteome

Perturbation of the MTBC core proteome was further assessed when adding an NTM, *M. avium* into the comparison. It was observed that the shared proteome decreases to from 1734 to 1255 proteins, henceforth referred to as the Mycobacterial core-proteome which was ID mapped to 830 Rv identifiers (Annexure table 4.3). A total of 479 proteins remain strictly shared by the MTBC and 102 remain strictly shared by the MTB group (Figure 4.10). A total of 82 from the 102 MTB specific proteins were mapped to Rv identifiers for TBDB annotation. These proteins fall in the categories of fatty acid metabolism, caprolactam degradation, propinoate metabolism, signal transduction and cell wall processes amongst others (Figure 4.11 and Annexure Table 4.5). The persisting uniqueness of some of these categories suggests that they may contain proteins of importance to *M. tuberculosis* pathogenesis. Only a single protein in this group (alpha Crystallin, ahpE) is annotated as a virulence protein. However other proteins that are known to be involved in some aspect of the pathogenesis phenotype are still found in this group including ESAT-6 like proteins and resuscitation promotion factors which are potentially interesting in the context of reactivation of latent infections as well as transmission studies [287,288].

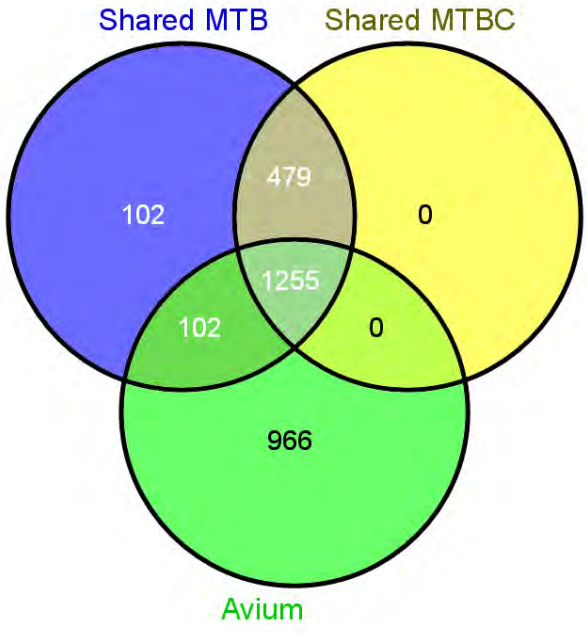

Figure 4.10: Qualitative cross species protein comparison across the 6 members of the MTBC. The venn diagram shows the overlap in the numbers of protein identifications between the 1938 MTB core

proteome (blue circle) and the MTBC proteome (yellow circle) and the total *M. avium* protein identifications that were ortholog mapped to *M. tuberculosis* H37Rv (green circle).

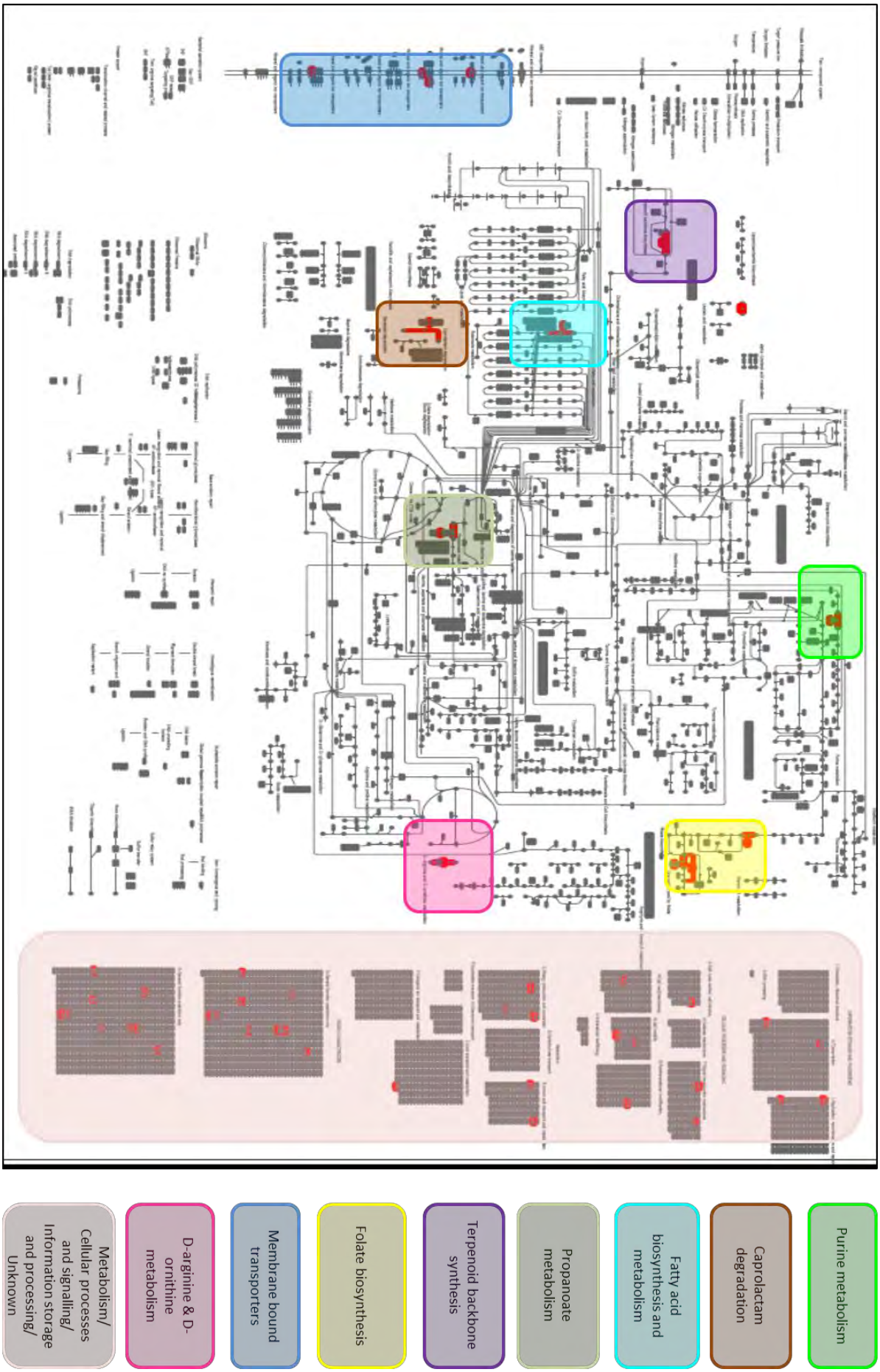
Purine metabolism
Caprolactam degradation
Fatty acid biosynthesis and metabolism
Propanoate metabolism
Terpenoid backbone synthesis
Folate biosynthesis
Membrane bound transporters
D-arginine & D-ornithine metabolism
Metabolism/ Cellular processes and signalling/ Information storage and processing/ Unknown

Figure 4.11: iTUBY functional and pathway placement of proteins that remain specific to shared *M. tuberculosis* core-proteome when including other members of the MTBC and *M. avium*.

The 1 255 proteins shared between *M. avium* and the MTBC group are enriched with intermediary respiration metabolism pathways (Figure 4.12). The number of those linked to virulence however decreases from 32 to 23 as seen in Table 4.5. These are classified as contributing to tuberculosis virulence by TBDB classification; however, they do provide a fundamental role in functioning of folded proteins in bacteria. However, virulence proteins stretch beyond the boundaries of those currently annotated as virulence or antigenic proteins. For example many proteins involved in cell wall processes and lipid metabolism as well as PE/PPE proteins may be involved in virulence. Taking this into consideration, there are a total of 155 further proteins with possible contributions to pathogenicity and virulence in these two categories. These include protein groups that are well known to be important for pathogenesis, including members of the polyketide synthesis (pks) family of proteins (pks10, pks13, pks16), mammalian cell entry (mce) family proteins (mce2 and mce4), secretion systems (sec) proteins (secF, secY, secA2), fibronectin binding proteins (fbpA and fbpC), as well as membrane protein family (MMPL) proteins (mmpl11, mmpl6, mmpl8). Some of the proteins in this table are conserved hypotheticals however, they are classified as virulence, detoxification and adaptation category possibly by association. For example Rv2521 lies in the middle of multiple PE/PPE/PGRS operons which are suspected to be virulence proteins and co-transcribed.

Members of these families of proteins have been shown to be useful in establishing successful entry into host cells, eliciting strong immune responses in human infection, as well as being virulence determinants in certain *M. tuberculosis* strains. Their presence in *M. avium* suggests that they are useful in a similar manner in this organism and could contribute to the reason why *M. avium* establishes a similar infection to *M. tuberculosis* in the lungs of immuno-compromised patients.

It is important to note that the comparison depicted here was based on the proteins in *M. avium* for which there were known *M. tuberculosis* H37Rv orthologs. As a result this comparison leaves out a large number of proteins apparently ‘unique’ to *M. avium* due to incomplete ortholog mapping and the fact that *M. avium* generally has a larger genome than *M. tuberculosis* which equates to a larger proteome by approximately 1 000 proteins.

Rv Loci	Protein name	Virulence association
RV3670	ephE epoxide hydrolase	Tuberculist and TBDB
RV3846	sodA superoxide dismutase	Tuberculist, TBDB, [289,290]
RV3660C	conserved hypothetical protein	Tuberculist, TBDB, [291]
RV1608C	bcpB peroxidoxin	Tuberculist, TBDB, [292]
RV0350	dnaK chaperone protein	Tuberculist, TBDB, [293]
RV2373C	dnaJ2 chaperone protein	Tuberculist, TBDB, l[153,292]
RV0440	groEL60 kda chaperonin 2 groEL2	Tuberculist, TBDB, [294,295]
RV2521	bcp bacterioferritin co-migratory protein	Tuberculist, TBDB, [292,296,297]
RV1901	cinA competence damage-inducible protein A	Tuberculist, TBDB
RV3497C	mce4CMCE-family protein	Tuberculist, TBDB, [298,299]
RV0554	bpoC non-haem peroxidase	Tuberculist, TBDB, [158,292,297]
RV3372	otsB 2trehalose-6-phosphate phosphatase	Tuberculist, TBDB
RV1477	invasion-associated protein	Tuberculist, TBDB, [300]
RV0384C	clpB endopeptidase ATP binding protein chain B	Tuberculist, TBDB, [153,295]
RV0351	grpE chaperone	Tuberculist, TBDB, [153,295]
RV1908C	katG catalase-peroxidase-peroxynitritase T	Tuberculist, TBDB, [301]
RV2701C	suhB extragenic suppressor protein	TBDB
RV2214C	ephD short-chain type dehydrogenase	Tuberculist, TBDB
RV1694	tlyA cytotoxin haemolysin	Tuberculist, TBDB, [302]
RV3490	otsA alpha, alpha-trehalose-phosphate synthase	Tuberculist, TBDB, [303]
RV0352	dnaJ1 chaperone protein	Tuberculist, TBDB, [153,295]
RV2299C	htpG chaperone protein	Tuberculist, TBDB
RV3417C	groEL60 kda chaperonin 1 groEL1	Tuberculist, TBDB, [153,295]

Table 4.5: List of proteins annotated as virulence proteins shared between all 7 organisms. All are listed by Tuberculist (www.tuberculist.org) and TBDB (www.tbdb.org) or the listed references.

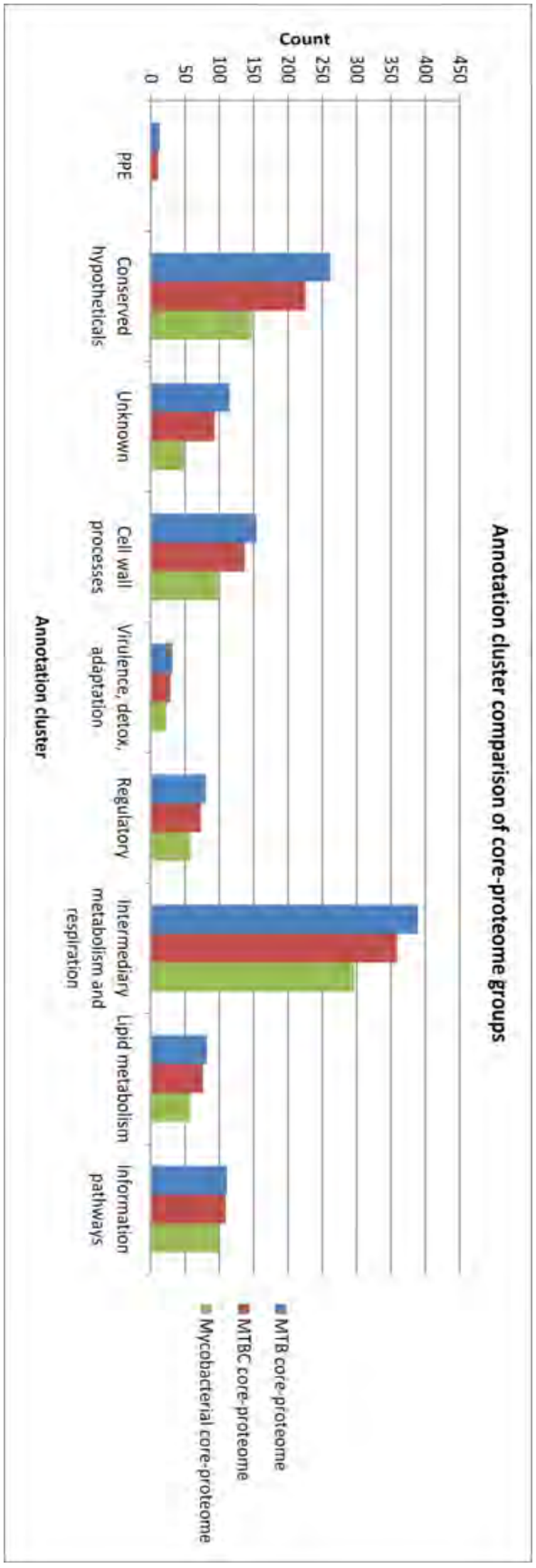

Figure 4.12: Comparison of major annotation group clusters of the MTB core proteome (blue bars), the MTBC core proteome (red bars) and the Mycobacterial core proteome (green bars) core proteome groups.

Generally for all the core proteomes observed, the intermediary metabolism and respiration pathways were the most enriched. This is consistent with the basic requirements of growth being conserved across the groups. The PE/PPE family of proteins is generally under-represented in each of these shared groups of proteins and the significant reduction in the numbers of these proteins in those shared by all 7 strains suggests that the PE/PPE group may be largely expressed only by the members of the MTBC which is probably the reason why they are largely reduced outside the MTBC. Interestingly, only two PE/PPE proteins are shared with *M. avium* (PPE4 and PPE58). All proteins identified in the discovery experiment are shown in Annexure 4.

4.4 Conclusion

Shortfalls were observed in ortholog mapping data between databases (Ensembl, UniProt and Tuberculist), as well as in orthologue mapping between strains. This suggests that discrepancies in the annotation of *Mycobacterium tuberculosis* strains, as well as consistent database nomenclatures, must still be ironed out to allow comprehensive proteomic studies that are database dependant.

This aim of this part of the work was to generate hypothesis with which to get a general idea of the protein expression in various mycobacterial strains. Due to the fact that each experiment was run once, it was challenging to draw conclusions on the quantitative aspect of the experiment from this data without biological or technical replicates. It was deemed unnecessary at this point to obtain replicates from these experiments as this chapter was basically a hypothesis searching qualitative study. No solid quantitative conclusions were meant to be drawn from this chapter but instead it was to be used as a stepping stone towards semi-quantitative replicated experiments from which solid conclusions could be drawn. These experiments are described in detail in chapter 5. Furthermore, the stochastic nature of the sampling used in discovery MS, strong conclusions about the proteins that were observed in some but not other strains cannot be made at this point. However the consistent expression of the 1255 proteins across 7 strains beyond the boundaries of the MTBC suggests a general level of conservation at the protein expression level of the genus Mycobacterium. These proteins represent just under $^1/_3$ of the H37Rv proteome and about a $^1/_5$ of the *M. avium* proteome.

Across the shared proteomes, the intermediary metabolism and respiration annotation category is dominant, whilst the PE/PPE group is the most under-represented. The information pathways

annotation cluster is the least perturbed across the core proteomes beyond the MTBC, with only 10 proteins lost between MTBC and Mycobacterial core proteome. A complete functional assessment of what biological pathways the shared proteomes underpin is hindered by the large number of proteins in the 'unknown' and 'conserved hypotheticals' annotation clusters. Proteins in these annotation clusters together make approximately $^{1}/_{3}$ of the H37Rv proteome. Complete functional annotation of members of the genus *Mycobacterium* will therefore be invaluable in interpreting the minimum functional repertoire of proteins expressed across this group of organisms *in vitro*. Further analysis of the differentially expressed proteins must still be assessed and validated using more sensitive MS approaches, such as selected reaction monitoring.

Chapter 5

Qualitative and quantitative validation of the expression of key proteins that influence the phenotype of *M. tuberculosis* using targeted Mass spectrometry.

5.1 Introduction

Mycobacterium tuberculosis, the aetiological agent of tuberculosis, is thought to infect about a third of the world's population. Current statistics from the world health organisation show that approximately 1.4 million people die from tuberculosis each year [5]. Although various studies have shown a link between certain strains to some aspects of virulence [13–17], the molecular contribution of strain variation to virulence remain poorly understood. In order to understand whether the molecular biology that contributes to the processes of infection and disease progression are consistent across strains, it is necessary to utilize a reproducible method to ascertain whether the proteins that drive these processes are consistently expressed across the strains. Moreover, proteins contributing to virulence and adaptation are potential diagnostic tools hence understanding their expression across strains could shed some light on new diagnostic opportunities.

Proteomic studies have been widely used in the biomarker discovery pipeline for the discovery of drug and diagnostic targets [304]. Proteomic based biomarker discovery strategies typically comprise two steps: the initial discovery stage usually involves comparing disease and normal samples to identify differential expression from which potential targets are chosen, based on qualitative and quantitative differences. The second stage then involves the validation of the targets obtained from the first stage *in vitro* and *in vivo* so as to ensure that only the most accurate and reproducible targets of high quality are taken forward to pre-clinical studies [262].

Mass spectrometry technology provides high throughput tools for both identification and validation of biomarker discovery. Discovery MS aims to unravel as much of the proteome as possible in any given sample [165]. Due to the nature of sampling in discovery MS platforms, not all differences observed in shotgun experiments are factual. Some differences arise from technical variability in sample processing, instrument variability or co-elution of target peptides with other peptides which results in under-sampling in some samples [305]. This can result in falsely discovered differences between samples, hence biomarkers obtained from

discovery experiments cannot be immediately used for clinical assays without further validation [306]. In the initial discovery experiment (Chapter 4), it was observed that about $^{1}/_{3}$ and $^{1}/_{5}$ of the *M. tuberculosis* complex and *M. avium* proteomes respectively is qualitatively expressed by all strains. The remaining proteins were found to be expressed differentially across the strains; however this observation was not validated.

Previously, immuno-assays such as antibody based ELISA have been successfully used for the validation of biomarkers. Despite such methods being well established, only a few Mycobacterial proteins have stable high affinity antibodies available that can be reliably used in a clinical validation assay [248,307]. Furthermore, the creation of antibodies by either immunisation or *in vitro* selection processes is expensive, time consuming and cannot be easily scaled to high throughput production. As a result, the number of Mycobacterial proteins that can be validated using these methods is limited.

Targeted mass spectrometry assays offer an appealing alternative to immuno-assays as they do not require antibodies and only a small sample volume is sufficient for an assay of multiple proteins in a single run. Targeted mass spectrometry assays seek to identify the presence or absence of a specific protein or group of proteins within a complex mixture of other proteins, hence they are termed 'selected reaction monitoring' (SRM) assays [183]. Typically, one targeted MS run can easily target up to 50 proteins simultaneously, hence this approach is alternatively called 'multiple reaction monitoring' (MRM).

The sensitivity and specificity of MRM allows this platform to provide relative quantitation in the absence of labelled peptide standards samples and absolute quantitation with labelled peptide standards. It has previously been shown that MRM technology can detect proteins in complex samples such as plasma over wide dynamic ranges with low limits of detection and quantification in biomarker discovery experiments [180,226].

The present chapter describes the development of MRM assays for *Mycobacterium tuberculosis* proteins that were identified in a prior discovery shotgun experiment (Chapter 4) as potential differential virulence and pathogenicity biomarkers based on variance in expression between Mycobacterial strains. Here, an MRM based validation experiment was carried out for 43 proteins across 7 strains of the genus *Mycobacterium* including *M. bovis*, *M. bovis* BCG, *M. avium* and 4 strains of *M. tuberculosis* representing lineages 2, 3 and 4 of *M. tuberculosis* classification. We obtained targeted reproducible relative quantitation measurements for all proteins across the 7 strains, providing evidence that the proteins are

indeed differentially expressed across different strains and thereby supporting the hypothesis that these proteins are potentially responsible for differential virulence.

5.2 Materials and methods

5.2.1 Shotgun MS

Mycobacterium tuberculosis isolates H37Rv, W-Beijing, CAS and LAM3 were obtained from the medical microbiology unit of the University of Cape Town (UCT), Stellenbosch University as well as the NHLS. These are described in Chapter 4 in Section 4.2.1. Cells were cultured for approximately 4-6 weeks in Sautons media as described in Section 4.2.2. Proteins were extracted and quantified from cell pellets and culture filtrates as described in section 4.2.3. Proteins were separated on a 1D SDS PAGE gel and visualised using Coomasie brilliant blue R250 as described in Section 4.2.4 and 4.2.5. Proteins were reduced and alkylated in gel in preparation for in gel tryptic digestion then digested in gel as described in Section 4.2.6. Shotgun MS was carried out on a LTQ Orbitrap Velos mass spectrometer as described in Section 4.2.7. Raw data was analysed as described in Section 4.2.8.

5.2.2 MRM-MS

5.2.2.1 Protein preparation for MRM-MS

Proteins were extracted in a biosafety level 3 facilities in line with health and safety guidelines as described in Section 4.2.3. Protein concentration was determined using a BCA assay according to manufacturer's protocol (#23227, Thermo Fisher Scientific). Protein preparation was carried out according to the filter aided sample preparation (FASP) method. Briefly, 200 µg of each protein sample was placed into a 10 kDa (MWCO) (Millipore). Protein cysteine residues were alkylated in the dark for 30 minutes in 10mM iodoacetamide (IAA). Iodoacteamide was then removed by centrifugation of the spin filter at 14 000g for 15 minutes. The remaining IAA was washed off twice by adding 8M urea in 0.1mM Tris-Cl pH 8.5 onto the column and spinning at 14 000 g for 15 minutes in a refrigerated bench-top centrifuge at 18ºC. The urea buffer was then washed off twice using 0.05 M ammonium bicarbonate to reduce the urea concentration to <2 M, which allows for tryptic digestion to efficiently take place. Sequencing-grade modified trypsin (#608-274-4330, Promega) was added at a ratio of 1:100 enzyme: substrate and incubated over-night at 37°C in a humid chamber. The tryptic peptides were collected by centrifugation of the filter at 14 000 g for 10 minutes.

To stop the tryptic digest the pH was lowered to 2 using an equal volume of 50% trifluoro acetic acid (TFA) followed by an incubation for 15 min at 37°C with shaking at 500 rpm. The peptide solution was desalted with C18 reverse-phase columns (Pierce #89870-25) according to the manufacturer's instructions. Briefly, the C18 columns were activated with 50% methanol, followed by equilibration with 5% ACN:0.5% TFA. After loading the sample, the columns were washed 3 times with 5% ACN:0.5% TFA. Finally, peptides were eluted with 70% ACN, dried under vacuum and re-solubilised in 0.1% FA to a final concentration of 8 µg/µl.

5.2.2.2 MRM-Mass spectrometry experiment

All MRM experiments were performed on a TSQ Vantage triple quadrupole mass spectrometer (Thermo Fisher Scientific) equipped with a heated electrospray II ion source. For liquid chromatography and separation of peptides, a Synergi 4µ Hydro RP 150 x 4.60 mm 80 Å pore size C18 column (serial # 630710-14) was used at a column flow rate of 300 µl/min. The gradient used was from 5-15% B in 5 minutes, 15-35% B in 90 minutes, 35-60% B in 10 minutes, 60-80% B in 5 minutes and kept at 80% B for 10 min. Solvent A was 100% water in 0.1% formic acid, and solvent B was 100% acetonitrile in 0.1% formic acid.

The mass spectrometer was operated in positive mode using electrospray ionisation with a voltage of 3,500 V. The capillary temperature was set to 350°C and the collision gas pressure to 1.2 mTorr. Up to 336 transitions per run were acquired with a cycle time of 3s and a dwell time of at least 20 ms. Collision energies were calculated per individual peptide transition ion using Skyline software and further optimized by a series of energy ramping experimental steps (10 steps of 5 V) to obtain the optimum energy of each transition. MS/MS data was acquired from the CID mode. Raw data was captured from the mass spectrometer and analysed using Skyline software.

To design MRM assays, peptides had to be chosen for analysis. For proteins that had previously been identified in a prior discovery experiment in chapter 4, selection was based on peptides that were physically observed in the prior experiment. Although each protein was typically observed by two or more peptides in the discovery experiment, two best performing peptides were chosen to confirm each protein in the MRM assay, with the exception of 2 proteins (Rv1818c and Rv0833) (Table 5.1). The proteins chosen for MRM analysis were based on relevance in pathogenicity and or virulence as stated in literature as shown in table 5.5. Due to the non-redundant nature of the *M. tuberculosis* proteome, 3 ion transitions were set as the minimum required to identify a peptide. As mentioned in chapter 2, other peptides are

not easily observable by MS due to the presence of MS incompatible peptide-centric properties [235]. This includes aspects such as the presence of methionine residues which are easily oxidized resulting in splitting of signal intensities between the oxidized and un-oxidized form. Peptides containing more than one cysteine residue were avoided due to the fact that these residues easily tend to form disulphide bonds hence altering their chemical properties and subsequently their elution properties. This is avoided in this type of MS as it is dependent on a pre-calculated elution time. Furthermore, the choice of peptides used for the proteins in this section was based on a collaboration with Schubert *et al* 2013 [248] who had previously run MRM experiments on the entire *M. tuberculosis* H37Rv proteome in an effort to characterise the total H37Rv proteome by MRM in order to build a peptide library for *M. tuberculosis*. Peptide data obtained from Schubert *et al* [248] and is also now present in peptide atlas; http://www.PeptideAtlas.org) was also used as an additional tool in the choice of peptides over and above our observation of these peptides in the discovery experiment.

After removing these filters the peptides were compared within a background of the total human and total Mycobacterial proteome. This was done to ensure that the peptides were unique to M. tuberculosis. This is essential in the event that this assay is run on clinical specimen which contains human proteins and a host of other bacterial proteins. The Mycobacterial proteome was used as a reference proteome to eliminate background from homologous proteins from other species of Mycobacteria so as to ensure that the targets were truly unique. After ensuring uniqueness of peptides, we then assessed to see those which had been found in the discovery experiment as well as in Schubert *et al* 2013. These were the basis of the peptides selected (Table 5.1).

Rv locus	Protein name	Total peptides	Peptide 1	#Transitions	Peptide 2	# Transitions
Rv0301	vapC2	3	DFDAIAALTGQK	5	EPPLSAMPVEYLTPR	3
Rv0899	arfA	2	GASALSLSLLSISR	3	SGNTVTLIGDFPDEAAK	4
Rv0901	arfC	2	AGADGSGPQGWLVK	5	IPVVPYAPYGPGSAR	4
Rv0966	Unknown	2	LTTFTLWGSGVLDLR	6	ADLPGAAIGPR	3
Rv1002C	pmt	2	FLNLGSLTDAGTPIFDEK	5	NSVVPLPDAVR	5
Rv1346	mbtN	2	AGTGLAAISWGLAHER	5	FVSLSPIADHIMVVAR	5
Rv1380	pyrB	3	QAMLPGHAVVLHPGPMVR	4	TVVTMFYENSTR	4
Rv1381	pyrC	2	LGLAGWPR	3	LTVGAVAHEGPMAAR	6
Rv1383	carA	2	AGVFSDGALAEPADLIAR	9	IVGIAGIDTR	3
Rv1384	carB	2	AEGLLAVTGDGAHAAR	10	GAFGDLLSAAGLPAPK	4
Rv1980c	mpt64	2	VYQNAGGTHPTTTYK	4	AFDWDQAYR	3
Rv1997	ctpF	2	FGPNTLAVVTR	3	AAAASAVAACHSAGIAVK	5
Rv2108	PPE36	2	LVYDGEPTFSYK	3	EEVIHLVPDVNK	4
Rv2126c	PE_PGRS_37	2	AGAPGTQGDSGDPGPPG	4	GGFADEFTGGFAQGGR	5
Rv2136c	uppP	3	DAVVVGIAQTLALVPGVSR	9	ILSAWLHGLVVK	5
Rv2156	mraY	3	IFMGDTGSLALGGVIAGLSVTSR	7	MAPFHHHFELVGWAETTVIIR	3
Rv2703	sigA	7	DAELTASADSVR	4	EMDITPEK	3
Rv3340	Unknown	3	IGNPTTDVVEQR	4	LYGGTYNLFHYSLAK	5
Rv3412	Unknown	3	GYADASLNEAAPDADR	3	MAVEADLADLAVYEALLAHK	4
Rv3621c	PPE65	2	AFNNFAAPR	3	YGFKPTVIAQPPAGG	3
Rv3709c	ask	2	SSYSDRPGTVVVGSIK	5	TDITFTCSR	3
Rv1818	PE_PGRS33	1	AGLIGDGGDGGAGGNGTGAK	8		
Rv0833	PE_PGRS13	1	TDLGGAGGAGGK	4		

Table 5.1: Peptides observed in shotgun discovery experiment shortlisted for MRM analyses

For the design of MRM assays for proteins that had not been previously observed in the discovery experiment, a minimum of 1 and a maximum of 3 tryptic peptides where possible were assessed and the best were chosen for relative quantitative comparison analysis. Three transitions were set as minimum to confirm the peptide (Annexure Table 5.1 and 5.2).

Limit of detection analysis were done on pure peptide standards by serial dilutions to determine the minimum concentration at which peptide signal could still be observed. A thousand times serial dilutions beginning from a concentration of 1mg/ml of peptide to 1fg/ml was reconstituted in mobile phase A. For each reconstituted peptide, 10µl was injected and separated on the LC beginning with a blank run and following on from the lowest concentration to the highest concentration. It was observed that for any peptide, 1mg/ml concentration resulted in a large amount of residual peptides in the column which required multiple washes to remove residual peptide. Further experiments were then carried out up to a concentration of 0.1ng/µl (which equals an amount of 1ng) to avoid column blockage. Figure 5.1a below shows the results obtained from peptide GAFGDLLSAAGLPAPK (both 2+ and 3+ species). This was used to formulate an equation with which to calculate limit of detection as shown in Figure 1.5b after having defined the signal to noise threshold of 20.

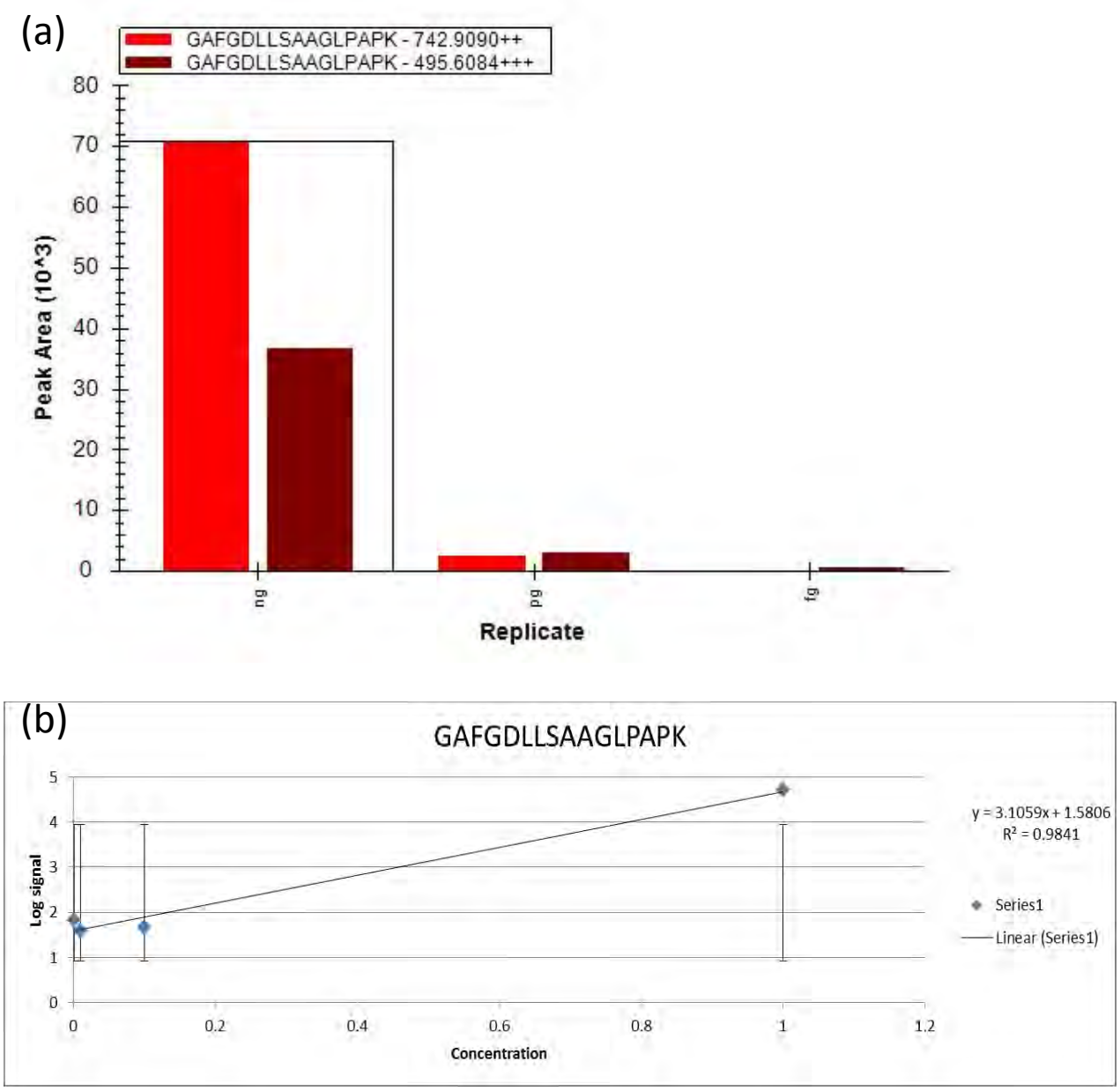

Figure 5.1: LOD experiments showing triplicate experiments of peptide GAFGDLLSAAGLPAPK from Rv1384 (2+ species in red and 3+ species in maroon). All experiments with 'ng' prefix represents experiments where 1ng was analyzed, 'pg' prefix represents 1pg and 'fg' prefix represent 1fg.

The histogram shows that the +3 species was more effective for quantification than the +2 species and that signal for this peptide was obtained up to 1pg (denoted pg in Figure 5.1). Very low signal was observed at the lowest dilution which represents 1fg. The LOD for the peptide standards is represented in Table 5.2 below.

Peptide	LOD (pg/µl)
AGVFSDGALAEPADLIAR	0.032
AEGLLAVTGDGAHAAR	0.025
GAFGDLLSAAGLPAPK	0.001
IVGIAGIDTR	8.28
LTVGAVAHEGPMAAR	0.07
LGLAGWPR	5.76
TVVTMFYENSTR	3.37
DDATAILDDADR	0.54

Table 5.2: LOD calculations of 8 peptide standards of proteins Rv1380-Rv1384

5.2.3 MRM data analysis

Data analysis was carried out using Skyline software (MacCoss Lab software). A total of eight data points were obtained per curve. An initial run was performed for all the peptides to determine elution time. The elution time of each peptide was divided by 8 to obtain the cycle time that allows for 8 data points to be collected per curve. Scan times below 5 milli seconds (ms) are normally considered good. Scan time then incorporates the number of transitions assessed per protein. Scan time of above 10 is good. Scan time was calculated by dividing the cycle time by the number of transitions (CT/total number of transitions). Table 5.3 illustrates the cycle times and scan times of peptide standards obtained from peptide standards.

Protein	Peptide	Number of transitions	Elution time (Experimentally observed)	Cycle time (ET/8) (ms)	Scan time (CT/# transitions*1000)
1380	DDATAILDDADR	129	18	2.25	17.44
1380	TVVTMFYENSTR	120	21	2.625	21.875
1381	LGLAGWPR	28	18	2.25	80.35
1381	LTVGAVAHEGPMAAR	199	21	2.625	13.19
1383	AGVFSDGALAEPADLIAR	214	18	2.25	10.51
1383	IVGIAGIDTR	214	21	2.625	12.26
1384	AEGLLAVTGDGAHAAR	276	18	2.25	8.15
1384	GAFGDLLSAAGLPAPK	84	18	2.25	26.78

Table 5.3: Determination of cycle time and can time based on elution time of standards. Cycle time measured in milliseconds

Quantitation of each signal was carried out using the area under the curve for the peptide transitions assayed. Retention times for the peptide standards were obtained by pre-assessment on the MS. For peptides without standards, the retention times were obtained from predictions from skyline software and gated at 5 seconds from the predicted retention time. Intra-assay ambiguity (CV) for each peptide was based on the calculated average protein concentration for

a set of technical duplicate injections of each sample. Inter-assay CV was calculated for each peptide from across biological replicates of the 7 strains. The peptide with the overall lowest inter-assay (biological replicate) CV per protein was chosen for relative quantification comparison.

5.3 Results

5.3.1 Shotgun MS qualitative assessment

Prior discovery MS results show that whilst a basal core proteome exists for the 7 strains, a substantial number of up to $^{2}/_{3}$ of the theoretical H37Rv proteome is differentially expressed. However, due to the stochastic nature of discovery MS, it was not possible to make concrete conclusions about these differentially expressed proteins. Thus to quantify sample a subset of the differentially expressed proteins, SRM technique was chosen as it is a more sensitive and reproducible MS technique. Because the design of SRM assays for such a large number of proteins is a laborious process, we sought to find a strategy to create a shorter list of candidate proteins to design assays for. We chose our starting point as the proteins that were found to be unique to the 4 strains of *Mycobacterium tuberculosis* based on the assumption that if they are truly only in *M. tuberculosis* then they are of immediate potential importance as they could be biomarkers for *M. tuberculosis* disease specific diagnosis.

A total of 168 proteins were found differentially expressed and unique to the *M. tuberculosis* human clinical strains in the shotgun proteomics study described previously in chapter 4. This qualitative analysis is shown in Figure 5.2 below. Gene expression data for each of these proteins was analysed using the TBDB repository. To shortlist proteins of possible relevance in differential clinical phenotype observed between *M. tuberculosis* isolates, we chose 7 experiments in TBDB where over-expression of the protein in that category would confer a selective advantage to the bacterium in *in vitro* disease models. The categories chosen are described in Table 5.3.

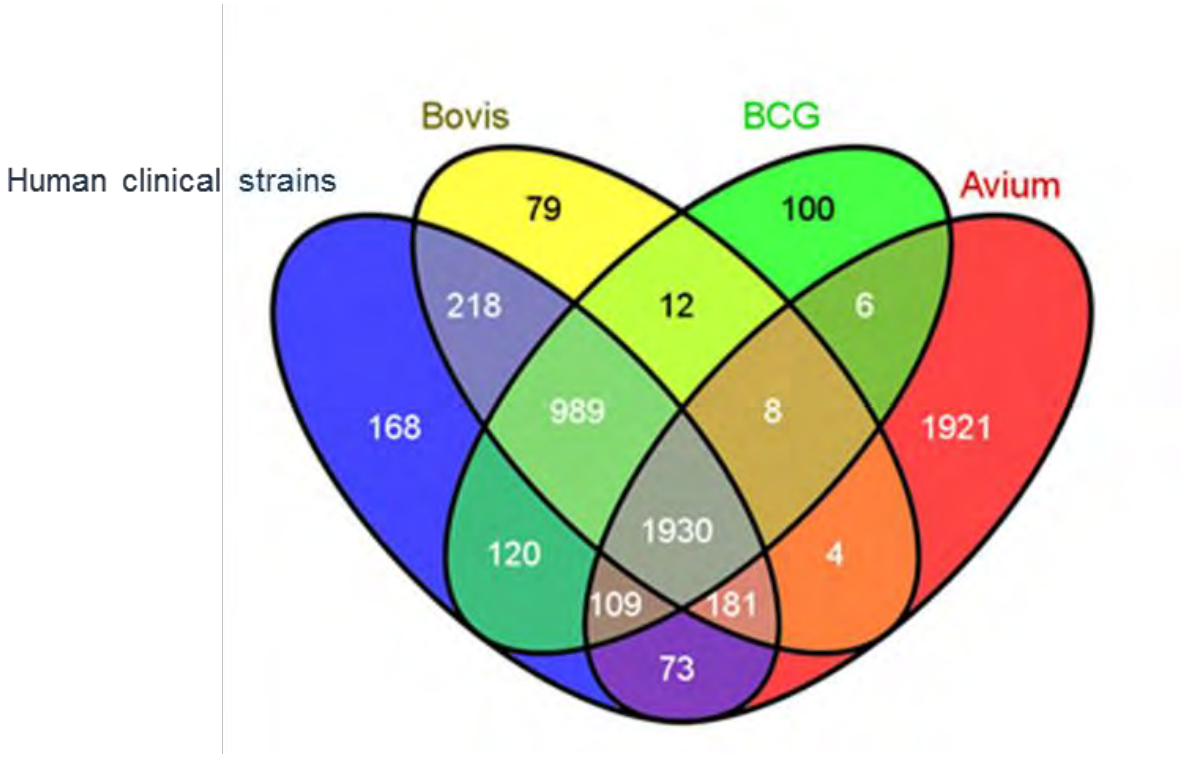

Figure 5.2: Qualitative cross strain/species data analysis. The analysis shows the overlap in the numbers of protein identifications between *M. bovis*, *M. bovis* BCG, *M. avium* and the 4 strictly *Mycobacterium tuberculosis* strains CAS, LAM, W-Beijing and H37Rv grouped into the 'human clinical strains' group.

5.3.2 Strategy on shortlisting of candidates for MRM analysis

Category	Disease model
Acid media	Acidified macrophage
Macrophage	Macrophage model
Hypoxia	Oxygen starvation in granulomas
NO treatment	Reactive nitrogen species RNS in macrophages
Starvation	Nutrient starvation in macrophages
Persistence	Latent TB infection
Antibiotics	Chemotherapeutic attack

Table 5.3: Table shows the 7 categories shortlisted from TBDB gene expression experiments for analysis of the 168 proteins unique to the human clinical strains, *M. tuberculosis* H37Rv, CAS, LAM and W-Beijing.

The gene expression of these proteins was then assessed in the 7 conditions that depict survival in the macrophage environment. Statistical analysis was carried out on the gene expression values obtained from the TBDB experiments using statistics packages in R (strategy depicted in Figure 5.3). Proteins whose average fold change averaged across all experiments for a given condition was ±2 SD from the mean were taken as significantly differentially expressed in that condition. Proteins that had significant fold change for less than 4 out of the 7 categories were removed from this list resulting in a shorter list of 72 proteins.

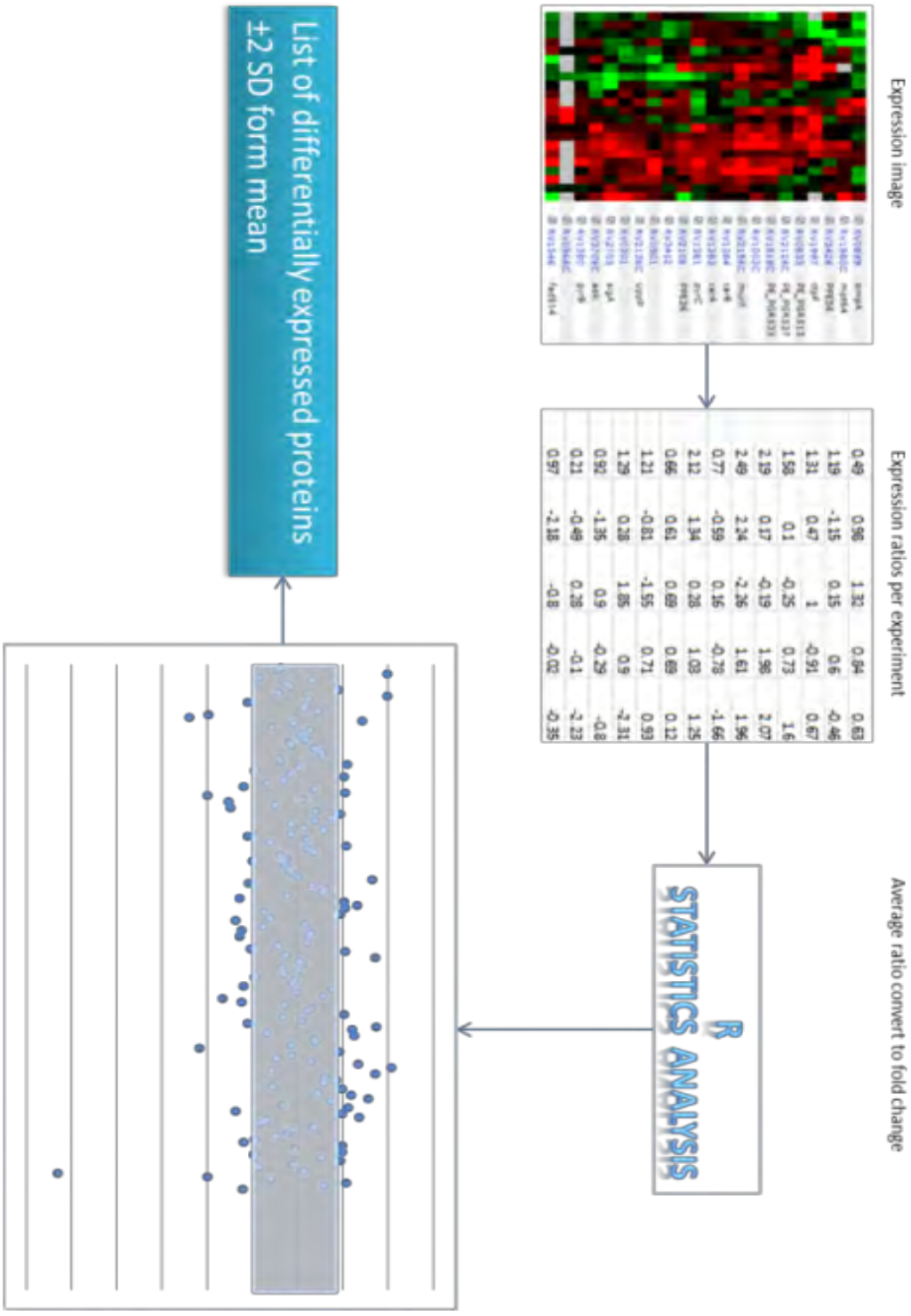

Figure 5.3: Gene expression analysis approach of the short list of 168 proteins expressed in human clinical strains. Expression ratio data was obtained from the chosen TBDB experiments and statistical packages in R were used to convert the ratios into fold changes. Analysis of the fold changes was done in R to identify proteins that have significant fold changes (±2SD from the mean) which are shown in the scatterplot above and below the shaded area.

Experiment	Up regulated	Down regulated
Acid media	58	38
Macrophage	18	53
Hypoxia	59	49
NO treatment	78	32
Starvation	51	26
Persistence	23	43
Antibiotics	40	54

Table 5.4: The number of significantly differentially expressed proteins from the 168 proteins unique to human clinical strains segregated into up-regulated and down-regulated per category assessed (www.tbdb.org)

The significantly differentially expressed proteins (Table 5.4) were assessed in the light of SRM assays that had previously been designed [248]. In that study, SRM assays had been successfully designed for 2 884 H37Rv proteins and these were used as a starting point to determine which proteins from the list might have pre-configured SRM assays. A total of 22 proteins in the shortlisted 72 candidates from the gene expression analysis had no previous SRM assays designed and these were removed from the analysis. From the remaining proteins, a shortlist of 23 proteins was picked and summarised in Figure 5.4 and Table 5.5.

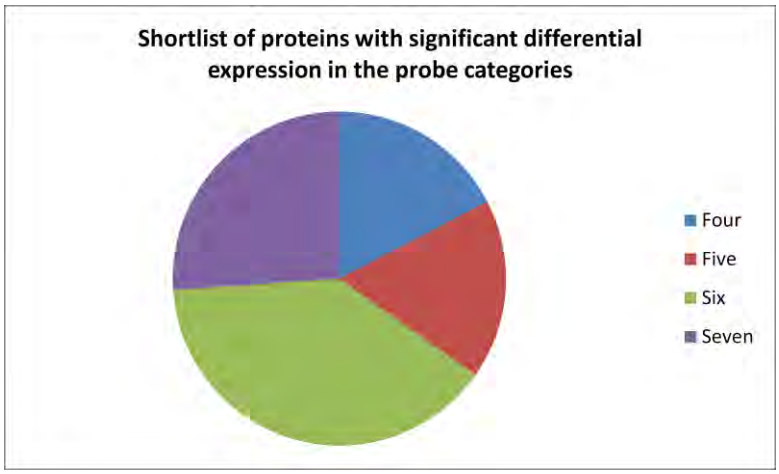

Figure 5.4: Representation of the shortlist of 23 proteins in the TBDB categories that were chosen for analysis. Approximately $^{2}/_{3}$ of the proteins had significant expression changes in 6 or all 7 of the categories assessed in TBDB and $^{1}/_{3}$ had significant expression changes in 4 and 5 categories.

In general, the proteins were involved in at least one aspect that potentially confers a selective advantage in establishing successful infection. This means that it is likely that differential expression of these proteins between strains potentially affects aspects of the pathogenic

process or virulence. Furthermore, these proteins are currently listed either in the category of high confidence drug targets as well as essential genes [297,308] further implying that differential expression could result in variations in survival in the host as well as response to drugs.

Locus	Protein name	Function	Associated phenotype
Rv0301	Toxic component of toxin-anti toxin system	Negative regulation of translation	Impaired growth when expressed
Rv0833	PE_PGRS13	Unknown	Possible virulnce/adaptation
Rv0899	Outer membrane porin A	Ammonia secretion	Tolerance to acidic conditions, impaired growth at ph 5.5
Rv0901	Uncharacterised membrane protein	Ammonia secretion	Tolerance to acidic conditions, impaired growth at ph 5.5
Rv0966c	Uncharacterised protein	unknown	Highly activated in the early stages of tuberculosis blood brain barrier invasion (CNS TB)
Rv1002c	Probable mannosyl-transferase	protein O-linked mannosylation	Growth and survival in host
Rv1346	Acyl dehydogenase mbtN	Mycobactin synthesis	Tolerance to low nutrient environment, adaptation to intracellular environment
Rv1380	Aspartate carbamoyltransferase	transporter activity	High confidence drug target possibly used for drug transport/modification, essential for growth
Rv1381	Dihydroorotase	hydrolase	Growth and survival in host
Rv1383	Carbamoyl-phosphate synthase small chain	amino acid biosynthesis	Growth and survival in host
Rv1384	Carbamoyl-phosphate synthase large chain	amino acid biosynthesis	Growth and survival in host
Rv1818c	PE_PGRS33	carrier protein	Modulation of host immune response, pathogenesis, response to oxygen and starvation
Rv1980c	Immunogenic protein 64	unknown	Tolerance to starvation, highly immunogenic, diagnostic, vaccine and drug target potential
Rv1997	Probable cation-transporting ATPase F	hydrolase	Implicated in domancy/persistance, immunogenic, response to hypoxia, NO, CO
Rv2108	PPE36	unknown	Immuno-active membrane component, diagnostic and vaccine target potential
Rv2126c	PE_PGRS_37	unknown	Possible virulnce/adaptation
Rv2136c	Undecaprenyl-diphosphatase	Dephosphorylase, hydrolase	Response to NO and antibiotic, high confidence drug target
Rv2156c	Phospho-N-acetylmuramoyl-pentapeptide-transferase	Lipid synthesis	Growth and survival in host, high confidence drug target
Rv2703	RNA polymerase sigA	Sigma factor for virulence factors	Host immune response modulator, virulence, growth in host, high confidence drug target
Rv3340	metC	methionine biosyntheisis	Growth in host
Rv3412	Uncharacterised protein	Unknown	Difference between clinical and laboratory strains
Rv3621c	PPE65	Unknown	Possible virulnce/adaptation
Rv3709c	Aspartate kinase	Phosphorylation for amino acid synthesis	Growth and survival in host

Table 5.5: The table shows the 23 proteins shortlisted for MRM analysis based on prior observation in a discovery MS experiment. The phenotype associated with the expression of each protein is shown in column 4.

5.3.3 MRM assessment of shortlisted candidates that were observed in shotgun-MS

Crude peptide samples were analyzed without pre-fractionation. Sample injection of 20 µl per sample amounting to 3.2 µg of protein was analyzed by LC MS/MS to measure the specific peptides using a single finalised method after optimizations. A minimum of 2 peptides per protein and 3 transitions per peptide were assessed for enhanced specificity and sensitivity (Annexure Table 5.2). Method development for each protein, the MRM assay involved multiple steps of optimization. Initial MS runs determined subsequent aspects such as cycle time as described in section 5.2.2.1 (Table 5.1).

Optimization for collision energies was carried out by successive 5 V increases and decreases of voltage from the initial voltage used which was obtained from theoretical voltage prediction carried out on Skyline software. The step size of 5V was carried out for a total step count of 10 (5 times increase and 5 times decrease from prediction). This allowed us to determine the optimum voltage to use per peptide to obtain the best fragmentation to identify each transition. This is depicted in Figure 5.5 below for the IVGIAGIDTR peptide derived from Rv1380 (PyrA). The peak with the largest peak area depicts the best collision energy (CE) to fragment the peptide. The figure illustrates that for the replicates, the optimum (CE) for this peptide is the ‘step -2’ (CE) (shown in light brown), which is 5V less than that which was predicted by Skyline software (shown in red). Optimized collision energies for each peptide are shown in the final method that was used for all peptides shown in Annexure Table 5.1.

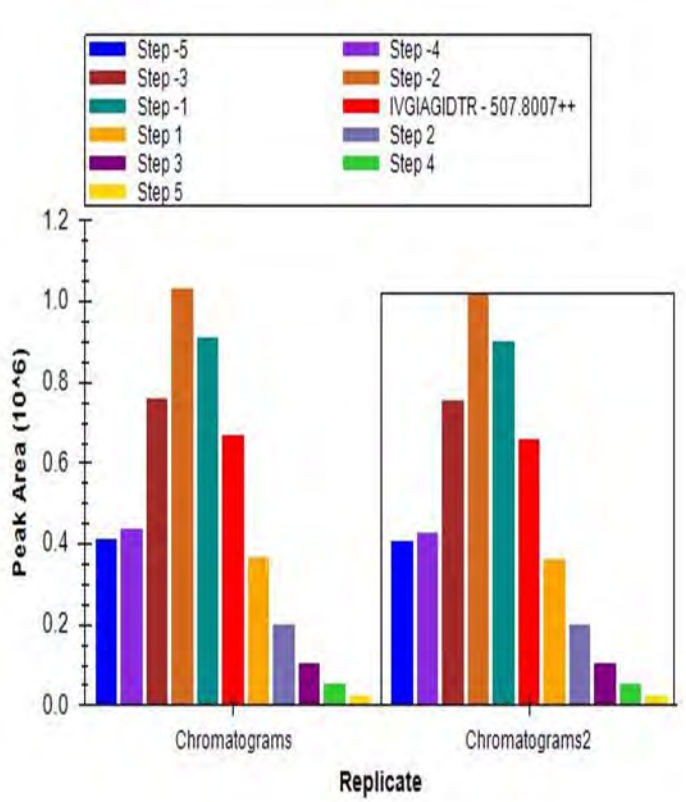

Figure 5.5: Illustration of collision energy optimisation for peptide IVGIAGIDTR from Rv1380. Each bar colour represents a 5V increase or decrease relative to the initial CE as depicted by the key.

Data analysis was carried out using Skyline™ software. For each peptide, each spectra was individually inspected from each strain to remove false data points and to assess if retention time was standard across samples and transitions as shown in Figure 5.6 below. Each colored bar represents a single transition for the respective peptide. In the panel above, the transitions are not lined up at the same retention time indicating that initially, the software picked the wrong transition. Following data clean-up, all transitions of each peptide align at the same retention time which is consistent with transitions belonging to the same peptide as seen in the bottom panel. The peptides and transitions are also summarised in Figure 5.6 below. Further chosen peptides and the associated transitions can be seen in Annexure table 5.1.

Peptide	Transitions
DDATAILDDADR	y4- y8
TVVTMFYENSTR	y5-y8
LGLAGWPR	y3-y5
LTVGAVAHEGPMAAR	y5-y11
AEGLLAVTGDGAHAAR	y5-y12
GAFGDLLSAAGLPAPK	y6-y12
AGVFSDGALAEPADLIAR	y7-y14
IVGIAGIDTR	y3-y6

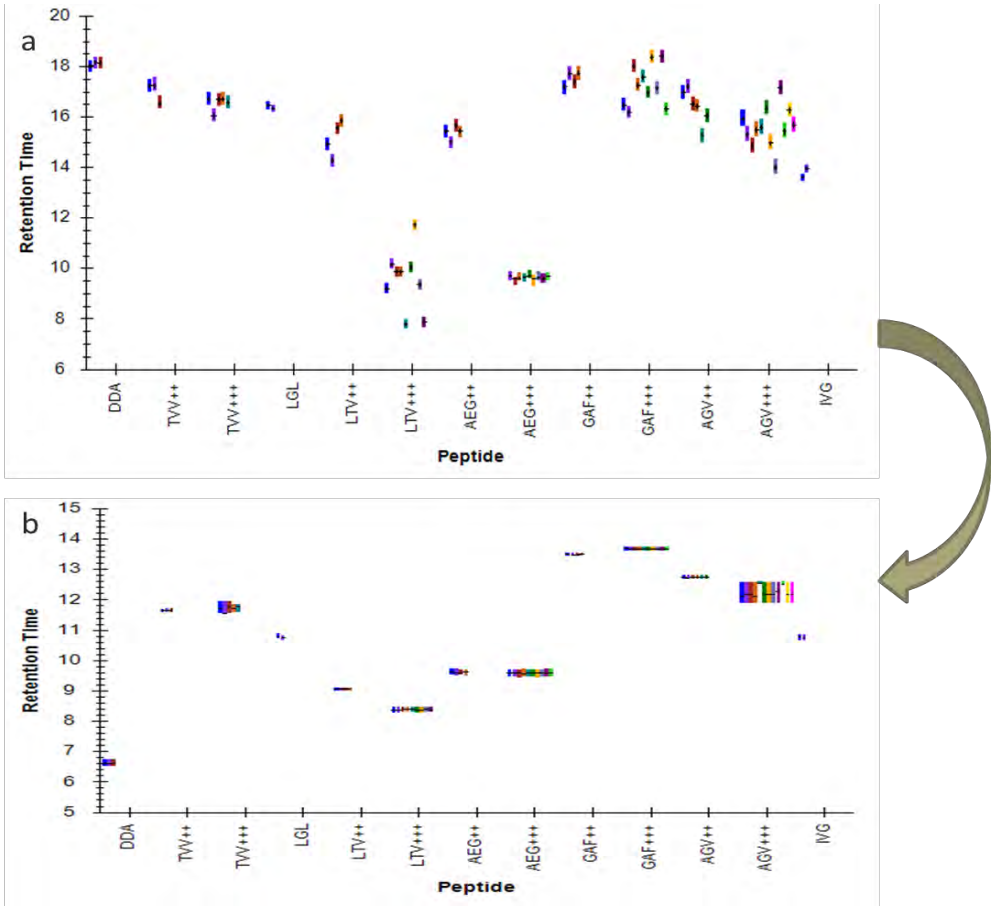

Figure 5.6: Spectra inspection clean-up for peptides depicted in Table 5.1. (a) shows scattered retention times the transitions that were observed for each peptide, suggestive of the picking of incorrect transitions from different peptides. (b) shows aligned transitions per peptide all eluting at the same retention time per peptide indicative of transitions from the same peptide. Each colour represents a single transition for the particular peptide.

For each peptide assessed, the output spectra contains retention time, peak area under the curve for all transitions as seen in Figure 5.7 depicting the spectrum obtained for Rv3412 from the Beijing strain. The area under the curve for each single transition was used as the surrogate for the amount of peptide and all individual areas under the curve for each transition per peptide were summed to give the total area under the curve per peptide. The area under the curve for

each single transition per strain was obtained from the results in skyline as shown in Figure 5.8 below.

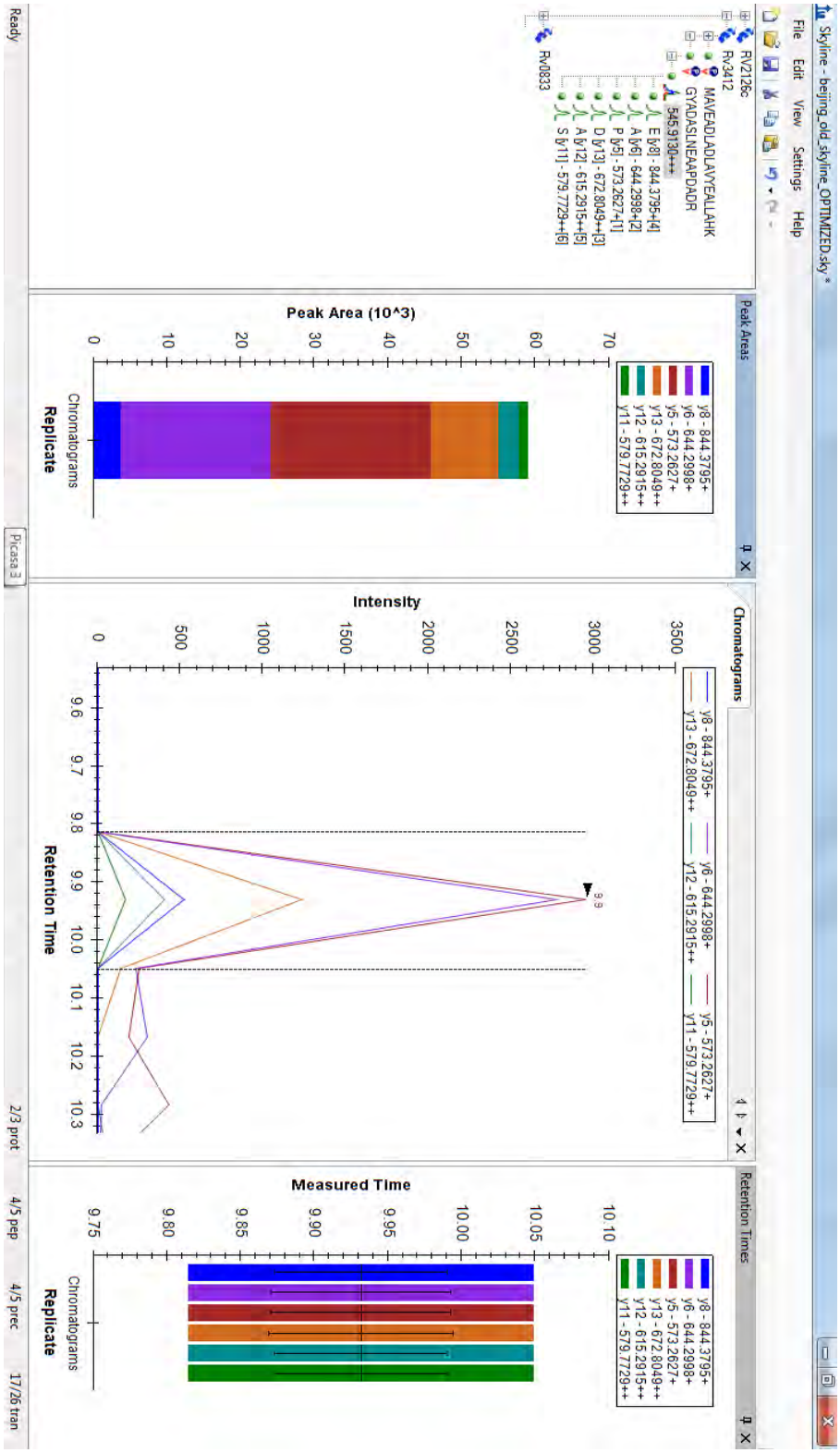

Figure 5.7: Typical output obtained from Skyline software using the example of the GYADASLNEAAPDADR peptide from the Rv3412 protein assessed in the W-Beijing strain. The bar graph shows the contribution of each transition to the summed peak area. The 'measured time' panel shows the retention time of each transition.

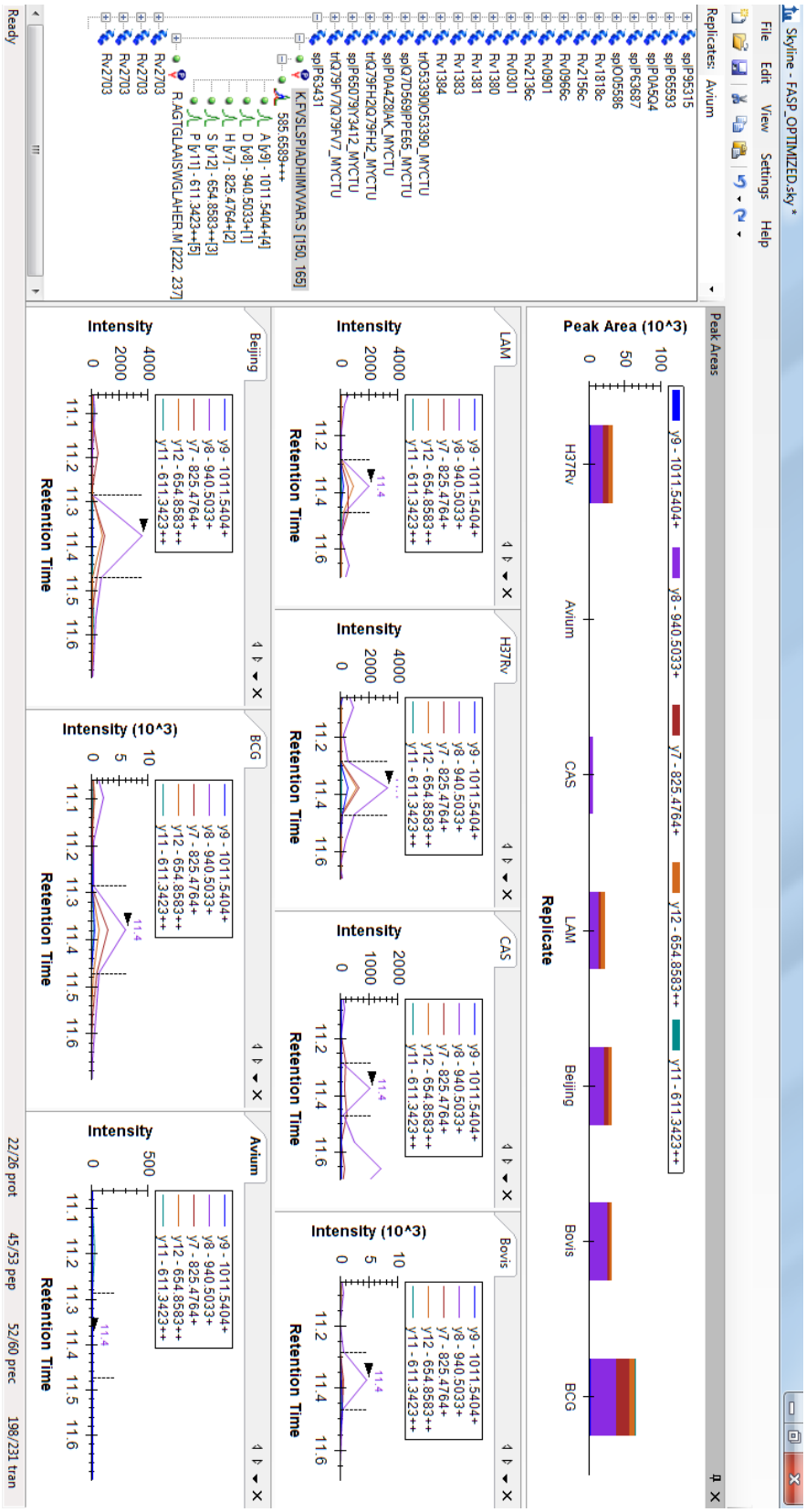

Figure 5.8: Screenshot obtained from Skyline software showing the spectra output for the K.FVSLSPIADHIMVVAR.S peptide from Rv1346 across the 7 strains. The figure shows that 5 transitions were used to identify this peptide. The spectral output shows that *M. avium* has the lowest signal as shown in the spectrum and in the corresponding peak area.

Having obtained the spectra and individually assessed them to remove incorrect transitions as described, the peak areas of each individual transition per peptide were then further assessed to separate signal from machine generated noise. The total signal to noise ratio was set at 5 to so as to eliminate the endogenous machine signal. Protein normalization was carried out based on the essential number of cells of each individual culture at extraction. Intra-assay and inter-assay coefficients of variation were determined for each individual peptide (Table 5.6). Intra assay variability was based on 3 technical replicates per strain whilst inter assay variability was assessed based on 2 biological replicates. Two peptides were used for the confirmation of each protein however for the purpose of relative quantification; a single peptide per protein with the lowest overall CV across samples was used to compare samples and to infer differential expression of the parent protein.

	Intra-assay variability (technical replicates)		
	Peptides with CV<10%	Peptides with CV>10%<20%	Peptides with CV<20%
H37Rv	29	11	1
Avium	39	3	1
CAS	34	8	2
LAM	34	4	4
Beijing	44	1	1
Bovis	37	7	3
BCG	41	4	2
	Inter-assay variability (biological replicates)		
	Peptides with CV<10%	Peptides with CV>10%<20%	Peptides with CV<20%
H37Rv	18	27	2
Avium	27	14	6
CAS	18	21	11
LAM	20	24	6
Beijing	26	11	11
Bovis	25	17	10
BCG	28	12	11

Table 5.6: The table shows inter and intra assay comparison of the 52 peptides from shortlisted proteins from the discovery experiment. Intra-assay and inter-assay variability was assessed for all assays. The assays were carried out in technical triplicates (intra-assay) and biological duplicates (inter-assay).

The peptide with the lowest CV across strains was chosen based on the assumption that the ionization and elution of the peptide remains similar across strains under similar conditions. This in turn results in the reduction of differences arising from inconsistencies in peptide behaviour in the LC MS column, which could otherwise cause sampling irregularities. For the proteins that were not found in the prior discovery experiment, only a single peptide had a successful assay for 19 of the 21 proteins. Intra-assay and inter-assay CV's of these peptides were more dispersed than those of the proteins that were observed in the prior discovery experiment suggesting that there are wider discrepancies in the behaviour of these peptides in the LC-MS column. Relative quantities were assessed by comparing the log signal intensities of each peptide (sum of all transitions of the peptide) per strain.

The signal for each peptide observed was obtained by summing up the peak areas of each transition of that peptide and then normalizing by the total number of cells per strain at the point of protein extraction. The number of cells was determined using the OD of each culture at extraction based on experimental evidence that OD_{600} 1 equals approximately 10^8 cells [309]. All proteins were observed in each sample albeit at different levels (Figure 5.9). The proteins were broadly classified into 4 groups denoting some aspect of the organisms' success in the host.

In general, clinical strains stood out in terms of expression of all the proteins in each group. Protein expression of the *M. tuberculosis* LAM strain stood out in the category of 'growth in host' with it being we observed that this strain had the highest protein signal per cell for half of the proteins in this category. This suggests that amongst these study strains, the LAM strain is possibly the most superior to grow in the host.

The contrasting down-regulation of Rv0301 in the LAM strain is plausible given that this protein is associated with negative regulation of growth meaning that it decreases the growth rate. With the exception of the Beijing strain, all other strains express this protein at a low level *in vitro* suggesting that only the Beijing strain has a propensity for reduced *in vitro* growth. Whether this is repeated *in vivo* remains to be determined. Another factor that could affect the phenotypic effect of this protein is the neutralising anti-toxin counterpart Rv0300 which was not assessed in this study.

In the category of 'response to stress conditions', there is no distinct repetitive theme, suggesting that within and outside the MTBC, there is a competitive level of resilience to various stress conditions. This comes as no surprise as members of the genus Mycobacterium are generally well equipped to survive in diverse environments [11]. Due to the fact that these conditions are not limited to infection environments, it is expected that they could be useful in other mycobacteria other than clinical strains.

In the 'host immune system evasion and virulence' category, for this particular set of proteins, the dominating strain is the Beijing strain. The expression of 4 of the 6 proteins in this group is highest in the Beijing strain (Rv2136c, Rv1002c, Rv2108 and Rv2703). Although protein Rv0966 is down-regulated in the Beijing strain, it is up-regulated in the LAM strain which is a competing clinical strain in terms of abundance in the South African context [310,311]. The function of this protein is unknown but it is thought to be up-regulated in the early stages of blood brain barrier invasion in central nervous system tuberculosis [312–314]. Rv2156c which encodes mpt64 is also present at elevated levels in the Beijing and CAS strain but it is highest in *M. avium*.

With the exception of Rv1818c, the drug response proteins assessed in this study form part of an operon (Rv1380-1384) which encodes the proteins pyrA, pyrB, pyrC, carA and carB. Although the primary function of this operon is not drug related, studies to ascertain its involvement in 5-fluoro uracil treatment are in progress (Mizrahi *et al*, unpublished data). For the 4 protein members of this operon assessed in this study, *M. avium* was showed the highest protein expression for all except Rv1384. Rv1818c had the highest expression in the CAS clinical strain but remained relatively low in other strains.

Drug Response

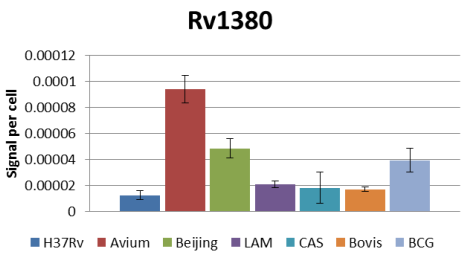

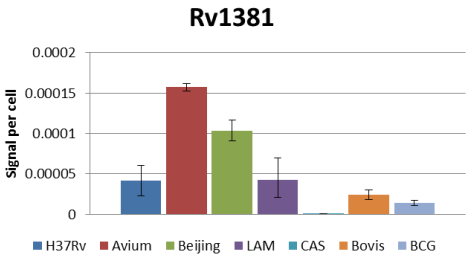

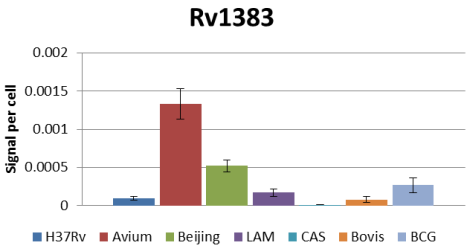

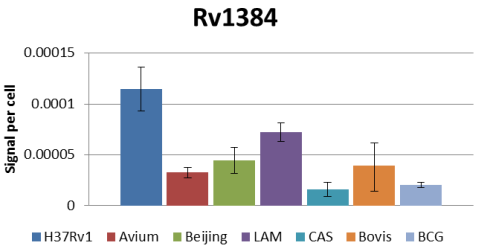

Modulation of immune response

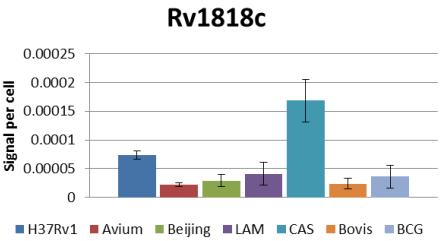

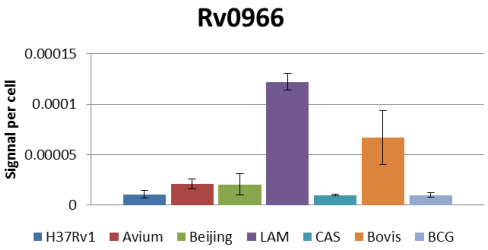

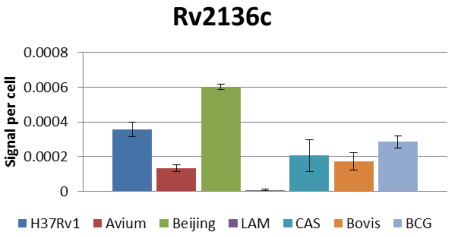

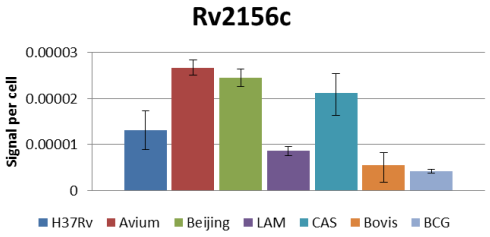

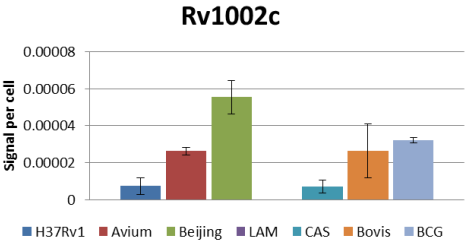

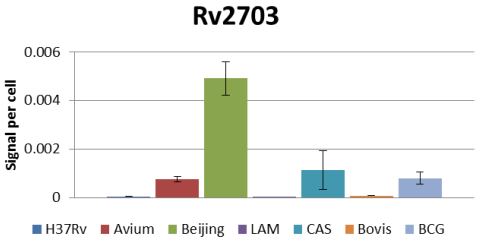

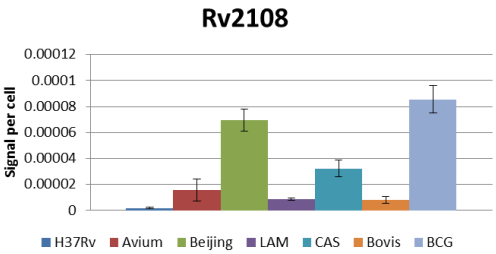

Growth in host

Rv0301

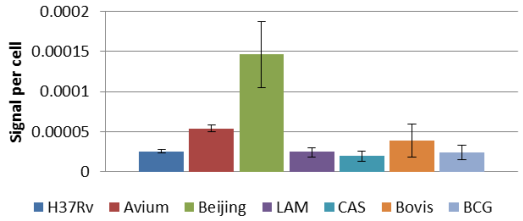

Rv0833

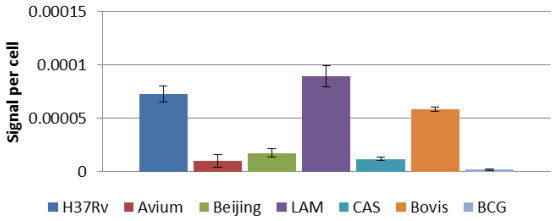

Rv3621c

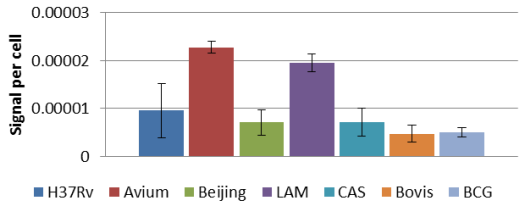

Rv3412

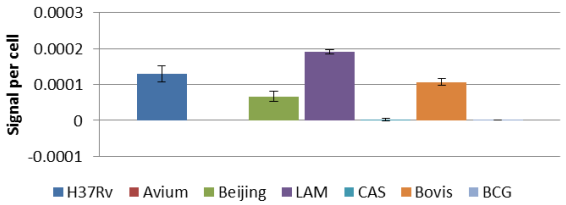

Rv2126c

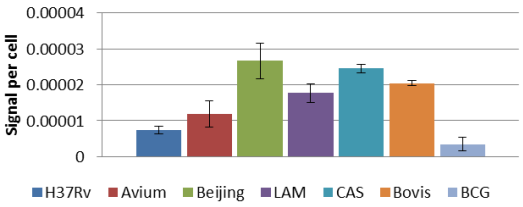

Rv3340

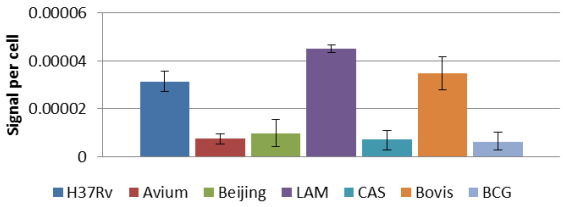

Adaptation to stress

Rv0899

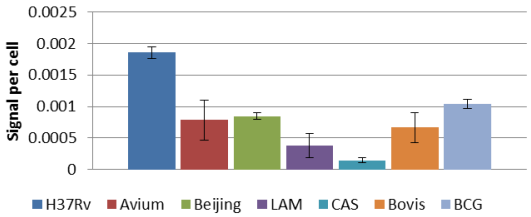

Rv1997

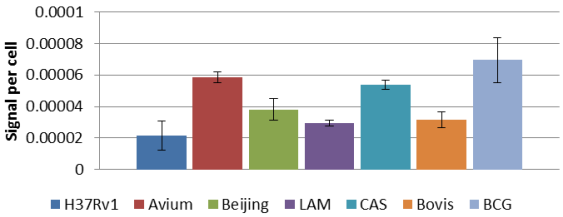

Rv3709c

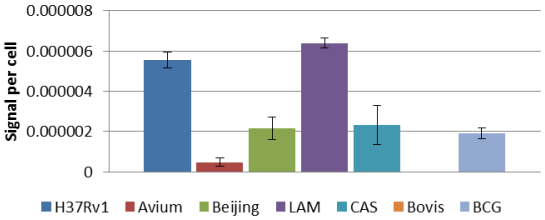

Rv1980c

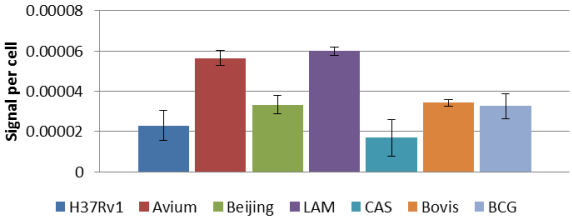

Rv0901

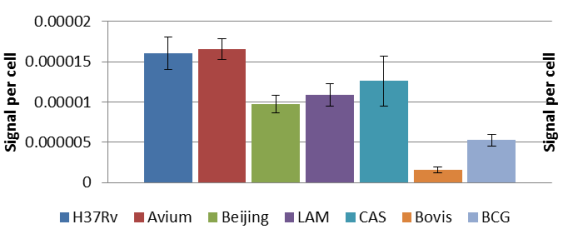

Rv1346

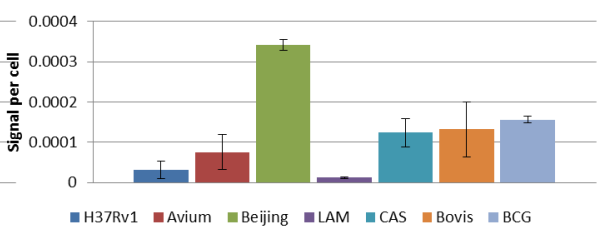

Figure 5.9: Relative quantitation of 23 proteins in in-vitro grown culture. The bar graphs represent signal per cell of each protein per strain based on the area under the curve as measured by MRM assay using one representative signature peptide.

An ANOVA test was used to determine if there was a significant difference in the expression of each of the peptides representing each protein. The single factor ANOVA results (Table 5.8) shows that of the 23 peptides assessed, 18 had a significant difference in expression amongst the 7 strains. Although the ANOVA test does not directly identify which strains the significant difference comes from, it becomes clearer when looking at the individual graphs (Figure 5.9) which strain or strains are responsible for the significance in the difference in expression.

Fold	Rv locus	Function & prediction from gene expression data	*p-value*
>5	Rv0301	VapC2; toxin; possible mRNAse; impaired growth when expressed | macrophage infection models	6,75E-07
	Rv0899	ArfA; outer membrane porin A; tolerance to acidic conditions, impaired growth at pH 5.5	6,42E-06
	Rv0901	ArfC; **unknown function**; tolerance to acidic conditions, impaired growth at pH 5.5	1,96E-05
	Rv0966	**Unknown function**; highly activated in the early stages of tuberculosis blood brain barrier invasion (CNS TB)	9,35E-07
	Rv1002C	Probable mannosyltransferase; sec dependant pathway, conserved membrane protein growth and survival in host	0,020716
>3	Rv1346	MbtN; mycobactin biosynthesis; iron scavenging, adaptation to intracellular environment |stress response models	0,039441
>2	Rv1380	PyrB; pyrimidine biosynthesis; essential for growth; high confidence drug target | drug response models	4,59E-09
>2	Rv1381	PyrC; pyrimidine biosynthesis; growth and survival in host | drug response models	1,08E-06
>2	Rv1383	Car A; pyrimidine biosynthesis; growth and survival in host | drug response models	4,47E-09
	Rv1384	CarB; pyrimidine biosynthesis; growth and survival in host	0,422015
	Rv1980c	Mpt64; **Unknown function**; tolerance to starvation, highly immunogenic; vaccine and drug target potential	0,876293
	Rv1997	CtpF; Metal cation-transporting ATPase; implicated in dormancy/persistance, response to hypoxia, NO	0,988059
	Rv2108	PPE36; **unknown function**; immuno-active membrane component; diagnostic and vaccine target	5,32E-12
	Rv2126c	PE_PGRS37; **unknown function**; possible virulence/adaptation	0,97868
>3	Rv2136c	UppP; undecaprenyl pyrophosphatase; high confidence drug target | host immune evasion &virulence models	0,026023
	Rv2156	MraY; peptidoglycan biosynthesis; growth and survival in host, high confidence drug target	0,649041
>5	Rv2703	Sig A; primary sigma factor in M.tb; host immune response modulator, virulence, growth in host, high confidence drug target | host immune evasion &virulence models	3,27E-07
	Rv3340	MetC; methionine biosynthesis; growth and survival in host	0,035777
	Rv3412	**Unknown function**; hypothetical protein; essential for cholesterol metabolism, essential during infection	1,23E-05
	Rv3621c	PPE65; **unknown function**; possible virulence/adaptation	1,61E-06
	Rv3709c	Ask; asparate kinase; survival in host	9,79E-08
	Rv1818	PE-PGRS33; **unknown function**; modulation of host immune response, response to oxygen and starvation	6,10E-06
	Rv0833	PE_PGRS13; **unknown function**; possible virulence/adaptation	5,55E-08

Table 5.8: ANOVA analysis of the signal of each protein across strains. The analysis of variance shows that 18 of the 23 have significant differences in their expression as seen by the p-values below 0.05. The proteins depicted in blue are those with insignificant fold change. Those depicted in red are over expressed in the W-Beijing strain. Those in black are significantly differentially expressed in other strains.

5.3.4 Assessment of quantitative accuracy of shotgun label free quantitation

To assess the validity of the discovery experiment, spectral counting expression values (NSAF) of the target proteins that were obtained at 1% FDR in the previous chapter were compared to the relative quantitation results of the MRM analysis obtained in this chapter. This was done to

observe if the trends from the discovery experiment are maintained in the targeted MRM analysis and thereby to assess the extent to which the semi-quantitative predictions in the discovery experiment hold true.

Proteins chosen for analysis by MRM were previously found in the discovery experiment by two or more peptides as previously mentioned. It must be clarified that these were part of the 168 proteins that were observed only in *M. tuberculosis* strains. However, they were differentially found among the *M. tuberculosis* isolates in the discovery experiment as their expression was observed variably in some but not all strains in some instances as shown in Figure 5.20. The results demonstrate a shortfall in the sampling of proteins in the discovery experiment. Most of the proteins were observed in the pathogenic clinical strains in the discovery experiment with the exception of Rv2156c which was chosen as a control expected to be found in all strains. The MRM experiment however observed all the proteins in all the strains. This can be justified by the sensitivity and the specificity of the MRM experimental platform which has two levels of selectivity, namely the precursor and product ion level. This allows for the precise selection of the specific peptide even in the presence of incorrect co-eluting peptides, regardless of their abundance.

The second observation made in comparing the 2 types of mass spectrometry approaches was that in most cases where a single observation was made in the discovery experiment e.g. Rv0301 and Rv1002c which were observed only in the Beijing strain in the discovery experiment, the targeted MRM experiment showed expression in all the strains, but with the Beijing strain showing the highest level of expression. This data points towards a concentration issue in the sampling of the discovery experiment. Where the concentration of the protein in a particular sample is lower, it is not easily sampled in the discovery experiment hence it is artificially absent. This appears to be clearly the case for 14 of the 23 proteins assessed (Rv0301, Rv1381, Rv1383, Rv1002c, Rv3709c, Rv1346, Rv3412, Rv2108, Rv3621, Rv0833, Rv0966c, Rv1818c, Rv2136c, and Rv3340).

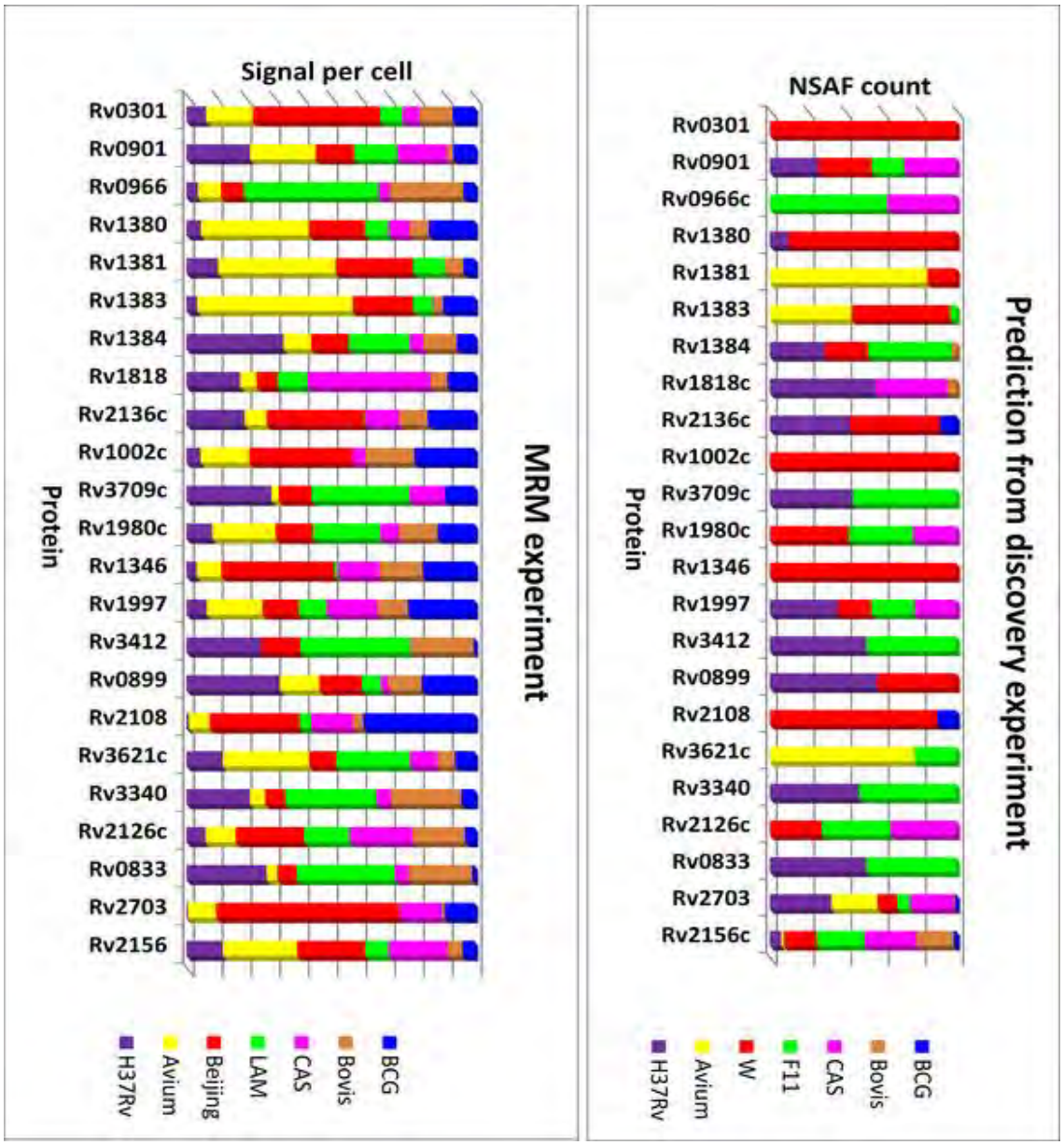

Figure 5.20: Comparison of relative protein signal between discovery and targeted MS experiments. The colour coded stacked bar graphs represent the contribution of each strain to the total signal of the specific protein.

The discovery experiment carried out across the 7 strains collectively found all but 178 proteins in the total H37Rv fasta file. Analysis of the 178 proteins for which we obtained no previous discovery data showed that approximately half had ≤1 tryptic peptides per protein (Figure 5.21) which limits the chances to find those peptides using the shotgun proteomics methodology. A total of 45 of these proteins were randomly assessed without any prior filter criteria except the presence of at least one tryptic peptide. The reason for the random choice was that these were not observed in the discovery experiment in any of the strains assessed. However, these proteins were still put through the filtering process of removing non-unique peptides against the background of the human and Mycobacterial proteome, removal of

peptides with methionine's and multiple cysteine residues as before. A maximum of 3 peptides per protein was initially sampled where possible, however for 90%, 1 peptide passed the assessment phase even after multiple rounds of optimization. Table 5.10 shows the 20 proteins out of the 45 that were sampled for which SRM assays were successfully designed. The successful peptides and transitions are that were assessed is shown in the assay in Annexure Table 5.1. It is noteworthy that almost half of the proteins that were not observed in the discovery experiment have either one or no tryptic peptide at all which reduces the chances of those proteins to be found using MS hence possibly explaining their absence from the discovery experiment data.

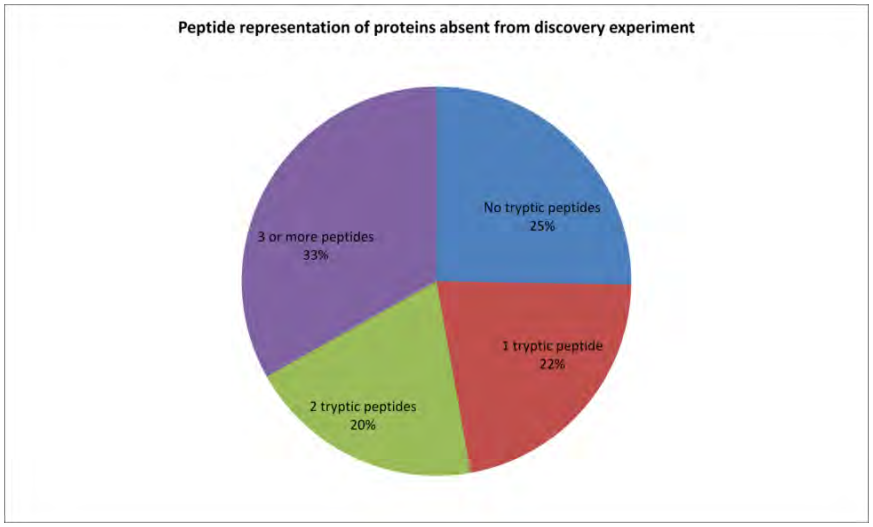

Figure 5.21: Pie chart depicting the peptide statistics of proteins that were not observed in the discovery experiment.

5.3.5 MRM assessment of shortlisted candidates that were not observed in shotgun-MS

Contrary to the proteins that were previously found in one strain in the discovery experiment, these proteins were observed in some but not all strains hence the difference in their expression is not only quantitative but also binary (i.e. present/absent). Analysis of variance was carried out and it was observed that there was significant differential expression for all the 20 proteins assessed (Table 5.10; Figure 5.22).

Rv locus/ Protein	Name	Biological role	Possible phenotype association	Evidence
RvBD_2894	Polyphosphate kinase ppk1	kinase/transferase, phosphoprotein	Unknown	Inferred from homology
A6ZI23	RNA polymerase beta subunit (Fragment) rpoB	DNA dependant transcription (fragment)	Possible association with drug resistance	Inferred from homology
A9X5B9	Gyrase B (Fragment) gyrB	DNA topoisomerase (fragment)	Possible association with drug resistance	Inferred from homology
RvBD_0304c	PPE Family protein	Unknown	Unknown	Predicted
RvBD_1651c	PE-PGRS Family protein	Unknown	Unknown	Predicted
Rv0834c	PE-PGRS14	Unknown	Unknown	Predicted
P72016	SecA protein	Transporter, secretion system	Virulence	Predicted
D9YMC3	RNA polymerase beta subunit (Fragment) rpoB	DNA dependant transcription (fragment)	Possible association with drug resistance	Predicted
Rv2519	PE 26	Unknown	Unknown	Predicted
Rv1983	Uncharacterized PE-PGRS family protein PE_PGRS35	Unknown	Unknown	Inferred from homology
Rv1198	ESAT-6-like protein esxL	Unknown	Unknown	Inferred from homology
Rv0603	Possible exported protein	Unknown	Unknown	Evidence at protein level
O33172	Hypothetical invasion protein INV2	Possible hydrolase	Attachment and entry of the bacterium into host cell, drug resistance	Predicted
O52051	PGB14T-P (Fragment)	Unknown	Signal protein, Response to antibiotic	Predicted
Rv3021c	Uncharacterized PPE family protein PPE47	Unknown	Highly activated in the early stages of blood brain barrier invasion	Evidence at transcr level
Rv2376c	Low molecular weight antigen MTB12 cfp2	Unknown	Immunogenic	Evidence at protein level
P96292	FtsE (Fragment)	ABC transporter (fragment)	involvement in cell division	Inferred from homology
Rv1037c	ESAT-6-like protein esxI	Unknown	immunogenic	Evidence at protein level
Rv3286c	SigF stress response factor fragment	DNA dependant transcription (fragment)	stationary phase response	Predicted
Rv0827c	Transcription regulation	Unknown	Response to metal cations	Evidence at protein level

Table 5.9: The proteins that were not found in the discovery experiment in any strain for which successful SRM assays were designed and carried out. ID mapping of some of the proteins from UniProt to Tuberculist Rv numbers was not possible hence where Rv numbers were not present, the UniProt ID was maintained.

Fold change	Rv locus/Uniprot ID	Function & prediction from gene expression data	p-value
>3	RvBD_2894	Polyphosphate kinase ppk1	1.79945E-06
>2	A6ZI23	RNA polymerase beta subunit (Fragment) rpoB	1.68806E-07
>5	A9X5B9	Gyrase B (Fragment) gyrB	1.64152E-10
>2	RvBD_0304c	PPE FAMILY PROTEIN	1.54805E-07
>2	RvBD_1651c	PE-PGRS FAMILY PROTEIN	2.58259E-13
>2	Rv0834c	PE-PGRS14	7.35049E-16
>3	P72016	SecA protein	0.000344283
>2	D9YMC3	RNA polymerase beta subunit (Fragment) rpoB	1.09876E-11
>3	Rv2519	PE 26	2.05188E-12
>2	Rv1983	Uncharacterized PE-PGRS family protein PE_PGRS35	1.14859E-06
>2	Rv1198	ESAT-6-like protein esxL	1.2092E-12
>3	Rv0603	Possible exported protein	1.89818E-11
>3	O33172	Hypothetical invasion protein INV2	5.78381E-14
~2	O52051	PGB14T-P (Fragment)	6.16316E-06
~2	Rv3021c	Uncharacterized PPE family protein PPE47	0.000204594
>2	Rv2376c	Low molecular weight antigen MTB12 cfp2	1.92486E-14
>2	P96292	FtsE (Fragment)	0.000344283
>3	Rv1037c	ESAT-6-like protein esxI	9.65808E-13
>3	Rv3286c	SigF stress response factor fragment	1.95137E-06
>2	Rv0827c	Transcription regulation	2.58432E-09

Table 5.10: ANOVA analysis of the signal of each protein across strains. Analysis shows that all the proteins have significant differences in their expression as seen by the p-values below 0.05

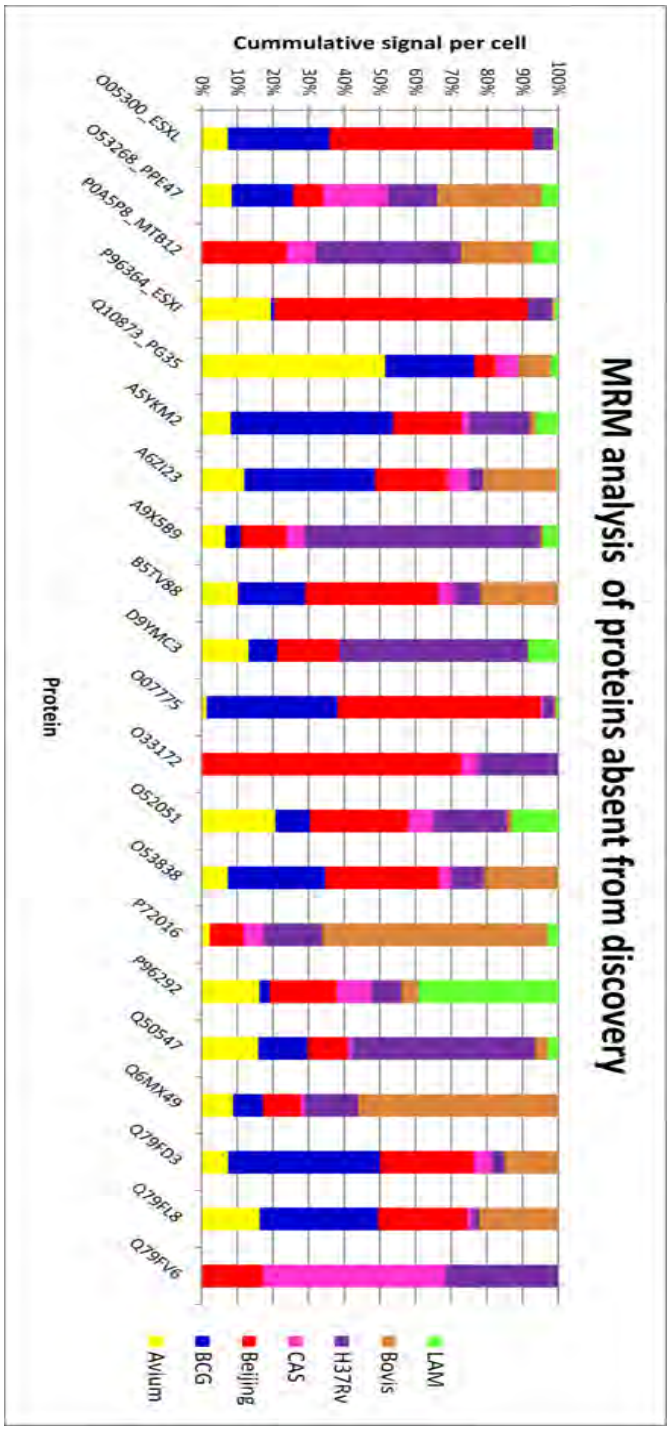

5.11: MRM MS protein signal of proteins that were not found in the discovery MS experiments: the colour coded stacked bar graphs represent the contribution of each strain to the total signal of the specific protein.

5.4 Discussion: Implication of differential expression

We utilised mass spectrometry tools to validate a total of 43 proteins in 7 strains of mycobacterial cultures *in vitro*. 23 of the proteins had previously been observed in a prior

discovery experiment and the remaining 20 had not been previously observed in any strain. The first 23 proteins were assessed based on their differential presence in the prior discovery experiment and were chosen based on filter criteria linking to enhanced pathogenicity or virulence; the second set of 20 proteins were randomly chosen.

In the South African context, the Beijing and LAM strains are known to have highly virulent phenotypes. An in depth literature survey of the significant differentially expressed proteins in these 2 strains was carried out to determine how those proteins might impact on virulence and establish possible phenotype links. Significant proteins that are up-regulated in the LAM strain include Rv3340, Rv0833, Rv3621c, Rv3709c, Rv3412 and Rv0966c.

A transcriptomic study by Jain *et al*, identified a group of genes up-regulated in the early stages of blood brain barrier (BBB) invasion of tuberculosis in a CNS invasion model. This study identified a group of 18 genes that belong to a genomic island that was previously described as expressed in *in vivo* models [315]. The genomic Rv0960-Rv1001 was found to contain genes whose mutations resulted in the failure of BBB invasion in the invasion model. Our MRM assay assessed one of those genes, and although expressed in every strain, it was more highly expressed in the LAM strain by several orders of magnitude higher than other clinical strains. In the model by Jain *et al*, this specific protein had an 18 fold change in expression, identifying it as potentially important in the mechanism of invasion.

This protein was found to be non-essential for *in vitro* growth hence suggesting its possible utility in *in vivo* survival or virulence. The amount of the protein in the gene expression study model was found to be congruent with the ability to traverse the BBB as seen by the difference between *M. smegmatis* and *M. tuberculosis*. Furthermore, they found no difference in the gene expression signal of this protein between *M. tuberculosis* and *M. bovis* BCG, which is consistent with the result in this proteomic MS study (Figure 5.9). This reiterates that BCG exhibits an equal propensity of invasion hence its major difference with clinical strains is surviving the immune response. It is known that approximately 1% to 10% of active TB patients develop TB-meningitis especially in HIV co-infected persons [316–318]. Although it is not widely documented which strains are found associated with CNS tuberculosis, a study of CNS-TB by Arvanitakis *et al* 2008 used RFLP analysis to demonstrate that there was a predominance of type 1 RFLP pattern in individuals with CNS-TB compared to any other type of restriction pattern [318]. In a simple study in guinea pigs, it was demonstrated that while invasion of the lungs by *M. tuberculosis* is comparable between H37Rv and CDC1551 strains,

CNS invasion of the two strains is largely different alluding to the notion that certain strains invade the CNS more efficiently than others [312].

Toxin antitoxin (TA) systems have been widely studied in bacteria and it has been proven that they are associated with programmed cell death under stress conditions such as starvation, antibiotics exposure, oxidative stress and DNA damage exposure amongst others [319–323]. Toxin Rv0301 is a component of the vapBC TA system, which is one of the most well characterised TA systems in *M. tuberculosis*. The toxin component Rv0301 (vapB) acts as a negative regulator of transcription by enabling mRNA cleavage [324,325]. The overproduction of MazF, a similar toxin component of a TA system found in *E. coli* causes complete cell growth arrest, resulting in a quasi-dormant state in which the cells still retain full capacity for protein synthesis [326,327]. Whilst negative growth regulation may at first sight be considered detrimental for pathogenesis or virulence, activation of these proteins actually allows the bacterium to readily adapt to stress in two ways. Firstly they inhibit cellular replication, which is protective to the bacterium, and secondly they degrade existing transcripts which allows them to rapidly change the metabolic program of the bacterium into a program that suits the new environment [328]. This present study suggests that the W-Beijing strain may be the most capable of stabilising in a new environment due to the elevated amount of Rv0301 expressed.

Rv1346 is a mycobactin biosynthesis protein (mbtN) which is regulated by a conserved iron acquisition locus in response to low iron conditions, such as those experienced in the host macrophage. Mycobactins are cell surface lipids that are indispensable for the growth of the tubercle bacillus and are required for the establishment and maintenance of tuberculosis infection [329,330]. They are responsible for scavenging iron from the host cell which is required since iron is a co-factor for many enzymatic reactions of the pathogen [331,332]. Mycobactin biosynthesis is a known virulence pathway which, when deleted or perturbed, results in the attenuation of the organism and failure to establish infection [120,333].

The unique role of Rv1346 (mbtN) in this virulence pathway is the production of acyl-S-ACP intermediates which are required for the formation of di-dehydroxy-mycobactins (DDM), the precursors to mycobactin [329]. In this study, mbtN was found to be highly up-regulated in the Beijing strain compared to any other strain, suggesting that this strain may have superior predisposition to form mycobactin intermediates which are then converted to mycobactin. This suggests that this strain is more adapted to the intracellular habitat and that it may be more capable of establishing infection and survives longer under host pressure of iron starvation.

Another significantly differentially expressed protein that is over-expressed in the W-Beijing strain is Rv2136c which encodes an undecaprenol pyro-phosphatase30 protein that is involved in peptidoglycan assembly. It is known to be involved in acid resistance/tolerance mechanisms of the pathogen that enable it to survive the low pH of activated macrophages. Induction of acid tolerance is known to be required for virulence in numerous organisms such as *Salmonella, Staphyloccocus*, *Streptococcus* and *Mycobacterium tuberculosis* [334,335]. It has previously been shown that mutation of a known acid tolerance gene, mgtC, in *M. tuberculosis* results in attenuation and failure to establish infection in mice [118]. Likewise, the mutation of Rv2136c resulted in a similar attenuation outcome, indicating that Rv2136c is important for establishing infection and conferring several stress resistance properties over and above acid tolerance [335].

Mutations to 5 acid tolerance genes, including Rv2136c, showed that the resultant phenotypes were not only hypersensitive to acidic conditions but also showed hypersensitivity to antibiotics, heat shock as well as reactive oxygen and nitrogen intermediates. This further suggested that the acid tolerance/resistance associated with this gene is coupled to resilience to other forms of stress [335].

Rv2703 (sigA/rpoV) is one of the major transcription factors in *Mycobacterium tuberculosis*. The significance of this transcription factor in defining virulence was displayed by a single point mutation (R515H) in H37Ra and *M. bovis* strain which converted the strains to avirulent forms thus suggesting that this sigma factor is important in transcribing a repertoire of housekeeping genes including genes involved aroA, rpoB, dnaJ, grpE and the 35 kDa protein amongst others [336,337]. Furthermore, the failure to create a knockout mutant of this gene unless complemented by inserting another copy elsewhere into the chromosome reiterates the essentiality of this gene [136]. This sigma factor is not limited to the transcription of virulence factors however specific mutations in it result in the failure to recognise and bind to promoters of certain virulence genes hence halting their expression.

It was initially assumed that this gene would be equally expressed across all strains since it is a principal sigma factor. However this study shows that this protein is significantly differentially expressed, with the Beijing strain exceeding other strains by more than 5 fold. Since this protein is in part indirectly responsible for virulence, this could imply that the W-Beijing strain has a level of virulence above others due to a higher rate of synthesis of the sigA regulated virulence factors. It has also been previously been reported in a separate study by Wu *et al*, that

SigA is over-expressed in a W-Beijing strains cultured in macrophages compared to H37Rv [338].

Rv2108 is a member of the PPE family of genes which encodes a putative p27 protein. Little is known about this protein although it has been cloned and expressed in bacterial vectors. The recombinant protein has been used to show that there are anti-Rv2108 antibodies in TB patient serum, hence suggesting that this protein contributes to the elicitation of the host immune response by *M. tuberculosis*. This comes as no surprise as PPE proteins have been predicted to be targets for the protective immune response [339]. Immuno-blot analysis also found this protein to be present in *M. bovis* BCG and other human clinical isolates of the MTBC [48,340,341].

This literature suggestion of specificity to the MTBC, coupled with the strong immunogenic nature of the protein led to the idea that it can be used as a biomarker or possible vaccine target. Here, it was found to be strongly expressed in BCG and the Beijing strain over other strains in but it was also found to be present in *M. avium*, a Mycobacterial species outside the MTBC, albeit at a lower amount. This observation is consistent with the fact BCG is active enough to produce sufficient responses that mimic infection to prepare the host for genuine infection. Alongside BCG, the Beijing strain has competing levels of Rv2108 suggesting that it elicits the p27 specific immune response in a similar manner to BCG but enhanced compared to the other strains under study. This could relate to a mechanism whereby Beijing strains are able to evade BCG immunization as has previously been recorded in literature [342].

Rv1002c is a membrane phosphate-O-mannosyltransferase which is part of the secA dependant protein export pathway. It is used for the post translational modification of protein by the addition of mannosyl groups in mannoprotein assembly. This mannosyl dependant pathway has largely been described in eukaryotes and members of the genus *Mycobacterium* are the only bacteria currently known to have this pathway [343]. Rv1002c is a homolog of a conserved eukaryotic protein which is known to catalyse the first step in the mannosylation process, meaning that this process is conserved between the eukaryotes and *M. tuberculosis*. Rv1002c and its homologs are normally used for protein glycosylation through secretory pathways, hence they are secreted or membrane proteins [344]. It is well known that most glycosylated *M. tuberculosis* culture filtrate proteins play important roles in infection and are recognised by the host immune system and their antigenic nature makes them possible vaccine targets.

The importance of the O-mannosylation pathway in *M. tuberculosis* and its homolog in *M. smegmatis* were assessed by inactivating Rv1002c and Msmeg_5437 respectively. Although there was no associated change in the *M. smegmatis* mutant, the *M. tuberculosis* mutant suffered highly reduced growth *in vitro* and attenuation of pathogenicity in *in vivo* mice models [345]. This immediately suggests a central role for this post translational modification, not only in the general physiological growth of the pathogen but also in its virulence in the host.

The T-cell response induced by anti-polymer antibody assays (APA) is dependent on its glycosylation status, specifically of the O-mannosylation of four of their threonines [346] which is made possible by Rv1002c. This further illustrates the importance of this protein during the infection process and suggests that differences in levels of this protein would thus have an effect on the virulence in the host. The present study shows that there is significant differential expression of this protein amongst the study strains. The Beijing strain is seen to produce the highest levels, exceeding other strains by up to 6-fold difference. This suggests that this specific O-mannosylation could occur more readily in W-Beijing strain compared to other strains thus resulting in a more pronounced immune response and the pathology that comes with it.

PE_PGRS33 was the only protein which was highly up-regulated in the CAS strain. This is a cell surface protein that has been shown to be involved in host cell attachment and invasion of host [347]. Like many PE_PGRS proteins, it has been shown by transposon hybridization experiments to be essential for adaptation to stress conditions, specifically nutrient starvation and anoxic conditions [40]. More recently it was shown to be involved in immuno-modulatory functions that promote the release of TNF-α from macrophages in a toll like receptor 2 dependant manner [348].

It is widely known that TNF-α is essential for the maintenance of the granuloma and the control of tuberculosis [349]. TNF-α is also known to be essential for successfully combating tuberculosis infection by triggering apoptosis of infected macrophages using classical caspase pathways [348]. Importantly, it has been shown that mutations [350,351] of this protein, such as those present in some clinical strains, results in the attenuation of this TNF-α killing pathway. Furthermore, inactivation of TNF-α is linked to the ability of *M. tuberculosis* to evade apoptosis of host macrophages.

It becomes clear that the mechanisms that mycobacteria use to regulate TNF-α induction are related to the regulation of key events such as the induction of pro-inflammatory cytokines/chemokines, which in turn determine whether the disease will take a protective or progressive nature [348]. In light of this knowledge, it can be postulated that strains that have a reduction in this protein could possibly have a similar reduction in the TNF-α killing pathway. This possibly results in reduced killing of these strains in macrophages and subsequently longer term survival. It is noteworthy that the most widespread strains in our context (LAM and Beijing) have highly reduced levels of this protein in this study which possibly enables them to evade killing by the TNF-α mediated pathway.

For the proteins that had not been observed in the discovery proteomics experiments (Chapter 4), targeted proteomics described here allowed the acquisition of semi-quantitative information on 20 proteins. Unlike the proteins that were previously found in the discovery analysis, some of these proteins were not found to be present in all strains in the MRM analyses, as shown in Figure 5.7. Using an ANOVA analysis, it was further shown that all the proteins have significant differential expression, as shown in Table 5.10.

Less than half of these previously unobserved proteins are functionally unannotated, thus restricting the ability to infer possible phenotypic effect based on differential expression. Some of the proteins that are functionally assigned are components of larger protein complexes, including A6ZI23, A9X5B9, C7FFT9, D9YMC3, O52051 and P96292 which form complexes with other well-known proteins such as RpoB, GyrB and KatG amongst others (Table 5.9). The functional contribution of these components to the performance of the whole protein complex is not yet known however. Thus although differential expression may be observed for these proteins, it is challenging to determine possible phenotypic differences that may result from these differences.

Protein O033172 was also observed in this study to be significantly overexpressed in the W-Beijing strains and furthermore, only expressed in *M. tuberculosis* strains. This is a protein thought to be required for the initial invasion of mammalian cells in mycobacterial strains. Proteins required for the initial attachment of mycobacterial cells to host cells were first recognised in *M. leprae* and more recently in *M. avium* [352,353]. The *M. tuberculosis* proteome was subsequently screened for homologs of these proteins and 2 homologs were found, denoted invA and invB. The conservation of the essential catalytic residue (Cys39) amongst others suggested that these proteins had conserved function across the organisms

[354]. Enhanced attachment of the pathogen to the host cell may enable infection to be established easier, thus suggesting that strains with higher levels of this protein per cell are likely more infective. This may begin to shed further light from a pathogen-centred molecular biology perspective to explain why W-Beijing strains are seemingly in the fore-front of establishing wide-spread disease in the South African context.

Rv2376c is one of the proteins that is actively secreted into the culture filtrate of *in vitro* grown culture, and like many other CF proteins, it invokes a strong immune response in human study donors stimulated with purified protein derivative (PPD) [355,356]. PPD is taken from culture filtrates of actively growing *M. bovis* BCG cells and contains a host of molecules including proteins, lipids, and a host of polysaccharides [357]. This immediately indicates that this protein is expressed *in vivo* as well. It elicits an immune response in a dose dependant manner, hence the more it is produced the stronger the immune response. Antibodies against this protein are found in healthy, TB disease free but PPD+ donors meaning that this protein either provides long lasting protective immune response for the host after exposure or that it is actively secreted by latent organisms (LTBI). As a result, this protein is a potential vaccine target for long term immunity against TB. In this study this protein was found in all except *M. avium* and BCG, with over-expression being observed in the H37Rv, W-beijing and M. bovis strains suggesting that it might infact represent an effective immunological decay.

Sigma factor F (sigF) is a transcription factor that was originally observed at the beginning of stationery phase in *in vitro* cultures of *M. tuberculosis* [152]. It was then initially postulated to be formed under conditions of nutritional stress however it was also detected under several other stress conditions such as oxidative stress, heat shock and acid stress [358]. SigF shows similarity to sporulation factors of *Streptomyces coelicolor* and *Bacillus subtilis* [139] that are produced under similar conditions, which led to the conclusion that this sigma factor is expressed *in vivo* under other stress conditions to transcribe genes that enable the organism to adapt to stress conditions. This suggests that this protein is produced in preparation for the pathogen to survive outside the host (synonymous with sporulation) or in preparation for a dormant-like phase, which is characterised by settling in a harsh environment [139]. This protein is produced in all strains however over-expressed in H37Rv by 3 fold difference.

Rv3021c also encodes the PPE47 protein which was also shown by Jain *et al*, to be up-regulated by a fold change of above 8 in CNS infection models [359]. It is also essential for *in vitro* growth, but its mode of action is unknown. Just like Rv0966c, this protein is present in

every strain, but Rv3021 is up-regulated in the *M. bovis* strain suggesting that the process of CNS invasion is standard across Mycobacterial strains yet different species may have different tendencies to the development of CNS infection.

Rv1037c encodes a possible component of a 2-component signalling system, based on inference from homology. These systems are useful for signal transduction, informing the pathogen on the state of its environment and allowing it to respond with respect to the surroundings. This protein is an ESAT-6-like protein and it is predicted to be part of the immuno-dominant family of proteins that, like ESAT-6, are secreted from the cell to invoke immune response [360,361]. Not much is known about this protein as it is currently inferred from homology. The remaining proteins studied here by MRM were of unknown function and although they exhibited significant differential expression between the strains, it remains to be determined whether they contribute a tangible phenotypic effect and if so, the mechanisms they may utilize to accomplish this.

5.5 Conclusion

Gene expression experiments deposited in TBDB were used as a reference template for the expression of candidate markers. However, it was also observed in this study that gene expression studies in TBDB are not necessarily transferable to other strains as we have observed here that protein expression differs between H37Rv and other strains.

Whilst the shotgun study was a hypothesis generating platform, the targeted MS technique that was used in this part of the study is a validation platform. A subset of the data obtained from the discovery experiment was validated using the SRM technology. The results obtained using this more sensitive and specific MS platform was not entirely identical to the shotgun experiment outcome. Although there were some parallels in the output between the two MS platforms, it became clear that some proteins that were not observed in some strains in the discovery experiment due to under-sampling that comes about as a result of concentration differences rather than actual absence. This can be in future overcome by further fractionation in the discovery experiment. The discovery MS experiment reported here analysed the sample in 10 fractions however some studies have reported up to 35 fractions [248]which enables greater separation of proteins resulting in the decrease in dynamic range. This then allows some peptides whose signal was previously clouded by more abundant peptides to be sampled.

The superiority of targeted MS SRM assays was established by its ability to detect proteins that were not observed in the previous shotgun experiment as well as identifying proteins in strains where the discovery experiment deemed them absent. This study suggests that it is most likely differences in the amount of proteins expressed rather than presence or absence of proteins that influences phenotype of strains.

Targeted quantitative MS analysis of the short list of candidate proteins across the strains uncovered previously unknown differences in the expression of several proteins which began to shed light as to which proteins to assess further when it comes to differential virulence. An in depth analysis of each of these proteins in disease models would be the next step in validating these proteins and possibly explaining mechanisms leading to clinical differential virulence. More-over, some of these proteins could potentially be utilised as biomarkers since the MRM assays for these proteins have now been established and can be used in any sample type.

In conclusion, although the LAM and Beijing strains are dominant in the South African populations, their mechanisms of action to achieve their success are quite different. This study uncovered possible proteomic basis of the success of W-Beijing strains, further suggesting strain specific selective bacterial fitness proteins semi-quantitatively and qualitatively. Factors involved in successful transmission dynamics of the W-Beijing strains may include: the ability to rapidly remodel the *M. tuberculosis* proteome in response to altered environments, upregulation of key sigma factors to support rapid transcriptional responses, upregulation of enzymes involved in pyrimidine biosynthesis to support transcription, upregulation of enzymes involved in cell wall biosynthesis to promote rapid growth, upregulation of mycobactin biosynthesis to promote iron scavenging in the new host and enhanced ability to establish primary infection and active TB disease in new host.

Whilst the mechanisms of added success of the Beijing strain are clear with respect to the proteins in this study, those of the LAM strain are quite elusive since most of the significantly up-regulated proteins in the LAM strain are not yet clearly understood in terms of function and mode of action. For such proteins, it becomes challenging to define possible phenotype associated with the up-regulation of that protein unless knock-out studies on mouse models are carried out. This means that a minor annotation gap must still be filled in order to fully understand the success of all strains. Furthermore, quantitative analysis of all proteins in a

high-throughput manner may further reveal similar biomarkers that contribute to differential phenotype.

Chapter 6

Semi-quantitative analysis of the expressed proteomes in clinical strains of *M. tuberculosis.*

6.1 Introduction

Liquid chromatography mass spectrometry (LC-MS) has become routinely used for the analysis of proteomes from complex samples. In proteomics, high resolution shotgun mass spectrometry has become the backbone for identification of thousands of proteins in given cell lysates. Quantitation of proteins in shotgun MS can be absolute or relative [219,220]. In absolute quantitation, accurate exact quantities of each protein in a sample can be determined for example by isotopically labelling the peptide samples before mass spectrometry using ICAT, SILAC or iTRAQ [241–244]. Whilst these methods are reasonably well established for absolute quantitation, they are expensive and require time consuming and complex sample preparation approaches [242].

Relative quantification of proteins in MS is a simpler, cheaper and time efficient alternative approach to absolute quantitation that does not involve any form of labelling of the peptides prior to MS assessment. This means that these methods are cheaper and faster as they do not require any additional steps in protein preparation. Although the quantitation output values obtained using relative quantitation are not exact protein concentrations, they do give an indication of relative protein abundance and by so doing quantitatively characterising changes in the expression of the proteins in different conditions or treatments [242].

There are two basic approaches to relative quantitation including spectral counting based and the spectral intensity based approaches. Intensity based approaches are based on the fact that mass spectral peak intensities of individual peptide ions correlate in a linear manner with the amount of the peptide and subsequently the amount of protein in the sample [250]. In intensity based absolute quantitation (iBAQ), the sum of intensities of all tryptic peptides for each protein is divided by the number of theoretically observable peptides. This is then normalised using the total ion count in that particular sample. The resulting iBAQ intensities provide an accurate determination of the relative of the proteins identified in a sample [362]. Relative abundance of different proteins in the same sample is theoretically less robust by iBAQ and yet has been used to estimate absolute copy number of each

protein per cell. iBAQ provides for relatively robust determination of the relative abundance of the same protein in different samples.

Spectral counting on the other hand is a form of label free quantitation that relies on the number of MS/MS spectra observed per protein as a measure of protein abundance. A number of tools are available for spectral counting based relative quantification of proteins which include normalized spectral abundance factor (NSAF), spectral index (SIn) and exponentially modified protein abundance index (emPAI) [198,218] that are described in Section 2.9.4.

High throughput qualitative and quantitative assessment of the proteome maps of *M. tuberculosis* strains may facilitate the identification of more markers of differential phenotype amongst strains of *M. tuberculosis* at global proteome level. This chapter therefore describes studies aimed at quantitation of the proteomes of 4 human clinical strains of *M. tuberculosis* strains, utilising state of the art MS instrumentation to relatively quantify the proteomic complement of the clinical strains using both spectral counting and intensity based relative quantitation approaches.

6.2 Materials and methods

6.2.1 Cell culture and protein extraction

Mycobacterium tuberculosis isolates H37Rv, W-Beijing, CAS and LAM3 were obtained from the medical microbiology unit of the University of Cape Town (UCT), Stellenbosch University, as well as the NHLS. These strains are described in Chapter 4 in Section 4.2.1 (Table 4.1). Cells were cultured for approximately 4-6 weeks in Sautons media as described in Section 4.2.2. Proteins were extracted and quantified from cell pellets and culture filtrates as described in section 4.2.3. Proteins from each of the four separate cultures were prepared for MS/MS using the FASP method as described in Section 5.2.2.1.

6.2.2.1 Data dependant acquisition Q-Exactive

Protein yields across replicates ranged between 2-20 mg/ml. 100 ng of each unfractionated peptide sample was loaded on a 15 cm silica column with a diameter of 75 µm packed in-house with 5 µm C18 particles packed in-house. Reverse phase chromatography was performed using a Thermo EASY-nLC 1000 with a binary buffer system consisting 0.1% FA in water (buffer A) and 0.1% FA in acetonitrile (buffer B). The peptides were separated using a linear gradient shown in Table 6.1 below at a flow rate of 300 nl/min.

time	duration	Flow [nL/min]	%B
00:00	N/A	300	5
160:00	160:00	300	33
166:00	06:00	300	50
172:00	06:00	300	90
180:00	08:00	500	90

Table 6.1: LC gradient used for peptide ion separation

The column was operated at a constant temperature of 21°C. The LC was coupled to a Q Exactive mass spectrometer [363] through a nano-electrospray source (Thermo Fisher Scientific). The Q Exactive was operated in data dependent mode with survey scans acquired at a resolution of 17,500 and MS/MS resolution at 70 000 between 300 to 1750 *m/z*. The top 20 most abundant isotope patterns were selected with an isolation window of 4.0 *m/z* and fragmented by higher energy collisional dissociation with normalized collision energies of 25V. The maximum ion injection times for the survey scan and the MS/MS scans were 250 ms and 120 ms, respectively. Repeat sequencing of peptides was kept to a minimum by dynamic exclusion of the sequenced peptides for 30 s. Three biological replicates were run per sample.

Data Analysis of the raw files were processed using the MaxQuant computational proteomics platform version 1.3.0.5 [364]. The fragmentation spectra were searched against a single concatenated fasta file containing complete protein fasta files obtained from UniProt for *M. bovis*, *M. bovis* BCG, *M. avium*, *M. tuberculosis* F11, *M. tuberculosis* H37Rv, *M. tuberculosis* KZN and *M. tuberculosis* W-Beijing (Broad institute) using the Andromeda search engine [365]. Carbamidomethylation of cysteine was set as a fixed modification and FDR was set at 0.01 at peptide and protein level.

6.2.2.2 Data independent acquisition SWATH-MS

An ABsciex 5600 QqTOF^{TM} (ABSciex, Concord, Canada) was used for the SWATH-MS experiment. The instrument was coupled with an Eksigent NanoLC-2DPlus with nanoFlex cHiPLC system for the diauxic shift sample acquisition. 10 ng of each unfractionated peptide sample from three biological replicates per strain was loaded onto the LC system. 0.1% (v/v) formic acid in water was used as solvent A and solvent B comprising 95% (v/v) acetonitrile

with 0.1% (v/v) formic acid. The mass spectrometer was operated in a data independent acquisition mode according to previous specifications [247] in a looped product ion mode where the instrument was tuned to allow a quadrupole resolution of 25 Da/mass selection. Using an isolation width of 26 Da (25 Da of optimal ion transmission efficiency + 1 Da for the window overlap), a set of 32 overlapping windows was constructed from the dataset covering the mass range 400–1200 Da. Consecutive Swaths were acquired with a ±0.5Da precursor isolation window overlap to ensure the transfer of the complete isotopic pattern of any given precursor ion in at least one isolation window and thereby to maintain optimal correlation between parent and fragment isotopes peaks at any LC time point. An accumulation time of 100 ms was used for each fragment ion scan and for the (optional) survey scans acquired at the beginning of each cycle resulting in a total duty cycle of 3.3 s, with a mass resolution of up to 30 000 for the MS/MS scans and fragment ion mass accuracy of 10 ppm.

To determine retention time, equal amounts of 11 standard peptides with known retention times across a number of MS platforms, known as iRT peptides, were spiked into each sample. iRT is an empirically derived dimensionless peptide specific value that is given to each of these standard peptide that is not MS platform dependant, hence can be maintained across LC platforms [240]. iRT values from the spiked iRT standard peptides were determined based on the auto-calculate regression implemented in the iRT calculator described by Escher et al [240,366]. These values were used as the standard to convert retention time of the peptides in the experimental sample into retention time space (iRT) to standardise the elution time of the peptides across all the samples. This was done in order to place the retention time of all the peptides in each sample into iRT space in the context of each sample so that they can be compared, given that different matrix can result in different retention times for the same peptide.

Spectra from an *M. tuberculosis* experimental peptide library created by Schubert *et al* [248] was used as a search database. The dataset consists of a total of 97% of the 4,012 annotated *M tuberculosis* proteins obtained from exhaustive mining the total *M. tuberculosis* proteome by shotgun MS and targeted MS platforms using whole cell lysates and synthetic peptides. The dataset contained 258 851 peptides (corresponding to 3,898 proteins), resulting from +2, +3 and +4 charged precursors.

6.2.2.3 Data analysis

For Skyline analysis, the background proteome was obtained from the *M. tuberculosis* protein fasta file downloaded from Tuberculist (version 2.6). The peptide set resulting from trypsin proteolysis (no missed cleavages) was generated *in silico*, using carbamidomethylation of cysteine as a fixed modification; variable modifications included ammonia loss, water loss and methionine oxidation. Due to the complexity of the spectra obtained from this method of data acquisition, the data could only be analysed using the openSWATH search algorithm described by Rost *et al* [249]. The same modification settings that were employed for Skyline analysis were set for the openSWATH search analysis. Experimental spectra were searched against the spectral library and each spectrum was scored according to similarity to the corresponding spectra in the spectral library. Multiple scores for each PSM were combined to choose the best matches for each peptide and these were used to determine the FDR for each PSM. Proteins were selected if there was at least one peptide obtained with an FDR of 0.001. Further peptides were then selected up to FDR 0.1 provided that there was at last one peptide with 0.001 FDR.

6.3 Results and discussion

6.3.1 iBAQ quantitation using Q-Exactive data dependant acquisition

Analysis of the QE data was carried out using MaxQuant database search software. The analysis showed the number of MS and MS/MS scans per strains depicted in Table 6.2 below. The number of MS and MS/MS were averagely 5 000 and 17 000 respectively, with the LAM strain exhibiting the lowest number of MS and MS/MS spectra and H37Rv having the highest. The total number of spectra is lower in this chapter compared to that observed in Chapter 4 due to the fact that no fractionation was carried out for this study sample. The number of MS and MS/MS scans were reproducibly observed across biological replicates for each strain suggesting consistency in the extraction method.

	MS	MS/MS
C1	8 500	18 132
C2	8 000	17 851
C3	8 000	17 759
L1	5 500	12 273
L2	5 000	14 434
L3	4 900	16 115
H1	7 000	23 781
H2	7 000	23 964
H3	7 000	23 503
B1	8 000	19 449
B2	8 500	19 015
B3	8 500	19 011

Table 6.2: Total number of MS and MS/MS scans per strain per replicate obtained using the Q-Exactive.

The percentage of spectra assigned per replicate per strain is shown in Figure 6.2 below. These analyses showed that while the number of MS and MS/MS spectra obtained across strains was roughly comparable, the percentage of assigned spectra for the CAS strain was reduced by about 25% compared to other strains. Total peptide and protein identifications across the replicates are depicted in Figure 6.1 below. The figure also shows the number of shared peptides and proteins between pairwise comparisons of each replicate to other replicates of that strain as well as all replicates of every other stain in the study.

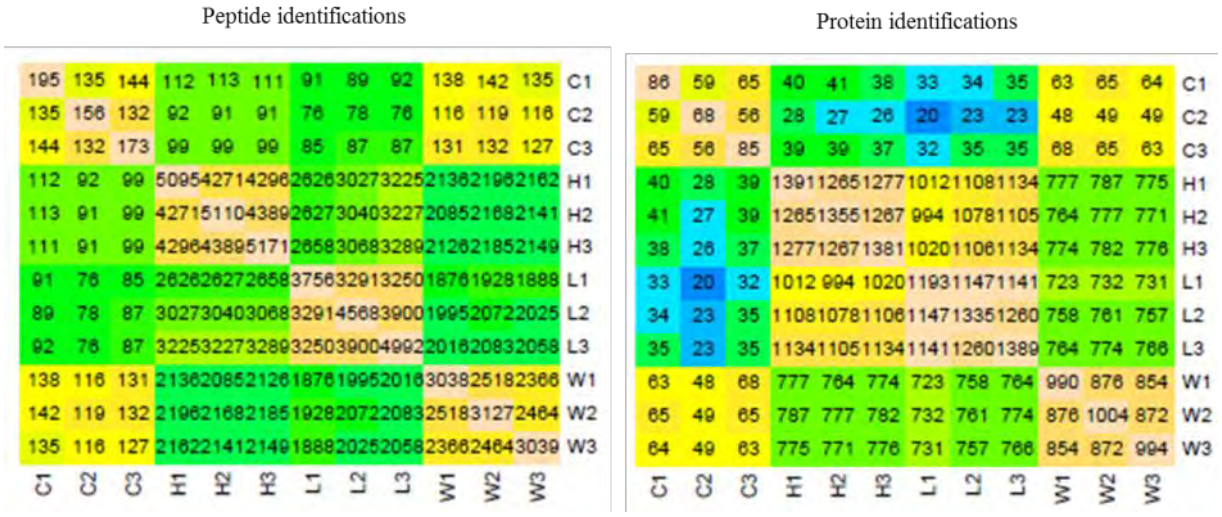

Figure 6.1: Number of peptide sequences and unique protein groups detected by unique evidences. C represents CAS strain, H represents H37Rv, L represents LAM strain and W represents W-beijing strain. The numbers 1, 2 and 3 represents the biological replicates of each strain.

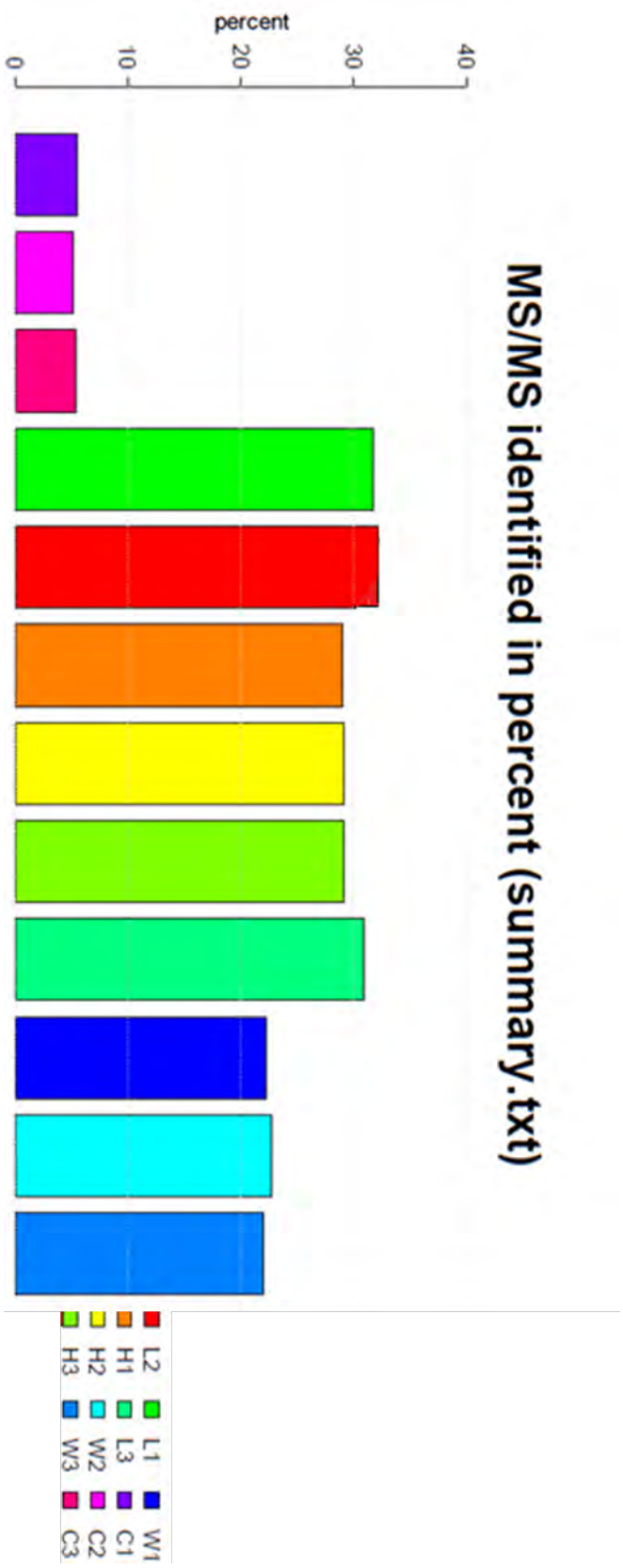

Figure 6.2: Percentage representation of MS/MS spectra assigned per replicate per strain.

Carbamidomethylation was set as a fixed modification whilst oxidation and N-acetylation were set as variable modifications. FDR was set at 0.01 and tryptic digest efficiency was determined to be 95% effective since 5% of the spectra had 2 or more missed cleavages. The number of proteins identified per mycobacterial strain across biological replicates was fairly reproducible, indicating that sample preparation across biological replicates was maintained equally standard. The number of overlaps between spectra from biological replicates of a single strain and among strains analysed on MaxQuant is also shown in Figure 6.1 above.

The complete dataset for all the 4 strains identified a total of 1919 unique protein groups derived from the database search based on comparison to the concatenated theoretical data file. Proteins are grouped together based on the number of shared peptides due to the fact that proteins are inferred using identified peptides, and some peptides are shared by many proteins. Such proteins that share peptides are then bracketed to form a single unique protein group. The proteins were then filtered for redundant proteins as the theoretical fasta file was made from a composite of 7 fasta files including *M. bovis*, *M bovis* BCG Pasteur, *M. avium*, *M. tuberculosis* H37Rv, *M. tuberculosis* F11, *M. tuberculosis* KZN and *M. tuberculosis* W-Beijing (Broad Institute strain). This means that each protein group theoretically had 7 identifications of the same protein from the 7 protein fasta files assuming that each protein is annotated in each fasta file.

The total non-redundant number of proteins identified across the 3 replicates for each strain using this MS approach is shown in Figure 6.3 below. The number of proteins obtained in this dataset (with the exception of the CAS strain) is similar to that obtained in the discovery shotgun experiments from unfractionated lysates at 1% FDR using the Orbitrap Velos (Chapter 3) thus suggesting that there may be a level of saturation in protein identifications from spectra acquired in a data dependant manner from unfractionated samples, regardless of how they are analysed. However, analysis of the protein lists by gene ontology indicated that there was a correlation in the proteomes between the two experiments although less was obtained in this experiment (Figure 6.4 and Figure 4.12). Furthermore, this data obtained using QE was obtained without optimization of LC or MS acquisition parameters suggesting two things; firstly, due to the compatibility of this data to the discovery data obtained under optimized machine parameters, we can conclude that the MS instrumentation used in this present work is more sensitive. The low identifications in the CAS strain were unexpected given that the number of MS and MS/MS scans as well as the total ion count was similar to that of the other strains. This means that the low identification rate is due to an anomaly in spectral assignment

of this rather than protein extractions or incomplete tryptic digestion. This data was however not excluded from future analysis.

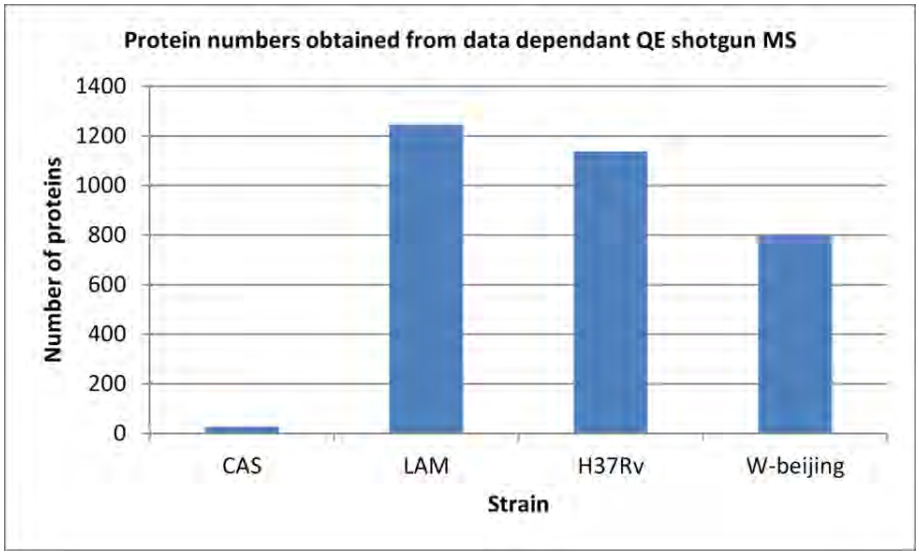

Figure 6.3: The total non-redundant number of protein identifications obtained per strain across 3 biological replicates. Note that the identifications represented here are only those found using the M. tuberculosis H37Rv fasta file.

Using MaxQuant, the summed MS1 intensities of the peptides for each individual protein were used to calculate an overall expression value, termed the intensity based absolute quantitation (iBAQ) value. Mean iBAQ values were calculated across the 3 biological replicates of each sample to obtain a single quantitation value for each protein. Following normalisation and log transformation of the data using R version 3.0.2, statistical assessment of the expression data was used to calculate means and standard deviation for proteins present in two or more strains. Proteins with ±2 SD from the mean were regarded as significantly differentially expressed.

A total of 344 proteins representing approximately 18% of the total identifications were found to be significantly differentially expressed amongst the strains. Functional annotation of the proteins showed that most of the proteins were classified in the intermediary metabolism and respiration and conserved hypotheticals (Figure 6.4). The classes of ‘Intermediary respiration’ and ‘conserved hypothetical’ proteins represent over half of the significantly differentially expressed proteins, followed by the information pathways and cell wall processes categories. Represented to a lesser extent are the classes ‘lipid metabolism’, ‘unknown’, ‘regulatory’, ‘virulence’ and ‘PE/PPE’ categories, which together make approximately 20% of the total

significantly differentially expressed proteome in comparison to the classification of the total theoretical proteome according to TBDB (Figure 6.5).

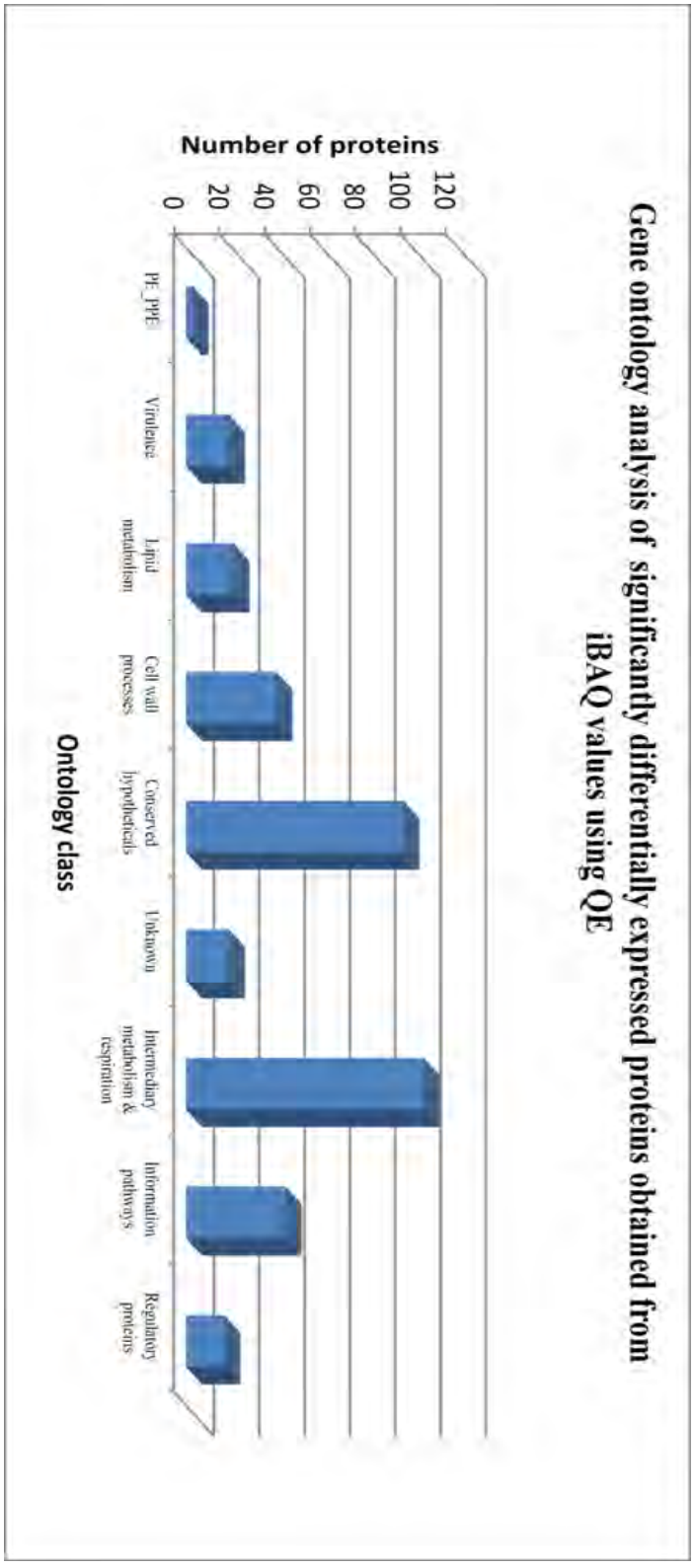

Figure 6.4: Functional annotation of 344 proteins that are significantly differentially expressed among the proteins

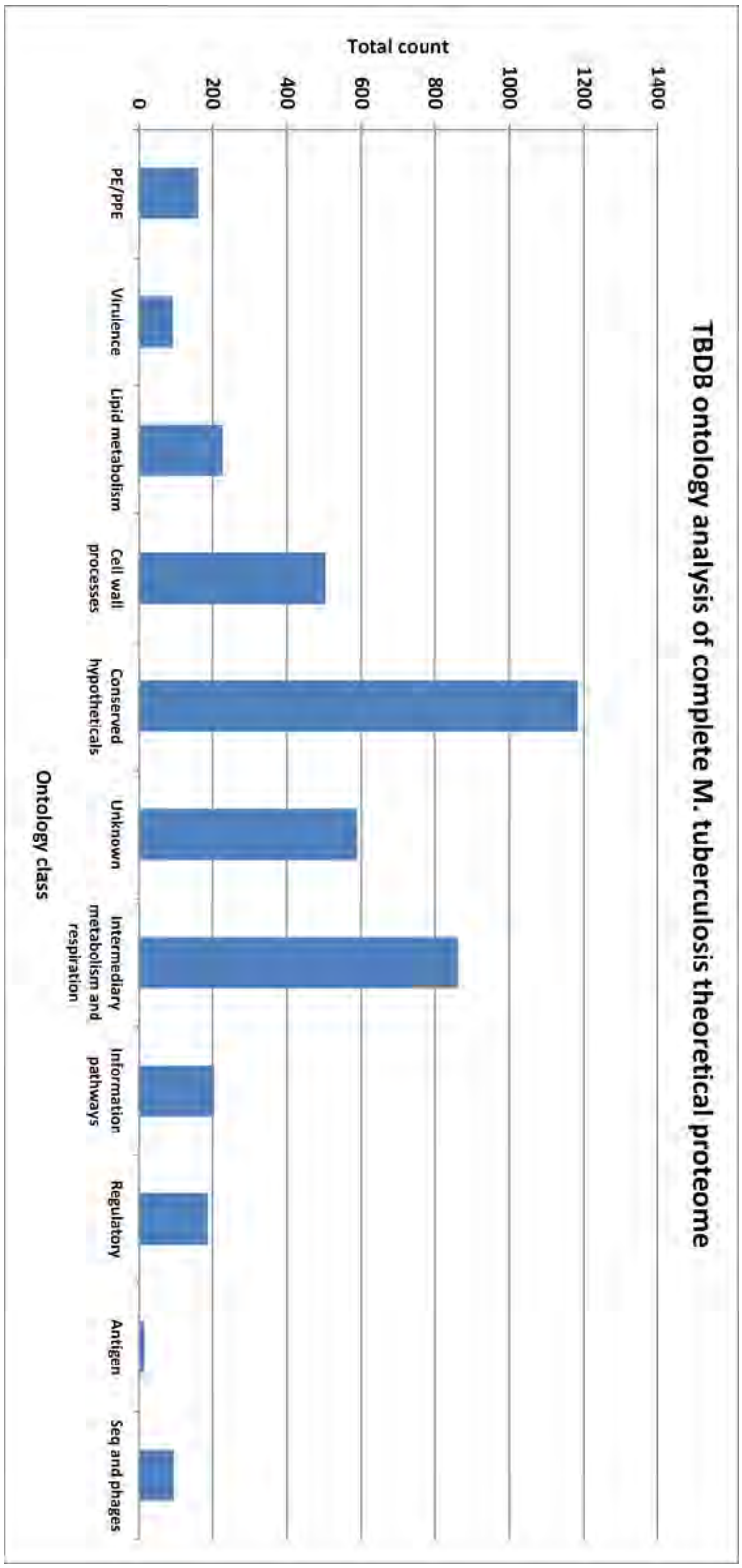

Figure 6.5: Functional annotation of 344 proteins that are significantly differentially expressed among the proteins

A small proportion of the differentially expressed proteins were classified as virulence proteins. These include well known virulence and antigenic proteins such as alpha crystallin and cfp29 amongst others, as shown in Table 6.3 below. However other proteins that are not classified in TBDB as virulence proteins are also found to be differentially expressed, including ESAT-6 and CFP10 which are currently annotated in the cell wall processes category and conserved hypotheticals respectively.

The significant differential expression of these important proteins that are implicated in determining the course of disease suggests that many of the other qualitative differences in protein expression identified here may also play a role in determining clinical phenotype of strains. In particular, this highlights the potential importance of proteins in the cell wall processes and conserved hypotheticals category in virulence and also indicates that pathogenicity and virulence may be determined by proteins that are not necessarily annotated as virulence proteins.

There are however a number of other proteins in families that contain well-known virulence proteins that are represented in other categories such as conserved hypotheticals, cell wall processes and lipid biosynthesis amongst others. These proteins families include the polyketide synthesis (pks), mammalian cell entry (mce), membrane proteins (mmpl), mycobactin synthesis (mbt), lipoproteins (lpr) and proteins belonging to secretion systems (sec) (Annexure Table 6.1). These could be involved in certain aspects of virulence that are not yet known or thoroughly understood hence are not currently classified as virulence proteins. Furthermore, some of these proteins such as Rv0350-Rv0352, Rv3490-Rv3499c and Rv3417c-Rv3418c are members of respective operons suggesting that they were co-expressed hence also supporting why their expression is collectively significantly differentially expressed.

Rv loci	Protein name	Function	Phenotype affected
Rv0350	dnaK	Chaperone: Response to heat, superoxide, antibiotics,	Virulence and growth
Rv0351	grpE	Chaperone: Response to hyperosmotic shock, heat and protein aggregation, transcription cofactor	Growth
Rv0352	dnaJ1	Chaperone: Response to heat and hyperosmotic shock, DNA replication, protein folding, regulation of transcription	Growth
Rv0384c	clpB	Chaperone: Response to stress, protein processing and folding	Growth
Rv0440	groEL	Chaperone: Response to stress conditions, adherence to host, immunogenic	Growth
Rv0798c	cfp29	Defense response	Growth
Rv1608c	bcpB	Oxidoreductase, peroxidase, response to ROS	
Rv1932	tpx	Anti-oxidant, oxidoreductase, evasion of immune response, response to ROS & RNS	Pathogenesis and Growth
Rv2031c	hspX	Chaperone: Response to hypoxia, starvation, ROS, heat, immune response, iron starvation	Virulence
Rv2214c	ephD	Inferred from homology: Oxidoreductase	
Rv2299c	htpG	Chaperone: Response to stress, inferred from homology	
Rv2373c	dnaJ2	Response to heat shock and hyperosmotic shock, Required for replication	Growth
Rv3417c	groEL1	Chaperone: Response to stress, nucleoid organisation, protein folding, DNA protection	Growth
Rv3418c	groES	Chaperone: Response to heat, antibiotic, protein folding,	Growth
Rv3490	otsA	Glycosyl transferase: trehalose biosynthesis	Growth
Rv3497c	mce4C	Predicted mammalian cell entry protein	
Rv3499c	mce4A	Predicted mammalian cell entry protein	
Rv3648c	cspA	Transcription factor: Regulation of transcription under temperature fluctuations	Growth

Table 6.3: Significantly differentially expressed proteins annotated in the virulence category by TBDB. All proteins affecting growth are determined by TraSH experiments described by Sassetti *et al* [297].

Notably, the functions of approximately half of the significantly differentially expressed proteins are still unknown. This suggests that complete functional annotation of the *M. tuberculosis* proteome must still be carried out before we can understand the implications of their differential expression. The finding that 18% of the expressed proteins identified in this experiment (which represents roughly 9% of the total theoretical proteome) was significantly differentially expressed potentially challenges the postulation that only a handful of proteins are implicated in differential virulence. To determine if this result was maintained across different label free quantitation platforms, this result was compared to the outcome from a similar intensity based label free quantitation using data independent MS acquisition (SWATH-MS) and shotgun orbitrap NSAF data. Although there are newer methods of quantitatively and qualitatively analysing Q-Exactive data such as Progenesis, this software was still under

development and was not yet publically available at the time that this data was analysed hence it was not used.

6.3.2 Intensity based quantitation from SWATH-MS analysis

10 ng of the peptide samples from the same biological replicates of the samples obtained previously in Section 6.2.1 , were analysed using SWATH-MS. Analysis of the spectra was carried out using openSWATH software described by Rost *et al* [249]. The analysis was run using a TB proteome experimental spectra database created by Schubert *et al* [248] as a reference standard for spectral matching. Retention time calibration of each sample was carried out using 11 well characterised reference standard peptides whose RT have been recorded across various machines in various sample mixtures which were spiked into each sample at a known fixed concentration. A 0.05Da extraction window was set for the selection of precursor ions and a 300 seconds window was set as the retention time window for the identification of spectra. A protein was accepted if at least one of the peptides was obtained with 0.1% FDR. Other peptides could then be accepted up to 10% FDR after at least a single peptide with 0.1% FDR was observed for that protein.

The feature alignment output table from openSWATH was then used as the input for MS-Stats for the statistical analysis of the MS output data. Normalisation was carried out using quantile normalisation in R. Analysis of the SWATH-MS data using openSWATH software under the parameters specified identified between 700 up to 2166 proteins per strain. These protein numbers depicted in Figure 6.8 below are from unfractionated samples obtained using at least one peptide identified with an FDR 0.1%. The CAS strain had the lowest number of proteins by over half while H37Rv, LAM and W-beijing had fairly similar protein identifications. The total ion count per strain (Figure 6.6) was obtained showing roughly similar ion counts across the strains, indicating that the sample processing methodology was standardized across strains.

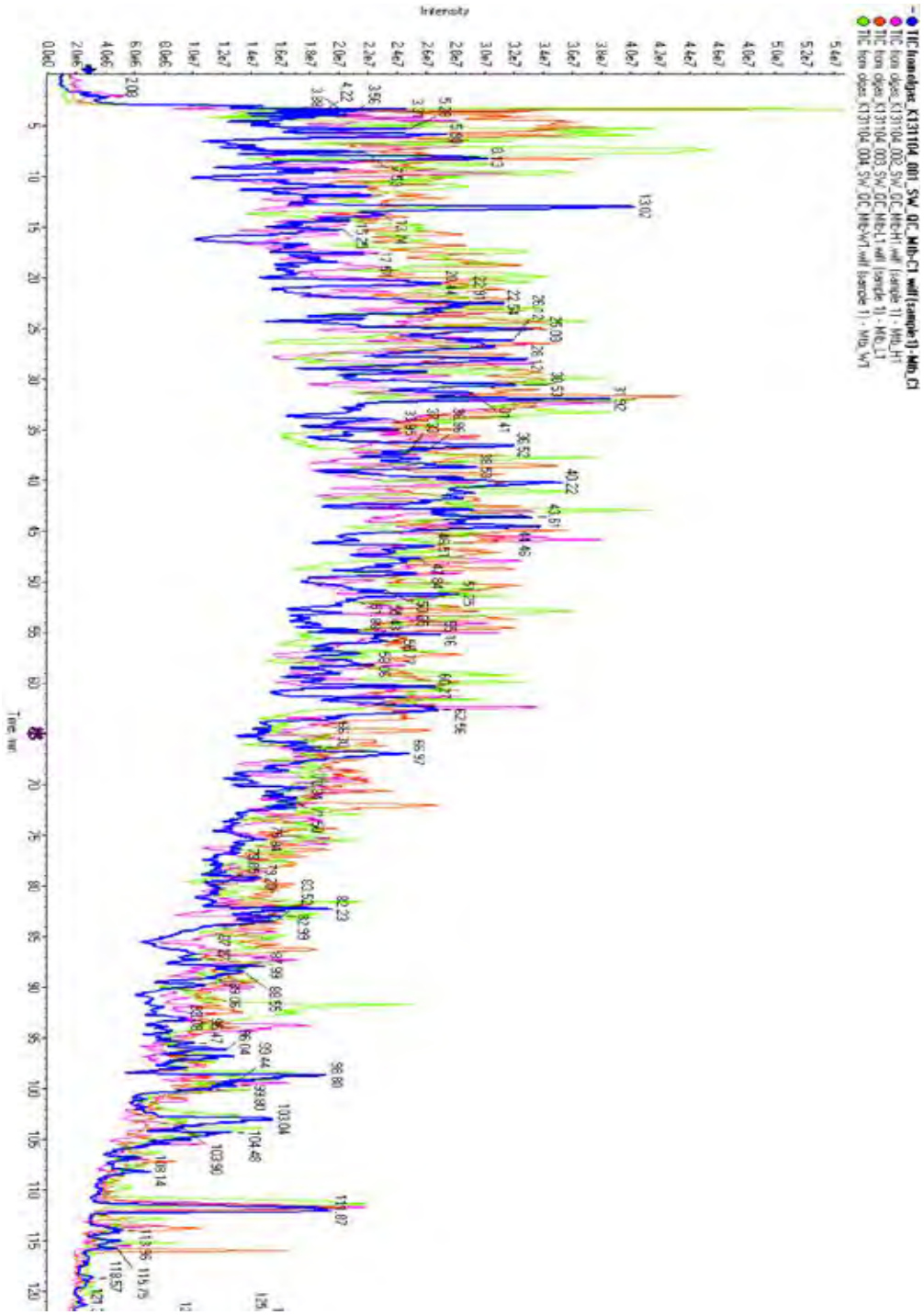

Figure 6.6: Total ion count of replicate 1for each the 4 clinical strains across the 120 minutes gradient.

Individual spectra were viewed using Skyline software as before. The Tuberculist *M. tuberculosis* proteome was set as the background proteome and retention time predictor was selected on the specified 11 iRT peptides described previously in Section 6.2.2.2. Modifications to peptides specified in the settings included the following; Carbamidomethylation as a fixed modification, and water loss, oxidation and ammonia loss as variable modifications. The MS/MS filtering setting was set to data independent acquisition,

using the SWATH isolation scheme. SWATH windows of 25 Da were specified in the settings and raw file were then imported and viewed directly under these settings. Each spiked standard was initially analyzed prior to any other peptides to ensure that they eluted within at the appropriate predicted retention time. This is essential because the accuracy of the retention time of the standards determines if the predicted retention times for the experimental peptides are correct. Analysis of the spiked standards on Skyline showed that these peptides were eluted at the predicted retention time across all peptide samples as shown in the spectra in Figure 6.7. Spectra from *M. tuberculosis* strains were then viewed using Skyline as shown in Figure 6.8, depicting the spectra from ESAT-6, an *M. tuberculosis* specific protein. The presence of these spectra within the predicted retention time indicates that this protein is present across all strains and also confirms that all four strains are *M. tuberculosis* strains as this protein is known to be found only in the *M. tuberculosis*.

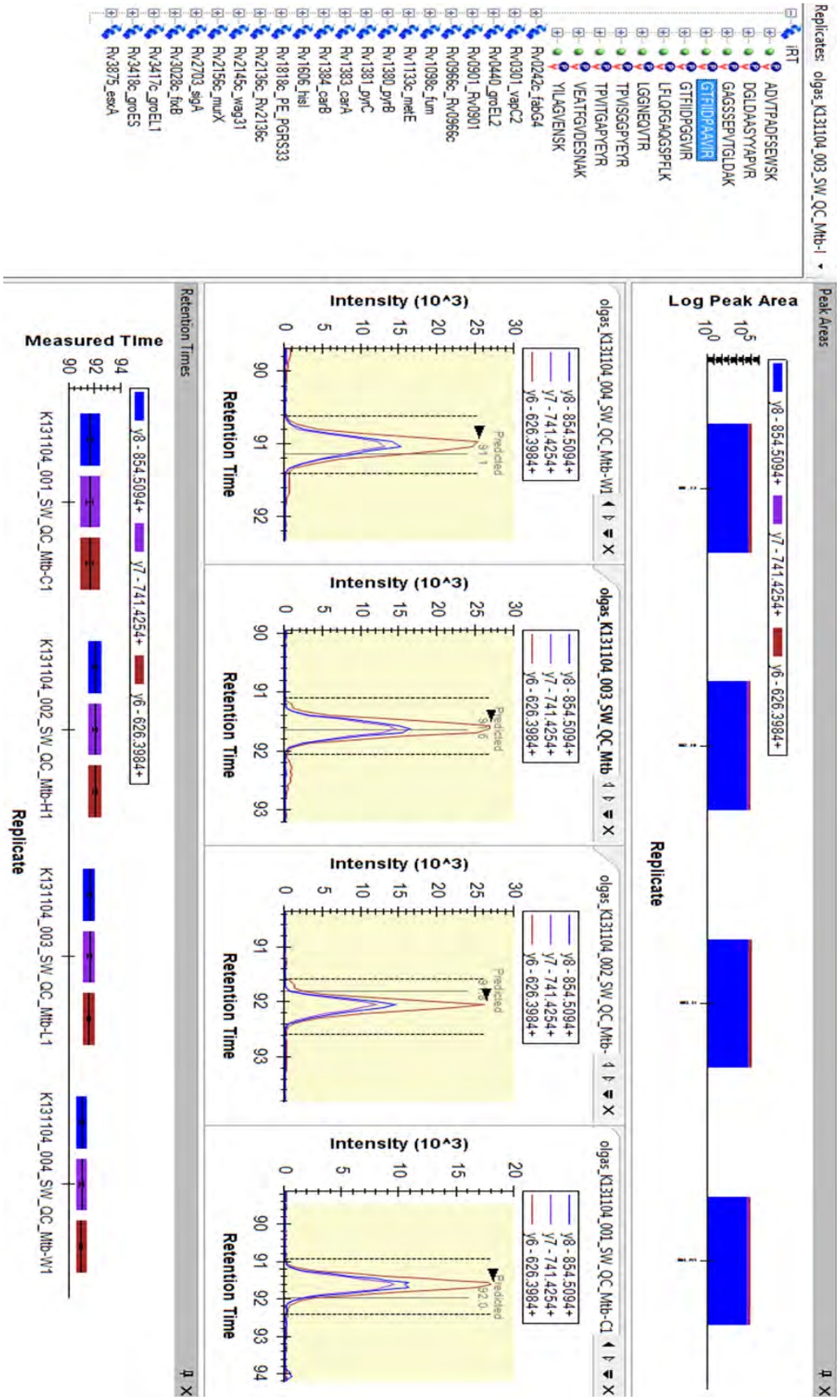

Figure 6.7: Spectra of iRT peptide GTFIIDPAAVIR showing that in each of the four strains, the peptide is eluted within a 5 seconds window from the prediction.

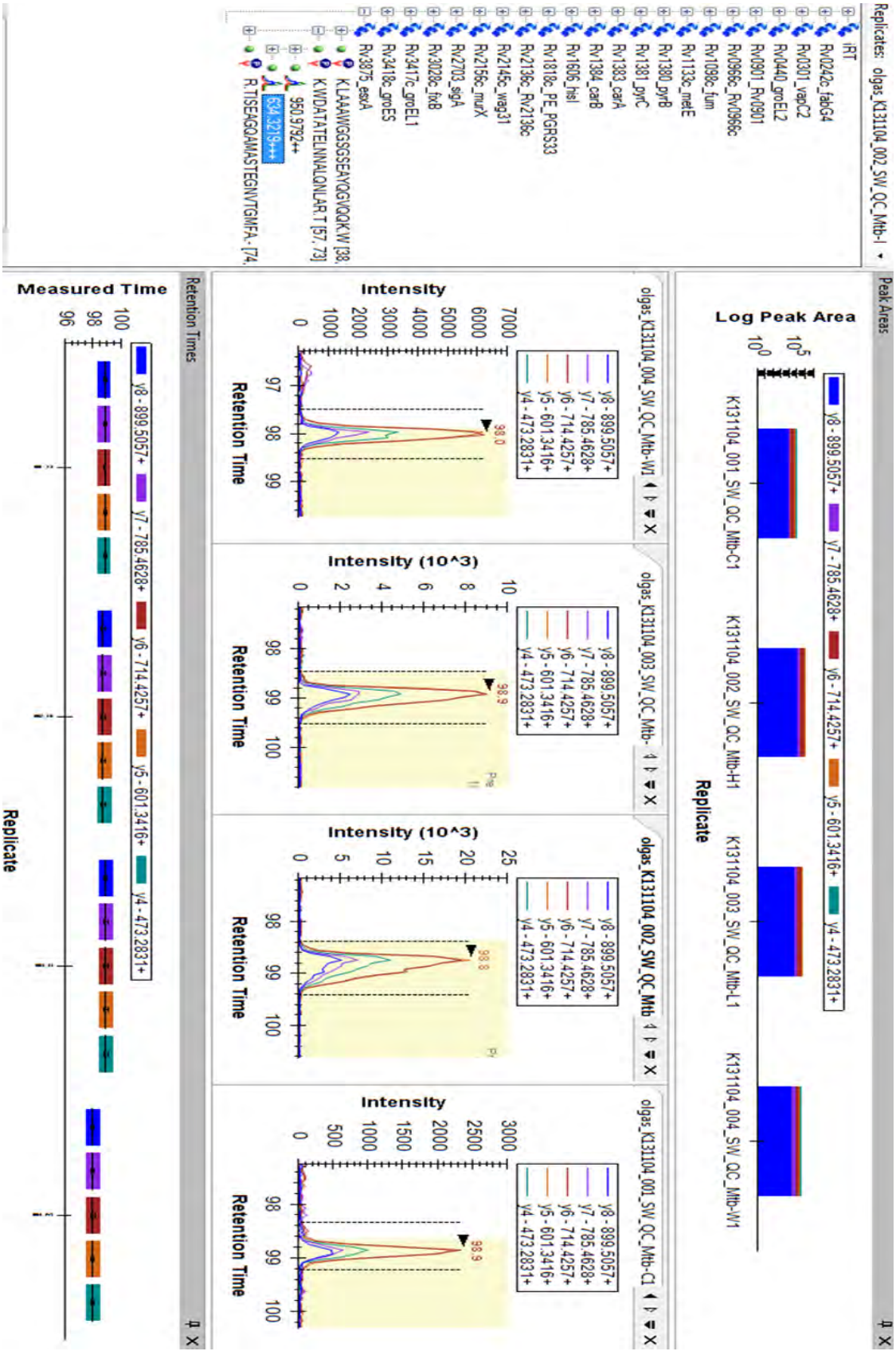

Figure 6.8: Spectra of the +3 species of the WDATATELNNALQNLARK peptide of ESAT-6 protein showing that in each of the four strains, the peptide is eluted within a 5 seconds window from the prediction.

Analysis of the datasets showed that although QE analysis identified fewer proteins, the trend in the SWATH-MS output (Figure 6.9) was similar to that obtained from QE data (Figure 6.3). Comparison of the non-redundant protein datasets between the 2 MS platforms shows that whilst W-Beijing, LAM and H37Rv strains identified a comparable number of proteins, the CAS strain similarly identified less proteins, although more were identified using SWATH-MS in comparison to QE.

The overlap of 1 689 non-redundant protein groups between the H37Rv, LAM and W-beijing strains was similar to the *M. tuberculosis* core-proteome observed in the discovery experiment (Chapter 4). Although this corroborates the data from the discovery experiment in Chapter 4, it also demonstrates the power of data independent acquisition SWATH-MS over the data dependant discovery MS experiment that was previously used. This is because the core proteome described in Chapter 4 was obtained at a protein FDR of 5% across 10 fractions of each sample whilst the proteins obtained in SWATH-MS were obtained under more stringent conditions where proteins had to be identified by at least one peptide with an FDR of 0.1% from unfractionated samples.

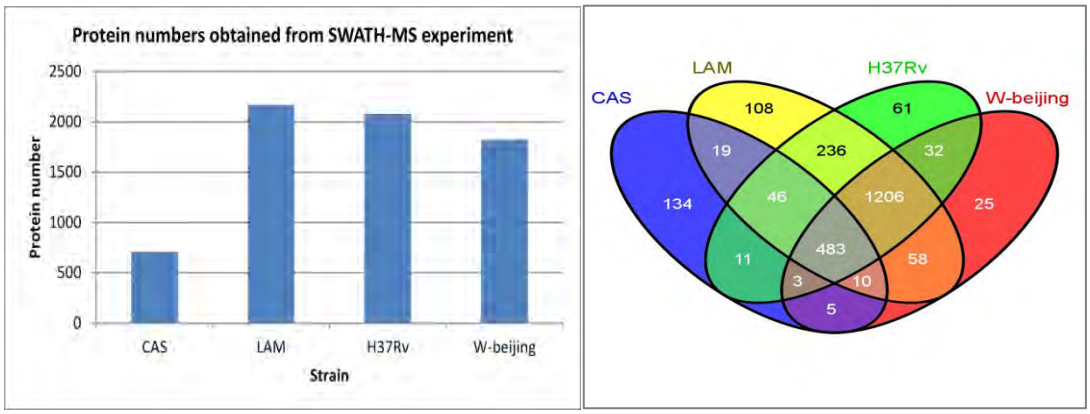

Figure 6.9: The bar graph shows the total number of proteins obtained in each strain using SWATH-MS data independent acquisition. The venn diagram shows the overlap in the protein identifications between the strains.

The amounts of each individual peptide identified for each protein were assessed using trellis plots to give an indication of the general protein expression trend across samples at the peptide level as shown in Figure 6.10 which gives illustrative data on the GroEL2 protein. Spectra from peptides that did not conform to the general observed trend on the trellis plot were re-checked using Skyline software version 2.1 to ensure that the right peptides were picked. It was observed that most peptides that did not follow the general observed trend were erroneous or

low confidence peptides and these were removed from the result. This was done across all the shared peptides. Figure 6.10 effectively shows that peptides of the same protein are expected to have relatively the same abundance pattern of expression across the strains. This is shown nicely in this figure that groEL2 constantly has lower expression in the CAS strain than all other strains as shown by the pattern of multiple peptides.

Statistical analysis of the expression values was carried out using MS Stats in R version 3.0.2 to determine proteins with significant expression changes. For each protein, the adjusted means of signal intensity across all the identified peptides were calculated to give a single signal intensity expression value. Proteins that were found in single strains were removed from the analysis and means and standard deviations were calculated based on the number of strains that expressed each protein. Proteins with a fold change of ±2 at a p-value of differential expression of below 0.05 were considered differentially expressed between the 4 strains. From this analysis 211 proteins were found to be significantly differentially expressed.

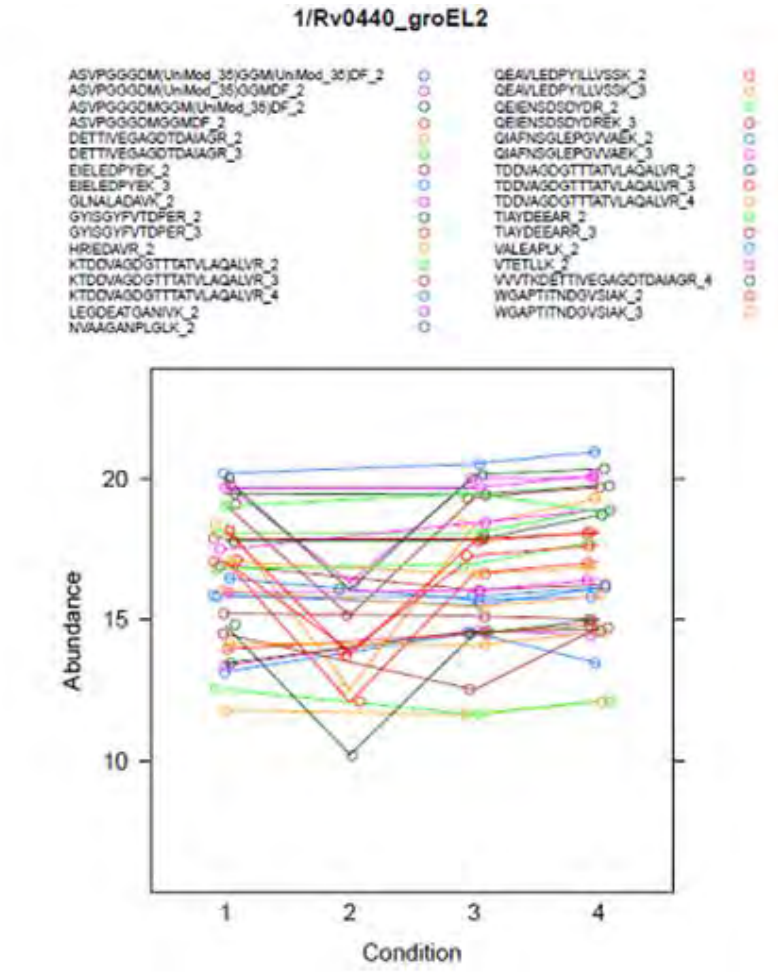

Figure 6.10: The trellis plot in shows all the peptides that were found for the groEL2 protein according to the color code. The condition depicts the strain where 1=LAM, 2=CAS, 3-W-beijing and 4=H37Rv. The abundance is the relative quantity of each peptide in each strain.

Functional annotation of this proteome set was carried out as before using TBDB functional categories (Figure 6.11). The functional analysis in this section mirrored that obtained from iBAQ values using data dependant acquisition by means of Q-Exactive (Figure 6.4) and also mirrored the proportions of these categories in the theoretical proteome as shown in (Figure 6.5).

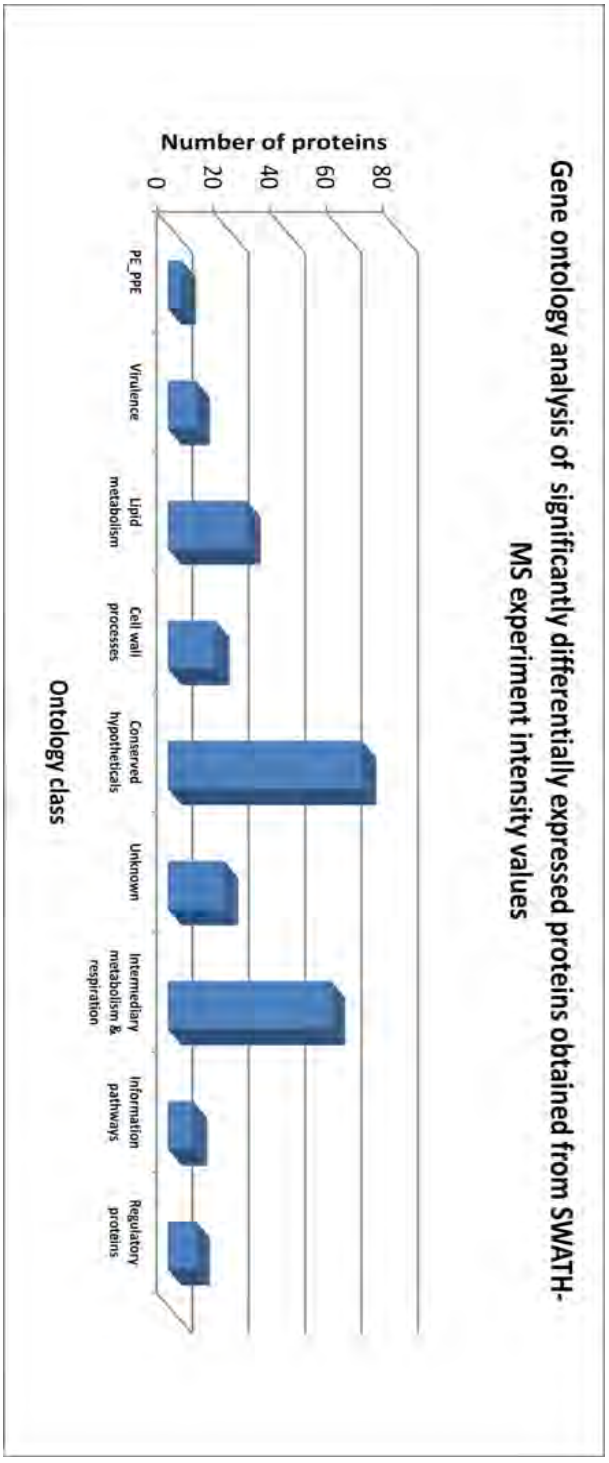

Figure 6.11: Functional annotation of 215 proteins identified in the SWATH-MS experiment that are significantly differentially expressed among the strains.

The virulence proteins observed include Rv0350, Rv0440, Rv1566c, Rv1908c, Rv3418c, Rv0251c, Rv1932 and Rv0174 (Table 6.4). Four of these proteins had previously been listed in Table 6.3 as significantly differentially expressed. This analysis thus added a further 4 proteins that were not observed in the iBAQ analysis, including Rv1566c, Rv1908c, Rv0251c and Rv0174 (Table 6.4). The additional proteins include a heat shock protein, katG protein and two

proteins that are required for entry into the host cell including an invasion protein (inv) and a mammalian cell entry protein (mce). Furthermore, CFP10 was also observed in this study as significantly differentially expressed (Annexure Table 6.2). Similarly a unique cohort of proteins in previously mentioned well-known protein families that harbour virulence proteins were observed in this assessment. Overall, this SWATH-MS analysis added a further 159 proteins that were not identified as significantly differentially expressed in the QE analysis. The data was then compared to the spectral counting NSAF values obtained in Chapter 4.

Rv loci	Protein name	Function	Phenotype affected
Rv0350	**dnaK**	**Chaperone: Response to heat, superoxide, antibiotics,**	**Virulence and growth**
Rv0440	**groEL2**	**Chaperone: Response to stress conditions, adherence to host, immunogenic**	**Growth**
Rv3418c	**groES**	**Chaperone: Response to heat, antibiotic, protein folding,**	**Growth**
Rv1932	**tpx**	**Anti-oxidant, oxidoreductase, evasion of immune response, response to ROS & RNS**	**Pathogenesis and Growth**
Rv1566c	inv	Possible invasion protein: Inferred from homolgy	
Rv1908c	katG	Broad spectrum peroxide resistance, drug resistance, evasion of host immune system	
Rv0251c	hsp20 family protein	Inferred from homology: stress response	
Rv0174	mce1F	Predicted mammalian cell entry	

Table 6.4: Significantly differentially expressed proteins in the virulence category. These proteins together with those in Table 6.2 above were found to be significantly differentially expressed using SWATH-MS experiments. The proteins that are shown in bold were found in the QE analysis as significantly differentially expressed (Table 6.2).

6.3.3 NSAF label free quantitation

Quantitation values described in this section were obtained from the initial shotgun discovery experiment described in chapter 4. NSAF values of proteins obtained at 1% FDR in the discovery experiment in chapter 4 were normalised and log transformed in R (version 3.0.2) as described before. Fold changes in expression were also calculated in R based on the number of strains that expressed each protein. Means and standard deviation were calculated and proteins with ±2SD from the mean at a p-value of below 0.05 were considered differentially expressed. In this analysis, 130 proteins, representing 8% of the proteins assessed had significant differential expression as shown in Annexure Table 6.3. This data also echoes the finding that only a relatively small number of proteins are possibly responsible for the phenotypic differences observed between strains at the quantitative level.

Functional annotation of these 130 proteins was carried out as before and showed that the pattern mimicked the 2 previous analyses where conserved hypotheticals and intermediary

metabolism classes of proteins still dominated the list as before (Figure 6.11). Only 7 virulence proteins were found to be significantly differentially expressed amongst the proteins shared by all 4 strains including Rv2031v, Rv2428, Rv2373v, Rv0440, Rv0171 Rv0351 and Rv3418c, all of which were already identified in Sections 6.3.1 and 6.3.2 as significantly differentially expressed.

In agreement with the two previous sections, this data further restates that differential virulence is likely to be more governed by proteins in classes other than those classified as virulence proteins. As with the intensity based quantitation, the spectral counting method of quantitation used in this part of the work also found ESAT-6 as well as CFP-10 to be significantly differentially expressed. This recurrent finding across quantitation platforms is notable because these proteins determine the course of disease and are already being used as diagnostic targets in IGRA tests and Quantiferon test [367,368].

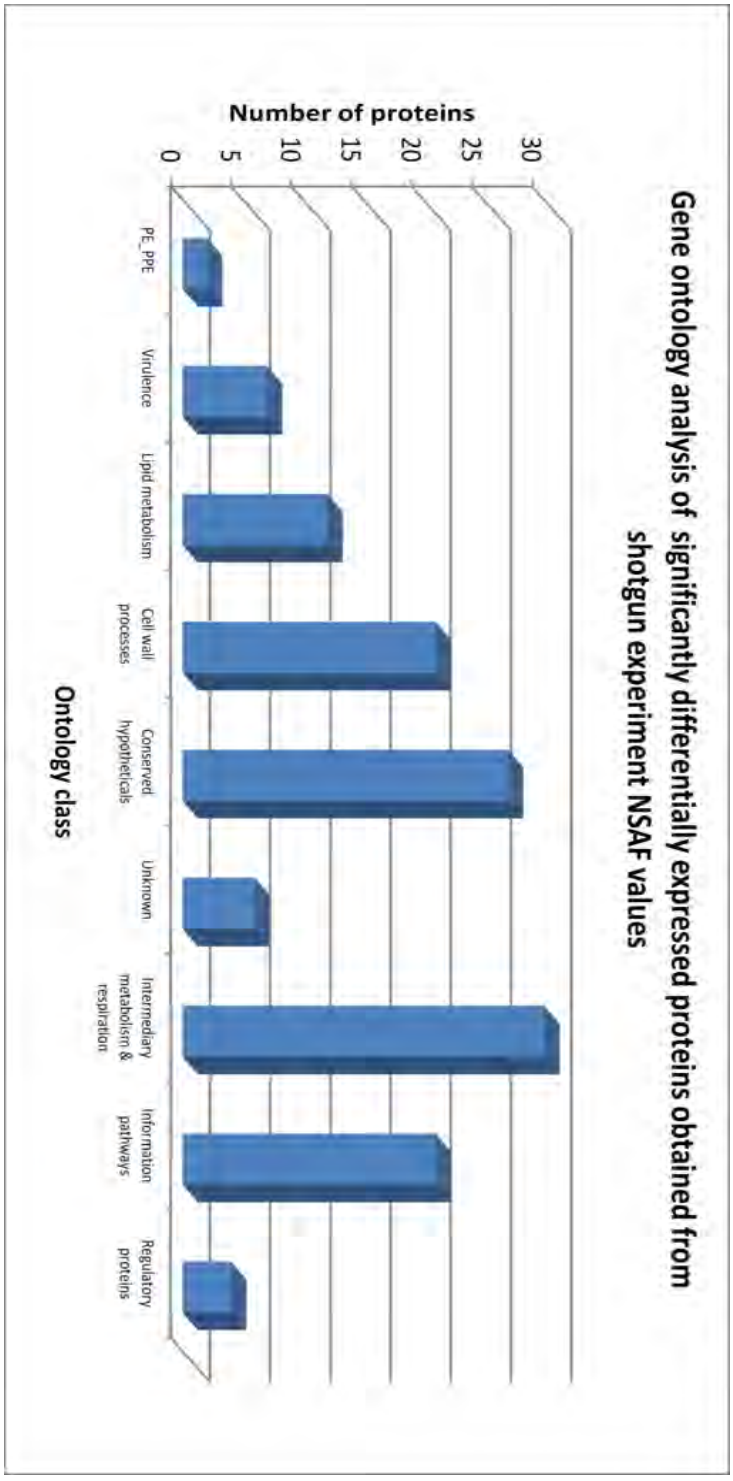

Figure 6.11: Functional annotation of 130 proteins that are significantly differentially expressed among the proteins shared by all strains

6.3.4 Comparison of the label free quantitation methods

A simple direct way to compare the label free quantitation approaches used in this study was evaluated by assessing the expression pattern of a common protein GroEL2. This protein was

chosen since it is a highly abundant protein known to be found across strains with multiple easily ionisable peptides. This comparison is shown in Figure 6.12 below.

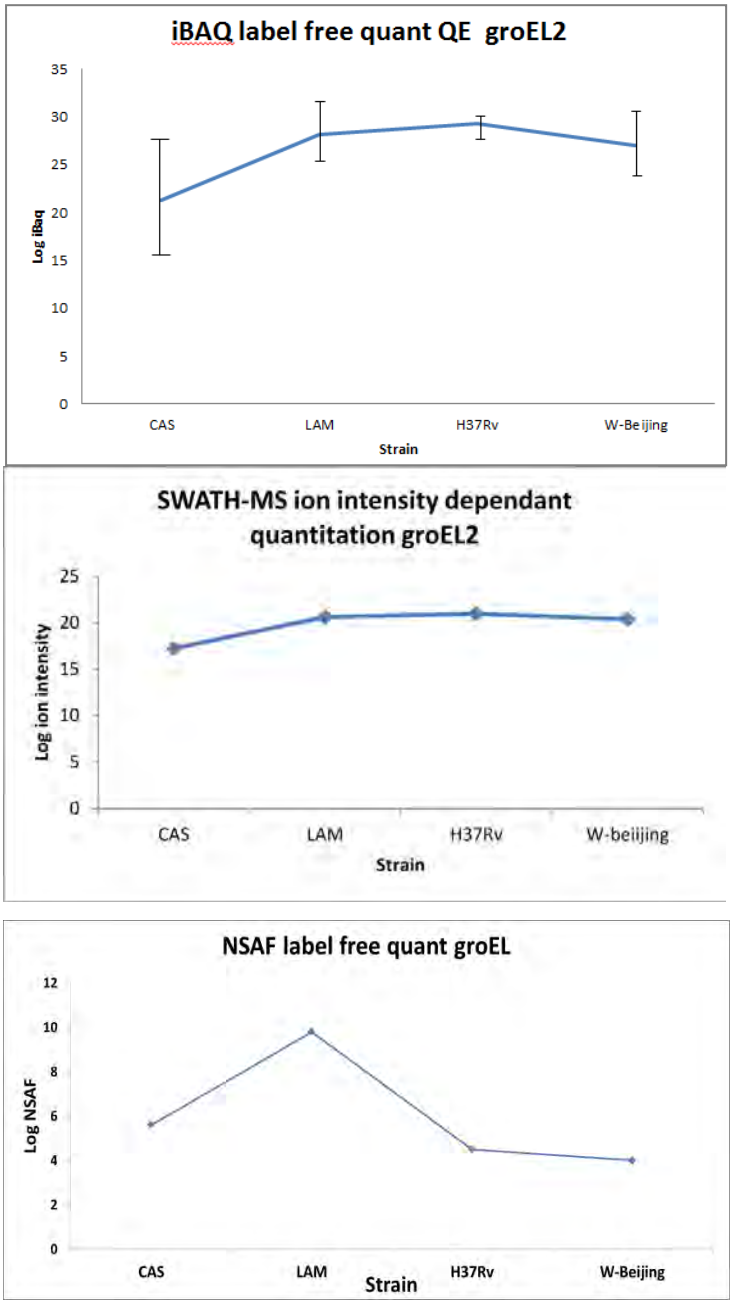

Figure 6.12: Comparison of protein quantitation techniques using iBAQ label free spectral counting on MaxQuant, NSAF based spectral counting and relative quantitation based on summed spectral intensity using openSWATH.

This simple visual comparison for one protein also indicated that that there is a correlation between the two intensity based label free methods used in QE analysis and SWATH MS experiments. However there is a clear discrepancy in the trend observed when using the

spectral counting based NSAF quantitation values. This gave an early indication of what to expect in terms of the numbers of overlapping differentially expressed proteins between quantitation platforms.

The overlap between the 3 quantitative datasets was assessed using venn diagrams (Figure 6.13). This assessment revealed that 82 significantly differentially expressed proteins are shared by 2 or more quantitation methods whilst only 8 are shared by all 3 methods (Table 6.5; Annexure table 6.4). Curiously, all the 8 shared by the 3 quantitation methods are associated with virulence, suggesting that these proteins are indeed differentially expressed regardless of MS platform or quantitation method.

Rv loci	Protein name	Function	Phenotype affected
Rv0440	**groEL2**	**Chaperone: Response to stress conditions, adherence to host, immunogenic**	**Growth**
Rv3418c	**groES**	**Chaperone: Response to heat, antibiotic, protein folding,**	**Growth**
Rv0475	hbhA	Cell adhesion, regulation of host receptor mediated endocytosis	Pathogenesis and Virulence
Rv0206c	mmpl3	Lipo-polysaccharide transport, cell wall biogenesis	Growth
Rv2346c	ESAT-6 like protein	Unknown	
Rv3874	esxB	Protein secretion via VII secretion system, adherence to host	Pathogenesis
Rv2357c	glyQ	Protein biosynthesis	Growth
Rv0667	rpoB	Transcription, response to antibiotic	Growth

Table 6.5: Significantly differentially expressed proteins in the virulence category shared by QE, SWATH-MS and shotgun NSAF experiments. Proteins in bold were found differentially expressed in SWATH-MS and QE data.

Notably, these are proteins whose functions are well understood and have been shown in various studies to be essential for pathogenesis, immune responses and virulence. The discovery that these proteins are significantly differentially expressed between strains that display different clinical phenotype, particularly virulence, suggests that these proteins could play a significant role in the observed variations in clinical phenotype.

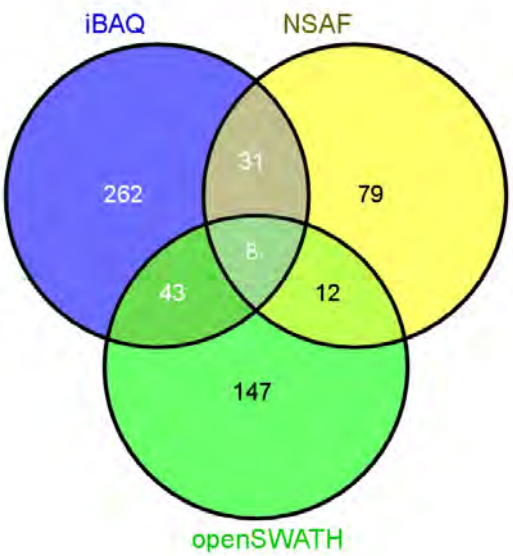

Figure 6.13: Overlap between proteins calculated to be significantly differentially expressed using the 3 label free quantitation platforms. All proteins in each circle are differentially expressed within the experiment in question. The analysis also shows proteins that were uniquely identified and significantly differentially expressed using each MS platform at an FDR of 0.01.

As expected, iBAQ and openSWATH shared more proteins than any comparison with NSAF. Differences were to be expected between NSAF and the two intensity based methods for two main reasons: Firstly, the NSAF algorithm is based on the total number of spectra observed per protein (spectral counting) rather than intensity of each peptide spectrum as with iBAQ and openSWATH intensity; Secondly, the sample processing method that was used in the acquisition of NSAF values was different from that which was used with the intensity based methods. NSAF values were obtained from pre-fractionated samples prepared using in gel digestion, whilst intensity based quantitation values were all obtained from unfractionated samples processed using the FASP protocol.

These dissimilarities could underlie the difference observed between the spectral counting based and intensity based methods. The large discrepancy between the two intensity based methods was however unanticipated. The main reason for this difference may lie in the nature of sampling of ions in the two MS platforms. Data dependant acquisition in SWATH-MS sampling allows the selection of all possible ions within successive 25Da windows across the retention time window without discrimination of ion intensity. However data dependant acquisition used for iBAQ quantitation repeatedly samples the most intense ions across the gradient meaning that less intense ions from less abundant proteins are missed. Consequently,

SWATH-MS identifies more peptides per protein than iBAQ, which could result in a difference in the quantitation. This also in part explains why SWATH-MS identifies more proteins than data dependant QE analysis. Secondly, the nature of downstream spectral assignment between the two methods differs substantially, which may result in more spectra being assigned in SWATH-MS approach compared to iBAQ. This may again lead to discrepancies in the quantitation. Furthermore, the QE and SWATH experiments were carried out in triplicate biological replicates while the NSAF data was obtained without biological replicates. This means that each of the iBAQ and SWATH-MS experiments independently seem reproducible and statistically significant and thus the differences in observed in these experiments would require further study.

6.4 Conclusion

This study has used various MS based approaches to identify and quantify the proteome of *M. tuberculosis* clinical isolates. The development of powerful MS platforms and techniques has seen an improvement in proteome mapping and quantitation. Proteomes that have previously been mapped using older approaches have been re-mapped to yield improved results [247,249,369]. The data obtained using the Q-Exactive at 1% FDR was similar to that observed in chapter four at 1% FDR. However, chapter 4 dealt with fractionated samples whilst this data in this chapter is obtained from unfractionated samples. This demonstrates the superiority of the Q-Exactive MS over the Orbitrap Velos that was previously used in this work and suggests that similar fractionation of the samples in this part of the study as was done in Chapter 4 could have produced even higher protein numbers using the Q-Exactive. Alternatively, searching this dataset at 5% FDR as was done in Chapter 4 could have returned higher protein numbers as well. This also reiterates the inference made in Chapter 3 where we concluded that there may be an upper limit or saturation in the number of proteins that can be identified from unfractionated cell lysates which can only be overcome by fractionating the sample to lower the dynamic range, hence increasing the chances of sampling lower abundance ions.

This study indicates that over and above presence or absence of proteins, the relative quantity of proteins expressed among strains may well have an impact on the resultant phenotype of the strains. Direct comparisons of the quantities of the expressed proteome of strains that occur in a clinical setting could shed light on possible reasons for the observed clinical phenotypes. In this study, the pairwise comparison that exhibited the highest number of significantly differentially expressed proteins was the Beijing-CAS pair, which was perhaps to be expected as the Beijing

strain is the most clinically dominant and virulent in the South African setting whilst the CAS strain is almost totally absent. In this pairwise comparison, most of the variation came from down-regulation of protein expression in the CAS strain (83%), predominantly in the intermediary metabolism and respiration group as well as cell wall processes. Curiously, only two of these significantly differentially expressed proteins fell into the virulence class, suggesting that alternative mechanisms other than those that are already marked as virulence associated could be responsible for the difference between these strains.

Another curious observation is that the Beijing and H37R pair shows the smallest significant differential expression, meaning that most shared proteins between the two are expressed in a similar manner. This is interesting because H37Rv does not occur in the clinical setting, hence it was anticipated that its expression profile would be distant from a strain that is considered highly virulent. Furthermore, H37Rv belongs to lineage 4 which is the same as the LAM strain, hence such a similarity rather with the Beijing strain (lineage 2) was unexpected. Among the significant differentially expressed proteins in this pair, only 2 proteins classified in the virulence category were significantly down-regulated: Rv3763 and Rv2373c. These encode the 19kDa antigen precursor protein and a chaperone (dnaJ) protein respectively. This also indicates that proteins other than virulence proteins could be responsible for differential virulence.

Analysis of the Beijing-LAM pair saw the largest difference in proteins that are categorised in the virulence, antigen and adaptation category. Seven of the proteins in this category are significantly down-regulated in Beijing compared to the LAM, including groES, groEL, hspX, tpx and antigen 85. Because these are major immuno-stimulatory proteins, they are bound to influence the course of disease, so finding them differentially expressed amongst major competing clinical strains could have noteworthy effects on the phenotypes of the strains.

Using the iBAQ quantitation experiment alone, the number of significantly differentially expressed proteins is 18% of the total proteins sampled. Overall, the numbers of proteins significantly differentially expressed in the entire comparison analysis represent about 14% of the total theoretical *M. tuberculosis* proteome, suggesting that relatively a small proportion of the proteome is responsible for differential phenotype at the quantitative level. Another observation that is clear in the quantitation assessment is that a large number of proteins that are most likely responsible for differential virulence are those that are annotated to categories other than the virulence. In other words, proteins annotated in the lipid metabolism and PE/PPE

categories for example are not annotated in gene ontology as virulence proteins however various studies have shown them to be useful for virulence. Whilst the functions of some of these proteins are known, over half are still of unknown function suggesting that complete annotation of these proteins must first take place before it is known how they affect virulence.

Preliminary ground work of method development carried out in chapter 3 described the use of fractionation as well as Rescore algorithm as useful in the increase in protein identification. These methods are however not used in this chapter for two reasons. Firstly, SWATH-MS spectra are not yet transferrable to any other algorithm except open-SWATH software. Hence the MS data produced from the SWATH-MS experimental runs could not be analysed by Rescore or any other algorithm. Secondly, although the main algorithm for Rescore has been published, the tool is not yet readily available online as it is still under development. Time constraints at this point did not allow us to send our Q-Exactive generated MS data to Ghent university to be analysed using Rescore. Hence it was thought more valuable to use Max-Quant as it also enables sound identifications and also additionally performs MS1 quantitation which Rescore does not have. Furthermore, fractionation was deemed unnecessary as the peptide sample was to be analysed by SWATH-MS which had been shown already to be able to identify large numbers of spectra from complex samples without fractionation. Furthermore, we decided against quantitation from fractionated samples as the fractions would be processed individually with variable loss in signal per fragment. Hence it was deemed to be more appropriate to quantitate from whole unfractionated samples to obtain a single quantification value. The peptide samples analysed on the Q-Exactive were subsequently not fractionated as this data was meant to be compared to the SWATH-MS data. Hence for compatibility, the Q-Exactive samples were not fractionated as well.

6.5 Future work

This study points us in the direction of which proteins to assess when it comes to differential virulence as a result of differential protein expression. Future studies could involve i*n vivo* assessment of proteins that were found as differentially expressed in this study and could be carried out in infection models of various strains to determine if their expression pattern *in vivo* mimics that observed *in vitro*. Elegant experiments could be designed whereby these proteins are individually conditionally inactivated in parent strains and controlled amounts are used in infection models to observe if the amount of expressed protein is directly proportional to the virulence observed. Furthermore, if reproducible expression pattern signatures of these proteins

in strains can be established, they might be used as diagnostic targets. This would be useful in the control of tuberculosis because knowing immediately the strain responsible for infection promptly gives health workers information on morbidity, epidemiology as well as tendency to drug resistance. This type of information has thus far only been available at the genomic level using genetic markers so protein markers could potentially act as a complementary diagnostic tool that offers a level of information above merely confirming the presence or absence of tuberculosis.

References

1. Palomino JC, Leao SC, Ritacco V (2007) Tuberculosis: From Basic Science to Patient Care. 1st ed. BourcillierKamps.

2. Davies PDO, Pai M (2008) The Diagnosis and Misdiagnosis ofTtuberculosis. Int J Tuber Lung Dis 12: 1226–1234.

3. Friedland G (2009) Tuberculosis Immune Reconstitution Inflammatory Syndrome : Drug Resistance and the Critical Need for Better Diagnostics. Clin Infect Dis 48: 677–679. doi:10.1086/596765.

4. Martinson N (2009) Tuberculosis in South Africa : Pandora ' s box ?

5. WHO (2012) Global Tuberculosis Report 2012.

6. Schluger NW, Rom WN (1998) State of the Art The Host Immune Response to Tuberculosis. Am J Respir Crit Care Med 157: 679–691.

7. Ulrichs T, Munk ME, Mollenkopf H, Behr-perst S, Gennaro ML, et al. (1998) Differential T cell Responses to Mycobacterium tuberculosis ESAT6 in Tuberculosis Patients and Healthy Donors. Eur J Immunol 28: 3949–3958.

8. Ravn P, Demissie A, Eguale T, Wondwosson H, Lein D, et al. (1999) Human T Cell Responses to the ESAT-6 Antigen From Mycobacterium. J Infect Dis 179: 637–645.

9. Guidry T V, Hunter RL, Actor JK (2007) Mycobacterial Glycolipid Trehalose 6,6'-Dimycolate-Induced Hypersensitive Granulomas : Contribution of CD4+ Lymphocytes. Microbiology 153: 3360–3369. doi:10.1099/mic.0.2007/010850-0.

10. Manabe YC, Kesavan AK, Lopez-Molina J, Hatem CL, Brooks M, et al. (2008) The Aerosol Rabbit Model of TB Latency, Reactivation and Immune Reconstitution Inflammatory Syndrome. Tuberculosis 88: 187–196. Available: http://www.ncbi.nlm.nih.gov/pubmed/18068491. Accessed 29 January 2013.

11. Cole ST, Brosch R, Garnier PT, Churcher DH, Harris S V, et al. (1998) Deciphering the biology of Mycobacterium tuberculosis from the Complete Genome Sequence. Nature 393: 537–544.

12. Homolka S, Post E, Oberhauser B, George AG, Westman L, et al. (2008) High Genetic Diversity Among Mycobacterium tuberculosis Complex Strains From Sierra Leone. BMC Microbiol 8. doi:10.1186/1471-2180-8-103.

13. Baker L, Brown T, Maiden MC, Drobniewski F (2004) Silent Nucleotide Polymorphisms and a Phylogeny for Mycobacterium tuberculosis. Emerg Infect Dis 10: 1568–1577.

14. Gagneux S, Small PM (2007) Global Phylogeography of Mycobacterium tuberculosis and Implications for Tuberculosis Product Development. Lancet Infect Dis 7: 328–337.

15. Shimono N, Morici L, Casali N, Cantrell S, Sidders B, et al. (2003) Hypervirulent Mutant of Mycobacterium tuberculosis Resulting From Disruption of the mce1 Operon. Proc Natl Acad Sci 100: 15918–15923.

16. Reed MB, Gagneux S, Deriemer K, Small PM, Iii CEB (2007) The W-Beijing Lineage of Mycobacterium tuberculosis Overproduces Triglycerides and Has the DosR Dormancy Regulon Constitutively Upregulated. J Bacteriol 189: 2583–2589. doi:10.1128/JB.01670-06.

17. Nicol MP, Wilkinson RJ (2008) The Clinical Consequences of Strain Diversity in Mycobacterium tuberculosis. Trans R Soc Trop Med Hygeine 102: 955–965.

18. Smith I (2003) Mycobacterium tuberculosis Pathogenesis and Molecular Determinants of Virulence. Clin Microbiol Rev 16: 463–496. doi:10.1128/CMR.16.3.463.

19. Van der Spuy GD, Kremer K, Ndabambi SL, Beyers N, Dunbar R, et al. (2009) Changing Mycobacterium tuberculosis Population Highlights Clade-specific Pathogenic Characteristics. Tuberculosis 89: 120–125. Available: http://dx.doi.org/10.1016/j.tube.2008.09.003.

20. Manca C, Tsenova L, Bergtold A, Freeman S, Tovey M, et al. (2001) Virulence of a Mycobacterium tuberculosis Clinical Isolate in Mice is Determined by Failure to Induce Th1 Type Immunity and is Associated With Induction of IFN-Alpha or Beta. Proc Natl Acad Sci 98: 5752–5757.

21. Brodin P (1998) Virulence Mechanisms in Tuberculosis.

22. Gagneux S, Narayanan S, Nicol M, Niemann S, Kremer K, et al. (2006) Variable Host – Pathogen Compatibility in Mycobacterium tuberculosis. Proc Natl Acad Sci 103: 2869–2873. doi:10.1073.

23. Kato-Maeda M, Rhee JT, Gingeras TR, Salamon H, Drenkow J, et al. (2001) Comparing Genomes Within The Species Mycobacterium tuberculosis. Genome Res 11: 547–554. Available: http://www.pubmedcentral.nih.gov/articlerender.fcgi?artid=311074&tool=pmcentrez&rendertype=abstract. Accessed 16 February 2013.

24. Kozak RA, Alexander DC, Liao R, Sherman DR, Behr MA (2011) Region of Difference 2 Contributes to Virulence of Mycobacterium tuberculosis. Infect Immun 79: 59–66. doi:10.1128/IAI.00824-10.

25. Dormans J, Roholl P (2004) Correlation of virulence , lung pathology , bacterial load and delayed type hypersensitivity responses after infection with different Mycobacterium tuberculosis genotypes in a BALB/c mouse model. Clin Exp Immunol 137: 460–468. doi:10.1111/j.1365-2249.2004.02551.x.

26. Chacon-Salinas R, Serafin-Lopez J, Ramos-Payan R, Mendez-Aragon P, Hernandez-Pando R, et al. (2005) Differential pattern of cytokine expression by macrophages infected in vitro with different Mycobacterium tuberculosis genotypes. Clin Exp Immunol 140: 443–449. doi:10.1111/j.1365-2249.2005.02797.x.

27. Aguilar DL, Hanekom M, Mata D, Pittius NCG Van, Helden PD Van, et al. (2010) Mycobacterium tuberculosis strains with the Beijing genotype demonstrate variability in virulence associated with transmission. Tuberculosis 90: 319–325. Available: http://dx.doi.org/10.1016/j.tube.2010.08.004.

28. Huet G, Constant P, Lanéelle M, Soolingen D Van, Daffé M, et al. (2009) A Lipid Profile Typifies the Beijing Strains of Mycobacterium tuberculosis: Identification of a Mutation Responsible For Modification of the Structures of Pthiocerol Dimycocerosates and the Phenolic Glycolipids. J Biol Chem 284: 27101–27113. doi:10.1074/jbc.M109.041939.

29. Fleischmann RD, Alland D, Eisen JA, Carpenter L, White O, et al. (2002) Whole-Genome Comparison of Mycobacterium tuberculosis Clinical and Laboratory Strains. J Bacteriol 184: 5479–5490. doi:10.1128/JB.184.19.5479.

30. Wu T, Lu C, Lai H (2009) Current Situations on Identification of Nontuberculous Mycobacteria. J Biomed Lab Sci 21: 1–6.

31. Griffith DE, Aksamit T, Brown-elliott BA, Catanzaro A, Daley C, et al. (2007) An Official ATS / IDSA Statement : Diagnosis , Treatment , and Prevention of Nontuberculous Mycobacterial Diseases. Am J Respir Crit Care Med 175: 367–414. doi:10.1164/rccm.200604-571ST.

32. Bahram NE, Ensieh S, Shrareh M, Jamshid F, Hossein F, et al. (2012) Isolation and phenotypic identification of non-tuberculous mycobacteria existing in Isfahan different water samples. Adv Biomed Res 1: 1–5. doi:10.4103/2277-9175.98115.

33. Kartalija M, Ovrutsky AR, Bryan CL, Pott GB, Al E (2012) Patients With Non-tuberculous Mycobacterial Lung Disease Exhibit Unique Body and Immune Phenotypes.: 1–44. doi:10.1164/rccm.201206-1035OC.

34. Kitada S, Levin A, Hiserote M, Harbeck R, Czaja C, et al. (2012) Serodiagnosis of Mycobacterium avium Complex Pulmonary Disease In The United States. Eur Respir J 10: 1–23. doi:10.1183/09031936.00098212.

35. Gutierrez MC, Ahmed N, Willery E, Narayanan S, Hasnain SE, et al. (2006) Predominance of Ancestral Lineages of Mycobacterium tuberculosis in India. Emerg Infect Dis 12: 1367–1374.

36. Graff J, Rei D, Guan J, Wang W, Seo J, et al. (2012) An epigenetic blockade of cognitive functions in the neurodegenerating brain. Nature. doi:10.1038/nature10849.

37. Krzywinska E, Krzywinski J, Schorey JS (2004) Naturally Occurring Horizontal Gene Transfer and Homologous Recombination in Mycobacterium. Microbiology 150: 1707–1712. doi:10.1099/mic.0.27088-0.

38. Cubillos-ruiz A, Morales J, Zambrano MM (2008) Analysis of the Genetic Variation in Mycobacterium tuberclosis Strains by Multiple Genome Alignments. BMC Res Notes 1: 1–10. doi:10.1186/1756-0500-1-110.

39. Bhanu NV, VanSoolingen D, VanEmbden JD, Dar L, Pandey RM, et al. (2002) Predominace of a novel Mycobacterium tuberculosis genotype in the Delhi region of India. Tuberculosis 82: 105–112. doi:10.1054/tube.332.

40. Delogu G, Brennan MJ (2001) Comparative Immune Response to PE and PE _ PGRS Antigens of Mycobacterium tuberculosis. Infect Immun 69: 5606–5611. doi:10.1128/IAI.69.9.5606.

41. Brosch R, Gordon S V, Marmiesse M, Brodin P, Buchrieser C, et al. (2002) A new evolutionary scenario for the Mycobacterium tuberculosis complex. Proc Natl Acad Sci U S A 99: 3384–3689.

42. Ribón W (2012) Biochemical Isolation and Identification of Mycobacteria. Dr. Jose C. Jimenez-Lopez (Ed). pp. 21–33. Available: http://www.intechopen.com/books/biochemical-testing/bochemical-isolation-and-identification-of-Mycobacteria.

43. Kamerbeek J, Schouls L, Kolk A, Agterveld M, VanSoolingen D, et al. (1997) Simultaneous Detection and Strain Differentiation of Mycobacterium tuberculosis for Diagnosis and Epidemiology. J Clin Microbiol 35: 907–914.

44. Saunders NA (1999) Strain Typing of Mycobacterium tuberculosis. J Infect 38: 80–86.

45. Fang Z, Doig C, Kenna DT, Smittipat N, Watt B, et al. (1999) IS 6110 -Mediated Deletions of Wild-Type Chromosomes of Mycobacterium tuberculosis. J Bacteriol 181: 1014–1020.

46. Hermans PWM, VanSoolingen D, VanEmbden J (1992) Characterization of a Major Polymorphic Tandem Repeat in Mycobacterium tuberculosis and Its Potential Use in the Epidemiology of Mycobacterium kansasii and Mycobacterium gordonae. J Bacteriol 174: 4157–4165.

47. Van Soolingen D, Hermans PWM, DeHaas P, Soll DR, Embdenl J (1991) Occurrence and Stability of Insertion Sequences in Mycobacterium tuberculosis Complex Strains : Evaluation of an Insertion Sequence-Dependent DNA Polymorphism as a Tool in the Epidemiology of Tuberculosis. J Clin Microbiol 29: 2578–2586.

48. Thierry D, Chavarot P, Marchal G, Le Thi KT, Ho ML, et al. (1995) Mycobacterium tuberculosis Strains Unidentified Using the IS6110 Probe Can Be Detected By Oligonucleotides Derived From the Mt308 Sequence. Res Microbiol 146: 325–328. Available: http://www.ncbi.nlm.nih.gov/pubmed/7569326.

49. Van Embden JDA, Cave MD, Crawford JT, Dale JW, Eisenach KD, et al. (1993) Strain Identification of Mycobacterium tuberculosis by DNA Fingerprinting : Recommendations for a Standardized Methodology. J Clin Microbiol 31: 406–409.

50. Otal I, Martin C, Vincent-levy-frebault V, Thierry D, Gicquel B (1991) Restriction Fragment Length Polymorphism Analysis Using IS6110 as an Epidemiological Marker in Tuberculosis. J Clin Microbiol 29: 1252–1254.

51. Lok KH, Benjamin WH, Kimerling ME, Pruitt V, Lathan M, et al. (2002) Molecular Differentiation of Mycobacterium tuberculosis Strains Without IS6110 Insertions. Emerg Infect Dis 8: 1310–1313.

52. Goyal M, Saunders NA, Young DB, VanEmbden JDA, Shaw RJ (1997) Differentiation of Mycobacterium tuberculosis Isolates by Spoligotyping and IS6110 Restriction Fragment Length Polymorphism. J Clin Microbiol 35: 647–651.

53. Groenen PMA, Bunschoten AE, van Soolingen D, Errtbden JDA (2006) Nature of DNA Polymorphsm in the Direct Repeat Cluster of Mycobacterium tuberculosis:Application for Strain Differentiation by a Novel Typing Method. Mol Microbiol 10: 1057–1065. doi:10.1111/j.1365-2958.1993.tb00976.x.

54. Brudey K, Driscoll JR, Rigouts L, Prodinger WM, Gori A, et al. (2006) Mycobacterium tuberculosis complex genetic diversity : mining the fourth international spoligotyping database (SpolDB4) for classification , population genetics and epidemiology. BMC Microbiol 6: 1–17. doi:10.1186/1471-2180-6-23.

55. Bifani PJ, Mathema B, Kurepina NE, Kreiswirth BN (2002) Global dissemination of the Mycobacterium tuberculosis W-Beijing family strains. Trends Microbiol 10: 45–52.

56. Filliol I, Motiwala AS, Cavatore M, Qi W, Hernando M, et al. (2006) Global Phylogeny of Mycobacterium tuberculosis Based on Single Nucleotide Polymorphism (SNP) Analysis : Insights into Tuberculosis Evolution , Phylogenetic Accuracy of Other DNA Fingerprinting Systems , and Recommendations for a Minimal Standard SNP Set. J Bacteriol 188: 759–772. doi:10.1128/JB.188.2.759-772.2006.

57. Frothingham R (1999) Evolutionary Bottlenecks in the Agents of Tuberculosis , Leprosy , and Paratuberculosis. Med Hypothesis 52: 95–99.

58. Sun Y, Bellamy R, Lee ASG, Ng ST, Ravindran S, et al. (2004) Use of Mycobacterial Interspersed Repetitive Unit – Variable-Number Mycobacterium tuberculosis in Singapore. J Clin Microbiol 42: 1986–1993. doi:10.1128/JCM.42.5.1986.

59. Supply P, Warren RM, Bañuls A, Lesjean S, Spuy GD Van Der, et al. (2003) Linkage Disequilibrium Between Minisatellite Loci Supports Clonal Evolution of Mycobacterium tuberculosis in a High Tuberculosis Incidence Area. Mol Microbiol 47: 529–538.

60. Mazars E, Lesjean S, Banuls A, Tibayrenc M, Gicquel B, et al. (2001) High-resolution Minisatellite-based Typing as a Portable Approach to Global Analysis of Mycobacterium tuberculosis Molecular Epidemiology. Proc Natl Acad Sci 98: 1901–1906.

61. Supply P, Lesjean S, Savine E, Soolingen D Van, Locht C, et al. (2001) Automated High-Throughput Genotyping for Study of Global Epidemiology of Mycobacterium tuberculosis Based on Mycobacterial Interspersed Repetitive Units. J Clin Microbiol 39: 3563–3571. doi:10.1128/JCM.39.10.3563.

62. Sola C, Filliol I, Legrand E, Mokrousov I, Rastogi N (2001) Mycobacterium tuberculosis Phylogeny Reconstruction Based on Combined Numerical Analysis with IS1081 , IS6110 , VNTR , and DR-Based Spoligotyping Suggests the Existence of Two New Phylogeographical Clades. J Mol Evol 53: 680–689. doi:10.1007/s002390010255.

63. Sola C, Filliol I, Legrand E, Lesjean S, Locht C, et al. (2003) Genotyping of the Mycobacterium tuberculosis Complex Using MIRUs : Association With VNTR and Spoligotyping for Molecular Epidemiology and Evolutionary Genetics. Infect Genet Evol 3: 125–133. doi:10.1016/S1567-1348(03)00011-X.

64. Lee ASG, Tang LLH, Lim IHK, Bellamy R, Wong S (2002) Discrimination of Single-Copy IS6110 DNA Fingerprints of Mycobacterium tuberculosis Isolates by High-Resolution Minisatellite-Based Typing. J Clin Microbiol 40: 657–659. doi:10.1128/JCM.40.2.657.

65. Roring S, Scott A, Brittain D, Walker I, Hewinson G, et al. (2002) Development of Variable-Number Tandem Repeat Typing of Mycobacterium bovis : Comparison of Results with Those Obtained by Using Existing Exact Tandem Repeats and Spoligotyping. J Clin Microbiol 40: 2126–2133. doi:10.1128/JCM.40.6.2126-2133.2002.

66. Hirsh AE, Tsolaki AG, Deriemer K, Feldman MW, Small PM (2004) Stable Association Between Strains of Mycobacterium tuberculosis and Their Human Host Populations. Proc Natl Acad Sci 101: 4871–4876. doi:10.1073/pnas.0305627101.

67. Alland D, Lacher DW, Hazbón MH, Motiwala AS, Fleischmann RD, et al. (2007) Role of Large Sequence Polymorphisms (LSPs) in Generating Genomic Diversity among Clinical Isolates of Mycobacterium tuberculosis and the Utility of LSPs in Phylogenetic Analysis. J Clin Microbiol 45: 39–46. doi:10.1128/JCM.02483-05.

68. Tsolaki AG, Gagneux S, Pym AS, Salmoniere YLG De, Kreiswirth BN, et al. (2005) Genomic Deletions Classify the Beijing / W Strains as a Distinct Genetic Lineage of Mycobacterium tuberculosis. J Clin Microbiol 43: 3185–3191. doi:10.1128/JCM.43.7.3185.

69. Paustian ML, Zhu X, Sreevatsan S, Robbe- S, Kapur V, et al. (2008) Comarative Genomic Analysis of Mycobacterium avium Subspecies Obtained From Multiple Host Species. BMC Genomics 9: 1471. doi:10.1186/1471-2164-9-135.

70. Hershberg R, Lipatov M, Small PM, Sheffer H, Niemann S, et al. (2008) High Functional Diversity in Mycobacterium tuberculosis Driven by Genetic Drift and Human Demography. PLoS Biol 6: 2658–2671. doi:10.1371/journal.pbio.0060311.

71. Sreevatsan S, Pan X, Stockbauer KE, Connell ND, Kreinwirth BN, et al. (1997) Restricted Structural Gene Polymorphism in the Mycobacterium tuberculosis Complex Indicates Evolutionarily Recent. Proc Natl Acad Sci 94: 9869–9874.

72. Wirth T, Hilderbrand F, Allic-beguec C, Wolbeling F, Kubica T, et al. (2008) Origin , Spread and Demography of the Mycobacterium tuberculosis Complex. PLoS One 4. doi:10.1371/journal.ppat.1000160.

73. Comas I, Chakravartti J, Small PM, Galagan J, Niemann S, et al. (2010) Articles Human T Cell Epitopes of Mycobacterium tuberculosis are Evolutionarily Hyperconserved. Nat Genet 42: 498–505. doi:10.1038/ng.590.

74. Golby P, Hatch KA, Bacon J, Cooney R, Riley P, et al. (2007) Comparative Transcriptomics Reveals Key Gene Expression Differences Between the Human and Bovine Pathogens of the Mycobacterium tuberculosis Complex. Microbiology 153: 3323–3336. doi:10.1099/mic.0.2007/009894-0.

75. Behr MA, Wilson MA, Gill WP, Small PM, Schoolnik GK, et al. (1999) Comparative Genomics of BCG Vaccines by Whole-Genome DNA Microarray. Science (80-) 284: 1520–1523. doi:10.1126/science.284.5419.1520.

76. Mostowy S, Cleto C, Sherman DR, Behr MA (2004) The Mycobacterium tuberculosis Complex Transcriptome of Attenuation. Tuberculosis 84: 197–204. doi:10.1016/j.tube.2004.02.022.

77. Koo M, Subbian S, Kaplan G (2012) Strain Specific Tanscriptional Response in Mycobacterium tuberculosis Infected Macrophages. Cell Commun Signal 10: 1–15. Available: http://www.biosignaling.com/content/10/1/2.

78. Homolka S, Niemann S, Russell DG, Rohde KH (2010) Functional Genetic Diversity among Mycobacterium tuberculosis Complex Clinical Isolates : Delineation of Conserved Core and Lineage-Specific Transcriptomes during Intracellular Survival. PLoS Pathog 6: e10000988. doi:10.1371/journal.ppat.1000988.

79. Rose G, Cortes T, Comas I, Coscolla M, Gagneux S, et al. (2013) Mapping of Genotype – Phenotype Diversity among Clinical Isolates of Mycobacterium tuberculosis by Sequence-based Transcriptional Profiling. Genome Biol Evol 5: 1849–1862. doi:10.1093/gbe/evt138.

80. Gandhi NR, Moll A, Sturm a W, Pawinski R, Govender T, et al. (2006) Extensively drug-resistant tuberculosis as a cause of death in patients co-infected with tuberculosis and HIV in a rural area of South Africa. Lancet 368: 1575–1580. Available: http://www.ncbi.nlm.nih.gov/pubmed/17084757. Accessed 5 April 2012.

81. Newton SM, Smith RJ, Wilkinson KA, Nicol MP, Garton NJ, et al. (2006) A Deletion Defining A Common Asian Lineage of Mycobacterium tuberculosis Associates With Immune Subversion. Proc Natl Acad Sci 103: 15594–15598.

82. Tsenova L, Ellison E, Harbacheuski R, Moreira AL, Kurepina N, et al. (2005) Virulence of Selected Mycobacterium tuberculosis Clinical Isolates in the Rabbit Model of Meningitis Is Dependent on Phenolic Glycolipid Produced by the Bacilli. J Infect Dis 192: 98–106.

83. Neufert C, Pai RK, Noss EH, Boom WH, Harding C V (2001) Mycobacterium tuberculosis 19-kDa Lipoprotein Promotes Neutrophil Activation. J Immunol 167: 1542–1549.

84. Tsolaki AG, Hirsh AE, Deriemer K, Enciso JA, Wong MZ, et al. (2004) Functional and Evolutionary Genomics of Mycobacterium tuberculosis : Insights from Genomic Deletions in 100 Strains. Proc Natl Acad Sci 101: 4865–4870.

85. Hovav A, Mullerad J, Davidovitch L, Bigi F, Cataldi A, et al. (2003) The Mycobacterium tuberculosis Recombinant 27-Kilodalton Lipoprotein Induces a Strong Th1-Type Immune Response Deleterious to Protection. Infect Immun 71: 3146–3154. doi:10.1128/IAI.71.6.3146.

86. Ramaswamy S, Musser JM (1998) Molecular Genetic Basis of Antimicrobial Agent Resistance In Mycobacterium tuberculosis : 1998 Update. Tuber Lung Dis 79: 3–29.

87. Tsenova L, Ellison E, Harbacheuski R, Moreira AL, Kurepina N, et al. (2005) Virulence of Selected Mycobacterium tuberculosis Clinical Isolates in the Rabbit Model of Meningitis Is Dependent on Phenolic Glycolipid Produced by the Bacilli. J Infect Dis 192: 98–106.

88. Lewis KN, Liao R, Guinn KM, Hickey MJ, Smith S, et al. (2006) Deletion of the RD1 from Mycobacterium tuberculosis Mimics Bacille Calmette-Geurin Attenuation. J Infect Dis 187: 117–123.

89. Pym AS, Brodin P, Brosch R, Huerre M, Cole ST (2002) Loss of RD1 Contributed to the Attenuation of the Live Tuberculosis Vaccines Mycobacterium bovis BCG and Mycobacterium microti. Mol Microbiol 46: 709–717.

90. Noss EH, Pai RK, Sellati TJ, Justin D, Belisle J, et al. (2001) Toll-Like Receptor 2-Dependent Inhibition of Macrophage Class II MHC Expression and Antigen Processing by 19-kDa Lipoprotein of Mycobacterium tuberculosis. J Immunol 167: 910–918. Available: http://www.jimmunol.org/content/167/2/910.

91. Lathigra R, Zhang Y, Hill M, Garcia MJ, Jackett PS, et al. (1996) Lack of Production of the 19-kDa Glycolipoprotein in Certain Strains of Mycobacterium tuberculosis. Res Microbiol 147: 237–249.

92. Mahairas GG, Sabo PJ, Hickey MJ, Singh DC, Stover CK (1996) Molecular Analysis of Genetic Differences Between Mycobacterium bovis BCG and Virulent M . bovis. J Bacteriol 178: 1274–1282.

93. Harth BG, Horwitz MA (1999) An Inhibitor of Exported Mycobacterium tuberculosis Glutamine Synthetase Selectively Blocks the Growth of Pathogenic Mycobacteria in Axenic Culture and in Human Monocytes : Extracellular Proteins as Potential Novel Drug Targets. J Exp Med 189: 1425–1435.

94. Harth G, Horwitz MA (2003) Inhibition of Mycobacterium tuberculosis Glutamine Synthetase as a Novel Antibiotic Strategy against Tuberculosis : Demonstration of Efficacy In Vivo. Infect Immun 71: 456–464. doi:10.1128/IAI.71.1.456.

95. Berthet F, Lagranderie M, Gounon P, Laurent-winter C, Ensergueix D, et al. (1998) Attenuation of virulence by disruption of the Mycobacterium tuberculosis erp gene. Science (80-) 282: 759–762. doi:10.1126/science.282.5389.759.

96. Azad AK, Sirakova TD, Norvin D, Kolattukudy PE (1997) Gene Knockout Reveals a Novel Gene Cluster for the Synthesis of a Class of Cell Wall Lipids Unique to Pathogenic Mycobacteria. J Biol Chem 272: 16741–16745. Available: http://www.jbc.org/content/272/27/16741.

97. Dubey VS, Sirakova TD, Kolattukudy PE (2002) Disruption of msl3 abolishes the synthesis of mycolipanoic and mycolipenic acids required for polyacyltrehalose synthesis in Mycobacterium tuberculosis H37Rv and causes cell aggregation. Mol Mirobiology 45: 1451–1459.

98. Cox JS, Chen B, Mcneil M, Jacobs WR (1999) Complex Lipid Determines Tissue-Specific Replication of Mycobacterium tuberculosis in Mice. Nature 402: 79–83. doi:10.1038/47042.

99. Camacho LR, Ensergueix D, Perez E, Gicquel B, Guilhot C (1999) Identification of a virulence gene cluster of Mycobacterium tuberculosis by signature-tagged transposon mutagenesis. Mol Microbiol 34: 257–267.

100. Converse PJ, Dannenberg AM, Estep JE, Sugisaki K, Abe Y, et al. (1996) Cavitary Tuberculosis Produced in Rabbits by Aerosolized Virulent Tubercle Bacilli. Infect Immun 64: 4776–4787.

101. Camacho LR, Constant P, Lanéelle M, Triccas A, Gicquel B, et al. (2001) Analysis of the Phthiocerol Dimycocerosate Locus of Mycobacterium tuberculosis : Evidence That This Lipid is Involved in the Cell Wall Permeability Barrier. J Biol Chem 276: 19845–19854. Available: http://www.jbc.org/content/276/23/19845.full.html#ref-list-1.

102. Belisle JT, Vissa VD, Sievert T, Takayama K, Brennan PJ, et al. (1997) Role of the major antigen of Mycobacterium tuberculosis in cell wall biogenesis. Science (80-) 276: 1420–1422.

103. Horwitz MA, Dillon BJ, Maslesa-Galic S (2000) Recombinant bacillus Calmette – Guerin (BCG) Vaccines Expressing The Mycobacterium tuberculosis 30-kDa Major Secretory Protein Induce Greater Protective Immunity Against Tuberculosis Than Conventional BCG Vaccines In A Highly Susceptible Animal Model. Proc Natl Acad Sci 97: 13853–13858.

104. Dubnau E, Lane M, Vaz T, Be A, Prome J (1997) Mycobacterium bovis BCG genes Involved in the Biosynthesis of Cyclopropyl Keto- and Hydroxy- Mycolic Acids. Mol Microbiol 23: 313–322.

105. Dubnau E, Chan J, Raynaud C, Mohan VP, Lane M (2000) Oxygenated Mycolic Acids Are Necessary for Virulence of Mycobacterium tuberculosis in Mice. Mol Microbiol 36: 630–637.

106. Yuan Y, Clifton BE (1996) A Common Mechanism for the Biosynthesis of Methoxy and Cyclopropyl Mycolic Acids in Mycobacterium tuberculosis. Proc Natl Acad Sci 93: 12828–12833.

107. Glickman MS, Cox JS, Jacobs WR (2000) A Novel Mycolic Acid Cyclopropane Synthetase Is Required for Cording , Persistence , and Virulence of Mycobacterium tuberculosis. Mol Cell 5: 717–727.

108. Raynaud C, Papavinasasundaram KG, Speight RA, Springer B, Sander P, et al. (2002) The Functions of OmpATb , A Pore-forming Protein of Mycobacterium tuberculosis. Mol Microbiol 46: 191–201.

109. Pethe K, Alonso S, Biet F, Delogu G, Brennan MJ, et al. (2001) The Heparin-binding Haemagglutinin of M . tuberculosis Is Required For Extrapulmonary Dissemination. Nature 412: 190–194. Available: http://www.nature.com/nature/journal/v412/n6843/full/41219a0.html.

110. Mckinney JD, Höner K, Muñoz-elías EJ, Miczak A, Chan W, et al. (2000) Persistance of Mycobacterim tuberculosis in Macrophages and Mice Requires the Glyoxalate Shunt Enzyme Isocitrate Lyase. Nature 406: 735–738. doi:10.1038/35021074.

111. Raynaud C, Guilhot C, Rauzier J, Bordat Y, Pelicic V, et al. (2002) Phospholipases C Are Involved In the Virulence of Mycobacterium tuberculosis. Mol Microbiol 45: 203–217.

112. Sambandamurthy VK, Wang X, Chen B, Russell RG, Derrick S, et al. (2002) A Pantothenate Auxotroph of Mycobacterium tuberculosis Is Highly Attenuated and Protects Mice Against Tuberculosis. Nat Med 8: 1171–1174. Available: http://www.nature.com/nm/journal/v8/n10/full/nm765.html.

113. McAdam R, Weisbrod TR, Martin J, Scuderi JD, Brown AM, et al. (1995) In Vivo Growth Characteristics of Leucine and Methionine Auxotrophic Mutants of Mycobacterium bovis BCG Generated by Transposon Mutagenesis. Infect Immun 63: 1004–1012.

114. Hondalus MK, Bardarov S, Russell R, Chan J, Jacobs WR, et al. (2000) Attenuation of and Protection Induced by a Leucine Auxotroph of Mycobacterium tuberculosis. Infect Immun 68: 2888–2898.

115. Parish T, Gordhan BG, Mcadam RA, Duncan K, Mizrahi V, et al. (1999) Production of Mutants In Amino Acid Biosynthesis Genes of Mycobacterium tuberculosis By Homologous Recombination. Microbiology 145: 3497–3503.

116. Smith DA, Parish T, Stoker NG, Bancroft GJ (2001) Characterization of Auxotrophic Mutants of Mycobacterium tuberculosis and Their Potential as Vaccine Candidates. Infect Immun 69: 1142–1150. doi:10.1128/IAI.69.2.1442.

117. Jackson M, Phalen SW, Lagranderie M, Ensergueix D, Chavarot P, et al. (1999) Persistence and Protective Efficacy of a Mycobacterium tuberculosis Auxotroph Vaccine. Infect Immun 67: 2867–2873.

118. Buchmeier N, Blanc-Potard A, Ehrt S, Piddington D, Riley L, et al. (2000) A parallel intraphagosomal survival strategy shared by mycobacterium tuberculosis and

Salmonella enterica. Mol Microbiol 35: 1375–1382. Available: http://www.ncbi.nlm.nih.gov/pubmed/10760138.

119. Moncrief MBC, Maguire ME (1998) Magnesium and the Role of mgtC in Growth of Salmonella typhimurium. Infect Immun 66: 3802–3809.

120. De Voss JJ, Rutter K, Schroeder BG, Su H, Zhu Y, et al. (2000) The Salicylate-derived Mycobactin Siderophores of Mycobacterium tuberculosis are Essential for Growth in Macrophages. Proc Natl Acad Sci 97: 1252–1257. Available: http://www.pubmedcentral.nih.gov/articlerender.fcgi?artid=15586&tool=pmcentrez&rendertype=abstract.

121. Litwin CM, Calderwood SB (1993) Role of Iron in Regulation of Virulence Genes. Clin Microbiol Rev 6: 137–149. doi:10.1128/CMR.6.2.137.Updated.

122. Lounis N, Truffot-Pernot C, Grosset J, Gordeuk VR, Boelaert JR (2001) Iron and Mycobacterium tuberculosis Infection. J Clin Virol 20: 123–126.

123. Rodriguez GM, Voskuil MI, Gold B, Schoolnik GK, Smith I (2002) ideR , an Essential Gene in Mycobacterium tuberculosis : Role of IdeR in Iron-Dependent Gene Expression , Iron Metabolism , and Oxidative Stress Response. Infect Immun 70: 3371–3381. doi:10.1128/IAI.70.7.3371.

124. Dellagostin OA, Esposito G, Eales L, Dale JW, Mcfadden J (1995) Activity of Mycobacterial Promoters During Intracellular and Extracellular Growth. Microbiology 141: 1785–1792.

125. Manabe YC, Saviola BJ, Sun L, Murphy JR, Bishai WR (1999) Attenuation of Virulence in Mycobacterium tuberculosis Expressing a Constitutively Active Iron Repressor. Proc Natl Acad Sci 96: 12844–12848.

126. Weber I, Fritz C, Ruttkowski S, Kreft A, Bange F (2000) Anaerobic Nitrate Reductase (narGHJI) Activity of Mycobacterium bovis BCG In vitro and its Contribution to Virulence in Immunodeficient Mice. Mol Microbiol 35: 1017–1025.

127. Fritz C, Maass S, Kreft A, Bange F (2002) Dependence of Mycobacterium bovis BCG on Anaerobic Nitrate Reductase for Persistence Is Tissue Specific. Infect Immun 70: 286–291. doi:10.1128/IAI.70.1.286.

128. Heym B, Domenech P, Stavropoulos E, Honore N, Saint-joanis B, et al. (1997) Effects of Overexpression of the Alkyl Hydroperoxide Reductase AhpC on the Virulence and Isoniazid Resistance of Mycobacterium tuberculosis. Infect Immun 65: 1395–1401.

129. Li Z, Kelley C, Collins F, Rouse D, Morris S (1998) Expression of katG in Mycobacterium tuberculosis Is Associated with Its Growth and Persistence in Mice and Guinea Pigs. J Infect Dis 177: 1030–1035.

130. Wilson T, Lisle GW De, Marcinkeviciene JA, Blanchard J, Collins DM (1996) Antisense RNA to ahpC, an Oxidative Stress Defence Gene Involved in Isoniazid

Resistance , Indicates That AhpC of Mycobacterium bovis Has Virulence Properties. Microbiology 144: 2687–2695.

131. Sherman DR, Sabo PJ, Hickey MJ, Arain TM, Mahairas GG, et al. (1995) Disparate Responses to Oxidative Stress in Saprophytic and Pathogenic Mycobacteria. Proc Natl Acad Sci 92: 6625–6629.

132. Dussurget O, Stewart G, Neyrolles O, Pescher P, Young D, et al. (2001) Role of Mycobacterium tuberculosis Copper-Zinc Superoxide Dismutase. Infect Immun 69: 529–533. doi:10.1128/IAI.69.1.529.

133. Edwards KM, Cynamon MH, Voladri Rama KR, Hager CC, Destefano MS, et al. (2001) Iron-cofactored Superoxide Dismutase Inhibits Host Responses to Mycobacterium tuberculosis. Am J Respir Crit Care Med 164: 2213–2219.

134. Piddington DL, Fang FC, Laessig T, Cooper AM, Orme IANM, et al. (2001) Cu , Zn Superoxide Dismutase of Mycobacterium tuberculosis Contributes to Survival in Activated Macrophages That Are Generating an Oxidative Burst. Infect Immun 69: 4980–4987. doi:10.1128/IAI.69.8.4980.

135. Predich M, Doukhan L, Nair G, Smith I (2006) Characterization of RNA Polymerase and Two Sigma Factors Genes From Mycobacterium smegmatis. Molcular Microbiol 15: 355–366. doi:10.1111/j.1365-2958.1995.tb02249.x.

136. Gomez M, Doukhan L, Nair G, Smith I (1998) SigA is an Essential Gene in Mycobacterium smegmatis. Mol Microbiol 29: 617–628.

137. Collins DM, Kawakami RP, Lisle GWDE, Pascopella L, Bloomt BR, et al. (1995) Mutation of the principal sigma factor causes loss of virulence in a strain of the Mycobacterium tuberculosis complex. 92: 8036–8040.

138. Chen P, Ruiz RE, Li Q, Silver RF, Bishai WR (2000) Construction and Characterization of a Mycobacterium tuberculosis Mutant Lacking the Alternate Sigma Factor Gene , sigF. Infect Immun 68: 5575–5580.

139. Demaio J, Zhang Y, Ko C, Youngt DB, Bishai WR (1996) A stationary-phase Stress-Response Mycobacterium tuberculosis Sigma Factor from Mycobacterium tuberculosis. Proc Natl Acad Sci 93: 2790–2794.

140. Jensen-cain DM, Quinn FD (2001) Differential Expression of SigE by Mycobacterium tuberculosis During Intracellular Growth. Microb Pathog 30: 271–278.

141. Manganelli R, Dubnau E, Kramer FR, Smith I (1999) Differential Expression of 10 Sigma Factor Genes in Mycobacterium tuberculosis. Mol Microbiol 31: 715–724.

142. Manganelli R, Voskuil MI, Schoolnik GK, Smith I (2001) The Mycobacterium tuberculosis ECF Sigma Factor E : Role in Global Gene Expression and Survival in Macrophages. Mol Microbiol 41: 423–437.

143. Manganelli R, Voskuil MI, Schoolnik GK, Dubnau E, Gomez M, et al. (2002) Role of the Extracytoplasmic-Function Sigma Factor H in Mycobacterium tuberculosis Global Gene Expression. Mol Microbiol 45: 365–374.

144. Kaushal D, Schroeder BG, Tyagi S, Yoshimatsu T, Scott C, et al. (2002) Reduced Immunopathology and Mortality Despite Tissue Persistence in a Mycobacterium tuberculosis Mutant Lacking Alternative Sigma Factor , SigH. Proc Natl Acad Sci 99: 8330–8335.

145. Groisman EA (2001) The Pleiotropic Two-Component Regulatory System PhoP-PhoQ . J Bacteriol 183: 1835–1842. doi:10.1128/JB.183.6.1835.

146. Perez E, Bordas Y, Guilhot C, Gicquel B, Martı C (2001) An Essential Role For phoP In Mycobacterium tuberculosis Virulence. Mol Microbiol 41: 179–187.

147. Graham JE, Clark-Curtiss JE (1999) Identification of Mycobacterium tuberculosis RNAs Synthesized in Response to Phagocytosis By Human Macrophages By Selective Capture of Transcribed Sequences (SCOTS). Proc Natl Acad 96: 11554–11559.

148. Zahrt TC, Deretic V (2001) Mycobacterium tuberculosis Signal Transduction System Required For Persistent Infections. Proc Natl Acad Sci 98: 12706–12711.

149. Wayne LG (1994) Dormancy of Mycobacterium tuberculosis and Latency of Disease. Eur J Microbiol Infect Dis 13: 908–914.

150. DeMaio J, Zhang Y, Bishai WR (1997) Mycobacterium tuberculosis sigF is Part of a Gene Cluster With Similarities to Bacillus subtilis sigF and sigB Operons. Tuber Lung Dis 78: 3–12.

151. Yuan Y, Crane DD, Simpson MR, Zhu, Ya Q, Hickey MJ, et al. (1998) The 16-kDa Alpha Crystallin (Acr) Protein of Mycobacterium tuberculosis is Required for Growth in Macrophages. Proc Natl Acad Sci 95: 9578–9583.

152. Yuan Y, Crane DD, Barry CE (1996) Stationary Phase-Associated Protein Expression in Mycobacterium tuberculosis : Function of the Mycobacterial alpha Crystallin Homolog. J Bacteriol 178: 4484–4492.

153. Stewart GR, Snewin VA, Walzl G, Hussell T, Tormay P, et al. (2001) Overexpression of Heat Shock Proteins Reduces Survival of Mycobacterium tuberculosis In the Chronic Phase of Infection. Nat Med 7: 732–737. doi:10.1038/89113.

154. Steyn AJC, Collins DM, Hondalus MK, Jacobs WR, Kawakami RP, et al. (2002) Mycobacterium tuberculosis WhiB3 Interacts With RpoV to Affect Host Survival But is Dispensable For In-vivo Growth. Proc Natl Acad Sci 99: 3147–3152.

155. Ferreras JA, Stirrett KL, Lu X, Ryu J, Soll CE, et al. (2009) Mycobacterial PGL Virulence Factor Biosynthesis : Mechanism and Small-molecule Inhibition of Polyketide Chain Initiation. Chem Biol 15: 51–61. doi:10.1016/j.chembiol.2007.11.010.

156. Reed MB, Domenech P, Manca C, Su H (2004) A Glycolipid of Hypervirulent Tuberculosis Strains That Inhibits the Innate Immune Response. Nature 431: 84–87.

157. Rindi L, Peroni I, Lari N, Bonanni D, Tortoli E, et al. (2007) Variation of the Expression of Mycobacterium tuberculosis ppe44 Gene Among Clinical Isolates. FEMS Immunol Med Microbiol 51: 381–387. doi:10.1111/j.1574-695X.2007.00315.x.

158. DeSouza GA, Fortuin S, Aguilar D, Pando RH, Mcevoy CRE, et al. (2010) Using a Label-free Proteomics Method to Identify Differentially Abundant Proteins in Closely Related Hypo- and Hypervirulent Clinical Mycobacterium tuberculosis Beijing Isolates. Mol Cell Proteomics 9: 2414–2423. doi:10.1074/mcp.M900422-MCP200.

159. Pheiffer C, Betts JC, Flynn HR, Lukey PT, Helden P Van (2005) Protein Expression By A Beijing Strain Differs From That of Another Clinical Isolate and Mycobacterium tuberculosis H37Rv. Microbiology 151: 1139–1150. doi:10.1099/mic.0.27518-0.

160. Ryoo SW, Park YK, Park S, Shim YS, Liew H (2007) Comparative Proteomic Analysis of Virulent Korean Mycobacterium tuberculosis K-strain with Other Mycobacteria Strain Following Infection of U-937 Macrophage. J Microbiol 45: 268–271.

161. Målen H, Souza GA De, Pathak S, Søfteland T, Wiker HG (2011) Comparison of Membrane Proteins of Mycobacterium tuberculosis H37Rv and H37Ra Strains. BMC Microbiol 11: 18–28. Available: http://www.biomedcentral.com/1471-2180/11/18.

162. Singhal N, Sharma P, Kumar M, Joshi B, Bisht D (2012) Analysis of Intracellular Expressed Proteins of Mycobacterium tuberculosis Clinical Isolates. Proteome Sci 10: 1–14. Available: http://www.proteomesci.com/content/10/1/14.

163. De Souza GA, Fortuin S, Aguilar D, Pando RH, Christopher R (2010) Using a Label-free Proteomics Method to Identify Differentially Abundant Proteins in Closely Related Hypo- and Hypervirulent Clinical Mycobacterium tuberculosis Beijing Isolates. Mol Cell Proteomics 9: 2414–2423. doi:10.1074/mcp.M900422-MCP200.

164. Dheenadhayalan V, Delogu G, Fadda G, Brennan MJ, Sanguinetti M (2006) Variable Expression Patterns of Mycobacterium tuberculosis PE _ PGRS Genes : Evidence that PE _ PGRS16 and PE _ PGRS26 Are Inversely Regulated In Vivo. J Bacteriol 188: 3721–3725. doi:10.1128/JB.188.10.3721.

165. Molloy MP, Witzmann FA (2002) Proteomics : Technologies and Applications. Brief Funct Genomic Proteomic 1: 23–39.

166. Monteoliva L, Albar JP (2004) Differential Proteomics : An Overview of Gel and Non-gel Based Approaches. Brief Funct Genomic Proteomic 3: 220–239.

167. Crick F (1970) Central Dogma of Molecular Biology. Nature 227: 561–563.

168. Corominas R, Yang X, Lin GN, Kang S, Shen Y, et al. (2014) Protein Interaction Networks of Alternatively Spliced Isoforms From Brain Links Genetic Risk Factors for Autism. Nat Commun 5: 1–12. Available: http://dx.doi.org/10.1038/ncomms4650.

169. Tress ML, Bodenmiller B, Aebersold R, Valencia A (2008) Proteomics studies confirm the presence of alternative protein isoforms on a large scale. Genome Biol 9: R162–R172. doi:10.1186/gb-2008-9-11-r162.

170. Chang K (2011) Identification of Protein Isoformss in Mass Spectrometry Based Proteomics Analyses Using Alternative Splicing Databases.

171. Villanueva-can L, Laurie S, Alba MM (2013) Improving Genome-Wide Scans of Positive Selection by Using Protein Isoforms of Similar Length. Genome Biol Evol 5: 457–467. doi:10.1093/gbe/evt017.

172. Howe I, Williams D., Bowen RD (1972) Mass Spectrometry: Principles and Applications. 2nd ed. New York: McGraw-Hill.

173. Wittmer D, Chen YH, Luckenmii WK, Hill HH (1994) Electrospray Ionization Ion Mobility Spectrometry. Anal Chem 66: 2348–2355.

174. Tanaka K, Waki H, Yutaka I, Akita S, Yoshida Y, et al. (1988) Protein and Polymer Analyses up to m/z 100 000 by Laser Desorption Time of Flight Mass Spectrometry. Rapid Commun Mass Spectrom 2: 151–153.

175. Mann M, Hendrickson RC, Pandey A (2001) Analysis of Proteins and Proteomes by Mass Spectrometry. Annu Rev Biochem 70: 437–473.

176. Yang Y, Zhang S, Howe K, Wilson DB, Moser F, et al. (2007) AB R F A Comparison of nLC-ESI-MS/MS and nLC-MALDI-MS/MS for GeLC-Based Protein Identification and iTRAQ-Based Shotgun Quantitative Proteomics. J Biomol Tech 18: 226–237.

177. Guilhaus M (1995) Principles and Instrumentation in Time-of-flight Mass Spectrometry. J Mass Spectrom 30: 1519–1532.

178. Brunee C (1987) The ideal mass analyzer: Fact or fiction. Int J Mass Spectrom 76: 125–237.

179. Wong PSH, Cooks GR (n.d.) Ion Trap Mass Spectrometry.

180. Schaeffer-reiss C (2008) A brief summary of the different types of mass spectrometers used in proteomics. Methods Mol Biol 484: 3–16. Available: http://www.springerlink.com/index/10.1007/978-1-59745-398-1. Accessed 6 August 2013.

181. Hu Q, Noll RJ, Li H, Makarov A, Cooks RG (2005) The Orbitrap : A New Mass Spectrometer. J Mass Spectrom 40: 430–443. doi:10.1002/jms.856.

182. Perry RH, Cooks RG, Noll RJ (2008) ORBITRAP MASS SPECTROMETRY : INSTRUMENTATION , ION MOTION AND APPLICATIONS. Mass Spectrom Rev 27: 661–699. doi:10.1002/mas.

183. Lange V, Picotti P, Domon B, Aebersold R (2008) Selected Reaction Monitoring for Quantitative Proteomics: A Tutorial. Mol Syst Biol 4: 222. Available:

http://www.pubmedcentral.nih.gov/articlerender.fcgi?artid=2583086&tool=pmcentrez&rendertype=abstract.

184. Anderson NL, Anderson NG (2002) The human plasma proteome. Mol Cell Proteomics 1: 845–855.

185. Muth T (2011) Cloud Computing in Proteomics for the In-depth Analysis of High Quality Unidentified Spectra. U-Ghent.

186. Ettre L (1993) Nomenclature for Chromatography. Pure Appl Chem 65: 819–872.

187. Washburn MP, Wolters D, Yates JR (2001) Large-scale Analysis of the Yeast Proteome by Multidimensional Protein Identification Technology. Nat Biotechnol 19: 242–247.

188. Motoyama A, Yates JR (2008) Multidimensional LC Sepa.rations in Shotgun Proteomics. Anal Chem 80: 7187–7193.

189. Henzel WJ, Watanabe C, Stults JT (2003) Protein Identification : The Origins of Peptide Mass Fingerprinting. J Am Soc Mass Spectrom 14: 931–942. doi:10.1016/S1044-0305(03)00214-9.

190. Soares R, Pires E, Almeida AM, Santos R, Gomes R, et al. (2001) Tandem Mass Spectrometry of Peptides.

191. Thiede B, Höhenwarter W, Krah A, Mattow J, Schmid M, et al. (2005) Peptide Mass Fingerprinting. Methods 35: 237–247. doi:10.1016/j.ymeth.2004.08.015.

192. Flora J., Null A., Muddiman D. (2002) Dual-micro-ESI source for precise mass determination on a quadrupole time-of-flight mass spectrometer for genomic and proteomic applications. Anal Bioanal Chem 373: 538–546.

193. Zubarev R., Haselmann K, Budnik B., Kjeldsen F, Jensen F (2002) Towards An Understanding of the Mechanism of Electron Capture Dissociation: A Historical Perspective and Modern Ideas. Eur J Mass Spectrom 8: 337–349.

194. Breuker K, Oh H, Horn D., Cerda B, McLafferty F. (2002) Detailed unfolding and folding of gaseous ubiquitin ions characterized by electron capture dissociation. J Am Chem Soc 124: 6407–6420.

195. Duncan DT, Craig R, Link AJ (2005) Parallel Tandem : A Program for Parallel Processing of Tandem Mass Spectra Using PVM or MPI and X ! Tandem. J Proteome Res 4: 1842–1847.

196. Geiger T, Wehner A, Schaab C, Cox J, Mann M (2012) Comparative Proteomic Analysis of Eleven Common Cell Lines Reveals Ubiquitous but Varying Expression of Most Proteins. Mol Cell Proteomics 11: M111.014050. doi:10.1074/mcp.M111.014050.

197. Rosenberger G, Koh CC, Guo T, Röst HL, Kouvonen P, et al. (2014) A repository of assays to quantify 10 , 000 human proteins by SWATH-MS. Sci Data 1: 1–15. doi:10.1038/sdata.2014.31.

198. Park CY, Klammer AA, Ka L, Maccoss MJ, Noble WS (2008) Rapid and Accurate Peptide Identification from Tandem Mass Spectra. J Proteome Res 7: 3022–3027.

199. Frank A, Tanner S, Bafna V, Pevzner P (2005) Peptide Sequence Tags for Fast Database Search in Mass-Spectrometry. J Proteome Res 4: 1287–1295.

200. Zhang J, Xin L, Shan B, Chen W, Xie M, et al. (2011) PEAKS DB : De Novo Sequencing Assisted Database Search for Sensitive and Accurate Peptide Identification. Mol Cell proteomics 11: 1–27.

201. Sezonov G, Joseleau-petit D, Ari D, Ari RD (2007) Escherichia coli Physiology in Luria-Bertani Broth Escherichia coli Physiology in Luria-Bertani Broth. J Bacteriol 189: 8746–8749. doi:10.1128/JB.01368-07.

202. Eng JK, Mccormack AL, Yates JR (1994) An Approach to Correlate Tandem Mass Spectral Data of Peptides with Amino Acid Sequences in a Protein Database. J Am Soc Mass Spectrom 5: 976–989.

203. Shteynberg D, Deutsch EW, Lam H, Eng JK, Sun Z, et al. (2011) iProphet: Multi-level Integrative Analysis of Shotgun Proteomic Data Improves Peptide and Protein Identification Rates and Error Estimates. Mol Cell proteomics 10: 1–44. Available: http://www.ncbi.nlm.nih.gov/pubmed/21876204.

204. Tanner S, Shu H, Frank A, Wang L, Zandi E, et al. (2005) InsPecT : Identification of Posttranslationally Modified Peptides From Tandem Mass Spectra. Anal Chem 77: 4626–4639. doi:10.1021/ac050102d.

205. Dancik V, Addona TA, Clauser KR, Vath JE, Pevzner PA (1999) De Novo Peptide Sequencing via Tandem Mass Spectrometry. J Comput Biol 6: 327–342.

206. Perkins DN, Pappin DJC, Creasy DM, Cotrell JS (1999) Probability Based Protein Identification By Searching Sequence Databases Using Mass Spectrometry Data. Electrophoresis 20: 3551–3567.

207. Geer LY, Markey SP, Kowalak J, Wagner L, Xu M, et al. (2004) Open Mass Spectrometry Search Alogorithm. J Proteome Res 3: 958–964.

208. Spivak M, Weston J, Ka L, Noble WS (2009) Improvements to the Percolator Algorithm for Peptide Identification From Shotgun Proteomics Data Sets. J Proteome Res 8: 3737–3745.

209. Kall L, Canterbury JD, Weston J, Noble WS, Maccoss MJ (2007) Semi-supervised Learning For Peptide Identification From Shotgun Proteomics Datasets. Nat Methods 4: 923–925. doi:10.1038/NMETH1113.

210. Gui J, Tosteson TD, Borsuk M (2012) Weighted Multiple Testing Procedures for Genomic Studies. BioData Min 5: 1–9.

211. Granholm V, Kall L (2010) Quality Assessment of Peptide-Spectrum Matches in Shotgun Proteomics. Proteomics 11: 1086–1093.

212. Benjamini Y, Hochberg Y (1995) Controlling the false discovery rate: a practical and powerful approach to multiple testing. J R Stat Soc Ser B Stat Methodol 57: 289–300.

213. Evans SR (2010) Common Statistical Concerns in Clinical Trials. J Exp Stroke &Translational Med 3: 1–7.

214. Deutsch EW, Mendoza L, Shteynberg D, Farrah T, Lam H, et al. (2010) A guided tour of the Trans-Proteomic Pipeline. Proteomics 10: 1150–1159. Available: http://www.ncbi.nlm.nih.gov/pubmed/20101611. Accessed 2 November 2010.

215. Nesvizhskii AI, Keller A, Kolker E, Aebersold R (2003) A Statistical Model for Identifying Proteins by Tandem Mass Spectrometry. Anal Chem 75: 4646–4658. Available: http://pubs.acs.org/doi/abs/10.1021/ac0341261. Accessed 26 July 2011.

216. Keller A (2009) Validation of Peptide Assignments to MS / MS Spectra PeptideProphet : Next TPP Step : PeptideProphet.

217. Keller A, Eng J, Zhang N, Li X, Aebersold R (2005) A uniform proteomics MS/MS Analysis Platform Utilizing Open XML File Formats. Mol Syst Biol 1: 2005.0017. Available: http://www.pubmedcentral.nih.gov/articlerender.fcgi?artid=1681455&tool=pmcentrez&rendertype=abstract. Accessed 16 February 2013.

218. Choi H, Fermin D, Nesvizhskii AI (2008) Significance Analysis of Spectral Count Data in Label-free Shotgun Proteomics. Mol Cell Proteomics 7: 2373–2385. doi:10.1074/mcp.M800203-MCP200.

219. Old WM, Meyer-arendt K, Aveline-wolf L, Pierce KG, Mendoza A, et al. (2005) Comparison of Label-free Methods for Quantifying Human Proteins by Shotgun Proteomics. Mol Cell Proteomics 4: 1487–1502. doi:10.1074/mcp.M500084-MCP200.

220. Zhu W, Smith JW, Huang C (2010) Mass Spectrometry-Based Label-Free Quantitative Proteomics. J Biomed Biotechnol: 1–6. doi:10.1155/2010/840518.

221. Lebert D, Dupuis A, Garin J, Bruley C, Brun V (2011) Production and Use of Stable Isotope-labeled Proteins for Absolute Quantitative Proteomics. Methods Mol Biol 753: 93–115. doi:10.1007/978-1-61779-148-2.

222. Ong SE, Blagoev B, Kratchmarova I, Kristensen DB, Steen H, et al. (2002) Stable Isotope Labeling By Amino Acids In Cell Culture, SILAC, As A Simple and Accurate Approach to Expression Proteomics. Mol Cell Proteomics 1: 376–386.

223. Mc Alister GC, Huttlin EL, Haas W, Ting L, Mark P, et al. (2013) Increasing the multiplexing capacity of TMT using reporter ion isotopes with isobaric masses. Anal Chem 84: 7469–7478. doi:10.1021/ac301572t.Increasing.

224. Viner R, Bomgarden R, Blank M, Rogers J (2010) Increasing the Multiplexing of Protein Quantitation from 6- to 10-Plex with Reporter Ion Isotopologues.

225. Hung C, Tholey A (2012) Tandem Mass Tag Protein Labeling for Top-Down Identification and Quantification. Anal Chem 84: 161–170.

226. Yates JR, Ruse CI, Nakorchevsky A (2009) Proteomics by Mass Spectrometry: Approaches, Advances, and Applications. Annu Rev Biomed Eng 11: 49–79. Available: http://www.ncbi.nlm.nih.gov/pubmed/19400705. Accessed 12 August 2013.

227. Ting L, Rad R, Gygi SP, Haas W (2012) MS3 Eliminates Ratio Distortion in Isobaric Labeling-based Multiplexed Quantitative Proteomics. Nat Methods 8: 937–940. doi:10.1038/nmeth.1714.MS3.

228. Trudgian DC, Ridlova G, Fischer R, Mackeen MM, Ternette N, et al. (2011) Comparative Evaluation of Label-free SINQ Normalized Spectral Index Quantitation in the Central Proteomics Facilities Pipeline. Proteomics 11: 1–8. doi:10.1002/pmic.201000800.

229. Paoletti AC, Parmely TJ, Tomomori-sato C, Sato S, Zhu D, et al. (2006) Quantitative Proteomic Analysis of Distinct Mammalian Mediator Complexes Using Normalized Spectral Abundance Factors. Proc Natl Acad Sci 103: 18928–18933.

230. Ishihama Y, Oda Y, Tabata T, Sato T, Nagasu T, et al. (2005) Index (emPAI) for Estimation of Absolute Protein Amount in Proteomics by the Number of Sequenced Peptides Per Protein. Mol Cell Proteomics 4: 1265–1272. doi:10.1074/mcp.M500061-MCP200.

231. Trudgian DC, Ridlova G, Fischer R, Mackeen MM, Ternette N, et al. (2011) Comparative evaluation of label-free SINQ normalized spectral index quantitation in the central proteomics facilities pipeline. Proteomics 11: 2790–2797. Available: http://www.ncbi.nlm.nih.gov/pubmed/21656681. Accessed 3 August 2011.

232. Colaert N, Vandekerckhove J, Gevaert K, Martens L (2011) A comparison of MS2-based label-free quantitative proteomic techniques with regards to accuracy and precision. Proteomics 11: 1110–1113. Available: http://www.ncbi.nlm.nih.gov/pubmed/21365758. Accessed 17 August 2011.

233. Tambor V, Fučíková A, Lenčo J, Kacerovský M, Řeháček V (2010) Application of Proteomics in Biomarker Discovery : a Primer for the Clinician. Physiol Res 59: 471–497.

234. Wolf-yadlin A, Hautaniemi S, Lauffenburger DA, White FM (2007) Multiple Reaction Monitoring For Robust Quantitative Proteomic Analysis of Cellular Signaling Networks. Proc Natl Acad Sci 104: 5860–5865.

235. Deutsch EW, Lam H, Aebersold R (2008) PeptideAtlas: a resource for target selection for emerging targeted proteomics workflows. EMBO Rep 9: 429–434. Available: http://www.pubmedcentral.nih.gov/articlerender.fcgi?artid=2373374&tool=pmcentrez&rendertype=abstract. Accessed 14 July 2010.

236. Blow N (2008) Mass spectrometry and proteomics: hitting the mark. Nat Methods 5: 741–747. Available: http://www.nature.com/doifinder/10.1038/nmeth0808-741.

237. Han B, Higgs RE (2008) Proteomics: From Hypothesis to Quantitative Assay on a Single Platform. Guidelines For Developing MRM Assays Using Ion Trap Mass Spectrometers. Brief Funct Genomic Proteomic 7: 340–354. Available: http://www.ncbi.nlm.nih.gov/pubmed/18579614. Accessed 24 April 2012.

238. Anderson L, Hunter CL (2006) Quantitative Mass Spectrometric Multiple Reaction Monitoring Assays for Major Plasma Proteins. Mol Cell Proteomics 5: 573–588. doi:10.1074/mcp.M500331-MCP200.

239. Malik A, Godfrey-Faussett P (2005) Effects of Genetic Variability of Mycobacterium tuberculosis. Lancet Infect Dis 5: 174–183.

240. Escher C, Reiter L, Maclean B, Ossola R, Herzog F, et al. (2012) Using iRT, a Normalized Retention Time for More Targeted Measurement of Peptides. Proteomics 12: 1111–1121. Available: http://www.ncbi.nlm.nih.gov/pubmed/22577012. Accessed 15 May 2012.

241. Shevshencko A, Chernushevich I, Ens W, Standing KG, Wilm TB, et al. (1999) Rapid De-novo Peptide Sequencing by a Combination of Nano-elctrospray Isotopic Labelling and a Quadrupole/Time-of-flight Mass Spectrometer. Rapid Commun Mass Spectrom 11: 1015–1024.

242. Silva JC, Gorenstein M V, Li G, Vissers JP, Geromanos SJ (2006) Absolute Quantification of Proteins by LCMS. Mol Cell Proteomics 5: 144–156.

243. Ross R, Huang YN, Marhese J, Al E (2002) Multiplex Protein Quantification Saccharomyes cerevisiae Using Amine Reactive Isobaric Tagging Reagent. Mol Cell Proteomics 3: 1154–1169.

244. Gygi S, Rist B, Gerber S, Turecek F, Gelb MH, et al. (1999) Quantitative Analysis of Protein Mixures Using Isotope Coded Affinity Tags. Nat Biotechnol 17: 994–999.

245. Plumb RS, Johnson KA, Rainville P, Smith BW, Wilson ID, et al. (2006) UPLC/MSE ; a new approach for generating molecular fragment information for biomarker structure elucidation. Rapid Commun Mass Spectrom 20: 1989–1994. doi:10.1002/rcm.

246. Egertson JD, Kuehn A, Merrihew GE, Bateman NW, Maclean BX, et al. (2014) Multiplexed MS/MS for Improved Data Independant Acquisition. Nat Methods 10: 1–10. doi:10.1038/nmeth.2528.Multiplexed.

247. Gillet LC, Navarro P, Tate S, Rost H, Selevsek N, et al. (2012) Targeted Data Extraction of the MS / MS Spectra Generated by Data- independent Acquisition : A New Concept for Consistent and Accurate Proteome Analysis. Mol Cell Proteomics 11: 1–28. doi:10.1074/mcp.O111.016717.

248. Schubert OT, Mouritsen J, Rosenberger G, Arthur PK, Ludwig C, et al. (2013) The Mtb Proteome Library : A Resource of Assays to Quantify the Complete Proteome of Mycobacterium tuberculosis. Cell Host Microbe 13: 602–612. doi:10.1016/j.chom.2013.04.008.

249. Roest HL, Rosenberger G, Navarro P, Schubert OT, Wolski W, et al. (2012) OpenSWATH : Automated , targeted analysis of mass spectrometric data generated by data-independent acquisition: 1–26. Available: http://www.openswath.org.

250. Ludwig C, Claassen M, Schmidt A, Aebersold R (2012) Estimation of Absolute Protein Quantities of Unlabeled Samples by Selected Reaction Monitoring Mass Spectrometry. Mol Cell Proteomics 11.

251. Medini D, Masignani V, Donati C, Rappuoli R (2005) The Microbial Pan-genome. Curr Opin Genet Dev 15: 589–594. doi:10.1016/j.gde.2005.09.006.

252. Reed MB, Gagneux S, Deriemer K, Small PM, Iii CEB, et al. (2007) The W-Beijing Lineage of Mycobacterium tuberculosis Overproduces Triglycerides and Has the DosR Dormancy Regulon Constitutively Upregulated The W-Beijing Lineage of Mycobacterium tuberculosis Overproduces Triglycerides and Has the DosR Dormancy Regulon. J Bacterriology 189: 2583–2589. doi:10.1128/JB.01670-06.

253. Hett EC, Rubin EJ (2008) Bacterial Growth and Cell Division : a Mycobacterial Perspective. Microbiol Mol Biol Rev 72: 126–156. doi:10.1128/MMBR.00028-07.

254. Sandri M, Rizzi C, Catani C, Carraro U (1993) Small and Large Scale Preparative Purification of Myosin Light and Heavy Chains By Selective KDS Precipitation of Myosin Subunits: Yield by SDS PAGE and Quantitative Orthogonal Densitometry. BAM 2: 107–114.

255. Shilov I V, Seymour SL, Patel AA, Loboda A, Tang WH, et al. (2007) The Paragon Algorithm , a Next Generation Search Engine That Uses Sequence Temperature Values and Feature Probabilities to Identify Peptides from Tandem Mass Spectra. Mol Cell Proteomics 6: 1638–1655. doi:10.1074/mcp.T600050-MCP200.

256. Muth T, Peters J, Blackburn J, Rapp E, Martens L (2013) ProteoCloud: A Full-Featured Open Source Proteomics Cloud Computing Pipeline. Proteomics 88: 104–108.

257. Käll L, Storey JD, Noble WS (2009) QVALITY: Non-parametric Estimation of Q-values and Posterior Error Probabilities. Bioinformatics 25: 964–966. Available: http://www.pubmedcentral.nih.gov/articlerender.fcgi?artid=2660870&tool=pmcentrez&rendertype=abstract. Accessed 16 March 2012.

258. Muth T, Vaudel M, Barsnes H, Martens L, Sickmann A (2010) XTandem Parser: An Open-source Library to Parse and Analyse X!Tandem MS/MS Search Results. Proteomics 7: 1522–1524.

259. Barsnes H, Huber S, Sickmann A, Eidhammer I, Martens L (2009) OMSSA Parser: an open-source library to parse and extract data from OMSSA MS/MS search results. Proteomics 9: 3772–3774.

260. Degroeve S, Martens L (2013) MS 2 PIP : a Tool for MS / MS Peak Intensity Prediction. Bioinformatics 29: 3199–3203. doi:10.1093/bioinformatics/btt544.

261. Adkins JN, Varnum SM, Auberry KJ, Moore RJ, Angell NH, et al. (2002) Toward a Human Blood Serum Proteome. Mol Cell Proteomics 1: 947–955. doi:10.1074/mcp.M200066-MCP200.

262. Scheiss R, Wollscheid B, Aebersold R (2009) Targeted Proteomic Strategy For Clinical Biomarker Dscovery. Mol Oncol 3: 33–44. doi:10.1016/j.molonc.2008.12.001.Targeted.

263. Peiper R, Su Q, Gatlin CL, Huang S, Anderson NL, et al. (2003) Multi-component immunoaffinity Iubtraction Chromatography : An Innovative Step Towards A Comprehensive Survey of the Human Plasma Proteome. Proteomics 3: 422–432.

264. Issaq HJ, Conrads TP, Janini GM, Veenstra TD (2002) Methods For Fractionation, Separation and Profiling of Proteins and Peptides. Electrophoresis 23: 3048–3061.

265. Brosch R, Gordon S V, Pym A, Eiglmeier K, Garnier T, et al. (2000) Comparative genomics of the mycobacteria. Int J Med Microbiol 290: 143–152. Available: http://www.ncbi.nlm.nih.gov/pubmed/11045919. Accessed 2 March 2013.

266. Uzoigwe JC, Khaitsa ML, Gibbs PS (2007) Epidemiological Evidence For Mycobacterium avium Subspecies paratuberculosis as a Cause of Crohn ' s Disease. Epidemiol Infect 135: 1057–1068. doi:10.1017/S0950268807008448.

267. Hagiwara E, Komatsu S, Nishihira R, Shinohara T, Baba T, et al. (2012) Clinical Characteristics and Prevalence of Pneumothorax in Patients With Pulmonary Mycobacterium avium Complex Disease. J Infect Chemother: 16–20. doi:10.1007/s10156-012-0518-0.

268. Takahashi M, Tsukamoto H, Kawamura T (2012) Mycobacterium kansasii Pulmonary Infection : CT Findings in 29 Cases. Jpn J Radiol 30: 398–406. doi:10.1007/s11604-012-0061-z.

269. Tortoli E, Simonetti TM, Lacchini C, Penati V, Urban P (1994) Tentative Evidence of AIDS-Associated Biotype of Mycobacterium kansasii. J Clin Microbiol 32: 1779–1782.

270. Stinear TP, Mve-obiang A, Small PLC, Frigui W, Pryor MJ, et al. (2004) Giant Plasmid Encoded Polyketide Synthases Produce the Macrolide Toxin of Mycobacterium ulcerans. Proc Natl Acad Sci 101: 1345–1349.

271. Tb I (2011) World Health Organization HIV / TB Facts 2011.

272. Richter E, Niemann S, Rusch-Gerdes S, Hoffner S (1999) Identification of Mycobacterium kansasii by Using a DNA Probe (AccuProbe) and Molecular Techniques. J Clin Microbiol 37: 964–970.

273. Park HK, Koh W-J, Shim TS, Kwon OJ (2010) Clinical Characteristics and Treatment Outcomes of Mycobacterium kansasii Lung Disease In Korea. Yonsei Med J 51: 552–556. Available: http://www.pubmedcentral.nih.gov/articlerender.fcgi?artid=2880268&tool=pmcentrez&rendertype=abstract. Accessed 6 April 2013.

274. Han SH, Kim KM, Chin BS, Choi SH, Lee HS, et al. (2010) Disseminated Mycobacterium kansasii Infection Associated With Skin Lesions: A Case Report and Comprehensive Review of the literature. J Korean Med Sci 25: 304–308. Available: http://www.pubmedcentral.nih.gov/articlerender.fcgi?artid=2811302&tool=pmcentrez&rendertype=abstract. Accessed 6 April 2013.

275. Ghazalpour A, Bennett B, Petyuk VA, Orozco L, Hagopian R, et al. (2011) Comparative Analysis of Proteome and Transcriptome Variation in Mouse. PLoS Genet 7: 1–17. doi:10.1371/journal.pgen.1001393.

276. Vogel C, Marcotte EM (2013) Insights Into the Regulation of Protein Abundance From Transcriptomic Analyses. Nat Rev Genet 13: 227–232. doi:10.1038/nrg3185.Insights.

277. Foss EJ, Radulovic D, Shaffer SA, Goodlett DR, Kruglyak L (2011) Genetic Variation Shapes Protein Networks Mainly through Non-transcriptional Mechanisms. PLoS Biol 9: 1–11. doi:10.1371/journal.pbio.1001144.

278. Maier T, Güell M, Serrano L (2009) Correlation of mRNA and Protein Complex Biological Samples. FEBS Lett 583: 3966–3973. Available: http://dx.doi.org/10.1016/j.febslet.2009.10.036.

279. Raju RM, Jedrychowski MP, Wei J, Pinkham JT, Park AS, et al. (2014) Post-Translational Regulation via Clp Protease Is Critical for Survival of Mycobacterium tuberculosis. PLoS Pathog 10: 1–10. doi:10.1371/journal.ppat.1003994.

280. Karve TM, Cheema AK (2011) Small Changes Huge Impact : The Role of Protein Posttranslational Modifications in Cellular Homeostasis and Disease. J Amino Acids: 1–13. doi:10.4061/2011/207691.

281. Wang Y, Peterson SE, Loring JF (2013) Protein Post-translational Modifications and Regulation of Pluripotency in Human Stem Cells. Cell Res 24: 143–160. Available: http://dx.doi.org/10.1038/cr.2013.151.

282. Sarkar R, Lenders L, Wilkinson K, Wilkinson RJ, Nicol MP (2012) Modern Lineages of Mycobacterium tuberculosis Exhibit Lineage-specific Patterns of Growth and Cytokine Induction in Human Monocyte-derived Macrophages. PLoS One 7: e43170. Available: http://www.pubmedcentral.nih.gov/articlerender.fcgi?artid=3420893&tool=pmcentrez&rendertype=abstract. Accessed 21 March 2013.

283. Rajaonarifara E (2013) A Bioinformatic Study on the Feasibility of a Cross-species Proteomics Analyses of Mycobacteria. University of Cape Town.

284. Oliveros JC (2007) Venny: An interactive tool for comparing lists with venn diagrams. Available: http://bioinfogp.cnb.csic.es/tools/venny/index.html.

285. Huang DW, Sherman BT, Lempicki RA (2009) Bioinformatics Enrichment Tools: Path Toward The Comprehensive Functional Analysis of Large Gene Lists. Nucleic Acid Res 37: 1–13.

286. Huang DW, Sherman BT, Lempicki RA (2009) Systematic and Intergrative Analysis of Large Gene Lists Using DAVID Bioinformatics Resources. Nat Protoc 4: 44–57.

287. Kana BD, Gordhan BG, Downing KJ, Sung N, Vostroktunova G, et al. (2008) The resuscitation-promoting factors of Mycobacterium tuberculosis Are RequiredFfor Virulence and Resuscitation From Dormancy But Are Collectively Dispensable For Growth In vitro. Mol Microbiol 67: 672–684. doi:10.1111/j.1365-2958.2007.06078.x.

288. Kana BD, Mizrahi V (2010) Mycobacterial Infections Resuscitation-promoting Factors In Bacterial Population Dynamics During TB Infection. Drug Discov Today Dis Mech 7: e13–e18. Available: http://dx.doi.org/10.1016/j.ddmec.2010.08.003.

289. Harth G, Horwitz MA (1999) Export of Recombinant Mycobacterium tuberculosis Superoxide Dismutase Is Dependent upon Both Information in the Protein and Mycobacterial Export Machinery : A Model For Studying Export of Leaderless Proteins by Pathogenic Mycobacteria. J Biol Chem 274: 4281–4292. doi:10.1074/jbc.274.7.4281.

290. Braunstein M, Espinosa BJ, Belisle JT, Jacobs WR (2003) SecA2 functions in the secretion of superoxide dismutase A and in the virulence of Mycobacterium tuberculosis. Mol Microbiol 48: 453–464.

291. Parish T, Smith DA, Roberts G, Betts J, Stoker NG, et al. (2003) The senX3-regX3 two-component resulatory system of Mycobacterium tuberculosis is required for virulence. Microbiology 149: 1423–1435. doi:10.1099/mic.0.26245-0.

292. Griffin JE, Gawronski JD, Dejesus MA, Ioerger TR, Akerley BJ, et al. (2011) High-Resolution Phenotypic Profiling Defines Genes Essential for Mycobacterial Growth and Cholesterol Catabolism. PLoS Pathog 7: 1–9. doi:10.1371/journal.ppat.1002251.

293. Covert BA, Spencer JS, Orme IM, Belisle JT (2001) The application of proteomics in defining the T cell antigens of Mycobacterium tuberculosis. Proteomics 1: 574–586.

294. Qamra R, Mande SC (2004) Crystal Structure of the 65-Kilodalton Heat Shock Protein , Chaperonin 60.2 , of Mycobacterium tuberculosis. J Bacteriol 186: 8105–8113. doi:10.1128/JB.186.23.8105.

295. Stewart GR, Wernisch L, Stabler R, Mangan JA, Hinds J, et al. (2002) Dissection of the heat-shock response in Mycobacterium tuberculosis using mutants and microarrays. Microbiology 148: 3129–3138.

296. De Souza GA, Leversen NA, Målen H, Wiker HG (2011) Bacterial proteins with cleaved or uncleaved signal peptides of the general secretory pathway. J Proteomics 75: 502–510. Available: http://dx.doi.org/10.1016/j.jprot.2011.08.016.

297. Sassetti CM, Rubin EJ (2003) Genetic Requirements for Mycobacterial Survival During Infection. Proc Natl Acad Sci 100: 12989–12994. Available: http://www.pubmedcentral.nih.gov/articlerender.fcgi?artid=240732&tool=pmcentrez&rendertype=abstract.

298. Van der Geize R, Yam K, Heuser T, Wilbrink MH, Hara H, et al. (2007) A gene cluster encoding cholesterol catabolism in a soil actinomycete provides insight into Mycobacterium tuberculosis survival in macrophages. Proc Natl Acad Sci 104: 1947–1952.

299. Haile Y, Caugant DA, Bjune G, Wiker HG (2002) Mycobacterium tuberculosis mammalian cell entry operon (mce) homologs in Mycobacterium other than tuberculosis (MOTT). FEMS Immunol Med Microbiol 33: 123–132.

300. Dahl JL, Kraus CN, Boshoff HIM, Doan B, Foley K, et al. (2003) The role of Rel Mtb - mediated adaptation to stationary phase in long-term persistence of Mycobacterium tuberculosis in mice. Proc Natl Acad Sci U S A 100: 10026–10031.

301. Pym AS, Saint-joanis B, Cole ST (2002) Effect of katG Mutations on the Virulence of Mycobacterium tuberculosis and the Implication for Transmission in Humans. Infect Immun 70: 4955–4960. doi:10.1128/IAI.70.9.4955.

302. Wren BW, Stabler RA, Das S, Butcher PD, Mangan JA, et al. (1998) Characterization of a haemolysin f rom Mycobacterium tuberculosis with homology to a virulence factor of Serpulina hyodysenteriae. Microbiology 144: 1205–1211.

303. Smet KAL De, Weston A, Brown IN, Young DB, Robertson BD (2000) Three pathways for trehalose biosynthesis in mycobacteria. Microbiology 146: 199–208.

304. Chao T, Hansmeier N, Halden RU (2010) Towards proteome standards: The use of absolute quantitation in high-throughput biomarker discovery. J Proteomics 73: 1641–1646. doi:10.1016/j.jprot.2010.04.004.Towards.

305. White CN, Chan DW, Zhang Z (2004) Bioinformatics Strategies For Proteomic Profiling. Clin Biochem 37: 636–641. Available: http://www.ncbi.nlm.nih.gov/pubmed/15234244. Accessed 27 August 2013.

306. Rifai N, Gillette M a, Carr S a (2006) Protein Biomarker Discovery and Validation: The Long and Uncertain Path to Clinical Utility. Nat Biotechnol 24: 971–983. Available: http://www.ncbi.nlm.nih.gov/pubmed/16900146. Accessed 9 August 2013.

307. Keshishian H, Addona T, Burgess M, Mani DR, Shi X, et al. (2009) Quantification of Cardiovascular Biomarkers in Patient Plasma by Targeted Mass Spectrometry and Stable Isotope Dilution. Mol Cell Proteomics 8: 2339–2349. doi:10.1074/mcp.M900140-MCP200.

308. Raman K, Yeturu K, Chandra N (2008) targetTB : A target identification pipeline for Mycobacterium tuberculosis through an interactome , reactome and genome-scale structural analysis. BMC Syst Biol 2: 1–21. doi:10.1186/1752-0509-2-109.

309. Shin SJ, Han JH, Manning EJB, Collins MT (2007) Rapid and Reliable Method for Quantification of Mycobacterium paratuberculosis by Use of the BACTEC MGIT 960 System. J Cinical Microbiol 45: 1941–1948. doi:10.1128/JCM.02616-06.

310. Nicol MP, Sola C, February B, Steyn L, Wilkinson RJ, et al. (2005) Distribution of Strain Families of Mycobacterium tuberculosis Causing Pulmonary and Extrapulmonary Disease in Hospitalized Children in Cape Town , South Africa. J Clin Microbiol 43: 5779–5781. doi:10.1128/JCM.43.11.5779.

311. Hove P, Molepo J, Dube S, Nchabeleng M (2012) Genotypic Diversity of Mycobacterium tuberculosis in Pretoria. South Afr J Epidemiol Infect 27: 77–83.

312. Be NA, Lamichhane G, Grosset J, Tyagi S, Cheng Q, et al. (2008) Murine Model to Study the Invasion and Survival of Mycobacterium tuberculosis in the Central Nervous System. J Infect Dis 198: 1–8. doi:10.1086/592447.

313. Jain SK, Paul-satyaseela M, Lamichhane G, Kim KS, Bishai WR (2006) Mycobacterium tuberculosis Invasion and Traversal Across an In Vitro Human Blood-Brain Barrier as a Pathogenic Mechanism for Central Nervous System Tuberculosis. J Infect Dis 21231: 1287–1295.

314. Rock RB, Olin M, Baker CA, Thomas W, Peterson PK, et al. (2008) Central Nervous System Tuberculosis : Pathogenesis and Clinical Aspects Central Nervous System Tuberculosis : Pathogenesis and Clinical Aspects. Clin Microbiol Rev 21: 243–261. doi:10.1128/CMR.00042-07.

315. Jain SK, Paul-satyaseela M, Lamichhane G, Kim KS, Bishai WR (2006) Mycobacterium tuberculosis Invasion and Traversal Across an In Vitro Human Blood-Brain Barrier as a Pathogenic Mechanism for Central Nervous System Tuberculosis. J Infect Dis 193: 1287–1295.

316. Thwaites G, Fisher M, Hemingway C, Scott G, Solomon T, et al. (2009) British Infection Society guidelines for the diagnosis and treatment of tuberculosis of the central nervous system in adults and children. J Infect 59: 167–187. Available: http://dx.doi.org/10.1016/j.jinf.2009.06.011.

317. Rock RB, Olin M, Baker CA, Molitor TW, Peterson PK (2008) Central Nervous System Tuberculosis : Pathogenesis and Clinical Aspects. Clin Microbiol Rev 21: 243–261. doi:10.1128/CMR.00042-07.

318. Arvanitakis Z, Long RL, Hershfield ES, Manfreda J (1998) M. tuberculosis Molecular Variation in CNS Infection: Evidence for Strain Dependent Neuro-virulence. Neurology 50: 1827–1832.

319. Christensen SK, Mikkelsen M, Pedersen K, Gerdes K (2001) RelE, a Global Inhibitor of Translation, is Activated During Nutritional Stress. Proc Natl Acad Sci U S A 98: 14328–14333. Available: http://www.pubmedcentral.nih.gov/articlerender.fcgi?artid=64681&tool=pmcentrez&rendertype=abstract.

320. Christensen SK, Gerdes K (2003) RelE toxins from Bacteria and Archaea cleave mRNAs on translating ribosomes, which are rescued by tmRNA. Mol Microbiol 48: 1389–1400. Available: http://doi.wiley.com/10.1046/j.1365-2958.2003.03512.x. Accessed 27 August 2013.

321. Sat B, Hazan R, Fisher T, Khaner H, Engelberg-kulka H, et al. (2001) Programmed Cell Death in Escherichia coli : Some Antibiotics Can Trigger mazEF Lethality. J Bacteriol 183: 2041–2045. doi:10.1128/JB.183.6.2041.

322. Hazan R, Sat B, Engelberg-kulka H (2004) Escherichia coli mazEF -Mediated Cell Death Is Triggered by Various Stressful Conditions Escherichia coli mazEF-Mediated Cell Death Is Triggered by Various Stressful Conditions. J Bacteriol 186: 3663–3669. doi:10.1128/JB.186.11.3663.

323. Engelberg-Kulka H, Sat B, Reches M, Amitai S, Hazan R (2004) Bacterial Programmed Cell Death Systems as Targets for Antibiotics. Trends Microbiol 12: 66–71. Available: http://www.ncbi.nlm.nih.gov/pubmed/15036322. Accessed 27 August 2013.

324. Arcus VL, Rainey PB, Turner SJ (2005) The PIN-domain toxin-antitoxin array in mycobacteria. Trends Microbiol 13: 360–365. Available: http://www.ncbi.nlm.nih.gov/pubmed/15993073. Accessed 27 August 2013.

325. Robson J, McKenzie JL, Cursons R, Cook GM, Arcus VL (2009) The vapBC Operon From Mycobacterium smegmatis Is An Autoregulated Toxin-antitoxin Module That Controls Growth Via Inhibition of Translation. J Mol Biol 390: 353–367. Available: http://www.ncbi.nlm.nih.gov/pubmed/19445953. Accessed 11 August 2013.

326. Suzuki M, Zhang J, Liu M, Woychik N a, Inouye M (2005) Single Protein Production in Living Cells Facilitated by an mRNA Interferase. Mol Cell 18: 253–261. Available: http://www.ncbi.nlm.nih.gov/pubmed/15837428. Accessed 27 August 2013.

327. Zhang Y, Zhang J, Hoeflich KP, Ikura M, Qing G, et al. (2003) MazF Cleaves Cellular mRNAs Specifically at ACA to Block Protein Synthesis in Escherichia coli. Mol Cell 12: 913–923. Available: http://www.ncbi.nlm.nih.gov/pubmed/14580342.

328. Ramage HR, Connolly LE, Cox JS (2009) Comprehensive Functional Analysis of Mycobacterium tuberculosis Toxin-Antitoxin Systems : Implications for Pathogenesis , Stress Responses , and Evolution. PLoS Genet 5: 1–14. doi:10.1371/journal.pgen.1000767.

329. Krithika R, Marathe U, Saxena P, Ansari MZ, Mohanty D, et al. (2006) A Genetic Locus Required For Iron Acquisition in Mycobacterium tuberculosis. Proc Natl Acad Sci 103: 2069–2074. Available: http://www.pubmedcentral.nih.gov/articlerender.fcgi?artid=1413701&tool=pmcentrez&rendertype=abstract.

330. Lamarca BBD, Zhu W, Arceneaux JEL, Byers BR, Lundrigan MD (2004) Participation of fad and mbt Genes in Synthesis of Mycobactin in Mycobacterium smegmatis. J Bacteriol 186: 374–382. doi:10.1128/JB.186.2.374.

331. Schaible UE, Kaufmann SHE (2004) Iron and Microbial Infection. Nat Rev Microbiol 2: 946–953. Available: http://www.ncbi.nlm.nih.gov/pubmed/15550940. Accessed 12 August 2013.

332. Ratledge C (2004) Iron, Mycobacteria and Tuberculosis. Tuberculosis 84: 110–130. Available: http://linkinghub.elsevier.com/retrieve/pii/S1472979203000945. Accessed 12 August 2013.

333. Siegrist MS, Unnikrishnan M, McConnell MJ, Borowsky M, Cheng T-Y, et al. (2009) Mycobacterial Esx-3 Is Required For Mycobactin-mediated Iron Acquisition. Proc Natl Acad Sci 106: 18792–18797. Available: http://www.pubmedcentral.nih.gov/articlerender.fcgi?artid=2774023&tool=pmcentrez&rendertype=abstract.

334. Chalker a F, Ingraham K a, Lunsford RD, Bryant a P, Bryant J, et al. (2000) The bacA gene, which determines bacitracin susceptibility in Streptococcus pneumoniae and Staphylococcus aureus, is also required for virulence. Microbiology 146: 1547–1553. Available: http://www.ncbi.nlm.nih.gov/pubmed/10878119.

335. Vandal OH, Roberts JA, Odaira T, Schnappinger D, Nathan CF, et al. (2009) Acid-Susceptible Mutants of Mycobacterium tuberculosis Share Hypersusceptibility to Cell Wall and Oxidative Stress and to the Host Environment. J Bacteriol 191: 625–631. doi:10.1128/JB.00932-08.

336. Collins DM, Kawakami RP, Lisle GWDE, Pascopella L, Bloomt BR, et al. (1995) Mutation of the principal sigma factor causes loss of virulence in a strain of the Mycobacterium tuberculosis complex. Proc Natl Acad Sci 92: 8036–8040.

337. Manganelli R, Proveddi R, Beaucher J, Gaudreau L, Smith I, et al. (2004) σ Factors and Global Gene Regulation in Mycobacterium tuberculosis. J Bacteriol 186: 895–902. doi:10.1128/JB.186.4.895.

338. Wu S, Howard ST, Lakey DL, Kipnis A, Samten B, et al. (2004) The Principal Sigma Factor SigA Mediates Enhanced Growth of Mycobacterium tuberculosis In-vivo. Mol Microbiol 51: 1551–1562. doi:10.1111/j.1365-2958.2003.03922.x.

339. Skeiky Y a, Ovendale PJ, Jen S, Alderson MR, Dillon DC, et al. (2000) T-cell Expression Cloning of a Mycobacterium tuberculosis Gene Encoding a Protective Antigen Associated With the Early Control of Infection. J Immunol 165: 7140–7149. Available: http://www.ncbi.nlm.nih.gov/pubmed/11120845.

340. Chevrier D, Casadémont I, Guesdon JL (2000) Cloning of a gene from Mycobacterium tuberculosis Coding for a Hypothetical 27 kDa Protein and its use for the Specific PCR Identification of these Mycobacteria. Mol Cell Probes 14: 241–248. Available: http://www.ncbi.nlm.nih.gov/pubmed/10970728. Accessed 27 August 2013.

341. Yuen LK, Ross BC, Jackson KM, Dwyer B (1993) Characterization of Mycobacterium tuberculosis Strains From Vietnamese Patients by Southern Blot Hybridization. J Clin Microbiol 31: 1615–1618. Available: http://www.pubmedcentral.nih.gov/articlerender.fcgi?artid=265589&tool=pmcentrez&rendertype=abstract.

342. Grode L, Seiler P, Baumann S (2005) Increased vaccine efficacy against tuberculosis of recombinant Mycobacterium bovis bacille Calmette- Guerin mutants that secrete listeriolysin. J Clin Investig 115: 2472–2479.

343. VanderVen BC, Harder JD, Crick DC, Belisle JT (2005) Export-mediated Assembly of Mycobacterial Glycoproteins Parallels Eukaryotic Pathways. Science (80-) 309: 941–943. Available: http://www.ncbi.nlm.nih.gov/pubmed/16081738. Accessed 7 August 2013.

344. Ihara Y, Manabe S, Kanda M, Kawano H, Nakayama T, et al. (2005) Increased Expression of Protein C-mannosylation in the Aortic Vessels of Diabetic Zucker rats. Glycobiology 15: 383–392. Available: http://www.ncbi.nlm.nih.gov/pubmed/15525818. Accessed 27 August 2013.

345. Liu C-F, Tonini L, Malaga W, Beau M, Stella A, et al. (2013) Bacterial protein-O-mannosylating Enzyme is Crucial for Virulence of Mycobacterium tuberculosis. Proc Natl Acad Sci 110: 6560–6565. Available: http://www.ncbi.nlm.nih.gov/pubmed/23550160. Accessed 22 August 2013.

346. Horn C (1999) Decreased Capacity of Recombinant 45/47-kDa Molecules (Apa) of Mycobacterium tuberculosis to Stimulate T Lymphocyte Responses Related to Changes in Their Mannosylation Pattern. J Biol Chem 274: 32023–32030. Available: http://www.jbc.org/cgi/doi/10.1074/jbc.274.45.32023. Accessed 27 August 2013.

347. Vallecillo AJ, Espitia C (2009) Microbial Pathogenesis Expression of Mycobacterium tuberculosis pe _ pgrs33 is Repressed During Stationary Phase and Stress Conditions, and its Transcription is Mediated By Sigma Factor A. Microb Pathog 46: 119–127. Available: http://dx.doi.org/10.1016/j.micpath.2008.11.003.

348. Basu S, Pathak SK, Banerjee A, Pathak S, Bhattacharyya A (2007) Execution of Macrophage Apoptosis by PE _ PGRS33 of Mycobacterium tuberculosis Is Mediated by Toll-like Receptor 2-dependent Release of Tumor Necrosis Factor alpha. J Biol Chem 282: 1039–1050. doi:10.1074/jbc.M604379200.

349. Flynn JL, Goldstein MM, Chan J, Triebold KJ, Pfeffersps K, et al. (1995) Tumor Necrosis Factor-u Is Required in the Protective Immune Response Against Mycobacterium tuberculosis in Mice. Immunity 2: 561–572.

350. Balcewicz-Sablinska MK, Keane J, Kornfeld H, Remold HG (1998) Pathogenic Mycobacterium tuberculosis evades apoptosis of host macrophages by release of TNF-R2, resulting in inactivation of TNF-alpha. J Imunol 161: 2636–2641. Available: http://www.ncbi.nlm.nih.gov/pubmed/9725266.

351. Rojas M, Olivier M, Gros P, Barrera LF, García LF (1999) TNF-alpha and IL-10 Modulate the Induction of Apoptosis By Virulent Mycobacterium tuberculosis In Murine Macrophages. J Immunol 162: 6122–6131. Available: http://www.ncbi.nlm.nih.gov/pubmed/10229855.

352. Rambukkana a, Salzer JL, Yurchenco PD, Tuomanen EI (1997) Neural Targeting of Mycobacterium leprae Mediated by the G-domain of the Laminin-alpha2 Chain. Cell 88: 811–821. Available: http://www.ncbi.nlm.nih.gov/pubmed/9118224.

353. Hayashi T, Rao SP, Catanzaro A (1997) Binding of the 68-Kilodalton Protein of Mycobacterium avium to Alpha(v)Beta3 on Human Monocyte-derived Macrophages Enhances Complement Receptor Type 3 Expression. Infect Immun 65: 1211–1216. Available: http://www.pubmedcentral.nih.gov/articlerender.fcgi?artid=175119&tool=pmcentrez&rendertype=abstract.

354. Labo M, Gusberti L, Rossi E De, Speziale P, Riccardi G (1998) Determination of a 15437 bp Nucleotide Sequence Around The inhA Gene of Mycobacterium avium and Similarity Analysis of the Products of Putative ORFs. Microbiology 144: 807–814.

355. Bhaskar S, Khanna SP, Mukherjee R (2000) Isolation , purification and immunological characterization of novel low molecular weight protein antigen CFP 6 from culture filtrate of M . tuberculosis. Vaccine 18: 2856–2866.

356. Webb JR, Vedvick TS, Alderson MR, Guderian JA, Jen SS, et al. (1998) Molecular Cloning, Expression and Immunogenicity of MTB12, a Novel Low-Molecular-Weight Antigen Secreted by Mycobacterium tuberculosis. Infect Immun 66: 4208–4214.

357. American Thoracic Society & Centers for Disease control and Prevention (2000) Diagnostic Standards and Classification of Tuberculosis in Adults and Children.

358. Gebhard S, Hümpel A, McLellan AD, Cook GM (2008) The Alternative Sigma Factor SigF of Mycobacterium smegmatis Is Required for Survival of Heat Shock, Acidic pH and Oxidative Stress. Microbiology 154: 2786–2795. Available: http://www.ncbi.nlm.nih.gov/pubmed/18757812. Accessed 27 August 2013.

359. Jain SK, Paul-Satyaseela M, Lamichhane G, Kim KS, Bishai WR (2006) Mycobacterium tuberculosis Invasion and Traversal Across an In-vitro Human Blood-brain Barrier as a Pathogenic Mechanism For Central Nervous System Tuberculosis. J Infect Dis 193: 1287–1295. Available: http://www.ncbi.nlm.nih.gov/pubmed/16586367.

360. Målen H, Berven FS, Fladmark KE, Wiker HG (2007) Comprehensive Analysis of Exported Proteins From Mycobacterium tuberculosis H37Rv. Proteomics 7: 1702–1718. Available: http://www.ncbi.nlm.nih.gov/pubmed/17443846. Accessed 12 August 2013.

361. Gey Van Pittius NC, Gamieldien J, Hide W, Brown GD, Siezen RJ, et al. (2001) The ESAT-6 Gene Cluster of Mycobacterium tuberculosis and Other High G+C Gram-Positive Bacteria. Genome Biol 2. Available: http://www.pubmedcentral.nih.gov/articlerender.fcgi?artid=57799&tool=pmcentrez&rendertype=abstract.

362. Smits AH, Jansen PWTC, Poser I, Hyman AA, Vermeulen M (2013) Stoichiometry of Chromatin-associated Protein Complexes Revealed By Label-free Quantitative Mass Spectrometry-based Proteomics. Nucleic Acid Res 41: 1–8. doi:10.1093/nar/gks941.

363. Michalski A, Damoc E, Hauschild JP, Lange O, Wieghaus A, et al. (2011) Mass spectrometry-based Proteomics Using Q-Exactive, A High-performance Benchtop Quadrupole Orbitrap Mass Spectrometer. Mol Cell Proteomics 10: 1074/mcp.M111.011015.

364. Cox J, Mann M (2008) MaxQuant enables high peptide identification rates, individualized p.p.b.-range mass accuracies and proteome-wide protein quantification. Nat Biotechnol 26: 1367–1372.

365. Cox J, Neuhauser N, Michalski A, Scheltema RA, Olsen J V, et al. (2011) Andromeda: A Peptide Search Engine Integrated into the MaxQuant Environment. J Proteome Res 10: 1794–1805.

366. Krokhin VO, Craig R, Spicer V, Ens W, Standing KG, et al. (2004) An Improved Model For Prediction of Retention Times of Tryptic Peptides in Ion Pair Reversed-phase HPLC: Its Application to Protein-peptide Mapping By Off-line HPLC-MALDI MS. Mol Cell Proteomics: 908–919.

367. Gineys R, Bodaghi B, Carcelain G, Cassoux N, le Boutin TH, et al. (2011) QuantiFERON-TB Gold Cut-offVvalue: Implications for the Management of Tuberculosis-Related Ocular Inflammation. Ophthalmology 152: 433–440.

368. Babu K, Philips M, Subbakrishna DK (2013) Perspectives of Quantiferon TB Gold test among Indian practitioners: a survey. J Ophthalmic Inflamm Infect 3: 1–5. Available: http://www.pubmedcentral.nih.gov/articlerender.fcgi?artid=3605069&tool=pmcentrez&rendertype=abstract. Accessed 7 April 2013.

369. Michalski A, Damoc E, Hauschild J, Lange O, Wieghaus A, et al. (2011) Mass Spectrometry-based Proteomics Using Q-Exactive , A High-performance Benchtop Quadrupole Orbitrap Mass Spectrometer. Mol Cell Proteomics 10: 1–11. doi:10.1074/mcp.M111.011015.

Appendix: Media and chemicals

7H9 broth: Dissolve 4.7g of media in 900ml of distilled water. Add 50µl Tween 20 and 50ml of 50% glycerol. Autoclave for 30 minutes then cool and add 50ml ADC supplement

7H11 agar: Dissolve 19g of media in 900ml distilled water; heat to dissolve and autoclave for 30 min. Add 100ml of OADC supplement

Sautons media: 2% glycerol, 0.4% L-asparagine, 0.2% glucose, 0.2% citric acid, 0.05% monopotassium phosphate, 0.05% magnesium sulphate, 0.015% tween 80, 0.005% ferric citrate, 0.00001% zinc sulphate at pH 7.4

Lysis buffer (pH 8.3): 1% SDS, 100 mM Tris-Cl pH 7.6, 0.1 mM dithiothreitol (DTT), 1 mM PMSF

Acrylamide: 30% (w/v) acrylamide, 0.8% (w/v) bis-acrylamide and 0.1 g (w/v) SDS O

Stacking Buffer (pH 6.3): 0.5 M Tris, 0.4% (w/v) SDS pH to 8.0

Resolving buffer (pH 8.8): 1.5 M Tris and 0.4% (w/v) SDS

To make up 36ml of 12% SDS-PAGE: 14.4ml of acrylamide in 9ml of resolving buffer and 12.6ml of water.

10X Electrophoresis buffer: 4% (w/v) glycine, 6.32% (w/v) Tris and 1% SDS. Dilute 1 in 10 for 1x running buffer

TCA stock solution: 10g TCA in 10ml distilled water

Coomassie Blue staining solution: 50% (v/v) methanol, 10% (v/v) acetic acid and 0.25% (w/v)

De-staining solution: 10% (v/v) methanol and 7.5% (v/v) acetic acid

DTT stock solution: To make 10 mL of a 1M solution, dissolve 1.54g DTT in distilled water

IAA: 0.2g in 20ml of distilled water

Ammonium bicarbonate: Dissolve 0.08g of ABC in 20ml Millipore water

Dilution buffer stock: 25 mM Tris, 192 mM glycine, pH 8.3

5x Loading Buffer (pH 6.8): 3.5% (w/v) Tris, 60% (v/v) glycine and 5% (w/v) SDS

Loading Dye: 200µl 5x loading buffer, 100µl β-mercaptoethanol, 100µl saturated, filtered bromophenol blue

Gradient for MS buffer A: 1ml of 100% Formic acid in 999ml of ultra-pure milli-pore water

Gradient for MS buffer B: 1ML of 100% Formic acid in 999ml of ultra-pure Chromasolv acetonitrile

All protein ID's obtained from shotgun MS

LAM	H37Rv	CAS	Beijing	Bovis	BCG	Avium
Rv0001	Rv0001	Rv0001	Rv0001	Rv0001	Rv0001	Rv0001
Rv0002	Rv0002	Rv0003	Rv0002	Rv0002	Rv0002	Rv0002
Rv0004	Rv0003	Rv0004	Rv0003	Rv0003	Rv0003	Rv0003
Rv0007	Rv0004	Rv0005	Rv0004	Rv0004	Rv0004	Rv0004
Rv0008c	Rv0005	Rv0006	Rv0005	Rv0005	Rv0005	Rv0005
Rv0009	Rv0006	Rv0007	Rv0006	Rv0006	Rv0006	Rv0006
Rv0011c	Rv0007	Rv0009	Rv0007	Rv0007	Rv0007	Rv0007
Rv0013	Rv0008c	Rv0011c	Rv0008c	Rv0008c	Rv0008c	Rv0008c
Rv0014c	Rv0009	Rv0012	Rv0009	Rv0009	Rv0010c	Rv0009
Rv0015c	Rv0010c	Rv0014c	Rv0010c	Rv0010c	Rv0012	Rv0010c
Rv0016c	Rv0011c	Rv0016c	Rv0012	Rv0011c	Rv0014c	Rv0012
Rv0017c	Rv0012	Rv0017c	Rv0014c	Rv0012	Rv0015c	Rv0014c
Rv0019c	Rv0014c	Rv0018c	Rv0015c	Rv0014c	Rv0016c	Rv0015c
Rv0020c	Rv0015c	Rv0019c	Rv0016c	Rv0015c	Rv0018c	Rv0016c
Rv0021c	Rv0016c	Rv0020c	Rv0018c	Rv0016c	Rv0019c	Rv0017c
Rv0022c	Rv0018c	Rv0022c	Rv0019c	Rv0017c	Rv0020c	Rv0018c
Rv0023	Rv0019c	Rv0023	Rv0020c	Rv0018c	Rv0022c	Rv0019c
Rv0024	Rv0020c	Rv0024	Rv0021c	Rv0019c	Rv0023	Rv0020c
Rv0025	Rv0021c	Rv0025	Rv0022c	Rv0020c	Rv0024	Rv0021c
Rv0026	Rv0022c	Rv0026	Rv0023	Rv0021c	Rv0025	Rv0022c
Rv0027	Rv0023	Rv0027	Rv0024	Rv0022c	Rv0026	Rv0023
Rv0029	Rv0024	Rv0029	Rv0025	Rv0023	Rv0027	Rv0024
Rv0032	Rv0025	Rv0030	Rv0026	Rv0024	Rv0029	Rv0025
Rv0034	Rv0026	Rv0032	Rv0027	Rv0025	Rv0030	Rv0026
Rv0035	Rv0029	Rv0035	Rv0029	Rv0026	Rv0031	Rv0027
Rv0036c	Rv0030	Rv0036c	Rv0030	Rv0027	Rv0032	Rv0029
Rv0037c	Rv0031	Rv0038	Rv0032	Rv0029	Rv0033	Rv0030
Rv0038	Rv0032	Rv0041	Rv0033	Rv0030	Rv0034	Rv0037c
Rv0040c	Rv0033	Rv0043c	Rv0034	Rv0031	Rv0035	Rv0038
Rv0041	Rv0034	Rv0044c	Rv0035	Rv0032	Rv0036c	Rv0040c
Rv0042c	Rv0035	Rv0045c	Rv0036c	Rv0033	Rv0037c	Rv0041
Rv0043c	Rv0036c	Rv0046c	Rv0037c	Rv0034	Rv0038	Rv0042c
Rv0044c	Rv0037c	Rv0047c	Rv0038	Rv0035	Rv0040c	Rv0043c
Rv0045c	Rv0038	Rv0048c	Rv0040c	Rv0036c	Rv0041	Rv0044c
Rv0046c	Rv0040c	Rv0050	Rv0041	Rv0037c	Rv0042c	Rv0045c
Rv0047c	Rv0041	Rv0051	Rv0042c	Rv0038	Rv0043c	Rv0046c
Rv0048c	Rv0042c	Rv0052	Rv0043c	Rv0040c	Rv0044c	Rv0047c
Rv0049	Rv0043c	Rv0054	Rv0044c	Rv0041	Rv0046c	Rv0048c
Rv0051	Rv0044c	Rv0055	Rv0045c	Rv0042c	Rv0047c	Rv0049
Rv0054	Rv0045c	Rv0056	Rv0046c	Rv0043c	Rv0048c	Rv0050
Rv0055	Rv0046c	Rv0057	Rv0047c	Rv0044c	Rv0049	Rv0051
Rv0056	Rv0047c	Rv0058	Rv0048c	Rv0045c	Rv0050	Rv0052
Rv0057	Rv0048c	Rv0059	Rv0049	Rv0046c	Rv0051	Rv0053
Rv0058	Rv0049	Rv0060	Rv0050	Rv0047c	Rv0052	Rv0055
Rv0060	Rv0050	Rv0062	Rv0051	Rv0048c	Rv0053	Rv0056
Rv0062	Rv0051	Rv0064	Rv0052	Rv0049	Rv0054	Rv0058
Rv0063	Rv0052	Rv0066c	Rv0053	Rv0050	Rv0055	Rv0063
Rv0065	Rv0053	Rv0067c	Rv0054	Rv0051	Rv0056	Rv0066c
Rv0066c	Rv0054	Rv0068	Rv0056	Rv0052	Rv0057	Rv0067c

Rv0067c	Rv0055	Rv0069c	Rv0057	Rv0053	Rv0058	Rv0073
Rv0068	Rv0056	Rv0070c	Rv0058	Rv0054	Rv0060	Rv0077c
Rv0069c	Rv0057	Rv0071	Rv0060	Rv0055	Rv0061	Rv0078
Rv0070c	Rv0058	Rv0072	Rv0062	Rv0056	Rv0062	Rv0081
Rv0072	Rv0059	Rv0073	Rv0063	Rv0057	Rv0063	Rv0082
Rv0073	Rv0060	Rv0074	Rv0064	Rv0058	Rv0064	Rv0083
Rv0074	Rv0061	Rv0075	Rv0065	Rv0059	Rv0065	Rv0084
Rv0075	Rv0062	Rv0077c	Rv0066c	Rv0060	Rv0066c	Rv0087
Rv0077c	Rv0063	Rv0078	Rv0067c	Rv0062	Rv0067c	Rv0088
Rv0078	Rv0064	Rv0078.1	Rv0068	Rv0063	Rv0068	Rv0090
Rv0078.1	Rv0065	Rv0079	Rv0069c	Rv0064	Rv0069c	Rv0102
Rv0079	Rv0066c	Rv0084	Rv0070c	Rv0065	Rv0070c	Rv0106
Rv0080	Rv0067c	Rv0085	Rv0071	Rv0066c	Rv0071	Rv0107c
Rv0081	Rv0068	Rv0086	Rv0072	Rv0067c	Rv0072	Rv0111
Rv0082	Rv0069c	Rv0087	Rv0073	Rv0068	Rv0073	Rv0113
Rv0083	Rv0070c	Rv0088	Rv0074	Rv0069c	Rv0074	Rv0114
Rv0084	Rv0071	Rv0090	Rv0075	Rv0070c	Rv0075	Rv0115
Rv0085	Rv0072	Rv0091	Rv0076c	Rv0071	Rv0077c	Rv0116c
Rv0087	Rv0073	Rv0092	Rv0077c	Rv0072	Rv0078.1	Rv0117
Rv0088	Rv0074	Rv0093c	Rv0078	Rv0073	Rv0079	Rv0119
Rv0089	Rv0075	Rv0094c	Rv0078.1	Rv0074	Rv0080	Rv0120c
Rv0090	Rv0076c	Rv0097	Rv0079	Rv0075	Rv0081	Rv0121c
Rv0091	Rv0077c	Rv0098	Rv0080	Rv0077c	Rv0083	Rv0125
Rv0093c	Rv0078	Rv0099	Rv0081	Rv0078	Rv0087	Rv0126
Rv0097	Rv0078.1	Rv0100	Rv0083	Rv0078.1	Rv0088	Rv0127
Rv0098	Rv0079	Rv0101	Rv0085	Rv0079	Rv0089	Rv0129c
Rv0099	Rv0080	Rv0103c	Rv0087	Rv0081	Rv0090	Rv0130
Rv0102	Rv0081	Rv0104	Rv0088	Rv0082	Rv0091	Rv0131c
Rv0103c	Rv0082	Rv0105c	Rv0089	Rv0083	Rv0092	Rv0132c
Rv0104	Rv0083	Rv0106	Rv0090	Rv0084	Rv0093c	Rv0133
Rv0105c	Rv0084	Rv0107c	Rv0091	Rv0085	Rv0094c	Rv0134
Rv0106	Rv0085	Rv0110	Rv0092	Rv0086	Rv0095c	Rv0135c
Rv0107c	Rv0087	Rv0111	Rv0093c	Rv0087	Rv0097	Rv0136
Rv0110	Rv0088	Rv0112	Rv0094c	Rv0088	Rv0098	Rv0139
Rv0111	Rv0089	Rv0114	Rv0097	Rv0089	Rv0099	Rv0140
Rv0112	Rv0090	Rv0115	Rv0098	Rv0090	Rv0100	Rv0141c
Rv0114	Rv0091	Rv0116c	Rv0099	Rv0091	Rv0101	Rv0142
Rv0115	Rv0092	Rv0117	Rv0100	Rv0092	Rv0102	Rv0143c
Rv0116c	Rv0094c	Rv0118c	Rv0101	Rv0093c	Rv0103c	Rv0144
Rv0117	Rv0095c	Rv0119	Rv0102	Rv0094c	Rv0104	Rv0145
Rv0118c	Rv0096	Rv0120c	Rv0103c	Rv0095c	Rv0105c	Rv0146
Rv0121c	Rv0097	Rv0124	Rv0104	Rv0096	Rv0106	Rv0147
Rv0122	Rv0099	Rv0126	Rv0105c	Rv0097	Rv0107c	Rv0148
Rv0123	Rv0100	Rv0127	Rv0106	Rv0098	Rv0108c	Rv0153c
Rv0125	Rv0101	Rv0129c	Rv0107c	Rv0099	Rv0110	Rv0154c
Rv0126	Rv0102	Rv0130	Rv0110	Rv0101	Rv0111	Rv0155
Rv0127	Rv0103c	Rv0131c	Rv0111	Rv0102	Rv0112	Rv0157
Rv0128	Rv0104	Rv0132c	Rv0112	Rv0103c	Rv0113	Rv0158
Rv0129c	Rv0105c	Rv0133	Rv0115	Rv0104	Rv0115	Rv0161
Rv0130	Rv0106	Rv0134	Rv0116c	Rv0105c	Rv0116c	Rv0162c
Rv0131c	Rv0107c	Rv0135c	Rv0117	Rv0106	Rv0117	Rv0163

Rv0132c	Rv0110	Rv0136	Rv0118c	Rv0107c	Rv0118c	Rv0164
Rv0133	Rv0111	Rv0137c	Rv0119	Rv0108c	Rv0119	Rv0165c
Rv0135c	Rv0112	Rv0138	Rv0120c	Rv0110	Rv0120c	Rv0166
Rv0136	Rv0114	Rv0139	Rv0123	Rv0111	Rv0121c	Rv0167
Rv0137c	Rv0115	Rv0142	Rv0124	Rv0112	Rv0123	Rv0168
Rv0139	Rv0116c	Rv0144	Rv0126	Rv0114	Rv0127	Rv0169
Rv0142	Rv0117	Rv0145	Rv0127	Rv0115	Rv0128	Rv0170
Rv0143c	Rv0118c	Rv0146	Rv0128	Rv0116c	Rv0129c	Rv0171
Rv0144	Rv0119	Rv0147	Rv0129c	Rv0117	Rv0130	Rv0172
Rv0146	Rv0120c	Rv0153c	Rv0130	Rv0118c	Rv0131c	Rv0174
Rv0147	Rv0121c	Rv0154c	Rv0131c	Rv0119	Rv0132c	Rv0175
Rv0148	Rv0122	Rv0155	Rv0132c	Rv0120c	Rv0133	Rv0176
Rv0151c	Rv0123	Rv0156	Rv0133	Rv0121c	Rv0135c	Rv0177
Rv0153c	Rv0125	Rv0157	Rv0134	Rv0122	Rv0136	Rv0178
Rv0154c	Rv0126	Rv0158	Rv0135c	Rv0123	Rv0137c	Rv0181c
Rv0155	Rv0127	Rv0159c	Rv0136	Rv0124	Rv0138	Rv0182c
Rv0157	Rv0128	Rv0160c	Rv0138	Rv0126	Rv0139	Rv0183
Rv0158	Rv0129c	Rv0161	Rv0139	Rv0127	Rv0140	Rv0184
Rv0161	Rv0130	Rv0162c	Rv0142	Rv0128	Rv0141c	Rv0185
Rv0162c	Rv0131c	Rv0163	Rv0143c	Rv0129c	Rv0142	Rv0186
Rv0163	Rv0132c	Rv0164	Rv0144	Rv0130	Rv0143c	Rv0187
Rv0164	Rv0133	Rv0165c	Rv0145	Rv0131c	Rv0144	Rv0189c
Rv0165c	Rv0134	Rv0166	Rv0146	Rv0132c	Rv0145	Rv0190
Rv0166	Rv0135c	Rv0167	Rv0147	Rv0133	Rv0146	Rv0191
Rv0167	Rv0136	Rv0168	Rv0148	Rv0135c	Rv0147	Rv0196
Rv0168	Rv0137c	Rv0169	Rv0152c	Rv0136	Rv0148	Rv0197
Rv0169	Rv0138	Rv0170	Rv0153c	Rv0138	Rv0150c	Rv0198c
Rv0173	Rv0139	Rv0171	Rv0154c	Rv0139	Rv0151c	Rv0199
Rv0174	Rv0141c	Rv0172	Rv0155	Rv0142	Rv0153c	Rv0201c
Rv0176	Rv0142	Rv0173	Rv0156	Rv0143c	Rv0154c	Rv0202c
Rv0177	Rv0143c	Rv0174	Rv0157	Rv0144	Rv0155	Rv0204c
Rv0178	Rv0144	Rv0175	Rv0158	Rv0145	Rv0157	Rv0205
Rv0179c	Rv0145	Rv0176	Rv0160c	Rv0146	Rv0158	Rv0206c
Rv0180c	Rv0146	Rv0177	Rv0161	Rv0147	Rv0159c	Rv0207c
Rv0182c	Rv0147	Rv0179c	Rv0162c	Rv0148	Rv0160c	Rv0208c
Rv0183	Rv0148	Rv0180c	Rv0163	Rv0149	Rv0161	Rv0209
Rv0184	Rv0149	Rv0182c	Rv0164	Rv0151c	Rv0162c	Rv0210
Rv0185	Rv0151c	Rv0183	Rv0165c	Rv0152c	Rv0163	Rv0211
Rv0186	Rv0153c	Rv0184	Rv0166	Rv0153c	Rv0164	Rv0214
Rv0187	Rv0154c	Rv0186	Rv0168	Rv0154c	Rv0165c	Rv0215c
Rv0189c	Rv0155	Rv0187	Rv0169	Rv0155	Rv0166	Rv0216
Rv0191	Rv0157	Rv0189c	Rv0170	Rv0156	Rv0167	Rv0217c
Rv0196	Rv0158	Rv0190	Rv0171	Rv0157	Rv0169	Rv0218
Rv0198c	Rv0159c	Rv0191	Rv0172	Rv0158	Rv0170	Rv0219
Rv0199	Rv0161	Rv0193c	Rv0173	Rv0159c	Rv0171	Rv0220
Rv0200	Rv0162c	Rv0194	Rv0175	Rv0160c	Rv0172	Rv0221
Rv0201c	Rv0163	Rv0196	Rv0176	Rv0161	Rv0173	Rv0222
Rv0202c	Rv0164	Rv0197	Rv0177	Rv0162c	Rv0174	Rv0223c
Rv0203	Rv0165c	Rv0198c	Rv0178	Rv0163	Rv0175	Rv0224c
Rv0207c	Rv0166	Rv0199	Rv0179c	Rv0164	Rv0176	Rv0225
Rv0208c	Rv0168	Rv0202c	Rv0180c	Rv0165c	Rv0177	Rv0226c

Rv0209	Rv0169	Rv0204c	Rv0181c	Rv0166	Rv0178	Rv0227c
Rv0210	Rv0170	Rv0205	Rv0182c	Rv0168	Rv0179c	Rv0228
Rv0211	Rv0171	Rv0206c	Rv0183	Rv0169	Rv0180c	Rv0230c
Rv0212c	Rv0172	Rv0207c	Rv0184	Rv0170	Rv0181c	Rv0231
Rv0213c	Rv0173	Rv0208c	Rv0185	Rv0171	Rv0182c	Rv0232
Rv0214	Rv0174	Rv0209	Rv0186	Rv0172	Rv0183	Rv0233
Rv0215c	Rv0175	Rv0210	Rv0187	Rv0173	Rv0184	Rv0234c
Rv0216	Rv0176	Rv0211	Rv0189c	Rv0174	Rv0185	Rv0235c
Rv0217c	Rv0177	Rv0212c	Rv0190	Rv0175	Rv0186	Rv0236c
Rv0218	Rv0178	Rv0213c	Rv0192	Rv0176	Rv0187	Rv0237
Rv0220	Rv0179c	Rv0214	Rv0193c	Rv0177	Rv0188	Rv0238
Rv0222	Rv0180c	Rv0215c	Rv0194	Rv0178	Rv0189c	Rv0241c
Rv0223c	Rv0181c	Rv0216	Rv0195	Rv0179c	Rv0190	Rv0242c
Rv0224c	Rv0182c	Rv0217c	Rv0196	Rv0180c	Rv0191	Rv0243
Rv0225	Rv0183	Rv0220	Rv0197	Rv0181c	Rv0192	Rv0244c
Rv0226c	Rv0184	Rv0221	Rv0198c	Rv0182c	Rv0194	Rv0245
Rv0227c	Rv0185	Rv0222	Rv0199	Rv0183	Rv0196	Rv0247c
Rv0228	Rv0186	Rv0223c	Rv0200	Rv0184	Rv0197	Rv0248c
Rv0229c	Rv0187	Rv0225	Rv0201c	Rv0185	Rv0198c	Rv0249c
Rv0230c	Rv0189c	Rv0226c	Rv0202c	Rv0186	Rv0199	Rv0250c
Rv0231	Rv0190	Rv0227c	Rv0204c	Rv0187	Rv0201c	Rv0251c
Rv0232	Rv0191	Rv0229c	Rv0205	Rv0189c	Rv0202c	Rv0252
Rv0233	Rv0192	Rv0231	Rv0206c	Rv0190	Rv0203	Rv0255c
Rv0235c	Rv0193c	Rv0232	Rv0207c	Rv0191	Rv0204c	Rv0256c
Rv0238	Rv0194	Rv0234c	Rv0208c	Rv0192	Rv0205	Rv0258c
Rv0239	Rv0196	Rv0236A	Rv0209	Rv0193c	Rv0206c	Rv0259c
Rv0240	Rv0197	Rv0236c	Rv0210	Rv0194	Rv0207c	Rv0260c
Rv0241c	Rv0198c	Rv0237	Rv0211	Rv0195	Rv0208c	Rv0263c
Rv0242c	Rv0199	Rv0241c	Rv0212c	Rv0196	Rv0209	Rv0264c
Rv0243	Rv0200	Rv0243	Rv0213c	Rv0197	Rv0210	Rv0265c
Rv0244c	Rv0201c	Rv0244c	Rv0214	Rv0198c	Rv0211	Rv0267
Rv0245	Rv0202c	Rv0246	Rv0215c	Rv0200	Rv0212c	Rv0269c
Rv0246	Rv0203	Rv0247c	Rv0216	Rv0201c	Rv0213c	Rv0270
Rv0247c	Rv0204c	Rv0248c	Rv0217c	Rv0202c	Rv0214	Rv0271c
Rv0248c	Rv0205	Rv0249c	Rv0218	Rv0203	Rv0215c	Rv0272c
Rv0249c	Rv0206c	Rv0250c	Rv0219	Rv0204c	Rv0216	Rv0273c
Rv0250c	Rv0207c	Rv0251c	Rv0220	Rv0206c	Rv0217c	Rv0274
Rv0251c	Rv0208c	Rv0252	Rv0221	Rv0207c	Rv0218	Rv0275c
Rv0252	Rv0209	Rv0253	Rv0222	Rv0208c	Rv0219	Rv0276
Rv0253	Rv0210	Rv0254c	Rv0223c	Rv0209	Rv0220	Rv0280
Rv0255c	Rv0211	Rv0255c	Rv0224c	Rv0210	Rv0221	Rv0281
Rv0257	Rv0212c	Rv0257	Rv0225	Rv0211	Rv0223c	Rv0282
Rv0258c	Rv0213c	Rv0258c	Rv0226c	Rv0212c	Rv0225	Rv0283
Rv0259c	Rv0214	Rv0259c	Rv0227c	Rv0213c	Rv0226c	Rv0286
Rv0260c	Rv0215c	Rv0260c	Rv0228	Rv0214	Rv0227c	Rv0289
Rv0262c	Rv0216	Rv0263c	Rv0231	Rv0215c	Rv0228	Rv0290
Rv0263c	Rv0217c	Rv0264c	Rv0232	Rv0217c	Rv0230c	Rv0291
Rv0265c	Rv0218	Rv0265c	Rv0233	Rv0218	Rv0231	Rv0292
Rv0266c	Rv0220	Rv0266c	Rv0234c	Rv0220	Rv0232	Rv0293c
Rv0267	Rv0221	Rv0267	Rv0235c	Rv0221	Rv0233	Rv0294
Rv0268c	Rv0222	Rv0268c	Rv0236A	Rv0223c	Rv0234c	Rv0295c

Rv0269c	Rv0223c	Rv0269c	Rv0236c	Rv0224c	Rv0235c	Rv0296c
Rv0270	Rv0224c	Rv0270	Rv0237	Rv0225	Rv0236c	Rv0306
Rv0271c	Rv0225	Rv0271c	Rv0238	Rv0226c	Rv0237	Rv0308
Rv0272c	Rv0226c	Rv0272c	Rv0239	Rv0227c	Rv0238	Rv0309
Rv0273c	Rv0227c	Rv0273c	Rv0242c	Rv0228	Rv0239	Rv0310c
Rv0275c	Rv0228	Rv0275c	Rv0243	Rv0229c	Rv0241c	Rv0311
Rv0276	Rv0229c	Rv0276	Rv0244c	Rv0230c	Rv0242c	Rv0312
Rv0277c	Rv0230c	Rv0281	Rv0245	Rv0231	Rv0243	Rv0313
Rv0281	Rv0231	Rv0282	Rv0246	Rv0232	Rv0244c	Rv0314c
Rv0282	Rv0232	Rv0283	Rv0247c	Rv0233	Rv0245	Rv0315
Rv0283	Rv0233	Rv0284	Rv0248c	Rv0234c	Rv0246	Rv0316
Rv0284	Rv0234c	Rv0286	Rv0250c	Rv0235c	Rv0247c	Rv0321
Rv0286	Rv0235c	Rv0288	Rv0251c	Rv0236A	Rv0248c	Rv0322
Rv0287	Rv0236c	Rv0291	Rv0252	Rv0236c	Rv0249c	Rv0323c
Rv0289	Rv0237	Rv0292	Rv0253	Rv0237	Rv0250c	Rv0329c
Rv0290	Rv0238	Rv0294	Rv0254c	Rv0238	Rv0251c	Rv0332
Rv0291	Rv0240	Rv0296c	Rv0255c	Rv0239	Rv0252	Rv0333
Rv0292	Rv0241c	Rv0297	Rv0256c	Rv0241c	Rv0253	Rv0334
Rv0293c	Rv0242c	Rv0299	Rv0257	Rv0242c	Rv0254c	Rv0336
Rv0294	Rv0243	Rv0300	Rv0258c	Rv0243	Rv0255c	Rv0337c
Rv0295c	Rv0244c	Rv0302	Rv0259c	Rv0244c	Rv0256c	Rv0338c
Rv0296c	Rv0245	Rv0305c	Rv0260c	Rv0246	Rv0257	Rv0344c
Rv0299	Rv0246	Rv0306	Rv0262c	Rv0247c	Rv0258c	Rv0350
Rv0301	Rv0248c	Rv0307c	Rv0263c	Rv0248c	Rv0259c	Rv0351
Rv0302	Rv0249c	Rv0312	Rv0264c	Rv0249c	Rv0260c	Rv0352
Rv0303	Rv0250c	Rv0317c	Rv0265c	Rv0250c	Rv0261c	Rv0357c
Rv0306	Rv0251c	Rv0318c	Rv0266c	Rv0252	Rv0262c	Rv0358
Rv0307c	Rv0252	Rv0319	Rv0267	Rv0253	Rv0263c	Rv0359
Rv0309	Rv0255c	Rv0320	Rv0268c	Rv0254c	Rv0265c	Rv0360c
Rv0311	Rv0257	Rv0321	Rv0269c	Rv0255c	Rv0266c	Rv0361
Rv0312	Rv0258c	Rv0322	Rv0270	Rv0257	Rv0267	Rv0364
Rv0313	Rv0259c	Rv0324	Rv0271c	Rv0258c	Rv0268c	Rv0365c
Rv0314c	Rv0260c	Rv0326	Rv0272c	Rv0260c	Rv0269c	Rv0366c
Rv0315	Rv0261c	Rv0327c	Rv0273c	Rv0261c	Rv0270	Rv0367c
Rv0316	Rv0262c	Rv0328	Rv0275c	Rv0262c	Rv0271c	Rv0380c
Rv0317c	Rv0263c	Rv0330c	Rv0276	Rv0263c	Rv0272c	Rv0382c
Rv0318c	Rv0264c	Rv0332	Rv0281	Rv0264c	Rv0273c	Rv0383c
Rv0319	Rv0265c	Rv0334	Rv0282	Rv0265c	Rv0275c	Rv0384c
Rv0320	Rv0266c	Rv0335c	Rv0283	Rv0266c	Rv0276	Rv0385
Rv0321	Rv0267	Rv0336	Rv0284	Rv0267	Rv0277c	Rv0389
Rv0322	Rv0268c	Rv0337c	Rv0286	Rv0268c	Rv0280	Rv0391
Rv0323c	Rv0269c	Rv0338c	Rv0289	Rv0269c	Rv0281	Rv0392c
Rv0324	Rv0270	Rv0339c	Rv0290	Rv0270	Rv0282	Rv0393
Rv0328	Rv0271c	Rv0342	Rv0291	Rv0271c	Rv0283	Rv0397
Rv0329c	Rv0272c	Rv0343	Rv0292	Rv0272c	Rv0284	Rv0398c
Rv0330c	Rv0273c	Rv0344c	Rv0293c	Rv0273c	Rv0286	Rv0400c
Rv0331	Rv0274	Rv0345	Rv0295c	Rv0275c	Rv0287	Rv0406c
Rv0332	Rv0276	Rv0346c	Rv0298	Rv0276	Rv0289	Rv0407
Rv0334	Rv0277c	Rv0347	Rv0299	Rv0277c	Rv0290	Rv0408
Rv0335c	Rv0280	Rv0350	Rv0302	Rv0281	Rv0291	Rv0409
Rv0337c	Rv0281	Rv0351	Rv0303	Rv0282	Rv0292	Rv0410c

Rv0338c	Rv0282	Rv0352	Rv0305c	Rv0283	Rv0293c	Rv0411c
Rv0339c	Rv0283	Rv0355c	Rv0306	Rv0284	Rv0294	Rv0412c
Rv0340	Rv0284	Rv0357c	Rv0307c	Rv0286	Rv0295c	Rv0413
Rv0341	Rv0286	Rv0359	Rv0308	Rv0289	Rv0296c	Rv0414c
Rv0342	Rv0288	Rv0360c	Rv0310c	Rv0290	Rv0297	Rv0415
Rv0343	Rv0289	Rv0362	Rv0311	Rv0291	Rv0298	Rv0416
Rv0344c	Rv0290	Rv0363c	Rv0312	Rv0292	Rv0299	Rv0417
Rv0345	Rv0291	Rv0365c	Rv0313	Rv0293c	Rv0301	Rv0418
Rv0346c	Rv0292	Rv0366c	Rv0314c	Rv0294	Rv0302	Rv0419
Rv0347	Rv0293c	Rv0367c	Rv0315	Rv0295c	Rv0303	Rv0421c
Rv0348	Rv0294	Rv0368c	Rv0316	Rv0296c	Rv0305c	Rv0422c
Rv0349	Rv0295c	Rv0369c	Rv0317c	Rv0297	Rv0306	Rv0423c
Rv0350	Rv0296c	Rv0373c	Rv0318c	Rv0298	Rv0307c	Rv0424c
Rv0351	Rv0297	Rv0375c	Rv0319	Rv0299	Rv0308	Rv0426c
Rv0352	Rv0299	Rv0380c	Rv0320	Rv0300	Rv0309	Rv0427c
Rv0353	Rv0300	Rv0381c	Rv0321	Rv0301	Rv0310c	Rv0428c
Rv0356c	Rv0301	Rv0382c	Rv0322	Rv0302	Rv0311	Rv0430
Rv0357c	Rv0302	Rv0383c	Rv0324	Rv0303	Rv0312	Rv0431
Rv0360c	Rv0303	Rv0384c	Rv0325	Rv0305c	Rv0313	Rv0433
Rv0361	Rv0305c	Rv0385	Rv0326	Rv0306	Rv0315	Rv0434
Rv0362	Rv0306	Rv0386	Rv0327c	Rv0307c	Rv0316	Rv0435c
Rv0363c	Rv0307c	Rv0387c	Rv0328	Rv0308	Rv0317c	Rv0437c
Rv0365c	Rv0308	Rv0388c	Rv0330c	Rv0309	Rv0318c	Rv0438c
Rv0367c	Rv0309	Rv0389	Rv0331	Rv0310c	Rv0319	Rv0439c
Rv0368c	Rv0310c	Rv0390	Rv0332	Rv0311	Rv0320	Rv0440
Rv0369c	Rv0311	Rv0391	Rv0333	Rv0314c	Rv0321	Rv0441c
Rv0370c	Rv0312	Rv0392c	Rv0334	Rv0315	Rv0322	Rv0442c
Rv0371c	Rv0313	Rv0393	Rv0335c	Rv0316	Rv0324	Rv0443
Rv0372c	Rv0314c	Rv0394c	Rv0336	Rv0317c	Rv0326	Rv0450c
Rv0373c	Rv0315	Rv0397	Rv0337c	Rv0318c	Rv0327c	Rv0451c
Rv0374c	Rv0316	Rv0399c	Rv0338c	Rv0319	Rv0328	Rv0452
Rv0375c	Rv0317c	Rv0400c	Rv0339c	Rv0320	Rv0329c	Rv0453
Rv0377	Rv0318c	Rv0402c	Rv0340	Rv0321	Rv0330c	Rv0455c
Rv0381c	Rv0319	Rv0404	Rv0341	Rv0322	Rv0331	Rv0456c
Rv0382c	Rv0320	Rv0405	Rv0342	Rv0324	Rv0334	Rv0458
Rv0383c	Rv0321	Rv0407	Rv0343	Rv0326	Rv0335c	Rv0462
Rv0384c	Rv0322	Rv0408	Rv0344c	Rv0327c	Rv0337c	Rv0464c
Rv0385	Rv0323c	Rv0410c	Rv0345	Rv0328	Rv0338c	Rv0465c
Rv0387c	Rv0324	Rv0411c	Rv0346c	Rv0329c	Rv0339c	Rv0466
Rv0389	Rv0325	Rv0412c	Rv0347	Rv0330c	Rv0342	Rv0467
Rv0390	Rv0326	Rv0413	Rv0348	Rv0331	Rv0343	Rv0468
Rv0391	Rv0327c	Rv0415	Rv0349	Rv0332	Rv0345	Rv0469
Rv0392c	Rv0328	Rv0417	Rv0350	Rv0333	Rv0346c	Rv0470c
Rv0393	Rv0329c	Rv0418	Rv0351	Rv0334	Rv0348	Rv0473
Rv0394c	Rv0330c	Rv0419	Rv0352	Rv0335c	Rv0349	Rv0474
Rv0395	Rv0331	Rv0421c	Rv0354c	Rv0337c	Rv0350	Rv0475
Rv0396	Rv0334	Rv0422c	Rv0356c	Rv0338c	Rv0351	Rv0476
Rv0397	Rv0335c	Rv0423c	Rv0357c	Rv0339c	Rv0352	Rv0478
Rv0398c	Rv0336	Rv0425c	Rv0358	Rv0340	Rv0356c	Rv0479c
Rv0399c	Rv0337c	Rv0426c	Rv0359	Rv0342	Rv0357c	Rv0480c
Rv0400c	Rv0338c	Rv0427c	Rv0362	Rv0343	Rv0358	Rv0481c

Rv0402c	Rv0339c	Rv0430	Rv0363c	Rv0344c	Rv0359	Rv0482
Rv0404	Rv0340	Rv0431	Rv0365c	Rv0345	Rv0360c	Rv0483
Rv0406c	Rv0342	Rv0433	Rv0366c	Rv0346c	Rv0361	Rv0484c
Rv0407	Rv0343	Rv0434	Rv0367c	Rv0347	Rv0362	Rv0485
Rv0408	Rv0344c	Rv0435c	Rv0368c	Rv0348	Rv0363c	Rv0486
Rv0410c	Rv0345	Rv0436c	Rv0369c	Rv0349	Rv0364	Rv0487
Rv0411c	Rv0346c	Rv0438c	Rv0370c	Rv0350	Rv0365c	Rv0489
Rv0412c	Rv0347	Rv0439c	Rv0371c	Rv0351	Rv0367c	Rv0490
Rv0414c	Rv0348	Rv0440	Rv0372c	Rv0352	Rv0368c	Rv0491
Rv0415	Rv0349	Rv0441c	Rv0373c	Rv0353	Rv0369c	Rv0492c
Rv0417	Rv0350	Rv0444c	Rv0374c	Rv0355c	Rv0371c	Rv0493c
Rv0418	Rv0351	Rv0446c	Rv0375c	Rv0356c	Rv0372c	Rv0495c
Rv0419	Rv0352	Rv0447c	Rv0376c	Rv0357c	Rv0373c	Rv0496
Rv0420c	Rv0353	Rv0448c	Rv0377	Rv0358	Rv0375c	Rv0497
Rv0421c	Rv0355c	Rv0449c	Rv0378	Rv0361	Rv0376c	Rv0499
Rv0422c	Rv0356c	Rv0450c	Rv0379	Rv0362	Rv0380c	Rv0500
Rv0423c	Rv0357c	Rv0451c	Rv0380c	Rv0363c	Rv0381c	Rv0500A
Rv0424c	Rv0358	Rv0452	Rv0381c	Rv0365c	Rv0382c	Rv0501
Rv0426c	Rv0359	Rv0455c	Rv0382c	Rv0366c	Rv0383c	Rv0502
Rv0427c	Rv0360c	Rv0456A	Rv0383c	Rv0368c	Rv0384c	Rv0503c
Rv0428c	Rv0361	Rv0456c	Rv0384c	Rv0369c	Rv0385	Rv0504c
Rv0429c	Rv0362	Rv0457c	Rv0385	Rv0370c	Rv0386	Rv0505c
Rv0430	Rv0363c	Rv0461	Rv0386	Rv0371c	Rv0387c	Rv0506
Rv0431	Rv0364	Rv0462	Rv0389	Rv0372c	Rv0388c	Rv0509
Rv0433	Rv0365c	Rv0464c	Rv0390	Rv0373c	Rv0389	Rv0510
Rv0434	Rv0366c	Rv0465c	Rv0391	Rv0374c	Rv0391	Rv0511
Rv0435c	Rv0367c	Rv0466	Rv0392c	Rv0375c	Rv0392c	Rv0512
Rv0436c	Rv0368c	Rv0467	Rv0393	Rv0376c	Rv0393	Rv0513
Rv0437c	Rv0369c	Rv0468	Rv0395	Rv0377	Rv0395	Rv0515
Rv0438c	Rv0370c	Rv0469	Rv0396	Rv0379	Rv0398c	Rv0516c
Rv0439c	Rv0371c	Rv0470c	Rv0398c	Rv0381c	Rv0399c	Rv0517
Rv0440	Rv0372c	Rv0471c	Rv0399c	Rv0382c	Rv0400c	Rv0518
Rv0443	Rv0373c	Rv0472c	Rv0400c	Rv0383c	Rv0403c	Rv0519c
Rv0444c	Rv0375c	Rv0473	Rv0401	Rv0384c	Rv0404	Rv0522
Rv0445c	Rv0376c	Rv0475	Rv0402c	Rv0385	Rv0405	Rv0523c
Rv0447c	Rv0377	Rv0478	Rv0403c	Rv0386	Rv0406c	Rv0524
Rv0448c	Rv0378	Rv0481c	Rv0404	Rv0387c	Rv0407	Rv0525
Rv0449c	Rv0379	Rv0482	Rv0405	Rv0388c	Rv0408	Rv0526
Rv0452	Rv0380c	Rv0484c	Rv0406c	Rv0389	Rv0409	Rv0528
Rv0456c	Rv0381c	Rv0485	Rv0407	Rv0391	Rv0410c	Rv0529
Rv0456A	Rv0382c	Rv0486	Rv0408	Rv0392c	Rv0411c	Rv0530
Rv0457c	Rv0383c	Rv0487	Rv0409	Rv0393	Rv0412c	Rv0531
Rv0458	Rv0384c	Rv0488	Rv0410c	Rv0394c	Rv0413	Rv0533c
Rv0461	Rv0385	Rv0490	Rv0411c	Rv0395	Rv0414c	Rv0534c
Rv0462	Rv0386	Rv0492c	Rv0412c	Rv0397	Rv0415	Rv0535
Rv0464c	Rv0389	Rv0493c	Rv0413	Rv0398c	Rv0416	Rv0536
Rv0465c	Rv0390	Rv0494	Rv0414c	Rv0399c	Rv0418	Rv0537c
Rv0466	Rv0391	Rv0496	Rv0415	Rv0400c	Rv0419	Rv0538
Rv0467	Rv0392c	Rv0497	Rv0417	Rv0401	Rv0420c	Rv0539
Rv0468	Rv0393	Rv0498	Rv0418	Rv0402c	Rv0421c	Rv0540
Rv0470c	Rv0395	Rv0499	Rv0419	Rv0403c	Rv0422c	Rv0541c

Rv0470.1	Rv0397	Rv0500	Rv0420c	Rv0404	Rv0423c	Rv0542c
Rv0471c	Rv0398c	Rv0500A	Rv0421c	Rv0405	Rv0425c	Rv0543c
Rv0473	Rv0399c	Rv0500B	Rv0422c	Rv0406c	Rv0426c	Rv0546c
Rv0474	Rv0400c	Rv0501	Rv0423c	Rv0407	Rv0428c	Rv0547c
Rv0475	Rv0401	Rv0502	Rv0425c	Rv0408	Rv0430	Rv0548c
Rv0478	Rv0402c	Rv0503c	Rv0426c	Rv0409	Rv0431	Rv0551c
Rv0479c	Rv0403c	Rv0505c	Rv0427c	Rv0410c	Rv0433	Rv0552
Rv0481c	Rv0404	Rv0506	Rv0428c	Rv0411c	Rv0434	Rv0553
Rv0482	Rv0405	Rv0507	Rv0430	Rv0412c	Rv0435c	Rv0554
Rv0483	Rv0406c	Rv0508	Rv0431	Rv0413	Rv0436c	Rv0555
Rv0484c	Rv0407	Rv0509	Rv0433	Rv0414c	Rv0437c	Rv0557
Rv0485	Rv0408	Rv0510	Rv0434	Rv0415	Rv0438c	Rv0558
Rv0487	Rv0409	Rv0511	Rv0435c	Rv0417	Rv0439c	Rv0560c
Rv0488	Rv0410c	Rv0512	Rv0436c	Rv0418	Rv0440	Rv0561c
Rv0489	Rv0411c	Rv0514	Rv0438c	Rv0419	Rv0441c	Rv0562
Rv0490	Rv0412c	Rv0516c	Rv0439c	Rv0420c	Rv0442c	Rv0563
Rv0491	Rv0413	Rv0517	Rv0440	Rv0421c	Rv0443	Rv0564c
Rv0492c	Rv0414c	Rv0518	Rv0441c	Rv0422c	Rv0444c	Rv0565c
Rv0492.1	Rv0415	Rv0519c	Rv0444c	Rv0423c	Rv0445c	Rv0566c
Rv0494	Rv0417	Rv0521	Rv0445c	Rv0425c	Rv0447c	Rv0579
Rv0495c	Rv0418	Rv0522	Rv0447c	Rv0426c	Rv0448c	Rv0584
Rv0496	Rv0419	Rv0523c	Rv0448c	Rv0427c	Rv0449c	Rv0585c
Rv0497	Rv0420c	Rv0526	Rv0449c	Rv0428c	Rv0450c	Rv0588
Rv0498	Rv0421c	Rv0528	Rv0450c	Rv0430	Rv0451c	Rv0590
Rv0499	Rv0422c	Rv0529	Rv0452	Rv0431	Rv0452	Rv0591
Rv0500	Rv0423c	Rv0531	Rv0454	Rv0433	Rv0454	Rv0592
Rv0501	Rv0425c	Rv0533c	Rv0455c	Rv0434	Rv0456A	Rv0593
Rv0502	Rv0426c	Rv0538	Rv0456A	Rv0435c	Rv0456c	Rv0594
Rv0504c	Rv0427c	Rv0539	Rv0456c	Rv0436c	Rv0457c	Rv0600c
Rv0505c	Rv0428c	Rv0540	Rv0458	Rv0437c	Rv0458	Rv0602c
Rv0506	Rv0429c	Rv0541c	Rv0461	Rv0438c	Rv0459	Rv0614
Rv0508	Rv0430	Rv0542c	Rv0462	Rv0439c	Rv0461	Rv0618
Rv0509	Rv0431	Rv0543c	Rv0464c	Rv0440	Rv0462	Rv0619
Rv0510	Rv0432	Rv0545c	Rv0465c	Rv0441c	Rv0464c	Rv0620
Rv0511	Rv0433	Rv0546c	Rv0466	Rv0442c	Rv0465c	Rv0625c
Rv0512	Rv0434	Rv0547c	Rv0467	Rv0443	Rv0466	Rv0629c
Rv0513	Rv0435c	Rv0548c	Rv0468	Rv0444c	Rv0467	Rv0630c
Rv0514	Rv0436c	Rv0551c	Rv0469	Rv0445c	Rv0468	Rv0631c
Rv0516c	Rv0437c	Rv0552	Rv0470.1	Rv0446c	Rv0469	Rv0632c
Rv0517	Rv0438c	Rv0553	Rv0471c	Rv0447c	Rv0470c	Rv0633c
Rv0518	Rv0439c	Rv0554	Rv0472c	Rv0448c	Rv0471c	Rv0634A
Rv0520	Rv0440	Rv0555	Rv0473	Rv0449c	Rv0472c	Rv0634B
Rv0522	Rv0441c	Rv0556	Rv0474	Rv0450c	Rv0473	Rv0635
Rv0523c	Rv0443	Rv0557	Rv0475	Rv0452	Rv0474	Rv0636
Rv0524	Rv0444c	Rv0558	Rv0477	Rv0453	Rv0475	Rv0637
Rv0525	Rv0445c	Rv0561c	Rv0479c	Rv0454	Rv0476	Rv0638
Rv0526	Rv0446c	Rv0562	Rv0480c	Rv0455c	Rv0478	Rv0639
Rv0527	Rv0447c	Rv0563	Rv0482	Rv0456A	Rv0480c	Rv0640
Rv0528	Rv0448c	Rv0564c	Rv0483	Rv0456c	Rv0482	Rv0641
Rv0530	Rv0449c	Rv0566c	Rv0484c	Rv0457c	Rv0483	Rv0644c
Rv0531	Rv0450c	Rv0567	Rv0485	Rv0458	Rv0484c	Rv0645c

Rv0533c	Rv0452	Rv0568	Rv0486	Rv0461	Rv0485	Rv0646c
Rv0534c	Rv0453	Rv0569	Rv0488	Rv0462	Rv0486	Rv0648
Rv0535	Rv0454	Rv0570	Rv0489	Rv0464c	Rv0487	Rv0649
Rv0536	Rv0456A	Rv0572c	Rv0490	Rv0465c	Rv0488	Rv0651
Rv0537c	Rv0456c	Rv0574c	Rv0491	Rv0466	Rv0489	Rv0652
Rv0538	Rv0457c	Rv0575c	Rv0492.1	Rv0467	Rv0490	Rv0654
Rv0539	Rv0458	Rv0578c	Rv0492c	Rv0468	Rv0491	Rv0655
Rv0540	Rv0459	Rv0579	Rv0493c	Rv0469	Rv0492c	Rv0663
Rv0541c	Rv0461	Rv0580c	Rv0494	Rv0470c	Rv0493c	Rv0667
Rv0542c	Rv0462	Rv0582	Rv0495c	Rv0471c	Rv0494	Rv0668
Rv0544c	Rv0464c	Rv0583c	Rv0496	Rv0472c	Rv0495c	Rv0670
Rv0545c	Rv0465c	Rv0584	Rv0497	Rv0473	Rv0496	Rv0671
Rv0546c	Rv0466	Rv0585c	Rv0499	Rv0474	Rv0497	Rv0672
Rv0547c	Rv0467	Rv0586	Rv0500	Rv0476	Rv0498	Rv0673
Rv0548c	Rv0468	Rv0587	Rv0500A	Rv0478	Rv0499	Rv0674
Rv0549c	Rv0469	Rv0588	Rv0501	Rv0479c	Rv0500	Rv0675
Rv0551c	Rv0470.1	Rv0589	Rv0502	Rv0480c	Rv0500A	Rv0676c
Rv0553	Rv0470c	Rv0590	Rv0503c	Rv0481c	Rv0501	Rv0678
Rv0554	Rv0471c	Rv0591	Rv0505c	Rv0482	Rv0502	Rv0679c
Rv0556	Rv0472c	Rv0593	Rv0506	Rv0483	Rv0503c	Rv0680c
Rv0557	Rv0473	Rv0594	Rv0507	Rv0484c	Rv0505c	Rv0681
Rv0558	Rv0474	Rv0597c	Rv0508	Rv0485	Rv0506	Rv0682
Rv0559c	Rv0475	Rv0598c	Rv0509	Rv0486	Rv0507	Rv0683
Rv0560c	Rv0476	Rv0599c	Rv0510	Rv0487	Rv0508	Rv0684
Rv0561c	Rv0478	Rv0600c	Rv0511	Rv0489	Rv0509	Rv0685
Rv0562	Rv0479c	Rv0602c	Rv0512	Rv0490	Rv0510	Rv0686
Rv0563	Rv0480c	Rv0604	Rv0513	Rv0491	Rv0511	Rv0687
Rv0565c	Rv0481c	Rv0607	Rv0515	Rv0492c	Rv0512	Rv0688
Rv0566c	Rv0482	Rv0608	Rv0517	Rv0493c	Rv0513	Rv0690c
Rv0567	Rv0484c	Rv0609.1	Rv0518	Rv0494	Rv0515	Rv0691c
Rv0568	Rv0485	Rv0610c	Rv0519c	Rv0495c	Rv0517	Rv0693
Rv0570	Rv0486	Rv0612	Rv0521	Rv0496	Rv0518	Rv0694
Rv0571c	Rv0487	Rv0613c	Rv0522	Rv0497	Rv0519c	Rv0695
Rv0572c	Rv0489	Rv0614	Rv0523c	Rv0499	Rv0520	Rv0696
Rv0573c	Rv0490	Rv0616c	Rv0524	Rv0500	Rv0521	Rv0697
Rv0574c	Rv0491	Rv0618	Rv0525	Rv0500A	Rv0522	Rv0700
Rv0575c	Rv0492c	Rv0620	Rv0526	Rv0501	Rv0523c	Rv0701
Rv0576	Rv0493c	Rv0623	Rv0530	Rv0502	Rv0524	Rv0702
Rv0577	Rv0494	Rv0624	Rv0531	Rv0503c	Rv0525	Rv0703
Rv3514	Rv0495c	Rv0625c	Rv0533c	Rv0504c	Rv0526	Rv0704
Rv0579	Rv0496	Rv0626	Rv0534c	Rv0506	Rv0528	Rv0705
Rv0580c	Rv0497	Rv0629c	Rv0536	Rv0507	Rv0529	Rv0706
Rv0582	Rv0498	Rv0630c	Rv0537c	Rv0508	Rv0530	Rv0707
Rv0584	Rv0499	Rv0631c	Rv0538	Rv0509	Rv0531	Rv0708
Rv0585c	Rv0500	Rv0633c	Rv0539	Rv0510	Rv0533c	Rv0709
Rv0586	Rv0501	Rv0634A	Rv0540	Rv0511	Rv0536	Rv0710
Rv0588	Rv0502	Rv0634B	Rv0541c	Rv0512	Rv0537c	Rv0711
Rv0589	Rv0503c	Rv0634c	Rv0542c	Rv0513	Rv0538	Rv0713
Rv0590	Rv0505c	Rv0640	Rv0543c	Rv0514	Rv0539	Rv0714
Rv0591	Rv0506	Rv0641	Rv0544c	Rv0515	Rv0540	Rv0715
Rv0592	Rv0507	Rv0642c	Rv0545c	Rv0516c	Rv0541c	Rv0716

Rv0593	Rv0508	Rv0643c	Rv0546c	Rv0517	Rv0542c	Rv0717
Rv0594	Rv0509	Rv0644c	Rv0547c	Rv0518	Rv0543c	Rv0718
Rv0596c	Rv0510	Rv0645c	Rv0548c	Rv0519c	Rv0545c	Rv0719
Rv0597c	Rv0511	Rv0646c	Rv0550c	Rv0520	Rv0547c	Rv0720
Rv0600c	Rv0512	Rv0648	Rv0551c	Rv0521	Rv0548c	Rv0721
Rv0602c	Rv0513	Rv0649	Rv0552	Rv0522	Rv0549c	Rv0722
Rv0604	Rv0515	Rv0650	Rv0553	Rv0524	Rv0550c	Rv0723
Rv0605	Rv0516c	Rv0651	Rv0554	Rv0525	Rv0551c	Rv0724
Rv0606	Rv0517	Rv0652	Rv0555	Rv0526	Rv0552	Rv0724.1
Rv0609	Rv0518	Rv0653c	Rv0556	Rv0528	Rv0553	Rv0726c
Rv0610c	Rv0519c	Rv0654	Rv0557	Rv0529	Rv0554	Rv0727c
Rv0611c	Rv0520	Rv0655	Rv0558	Rv0530	Rv0555	Rv0728c
Rv0612	Rv0521	Rv0656c	Rv0560c	Rv0531	Rv0558	Rv0729
Rv0616c	Rv0522	Rv0657c	Rv0561c	Rv0533c	Rv0561c	Rv0730
Rv0617	Rv0523c	Rv0659c	Rv0562	Rv0534c	Rv0562	Rv0732
Rv0618	Rv0524	Rv0662c	Rv0564c	Rv0535	Rv0563	Rv0733
Rv0622	Rv0525	Rv0663	Rv0565c	Rv0536	Rv0564c	Rv0734
Rv0623	Rv0526	Rv0665	Rv0566c	Rv0537c	Rv0565c	Rv0737
Rv0624	Rv0528	Rv0666	Rv0567	Rv0538	Rv0566c	Rv0738
Rv0625c	Rv0529	Rv0667	Rv0568	Rv0539	Rv0567	Rv0751c
Rv0626	Rv0530	Rv0668	Rv0569	Rv0540	Rv0568	Rv0752c
Rv0627	Rv0531	Rv0669c	Rv0570	Rv0541c	Rv0570	Rv0753c
Rv0628c	Rv0532	Rv0671	Rv0571c	Rv0542c	Rv0571c	Rv0754
Rv0629c	Rv0533c	Rv0674	Rv0572c	Rv0545c	Rv0572c	Rv0756c
Rv0630c	Rv0534c	Rv0675	Rv0573c	Rv0546c	Rv0573c	Rv0757
Rv0632c	Rv0535	Rv0676c	Rv0574c	Rv0547c	Rv0574c	Rv0758
Rv0633c	Rv0536	Rv0678	Rv0575c	Rv0548c	Rv0575c	Rv0759c
Rv0634c	Rv0537c	Rv0681	Rv0576	Rv0549c	Rv0576	Rv0760c
Rv0634A	Rv0538	Rv0682	Rv0577	Rv0550c	Rv0577	Rv0761c
Rv0635	Rv0539	Rv0683	Rv0578c	Rv0551c	Rv0578c	Rv0764c
Rv0636	Rv0540	Rv0684	Rv0579	Rv0552	Rv0580c	Rv0765c
Rv0637	Rv0541c	Rv0685	Rv0580c	Rv0553	Rv0581	Rv0767c
Rv0638	Rv0542c	Rv0686	Rv0581	Rv0554	Rv0582	Rv0768
Rv0639	Rv0543c	Rv0687	Rv0582	Rv0555	Rv0584	Rv0769
Rv0640	Rv0544c	Rv0690c	Rv0584	Rv0556	Rv0585c	Rv0770
Rv0641	Rv0546c	Rv0692	Rv0585c	Rv0557	Rv0586	Rv0772
Rv0645c	Rv0547c	Rv0693	Rv0586	Rv0558	Rv0587	Rv0773c
Rv0646c	Rv0548c	Rv0694	Rv0588	Rv0560c	Rv0588	Rv0774c
Rv0649	Rv0549c	Rv0696	Rv0589	Rv0561c	Rv0589	Rv0775
Rv0650	Rv0551c	Rv0697	Rv0590	Rv0562	Rv0590	Rv0776c
Rv0651	Rv0552	Rv0698	Rv0591	Rv0563	Rv0591	Rv0777
Rv0652	Rv0553	Rv0700	Rv0592	Rv0564c	Rv0592	Rv0778
Rv0653c	Rv0554	Rv0701	Rv0593	Rv0565c	Rv0593	Rv0780
Rv0654	Rv0555	Rv0702	Rv0594	Rv0566c	Rv0594	Rv0781
Rv0656c	Rv0556	Rv0704	Rv0596c	Rv0567	Rv0595c	Rv0782
Rv0659c	Rv0557	Rv0705	Rv0597c	Rv0568	Rv0596c	Rv0783c
Rv0660c	Rv0558	Rv0706	Rv0598c	Rv0569	Rv0597c	Rv0784
Rv0661c	Rv0560c	Rv0707	Rv0600c	Rv0570	Rv0598c	Rv0785
Rv0662c	Rv0561c	Rv0710	Rv0602c	Rv0571c	Rv0600c	Rv0787.1
Rv0663	Rv0562	Rv0711	Rv0604	Rv0572c	Rv0602c	Rv0792c
Rv0665	Rv0563	Rv0714	Rv0605	Rv0573c	Rv0604	Rv0797

Rv0668	Rv0564c	Rv0715	Rv0606	Rv0574c	Rv0605	Rv0798c
Rv0669c	Rv0565c	Rv0718	Rv0607	Rv0575c	Rv0606	Rv0799c
Rv0670	Rv0566c	Rv0719	Rv0608	Rv0576	Rv0607	Rv0800
Rv0671	Rv0567	Rv0720	Rv0609.1	Rv0577	Rv0608	Rv0803
Rv0672	Rv0568	Rv0723	Rv0610c	Rv0578c	Rv0609	Rv0804
Rv0673	Rv0570	Rv0724	Rv0612	Rv0579	Rv0609.1	Rv0807
Rv0674	Rv0571c	Rv0725c	Rv0613c	Rv0580c	Rv0610c	Rv0808
Rv0675	Rv0572c	Rv0726c	Rv0614	Rv0581	Rv0611c	Rv0809
Rv0677c	Rv0573c	Rv0727c	Rv0616c	Rv0582	Rv0612	Rv0811c
Rv0678	Rv0574c	Rv0729	Rv0617	Rv0583c	Rv0613c	Rv0812
Rv0679c	Rv0575c	Rv0731c	Rv0618	Rv0584	Rv0614	Rv0813c
Rv0680c	Rv0576	Rv0732	Rv0619	Rv0585c	Rv0617	Rv0814c
Rv0681	Rv0578c	Rv0733	Rv0620	Rv0586	Rv0620	Rv0815c
Rv0682	Rv0579	Rv0734	Rv0621	Rv0587	Rv0621	Rv0816c
Rv0683	Rv0580c	Rv0735	Rv0623	Rv0588	Rv0622	Rv0817c
Rv0684	Rv0581	Rv0737	Rv0624	Rv0589	Rv0623	Rv0818
Rv0685	Rv0582	Rv0739	Rv0625c	Rv0590	Rv0624	Rv0819
Rv0686	Rv0584	Rv0740	Rv0626	Rv0591	Rv0625c	Rv0820
Rv0687	Rv0585c	Rv0741	Rv0627	Rv0592	Rv0626	Rv0821c
Rv0688	Rv0586	Rv0743c	Rv0628c	Rv0593	Rv0627	Rv0822c
Rv0689c	Rv0587	Rv0748	Rv0629c	Rv0594	Rv0628c	Rv0823c
Rv0690c	Rv0588	Rv0750	Rv0630c	Rv0596c	Rv0629c	Rv0824c
Rv0693	Rv0589	Rv0751c	Rv0631c	Rv0597c	Rv0630c	Rv0825c
Rv0694	Rv0590	Rv0752c	Rv0632c	Rv0598c	Rv0631c	Rv0826
Rv0695	Rv0590.1	Rv0753c	Rv0633c	Rv0599c	Rv0632c	Rv0827c
Rv0697	Rv0591	Rv0755.1	Rv0634A	Rv0600c	Rv0634A	Rv0830
Rv0698	Rv0592	Rv0756c	Rv0634B	Rv0602c	Rv0634B	Rv0835
Rv0700	Rv0593	Rv0757	Rv0634c	Rv0604	Rv0634c	Rv0838
Rv0701	Rv0594	Rv0758	Rv0635	Rv0605	Rv0635	Rv0839
Rv0702	Rv0596c	Rv0760c	Rv0636	Rv0606	Rv0636	Rv0843
Rv0703	Rv0597c	Rv0761c	Rv0637	Rv0607	Rv0637	Rv0844c
Rv0704	Rv0598c	Rv0762c	Rv0639	Rv0608	Rv0638	Rv0845
Rv0705	Rv0599c	Rv0764c	Rv0640	Rv0609	Rv0639	Rv0846c
Rv0706	Rv0600c	Rv0765c	Rv0641	Rv0609.1	Rv0640	Rv0851c
Rv0707	Rv0601c	Rv0767c	Rv0642c	Rv0610c	Rv0641	Rv0852
Rv0708	Rv0602c	Rv0768	Rv0643c	Rv0612	Rv0642c	Rv0853c
Rv0710	Rv0604	Rv0769	Rv0644c	Rv0613c	Rv0643c	Rv0854
Rv0711	Rv0605	Rv0770	Rv0645c	Rv0614	Rv0644c	Rv0855
Rv0712	Rv0606	Rv0771	Rv0646c	Rv0617	Rv0645c	Rv0856
Rv0714	Rv0608	Rv0772	Rv0647c	Rv0618	Rv0646c	Rv0858c
Rv0715	Rv0609	Rv0773c	Rv0648	Rv0619	Rv0648	Rv0859
Rv0716	Rv0609.1	Rv0774c	Rv0649	Rv0620	Rv0649	Rv0860
Rv0718	Rv0610c	Rv0775	Rv0651	Rv0621	Rv0650	Rv0861c
Rv0719	Rv0611c	Rv0777	Rv0652	Rv0622	Rv0651	Rv0862c
Rv0720	Rv0612	Rv0778	Rv0653c	Rv0624	Rv0652	Rv0864
Rv0723	Rv0613c	Rv0779c	Rv0654	Rv0625c	Rv0653c	Rv0865
Rv0724	Rv0614	Rv0780	Rv0655	Rv0626	Rv0654	Rv0868c
Rv0725c	Rv0616c	Rv0784	Rv0657c	Rv0628c	Rv0655	Rv0871
Rv0726c	Rv0619	Rv0785	Rv0659c	Rv0629c	Rv0656c	Rv0873
Rv0727c	Rv0620	Rv0787	Rv0661c	Rv0630c	Rv0657c	Rv0875c
Rv0728c	Rv0621	Rv0788	Rv0662c	Rv0631c	Rv0658c	Rv0876c

Rv0729	Rv0622	Rv0789c	Rv0663	Rv0633c	Rv0659c	Rv0877
Rv0730	Rv0623	Rv0791c	Rv0665	Rv0634c	Rv0661c	Rv0879c
Rv0731c	Rv0624	Rv0792c	Rv0667	Rv0635	Rv0662c	Rv0880
Rv0732	Rv0625c	Rv0795	Rv0668	Rv0636	Rv0663	Rv0881
Rv0733	Rv0626	Rv0799c	Rv0669c	Rv0637	Rv0667	Rv0883c
Rv0734	Rv0627	Rv0800	Rv0670	Rv0638	Rv0668	Rv0884c
Rv0735	Rv0628c	Rv0802c	Rv0671	Rv0640	Rv0669c	Rv0885
Rv0737	Rv0629c	Rv0803	Rv0672	Rv0641	Rv0671	Rv0886
Rv0738	Rv0630c	Rv0804	Rv0673	Rv0642c	Rv0672	Rv0887c
Rv0741	Rv0631c	Rv0805	Rv0675	Rv0643c	Rv0673	Rv0889c
Rv0743c	Rv0632c	Rv0806c	Rv0676c	Rv0644c	Rv0674	Rv0897c
Rv0744c	Rv0633c	Rv0808	Rv0677c	Rv0645c	Rv0675	Rv0898c
Rv0748	Rv0634A	Rv0809	Rv0678	Rv0646c	Rv0676c	Rv0902c
Rv0749	Rv0634B	Rv0811c	Rv0681	Rv0648	Rv0677c	Rv0903c
Rv0751c	Rv0634c	Rv0812	Rv0682	Rv0649	Rv0678	Rv0905
Rv0752c	Rv0635	Rv0813c	Rv0683	Rv0650	Rv0680c	Rv0906
Rv0753c	Rv0636	Rv0815c	Rv0684	Rv0651	Rv0681	Rv0907
Rv0755c	Rv0637	Rv0817c	Rv0686	Rv0652	Rv0682	Rv0908
Rv0756c	Rv0639	Rv0819	Rv0688	Rv0653c	Rv0683	Rv0909
Rv0757	Rv0640	Rv0820	Rv0689c	Rv0654	Rv0684	Rv0910
Rv0758	Rv0641	Rv0821c	Rv0690c	Rv0655	Rv0685	Rv0912
Rv0759c	Rv0642c	Rv0822c	Rv0691c	Rv0656c	Rv0686	Rv0914c
Rv0760c	Rv0643c	Rv0823c	Rv0692	Rv0657c	Rv0687	Rv0916c
Rv0761c	Rv0644c	Rv0824c	Rv0693	Rv0659c	Rv0688	Rv0920c
Rv0762c	Rv0645c	Rv0825c	Rv0694	Rv0660c	Rv0689c	Rv0923c
Rv0764c	Rv0646c	Rv0826	Rv0695	Rv0661c	Rv0690c	Rv0924c
Rv0765c	Rv0647c	Rv0827c	Rv0696	Rv0662c	Rv0691c	Rv0926c
Rv0766c	Rv0648	Rv0831c	Rv0697	Rv0663	Rv0693	Rv0928
Rv0767c	Rv0649	Rv0837c	Rv0699	Rv0665	Rv0694	Rv0929
Rv0768	Rv0650	Rv0838	Rv0701	Rv0666	Rv0695	Rv0931c
Rv0769	Rv0651	Rv0839	Rv0702	Rv0667	Rv0696	Rv0932c
Rv0770	Rv0652	Rv0840c	Rv0703	Rv0668	Rv0697	Rv0937c
Rv0772	Rv0653c	Rv0841	Rv0704	Rv0669c	Rv0698	Rv0938
Rv0773c	Rv0654	Rv0842	Rv0705	Rv0671	Rv0699	Rv0939
Rv0774c	Rv0655	Rv0843	Rv0706	Rv0672	Rv0700	Rv0941c
Rv0775	Rv0656c	Rv0845	Rv0707	Rv0673	Rv0701	Rv0944
Rv0776c	Rv0658c	Rv0847	Rv0708	Rv0674	Rv0702	Rv0945
Rv0777	Rv0659c	Rv0849	Rv0709	Rv0675	Rv0703	Rv0946c
Rv0778	Rv0661c	Rv0852	Rv0710	Rv0676c	Rv0704	Rv0948c
Rv0779c	Rv0662c	Rv0853c	Rv0711	Rv0677c	Rv0705	Rv0949
Rv0780	Rv0663	Rv0854	Rv0712	Rv0678	Rv0706	Rv0950c
Rv0782	Rv0664	Rv0855	Rv0713	Rv0679c	Rv0707	Rv0951
Rv0783c	Rv0665	Rv0856	Rv0714	Rv0681	Rv0708	Rv0952
Rv0784	Rv0667	Rv0857	Rv0715	Rv0682	Rv0709	Rv0953c
Rv0785	Rv0668	Rv0858c	Rv0716	Rv0683	Rv0710	Rv0957
Rv0787	Rv0669c	Rv0860	Rv0718	Rv0684	Rv0711	Rv0959
Rv0788	Rv0670	Rv0861c	Rv0719	Rv0685	Rv0712	Rv0966c
Rv0789c	Rv0671	Rv0862c	Rv0720	Rv0686	Rv0713	Rv0971c
Rv0790c	Rv0672	Rv0864	Rv0721	Rv0687	Rv0714	Rv0972c
Rv0792c	Rv0673	Rv0866	Rv0722	Rv0688	Rv0715	Rv0973c
Rv0793	Rv0674	Rv0867c	Rv0723	Rv0689c	Rv0716	Rv0974c

Rv0794c	Rv0675	Rv0869c	Rv0724	Rv0690c	Rv0717	Rv0975c
Rv0798c	Rv0676c	Rv0873	Rv0725c	Rv0691c	Rv0718	Rv0976c
Rv0799c	Rv0677c	Rv0874c	Rv0726c	Rv0692	Rv0719	Rv0981
Rv0800	Rv0678	Rv0876c	Rv0727c	Rv0693	Rv0720	Rv0982
Rv0801	Rv0681	Rv0877	Rv0728c	Rv0694	Rv0721	Rv0983
Rv0802c	Rv0682	Rv0878c	Rv0729	Rv0696	Rv0723	Rv0984
Rv0803	Rv0683	Rv0880	Rv0730	Rv0697	Rv0724	Rv0985c
Rv0804	Rv0684	Rv0884c	Rv0731c	Rv0701	Rv0725c	Rv0987
Rv0805	Rv0685	Rv0885	Rv0732	Rv0702	Rv0726c	Rv0990c
Rv0806c	Rv0686	Rv0886	Rv0733	Rv0703	Rv0727c	Rv0991c
Rv0807	Rv0687	Rv0887c	Rv0734	Rv0704	Rv0728c	Rv0992c
Rv0808	Rv0688	Rv0888	Rv0735	Rv0705	Rv0729	Rv0993
Rv0809	Rv0689c	Rv0889c	Rv0737	Rv0706	Rv0730	Rv0994
Rv0811c	Rv0690c	Rv0890c	Rv0738	Rv0707	Rv0731c	Rv0995
Rv0812	Rv0691c	Rv0892	Rv0739	Rv0709	Rv0732	Rv0996
Rv0813c	Rv0692	Rv0893c	Rv0740	Rv0710	Rv0733	Rv0998
Rv0815c	Rv0693	Rv0894	Rv0741	Rv0711	Rv0734	Rv0999
Rv0816c	Rv0694	Rv0895	Rv0743c	Rv0712	Rv0735	Rv1000c
Rv0817c	Rv0695	Rv0896	Rv0744c	Rv0713	Rv0737	Rv1001
Rv0818	Rv0696	Rv0897c	Rv0748	Rv0714	Rv0738	Rv1002c
Rv0820	Rv0697	Rv0902c	Rv0750	Rv0715	Rv0739	Rv1003
Rv0822c	Rv0698	Rv0903c	Rv0751c	Rv0716	Rv0740	Rv1005c
Rv0823c	Rv0699	Rv0904c	Rv0752c	Rv0717	Rv0741	Rv1006
Rv0824c	Rv0700	Rv0905	Rv0753c	Rv0718	Rv0743c	Rv1007c
Rv0825c	Rv0701	Rv0906	Rv0754	Rv0719	Rv0744c	Rv1008
Rv0826	Rv0702	Rv0907	Rv0755.1	Rv0720	Rv0745	Rv1009
Rv0827c	Rv0703	Rv0908	Rv0758	Rv0721	Rv0748	Rv1010
Rv0828c	Rv0704	Rv0910	Rv0759c	Rv0722	Rv0749	Rv1011
Rv0830	Rv0705	Rv0912	Rv0762c	Rv0723	Rv0751c	Rv1013
Rv0831c	Rv0706	Rv0913c	Rv0763c	Rv0724	Rv0752c	Rv1014c
Rv0795	Rv0707	Rv0914c	Rv0764c	Rv0725c	Rv0753c	Rv1017c
Rv2815c	Rv0709	Rv0915c	Rv0765c	Rv0726c	Rv0755.1	Rv1018c
Rv3186	Rv0710	Rv0918	Rv0766c	Rv0727c	Rv0756c	Rv1019
Rv2168c	Rv0711	Rv0919	Rv0767c	Rv0728c	Rv0757	Rv1021
Rv2105	Rv0712	Rv0920c	Rv0768	Rv0729	Rv0758	Rv1022
Rv2354	Rv0713	Rv0921	Rv0769	Rv0730	Rv0759c	Rv1023
Rv3325	Rv0714	Rv0922	Rv0770	Rv0731c	Rv0762c	Rv1024
Rv3474	Rv0715	Rv0923c	Rv0771	Rv0732	Rv0764c	Rv1025
Rv1370c	Rv0716	Rv0924c	Rv0772	Rv0733	Rv0765c	Rv1026
Rv2648	Rv0717	Rv0925c	Rv0773c	Rv0734	Rv0766c	Rv1027c
Rv2278	Rv0718	Rv0927c	Rv0774c	Rv0735	Rv0767c	Rv1028c
Rv3184	Rv0719	Rv0928	Rv0775	Rv0736	Rv0768	Rv1029
Rv1763	Rv0720	Rv0929	Rv0776c	Rv0737	Rv0769	Rv1030
Rv2480c	Rv0721	Rv0930	Rv0777	Rv0738	Rv0770	Rv1031
Rv1757c	Rv0722	Rv0931c	Rv0778	Rv0739	Rv0772	Rv1032c
Rv3381c	Rv0723	Rv0933	Rv0779c	Rv0744c	Rv0773c	Rv1033c
Rv0836c	Rv0724	Rv0935	Rv0780	Rv0745	Rv0774c	Rv1040c
Rv0837c	Rv0724.1	Rv0936	Rv0782	Rv0747	Rv0775	Rv1044
Rv0838	Rv0725c	Rv0937c	Rv0783c	Rv0748	Rv0776c	Rv1045
Rv0839	Rv0726c	Rv0938	Rv0784	Rv0749	Rv0777	Rv1051c
Rv0840c	Rv0727c	Rv0939	Rv0785	Rv0751c	Rv0778	Rv1056

Rv0842	Rv0728c	Rv0940c	Rv0787	Rv0752c	Rv0779c	Rv1057
Rv0843	Rv0729	Rv0941c	Rv0788	Rv0753c	Rv0780	Rv1058
Rv0844c	Rv0730	Rv0944	Rv0789c	Rv0754	Rv0782	Rv1059
Rv0845	Rv0731c	Rv0945	Rv0790c	Rv0755.1	Rv0783c	Rv1060
Rv0846c	Rv0732	Rv0946c	Rv0791c	Rv0756c	Rv0784	Rv1061
Rv0847	Rv0733	Rv0949	Rv0792c	Rv0757	Rv0785	Rv1062
Rv0849	Rv0734	Rv0950c	Rv0793	Rv0758	Rv0787	Rv1063c
Rv0851c	Rv0735	Rv0951	Rv0794c	Rv0759c	Rv0787.1	Rv1065
Rv0852	Rv0737	Rv0952	Rv0795	Rv0760c	Rv0788	Rv1066
Rv0853c	Rv0738	Rv0953c	Rv0796	Rv0762c	Rv0790c	Rv1069c
Rv0854	Rv0739	Rv0954	Rv0797	Rv0763c	Rv0791c	Rv1070c
Rv0855	Rv0740	Rv0955	Rv0798c	Rv0764c	Rv0792c	Rv1072
Rv0856	Rv0741	Rv0956	Rv0799c	Rv0765c	Rv0793	Rv1073
Rv0857	Rv0743c	Rv0957	Rv0800	Rv0766c	Rv0794c	Rv1074c
Rv0858c	Rv0744c	Rv0958	Rv0802c	Rv0767c	Rv0796	Rv1076
Rv0860	Rv0745	Rv0959	Rv0803	Rv0768	Rv0798c	Rv1077
Rv0861c	Rv0748	Rv0963c	Rv0804	Rv0769	Rv0800	Rv1078
Rv0862c	Rv0749	Rv0964c	Rv0805	Rv0770	Rv0801	Rv1080c
Rv0864	Rv0750	Rv0966c	Rv0806c	Rv0771	Rv0802c	Rv1082
Rv0865	Rv0751c	Rv0968	Rv0807	Rv0772	Rv0803	Rv1084
Rv0866	Rv0752c	Rv0969	Rv0808	Rv0773c	Rv0804	Rv1086
Rv0867c	Rv0753c	Rv0971c	Rv0809	Rv0774c	Rv0805	Rv1092c
Rv0868c	Rv0755.1	Rv0972c	Rv0811c	Rv0775	Rv0806c	Rv1093
Rv0869c	Rv0756c	Rv0973c	Rv0812	Rv0776c	Rv0807	Rv1094
Rv0873	Rv0757	Rv0975c	Rv0813c	Rv0777	Rv0808	Rv1095
Rv0874c	Rv0758	Rv0976c	Rv0814c	Rv0778	Rv0811c	Rv1096
Rv0876c	Rv0759c	Rv0979A	Rv0815c	Rv0780	Rv0812	Rv1097c
Rv0879c	Rv0760c	Rv0982	Rv0816c	Rv0781	Rv0813c	Rv1098c
Rv0880	Rv0761c	Rv0983	Rv0817c	Rv0783c	Rv0815c	Rv1099c
Rv0883c	Rv0762c	Rv0984	Rv0818	Rv0784	Rv0817c	Rv1100
Rv0884c	Rv0764c	Rv0985c	Rv0819	Rv0785	Rv0818	Rv1104
Rv0885	Rv0765c	Rv0986	Rv0820	Rv0786c	Rv0819	Rv1105
Rv0886	Rv0766c	Rv0987	Rv0822c	Rv0787	Rv0820	Rv1106c
Rv0887c	Rv0767c	Rv0990c	Rv0823c	Rv0787.1	Rv0821c	Rv1107c
Rv0889c	Rv0768	Rv0992c	Rv0824c	Rv0788	Rv0822c	Rv1108c
Rv0890c	Rv0769	Rv0993	Rv0826	Rv0789c	Rv0823c	Rv1109c
Rv0891c	Rv0770	Rv0995	Rv0827c	Rv0790c	Rv0824c	Rv1110
Rv0893c	Rv0771	Rv0996	Rv0829	Rv0791c	Rv0825c	Rv1111c
Rv0894	Rv0772	Rv0998	Rv0830	Rv0792c	Rv0826	Rv1112
Rv0895	Rv0773c	Rv0999	Rv0831c	Rv0793	Rv0827c	Rv1113
Rv0896	Rv0774c	Rv1000c	Rv0832	Rv0794c	Rv0828c	Rv1117
Rv0897c	Rv0775	Rv1001	Rv0833	Rv0796	Rv0829	Rv1118c
Rv0898c	Rv0776c	Rv1002c	Rv0837c	Rv0798c	Rv0830	Rv1120c
Rv0899	Rv0777	Rv1003	Rv0838	Rv0799c	Rv0831c	Rv1121
Rv0901	Rv0778	Rv1005c	Rv0840c	Rv0800	Rv0836c	Rv1122
Rv0902c	Rv0779c	Rv1006	Rv0841	Rv0801	Rv0837c	Rv1123c
Rv0903c	Rv0780	Rv1007c	Rv0842	Rv0802c	Rv0838	Rv1124
Rv0904c	Rv0781	Rv1008	Rv0843	Rv0803	Rv0839	Rv1125
Rv0905	Rv0782	Rv1009	Rv0844c	Rv0805	Rv0840c	Rv1126c
Rv0906	Rv0783c	Rv1010	Rv0845	Rv0806c	Rv0842	Rv1127c
Rv0907	Rv0784	Rv1011	Rv0846c	Rv0807	Rv0843	Rv1128c

Rv0908	Rv0785	Rv1012	Rv0848	Rv0808	Rv0844c	Rv1129c
Rv0910	Rv0786c	Rv1013	Rv0852	Rv0809	Rv0845	Rv1130
Rv0911	Rv0787	Rv1015c	Rv0853c	Rv0811c	Rv0846c	Rv1131
Rv0913c	Rv0787.1	Rv1016c	Rv0855	Rv0812	Rv0847	Rv1132
Rv0914c	Rv0788	Rv1017c	Rv0856	Rv0813c	Rv0848	Rv1133c
Rv0915c	Rv0789c	Rv1018c	Rv0858c	Rv0815c	Rv0849	Rv1138c
Rv0918	Rv0790c	Rv1019	Rv0860	Rv0816c	Rv0850	Rv1139c
Rv0919	Rv0791c	Rv1020	Rv0861c	Rv0817c	Rv0851c	Rv1140
Rv0920c	Rv0792c	Rv1021	Rv0862c	Rv0818	Rv0853c	Rv1141c
Rv0921	Rv0793	Rv1022	Rv0863	Rv0819	Rv0855	Rv1142c
Rv0922	Rv0794c	Rv1023	Rv0864	Rv0820	Rv0856	Rv1143
Rv0923c	Rv0795	Rv1024	Rv0866	Rv0821c	Rv0857	Rv1144
Rv0925c	Rv0796	Rv1025	Rv0868c	Rv0822c	Rv0858c	Rv1145
Rv0926c	Rv0797	Rv1026	Rv0869c	Rv0823c	Rv0859	Rv1146
Rv0927c	Rv0798c	Rv1027c	Rv0873	Rv0824c	Rv0860	Rv1147
Rv0928	Rv0799c	Rv1028c	Rv0874c	Rv0825c	Rv0861c	Rv1151c
Rv0929	Rv0800	Rv1030	Rv0876c	Rv0826	Rv0862c	Rv1152
Rv0930	Rv0801	Rv1032c	Rv0877	Rv0827c	Rv0863	Rv1154c
Rv0931c	Rv0802c	Rv1033c	Rv0878c	Rv0828c	Rv0864	Rv1155
Rv0932c	Rv0803	Rv1034c	Rv0879c	Rv0829	Rv0865	Rv1156
Rv0933	Rv0804	Rv1035c	Rv0880	Rv0830	Rv0866	Rv1157c
Rv0934	Rv0805	Rv1036c	Rv0881	Rv0831c	Rv0867c	Rv1159
Rv0935	Rv0806c	Rv1038c	Rv0883c	Rv0836c	Rv0869c	Rv1160
Rv0936	Rv0807	Rv1041c	Rv0884c	Rv0837c	Rv0871	Rv1161
Rv0937c	Rv0808	Rv1043c	Rv0885	Rv0838	Rv0873	Rv1162
Rv0939	Rv0809	Rv1044	Rv0886	Rv0840c	Rv0874c	Rv1163
Rv0940c	Rv0811c	Rv1045	Rv0887c	Rv0841	Rv0876c	Rv1164
Rv0941c	Rv0812	Rv1046c	Rv0888	Rv0842	Rv0877	Rv1165
Rv0943c	Rv0813c	Rv1048c	Rv0889c	Rv0843	Rv0878c	Rv1166
Rv0944	Rv0814c	Rv1049	Rv0890c	Rv0844c	Rv0879c	Rv1167c
Rv0945	Rv0815c	Rv1050	Rv0891c	Rv0845	Rv0880	Rv1170
Rv0946c	Rv0816c	Rv1051c	Rv0892	Rv0846c	Rv0883c	Rv1171
Rv0948c	Rv0817c	Rv1057	Rv0893c	Rv0847	Rv0884c	Rv1173
Rv0949	Rv0818	Rv1058	Rv0894	Rv0848	Rv0885	Rv1174c
Rv0950c	Rv0819	Rv1059	Rv0895	Rv0849	Rv0886	Rv1176c
Rv0951	Rv0820	Rv1060	Rv0896	Rv0850	Rv0887c	Rv1177
Rv0952	Rv0821c	Rv1063c	Rv0897c	Rv0851c	Rv0888	Rv1180
Rv0955	Rv0822c	Rv1066	Rv0898c	Rv0852	Rv0889c	Rv1181
Rv0956	Rv0823c	Rv1068c	Rv0899	Rv0853c	Rv0890c	Rv1183
Rv0957	Rv0824c	Rv1069c	Rv0900	Rv0854	Rv0891c	Rv1184c
Rv0958	Rv0825c	Rv1070c	Rv0901	Rv0855	Rv0892	Rv1185c
Rv0959	Rv0826	Rv1071c	Rv0902c	Rv0857	Rv0893c	Rv1186c
Rv0960	Rv0827c	Rv1072	Rv0903c	Rv0858c	Rv0894	Rv1187
Rv0962c	Rv0828c	Rv1073	Rv0904c	Rv0859	Rv0895	Rv1188
Rv0964c	Rv0829	Rv1074c	Rv0905	Rv0860	Rv0896	Rv1189
Rv0968	Rv0830	Rv1075c	Rv0907	Rv0861c	Rv0897c	Rv1191
Rv0970	Rv0831c	Rv1076	Rv0908	Rv0862c	Rv0898c	Rv1193
Rv0971c	Rv0837c	Rv1077	Rv0910	Rv0863	Rv0899	Rv1200
Rv0972c	Rv0838	Rv1078	Rv0911	Rv0866	Rv0900	Rv1201c
Rv0973c	Rv0839	Rv1079	Rv0913c	Rv0867c	Rv0901	Rv1202
Rv0974c	Rv0840c	Rv1080c	Rv0914c	Rv0868c	Rv0902c	Rv1203c

Rv0975c	Rv0842	Rv1082	Rv0915c	Rv0869c	Rv0903c	Rv1204c
Rv0981	Rv0843	Rv1084	Rv0917	Rv0871	Rv0904c	Rv1205
Rv0982	Rv0844c	Rv1085c	Rv0918	Rv0873	Rv0905	Rv1206
Rv0983	Rv0845	Rv1086	Rv0919	Rv0874c	Rv0906	Rv1207
Rv0984	Rv0846c	Rv1088	Rv0920c	Rv0875c	Rv0907	Rv1208
Rv0985c	Rv0847	Rv1092c	Rv0921	Rv0876c	Rv0908	Rv1209
Rv0987	Rv0848	Rv1093	Rv0922	Rv0878c	Rv0910	Rv1210
Rv0988	Rv0849	Rv1094	Rv0923c	Rv0880	Rv0911	Rv1212c
Rv0989c	Rv0850	Rv1095	Rv0924c	Rv0881	Rv0913c	Rv1213
Rv0991c	Rv0851c	Rv1096	Rv0925c	Rv0883c	Rv0914c	Rv1215c
Rv0992c	Rv0852	Rv1098c	Rv0926c	Rv0884c	Rv0915c	Rv1216c
Rv0993	Rv0853c	Rv1099c	Rv0928	Rv0885	Rv0917	Rv1217c
Rv0994	Rv0854	Rv1101c	Rv0929	Rv0886	Rv0918	Rv1218c
Rv0996	Rv0855	Rv1106c	Rv0930	Rv0887c	Rv0919	Rv1219c
Rv0997	Rv0856	Rv1108c	Rv0931c	Rv0888	Rv0920c	Rv1220c
Rv0998	Rv0857	Rv1109c	Rv0933	Rv0889c	Rv0921	Rv1221
Rv0999	Rv0858c	Rv1110	Rv0935	Rv0890c	Rv0922	Rv1223
Rv1000c	Rv0859	Rv1111c	Rv0936	Rv0891c	Rv0923c	Rv1224
Rv1003	Rv0860	Rv1112	Rv0938	Rv0892	Rv0924c	Rv1229c
Rv1004c	Rv0861c	Rv1113	Rv0939	Rv0893c	Rv0926c	Rv1230c
Rv1005c	Rv0862c	Rv1114	Rv0940c	Rv0894	Rv0927c	Rv1232c
Rv1006	Rv0863	Rv1115	Rv0941c	Rv0895	Rv0928	Rv1234
Rv1007c	Rv0864	Rv1117	Rv0942	Rv0896	Rv0929	Rv1235
Rv1008	Rv0868c	Rv1118c	Rv0943c	Rv0897c	Rv0930	Rv1236
Rv1009	Rv0869c	Rv1120c	Rv0944	Rv0898c	Rv0931c	Rv1237
Rv1010	Rv0871	Rv1121	Rv0945	Rv0899	Rv0933	Rv1238
Rv1011	Rv0872c	Rv1122	Rv0946c	Rv0900	Rv0934	Rv1239c
Rv1013	Rv0873	Rv1124	Rv0949	Rv0901	Rv0935	Rv1240
Rv1014c	Rv0874c	Rv1125	Rv0950c	Rv0902c	Rv0936	Rv1244
Rv1015c	Rv0875c	Rv1126c	Rv0951	Rv0903c	Rv0937c	Rv1245c
Rv1016c	Rv0876c	Rv1128c	Rv0952	Rv0904c	Rv0938	Rv1249c
Rv1017c	Rv0877	Rv1129c	Rv0953c	Rv0905	Rv0939	Rv1250
Rv1018c	Rv0878c	Rv1130	Rv0954	Rv0906	Rv0940c	Rv1251c
Rv1019	Rv0879c	Rv1131	Rv0955	Rv0907	Rv0941c	Rv1253
Rv1020	Rv0880	Rv1132	Rv0956	Rv0908	Rv0942	Rv1254
Rv1021	Rv0881	Rv1133c	Rv0957	Rv0909	Rv0944	Rv1255c
Rv1022	Rv0883c	Rv1135.1	Rv0958	Rv0910	Rv0945	Rv1256c
Rv1024	Rv0884c	Rv1135c	Rv0959	Rv0911	Rv0946c	Rv1257c
Rv1025	Rv0885	Rv1138c	Rv0960	Rv0913c	Rv0948c	Rv1258c
Rv1026	Rv0886	Rv1139c	Rv0961	Rv0914c	Rv0949	Rv1259
Rv1027c	Rv0887c	Rv1140	Rv0962c	Rv0915c	Rv0950c	Rv1260
Rv1029	Rv0888	Rv1143	Rv0963c	Rv0917	Rv0951	Rv1261c
Rv1030	Rv0889c	Rv1144	Rv0964c	Rv0918	Rv0952	Rv1262c
Rv1031	Rv0890c	Rv1145	Rv0967	Rv0919	Rv0953c	Rv1263
Rv1033c	Rv0891c	Rv1146	Rv0968	Rv0920c	Rv0954	Rv1264
Rv1035c	Rv0892	Rv1147	Rv0969	Rv0921	Rv0955	Rv1265
Rv1038c	Rv0893c	Rv1148c	Rv0970	Rv0922	Rv0956	Rv1266c
Rv1039c	Rv0894	Rv1152	Rv0971c	Rv0924c	Rv0957	Rv1267c
Rv1040c	Rv0895	Rv1153c	Rv0972c	Rv0926c	Rv0958	Rv1272c
Rv1043c	Rv0896	Rv1154c	Rv0973c	Rv0927c	Rv0959	Rv1273c
Rv1044	Rv0897c	Rv1155	Rv0974c	Rv0928	Rv0960	Rv1275

Rv1045	Rv0898c	Rv1156	Rv0975c	Rv0929	Rv0963c	Rv1276c
Rv1046c	Rv0899	Rv1159	Rv0979A	Rv0931c	Rv0964c	Rv1277
Rv1048c	Rv0900	Rv1160	Rv0979c	Rv0932c	Rv0966c	Rv1278
Rv1049	Rv0902c	Rv1161	Rv0982	Rv0934	Rv0967	Rv1279
Rv1050	Rv0903c	Rv1162	Rv0983	Rv0935	Rv0968	Rv1280c
Rv1051c	Rv0904c	Rv1164	Rv0984	Rv0936	Rv0969	Rv1281c
Rv1052	Rv0905	Rv1165	Rv0986	Rv0937c	Rv0970	Rv1282c
Rv1054	Rv0907	Rv1168c	Rv0987	Rv0938	Rv0971c	Rv1283c
Rv1056	Rv0908	Rv1171	Rv0988	Rv0939	Rv0972c	Rv1284
Rv1058	Rv0910	Rv1173	Rv0989c	Rv0940c	Rv0973c	Rv1285
Rv1059	Rv0911	Rv1175c	Rv0990c	Rv0941c	Rv0974c	Rv1286
Rv1060	Rv0913c	Rv1178	Rv0992c	Rv0942	Rv0975c	Rv1287
Rv1061	Rv0914c	Rv1179c	Rv0993	Rv0943c	Rv0976c	Rv1293
Rv1062	Rv0915c	Rv1180	Rv0994	Rv0944	Rv0979c	Rv1294
Rv1063c	Rv0917	Rv1181	Rv0995	Rv0945	Rv0981	Rv1295
Rv1064c	Rv0919	Rv1182	Rv0996	Rv0946c	Rv0982	Rv1296
Rv1065	Rv0920c	Rv1183	Rv0997	Rv0949	Rv0983	Rv1297
Rv1066	Rv0921	Rv1184c	Rv0998	Rv0950c	Rv0984	Rv1298
Rv1067c	Rv0922	Rv1185c	Rv0999	Rv0951	Rv0987	Rv1299
Rv1068c	Rv0923c	Rv1186c	Rv1000c	Rv0952	Rv0988	Rv1300
Rv1069c	Rv0924c	Rv1187	Rv1001	Rv0953c	Rv0989c	Rv1301
Rv1070c	Rv0925c	Rv1188	Rv1002c	Rv0955	Rv0990c	Rv1302
Rv1071c	Rv0926c	Rv1189	Rv1003	Rv0957	Rv0991c	Rv1303
Rv1072	Rv0927c	Rv1190	Rv1005c	Rv0958	Rv0992c	Rv1304
Rv1073	Rv0928	Rv1191	Rv1006	Rv0959	Rv0993	Rv1306
Rv1074c	Rv0929	Rv1192	Rv1007c	Rv0963c	Rv0994	Rv1307
Rv1076	Rv0930	Rv1193	Rv1008	Rv0964c	Rv0995	Rv1308
Rv1077	Rv0931c	Rv1194c	Rv1009	Rv0966c	Rv0996	Rv1309
Rv1078	Rv0932c	Rv1201c	Rv1010	Rv0967	Rv0997	Rv1310
Rv1079	Rv0933	Rv1202	Rv1011	Rv0969	Rv0998	Rv1311
Rv1080c	Rv0935	Rv1203c	Rv1012	Rv0970	Rv0999	Rv1312
Rv1081c	Rv0936	Rv1204c	Rv1013	Rv0971c	Rv1000c	Rv1314c
Rv1082	Rv0937c	Rv1206	Rv1014c	Rv0972c	Rv1001	Rv1315
Rv1083	Rv0938	Rv1207	Rv1015c	Rv0973c	Rv1002c	Rv1316c
Rv1084	Rv0939	Rv1208	Rv1016c	Rv0974c	Rv1003	Rv1317c
Rv1085c	Rv0940c	Rv1209	Rv1017c	Rv0975c	Rv1004c	Rv1318c
Rv1086	Rv0941c	Rv1211	Rv1018c	Rv0976c	Rv1006	Rv1319c
Rv1087.1	Rv0942	Rv1212c	Rv1019	Rv0979A	Rv1007c	Rv1320c
Rv1088	Rv0943c	Rv1213	Rv1020	Rv0979c	Rv1008	Rv1321
Rv1089	Rv0944	Rv1215c	Rv1021	Rv0980c	Rv1009	Rv1322
Rv1092c	Rv0945	Rv1216c	Rv1022	Rv0981	Rv1010	Rv1323
Rv1093	Rv0946c	Rv1217c	Rv1023	Rv0982	Rv1011	Rv1324
Rv1094	Rv0948c	Rv1218c	Rv1024	Rv0983	Rv1012	Rv1327c
Rv1095	Rv0949	Rv1219c	Rv1025	Rv0984	Rv1013	Rv1328
Rv1096	Rv0950c	Rv1222	Rv1026	Rv0985c	Rv1014c	Rv1329c
Rv1097c	Rv0951	Rv1223	Rv1027c	Rv0986	Rv1015c	Rv1330c
Rv1098c	Rv0952	Rv1224	Rv1028c	Rv0987	Rv1017c	Rv1331
Rv1101c	Rv0953c	Rv1225c	Rv1029	Rv0988	Rv1018c	Rv1332
Rv1102c	Rv0955	Rv1226c	Rv1030	Rv0989c	Rv1019	Rv1333
Rv1105	Rv0956	Rv1229c	Rv1032c	Rv0990c	Rv1020	Rv1337
Rv1106c	Rv0957	Rv1230c	Rv1033c	Rv0991c	Rv1021	Rv1338

Rv1108c	Rv0958	Rv1232c	Rv1034c	Rv0992c	Rv1022	Rv1341
Rv1110	Rv0959	Rv1234	Rv1035c	Rv0994	Rv1023	Rv1343c
Rv1111c	Rv0960	Rv1235	Rv1039c	Rv0995	Rv1024	Rv1344
Rv1112	Rv0961	Rv1236	Rv1041c	Rv0996	Rv1025	Rv1345
Rv1114	Rv0962c	Rv1237	Rv1042c	Rv0997	Rv1026	Rv1346
Rv1115	Rv0963c	Rv1238	Rv1043c	Rv0998	Rv1027c	Rv1347c
Rv1117	Rv0964c	Rv1239c	Rv1044	Rv0999	Rv1028c	Rv1348
Rv1118c	Rv0966c	Rv1240	Rv1045	Rv1000c	Rv1029	Rv1349
Rv1120c	Rv0967	Rv1241	Rv1046c	Rv1001	Rv1030	Rv1350
Rv1121	Rv0968	Rv1246c	Rv1047	Rv1002c	Rv1031	Rv1353c
Rv1122	Rv0969	Rv1247c	Rv1048c	Rv1003	Rv1032c	Rv1354c
Rv1123c	Rv0971c	Rv1248c	Rv1049	Rv1005c	Rv1033c	Rv1355c
Rv1124	Rv0972c	Rv1250	Rv1050	Rv1006	Rv1034c	Rv1356c
Rv1125	Rv0973c	Rv1251c	Rv1051c	Rv1007c	Rv1035c	Rv1360
Rv1126c	Rv0974c	Rv1253	Rv1053c	Rv1008	Rv1038c	Rv1362c
Rv1127c	Rv0975c	Rv1257c	Rv1054	Rv1009	Rv1039c	Rv1363c
Rv1128c	Rv0976c	Rv1259	Rv1055	Rv1010	Rv1042c	Rv1364c
Rv1129c	Rv0978c	Rv1260	Rv1056	Rv1011	Rv1043c	Rv1367c
Rv1130	Rv0979A	Rv1261c	Rv1057	Rv1012	Rv1044	Rv1379
Rv1131	Rv0979c	Rv1262c	Rv1058	Rv1013	Rv1045	Rv1380
Rv1132	Rv0980c	Rv1264	Rv1059	Rv1014c	Rv1046c	Rv1381
Rv1135.1	Rv0981	Rv1265	Rv1060	Rv1015c	Rv1047	Rv1382
Rv1136	Rv0982	Rv1266c	Rv1061	Rv1016c	Rv1048c	Rv1383
Rv1138c	Rv0983	Rv1267c	Rv1062	Rv1017c	Rv1049	Rv1384
Rv1139c	Rv0984	Rv1268c	Rv1063c	Rv1018c	Rv1050	Rv1385
Rv1141c	Rv0985c	Rv1270c	Rv1064c	Rv1019	Rv1051c	Rv1387
Rv1142c	Rv0986	Rv1272c	Rv1065	Rv1020	Rv1053c	Rv1388
Rv1143	Rv0987	Rv1273c	Rv1066	Rv1021	Rv1054	Rv1391
Rv1144	Rv0988	Rv1274	Rv1067c	Rv1022	Rv1056	Rv1392
Rv1147	Rv0990c	Rv1275	Rv1068c	Rv1023	Rv1057	Rv1393c
Rv1152	Rv0991c	Rv1277	Rv1069c	Rv1024	Rv1058	Rv1400c
Rv1153c	Rv0992c	Rv1278	Rv1070c	Rv1025	Rv1059	Rv1402
Rv1154c	Rv0993	Rv1279	Rv1072	Rv1026	Rv1063c	Rv1404
Rv1155	Rv0994	Rv1280c	Rv1073	Rv1027c	Rv1064c	Rv1405c
Rv1156	Rv0995	Rv1281c	Rv1074c	Rv1028c	Rv1066	Rv1406
Rv1157c	Rv0996	Rv1282c	Rv1075c	Rv1029	Rv1068c	Rv1407
Rv1159	Rv0997	Rv1284	Rv1076	Rv1030	Rv1069c	Rv1408
Rv1160	Rv0998	Rv1285	Rv1077	Rv1031	Rv1070c	Rv1409
Rv1162	Rv0999	Rv1286	Rv1078	Rv1032c	Rv1071c	Rv1410c
Rv1163	Rv1000c	Rv1287	Rv1079	Rv1033c	Rv1072	Rv1411c
Rv1164	Rv1001	Rv1289	Rv1080c	Rv1034c	Rv1073	Rv1412
Rv1165	Rv1002c	Rv1290.1	Rv1081c	Rv1035c	Rv1074c	Rv1415
Rv1166	Rv1003	Rv1290c	Rv1082	Rv1036c	Rv1075c	Rv1416
Rv1167c	Rv1005c	Rv1292	Rv1084	Rv1039c	Rv1076	Rv1420
Rv1168c	Rv1006	Rv1293	Rv1085c	Rv1040c	Rv1077	Rv1421
Rv1169c	Rv1007c	Rv1294	Rv1088	Rv1042c	Rv1078	Rv1422
Rv1171	Rv1008	Rv1297	Rv1092c	Rv1043c	Rv1079	Rv1423
Rv1172c	Rv1009	Rv1298	Rv1093	Rv1044	Rv1080c	Rv1425
Rv1173	Rv1010	Rv1302	Rv1094	Rv1045	Rv1081c	Rv1426c
Rv1175c	Rv1011	Rv1303	Rv1095	Rv1048c	Rv1082	Rv1427c
Rv1176c	Rv1012	Rv1304	Rv1096	Rv1049	Rv1084	Rv1428c

Rv1178	Rv1013	Rv1307	Rv1097c	Rv1050	Rv1085c	Rv1431
Rv1179c	Rv1014c	Rv1308	Rv1098c	Rv1051c	Rv1086	Rv1432
Rv2940c	Rv1015c	Rv1309	Rv1099c	Rv1053c	Rv1087.1	Rv1436
Rv1182	Rv1016c	Rv1310	Rv1100	Rv1054	Rv1088	Rv1437
Rv1184c	Rv1017c	Rv1312	Rv1101c	Rv1056	Rv1092c	Rv1438
Rv1185c	Rv1018c	Rv1314c	Rv1105	Rv1057	Rv1093	Rv1445c
Rv1186c	Rv1020	Rv1315	Rv1106c	Rv1058	Rv1094	Rv1446c
Rv1187	Rv1021	Rv1316c	Rv1107c	Rv1059	Rv1095	Rv1447c
Rv1188	Rv1022	Rv1317c	Rv1108c	Rv1060	Rv1096	Rv1448c
Rv1189	Rv1023	Rv1318c	Rv1109c	Rv1061	Rv1098c	Rv1449c
Rv1190	Rv1024	Rv1319c	Rv1110	Rv1062	Rv1099c	Rv1454c
Rv1191	Rv1025	Rv1320c	Rv1111c	Rv1063c	Rv1104	Rv1455
Rv1192	Rv1026	Rv1322	Rv1112	Rv1065	Rv1105	Rv1456c
Rv1193	Rv1027c	Rv1323	Rv1113	Rv1066	Rv1106c	Rv1457c
Rv1194c	Rv1028c	Rv1325c	Rv1116	Rv1067c	Rv1108c	Rv1458c
Rv1197	Rv1029	Rv1326c	Rv1116.1	Rv1068c	Rv1109c	Rv1459c
Rv1201c	Rv1030	Rv1327c	Rv1117	Rv1069c	Rv1110	Rv1460
Rv1202	Rv1031	Rv1328	Rv1118c	Rv1070c	Rv1111c	Rv1461
Rv1203c	Rv1032c	Rv1329c	Rv1120c	Rv1071c	Rv1112	Rv1462
Rv1204c	Rv1033c	Rv1330c	Rv1121	Rv1072	Rv1113	Rv1463
Rv1205	Rv1034c	Rv1332	Rv1122	Rv1073	Rv1116	Rv1464
Rv1206	Rv1035c	Rv1333	Rv1124	Rv1074c	Rv1117	Rv1465
Rv1207	Rv1038c	Rv1336	Rv1125	Rv1075c	Rv1118c	Rv1467c
Rv1208	Rv1039c	Rv1337	Rv1126c	Rv1076	Rv1120c	Rv1471
Rv1209	Rv1040c	Rv1338	Rv1127c	Rv1077	Rv1121	Rv1472
Rv1210	Rv1041c	Rv1344	Rv1128c	Rv1078	Rv1122	Rv1473
Rv1213	Rv1042c	Rv1345	Rv1129c	Rv1079	Rv1123c	Rv1473.1
Rv1215c	Rv1043c	Rv1346	Rv1130	Rv1080c	Rv1124	Rv1474c
Rv1216c	Rv1044	Rv1347c	Rv1131	Rv1081c	Rv1125	Rv1475c
Rv1217c	Rv1045	Rv1348	Rv1132	Rv1083	Rv1126c	Rv1477
Rv1218c	Rv1046c	Rv1349	Rv1133c	Rv1084	Rv1127c	Rv1478
Rv1219c	Rv1047	Rv1350	Rv1134	Rv1085c	Rv1128c	Rv1479
Rv1222	Rv1048c	Rv1351	Rv1135c	Rv1086	Rv1129c	Rv1480
Rv1223	Rv1049	Rv1352	Rv1137c	Rv1087	Rv1130	Rv1481
Rv1224	Rv1050	Rv1353c	Rv1138c	Rv1088	Rv1131	Rv1482c
Rv1225c	Rv1051c	Rv1355c	Rv1140	Rv1091	Rv1132	Rv1483
Rv1226c	Rv1052	Rv1357c	Rv1141c	Rv1093	Rv1133c	Rv1484
Rv1227c	Rv1053c	Rv1358	Rv1143	Rv1094	Rv1135.1	Rv1485
Rv1228	Rv1054	Rv1359	Rv1144	Rv1095	Rv1136	Rv1487
Rv1229c	Rv1056	Rv1360	Rv1145	Rv1096	Rv1137c	Rv1488
Rv1231c	Rv1057	Rv1363c	Rv1146	Rv1097c	Rv1138c	Rv1489
Rv1232c	Rv1058	Rv1364c	Rv1147	Rv1098c	Rv1139c	Rv1490
Rv1234	Rv1059	Rv1367c	Rv1148c	Rv1099c	Rv1140	Rv1491c
Rv1235	Rv1061	Rv1368	Rv1149	Rv1100	Rv1141c	Rv1492
Rv1236	Rv1062	Rv1370c	Rv1152	Rv1101c	Rv1142c	Rv1493
Rv1237	Rv1063c	Rv1371	Rv1153c	Rv1102c	Rv1143	Rv1496
Rv1238	Rv1065	Rv1372	Rv1154c	Rv1104	Rv1144	Rv1497
Rv1239c	Rv1066	Rv1373	Rv1155	Rv1105	Rv1145	Rv1516c
Rv1241	Rv1067c	Rv1374c	Rv1156	Rv1106c	Rv1146	Rv1517
Rv1244	Rv1068c	Rv1375	Rv1157c	Rv1108c	Rv1147	Rv1520
Rv1245c	Rv1069c	Rv1376	Rv1158c	Rv1109c	Rv1148c	Rv1524

Rv1246c	Rv1070c	Rv1378c	Rv1159	Rv1110	Rv1149	Rv1527c
Rv1247c	Rv1072	Rv1379	Rv1160	Rv1112	Rv1152	Rv1531
Rv1248c	Rv1073	Rv1381	Rv1161	Rv1113	Rv1153c	Rv1532c
Rv1249c	Rv1074c	Rv1382	Rv1162	Rv1114	Rv1154c	Rv1533
Rv1251c	Rv1075c	Rv1383	Rv1163	Rv1115	Rv1155	Rv1535
Rv1253	Rv1076	Rv1384	Rv1165	Rv1116.1	Rv1156	Rv1536
Rv1254	Rv1077	Rv1388	Rv1166	Rv1117	Rv1157c	Rv1537
Rv1255c	Rv1078	Rv1389	Rv1167c	Rv1118c	Rv1159	Rv1538c
Rv1257c	Rv1079	Rv1391	Rv1168c	Rv1120c	Rv1159A	Rv1540
Rv1259	Rv1080c	Rv1392	Rv1170	Rv1121	Rv1160	Rv1542c
Rv1260	Rv1081c	Rv1393c	Rv1172c	Rv1122	Rv1161	Rv1543
Rv1261c	Rv1082	Rv1394c	Rv1173	Rv1123c	Rv1162	Rv1544
Rv1262c	Rv1083	Rv1395	Rv1175c	Rv1124	Rv1163	Rv1546
Rv1263	Rv1084	Rv1396c	Rv1178	Rv1125	Rv1164	Rv1547
Rv1264	Rv1085c	Rv1397c	Rv1179c	Rv1126c	Rv1165	Rv1549
Rv1265	Rv1086	Rv1399c	Rv1180	Rv1127c	Rv1166	Rv1551
Rv1266c	Rv1087.1	Rv1401	Rv1181	Rv1128c	Rv1167c	Rv1557
Rv1267c	Rv1088	Rv1402	Rv1182	Rv1129c	Rv1168c	Rv1558
Rv1268c	Rv1089	Rv1404	Rv1183	Rv1130	Rv1170	Rv1559
Rv1269c	Rv1091	Rv1405c	Rv1184c	Rv1131	Rv1171	Rv1562c
Rv1270c	Rv1092c	Rv1406	Rv1185c	Rv1132	Rv1172c	Rv1563c
Rv1272c	Rv1093	Rv1407	Rv1186c	Rv1133c	Rv1173	Rv1564c
Rv1273c	Rv1094	Rv1409	Rv1187	Rv1134	Rv1175c	Rv1565c
Rv1274	Rv1095	Rv1411c	Rv1188	Rv1135.1	Rv1176c	Rv1568
Rv1275	Rv1096	Rv1412	Rv1189	Rv1135c	Rv1178	Rv1569
Rv1277	Rv1097c	Rv1413	Rv1190	Rv1136	Rv1179c	Rv1570
Rv1279	Rv1098c	Rv1414	Rv1191	Rv1137c	Rv1180	Rv1586c
Rv1280c	Rv1099c	Rv1415	Rv1192	Rv1138c	Rv1181	Rv1589
Rv1281c	Rv1100	Rv1416	Rv1193	Rv1139c	Rv1182	Rv1590
Rv1282c	Rv1101c	Rv1417	Rv1194c	Rv1141c	Rv1183	Rv1591
Rv1283c	Rv1103c	Rv1418	Rv1199c	Rv1142c	Rv1184c	Rv1592c
Rv1284	Rv1104	Rv1420	Rv1201c	Rv1143	Rv1185c	Rv1593c
Rv1285	Rv1105	Rv1421	Rv1202	Rv1144	Rv1186c	Rv1594
Rv1287	Rv1106c	Rv1422	Rv1203c	Rv1145	Rv1187	Rv1595
Rv1288	Rv1107c	Rv1423	Rv1204c	Rv1146	Rv1188	Rv1596
Rv1289	Rv1108c	Rv1425	Rv1206	Rv1147	Rv1189	Rv1597
Rv1290c	Rv1109c	Rv1426c	Rv1207	Rv1148c	Rv1192	Rv1598c
Rv1290.1	Rv1110	Rv1427c	Rv1208	Rv1149	Rv1193	Rv1599
Rv1291c	Rv1111c	Rv1429	Rv1209	Rv1151c	Rv1194c	Rv1600
Rv1293	Rv1112	Rv1431	Rv1210	Rv1152	Rv1196	Rv1601
Rv1294	Rv1113	Rv1432	Rv1211	Rv1153c	Rv1197	Rv1602
Rv1295	Rv1114	Rv1433	Rv1212c	Rv1154c	Rv1199c	Rv1603
Rv1296	Rv1116	Rv1436	Rv1213	Rv1156	Rv1200	Rv1604
Rv1297	Rv1116.1	Rv1437	Rv1215c	Rv1157c	Rv1201c	Rv1605
Rv1298	Rv1117	Rv1438	Rv1216c	Rv1159	Rv1202	Rv1606
Rv1299	Rv1118c	Rv1439c	Rv1217c	Rv1160	Rv1203c	Rv1607
Rv1300	Rv1120c	Rv1440	Rv1219c	Rv1161	Rv1205	Rv1608c
Rv1301	Rv1121	Rv1442	Rv1220c	Rv1162	Rv1206	Rv1609
Rv1302	Rv1122	Rv1443c	Rv1223	Rv1163	Rv1207	Rv1610
Rv1303	Rv1123c	Rv1444c	Rv1224	Rv1165	Rv1208	Rv1611
Rv1306	Rv1124	Rv1445c	Rv1226c	Rv1166	Rv1210	Rv1612

Rv1307	Rv1125	Rv1446c	Rv1228	Rv1170	Rv1211	Rv1613
Rv1308	Rv1126c	Rv1447c	Rv1229c	Rv1172c	Rv1213	Rv1617
Rv1309	Rv1127c	Rv1448c	Rv1230c	Rv1173	Rv1215c	Rv1618
Rv1310	Rv1128c	Rv1449c	Rv1232c	Rv1175c	Rv1216c	Rv1619
Rv1311	Rv1129c	Rv1450c	Rv1234	Rv1176c	Rv1217c	Rv1620c
Rv1312	Rv1130	Rv1451	Rv1235	Rv1178	Rv1218c	Rv1621c
Rv1314c	Rv1131	Rv1453	Rv1236	Rv1179c	Rv1219c	Rv1622c
Rv1315	Rv1132	Rv1454c	Rv1237	Rv1180	Rv1220c	Rv1623c
Rv1316c	Rv1133c	Rv1455	Rv1238	Rv1181	Rv1222	Rv1625c
Rv1317c	Rv1135.1	Rv1456c	Rv1239c	Rv1182	Rv1223	Rv1626
Rv3475	Rv1135c	Rv1458c	Rv1240	Rv1183	Rv1224	Rv1629
Rv0796	Rv1136	Rv1460	Rv1241	Rv1184c	Rv1225c	Rv1630
Rv2479c	Rv1137c	Rv1461	Rv1244	Rv1185c	Rv1226c	Rv1631
Rv1369c	Rv1138c	Rv1462	Rv1245c	Rv1186c	Rv1229c	Rv1632c
Rv3187	Rv1140	Rv1463	Rv1246c	Rv1187	Rv1230c	Rv1633
Rv2814c	Rv1141c	Rv1464	Rv1247c	Rv1188	Rv1231c	Rv1634
Rv2279	Rv1142c	Rv1465	Rv1248c	Rv1189	Rv1232c	Rv1636
Rv2355	Rv1143	Rv1467c	Rv1249c	Rv1190	Rv1235	Rv1637c
Rv1764	Rv1144	Rv1469	Rv1250	Rv1191	Rv1236	Rv1638
Rv2167c	Rv1145	Rv1472	Rv1251c	Rv1192	Rv1237	Rv1639c
Rv1756c	Rv1146	Rv1473	Rv1252c	Rv1193	Rv1238	Rv1640c
Rv2649	Rv1147	Rv1474c	Rv1253	Rv1194c	Rv1239c	Rv1641
Rv3185	Rv1148c	Rv1475c	Rv1254	Rv1196	Rv1240	Rv1642
Rv2106	Rv1149	Rv1477	Rv1255c	Rv1199c	Rv1241	Rv1643
Rv3326	Rv1151c	Rv1478	Rv1256c	Rv1200	Rv1242	Rv1644
Rv3380c	Rv1152	Rv1479	Rv1257c	Rv1201c	Rv1244	Rv1645c
Rv1320c	Rv1153c	Rv1480	Rv1259	Rv1202	Rv1245c	Rv1647
Rv1321	Rv1154c	Rv1481	Rv1260	Rv1203c	Rv1246c	Rv1649
Rv1322	Rv1155	Rv1482c	Rv1261c	Rv1205	Rv1247c	Rv1650
Rv1323	Rv1156	Rv1483	Rv1262c	Rv1206	Rv1248c	Rv1652
Rv1324	Rv1157c	Rv1485	Rv1263	Rv1207	Rv1249c	Rv1653
Rv1326c	Rv1159	Rv1486c	Rv1264	Rv1208	Rv1251c	Rv1654
Rv1327c	Rv1160	Rv1488	Rv1265	Rv1209	Rv1252c	Rv1655
Rv1328	Rv1161	Rv1490	Rv1266c	Rv1210	Rv1253	Rv1656
Rv1329c	Rv1162	Rv1491c	Rv1267c	Rv1211	Rv1258c	Rv1657
Rv1331	Rv1163	Rv1492	Rv1268c	Rv1212c	Rv1259	Rv1658
Rv1332	Rv1164	Rv1493	Rv1269c	Rv1213	Rv1260	Rv1659
Rv1333	Rv1165	Rv1494	Rv1270c	Rv1214c	Rv1261c	Rv1660
Rv1337	Rv1166	Rv1495	Rv1272c	Rv1215c	Rv1263	Rv1661
Rv1338	Rv1168c	Rv1496	Rv1273c	Rv1216c	Rv1264	Rv1662
Rv1340	Rv1170	Rv1497	Rv1275	Rv1217c	Rv1265	Rv1663
Rv1341	Rv1171	Rv1498c	Rv1276c	Rv1218c	Rv1266c	Rv1664
Rv1345	Rv1172c	Rv1499	Rv1277	Rv1219c	Rv1267c	Rv1665
Rv1346	Rv1173	Rv1500	Rv1278	Rv1220c	Rv1269c	Rv1666c
Rv1348	Rv1174c	Rv1502	Rv1279	Rv1221	Rv1270c	Rv1667c
Rv1349	Rv1175c	Rv1503c	Rv1280c	Rv1222	Rv1272c	Rv1668c
Rv1350	Rv1176c	Rv1504c	Rv1281c	Rv1223	Rv1273c	Rv1682
Rv1351	Rv1178	Rv1507.1	Rv1282c	Rv1224	Rv1274	Rv1683
Rv1353c	Rv1179c	Rv1508c	Rv1284	Rv1225c	Rv1275	Rv1685c
Rv1354c	Rv1180	Rv1509	Rv1285	Rv1226c	Rv1276c	Rv1687c
Rv1355c	Rv1181	Rv1511	Rv1286	Rv1228	Rv1277	Rv1688

Rv1356c	Rv1182	Rv1512	Rv1287	Rv1229c	Rv1278	Rv1689
Rv1357c	Rv1183	Rv1513	Rv1288	Rv1230c	Rv1279	Rv1691
Rv1359	Rv1184c	Rv1514c	Rv1290.1	Rv1231c	Rv1280c	Rv1692
Rv1360	Rv1185c	Rv1515c	Rv1290c	Rv1232c	Rv1281c	Rv1693
Rv1361c	Rv1186c	Rv1516c	Rv1292	Rv1234	Rv1282c	Rv1694
Rv1362c	Rv1187	Rv1518	Rv1293	Rv1235	Rv1283c	Rv1695
Rv1363c	Rv1188	Rv1520	Rv1294	Rv1236	Rv1284	Rv1696
Rv1366	Rv1189	Rv1521	Rv1295	Rv1237	Rv1285	Rv1697
Rv1368	Rv1190	Rv1522c	Rv1296	Rv1238	Rv1286	Rv1698
Rv1371	Rv1191	Rv1523	Rv1297	Rv1239c	Rv1287	Rv1699
Rv1372	Rv1192	Rv1524	Rv1298	Rv1240	Rv1288	Rv1700
Rv1373	Rv1193	Rv1525	Rv1299	Rv1241	Rv1289	Rv1701
Rv1374c	Rv1194c	Rv1527c	Rv1300	Rv1244	Rv1290.1	Rv1702c
Rv1375	Rv1196	Rv1529	Rv1302	Rv1245c	Rv1290c	Rv1703c
Rv1376	Rv1197	Rv1530	Rv1306	Rv1246c	Rv1292	Rv1708
Rv1377c	Rv1199c	Rv1532c	Rv1307	Rv1247c	Rv1293	Rv1709
Rv1379	Rv1201c	Rv1534	Rv1308	Rv1248c	Rv1294	Rv1710
Rv1380	Rv1202	Rv1535	Rv1309	Rv1249c	Rv1295	Rv1711
Rv1381	Rv1203c	Rv1536	Rv1310	Rv1250	Rv1296	Rv1712
Rv1382	Rv1204c	Rv1537	Rv1312	Rv1251c	Rv1297	Rv1713
Rv1383	Rv1205	Rv1538c	Rv1313c	Rv1252c	Rv1298	Rv1722
Rv1384	Rv1206	Rv1540	Rv1314c	Rv1253	Rv1299	Rv1723
Rv1385	Rv1207	Rv1543	Rv1315	Rv1254	Rv1300	Rv1729c
Rv1386	Rv1208	Rv1544	Rv1316c	Rv1255c	Rv1301	Rv1733c
Rv1387	Rv1209	Rv1545	Rv1317c	Rv1259	Rv1302	Rv1746
Rv1388	Rv1210	Rv1547	Rv1318c	Rv1260	Rv1303	Rv1747
Rv1392	Rv1211	Rv1550	Rv1319c	Rv1261c	Rv1306	Rv1748
Rv1394c	Rv1212c	Rv1551	Rv1320c	Rv1262c	Rv1307	Rv1750c
Rv1395	Rv1213	Rv1552	Rv1321	Rv1263	Rv1308	Rv1751
Rv1397c	Rv1215c	Rv1553	Rv1322	Rv1264	Rv1309	Rv1752
Rv1399c	Rv1216c	Rv1554	Rv1322.1	Rv1265	Rv1310	Rv1760
Rv1400c	Rv1217c	Rv1555	Rv1323	Rv1266c	Rv1311	Rv1765c
Rv1402	Rv1218c	Rv1556	Rv1324	Rv1267c	Rv1312	Rv1776c
Rv1403c	Rv1219c	Rv1557	Rv1325c	Rv1269c	Rv1313c	Rv1777
Rv1404	Rv1220c	Rv1558	Rv1326c	Rv1270c	Rv1314c	Rv1779c
Rv1405c	Rv1221	Rv1559	Rv1327c	Rv1271c	Rv1315	Rv1780
Rv1406	Rv1222	Rv1561	Rv1328	Rv1272c	Rv1317c	Rv1781c
Rv1407	Rv1223	Rv1562c	Rv1329c	Rv1273c	Rv1318c	Rv1782
Rv1408	Rv1224	Rv1563c	Rv1330c	Rv1274	Rv1319c	Rv1783
Rv1409	Rv1225c	Rv1564c	Rv1331	Rv1275	Rv1320c	Rv1784
Rv1411c	Rv1226c	Rv1565c	Rv1332	Rv1276c	Rv1321	Rv1785c
Rv1412	Rv1227c	Rv1569	Rv1333	Rv1277	Rv1323	Rv1786
Rv1413	Rv1229c	Rv1570	Rv1336	Rv1278	Rv1324	Rv1787
Rv1414	Rv1230c	Rv1571	Rv1339	Rv1279	Rv1326c	Rv1789
Rv1415	Rv1231c	Rv1589	Rv1342c	Rv1280c	Rv1327c	Rv1790
Rv1416	Rv1232c	Rv1592c	Rv1345	Rv1281c	Rv1328	Rv1794
Rv1418	Rv1234	Rv1593c	Rv1346	Rv1282c	Rv1329c	Rv1795
Rv1420	Rv1235	Rv1594	Rv1348	Rv1283c	Rv1330c	Rv1796
Rv1421	Rv1236	Rv1595	Rv1349	Rv1284	Rv1331	Rv1797
Rv1422	Rv1238	Rv1598c	Rv1350	Rv1285	Rv1332	Rv1798
Rv1423	Rv1239c	Rv1600	Rv1351	Rv1286	Rv1333	Rv1806

Rv1424c	Rv1240	Rv1602	Rv1353c	Rv1287	Rv1334	Rv1809
Rv1425	Rv1241	Rv1603	Rv1354c	Rv1288	Rv1335	Rv1810
Rv1426c	Rv1242	Rv1604	Rv1355c	Rv1289	Rv1336	Rv1811
Rv1427c	Rv1244	Rv1605	Rv1356c	Rv1290.1	Rv1337	Rv1812c
Rv1428c	Rv1245c	Rv1608c	Rv1357c	Rv1290c	Rv1338	Rv1814
Rv1429	Rv1246c	Rv1609	Rv1358	Rv1291c	Rv1343c	Rv1815
Rv1430	Rv1247c	Rv1611	Rv1359	Rv1292	Rv1344	Rv1816
Rv1431	Rv1248c	Rv1612	Rv1360	Rv1293	Rv1345	Rv1817
Rv1432	Rv1249c	Rv1613	Rv1361c	Rv1294	Rv1346	Rv1819c
Rv1433	Rv1250	Rv1615	Rv1362c	Rv1295	Rv1347c	Rv1820
Rv1436	Rv1251c	Rv1617	Rv1363c	Rv1296	Rv1348	Rv1821
Rv1437	Rv1252c	Rv1618	Rv1364c	Rv1297	Rv1349	Rv1822
Rv1438	Rv1253	Rv1619	Rv1366	Rv1298	Rv1350	Rv1823
Rv1439c	Rv1254	Rv1621c	Rv1367c	Rv1299	Rv1351	Rv1825
Rv1442	Rv1255c	Rv1622c	Rv1368	Rv1300	Rv1352	Rv1828
Rv1443c	Rv1256c	Rv1624c	Rv1369c	Rv1301	Rv1353c	Rv1829
Rv1444c	Rv1257c	Rv1625c	Rv1370c	Rv1302	Rv1354c	Rv1830
Rv1445c	Rv1259	Rv1626	Rv1371	Rv1304	Rv1355c	Rv1832
Rv1447c	Rv1260	Rv1627c	Rv1372	Rv1306	Rv1356c	Rv1834
Rv1448c	Rv1261c	Rv1628c	Rv1373	Rv1307	Rv1357c	Rv1836c
Rv1449c	Rv1262c	Rv1629	Rv1374c	Rv1308	Rv1358	Rv1837c
Rv1453	Rv1263	Rv1630	Rv1375	Rv1309	Rv1360	Rv1841c
Rv1454c	Rv1264	Rv1631	Rv1376	Rv1310	Rv1362c	Rv1842c
Rv1455	Rv1265	Rv1633	Rv1377c	Rv1312	Rv1364c	Rv1843c
Rv1456c	Rv1266c	Rv1635c	Rv1378c	Rv1315	Rv1365c	Rv1844c
Rv1457c	Rv1267c	Rv1636	Rv1379	Rv1316c	Rv1366	Rv1845c
Rv1458c	Rv1268c	Rv1638	Rv1380	Rv1317c	Rv1367c	Rv1846c
Rv1459c	Rv1269c	Rv1638.1	Rv1381	Rv1318c	Rv1368	Rv1854c
Rv1460	Rv1270c	Rv1640c	Rv1382	Rv1319c	Rv1369c	Rv1855c
Rv1461	Rv1271c	Rv1641	Rv1383	Rv1320c	Rv1371	Rv1856c
Rv1462	Rv1272c	Rv1645c	Rv1384	Rv1321	Rv1372	Rv1857
Rv1463	Rv1273c	Rv1647	Rv1386	Rv1322.1	Rv1373	Rv1858
Rv1464	Rv1274	Rv1650	Rv1388	Rv1323	Rv1374c	Rv1859
Rv1465	Rv1275	Rv1653	Rv1389	Rv1324	Rv1375	Rv1860
Rv1467c	Rv1276c	Rv1655	Rv1391	Rv1325c	Rv1376	Rv1863c
Rv1469	Rv1277	Rv1656	Rv1392	Rv1326c	Rv1378c	Rv1865c
Rv1471	Rv1278	Rv1657	Rv1393c	Rv1327c	Rv1379	Rv1866
Rv1472	Rv1279	Rv1658	Rv1394c	Rv1328	Rv1380	Rv1867
Rv1473	Rv1280c	Rv1659	Rv1395	Rv1329c	Rv1381	Rv1868
Rv1474c	Rv1281c	Rv1660	Rv1396c	Rv1330c	Rv1382	Rv1869c
Rv1475c	Rv1282c	Rv1661	Rv1398c	Rv1331	Rv1383	Rv1870c
Rv1476	Rv1284	Rv1662	Rv1399c	Rv1332	Rv1384	Rv1871c
Rv1477	Rv1285	Rv1663	Rv1400c	Rv1333	Rv1385	Rv1872c
Rv1479	Rv1286	Rv1664	Rv1402	Rv1334	Rv1387	Rv1873
Rv1480	Rv1287	Rv1666c	Rv1403c	Rv1336	Rv1388	Rv1876
Rv1481	Rv1288	Rv1667c	Rv1404	Rv1337	Rv1389	Rv1877
Rv1482c	Rv1289	Rv1668c	Rv1406	Rv1338	Rv1391	Rv1878
Rv1483	Rv1290.1	Rv1671	Rv1407	Rv1340	Rv1392	Rv1879
Rv1484	Rv1290c	Rv1673c	Rv1408	Rv1342c	Rv1393c	Rv1880c
Rv1485	Rv1292	Rv1674c	Rv1409	Rv1343c	Rv1394c	Rv1882c
Rv1487	Rv1293	Rv1675c	Rv1410c	Rv1345	Rv1395	Rv1884c

Rv1488	Rv1294	Rv1676	Rv1411c	Rv1346	Rv1396c	Rv1885c
Rv1490	Rv1295	Rv1677	Rv1412	Rv1347c	Rv1397c	Rv1886c
Rv1491c	Rv1296	Rv1679	Rv1413	Rv1348	Rv1398c	Rv1887
Rv1493	Rv1297	Rv1680	Rv1414	Rv1349	Rv1399c	Rv1888c
Rv1494	Rv1298	Rv1681	Rv1415	Rv1350	Rv1400c	Rv1890c
Rv1495	Rv1299	Rv1682	Rv1416	Rv1351	Rv1402	Rv1892
Rv1496	Rv1300	Rv1683	Rv1417	Rv1352	Rv1403c	Rv1894c
Rv1497	Rv1301	Rv1685c	Rv1418	Rv1353c	Rv1404	Rv1895
Rv1498c	Rv1302	Rv1689	Rv1420	Rv1354c	Rv1405c	Rv1896c
Rv1499	Rv1303	Rv1692	Rv1421	Rv1355c	Rv1406	Rv1897c
Rv1500	Rv1306	Rv1694	Rv1422	Rv1356c	Rv1407	Rv1900c
Rv1504c	Rv1307	Rv1695	Rv1423	Rv1357c	Rv1408	Rv1901
Rv1506c	Rv1308	Rv1696	Rv1424c	Rv1358	Rv1409	Rv1902c
Rv1507c	Rv1309	Rv1697	Rv1425	Rv1359	Rv1411c	Rv1905c
Rv1507.1	Rv1310	Rv1699	Rv1426c	Rv1360	Rv1412	Rv1908c
Rv1508c	Rv1311	Rv1700	Rv1427c	Rv1362c	Rv1413	Rv1909c
Rv1508.1	Rv1312	Rv1701	Rv1428c	Rv1363c	Rv1415	Rv1910c
Rv1509	Rv1313c	Rv1706.1	Rv1429	Rv1364c	Rv1416	Rv1911c
Rv1511	Rv1314c	Rv1706c	Rv1430	Rv1366	Rv1417	Rv1913
Rv1512	Rv1315	Rv1710	Rv1431	Rv1367c	Rv1418	Rv1915
Rv1513	Rv1316c	Rv1711	Rv1432	Rv1368	Rv1420	Rv1916
Rv1514c	Rv1317c	Rv1712	Rv1433	Rv1369c	Rv1421	Rv1919c
Rv1515c	Rv1318c	Rv1713	Rv1435c	Rv1371	Rv1422	Rv1920
Rv1516c	Rv1319c	Rv1715	Rv1436	Rv1372	Rv1423	Rv1925
Rv1517	Rv1320c	Rv1716	Rv1437	Rv1373	Rv1424c	Rv1928c
Rv1521	Rv1321	Rv1718	Rv1438	Rv1374c	Rv1425	Rv1929c
Rv1522c	Rv1322	Rv1719	Rv1439c	Rv1375	Rv1426c	Rv1930c
Rv1523	Rv1322.1	Rv1721c	Rv1442	Rv1376	Rv1427c	Rv1931c
Rv1524	Rv1323	Rv1722	Rv1443c	Rv1377c	Rv1428c	Rv1935c
Rv1525	Rv1324	Rv1723	Rv1444c	Rv1378c	Rv1429	Rv1960c
Rv1526c	Rv1325c	Rv1724c	Rv1445c	Rv1379	Rv1431	Rv1963c
Rv1528c	Rv1326c	Rv1725c	Rv1446c	Rv1380	Rv1432	Rv1965
Rv1529	Rv1327c	Rv1726	Rv1447c	Rv1381	Rv1433	Rv1966
Rv1530	Rv1328	Rv1728c	Rv1448c	Rv1382	Rv1435c	Rv1967
Rv1531	Rv1329c	Rv1729c	Rv1449c	Rv1383	Rv1436	Rv1968
Rv1532c	Rv1330c	Rv1730c	Rv1450c	Rv1384	Rv1437	Rv1969
Rv1533	Rv1331	Rv1731	Rv1453	Rv1385	Rv1438	Rv1973
Rv1534	Rv1332	Rv1733c	Rv1454c	Rv1386	Rv1439c	Rv1974
Rv1536	Rv1333	Rv1736c	Rv1455	Rv1387	Rv1440	Rv1976c
Rv1538c	Rv1334	Rv1738	Rv1456c	Rv1388	Rv1441c	Rv1978
Rv1540	Rv1335	Rv1739c	Rv1457c	Rv1389	Rv1442	Rv1980c
Rv1541c	Rv1336	Rv1742	Rv1458c	Rv1391	Rv1443c	Rv1981c
Rv1542c	Rv1337	Rv1743	Rv1459c	Rv1392	Rv1444c	Rv1998c
Rv1543	Rv1338	Rv1744c	Rv1460	Rv1393c	Rv1445c	Rv2000
Rv1544	Rv1339	Rv1745c	Rv1461	Rv1394c	Rv1446c	Rv2002
Rv1546	Rv1340	Rv1746	Rv1462	Rv1395	Rv1447c	Rv2005c
Rv1547	Rv1341	Rv1747	Rv1464	Rv1398c	Rv1448c	Rv2007c
Rv1550	Rv1344	Rv1748	Rv1465	Rv1400c	Rv1449c	Rv2014
Rv1551	Rv1345	Rv1750c	Rv1466	Rv1401	Rv1450c	Rv2015c
Rv1552	Rv1346	Rv1751	Rv1467c	Rv1402	Rv1451	Rv2017
Rv1555	Rv1347c	Rv1752	Rv1468c	Rv1403c	Rv1452c	Rv2025c

Rv1556	Rv1348	Rv1754c	Rv1469	Rv1404	Rv1453	Rv2026c
Rv1557	Rv1349	Rv1757c	Rv1470	Rv1405c	Rv1454c	Rv2033c
Rv1558	Rv1350	Rv1760	Rv1471	Rv1406	Rv1455	Rv2034
Rv1559	Rv1351	Rv1762c	Rv1472	Rv1407	Rv1456c	Rv2036
Rv1562c	Rv1352	Rv1763	Rv1473	Rv1408	Rv1458c	Rv2037c
Rv1563c	Rv1353c	Rv1765c	Rv1473.1	Rv1409	Rv1460	Rv2038c
Rv1564c	Rv1354c	Rv1767	Rv1474c	Rv1411c	Rv1461	Rv2039c
Rv1565c	Rv1355c	Rv1769	Rv1475c	Rv1412	Rv1462	Rv2040c
Rv1566c	Rv1356c	Rv1770	Rv1476	Rv1414	Rv1463	Rv2041c
Rv1568	Rv1357c	Rv1771	Rv1477	Rv1415	Rv1464	Rv2042c
Rv1570	Rv1358	Rv1772	Rv1478	Rv1416	Rv1466	Rv2045c
Rv1571	Rv1359	Rv1773c	Rv1479	Rv1417	Rv1467c	Rv2046
Rv1588c	Rv1360	Rv1775	Rv1480	Rv1418	Rv1469	Rv2047c
Rv1591	Rv1361c	Rv1776c	Rv1481	Rv1420	Rv1470	Rv2048c
Rv1592c	Rv1362c	Rv1777	Rv1482c	Rv1421	Rv1471	Rv2052c
Rv1593c	Rv1363c	Rv1778c	Rv1483	Rv1422	Rv1472	Rv2053c
Rv1594	Rv1364c	Rv1779c	Rv1484	Rv1423	Rv1473	Rv2054
Rv1595	Rv1365c	Rv1780	Rv1485	Rv1424c	Rv1473.1	Rv2058c
Rv1597	Rv1366	Rv1781c	Rv1486c	Rv1425	Rv1474c	Rv2059
Rv1598c	Rv1367c	Rv1782	Rv1487	Rv1426c	Rv1475c	Rv2062c
Rv1601	Rv1368	Rv1784	Rv1488	Rv1427c	Rv1476	Rv2065
Rv1602	Rv1369c	Rv1785c	Rv1489.1	Rv1428c	Rv1477	Rv2066
Rv1603	Rv1370c	Rv1790	Rv1490	Rv1429	Rv1478	Rv2067c
Rv1604	Rv1371	Rv1796	Rv1491c	Rv1430	Rv1479	Rv2069
Rv1606	Rv1372	Rv1797	Rv1492	Rv1431	Rv1480	Rv2070c
Rv1608c	Rv1373	Rv1798	Rv1493	Rv1432	Rv1481	Rv2072c
Rv1609	Rv1374c	Rv1800	Rv1495	Rv1433	Rv1482c	Rv2073c
Rv1610	Rv1375	Rv1802	Rv1496	Rv1434	Rv1483	Rv2074
Rv1612	Rv1376	Rv1803c	Rv1497	Rv1436	Rv1484	Rv2077c
Rv1613	Rv1377c	Rv1805c	Rv1498c	Rv1437	Rv1486c	Rv2078
Rv1616	Rv1378c	Rv1808	Rv1499	Rv1438	Rv1487	Rv2079
Rv1617	Rv1379	Rv1809	Rv1500	Rv1439c	Rv1488	Rv2083
Rv1618	Rv1380	Rv1810	Rv1501	Rv1440	Rv1489.1	Rv2089c
Rv1619	Rv1381	Rv1811	Rv1502	Rv1442	Rv1490	Rv2090
Rv1620c	Rv1382	Rv1812c	Rv1503c	Rv1443c	Rv1492	Rv2094c
Rv1621c	Rv1383	Rv1814	Rv1504c	Rv1444c	Rv1493	Rv2095c
Rv1622c	Rv1384	Rv1815	Rv1505c	Rv1445c	Rv1494	Rv2096c
Rv1623c	Rv1385	Rv1816	Rv1507.1	Rv1446c	Rv1495	Rv2097c
Rv1625c	Rv1386	Rv1817	Rv1507c	Rv1447c	Rv1496	Rv2110c
Rv1626	Rv1388	Rv1819c	Rv1508c	Rv1448c	Rv1497	Rv2114
Rv1627c	Rv1389	Rv1820	Rv1509	Rv1449c	Rv1498c	Rv2115c
Rv1629	Rv1390	Rv1821	Rv1511	Rv1450c	Rv1499	Rv2117
Rv1630	Rv1391	Rv1824	Rv1512	Rv1451	Rv1500	Rv2118c
Rv1631	Rv1392	Rv1825	Rv1513	Rv1452c	Rv1501	Rv2119
Rv1635c	Rv1393c	Rv1827	Rv1514c	Rv1453	Rv1502	Rv2121c
Rv1636	Rv1394c	Rv1828	Rv1515c	Rv1454c	Rv1503c	Rv2122c
Rv1637c	Rv1395	Rv1830	Rv1516c	Rv1455	Rv1505c	Rv2129c
Rv1638.1	Rv1397c	Rv1832	Rv1518	Rv1456c	Rv1517	Rv2130c
Rv1641	Rv1399c	Rv1833c	Rv1520	Rv1457c	Rv1518	Rv2131c
Rv1644	Rv1400c	Rv1834	Rv1521	Rv1458c	Rv1519	Rv2133c
Rv1645c	Rv1401	Rv1835c	Rv1522c	Rv1459c	Rv1520	Rv2134c

Rv1647	Rv1402	Rv1837c	Rv1523	Rv1460	Rv1521	Rv2135c
Rv1649	Rv1403c	Rv1839c	Rv1524	Rv1461	Rv1522c	Rv2136c
Rv1652	Rv1404	Rv1841c	Rv1525	Rv1462	Rv1523	Rv2137c
Rv1653	Rv1405c	Rv1842c	Rv1526c	Rv1463	Rv1524	Rv2138
Rv1654	Rv1406	Rv1843c	Rv1527c	Rv1464	Rv1525	Rv2139
Rv1655	Rv1407	Rv1844c	Rv1528c	Rv1465	Rv1526c	Rv2141c
Rv1656	Rv1409	Rv1845c	Rv1529	Rv1466	Rv1527c	Rv2143
Rv1658	Rv1410c	Rv1846c	Rv1530	Rv1467c	Rv1528c	Rv2144c
Rv1659	Rv1411c	Rv1847	Rv1531	Rv1469	Rv1529	Rv2145c
Rv1660	Rv1412	Rv1848	Rv1532c	Rv1470	Rv1530	Rv2146c
Rv1664	Rv1413	Rv1849	Rv1534	Rv1472	Rv1531	Rv2147c
Rv1665	Rv1414	Rv1850	Rv1535	Rv1473	Rv1532c	Rv2148c
Rv1666c	Rv1415	Rv1851	Rv1536	Rv1473.1	Rv1533	Rv2149c
Rv1668c	Rv1417	Rv1852	Rv1537	Rv1474c	Rv1534	Rv2150c
Rv1670	Rv1418	Rv1854c	Rv1538c	Rv1475c	Rv1535	Rv2151c
Rv1672c	Rv1420	Rv1855c	Rv1541c	Rv1477	Rv1536	Rv2152c
Rv1673c	Rv1421	Rv1857	Rv1542c	Rv1478	Rv1537	Rv2153c
Rv1675c	Rv1422	Rv1859	Rv1543	Rv1479	Rv1538c	Rv2154c
Rv1676	Rv1423	Rv1862	Rv1544	Rv1480	Rv1540	Rv2155c
Rv1677	Rv1424c	Rv1863c	Rv1545	Rv1481	Rv1542c	Rv2156c
Rv1678	Rv1425	Rv1864c	Rv1546	Rv1482c	Rv1543	Rv2157c
Rv1679	Rv1426c	Rv1865c	Rv1547	Rv1483	Rv1544	Rv2158c
Rv1680	Rv1427c	Rv1867	Rv1549	Rv1484	Rv1547	Rv2163c
Rv1681	Rv1428c	Rv1868	Rv1550	Rv1485	Rv1549	Rv2164c
Rv1682	Rv1429	Rv1870c	Rv1551	Rv1486c	Rv1551	Rv2165c
Rv1683	Rv1431	Rv1871c	Rv1552	Rv1487	Rv1552	Rv2166c
Rv1685c	Rv1432	Rv1872c	Rv1553	Rv1488	Rv1553	Rv2169c
Rv1686c	Rv1433	Rv1875	Rv1556	Rv1490	Rv1556	Rv2170
Rv1687c	Rv1435c	Rv1876	Rv1557	Rv1491c	Rv1557	Rv2171
Rv1688	Rv1436	Rv1877	Rv1558	Rv1492	Rv1558	Rv2172c
Rv1689	Rv1437	Rv1878	Rv1559	Rv1493	Rv1559	Rv2173
Rv1690	Rv1438	Rv1879	Rv1561	Rv1494	Rv1560	Rv2175c
Rv1691	Rv1439c	Rv1880c	Rv1562c	Rv1495	Rv1562c	Rv2176
Rv1692	Rv1440	Rv1881c	Rv1563c	Rv1496	Rv1563c	Rv2178c
Rv1694	Rv1441c	Rv1882c	Rv1564c	Rv1497	Rv1564c	Rv2179c
Rv1695	Rv1442	Rv1883c	Rv1565c	Rv1498c	Rv1565c	Rv2180c
Rv1696	Rv1443c	Rv1884c	Rv1566c	Rv1500	Rv1566c	Rv2181
Rv1697	Rv1444c	Rv1885c	Rv1568	Rv1501	Rv1567c	Rv2182c
Rv1698	Rv1446c	Rv1887	Rv1569	Rv1502	Rv1569	Rv2184c
Rv1699	Rv1447c	Rv1889c	Rv1570	Rv1503c	Rv1570	Rv2185c
Rv1700	Rv1448c	Rv1890c	Rv1571	Rv1505c	Rv1571	Rv2186c
Rv1701	Rv1449c	Rv1892	Rv1574	Rv1517	Rv1587c	Rv2187
Rv1702c	Rv1450c	Rv1893	Rv1575	Rv1518	Rv1589	Rv2188c
Rv1703c	Rv1453	Rv1894c	Rv1576c	Rv1520	Rv1590	Rv2189c
Rv1704c	Rv1454c	Rv1895	Rv1577c	Rv1521	Rv1591	Rv2190c
Rv1705c	Rv1455	Rv1896c	Rv1578c	Rv1522c	Rv1592c	Rv2191
Rv1706c	Rv1456c	Rv1898	Rv1580c	Rv1523	Rv1593c	Rv2192c
Rv1707	Rv1457c	Rv1899c	Rv1581c	Rv1524	Rv1594	Rv2194
Rv1708	Rv1458c	Rv1900c	Rv1582c	Rv1525	Rv1595	Rv2195
Rv1710	Rv1459c	Rv1901	Rv1583c	Rv1526c	Rv1596	Rv2196
Rv1711	Rv1460	Rv1904	Rv1584c	Rv1527c	Rv1597	Rv2197c

Rv1712	Rv1461	Rv1907c	Rv1585c	Rv1528c	Rv1598c	Rv2198c
Rv1713	Rv1462	Rv1908c	Rv1586c	Rv1529	Rv1599	Rv2200c
Rv1714	Rv1463	Rv1911c	Rv1587c	Rv1530	Rv1600	Rv2201
Rv1715	Rv1464	Rv1912c	Rv1588c	Rv1531	Rv1601	Rv2202c
Rv1718	Rv1466	Rv1914c	Rv1589	Rv1532c	Rv1603	Rv2203
Rv1719	Rv1467c	Rv1915	Rv1590	Rv1533	Rv1605	Rv2204c
Rv1720c	Rv1469	Rv1916	Rv1592c	Rv1534	Rv1606	Rv2205c
Rv1723	Rv1472	Rv1920	Rv1593c	Rv1535	Rv1608c	Rv2206
Rv1725c	Rv1473	Rv1922	Rv1594	Rv1536	Rv1609	Rv2207
Rv1726	Rv1474c	Rv1923	Rv1595	Rv1537	Rv1610	Rv2208
Rv1727	Rv1475c	Rv1924c	Rv1598c	Rv1538c	Rv1611	Rv2210c
Rv1729c	Rv1477	Rv1925	Rv1599	Rv1539	Rv1612	Rv2211c
Rv1731	Rv1478	Rv1926c	Rv1600	Rv1540	Rv1613	Rv2213
Rv1732c	Rv1479	Rv1928c	Rv1601	Rv1542c	Rv1614	Rv2214c
Rv1733c	Rv1480	Rv1930c	Rv1602	Rv1543	Rv1617	Rv2215
Rv1734c	Rv1481	Rv1931c	Rv1604	Rv1544	Rv1618	Rv2216
Rv1736c	Rv1482c	Rv1933c	Rv1605	Rv1546	Rv1619	Rv2217
Rv1737c	Rv1483	Rv1934c	Rv1608c	Rv1547	Rv1620c	Rv2218
Rv1739c	Rv1484	Rv1936	Rv1609	Rv1549	Rv1621c	Rv2219
Rv1741	Rv1485	Rv1937	Rv1610	Rv1551	Rv1622c	Rv2219.1
Rv1742	Rv1486c	Rv1938	Rv1611	Rv1552	Rv1623c	Rv2220
Rv1743	Rv1487	Rv1940	Rv1612	Rv1553	Rv1624c	Rv2221c
Rv1744c	Rv1488	Rv1943c	Rv1613	Rv1555	Rv1625c	Rv2222c
Rv1745c	Rv1489	Rv1945	Rv1614	Rv1556	Rv1626	Rv2223c
Rv1746	Rv1489.1	Rv1947	Rv1615	Rv1557	Rv1627c	Rv2224c
Rv1747	Rv1490	Rv1949c	Rv1616	Rv1558	Rv1628c	Rv2225
Rv1748	Rv1491c	Rv1952	Rv1617	Rv1559	Rv1629	Rv2226
Rv1749c	Rv1492	Rv1955	Rv1618	Rv1560	Rv1630	Rv2227
Rv1750c	Rv1493	Rv1957	Rv1619	Rv1561	Rv1631	Rv2228c
Rv1751	Rv1495	Rv1958c	Rv1620c	Rv1562c	Rv1632c	Rv2229c
Rv1752	Rv1496	Rv1959c	Rv1621c	Rv1564c	Rv1633	Rv2230c
Rv1755c	Rv1497	Rv1960c	Rv1622c	Rv1565c	Rv1634	Rv2231c
Rv1761c	Rv1498c	Rv1962c	Rv1625c	Rv1566c	Rv1635c	Rv2232
Rv1762c	Rv1499	Rv1963c	Rv1626	Rv1567c	Rv1636	Rv2234
Rv2015c	Rv1500	Rv1964	Rv1627c	Rv1568	Rv1637c	Rv2235
Rv1766	Rv1501	Rv1966	Rv1628c	Rv1569	Rv1638	Rv2236c
Rv1767	Rv1502	Rv1967	Rv1629	Rv1570	Rv1638.1	Rv2241
Rv1770	Rv1503c	Rv1968	Rv1630	Rv1571	Rv1640c	Rv2242
Rv1771	Rv1504c	Rv1969	Rv1631	Rv1573	Rv1641	Rv2243
Rv1772	Rv1507.1	Rv1970	Rv1633	Rv1575	Rv1642	Rv2244
Rv1773c	Rv1507c	Rv1976c	Rv1635c	Rv1576c	Rv1643	Rv2245
Rv1774	Rv1508.1	Rv1977	Rv1636	Rv1577c	Rv1644	Rv2246
Rv1775	Rv1508c	Rv1979c	Rv1637c	Rv1578c	Rv1645c	Rv2247
Rv1776c	Rv1509	Rv1980c	Rv1638	Rv1580c	Rv1647	Rv2249c
Rv1778c	Rv1510	Rv1981c	Rv1638.1	Rv1581c	Rv1648	Rv2250c
Rv1779c	Rv1511	Rv1985c	Rv1639c	Rv1582c	Rv1649	Rv2251
Rv1780	Rv1512	Rv1987	Rv1640c	Rv1583c	Rv1650	Rv2252
Rv1781c	Rv1513	Rv1990c	Rv1641	Rv1584c	Rv1652	Rv2256c
Rv1782	Rv1514c	Rv1992c	Rv1642	Rv1586c	Rv1653	Rv2257c
Rv1784	Rv1515c	Rv1993c	Rv1643	Rv1587c	Rv1654	Rv2260
Rv1785c	Rv1516c	Rv1994c	Rv1644	Rv1589	Rv1655	Rv2263

Rv1788	Rv1517	Rv1995	Rv1645c	Rv1590	Rv1656	Rv2264c
Rv1789	Rv1518	Rv1996	Rv1647	Rv1591	Rv1657	Rv2266
Rv1790	Rv1520	Rv1997	Rv1649	Rv1592c	Rv1658	Rv2282c
Rv1793	Rv1521	Rv1998c	Rv1650	Rv1593c	Rv1659	Rv2284
Rv1794	Rv1522c	Rv1999c	Rv1652	Rv1594	Rv1660	Rv2287
Rv1795	Rv1523	Rv2000	Rv1653	Rv1595	Rv1661	Rv2290
Rv1797	Rv1524	Rv2002	Rv1654	Rv1596	Rv1662	Rv2291
Rv1798	Rv1525	Rv2003c	Rv1655	Rv1597	Rv1663	Rv2294
Rv1800	Rv1526c	Rv2004c	Rv1656	Rv1598c	Rv1664	Rv2296
Rv1802	Rv1527c	Rv2005c	Rv1657	Rv1599	Rv1665	Rv2298
Rv1804c	Rv1528c	Rv2006	Rv1658	Rv1600	Rv1666c	Rv2299c
Rv1807	Rv1529	Rv2008c	Rv1659	Rv1601	Rv1667c	Rv2301
Rv1808	Rv1530	Rv2012	Rv1660	Rv1603	Rv1668c	Rv2313c
Rv1810	Rv1531	Rv2013	Rv1661	Rv1605	Rv1670	Rv2314c
Rv1811	Rv1532c	Rv2016	Rv1662	Rv1606	Rv1671	Rv2315c
Rv1812c	Rv1533	Rv2017	Rv1663	Rv1608c	Rv1673c	Rv2316
Rv1813c	Rv1534	Rv2018	Rv1664	Rv1609	Rv1674c	Rv2317
Rv1816	Rv1535	Rv2020c	Rv1665	Rv1610	Rv1675c	Rv2318
Rv1817	Rv1536	Rv2021c	Rv1666c	Rv1611	Rv1676	Rv2320c
Rv1819c	Rv1537	Rv2022c	Rv1667c	Rv1612	Rv1677	Rv2321c
Rv1820	Rv1538c	Rv2023c	Rv1668c	Rv1613	Rv1678	Rv2322c
Rv1821	Rv1539	Rv2024c	Rv1669	Rv1614	Rv1679	Rv2323c
Rv1822	Rv1540	Rv2027c	Rv1672c	Rv1615	Rv1680	Rv2324
Rv1823	Rv1541c	Rv2029c	Rv1673c	Rv1617	Rv1681	Rv2325c
Rv1825	Rv1543	Rv2030c	Rv1674c	Rv1618	Rv1682	Rv2326c
Rv1826	Rv1544	Rv2031c	Rv1675c	Rv1619	Rv1683	Rv2327
Rv1827	Rv1546	Rv2032	Rv1676	Rv1620c	Rv1684	Rv2330c
Rv1828	Rv1547	Rv2033c	Rv1678	Rv1621c	Rv1685c	Rv2332
Rv1829	Rv1549	Rv2034	Rv1679	Rv1622c	Rv1686c	Rv2334
Rv1830	Rv1550	Rv2038c	Rv1680	Rv1623c	Rv1687c	Rv2335
Rv1832	Rv1551	Rv2039c	Rv1681	Rv1624c	Rv1688	Rv2343c
Rv1833c	Rv1552	Rv2041c	Rv1682	Rv1625c	Rv1689	Rv2344c
Rv1834	Rv1553	Rv2045c	Rv1683	Rv1626	Rv1691	Rv2345
Rv1835c	Rv1554	Rv2047c	Rv1685c	Rv1627c	Rv1692	Rv2357c
Rv1836c	Rv1556	Rv2048c	Rv1687c	Rv1629	Rv1694	Rv2358
Rv1838c	Rv1557	Rv2050	Rv1688	Rv1630	Rv1695	Rv2359
Rv1841c	Rv1558	Rv2051c	Rv1689	Rv1631	Rv1696	Rv2360c
Rv1842c	Rv1559	Rv2052c	Rv1690	Rv1632c	Rv1697	Rv2362c
Rv1844c	Rv1560	Rv2053c	Rv1691	Rv1633	Rv1698	Rv2363
Rv1845c	Rv1561	Rv2054	Rv1692	Rv1635c	Rv1699	Rv2364c
Rv1846c	Rv1562c	Rv2056c	Rv1694	Rv1636	Rv1700	Rv2366c
Rv1848	Rv1563c	Rv2057c	Rv1695	Rv1638	Rv1701	Rv2368c
Rv1850	Rv1564c	Rv2058c	Rv1696	Rv1638.1	Rv1702c	Rv2372c
Rv1851	Rv1565c	Rv2061c	Rv1697	Rv1639c	Rv1703c	Rv2373c
Rv1852	Rv1566c	Rv2062c	Rv1698	Rv1640c	Rv1704c	Rv2374c
Rv1854c	Rv1569	Rv2064	Rv1699	Rv1641	Rv1706c	Rv2378c
Rv1855c	Rv1570	Rv2065	Rv1700	Rv1642	Rv1707	Rv2379c
Rv1856c	Rv1571	Rv2066	Rv1701	Rv1643	Rv1708	Rv2380c
Rv1857	Rv1573	Rv2068c	Rv1702c	Rv1645c	Rv1710	Rv2381c
Rv1858	Rv1574	Rv2069	Rv1703c	Rv1646	Rv1711	Rv2382c
Rv1859	Rv1575	Rv2070c	Rv1704c	Rv1647	Rv1712	Rv2383c

Rv1860	Rv1576c	Rv2071c	Rv1705c	Rv1649	Rv1713	Rv2384
Rv1862	Rv1577c	Rv2072c	Rv1706c	Rv1650	Rv1714	Rv2385
Rv1864c	Rv1578c	Rv2073c	Rv1707	Rv1652	Rv1716	Rv2386c
Rv1865c	Rv1580c	Rv2074	Rv1708	Rv1653	Rv1717	Rv2387
Rv1867	Rv1581c	Rv2075c	Rv1710	Rv1654	Rv1718	Rv2388c
Rv1868	Rv1582c	Rv2079	Rv1711	Rv1655	Rv1719	Rv2390c
Rv1869c	Rv1583c	Rv2083	Rv1712	Rv1656	Rv1720c	Rv2391
Rv1871c	Rv1584c	Rv2084	Rv1713	Rv1657	Rv1721c	Rv2392
Rv1872c	Rv1585c	Rv2085	Rv1714	Rv1658	Rv1722	Rv2393
Rv1873	Rv1586c	Rv2086	Rv1715	Rv1659	Rv1723	Rv2398c
Rv1875	Rv1587c	Rv2088	Rv1716	Rv1660	Rv1724c	Rv2399c
Rv1877	Rv1588c	Rv2089c	Rv1718	Rv1661	Rv1725c	Rv2400c
Rv1878	Rv1589	Rv2090	Rv1719	Rv1662	Rv1726	Rv2402
Rv1879	Rv1591	Rv2091c	Rv1720c	Rv1663	Rv1727	Rv2403c
Rv1880c	Rv1592c	Rv2092c	Rv1722	Rv1664	Rv1729c	Rv2404c
Rv1881c	Rv1593c	Rv2095c	Rv1723	Rv1665	Rv1730c	Rv2405
Rv1882c	Rv1594	Rv2096c	Rv1725c	Rv1666c	Rv1731	Rv2406c
Rv1883c	Rv1595	Rv2097c	Rv1726	Rv1667c	Rv1732c	Rv2407
Rv1884c	Rv1596	Rv2100	Rv1727	Rv1668c	Rv1733c	Rv2409c
Rv1885c	Rv1597	Rv2101	Rv1729c	Rv1669	Rv1734c	Rv2410c
Rv1886c	Rv1599	Rv2102	Rv1730c	Rv1670	Rv1735c	Rv2412
Rv1887	Rv1600	Rv2103c	Rv1731	Rv1671	Rv1736c	Rv2413c
Rv1888c	Rv1601	Rv2104c	Rv1733c	Rv1672c	Rv1738	Rv2414c
Rv1889c	Rv1602	Rv2105	Rv1734c	Rv1674c	Rv1739c	Rv2415c
Rv1890c	Rv1603	Rv2108	Rv1736c	Rv1675c	Rv1740	Rv2416c
Rv1892	Rv1604	Rv2110c	Rv1737c	Rv1676	Rv1742	Rv2417c
Rv1895	Rv1605	Rv2112c	Rv1738	Rv1677	Rv1743	Rv2418c
Rv1896c	Rv1606	Rv2113	Rv1739c	Rv1679	Rv1744c	Rv2419c
Rv1897c	Rv1608c	Rv2114	Rv1742	Rv1680	Rv1746	Rv2425c
Rv1898	Rv1609	Rv2115c	Rv1743	Rv1681	Rv1747	Rv2426c
Rv1900c	Rv1610	Rv2116	Rv1745c	Rv1682	Rv1748	Rv2427c
Rv1901	Rv1611	Rv2119	Rv1747	Rv1683	Rv1749c	Rv2428
Rv1902c	Rv1612	Rv2121c	Rv1748	Rv1685c	Rv1750c	Rv2429
Rv1903	Rv1613	Rv2122c	Rv1749c	Rv1687c	Rv1751	Rv2434c
Rv1904	Rv1614	Rv2124c	Rv1750c	Rv1688	Rv1752	Rv2435c
Rv1905c	Rv1617	Rv2127	Rv1751	Rv1689	Rv1754c	Rv2436
Rv1906c	Rv1618	Rv2129c	Rv1752	Rv1690	Rv1755c	Rv2438c
Rv1907c	Rv1619	Rv2130c	Rv1754c	Rv1691	Rv1756c	Rv2439c
Rv1908c	Rv1620c	Rv2131c	Rv1755c	Rv1692	Rv1759c	Rv2440c
Rv1909c	Rv1621c	Rv2133c	Rv1756c	Rv1693	Rv1760	Rv2441c
Rv1912c	Rv1623c	Rv2135c	Rv1757c	Rv1694	Rv1762c	Rv2442c
Rv1913	Rv1624c	Rv2138	Rv1758	Rv1695	Rv1764	Rv2444c
Rv1914c	Rv1625c	Rv2140c	Rv1760	Rv1696	Rv1765c	Rv2445c
Rv1915	Rv1626	Rv2141c	Rv1761c	Rv1697	Rv1774	Rv2446c
Rv1916	Rv1627c	Rv2142c	Rv1762c	Rv1698	Rv1775	Rv2447c
Rv1918c	Rv1628c	Rv2143	Rv1763	Rv1699	Rv1776c	Rv2448c
Rv1919c	Rv1629	Rv2145c	Rv1764	Rv1700	Rv1777	Rv2449c
Rv1920	Rv1630	Rv2147c	Rv1765c	Rv1701	Rv1779c	Rv2453c
Rv1921c	Rv1631	Rv2148c	Rv1766	Rv1702c	Rv1780	Rv2454c
Rv1922	Rv1632c	Rv2149c	Rv1767	Rv1703c	Rv1781c	Rv2455c
Rv1923	Rv1633	Rv2150c	Rv1769	Rv1704c	Rv1782	Rv2457c

Rv1924c	Rv1634	Rv2151c	Rv1770	Rv1705c	Rv1784	Rv2458
Rv1925	Rv1635c	Rv2152c	Rv1771	Rv1706.1	Rv1785c	Rv2460c
Rv1926c	Rv1636	Rv2153c	Rv1773c	Rv1706c	Rv1786	Rv2461c
Rv1927	Rv1637c	Rv2154c	Rv1774	Rv1707	Rv1787	Rv2462c
Rv1928c	Rv1638	Rv2155c	Rv1775	Rv1708	Rv1789	Rv2463
Rv1929c	Rv1638.1	Rv2158c	Rv1776c	Rv1709	Rv1790	Rv2464c
Rv1930c	Rv1639c	Rv2159c	Rv1777	Rv1710	Rv1793	Rv2465c
Rv1931c	Rv1640c	Rv2163c	Rv1778c	Rv1711	Rv1794	Rv2466c
Rv1932	Rv1641	Rv2164c	Rv1779c	Rv1712	Rv1795	Rv2467
Rv1934c	Rv1642	Rv2165c	Rv1780	Rv1713	Rv1796	Rv2468c
Rv1935c	Rv1643	Rv2166c	Rv1781c	Rv1714	Rv1797	Rv2469c
Rv1936	Rv1644	Rv2168c	Rv1782	Rv1715	Rv1798	Rv2471
Rv1937	Rv1645c	Rv2170	Rv1783	Rv1716	Rv1800	Rv2474c
Rv1938	Rv1646	Rv2172c	Rv1784	Rv1717	Rv1802	Rv2475c
Rv1940	Rv1647	Rv2173	Rv1785c	Rv1718	Rv1805c	Rv2476c
Rv1941	Rv1649	Rv2175c	Rv1787	Rv1719	Rv1808	Rv2477c
Rv1942c	Rv1650	Rv2176	Rv1790	Rv1720c	Rv1810	Rv2478c
Rv1943c	Rv1652	Rv2178c	Rv1794	Rv1721c	Rv1812c	Rv2483c
Rv1946c	Rv1653	Rv2181	Rv1795	Rv1722	Rv1813c	Rv2484c
Rv1947	Rv1654	Rv2182c	Rv1796	Rv1723	Rv1814	Rv2485c
Rv1948c	Rv1655	Rv2183c	Rv1797	Rv1724c	Rv1816	Rv2495c
Rv1949c	Rv1657	Rv2184c	Rv1798	Rv1725c	Rv1817	Rv2496c
Rv1953	Rv1658	Rv2187	Rv1802	Rv1726	Rv1819c	Rv2497c
Rv1955	Rv1659	Rv2188c	Rv1803c	Rv1727	Rv1820	Rv2498c
Rv1956	Rv1660	Rv2189c	Rv1804c	Rv1728c	Rv1821	Rv2499c
Rv1957	Rv1661	Rv2190c	Rv1805c	Rv1729c	Rv1823	Rv2500c
Rv1959c	Rv1662	Rv2191	Rv1811	Rv1730c	Rv1824	Rv2501c
Rv1960c	Rv1663	Rv2195	Rv1812c	Rv1731	Rv1825	Rv2502c
Rv1961	Rv1664	Rv2196	Rv1813c	Rv1732c	Rv1827	Rv2503c
Rv1962c	Rv1665	Rv2197c	Rv1814	Rv1733c	Rv1828	Rv2505c
Rv1963c	Rv1666c	Rv2200c	Rv1816	Rv1735c	Rv1830	Rv2506
Rv1965	Rv1667c	Rv2201	Rv1817	Rv1736c	Rv1832	Rv2507
Rv1966	Rv1668c	Rv2202c	Rv1819c	Rv1738	Rv1833c	Rv2508c
Rv1967	Rv1669	Rv2205c	Rv1820	Rv1739c	Rv1834	Rv2509
Rv1968	Rv1671	Rv2207	Rv1821	Rv1740	Rv1835c	Rv2510c
Rv1969	Rv1672c	Rv2209	Rv1822	Rv1741	Rv1836c	Rv2511
Rv1970	Rv1673c	Rv2212	Rv1823	Rv1742	Rv1837c	Rv2518c
Rv1972	Rv1674c	Rv2213	Rv1825	Rv1743	Rv1839c	Rv2521
Rv1973	Rv1675c	Rv2214c	Rv1828	Rv1744c	Rv1841c	Rv2522c
Rv1974	Rv1676	Rv2215	Rv1830	Rv1745c	Rv1842c	Rv2524c
Rv1975	Rv1678	Rv2216	Rv1832	Rv1746	Rv1843c	Rv2525c
Rv1976c	Rv1679	Rv2217	Rv1833c	Rv1747	Rv1844c	Rv2531c
Rv1977	Rv1680	Rv2218	Rv1834	Rv1748	Rv1846c	Rv2533c
Rv1978	Rv1681	Rv2219	Rv1835c	Rv1749c	Rv1848	Rv2534c
Rv1980c	Rv1682	Rv2219.1	Rv1836c	Rv1750c	Rv1849	Rv2535c
Rv1985c	Rv1683	Rv2220	Rv1837c	Rv1751	Rv1850	Rv2536
Rv1986	Rv1684	Rv2221c	Rv1839c	Rv1752	Rv1851	Rv2538c
Rv1988	Rv1685c	Rv2222c	Rv1841c	Rv1754c	Rv1852	Rv2539c
Rv1989c	Rv1686c	Rv2224c	Rv1842c	Rv1755c	Rv1853	Rv2540c
Rv1990c	Rv1687c	Rv2225	Rv1843c	Rv1756c	Rv1854c	Rv2552c
Rv1990.1	Rv1688	Rv2226	Rv1844c	Rv1760	Rv1855c	Rv2553c

Rv1991c	Rv1689	Rv2227	Rv1846c	Rv1762c	Rv1856c	Rv2554c
Rv1992c	Rv1690	Rv2228c	Rv1848	Rv1764	Rv1858	Rv2555c
Rv1993c	Rv1691	Rv2229c	Rv1849	Rv1765.1	Rv1859	Rv2556c
Rv1994c	Rv1692	Rv2230c	Rv1850	Rv1765c	Rv1860	Rv2558
Rv1995	Rv1693	Rv2231c	Rv1851	Rv1766	Rv1862	Rv2559c
Rv1996	Rv1694	Rv2234	Rv1852	Rv1767	Rv1864c	Rv2564
Rv1997	Rv1695	Rv2235	Rv1854c	Rv1769	Rv1865c	Rv2567
Rv1998c	Rv1696	Rv2236c	Rv1855c	Rv1770	Rv1866	Rv2568c
Rv1999c	Rv1697	Rv2238c	Rv1856c	Rv1771	Rv1867	Rv2569c
Rv2000	Rv1698	Rv2240c	Rv1857	Rv1773c	Rv1868	Rv2570
Rv2001	Rv1699	Rv2241	Rv1859	Rv1774	Rv1869c	Rv2571c
Rv2002	Rv1700	Rv2242	Rv1862	Rv1775	Rv1870c	Rv2572c
Rv2003c	Rv1701	Rv2244	Rv1863c	Rv1776c	Rv1871c	Rv2573
Rv2004c	Rv1702c	Rv2246	Rv1864c	Rv1777	Rv1872c	Rv2574
Rv2005c	Rv1703c	Rv2247	Rv1865c	Rv1778c	Rv1876	Rv2575
Rv2006	Rv1704c	Rv2248	Rv1866	Rv1779c	Rv1877	Rv2577
Rv2008c	Rv1706c	Rv2249c	Rv1867	Rv1780	Rv1879	Rv2578c
Rv2010	Rv1707	Rv2250c	Rv1868	Rv1781c	Rv1880c	Rv2580c
Rv2011c	Rv1708	Rv2251	Rv1869c	Rv1782	Rv1882c	Rv2581c
Rv2012	Rv1710	Rv2252	Rv1870c	Rv1783	Rv1884c	Rv2582
Rv2013	Rv1711	Rv2253	Rv1871c	Rv1785c	Rv1885c	Rv2583c
Rv2014	Rv1712	Rv2256c	Rv1872c	Rv1787	Rv1887	Rv2585c
Rv2017	Rv1713	Rv2258c	Rv1875	Rv1790	Rv1888.1	Rv2586c
Rv2018	Rv1714	Rv2259	Rv1876	Rv1794	Rv1889c	Rv2587c
Rv2021c	Rv1715	Rv2260	Rv1877	Rv1796	Rv1890c	Rv2588c
Rv2022c	Rv1716	Rv2263	Rv1879	Rv1797	Rv1891	Rv2589
Rv2023c	Rv1717	Rv2265	Rv1880c	Rv1798	Rv1892	Rv2590
Rv2025c	Rv1718	Rv2266	Rv1882c	Rv1800	Rv1894c	Rv2592c
Rv2026c	Rv1719	Rv2268c	Rv1883c	Rv1802	Rv1895	Rv2593c
Rv2027c	Rv1721c	Rv2269c	Rv1884c	Rv1803c	Rv1896c	Rv2594c
Rv2028c	Rv1722	Rv2275	Rv1885c	Rv1804c	Rv1897c	Rv2597
Rv2029c	Rv1723	Rv2276	Rv1888.1	Rv1805c	Rv1898	Rv2601
Rv2030c	Rv1724c	Rv2277c	Rv1888c	Rv1808	Rv1899c	Rv2603c
Rv2032	Rv1725c	Rv2278	Rv1889c	Rv1810	Rv1900c	Rv2604c
Rv2033c	Rv1726	Rv2281	Rv1890c	Rv1811	Rv1901	Rv2605c
Rv2034	Rv1728c	Rv2282c	Rv1891	Rv1812c	Rv1902c	Rv2606c
Rv2035	Rv1729c	Rv2284	Rv1892	Rv1813c	Rv1904	Rv2607
Rv2036	Rv1730c	Rv2285	Rv1893	Rv1814	Rv1905c	Rv2609c
Rv2038c	Rv1731	Rv2286c	Rv1894c	Rv1815	Rv1906c	Rv2610c
Rv2039c	Rv1733c	Rv2287	Rv1895	Rv1816	Rv1907c	Rv2611c
Rv2040c	Rv1735c	Rv2289	Rv1896c	Rv1817	Rv1908c	Rv2612c
Rv2041c	Rv1736c	Rv2290	Rv1898	Rv1819c	Rv1909c	Rv2613c
Rv2042c	Rv1737c	Rv2291	Rv1899c	Rv1820	Rv1910c	Rv2614c
Rv2043c	Rv1738	Rv2294	Rv1900c	Rv1821	Rv1912c	Rv2616
Rv2045c	Rv1739c	Rv2295	Rv1901	Rv1822	Rv1914c	Rv2619c
Rv2046	Rv1741	Rv2296	Rv1903	Rv1823	Rv1915	Rv2620c
Rv2047c	Rv1742	Rv2297	Rv1904	Rv1824	Rv1916	Rv2621c
Rv2050	Rv1743	Rv2298	Rv1906c	Rv1825	Rv1919c	Rv2622
Rv2051c	Rv1744c	Rv2299c	Rv1908c	Rv1826	Rv1920	Rv2627c
Rv2052c	Rv1745c	Rv2300c	Rv1909c	Rv1827	Rv1921c	Rv2629
Rv2054	Rv1746	Rv2302	Rv1910c	Rv1828	Rv1922	Rv2633c

Rv2056c	Rv1747	Rv2303c	Rv1912c	Rv1829	Rv1923	Rv2637
Rv2058c	Rv1748	Rv2305	Rv1913	Rv1830	Rv1924c	Rv2640c
Rv2059	Rv1750c	Rv2306.2	Rv1914c	Rv1831	Rv1925	Rv2641
Rv2061c	Rv1751	Rv2307.2	Rv1915	Rv1832	Rv1926c	Rv2643
Rv2062c	Rv1752	Rv2307c	Rv1916	Rv1833c	Rv1927	Rv2646
Rv2064	Rv1754c	Rv2308	Rv1918c	Rv1834	Rv1928c	Rv2659c
Rv2065	Rv1755c	Rv2309c	Rv1919c	Rv1835c	Rv1929c	Rv2667
Rv2066	Rv1756c	Rv2310	Rv1920	Rv1836c	Rv1930c	Rv2668
Rv2067c	Rv1757c	Rv2311	Rv1922	Rv1837c	Rv1931c	Rv2669
Rv2068c	Rv1759c	Rv2312	Rv1923	Rv1839c	Rv1933c	Rv2670c
Rv2070c	Rv1760	Rv2313c	Rv1924c	Rv1841c	Rv1934c	Rv2671
Rv2071c	Rv1762c	Rv2314c	Rv1925	Rv1842c	Rv1935c	Rv2672
Rv2073c	Rv1763	Rv2315c	Rv1927	Rv1843c	Rv1936	Rv2673
Rv2074	Rv1764	Rv2318	Rv1928c	Rv1844c	Rv1937	Rv2676c
Rv2075c	Rv1765c	Rv2320c	Rv1929c	Rv1845c	Rv1938	Rv2678c
Rv2077c	Rv1766	Rv2321c	Rv1930c	Rv1846c	Rv1940	Rv2680
Rv2080	Rv1767	Rv2324	Rv1931c	Rv1847	Rv1942c	Rv2681
Rv2084	Rv1769	Rv2325c	Rv1932	Rv1849	Rv1943c	Rv2682c
Rv2086	Rv1770	Rv2326c	Rv1933c	Rv1850	Rv1944c	Rv2690c
Rv2088	Rv1771	Rv2327	Rv1934c	Rv1851	Rv1946c	Rv2691
Rv2089c	Rv1772	Rv2328	Rv1935c	Rv1852	Rv1947	Rv2692
Rv2091c	Rv1773c	Rv2329c	Rv1937	Rv1853	Rv1949c	Rv2694c
Rv2092c	Rv1774	Rv2330c	Rv1938	Rv1854c	Rv1952	Rv2696c
Rv2093c	Rv1775	Rv2331	Rv1939	Rv1855c	Rv1953	Rv2697c
Rv2095c	Rv1776c	Rv2331.1	Rv1940	Rv1856c	Rv1954c	Rv2700
Rv2096c	Rv1777	Rv2332	Rv1941	Rv1857	Rv1955	Rv2701c
Rv2100	Rv1778c	Rv2334	Rv1942c	Rv1858	Rv1956	Rv2703
Rv2102	Rv1779c	Rv2335	Rv1943c	Rv1859	Rv1957	Rv2704
Rv2104c	Rv1780	Rv2336	Rv1945	Rv1860	Rv1958c	Rv2705c
Rv2113	Rv1781c	Rv2337c	Rv1947	Rv1861	Rv1960c	Rv2707
Rv2114	Rv1782	Rv2338c	Rv1949c	Rv1862	Rv1961	Rv2708c
Rv2116	Rv1783	Rv2339	Rv1953	Rv1864c	Rv1962c	Rv2709
Rv2117	Rv1784	Rv2340c	Rv1954c	Rv1865c	Rv1963c	Rv2710
Rv2118c	Rv1785c	Rv2341	Rv1955	Rv1866	Rv1988	Rv2711
Rv2119	Rv1786	Rv2343c	Rv1956	Rv1867	Rv1989c	Rv2712c
Rv2121c	Rv1787	Rv2344c	Rv1958c	Rv1868	Rv1990c	Rv2713
Rv2124c	Rv1789	Rv2345	Rv1959c	Rv1869c	Rv1991c	Rv2715
Rv2125	Rv1790	Rv2346c	Rv1961	Rv1870c	Rv1992c	Rv2718c
Rv2127	Rv1793	Rv2347c	Rv1963c	Rv1871c	Rv1993c	Rv2719c
Rv2129c	Rv1794	Rv2349c	Rv1964	Rv1872c	Rv1994c	Rv2720
Rv2131c	Rv1795	Rv2350c	Rv1966	Rv1873	Rv1995	Rv2721c
Rv2133c	Rv1796	Rv2351c	Rv1967	Rv1875	Rv1997	Rv2722
Rv2134c	Rv1797	Rv2353c	Rv1968	Rv1877	Rv1998c	Rv2724c
Rv2135c	Rv1798	Rv2354	Rv1969	Rv1878	Rv1999c	Rv2725c
Rv2136c	Rv1800	Rv2356c	Rv1970	Rv1879	Rv2000	Rv2726c
Rv2137c	Rv1802	Rv2357c	Rv1971	Rv1880c	Rv2001	Rv2727c
Rv2138	Rv1805c	Rv2358	Rv1972	Rv1881c	Rv2002	Rv2729c
Rv2139	Rv1808	Rv2360c	Rv1974	Rv1882c	Rv2003c	Rv2731
Rv2140c	Rv1809	Rv2361c	Rv1976c	Rv1884c	Rv2004c	Rv2733c
Rv2142c	Rv1810	Rv2362c	Rv1977	Rv1885c	Rv2005c	Rv2736c
Rv2143	Rv1811	Rv2363	Rv1978	Rv1887	Rv2006	Rv2737.1

Rv2145c	Rv1812c	Rv2365c	Rv1979c	Rv1888c	Rv2008c	Rv2737c
Rv2148c	Rv1813c	Rv2366c	Rv1981c	Rv1889c	Rv2009	Rv2739c
Rv2149c	Rv1816	Rv2368c	Rv1985c	Rv1890c	Rv2010	Rv2740
Rv2150c	Rv1817	Rv2370c	Rv1987	Rv1891	Rv2011c	Rv2743c
Rv2151c	Rv1819c	Rv2371	Rv1988	Rv1893	Rv2012	Rv2744c
Rv2152c	Rv1820	Rv2373c	Rv1989c	Rv1894c	Rv2013	Rv2746c
Rv2154c	Rv1821	Rv2374c	Rv1990.1	Rv1895	Rv2014	Rv2747
Rv2155c	Rv1822	Rv2375	Rv1990c	Rv1896c	Rv2016	Rv2748c
Rv2157c	Rv1823	Rv2379c	Rv1991c	Rv1898	Rv2017	Rv2749
Rv2158c	Rv1824	Rv2380c	Rv1992c	Rv1899c	Rv2018	Rv2750
Rv2159c	Rv1825	Rv2381c	Rv1993c	Rv1900c	Rv2019	Rv2751
Rv2160.1	Rv1827	Rv2382c	Rv1994c	Rv1901	Rv2020c	Rv2752c
Rv2161c	Rv1829	Rv2383c	Rv1995	Rv1902c	Rv2021c	Rv2753c
Rv2163c	Rv1830	Rv2384	Rv1996	Rv1903	Rv2022c	Rv2754c
Rv2164c	Rv1831	Rv2385	Rv1997	Rv1905c	Rv2023c	Rv2756c
Rv2165c	Rv1832	Rv2386c	Rv1998c	Rv1906c	Rv2024c	Rv2764c
Rv2166c	Rv1833c	Rv2387	Rv1999c	Rv1907c	Rv2026c	Rv2765
Rv2169c	Rv1834	Rv2388c	Rv2000	Rv1908c	Rv2027c	Rv2766c
Rv2170	Rv1835c	Rv2389c	Rv2001	Rv1909c	Rv2029c	Rv2769c
Rv2171	Rv1836c	Rv2390c	Rv2002	Rv1910c	Rv2030c	Rv2771c
Rv2172c	Rv1837c	Rv2391	Rv2004c	Rv1911c	Rv2031c	Rv2772c
Rv2173	Rv1838c	Rv2393	Rv2005c	Rv1912c	Rv2032	Rv2773c
Rv2174	Rv1839c	Rv2396	Rv2006	Rv1913	Rv2033c	Rv2776c
Rv2175c	Rv1841c	Rv2397c	Rv2008c	Rv1914c	Rv2034	Rv2777c
Rv2178c	Rv1842c	Rv2399c	Rv2009	Rv1915	Rv2035	Rv2778c
Rv2179c	Rv1843c	Rv2401	Rv2011c	Rv1916	Rv2036	Rv2780
Rv2180c	Rv1844c	Rv2402	Rv2012	Rv1917c	Rv2037c	Rv2782c
Rv2181	Rv1845c	Rv2403c	Rv2014	Rv1919c	Rv2038c	Rv2783c
Rv2182c	Rv1846c	Rv2404c	Rv2015c	Rv1920	Rv2041c	Rv2785c
Rv2183c	Rv1847	Rv2405	Rv2016	Rv1921c	Rv2042c	Rv2788
Rv2184c	Rv1848	Rv2406c	Rv2017	Rv1922	Rv2043c	Rv2789c
Rv2185c	Rv1850	Rv2407	Rv2018	Rv1923	Rv2045c	Rv2790c
Rv2187	Rv1851	Rv2408	Rv2019	Rv1924c	Rv2047c	Rv2793c
Rv2188c	Rv1852	Rv2409c	Rv2021c	Rv1925	Rv2048c	Rv2794c
Rv2189c	Rv1853	Rv2410c	Rv2022c	Rv1926c	Rv2049c	Rv2795c
Rv2191	Rv1854c	Rv2411c	Rv2023c	Rv1927	Rv2050	Rv2799
Rv2192c	Rv1855c	Rv2412	Rv2024c	Rv1928c	Rv2051c	Rv2800
Rv2193	Rv1856c	Rv2413c	Rv2026c	Rv1929c	Rv2052c	Rv2825c
Rv2194	Rv1857	Rv2414c	Rv2027c	Rv1930c	Rv2053c	Rv2828c
Rv2195	Rv1858	Rv2415c	Rv2028c	Rv1931c	Rv2054	Rv2831
Rv2196	Rv1859	Rv2416c	Rv2029c	Rv1933c	Rv2055c	Rv2838c
Rv2198c	Rv1860	Rv2417c	Rv2030c	Rv1934c	Rv2056c	Rv2839c
Rv2200c	Rv1861	Rv2420c	Rv2031c	Rv1935c	Rv2057c	Rv2841c
Rv2201	Rv1862	Rv2421c	Rv2032	Rv1936	Rv2058c	Rv2844
Rv2202c	Rv1863c	Rv2423	Rv2033c	Rv1937	Rv2059	Rv2845c
Rv2203	Rv1864c	Rv2424c	Rv2034	Rv1938	Rv2061c	Rv2846c
Rv2204c	Rv1865c	Rv2425c	Rv2035	Rv1939	Rv2062c	Rv2847c
Rv2206	Rv1866	Rv2426c	Rv2037c	Rv1940	Rv2063	Rv2848c
Rv2207	Rv1867	Rv2427c	Rv2038c	Rv1941	Rv2064	Rv2849c
Rv2209	Rv1868	Rv2430c	Rv2040c	Rv1942c	Rv2065	Rv2850c
Rv2210c	Rv1869c	Rv2432c	Rv2041c	Rv1945	Rv2066	Rv2851c

Rv2211c	Rv1870c	Rv2435c	Rv2042c	Rv1947	Rv2067c	Rv2852c
Rv2212	Rv1871c	Rv2438c	Rv2043c	Rv1948c	Rv2068c	Rv2854
Rv2213	Rv1872c	Rv2439c	Rv2045c	Rv1949c	Rv2069	Rv2855
Rv2214c	Rv1873	Rv2440c	Rv2046	Rv1952	Rv2070c	Rv2857c
Rv2215	Rv1874	Rv2441c	Rv2047c	Rv1953	Rv2071c	Rv2860c
Rv2216	Rv1875	Rv2444c	Rv2048c	Rv1954c	Rv2077c	Rv2861c
Rv2217	Rv1876	Rv2445c	Rv2050	Rv1955	Rv2079	Rv2864c
Rv2218	Rv1877	Rv2447c	Rv2051c	Rv1956	Rv2081c	Rv2867c
Rv2219	Rv1878	Rv2448c	Rv2052c	Rv1957	Rv2082	Rv2868c
Rv2219.1	Rv1879	Rv2449c	Rv2054	Rv1958c	Rv2083	Rv2869c
Rv2220	Rv1880c	Rv2450c	Rv2055c	Rv1959c	Rv2084	Rv2870c
Rv2221c	Rv1881c	Rv2453c	Rv2056c	Rv1960c	Rv2085	Rv2874
Rv2222c	Rv1882c	Rv2454c	Rv2059	Rv1961	Rv2086	Rv2877c
Rv2223c	Rv1883c	Rv2455c	Rv2062c	Rv1962c	Rv2088	Rv2878c
Rv2224c	Rv1885c	Rv2456c	Rv2063	Rv1963c	Rv2089c	Rv2881c
Rv2228c	Rv1886c	Rv2457c	Rv2064	Rv1964	Rv2090	Rv2882c
Rv2229c	Rv1887	Rv2461c	Rv2065	Rv1978	Rv2091c	Rv2883c
Rv2230c	Rv1888.1	Rv2462c	Rv2066	Rv1979c	Rv2092c	Rv2884
Rv2231c	Rv1888c	Rv2463	Rv2067c	Rv1980c	Rv2093c	Rv2887
Rv2232	Rv1889c	Rv2466c	Rv2068c	Rv1981c	Rv2096c	Rv2888c
Rv2234	Rv1890c	Rv2467	Rv2069	Rv1984c	Rv2097c	Rv2889c
Rv2235	Rv1893	Rv2468c	Rv2070c	Rv1985c	Rv2100	Rv2890c
Rv2238c	Rv1894c	Rv2469c	Rv2071c	Rv1986	Rv2101	Rv2894c
Rv2240c	Rv1895	Rv2470	Rv2072c	Rv1987	Rv2102	Rv2895c
Rv2241	Rv1896c	Rv2471	Rv2073c	Rv1988	Rv2103c	Rv2896c
Rv2242	Rv1897c	Rv2473	Rv2074	Rv1989c	Rv2104c	Rv2897c
Rv2243	Rv1898	Rv2476c	Rv2075c	Rv1990.1	Rv2106	Rv2899c
Rv2244	Rv1899c	Rv2477c	Rv2077c	Rv1992c	Rv2108	Rv2901c
Rv2245	Rv1900c	Rv2478c	Rv2079	Rv1993c	Rv2110c	Rv2902c
Rv2246	Rv1901	Rv2480c	Rv2082	Rv1995	Rv2112c	Rv2903c
Rv2247	Rv1902c	Rv2481c	Rv2083	Rv1996	Rv2113	Rv2905
Rv2249c	Rv1903	Rv2482c	Rv2084	Rv1997	Rv2114	Rv2906c
Rv2251	Rv1904	Rv2483c	Rv2085	Rv1999c	Rv2115c	Rv2907c
Rv2252	Rv1905c	Rv2484c	Rv2086	Rv2000	Rv2117	Rv2908c
Rv2253	Rv1906c	Rv2485c	Rv2088	Rv2001	Rv2118c	Rv2909c
Rv2256c	Rv1907c	Rv2486	Rv2089c	Rv2002	Rv2119	Rv2911
Rv2257c	Rv1908c	Rv2488c	Rv2090	Rv2004c	Rv2121c	Rv2912c
Rv2258c	Rv1909c	Rv2490c	Rv2091c	Rv2005c	Rv2122c	Rv2913c
Rv2259	Rv1910c	Rv2491	Rv2092c	Rv2006	Rv2123	Rv2915c
Rv2263	Rv1912c	Rv2493	Rv2093c	Rv2008c	Rv2124c	Rv2916c
Rv2265	Rv1913	Rv2495c	Rv2095c	Rv2009	Rv2125	Rv2917
Rv2266	Rv1915	Rv2496c	Rv2096c	Rv2010	Rv2127	Rv2918c
Rv2267c	Rv1916	Rv2497c	Rv2097c	Rv2011c	Rv2128	Rv2919c
Rv2268c	Rv1919c	Rv2499c	Rv2100	Rv2012	Rv2129c	Rv2920c
Rv2270	Rv1920	Rv2500c	Rv2101	Rv2013	Rv2130c	Rv2921c
Rv2271	Rv1921c	Rv2501c	Rv2102	Rv2014	Rv2133c	Rv2922A
Rv2273	Rv1922	Rv2502c	Rv2104c	Rv2016	Rv2134c	Rv2922c
Rv2275	Rv1923	Rv2503c	Rv2105	Rv2017	Rv2135c	Rv2923c
Rv2276	Rv1924c	Rv2505c	Rv2106	Rv2018	Rv2137c	Rv2924c
Rv2280	Rv1925	Rv2506	Rv2108	Rv2019	Rv2139	Rv2925c
Rv2281	Rv1926c	Rv2510c	Rv2109c	Rv2020c	Rv2141c	Rv2926c

Rv2282c	Rv1927	Rv2511	Rv2110c	Rv2021c	Rv2142c	Rv2927c
Rv2284	Rv1928c	Rv2513	Rv2112c	Rv2022c	Rv2143	Rv2928
Rv2285	Rv1929c	Rv2515c	Rv2113	Rv2023c	Rv2145c	Rv2935
Rv2286c	Rv1930c	Rv2516c	Rv2114	Rv2024c	Rv2147c	Rv2936
Rv2287	Rv1931c	Rv2520c	Rv2115c	Rv2026c	Rv2148c	Rv2938
Rv2288	Rv1933c	Rv2521	Rv2116	Rv2027c	Rv2149c	Rv2951c
Rv2290	Rv1934c	Rv2522c	Rv2117	Rv2028c	Rv2150c	Rv2955c
Rv2293c	Rv1936	Rv2523c	Rv2118c	Rv2029c	Rv2152c	Rv2957
Rv2294	Rv1937	Rv2524c	Rv2119	Rv2030c	Rv2153c	Rv2963
Rv2295	Rv1938	Rv2525c	Rv2121c	Rv2031c	Rv2154c	Rv2965c
Rv2296	Rv1940	Rv2528c	Rv2122c	Rv2032	Rv2155c	Rv2966c
Rv2297	Rv1941	Rv2529	Rv2123	Rv2033c	Rv2157c	Rv2967c
Rv2298	Rv1942c	Rv2530A	Rv2124c	Rv2034	Rv2158c	Rv2969c
Rv2299c	Rv1943c	Rv2530c	Rv2126c	Rv2035	Rv2159c	Rv2973c
Rv2300c	Rv1945	Rv2531c	Rv2127	Rv2036	Rv2160.1	Rv2974c
Rv2302	Rv1946c	Rv2532c	Rv2130c	Rv2037c	Rv2161c	Rv2975c
Rv2303c	Rv1947	Rv2534c	Rv2134c	Rv2038c	Rv2163c	Rv2976c
Rv2305	Rv1948c	Rv2535c	Rv2135c	Rv2039c	Rv2164c	Rv2977c
Rv2306c	Rv1949c	Rv2536	Rv2137c	Rv2040c	Rv2165c	Rv2981c
Rv2307c	Rv1954c	Rv2537c	Rv2138	Rv2041c	Rv2166c	Rv2984
Rv2307.2	Rv1955	Rv2538c	Rv2139	Rv2042c	Rv2167c	Rv2985
Rv2308	Rv1956	Rv2540c	Rv2140c	Rv2044c	Rv2169c	Rv2986c
Rv2309c	Rv1957	Rv2541	Rv2141c	Rv2045c	Rv2170	Rv2987c
Rv2310	Rv1958c	Rv2542	Rv2142c	Rv2046	Rv2171	Rv2988c
Rv2311	Rv1959c	Rv2543	Rv2143	Rv2047c	Rv2172c	Rv2989
Rv2313c	Rv1960c	Rv2544	Rv2145c	Rv2048c	Rv2173	Rv2991
Rv2314c	Rv1961	Rv2545	Rv2147c	Rv2049c	Rv2174	Rv2994
Rv2315c	Rv1962c	Rv2546	Rv2148c	Rv2050	Rv2175c	Rv2995c
Rv2317	Rv1963c	Rv2547	Rv2149c	Rv2051c	Rv2176	Rv2996c
Rv2318	Rv1964	Rv2553c	Rv2150c	Rv2052c	Rv2177c	Rv2997
Rv2319c	Rv1966	Rv2555c	Rv2151c	Rv2053c	Rv2178c	Rv3001c
Rv2320c	Rv1967	Rv2557	Rv2152c	Rv2054	Rv2180c	Rv3003c
Rv2323c	Rv1968	Rv2559c	Rv2153c	Rv2055c	Rv2181	Rv3004
Rv2324	Rv1969	Rv2563	Rv2154c	Rv2056c	Rv2182c	Rv3006
Rv2325c	Rv1970	Rv2564	Rv2155c	Rv2058c	Rv2183c	Rv3007c
Rv2326c	Rv1971	Rv2565	Rv2156c	Rv2059	Rv2184c	Rv3009c
Rv2327	Rv1972	Rv2566	Rv2157c	Rv2062c	Rv2186c	Rv3010c
Rv2328	Rv1973	Rv2567	Rv2158c	Rv2063	Rv2187	Rv3011c
Rv2329c	Rv1974	Rv2568c	Rv2159c	Rv2064	Rv2188c	Rv3012c
Rv2331	Rv1975	Rv2569c	Rv2160.1	Rv2065	Rv2189c	Rv3013
Rv2331.1	Rv1976c	Rv2570	Rv2160c	Rv2066	Rv2190c	Rv3014c
Rv2332	Rv1977	Rv2571c	Rv2161c	Rv2067c	Rv2191	Rv3015c
Rv2333c	Rv1978	Rv2572c	Rv2162c	Rv2068c	Rv2192c	Rv3024c
Rv2334	Rv1979c	Rv2573	Rv2163c	Rv2069	Rv2193	Rv3025c
Rv2335	Rv1980c	Rv2577	Rv2164c	Rv2070c	Rv2194	Rv3026c
Rv2336	Rv1981c	Rv2578c	Rv2165c	Rv2071c	Rv2195	Rv3027c
Rv2337c	Rv1982c	Rv2579	Rv2166c	Rv2075c	Rv2196	Rv3028c
Rv2338c	Rv1984c	Rv2580c	Rv2167c	Rv2077c	Rv2197c	Rv3029c
Rv2339	Rv1985c	Rv2581c	Rv2168c	Rv2079	Rv2198c	Rv3030
Rv2340c	Rv1986	Rv2583c	Rv2169c	Rv2080	Rv2200c	Rv3031
Rv2343c	Rv1988	Rv2584c	Rv2170	Rv2082	Rv2201	Rv3032

Rv2344c	Rv1989c	Rv2585c	Rv2171	Rv2083	Rv2202c	Rv3034c
Rv2345	Rv1990.1	Rv2586c	Rv2172c	Rv2084	Rv2204c	Rv3035
Rv2346c	Rv1991c	Rv2587c	Rv2173	Rv2085	Rv2205c	Rv3036c
Rv2347c	Rv1992c	Rv2589	Rv2174	Rv2086	Rv2206	Rv3037c
Rv2350c	Rv1993c	Rv2590	Rv2175c	Rv2088	Rv2207	Rv3038c
Rv2351c	Rv1994c	Rv2592c	Rv2176	Rv2089c	Rv2209	Rv3039c
Rv2356c	Rv1995	Rv2593c	Rv2178c	Rv2090	Rv2210c	Rv3040c
Rv2357c	Rv1996	Rv2594c	Rv2179c	Rv2091c	Rv2211c	Rv3041c
Rv2359	Rv1997	Rv2597	Rv2180c	Rv2092c	Rv2212	Rv3043c
Rv2360c	Rv1998c	Rv2601A	Rv2181	Rv2093c	Rv2213	Rv3044
Rv2361c	Rv1999c	Rv2602	Rv2182c	Rv2094c	Rv2214c	Rv3045
Rv2362c	Rv2000	Rv2604c	Rv2183c	Rv2095c	Rv2215	Rv3046c
Rv2363	Rv2001	Rv2605c	Rv2184c	Rv2096c	Rv2216	Rv3048c
Rv2364c	Rv2002	Rv2606c	Rv2185c	Rv2097c	Rv2218	Rv3049c
Rv2366c	Rv2003c	Rv2609c	Rv2187	Rv2098c	Rv2219	Rv3050c
Rv2368c	Rv2004c	Rv2610c	Rv2188c	Rv2099c	Rv2219.1	Rv3051c
Rv2370c	Rv2005c	Rv2611c	Rv2189c	Rv2100	Rv2220	Rv3052c
Rv2373c	Rv2006	Rv2614c	Rv2190c	Rv2101	Rv2221c	Rv3053c
Rv2375	Rv2008c	Rv2615c	Rv2191	Rv2102	Rv2222c	Rv3054c
Rv2378c	Rv2009	Rv2617c	Rv2192c	Rv2104c	Rv2223c	Rv3055
Rv2381c	Rv2010	Rv2618	Rv2195	Rv2106	Rv2224c	Rv3056
Rv2382c	Rv2011c	Rv2621c	Rv2197c	Rv2107	Rv2225	Rv3057c
Rv2383c	Rv2012	Rv2622	Rv2198c	Rv2108	Rv2226	Rv3058c
Rv2384	Rv2013	Rv2624c	Rv2200c	Rv2109c	Rv2227	Rv3059
Rv2385	Rv2014	Rv2625c	Rv2201	Rv2110c	Rv2228c	Rv3060c
Rv2386c	Rv2015c	Rv2626c	Rv2202c	Rv2112c	Rv2229c	Rv3061c
Rv2387	Rv2016	Rv2627c	Rv2203	Rv2113	Rv2230c	Rv3062
Rv2389c	Rv2017	Rv2630	Rv2205c	Rv2114	Rv2231c	Rv3063
Rv2391	Rv2018	Rv2631	Rv2207	Rv2115c	Rv2232	Rv3070
Rv2392	Rv2019	Rv2632c	Rv2208	Rv2117	Rv2234	Rv3071
Rv2393	Rv2020c	Rv2633c	Rv2209	Rv2118c	Rv2235	Rv3073c
Rv2394	Rv2021c	Rv2636	Rv2210c	Rv2119	Rv2236c	Rv3074
Rv2395	Rv2022c	Rv2638	Rv2211c	Rv2121c	Rv2237	Rv3075c
Rv2396	Rv2023c	Rv2642	Rv2212	Rv2122c	Rv2240c	Rv3094c
Rv2397c	Rv2024c	Rv2643	Rv2213	Rv2123	Rv2241	Rv3095
Rv2399c	Rv2025c	Rv2646	Rv2214c	Rv2124c	Rv2242	Rv3096
Rv2400c	Rv2026c	Rv2647	Rv2215	Rv2125	Rv2243	Rv3101c
Rv2402	Rv2027c	Rv2648	Rv2216	Rv2127	Rv2244	Rv3102c
Rv2403c	Rv2028c	Rv2650c	Rv2217	Rv2129c	Rv2245	Rv3104c
Rv2404c	Rv2029c	Rv2651c	Rv2218	Rv2130c	Rv2246	Rv3105c
Rv2406c	Rv2030c	Rv2653c	Rv2219	Rv2131c	Rv2247	Rv3106
Rv2407	Rv2031c	Rv2654c	Rv2219.1	Rv2133c	Rv2248	Rv3118
Rv2408	Rv2032	Rv2655c	Rv2220	Rv2134c	Rv2249c	Rv3120
Rv2409c	Rv2033c	Rv2658c	Rv2221c	Rv2135c	Rv2250c	Rv3127
Rv2410c	Rv2034	Rv2659c	Rv2222c	Rv2137c	Rv2251	Rv3129
Rv2411c	Rv2035	Rv2662	Rv2223c	Rv2138	Rv2252	Rv3133c
Rv2412	Rv2036	Rv2667	Rv2224c	Rv2139	Rv2253	Rv3134c
Rv2413c	Rv2038c	Rv2669	Rv2226	Rv2140c	Rv2254c	Rv3135
Rv2414c	Rv2039c	Rv2670c	Rv2228c	Rv2141c	Rv2255c	Rv3136
Rv2415c	Rv2040c	Rv2671	Rv2229c	Rv2142c	Rv2257c	Rv3137
Rv2417c	Rv2041c	Rv2672	Rv2230c	Rv2143	Rv2258c	Rv3139

Rv2418c	Rv2042c	Rv2673	Rv2232	Rv2145c	Rv2259	Rv3140
Rv2419c	Rv2043c	Rv2676c	Rv2234	Rv2147c	Rv2260	Rv3141
Rv2420c	Rv2044c	Rv2677c	Rv2235	Rv2148c	Rv2262c	Rv3143
Rv2421c	Rv2045c	Rv2678c	Rv2236c	Rv2149c	Rv2263	Rv3145
Rv2422	Rv2046	Rv2679	Rv2237	Rv2150c	Rv2264c	Rv3146
Rv2423	Rv2047c	Rv2681	Rv2238c	Rv2151c	Rv2265	Rv3147
Rv2426c	Rv2048c	Rv2686c	Rv2240c	Rv2152c	Rv2266	Rv3148
Rv2427c	Rv2049c	Rv2687c	Rv2241	Rv2153c	Rv2267c	Rv3149
Rv2428	Rv2050	Rv2690c	Rv2242	Rv2154c	Rv2268c	Rv3150
Rv2429	Rv2051c	Rv2691	Rv2243	Rv2155c	Rv2271	Rv3151
Rv2430c	Rv2052c	Rv2692	Rv2244	Rv2157c	Rv2273	Rv3152
Rv2431c	Rv2053c	Rv2694c	Rv2245	Rv2158c	Rv2274c	Rv3153
Rv2434c	Rv2054	Rv2696c	Rv2246	Rv2159c	Rv2275	Rv3156
Rv2435c	Rv2058c	Rv2697c	Rv2247	Rv2160.1	Rv2276	Rv3157
Rv2436	Rv2059	Rv2698	Rv2248	Rv2161c	Rv2277c	Rv3158
Rv2437	Rv2062c	Rv2700	Rv2249c	Rv2162c	Rv2279	Rv3163c
Rv2439c	Rv2063	Rv2701c	Rv2250.1	Rv2163c	Rv2280	Rv3164c
Rv2440c	Rv2064	Rv2702	Rv2250c	Rv2164c	Rv2281	Rv3165c
Rv2441c	Rv2065	Rv2703	Rv2251	Rv2165c	Rv2282c	Rv3166c
Rv2443	Rv2066	Rv2708c	Rv2252	Rv2166c	Rv2283	Rv3167c
Rv2444c	Rv2067c	Rv2709	Rv2253	Rv2167c	Rv2284	Rv3168
Rv2445c	Rv2068c	Rv2710	Rv2255c	Rv2169c	Rv2285	Rv3169
Rv2447c	Rv2069	Rv2711	Rv2256c	Rv2170	Rv2286c	Rv3170
Rv2448c	Rv2070c	Rv2712c	Rv2257c	Rv2171	Rv2288	Rv3171c
Rv2449c	Rv2071c	Rv2713	Rv2258c	Rv2172c	Rv2289	Rv3173c
Rv2450c	Rv2072c	Rv2715	Rv2260	Rv2173	Rv2291	Rv3192
Rv2451	Rv2073c	Rv2717c	Rv2262c	Rv2174	Rv2293c	Rv3193c
Rv2453c	Rv2074	Rv2718c	Rv2263	Rv2175c	Rv2294	Rv3194c
Rv2454c	Rv2075c	Rv2719c	Rv2264c	Rv2176	Rv2296	Rv3195
Rv2455c	Rv2077c	Rv2720	Rv2265	Rv2177c	Rv2297	Rv3196
Rv2456c	Rv2078	Rv2721c	Rv2266	Rv2178c	Rv2298	Rv3197
Rv2457c	Rv2079	Rv2723	Rv2268c	Rv2179c	Rv2299c	Rv3197.1
Rv2458	Rv2080	Rv2724c	Rv2269c	Rv2181	Rv2300c	Rv3198A
Rv2459	Rv2081c	Rv2725c	Rv2270	Rv2182c	Rv2301	Rv3198c
Rv2460c	Rv2082	Rv2726c	Rv2273	Rv2183c	Rv2302	Rv3199c
Rv2461c	Rv2083	Rv2727c	Rv2275	Rv2184c	Rv2303c	Rv3200c
Rv2462c	Rv2084	Rv2728c	Rv2276	Rv2185c	Rv2305	Rv3201c
Rv2463	Rv2085	Rv2731	Rv2277c	Rv2186c	Rv2306.1	Rv3202c
Rv2464c	Rv2086	Rv2732c	Rv2278	Rv2187	Rv2307.2	Rv3203
Rv2465c	Rv2088	Rv2733c	Rv2279	Rv2188c	Rv2307.4	Rv3204
Rv2466c	Rv2089c	Rv2734	Rv2280	Rv2189c	Rv2307c	Rv3205c
Rv2467	Rv2090	Rv2735c	Rv2281	Rv2190c	Rv2308	Rv3206c
Rv2468c	Rv2091c	Rv2736c	Rv2282c	Rv2191	Rv2309.1	Rv3207c
Rv2469c	Rv2092c	Rv2737c	Rv2283	Rv2192c	Rv2311	Rv3208
Rv2470	Rv2093c	Rv2739c	Rv2284	Rv2193	Rv2313c	Rv3208.1
Rv2471	Rv2094c	Rv2742c	Rv2285	Rv2194	Rv2314c	Rv3210c
Rv2473	Rv2095c	Rv2743c	Rv2286c	Rv2195	Rv2315c	Rv3212
Rv2474c	Rv2096c	Rv2744c	Rv2288	Rv2196	Rv2316	Rv3213c
Rv2475c	Rv2097c	Rv2745c	Rv2289	Rv2197c	Rv2318	Rv3214
Rv2476c	Rv2100	Rv2748c	Rv2291	Rv2200c	Rv2319c	Rv3215
Rv2477c	Rv2101	Rv2749	Rv2294	Rv2201	Rv2320c	Rv3216

Rv2483c	Rv2102	Rv2750	Rv2296	Rv2202c	Rv2321c	Rv3218
Rv2486	Rv2103c	Rv2752c	Rv2297	Rv2203	Rv2322c	Rv3220c
Rv2488c	Rv2104c	Rv2753c	Rv2298	Rv2204c	Rv2324	Rv3224
Rv2489c	Rv2105	Rv2754c	Rv2299c	Rv2205c	Rv2325c	Rv3226c
Rv2491	Rv2106	Rv2756c	Rv2300c	Rv2206	Rv2326c	Rv3227
Rv2492	Rv2107	Rv2757c	Rv2302	Rv2207	Rv2327	Rv3228
Rv2494	Rv2108	Rv2758c	Rv2303c	Rv2209	Rv2329c	Rv3229c
Rv2496c	Rv2109c	Rv2759c	Rv2305	Rv2210c	Rv2330c	Rv3230c
Rv2497c	Rv2110c	Rv2761c	Rv2306.1	Rv2211c	Rv2331	Rv3231c
Rv2498c	Rv2112c	Rv2764c	Rv2306.2	Rv2212	Rv2331.1	Rv3232c
Rv2499c	Rv2114	Rv2767c	Rv2306c	Rv2213	Rv2332	Rv3233c
Rv2500c	Rv2115c	Rv2768c	Rv2307.2	Rv2214c	Rv2333c	Rv3234c
Rv2501c	Rv2117	Rv2772c	Rv2307.4	Rv2215	Rv2334	Rv3235
Rv2502c	Rv2118c	Rv2773c	Rv2307c	Rv2216	Rv2335	Rv3236c
Rv2503c	Rv2119	Rv2776c	Rv2308	Rv2217	Rv2336	Rv3238c
Rv2505c	Rv2120c	Rv2778c	Rv2309c	Rv2218	Rv2337c	Rv3241c
Rv2506	Rv2121c	Rv2779c	Rv2310	Rv2219	Rv2338c	Rv3242c
Rv2507	Rv2122c	Rv2780	Rv2311	Rv2219.1	Rv2339	Rv3245c
Rv2508c	Rv2123	Rv2781c	Rv2312	Rv2220	Rv2340c	Rv3247c
Rv2509	Rv2124c	Rv2782c	Rv2314c	Rv2221c	Rv2342	Rv3248c
Rv2510c	Rv2125	Rv2783c	Rv2315c	Rv2222c	Rv2343c	Rv3249c
Rv2511	Rv2127	Rv2784c	Rv2316	Rv2224c	Rv2344c	Rv3250c
Rv2513	Rv2129c	Rv2785c	Rv2318	Rv2225	Rv2345	Rv3252c
Rv2514c	Rv2130c	Rv2786c	Rv2319c	Rv2226	Rv2353c	Rv3253c
Rv2515c	Rv2131c	Rv2787	Rv2320c	Rv2228c	Rv2355	Rv3254
Rv2516c	Rv2132	Rv2788	Rv2321c	Rv2229c	Rv2357c	Rv3255c
Rv2518c	Rv2133c	Rv2789c	Rv2323c	Rv2230c	Rv2358	Rv3256c
Rv2521	Rv2134c	Rv2790c	Rv2324	Rv2231c	Rv2359	Rv3259
Rv2522c	Rv2135c	Rv2791c	Rv2325c	Rv2232	Rv2360c	Rv3260c
Rv2523c	Rv2137c	Rv2793c	Rv2326c	Rv2234	Rv2361c	Rv3261
Rv2524c	Rv2138	Rv2794c	Rv2327	Rv2235	Rv2362c	Rv3262
Rv2525c	Rv2139	Rv2796c	Rv2329c	Rv2236c	Rv2363	Rv3263
Rv2528c	Rv2140c	Rv2797c	Rv2330c	Rv2237	Rv2365c	Rv3264c
Rv2529	Rv2141c	Rv2800	Rv2331	Rv2238c	Rv2366c	Rv3265c
Rv2530c	Rv2142c	Rv2801c	Rv2331.1	Rv2240c	Rv2368c	Rv3266c
Rv2531c	Rv2143	Rv2802c	Rv2332	Rv2241	Rv2369c	Rv3267
Rv2532c	Rv2145c	Rv2803	Rv2334	Rv2242	Rv2370c	Rv3268
Rv2533c	Rv2147c	Rv2805	Rv2335	Rv2243	Rv2372c	Rv3269
Rv2534c	Rv2148c	Rv2807	Rv2336	Rv2245	Rv2373c	Rv3270
Rv2535c	Rv2149c	Rv2810c	Rv2337c	Rv2246	Rv2374c	Rv3272
Rv2536	Rv2150c	Rv2811	Rv2338c	Rv2247	Rv2375	Rv3274c
Rv2538c	Rv2151c	Rv2812	Rv2339	Rv2248	Rv2378c	Rv3275c
Rv2539c	Rv2152c	Rv2813	Rv2340c	Rv2249c	Rv2379c	Rv3276c
Rv2540c	Rv2153c	Rv2815c	Rv2342	Rv2250c	Rv2380c	Rv3277
Rv2542	Rv2154c	Rv2816c	Rv2343c	Rv2251	Rv2381c	Rv3278c
Rv2543	Rv2155c	Rv2817c	Rv2344c	Rv2252	Rv2382c	Rv3279c
Rv2544	Rv2156c	Rv2818c	Rv2345	Rv2253	Rv2383c	Rv3280
Rv2545	Rv2157c	Rv2819c	Rv2347c	Rv2254c	Rv2384	Rv3281
Rv2547	Rv2158c	Rv2820c	Rv2349c	Rv2255c	Rv2385	Rv3283
Rv2548	Rv2159c	Rv2821c	Rv2350c	Rv2256c	Rv2386c	Rv3284
Rv2549c	Rv2160.1	Rv2823c	Rv2351c	Rv2257c	Rv2387	Rv3285

Rv2550c	Rv2160c	Rv2825c	Rv2354	Rv2258c	Rv2390c	Rv3286c
Rv2551c	Rv2161c	Rv2826c	Rv2355	Rv2259	Rv2391	Rv3287c
Rv2552c	Rv2163c	Rv2827c	Rv2356c	Rv2260	Rv2392	Rv3290c
Rv2553c	Rv2164c	Rv2828c	Rv2357c	Rv2262c	Rv2393	Rv3291c
Rv2554c	Rv2165c	Rv2829c	Rv2358	Rv2263	Rv2394	Rv3292
Rv2555c	Rv2166c	Rv2830c	Rv2360c	Rv2264c	Rv2395	Rv3293
Rv2557	Rv2167c	Rv2831	Rv2361c	Rv2265	Rv2397c	Rv3295
Rv2558	Rv2168c	Rv2832c	Rv2362c	Rv2266	Rv2398c	Rv3296
Rv2559c	Rv2169c	Rv2833c	Rv2363	Rv2267c	Rv2399c	Rv3298c
Rv2560	Rv2170	Rv2834c	Rv2364c	Rv2268c	Rv2401	Rv3300c
Rv2563	Rv2171	Rv2835c	Rv2365c	Rv2274c	Rv2402	Rv3302c
Rv2564	Rv2172c	Rv2837c	Rv2366c	Rv2275	Rv2403c	Rv3305c
Rv2565	Rv2173	Rv2838c	Rv2368c	Rv2276	Rv2404c	Rv3306c
Rv2567	Rv2175c	Rv2839c	Rv2369c	Rv2277c	Rv2406c	Rv3307
Rv2568c	Rv2176	Rv2840c	Rv2370c	Rv2279	Rv2407	Rv3308
Rv2569c	Rv2177c	Rv2841c	Rv2372c	Rv2280	Rv2408	Rv3309c
Rv2570	Rv2178c	Rv2842c	Rv2373c	Rv2281	Rv2409c	Rv3310
Rv2571c	Rv2179c	Rv2843	Rv2374c	Rv2282c	Rv2410c	Rv3311
Rv2572c	Rv2180c	Rv2844	Rv2375	Rv2284	Rv2411c	Rv3313c
Rv2574	Rv2181	Rv2845c	Rv2378c	Rv2285	Rv2412	Rv3314c
Rv2575	Rv2182c	Rv2847c	Rv2379c	Rv2286c	Rv2413c	Rv3315c
Rv2576c	Rv2183c	Rv2848c	Rv2380c	Rv2287	Rv2414c	Rv3316
Rv2577	Rv2184c	Rv2849c	Rv2381c	Rv2288	Rv2415c	Rv3317
Rv2578c	Rv2185c	Rv2850c	Rv2382c	Rv2289	Rv2416c	Rv3318
Rv2579	Rv2187	Rv2854	Rv2383c	Rv2294	Rv2417c	Rv3319
Rv2580c	Rv2188c	Rv2855	Rv2384	Rv2295	Rv2418c	Rv3322c
Rv2582	Rv2189c	Rv2857c	Rv2385	Rv2296	Rv2419c	Rv3327
Rv2583c	Rv2190c	Rv2858c	Rv2386c	Rv2297	Rv2420c	Rv3328c
Rv2584c	Rv2191	Rv2859c	Rv2387	Rv2298	Rv2421c	Rv3329
Rv2585c	Rv2192c	Rv2862c	Rv2388c	Rv2299c	Rv2423	Rv3332
Rv2586c	Rv2193	Rv2864c	Rv2389c	Rv2300c	Rv2425c	Rv3336c
Rv2587c	Rv2194	Rv2865	Rv2391	Rv2301	Rv2426c	Rv3337
Rv2588c	Rv2195	Rv2867c	Rv2392	Rv2303c	Rv2427c	Rv3338
Rv2589	Rv2196	Rv2868c	Rv2393	Rv2304c	Rv2429	Rv3339c
Rv2590	Rv2197c	Rv2869c	Rv2394	Rv2305	Rv2430c	Rv3341
Rv2592c	Rv2198c	Rv2870c	Rv2395	Rv2306.1	Rv2431c	Rv3342
Rv2593c	Rv2200c	Rv2871	Rv2397c	Rv2306.2	Rv2434c	Rv3346c
Rv2594c	Rv2201	Rv2874	Rv2398c	Rv2307.4	Rv2435c	Rv3355c
Rv2596	Rv2202c	Rv2877c	Rv2399c	Rv2307c	Rv2436	Rv3356c
Rv2597	Rv2203	Rv2879c	Rv2401	Rv2308	Rv2438c	Rv3359
Rv2599	Rv2204c	Rv2880c	Rv2402	Rv2309.1	Rv2439c	Rv3361c
Rv2601	Rv2205c	Rv2883c	Rv2403c	Rv2309c	Rv2440c	Rv3362c
Rv2602	Rv2206	Rv2884	Rv2404c	Rv2310	Rv2441c	Rv3363c
Rv2603c	Rv2207	Rv2885c	Rv2405	Rv2311	Rv2442c	Rv3364c
Rv2604c	Rv2209	Rv2886c	Rv2406c	Rv2312	Rv2443	Rv3365c
Rv2605c	Rv2210c	Rv2887	Rv2407	Rv2313c	Rv2444c	Rv3366
Rv2606c	Rv2211c	Rv2888c	Rv2408	Rv2314c	Rv2445c	Rv3368c
Rv2607	Rv2212	Rv2889c	Rv2409c	Rv2315c	Rv2447c	Rv3370c
Rv2608	Rv2213	Rv2890c	Rv2410c	Rv2316	Rv2448c	Rv3371
Rv2609c	Rv2214c	Rv2891	Rv2411c	Rv2317	Rv2449c	Rv3372
Rv2610c	Rv2215	Rv2892c	Rv2412	Rv2318	Rv2451	Rv3389c

Rv2611c	Rv2216	Rv2893	Rv2413c	Rv2319c	Rv2453c	Rv3390
Rv2612c	Rv2217	Rv2894c	Rv2414c	Rv2320c	Rv2454c	Rv3391
Rv2613c	Rv2218	Rv2896c	Rv2415c	Rv2321c	Rv2455c	Rv3393
Rv2614c	Rv2219	Rv2897c	Rv2416c	Rv2322c	Rv2456c	Rv3394c
Rv2616	Rv2219.1	Rv2898c	Rv2417c	Rv2323c	Rv2457c	Rv3395c
Rv2617c	Rv2220	Rv2899c	Rv2419c	Rv2324	Rv2458	Rv3400
Rv2619c	Rv2221c	Rv2900c	Rv2421c	Rv2325c	Rv2459	Rv3401
Rv2620c	Rv2223c	Rv2902c	Rv2423	Rv2326c	Rv2460c	Rv3405c
Rv2621c	Rv2224c	Rv2903c	Rv2424c	Rv2327	Rv2461c	Rv3406
Rv2622	Rv2225	Rv2906c	Rv2425c	Rv2329c	Rv2462c	Rv3409c
Rv2623	Rv2226	Rv2908c	Rv2426c	Rv2331	Rv2463	Rv3410c
Rv2624c	Rv2227	Rv2909c	Rv2427c	Rv2331.1	Rv2464c	Rv3411c
Rv2625c	Rv2228c	Rv2910c	Rv2429	Rv2332	Rv2465c	Rv3413c
Rv2627c	Rv2229c	Rv2911	Rv2432c	Rv2333c	Rv2466c	Rv3414c
Rv2628	Rv2230c	Rv2912c	Rv2434c	Rv2334	Rv2467	Rv3415c
Rv2629	Rv2231c	Rv2913c	Rv2435c	Rv2335	Rv2469c	Rv3417c
Rv2630	Rv2232	Rv2914c	Rv2436	Rv2336	Rv2470	Rv3418c
Rv2631	Rv2234	Rv2915c	Rv2438c	Rv2337c	Rv2471	Rv3419c
Rv2632c	Rv2235	Rv2916c	Rv2439c	Rv2338c	Rv2472	Rv3420c
Rv2633c	Rv2236c	Rv2917	Rv2440c	Rv2339	Rv2473	Rv3421c
Rv2636	Rv2237	Rv2918c	Rv2442c	Rv2340c	Rv2474c	Rv3422c
Rv2638	Rv2238c	Rv2919c	Rv2443	Rv2341	Rv2476c	Rv3423c
Rv2640c	Rv2240c	Rv2921c	Rv2444c	Rv2343c	Rv2477c	Rv3427c
Rv2641	Rv2241	Rv2922A	Rv2445c	Rv2344c	Rv2478c	Rv3432c
Rv2642	Rv2242	Rv2922c	Rv2447c	Rv2345	Rv2479c	Rv3433c
Rv2643	Rv2243	Rv2924c	Rv2448c	Rv2353c	Rv2481c	Rv3434c
Rv2645	Rv2244	Rv2926c	Rv2449c	Rv2355	Rv2482c	Rv3436c
Rv2646	Rv2245	Rv2927c	Rv2450c	Rv2356c	Rv2483c	Rv3438
Rv2650c	Rv2246	Rv2930	Rv2453c	Rv2357c	Rv2484c	Rv3439c
Rv2651c	Rv2247	Rv2931	Rv2454c	Rv2358	Rv2485c	Rv3440c
Rv2652c	Rv2248	Rv2932	Rv2455c	Rv2359	Rv2486	Rv3441c
Rv2653c	Rv2249c	Rv2933	Rv2456c	Rv2360c	Rv2487c	Rv3442c
Rv2655c	Rv2250.1	Rv2934	Rv2457c	Rv2361c	Rv2488c	Rv3443c
Rv2656c	Rv2250c	Rv2935	Rv2458	Rv2362c	Rv2489c	Rv3445c
Rv2657c	Rv2251	Rv2936	Rv2459	Rv2363	Rv2490c	Rv3446c
Rv2659c	Rv2252	Rv2937	Rv2460c	Rv2365c	Rv2491	Rv3447c
Rv2661c	Rv2253	Rv2939	Rv2461c	Rv2366c	Rv2492	Rv3449
Rv2664	Rv2255c	Rv2940c	Rv2462c	Rv2367c	Rv2493	Rv3450c
Rv2667	Rv2257c	Rv2941	Rv2463	Rv2368c	Rv2495c	Rv3451
Rv2669	Rv2258c	Rv2942	Rv2464c	Rv2369c	Rv2496c	Rv3455c
Rv2670c	Rv2259	Rv2943	Rv2465c	Rv2370c	Rv2497c	Rv3457c
Rv2671	Rv2260	Rv2943.1	Rv2466c	Rv2371	Rv2498c	Rv3458c
Rv2673	Rv2262c	Rv2944	Rv2467	Rv2372c	Rv2499c	Rv3459c
Rv2674	Rv2263	Rv2945c	Rv2468c	Rv2373c	Rv2500c	Rv3460c
Rv2675c	Rv2264c	Rv2946c	Rv2469c	Rv2374c	Rv2501c	Rv3461c
Rv2676c	Rv2265	Rv2948c	Rv2470	Rv2378c	Rv2502c	Rv3462c
Rv2677c	Rv2266	Rv2949c	Rv2471	Rv2379c	Rv2503c	Rv3463
Rv2678c	Rv2267c	Rv2950c	Rv2474c	Rv2380c	Rv2505c	Rv3464
Rv2679	Rv2268c	Rv2951c	Rv2476c	Rv2381c	Rv2506	Rv3473c
Rv2681	Rv2269c	Rv2952	Rv2477c	Rv2382c	Rv2507	Rv3481c
Rv2682c	Rv2273	Rv2953	Rv2478c	Rv2383c	Rv2508c	Rv3484

Rv2683	Rv2274c	Rv2954c	Rv2479c	Rv2384	Rv2509	Rv3485c
Rv2684	Rv2275	Rv2955c	Rv2480c	Rv2385	Rv2510c	Rv3487c
Rv2685	Rv2276	Rv2957	Rv2481c	Rv2386c	Rv2511	Rv3489
Rv2686c	Rv2277c	Rv2958c	Rv2482c	Rv2387	Rv2512c	Rv3490
Rv2687c	Rv2278	Rv2960c	Rv2483c	Rv2388c	Rv2513	Rv3491
Rv2688c	Rv2279	Rv2962c	Rv2484c	Rv2389c	Rv2514c	Rv3492c
Rv2689c	Rv2280	Rv2964	Rv2485c	Rv2390c	Rv2515c	Rv3493c
Rv2691	Rv2281	Rv2966c	Rv2486	Rv2391	Rv2516c	Rv3495c
Rv2692	Rv2282c	Rv2967c	Rv2488c	Rv2392	Rv2517c	Rv3496c
Rv2693c	Rv2284	Rv2969c	Rv2489c	Rv2393	Rv2518c	Rv3497c
Rv2694c	Rv2285	Rv2970c	Rv2491	Rv2394	Rv2520c	Rv3498c
Rv2695	Rv2286c	Rv2971	Rv2492	Rv2395	Rv2521	Rv3500c
Rv2696c	Rv2287	Rv2973c	Rv2493	Rv2397c	Rv2522c	Rv3501c
Rv2697c	Rv2288	Rv2974c	Rv2494	Rv2398c	Rv2523c	Rv3502c
Rv2698	Rv2289	Rv2975c	Rv2495c	Rv2399c	Rv2524c	Rv3504
Rv2700	Rv2290	Rv2976c	Rv2496c	Rv2400c	Rv2528c	Rv3505
Rv2701c	Rv2292c	Rv2977c	Rv2497c	Rv2401	Rv2529	Rv3506
Rv2702	Rv2294	Rv2978c	Rv2498c	Rv2402	Rv2530A	Rv3509c
Rv2703	Rv2295	Rv2979c	Rv2499c	Rv2403c	Rv2531c	Rv3510c
Rv2704	Rv2296	Rv2981c	Rv2500c	Rv2404c	Rv2532c	Rv3513c
Rv2705c	Rv2297	Rv2982c	Rv2501c	Rv2405	Rv2533c	Rv3515c
Rv2707	Rv2298	Rv2983	Rv2502c	Rv2406c	Rv2534c	Rv3516
Rv2711	Rv2299c	Rv2984	Rv2503c	Rv2408	Rv2535c	Rv3517
Rv2713	Rv2300c	Rv2985	Rv2505c	Rv2409c	Rv2536	Rv3518c
Rv2714	Rv2303c	Rv2986c	Rv2506	Rv2410c	Rv2537c	Rv3519
Rv2715	Rv2304c	Rv2987c	Rv2507	Rv2411c	Rv2538c	Rv3521
Rv2716	Rv2305	Rv2988c	Rv2508c	Rv2412	Rv2539c	Rv3522
Rv2718c	Rv2306.2	Rv2989	Rv2509	Rv2413c	Rv2540c	Rv3523
Rv2719c	Rv2306c	Rv2990c	Rv2510c	Rv2414c	Rv2541	Rv3525c
Rv2720	Rv2307.2	Rv2991	Rv2511	Rv2415c	Rv2542	Rv3526
Rv2721c	Rv2307.4	Rv2992c	Rv2512c	Rv2416c	Rv2543	Rv3527
Rv2723	Rv2307c	Rv2993c	Rv2513	Rv2417c	Rv2544	Rv3529c
Rv2724c	Rv2308	Rv2994	Rv2514c	Rv2418c	Rv2545	Rv3530c
Rv2725c	Rv2309.1	Rv2996c	Rv2515c	Rv2419c	Rv2548	Rv3531c
Rv2726c	Rv2309c	Rv2997	Rv2516c	Rv2420c	Rv2549c	Rv3534c
Rv2727c	Rv2310	Rv2998	Rv2517c	Rv2421c	Rv2550c	Rv3535c
Rv2729c	Rv2311	Rv2998.1	Rv2521	Rv2422	Rv2551c	Rv3536c
Rv2730	Rv2313c	Rv3000	Rv2522c	Rv2423	Rv2552c	Rv3537
Rv2731	Rv2314c	Rv3001c	Rv2523c	Rv2425c	Rv2553c	Rv3538
Rv2732c	Rv2315c	Rv3002c	Rv2524c	Rv2426c	Rv2554c	Rv3542c
Rv2733c	Rv2316	Rv3003c	Rv2525c	Rv2427c	Rv2555c	Rv3543c
Rv2734	Rv2317	Rv3004	Rv2526	Rv2428	Rv2556c	Rv3544c
Rv2735c	Rv2318	Rv3006	Rv2527	Rv2429	Rv2557	Rv3545c
Rv2736c	Rv2319c	Rv3009c	Rv2528c	Rv2430c	Rv2558	Rv3546
Rv2737c	Rv2320c	Rv3010c	Rv2529	Rv2431c	Rv2559c	Rv3547
Rv2739c	Rv2321c	Rv3011c	Rv2530A	Rv2432c	Rv2560	Rv3548c
Rv2742c	Rv2322c	Rv3014c	Rv2530c	Rv2434c	Rv2561	Rv3549c
Rv2743c	Rv2323c	Rv3024c	Rv2531c	Rv2435c	Rv2562	Rv3550
Rv2744c	Rv2324	Rv3026c	Rv2534c	Rv2436	Rv2563	Rv3551
Rv2745c	Rv2325c	Rv3027c	Rv2535c	Rv2437	Rv2564	Rv3552
Rv2746c	Rv2326c	Rv3028c	Rv2536	Rv2438c	Rv2565	Rv3553

Rv2748c	Rv2327	Rv3030	Rv2537c	Rv2439c	Rv2566	Rv3555c
Rv2750	Rv2328	Rv3032	Rv2538c	Rv2440c	Rv2567	Rv3556c
Rv2751	Rv2329c	Rv3033	Rv2539c	Rv2442c	Rv2568c	Rv3557c
Rv2752c	Rv2330c	Rv3034c	Rv2540c	Rv2443	Rv2570	Rv3559c
Rv2753c	Rv2331	Rv3035	Rv2541	Rv2444c	Rv2572c	Rv3560c
Rv2754c	Rv2331.1	Rv3037c	Rv2542	Rv2445c	Rv2573	Rv3561
Rv2756c	Rv2332	Rv3038c	Rv2544	Rv2447c	Rv2574	Rv3562
Rv2757c	Rv2333c	Rv3039c	Rv2546	Rv2448c	Rv2575	Rv3563
Rv2758c	Rv2334	Rv3042c	Rv2547	Rv2449c	Rv2576c	Rv3564
Rv2759c	Rv2335	Rv3044	Rv2549c	Rv2450c	Rv2577	Rv3565
Rv2760c	Rv2336	Rv3045	Rv2550c	Rv2453c	Rv2578c	Rv3566c
Rv2761c	Rv2337c	Rv3048c	Rv2551c	Rv2454c	Rv2579	Rv3567c
Rv2762c	Rv2338c	Rv3049c	Rv2552c	Rv2455c	Rv2580c	Rv3568c
Rv2763c	Rv2339	Rv3050c	Rv2553c	Rv2456c	Rv2581c	Rv3569c
Rv2765	Rv2340c	Rv3052c	Rv2554c	Rv2457c	Rv2582	Rv3570c
Rv2766c	Rv2341	Rv3053c	Rv2555c	Rv2458	Rv2583c	Rv3571
Rv2772c	Rv2343c	Rv3054c	Rv2556c	Rv2459	Rv2584c	Rv3573c
Rv2773c	Rv2344c	Rv3056	Rv2557	Rv2460c	Rv2585c	Rv3574
Rv2774c	Rv2345	Rv3058c	Rv2558	Rv2461c	Rv2586c	Rv3575c
Rv2776c	Rv2347c	Rv3059	Rv2559c	Rv2462c	Rv2587c	Rv3577
Rv2777c	Rv2349c	Rv3060c	Rv2560	Rv2463	Rv2589	Rv3578
Rv2778c	Rv2350c	Rv3061c	Rv2561	Rv2464c	Rv2590	Rv3579c
Rv2779c	Rv2351c	Rv3062	Rv2562	Rv2465c	Rv2592c	Rv3580c
Rv2780	Rv2352c	Rv3063	Rv2563	Rv2466c	Rv2593c	Rv3581c
Rv2781c	Rv2354	Rv3066	Rv2564	Rv2467	Rv2594c	Rv3582c
Rv2782c	Rv2355	Rv3071	Rv2565	Rv2468c	Rv2595	Rv3583c
Rv2783c	Rv2356c	Rv3072c	Rv2566	Rv2469c	Rv2596	Rv3585
Rv2784c	Rv2357c	Rv3074	Rv2567	Rv2470	Rv2597	Rv3586
Rv2785c	Rv2359	Rv3076	Rv2569c	Rv2471	Rv2599	Rv3587c
Rv2786c	Rv2360c	Rv3077	Rv2570	Rv2472	Rv2601	Rv3588c
Rv2788	Rv2361c	Rv3079c	Rv2571c	Rv2473	Rv2601A	Rv3589
Rv2789c	Rv2362c	Rv3080c	Rv2572c	Rv2474c	Rv2602	Rv3591c
Rv2790c	Rv2363	Rv3081	Rv2573	Rv2475c	Rv2603c	Rv3593
Rv2792c	Rv2364c	Rv3083	Rv2574	Rv2476c	Rv2604c	Rv3596c
Rv2793c	Rv2366c	Rv3084	Rv2575	Rv2477c	Rv2605c	Rv3597c
Rv2794c	Rv2368c	Rv3085	Rv2578c	Rv2478c	Rv2606c	Rv3598c
Rv2795c	Rv2369c	Rv3086	Rv2579	Rv2479c	Rv2607	Rv3600c
Rv2796c	Rv2370c	Rv3087	Rv2580c	Rv2481c	Rv2608	Rv3602c
Rv2797c	Rv2371	Rv3088	Rv2581c	Rv2482c	Rv2609c	Rv3604c
Rv2798c	Rv2372c	Rv3089	Rv2582	Rv2483c	Rv2610c	Rv3606c
Rv2800	Rv2373c	Rv3090	Rv2583c	Rv2484c	Rv2611c	Rv3608c
Rv2802c	Rv2374c	Rv3091	Rv2584c	Rv2485c	Rv2613c	Rv3609c
Rv2803	Rv2375	Rv3092c	Rv2585c	Rv2486	Rv2614.1	Rv3610c
Rv2807	Rv2378c	Rv3093c	Rv2586c	Rv2488c	Rv2614c	Rv3617
Rv2808	Rv2379c	Rv3094c	Rv2587c	Rv2489c	Rv2616	Rv3618
Rv2809	Rv2380c	Rv3095	Rv2589	Rv2490c	Rv2617c	Rv3623
Rv2811	Rv2381c	Rv3100c	Rv2590	Rv2491	Rv2618	Rv3624c
Rv2812	Rv2382c	Rv3101c	Rv2592c	Rv2492	Rv2620c	Rv3625c
Rv2813	Rv2383c	Rv3102c	Rv2593c	Rv2493	Rv2621c	Rv3626c
Rv2816c	Rv2384	Rv3105c	Rv2594c	Rv2494	Rv2622	Rv3627c
Rv2817c	Rv2385	Rv3106	Rv2596	Rv2495c	Rv2623	Rv3628

Rv2819c	Rv2386c	Rv3109	Rv2597	Rv2496c	Rv2624c	Rv3629c
Rv2820c	Rv2388c	Rv3111	Rv2599	Rv2497c	Rv2625c	Rv3630
Rv2821c	Rv2389c	Rv3114	Rv2601A	Rv2498c	Rv2627c	Rv3632
Rv2822c	Rv2390c	Rv3116	Rv2603c	Rv2499c	Rv2628	Rv3633
Rv2823c	Rv2391	Rv3119	Rv2604c	Rv2500c	Rv2629	Rv3635
Rv2824c	Rv2392	Rv3122	Rv2605c	Rv2501c	Rv2631	Rv3640c
Rv2825c	Rv2393	Rv3124	Rv2606c	Rv2502c	Rv2632c	Rv3642c
Rv2826c	Rv2394	Rv3125c	Rv2607	Rv2503c	Rv2633c	Rv3644c
Rv2827c	Rv2395	Rv3126c	Rv2609c	Rv2504c	Rv2634c	Rv3645
Rv2828c	Rv2397c	Rv3127	Rv2610c	Rv2505c	Rv2635	Rv3646c
Rv2831	Rv2398c	Rv3130c	Rv2611c	Rv2506	Rv2636	Rv3647c
Rv2832c	Rv2399c	Rv3131	Rv2612c	Rv2507	Rv2638	Rv3649
Rv2833c	Rv2400c	Rv3132c	Rv2613c	Rv2508c	Rv2639c	Rv3651
Rv2834c	Rv2401	Rv3133c	Rv2614.1	Rv2509	Rv2643	Rv3654c
Rv2837c	Rv2402	Rv3134c	Rv2614c	Rv2510c	Rv2644c	Rv3655c
Rv2838c	Rv2403c	Rv3135	Rv2617c	Rv2511	Rv2649	Rv3657c
Rv2839c	Rv2404c	Rv3138	Rv2618	Rv2512c	Rv2660c	Rv3658c
Rv2840c	Rv2405	Rv3139	Rv2620c	Rv2513	Rv2661c	Rv3659c
Rv2841c	Rv2406c	Rv3140	Rv2621c	Rv2514c	Rv2663	Rv3660c
Rv2842c	Rv2407	Rv3142c	Rv2622	Rv2515c	Rv2665	Rv3661
Rv2843	Rv2408	Rv3143	Rv2623	Rv2516c	Rv2667	Rv3662c
Rv2844	Rv2409c	Rv3144c	Rv2624c	Rv2518c	Rv2668	Rv3663c
Rv2845c	Rv2410c	Rv3145	Rv2625c	Rv2520c	Rv2669	Rv3664c
Rv2846c	Rv2411c	Rv3146	Rv2626c	Rv2521	Rv2670c	Rv3665c
Rv2847c	Rv2412	Rv3147	Rv2627c	Rv2522c	Rv2671	Rv3668c
Rv2848c	Rv2413c	Rv3148	Rv2628	Rv2523c	Rv2672	Rv3669
Rv2849c	Rv2414c	Rv3150	Rv2629	Rv2524c	Rv2673	Rv3670
Rv2850c	Rv2415c	Rv3151	Rv2630	Rv2525c	Rv2676c	Rv3671c
Rv2851c	Rv2416c	Rv3152	Rv2631	Rv2526	Rv2677c	Rv3672c
Rv2852c	Rv2417c	Rv3153	Rv2632c	Rv2527	Rv2678c	Rv3673c
Rv2855	Rv2418c	Rv3157	Rv2633c	Rv2528c	Rv2679	Rv3674c
Rv2856	Rv2419c	Rv3158	Rv2635	Rv2529	Rv2680	Rv3675
Rv2857c	Rv2421c	Rv3159c	Rv2636	Rv2530A	Rv2681	Rv3676
Rv2858c	Rv2422	Rv3160c	Rv2637	Rv2531c	Rv2682c	Rv3677c
Rv2860c	Rv2423	Rv3161c	Rv2638	Rv2532c	Rv2683	Rv3678.1
Rv2861c	Rv2424c	Rv3163c	Rv2643	Rv2533c	Rv2684	Rv3678c
Rv2862c	Rv2425c	Rv3164c	Rv2644c	Rv2534c	Rv2685	Rv3679
Rv2863	Rv2426c	Rv3165c	Rv2646	Rv2535c	Rv2686c	Rv3680
Rv2865	Rv2427c	Rv3166c	Rv2647	Rv2536	Rv2687c	Rv3681c
Rv2867c	Rv2428	Rv3168	Rv2648	Rv2537c	Rv2688c	Rv3682
Rv2868c	Rv2429	Rv3170	Rv2649	Rv2538c	Rv2689c	Rv3683
Rv2869c	Rv2430c	Rv3171c	Rv2650c	Rv2539c	Rv2690c	Rv3684
Rv2870c	Rv2431c	Rv3173c	Rv2651c	Rv2540c	Rv2691	Rv3687c
Rv2872	Rv2432c	Rv3174	Rv2652c	Rv2541	Rv2692	Rv3688c
Rv2873	Rv2433c	Rv3175	Rv2653c	Rv2542	Rv2694c	Rv3689
Rv2874	Rv2434c	Rv3176c	Rv2655c	Rv2543	Rv2695	Rv3690
Rv2878c	Rv2435c	Rv3177	Rv2657c	Rv2544	Rv2696c	Rv3691
Rv2880c	Rv2436	Rv3179	Rv2658c	Rv2545	Rv2697c	Rv3693
Rv2879c	Rv2437	Rv3182	Rv2659c	Rv2546	Rv2698	Rv3694c
Rv2881c	Rv2438.1	Rv3183	Rv2662	Rv2547	Rv2700	Rv3695
Rv2882c	Rv2438c	Rv3184	Rv2665	Rv2549c	Rv2701c	Rv3696c

Rv2883c	Rv2439c	Rv3186	Rv2666	Rv2551c	Rv2702	Rv3698
Rv2884	Rv2440c	Rv3188	Rv2667	Rv2552c	Rv2703	Rv3699
Rv2885c	Rv2441c	Rv3190c	Rv2668	Rv2553c	Rv2704	Rv3700c
Rv2888c	Rv2442c	Rv3191c	Rv2669	Rv2554c	Rv2706c	Rv3701c
Rv2889c	Rv2443	Rv3193c	Rv2670c	Rv2555c	Rv2707	Rv3702c
Rv2890c	Rv2444c	Rv3194c	Rv2671	Rv2556c	Rv2708c	Rv3703c
Rv2891	Rv2445c	Rv3195	Rv2672	Rv2557	Rv2709	Rv3704c
Rv2892c	Rv2447c	Rv3196	Rv2673	Rv2558	Rv2710	Rv3706c
Rv2893	Rv2448c	Rv3197	Rv2674	Rv2559c	Rv2711	Rv3707c
Rv2894c	Rv2449c	Rv3197.1	Rv2676c	Rv2560	Rv2712c	Rv3708c
Rv2897c	Rv2450c	Rv3198A	Rv2677c	Rv2561	Rv2713	Rv3709c
Rv2899c	Rv2451	Rv3198c	Rv2678c	Rv2562	Rv2714	Rv3710
Rv2900c	Rv2452c	Rv3199c	Rv2679	Rv2563	Rv2715	Rv3711c
Rv2901c	Rv2453c	Rv3200c	Rv2681	Rv2564	Rv2716	Rv3712
Rv2902c	Rv2454c	Rv3201c	Rv2682c	Rv2565	Rv2717c	Rv3714c
Rv2903c	Rv2455c	Rv3202c	Rv2683	Rv2566	Rv2718c	Rv3717
Rv2904c	Rv2456c	Rv3203	Rv2684	Rv2567	Rv2719c	Rv3718c
Rv2907c	Rv2457c	Rv3205c	Rv2685	Rv2568c	Rv2720	Rv3719
Rv2909c	Rv2458	Rv3206c	Rv2686c	Rv2569c	Rv2721c	Rv3720
Rv2910c	Rv2459	Rv3207c	Rv2687c	Rv2570	Rv2722	Rv3721c
Rv2911	Rv2460c	Rv3208.1	Rv2688c	Rv2571c	Rv2723	Rv3722c
Rv2912c	Rv2461c	Rv3210c	Rv2690c	Rv2572c	Rv2724c	Rv3723
Rv2913c	Rv2462c	Rv3211	Rv2691	Rv2573	Rv2725c	Rv3726
Rv2914c	Rv2463	Rv3212	Rv2692	Rv2574	Rv2727c	Rv3727
Rv2915c	Rv2464c	Rv3213c	Rv2693c	Rv2577	Rv2728c	Rv3730c
Rv2916c	Rv2465c	Rv3215	Rv2694c	Rv2578c	Rv2730	Rv3731
Rv2917	Rv2466c	Rv3216	Rv2695	Rv2579	Rv2731	Rv3733c
Rv2918c	Rv2467	Rv3218	Rv2696c	Rv2580c	Rv2732c	Rv3734c
Rv2919c	Rv2468c	Rv3220c	Rv2698	Rv2581c	Rv2733c	Rv3745c
Rv2920c	Rv2469c	Rv3221.1	Rv2701c	Rv2583c	Rv2734	Rv3752c
Rv2921c	Rv2470	Rv3221c	Rv2702	Rv2584c	Rv2735c	Rv3753c
Rv2922A	Rv2471	Rv3223c	Rv2703	Rv2585c	Rv2736c	Rv3754
Rv2923c	Rv2473	Rv3224	Rv2704	Rv2586c	Rv2737.1	Rv3755c
Rv2924c	Rv2474c	Rv3224.1	Rv2705c	Rv2588c	Rv2737c	Rv3756c
Rv2925c	Rv2475c	Rv3224.2	Rv2706c	Rv2589	Rv2738c	Rv3758c
Rv2927c	Rv2476c	Rv3225c	Rv2707	Rv2590	Rv2739c	Rv3759c
Rv2928	Rv2477c	Rv3226c	Rv2709	Rv2592c	Rv2740	Rv3760
Rv2930	Rv2478c	Rv3227	Rv2710	Rv2593c	Rv2741	Rv3761c
Rv2935	Rv2479c	Rv3228	Rv2711	Rv2594c	Rv2742c	Rv3762c
Rv2936	Rv2480c	Rv3229c	Rv2712c	Rv2595	Rv2743c	Rv3764c
Rv2937	Rv2481c	Rv3230c	Rv2713	Rv2596	Rv2744c	Rv3765c
Rv2939	Rv2482c	Rv3232c	Rv2714	Rv2597	Rv2745c	Rv3767c
Rv2941	Rv2483c	Rv3234c	Rv2715	Rv2599	Rv2746c	Rv3773c
Rv2942	Rv2484c	Rv3235	Rv2717c	Rv2601	Rv2747	Rv3774
Rv2943	Rv2485c	Rv3236c	Rv2718c	Rv2601A	Rv2748c	Rv3775
Rv2944	Rv2486	Rv3237c	Rv2719c	Rv2602	Rv2750	Rv3777
Rv2945c	Rv2488c	Rv3239c	Rv2720	Rv2603c	Rv2751	Rv3778c
Rv2947c	Rv2489c	Rv3240c	Rv2721c	Rv2604c	Rv2752c	Rv3780
Rv2948c	Rv2490c	Rv3242c	Rv2722	Rv2605c	Rv2753c	Rv3781
Rv2949c	Rv2491	Rv3244c	Rv2723	Rv2606c	Rv2754c	Rv3782
Rv2950c	Rv2492	Rv3245c	Rv2724c	Rv2607	Rv2755c	Rv3787c

Rv2951c	Rv2493	Rv3247c	Rv2725c	Rv2608	Rv2756c	Rv3788
Rv2952	Rv2494	Rv3248c	Rv2726c	Rv2609c	Rv2757c	Rv3790
Rv2953	Rv2495c	Rv3249c	Rv2727c	Rv2610c	Rv2758c	Rv3791
Rv2954c	Rv2496c	Rv3250c	Rv2728c	Rv2611c	Rv2759c	Rv3792
Rv2955c	Rv2497c	Rv3252c	Rv2729c	Rv2613c	Rv2760c	Rv3793
Rv2956	Rv2498c	Rv3254	Rv2730	Rv2614.1	Rv2761c	Rv3794
Rv2957	Rv2499c	Rv3255c	Rv2731	Rv2614c	Rv2762c	Rv3797
Rv2959c	Rv2500c	Rv3256c	Rv2732c	Rv2615c	Rv2763c	Rv3799c
Rv2960c	Rv2501c	Rv3257c	Rv2733c	Rv2616	Rv2764c	Rv3800c
Rv2961	Rv2502c	Rv3259	Rv2734	Rv2618	Rv2765	Rv3801c
Rv2962c	Rv2503c	Rv3260c	Rv2735c	Rv2621c	Rv2766c	Rv3802c
Rv2963	Rv2504c	Rv3261	Rv2736c	Rv2622	Rv2769c	Rv3803c
Rv2964	Rv2505c	Rv3262	Rv2737c	Rv2623	Rv2772c	Rv3804c
Rv2965c	Rv2506	Rv3263	Rv2738c	Rv2624c	Rv2773c	Rv3805c
Rv2966c	Rv2507	Rv3264c	Rv2739c	Rv2625c	Rv2775	Rv3806c
Rv2967c	Rv2508c	Rv3265c	Rv2741	Rv2626c	Rv2776c	Rv3808c
Rv2969c	Rv2509	Rv3266c	Rv2742c	Rv2627c	Rv2777c	Rv3809c
Rv2970c	Rv2510c	Rv3267	Rv2743c	Rv2628	Rv2778c	Rv3811
Rv2971	Rv2511	Rv3269	Rv2744c	Rv2629	Rv2779c	Rv3813c
Rv2972c	Rv2512c	Rv3270	Rv2745c	Rv2630	Rv2780	Rv3814c
Rv2973c	Rv2513	Rv3272	Rv2746c	Rv2631	Rv2782c	Rv3815c
Rv2974c	Rv2514c	Rv3273	Rv2748c	Rv2632c	Rv2783c	Rv3816c
Rv2976c	Rv2515c	Rv3274c	Rv2750	Rv2633c	Rv2784c	Rv3818
Rv2977c	Rv2516c	Rv3275c	Rv2751	Rv2635	Rv2785c	Rv3819
Rv2978c	Rv2517c	Rv3276c	Rv2752c	Rv2636	Rv2786c	Rv3821
Rv2979c	Rv2518c	Rv3279c	Rv2753c	Rv2637	Rv2787	Rv3823c
Rv2980	Rv2520c	Rv3280	Rv2754c	Rv2638	Rv2788	Rv3829c
Rv2982c	Rv2521	Rv3282	Rv2755c	Rv2639c	Rv2789c	Rv3830c
Rv2985	Rv2522c	Rv3283	Rv2756c	Rv2640c	Rv2790c	Rv3832c
Rv2986c	Rv2524c	Rv3285	Rv2757c	Rv2641	Rv2791c	Rv3833
Rv2987c	Rv2525c	Rv3286c	Rv2758c	Rv2643	Rv2792c	Rv3834c
Rv2988c	Rv2526	Rv3287c	Rv2759c	Rv2649	Rv2793c	Rv3835
Rv2989	Rv2527	Rv3288c	Rv2760c	Rv2660c	Rv2794c	Rv3838c
Rv2990c	Rv2528c	Rv3289c	Rv2761c	Rv2662	Rv2795c	Rv3839
Rv2991	Rv2529	Rv3290c	Rv2763c	Rv2663	Rv2796c	Rv3840
Rv2992c	Rv2530A	Rv3291c	Rv2764c	Rv2664	Rv2797c	Rv3842c
Rv2993c	Rv2530c	Rv3292	Rv2765	Rv2665	Rv2798c	Rv3846
Rv2994	Rv2531c	Rv3293	Rv2766c	Rv2666	Rv2800	Rv3849
Rv2995c	Rv2532c	Rv3294c	Rv2767c	Rv2667	Rv2801c	Rv3850
Rv2996c	Rv2533c	Rv3295	Rv2772c	Rv2668	Rv2802c	Rv3853
Rv2997	Rv2534c	Rv3296	Rv2773c	Rv2669	Rv2803	Rv3854c
Rv3000	Rv2535c	Rv3298c	Rv2776c	Rv2670c	Rv2804c	Rv3855
Rv3001c	Rv2536	Rv3299c	Rv2777c	Rv2671	Rv2805	Rv3856c
Rv3002c	Rv2537c	Rv3300c	Rv2778c	Rv2672	Rv2807	Rv3858c
Rv3003c	Rv2538c	Rv3302c	Rv2779c	Rv2673	Rv2809	Rv3859c
Rv3009c	Rv2539c	Rv3303c	Rv2780	Rv2674	Rv2811	Rv3860
Rv3010c	Rv2541	Rv3306c	Rv2781c	Rv2676c	Rv2812	Rv3876
Rv3012c	Rv2542	Rv3308	Rv2782c	Rv2677c	Rv2813	Rv3884c
Rv3013	Rv2543	Rv3310	Rv2783c	Rv2678c	Rv2814c	Rv3885c
Rv3014c	Rv2544	Rv3311	Rv2785c	Rv2679	Rv2816c	Rv3886c
Rv3015c	Rv2545	Rv3312c	Rv2786c	Rv2680	Rv2817c	Rv3887c

Rv3016	Rv2546	Rv3313c	Rv2787	Rv2681	Rv2818c	Rv3888c
Rv3018c	Rv2547	Rv3314c	Rv2788	Rv2682c	Rv2819c	Rv3889c
Rv3020c	Rv2548	Rv3315c	Rv2790c	Rv2683	Rv2820c	Rv3891c
Rv3024c	Rv2549c	Rv3317	Rv2791c	Rv2684	Rv2821c	Rv3893c
Rv3025c	Rv2550c	Rv3318	Rv2792c	Rv2685	Rv2822c	Rv3895c
Rv3026c	Rv2551c	Rv3319	Rv2793c	Rv2686c	Rv2823c	Rv3896c
Rv3027c	Rv2552c	Rv3321c	Rv2794c	Rv2687c	Rv2824c	Rv3897c
Rv3028c	Rv2553c	Rv3324c	Rv2795c	Rv2688c	Rv2825c	Rv3898c
Rv3029c	Rv2554c	Rv3325	Rv2797c	Rv2689c	Rv2826c	Rv3899c
Rv3030	Rv2555c	Rv3327	Rv2798c	Rv2690c	Rv2827c	Rv3901c
Rv3031	Rv2557	Rv3329	Rv2799	Rv2691	Rv2830c	Rv3902c
Rv3033	Rv2558	Rv3331	Rv2800	Rv2692	Rv2831	Rv3903c
Rv3035	Rv2559c	Rv3332	Rv2801c	Rv2694c	Rv2832c	Rv3904c
Rv3037c	Rv2560	Rv3333c	Rv2802c	Rv2696c	Rv2833c	Rv3906c
Rv3038c	Rv2561	Rv3334	Rv2803	Rv2697c	Rv2836c	Rv3907c
Rv3039c	Rv2562	Rv3336c	Rv2804c	Rv2700	Rv2837c	Rv3908
Rv3040c	Rv2563	Rv3338	Rv2805	Rv2701c	Rv2838c	Rv3910
Rv3041c	Rv2564	Rv3339c	Rv2807	Rv2702	Rv2839c	Rv3912
Rv3042c	Rv2565	Rv3341	Rv2809	Rv2703	Rv2841c	Rv3913
Rv3043c	Rv2566	Rv3342	Rv2810c	Rv2704	Rv2842c	Rv3914
Rv3044	Rv2567	Rv3350c	Rv2811	Rv2705c	Rv2843	Rv3915
Rv3045	Rv2568c	Rv3353c	Rv2812	Rv2706c	Rv2844	Rv3916c
Rv3046c	Rv2569c	Rv3357	Rv2813	Rv2708c	Rv2845c	Rv3917c
Rv3047c	Rv2570	Rv3359	Rv2814c	Rv2709	Rv2847c	Rv3918c
Rv3048c	Rv2571c	Rv3360	Rv2815c	Rv2710	Rv2848c	Rv3919c
Rv3049c	Rv2572c	Rv3361c	Rv2816c	Rv2711	Rv2849c	Rv3920c
Rv3050c	Rv2573	Rv3362c	Rv2817c	Rv2712c	Rv2850c	Rv3921c
Rv3051c	Rv2574	Rv3365c	Rv2818c	Rv2713	Rv2851c	Rv3922c
Rv3052c	Rv2575	Rv3370c	Rv2819c	Rv2714	Rv2852c	Rv3923c
Rv3054c	Rv2576c	Rv3371	Rv2820c	Rv2715	Rv2853	Rv3924c
Rv3055	Rv2577	Rv3372	Rv2821c	Rv2716	Rv2854	
Rv3056	Rv2578c	Rv3373	Rv2822c	Rv2717c	Rv2855	
Rv3059	Rv2579	Rv3374	Rv2823c	Rv2718c	Rv2856	
Rv3060c	Rv2580c	Rv3375	Rv2824c	Rv2719c	Rv2858c	
Rv3061c	Rv2581c	Rv3376	Rv2825c	Rv2720	Rv2859c	
Rv3062	Rv2582	Rv3377c	Rv2826c	Rv2721c	Rv2860c	
Rv3066	Rv2583c	Rv3381c	Rv2827c	Rv2722	Rv2862c	
Rv3067	Rv2585c	Rv3382c	Rv2828c	Rv2723	Rv2863	
Rv3068c	Rv2586c	Rv3384c	Rv2830c	Rv2724c	Rv2864c	
Rv3071	Rv2587c	Rv3385c	Rv2831	Rv2725c	Rv2865	
Rv3072c	Rv2588c	Rv3386	Rv2832c	Rv2726c	Rv2866	
Rv3073c	Rv2589	Rv3389c	Rv2833c	Rv2727c	Rv2867c	
Rv3074	Rv2590	Rv3390	Rv2834c	Rv2728c	Rv2868c	
Rv3075c	Rv2592c	Rv3391	Rv2835c	Rv2729c	Rv2870c	
Rv3076	Rv2593c	Rv3393	Rv2837c	Rv2730	Rv2871	
Rv3077	Rv2594c	Rv3394c	Rv2838c	Rv2731	Rv2873	
Rv3079c	Rv2595	Rv3395.1	Rv2839c	Rv2732c	Rv2874	
Rv3080c	Rv2596	Rv3395c	Rv2840c	Rv2733c	Rv2879c	
Rv3081	Rv2597	Rv3396c	Rv2841c	Rv2734	Rv2880c	
Rv3082c	Rv2599	Rv3397c	Rv2842c	Rv2735c	Rv2881c	
Rv3083	Rv2601	Rv3398c	Rv2844	Rv2736c	Rv2883c	

Rv3084	Rv2601A	Rv3399	Rv2845c	Rv2737.1	Rv2884
Rv3088	Rv2603c	Rv3400	Rv2846c	Rv2737c	Rv2885c
Rv3089	Rv2604c	Rv3401	Rv2847c	Rv2738c	Rv2886c
Rv3091	Rv2605c	Rv3402c	Rv2848c	Rv2739c	Rv2887
Rv3093c	Rv2606c	Rv3403c	Rv2849c	Rv2741	Rv2888c
Rv3094c	Rv2607	Rv3405c	Rv2850c	Rv2743c	Rv2889c
Rv3095	Rv2608	Rv3406	Rv2851c	Rv2744c	Rv2890c
Rv3096	Rv2609c	Rv3407	Rv2852c	Rv2745c	Rv2892c
Rv3098c	Rv2610c	Rv3408	Rv2854	Rv2747	Rv2894c
Rv3099c	Rv2611c	Rv3409c	Rv2855	Rv2748c	Rv2895c
Rv3100c	Rv2612c	Rv3410c	Rv2856	Rv2749	Rv2896c
Rv3101c	Rv2613c	Rv3411c	Rv2857c	Rv2750	Rv2897c
Rv3102c	Rv2614.1	Rv3413c	Rv2858c	Rv2751	Rv2898c
Rv3104c	Rv2614c	Rv3417c	Rv2859c	Rv2752c	Rv2899c
Rv3105c	Rv2615c	Rv3420c	Rv2860c	Rv2753c	Rv2900c
Rv3106	Rv2616	Rv3423c	Rv2861c	Rv2754c	Rv2901c
Rv3107c	Rv2617c	Rv3424c	Rv2862c	Rv2756c	Rv2902c
Rv3108	Rv2618	Rv3430c	Rv2863	Rv2757c	Rv2903c
Rv3109	Rv2620c	Rv3432c	Rv2864c	Rv2758c	Rv2904c
Rv3110	Rv2621c	Rv3433c	Rv2865	Rv2759c	Rv2905
Rv3111	Rv2622	Rv3434c	Rv2867c	Rv2760c	Rv2906c
Rv3114	Rv2623	Rv3435c	Rv2868c	Rv2761c	Rv2907c
Rv3116	Rv2624c	Rv3436c	Rv2869c	Rv2762c	Rv2909c
Rv3119	Rv2625c	Rv3437	Rv2870c	Rv2763c	Rv2910c
Rv3120	Rv2626c	Rv3438	Rv2874	Rv2764c	Rv2911
Rv3123	Rv2627c	Rv3441c	Rv2878c	Rv2765	Rv2912c
Rv3125c	Rv2628	Rv3442c	Rv2879c	Rv2766c	Rv2913c
Rv3126c	Rv2629	Rv3443c	Rv2880c	Rv2767c	Rv2914c
Rv3127	Rv2630	Rv3444c	Rv2881c	Rv2768c	Rv2915c
Rv3129	Rv2631	Rv3446c	Rv2882c	Rv2772c	Rv2916c
Rv3131	Rv2632c	Rv3447c	Rv2883c	Rv2773c	Rv2917
Rv3132c	Rv2633c	Rv3448	Rv2884	Rv2774c	Rv2918c
Rv3133c	Rv2634c	Rv3449	Rv2885c	Rv2775	Rv2919c
Rv3134c	Rv2635	Rv3450c	Rv2886c	Rv2776c	Rv2921c
Rv3136	Rv2636	Rv3451	Rv2887	Rv2777c	Rv2922c
Rv3137	Rv2638	Rv3453	Rv2888c	Rv2779c	Rv2924c
Rv3138	Rv2641	Rv3455c	Rv2889c	Rv2780	Rv2925c
Rv3139	Rv2642	Rv3456c	Rv2890c	Rv2781c	Rv2926c
Rv3140	Rv2643	Rv3457c	Rv2891	Rv2782c	Rv2927c
Rv3141	Rv2644c	Rv3458c	Rv2892c	Rv2783c	Rv2928
Rv3143	Rv2645	Rv3460c	Rv2893	Rv2784c	Rv2929
Rv3146	Rv2646	Rv3461c	Rv2894c	Rv2785c	Rv2930
Rv3147	Rv2647	Rv3462c	Rv2896c	Rv2786c	Rv2931
Rv3148	Rv2648	Rv3463	Rv2897c	Rv2787	Rv2932
Rv3149	Rv2649	Rv3464	Rv2898c	Rv2788	Rv2933
Rv3150	Rv2650c	Rv3465	Rv2900c	Rv2789c	Rv2934
Rv3151	Rv2651c	Rv3466	Rv2901c	Rv2790c	Rv2935
Rv3154	Rv2654c	Rv3467	Rv2902c	Rv2791c	Rv2936
Rv3155	Rv2655c	Rv3468c	Rv2903c	Rv2792c	Rv2937
Rv3156	Rv2656c	Rv3470c	Rv2904c	Rv2793c	Rv2939
Rv3158	Rv2657c	Rv3472	Rv2905	Rv2794c	Rv2940c

Rv3159c	Rv2659c	Rv3473c	Rv2907c	Rv2795c	Rv2941
Rv3160c	Rv2660c	Rv3474	Rv2908c	Rv2796c	Rv2942
Rv3161c	Rv2661c	Rv3479	Rv2910c	Rv2797c	Rv2943
Rv3163c	Rv2662	Rv3480c	Rv2911	Rv2799	Rv2943.1
Rv3164c	Rv2663	Rv3486	Rv2912c	Rv2800	Rv2945c
Rv3165c	Rv2666	Rv3487c	Rv2913c	Rv2801c	Rv2948c
Rv3166c	Rv2667	Rv3490	Rv2914c	Rv2802c	Rv2949c
Rv3167c	Rv2669	Rv3493c	Rv2916c	Rv2803	Rv2950c
Rv3168	Rv2670c	Rv3494c	Rv2917	Rv2804c	Rv2951c
Rv3169	Rv2671	Rv3495c	Rv2918c	Rv2805	Rv2952
Rv3170	Rv2672	Rv3496c	Rv2920c	Rv2807	Rv2953
Rv3171c	Rv2673	Rv3497c	Rv2921c	Rv2808	Rv2954c
Rv3173c	Rv2674	Rv3498c	Rv2922A	Rv2809	Rv2955c
Rv3174	Rv2675c	Rv3499c	Rv2922c	Rv2811	Rv2956
Rv3175	Rv2676c	Rv3501c	Rv2923c	Rv2812	Rv2957
Rv3176c	Rv2677c	Rv3502c	Rv2924c	Rv2813	Rv2958c
Rv3177	Rv2678c	Rv3505	Rv2925c	Rv2814c	Rv2959c
Rv3178	Rv2679	Rv3506	Rv2926c	Rv2816c	Rv2960c
Rv3180c	Rv2680	Rv3510c	Rv2927c	Rv2817c	Rv2961
Rv3181c	Rv2681	Rv3512	Rv2928	Rv2818c	Rv2962c
Rv3182	Rv2682c	Rv3513c	Rv2929	Rv2819c	Rv2963
Rv3183	Rv2683	Rv3515c	Rv2930	Rv2820c	Rv2965c
Rv3188	Rv2684	Rv3516	Rv2931	Rv2821c	Rv2966c
Rv3189	Rv2685	Rv3517	Rv2932	Rv2822c	Rv2967c
Rv3193c	Rv2686c	Rv3519	Rv2933	Rv2823c	Rv2968c
Rv3194c	Rv2688c	Rv3521	Rv2934	Rv2824c	Rv2969c
Rv3196	Rv2689c	Rv3522	Rv2935	Rv2825c	Rv2970c
Rv3197	Rv2690c	Rv3523	Rv2936	Rv2826c	Rv2971
Rv3197.1	Rv2691	Rv3526	Rv2937	Rv2827c	Rv2972c
Rv3198c	Rv2692	Rv3528c	Rv2939	Rv2828c	Rv2973c
Rv3198A	Rv2693c	Rv3529c	Rv2940c	Rv2830c	Rv2974c
Rv3199c	Rv2694c	Rv3532	Rv2941	Rv2831	Rv2976c
Rv3200c	Rv2695	Rv3534c	Rv2942	Rv2832c	Rv2977c
Rv3201c	Rv2696c	Rv3535c	Rv2943	Rv2833c	Rv2978c
Rv3202c	Rv2697c	Rv3536c	Rv2944	Rv2834c	Rv2979c
Rv3204	Rv2698	Rv3537	Rv2945c	Rv2835c	Rv2980
Rv3205c	Rv2701c	Rv3538	Rv2946c	Rv2837c	Rv2981c
Rv3206c	Rv2703	Rv3539	Rv2947c	Rv2838c	Rv2984
Rv3208	Rv2704	Rv3541c	Rv2948c	Rv2839c	Rv2985
Rv3208.1	Rv2705c	Rv3542c	Rv2949c	Rv2840c	Rv2986c
Rv3209	Rv2706c	Rv3543c	Rv2950c	Rv2841c	Rv2987c
Rv3210c	Rv2707	Rv3545c	Rv2951c	Rv2842c	Rv2988c
Rv3211	Rv2708c	Rv3546	Rv2952	Rv2843	Rv2989
Rv3212	Rv2709	Rv3549c	Rv2953	Rv2844	Rv2990c
Rv3213c	Rv2710	Rv3550	Rv2954c	Rv2845c	Rv2991
Rv3214	Rv2711	Rv3551	Rv2955c	Rv2846c	Rv2992c
Rv3215	Rv2712c	Rv3552	Rv2956	Rv2847c	Rv2994
Rv3216	Rv2713	Rv3553	Rv2957	Rv2848c	Rv2995c
Rv3218	Rv2714	Rv3554	Rv2958c	Rv2849c	Rv2996c
Rv3221.1	Rv2715	Rv3555c	Rv2960c	Rv2850c	Rv2997
Rv3222c	Rv2718c	Rv3556c	Rv2962c	Rv2851c	Rv2998

Rv3224	Rv2719c	Rv3557c	Rv2963	Rv2852c	Rv2998.1
Rv3225c	Rv2720	Rv3558	Rv2965c	Rv2854	Rv2999
Rv3226c	Rv2721c	Rv3559c	Rv2966c	Rv2855	Rv3000
Rv3227	Rv2722	Rv3560c	Rv2967c	Rv2857c	Rv3001c
Rv3228	Rv2723	Rv3561	Rv2969c	Rv2858c	Rv3002c
Rv3229c	Rv2724c	Rv3562	Rv2970c	Rv2860c	Rv3003c
Rv3230c	Rv2725c	Rv3563	Rv2971	Rv2861c	Rv3005c
Rv3231c	Rv2726c	Rv3564	Rv2972c	Rv2862c	Rv3006
Rv3232c	Rv2727c	Rv3565	Rv2973c	Rv2864c	Rv3008
Rv3235	Rv2728c	Rv3566c	Rv2974c	Rv2865	Rv3009c
Rv3236c	Rv2729c	Rv3567c	Rv2975c	Rv2866	Rv3010c
Rv3237c	Rv2731	Rv3568c	Rv2977c	Rv2867c	Rv3011c
Rv3238c	Rv2732c	Rv3569c	Rv2978c	Rv2868c	Rv3012c
Rv3728	Rv2733c	Rv3570c	Rv2979c	Rv2869c	Rv3013
Rv3240c	Rv2734	Rv3571	Rv2981c	Rv2870c	Rv3014c
Rv3241c	Rv2735c	Rv3573c	Rv2982c	Rv2871	Rv3015c
Rv3242c	Rv2736c	Rv3574	Rv2983	Rv2872	Rv3016
Rv3243c	Rv2737c	Rv3575c	Rv2984	Rv2873	Rv3023c
Rv3244c	Rv2738c	Rv3579c	Rv2985	Rv2874	Rv3024c
Rv3245c	Rv2739c	Rv3580c	Rv2986c	Rv2875	Rv3025c
Rv3246c	Rv2740	Rv3583c	Rv2988c	Rv2877c	Rv3026c
Rv3247c	Rv2742c	Rv3588c	Rv2989	Rv2878c	Rv3027c
Rv3248c	Rv2743c	Rv3589	Rv2990c	Rv2879c	Rv3028c
Rv3249c	Rv2744c	Rv3591c	Rv2991	Rv2880c	Rv3029c
Rv3252c	Rv2745c	Rv3593	Rv2992c	Rv2881c	Rv3030
Rv3253c	Rv2746c	Rv3594	Rv2993c	Rv2882c	Rv3031
Rv3254	Rv2747	Rv3596c	Rv2994	Rv2883c	Rv3032
Rv3255c	Rv2748c	Rv3598c	Rv2995c	Rv2884	Rv3033
Rv3256c	Rv2750	Rv3602c	Rv2996c	Rv2885c	Rv3034c
Rv3257c	Rv2751	Rv3603c	Rv2997	Rv2886c	Rv3035
Rv3259	Rv2752c	Rv3604c	Rv2998	Rv2887	Rv3037c
Rv3261	Rv2753c	Rv3607c	Rv2999	Rv2888c	Rv3038c
Rv3262	Rv2754c	Rv3609c	Rv3000	Rv2889c	Rv3039c
Rv3263	Rv2756c	Rv3610c	Rv3001c	Rv2890c	Rv3040c
Rv3264c	Rv2757c	Rv3612c	Rv3002c	Rv2891	Rv3041c
Rv3265c	Rv2758c	Rv3614c	Rv3003c	Rv2892c	Rv3042c
Rv3266c	Rv2759c	Rv3620c	Rv3004	Rv2893	Rv3043c
Rv3267	Rv2760c	Rv3625c	Rv3006	Rv2894c	Rv3044
Rv3269	Rv2761c	Rv3628	Rv3008	Rv2895c	Rv3045
Rv3270	Rv2762c	Rv3631	Rv3009c	Rv2896c	Rv3046c
Rv3271c	Rv2763c	Rv3633	Rv3010c	Rv2897c	Rv3048c
Rv3272	Rv2764c	Rv3635	Rv3011c	Rv2898c	Rv3049c
Rv3273	Rv2765	Rv3636	Rv3012c	Rv2899c	Rv3050c
Rv3274c	Rv2766c	Rv3639c	Rv3014c	Rv2900c	Rv3051c
Rv3275c	Rv2767c	Rv3640c	Rv3015c	Rv2901c	Rv3052c
Rv3276c	Rv2770c	Rv3641c	Rv3023c	Rv2902c	Rv3054c
Rv3277	Rv2771c	Rv3642c	Rv3024c	Rv2903c	Rv3055
Rv3278c	Rv2772c	Rv3644c	Rv3025c	Rv2904c	Rv3056
Rv3279c	Rv2773c	Rv3645	Rv3026c	Rv2905	Rv3057c
Rv3280	Rv2776c	Rv3646c	Rv3027c	Rv2906c	Rv3058c
Rv3282	Rv2777c	Rv3647c	Rv3028c	Rv2907c	Rv3059

Rv3283	Rv2778c	Rv3648c	Rv3029c	Rv2908c	Rv3060c
Rv3284	Rv2779c	Rv3649	Rv3030	Rv2909c	Rv3061c
Rv3285	Rv2780	Rv3651	Rv3031	Rv2910c	Rv3062
Rv3286c	Rv2781c	Rv3658c	Rv3032	Rv2911	Rv3066
Rv3290c	Rv2782c	Rv3659c	Rv3033	Rv2912c	Rv3068c
Rv3291c	Rv2783c	Rv3660c	Rv3034c	Rv2913c	Rv3070
Rv3292	Rv2784c	Rv3662c	Rv3035	Rv2914c	Rv3071
Rv3293	Rv2785c	Rv3663c	Rv3037c	Rv2915c	Rv3072c
Rv3294c	Rv2786c	Rv3664c	Rv3038c	Rv2916c	Rv3073c
Rv3295	Rv2787	Rv3665c	Rv3039c	Rv2917	Rv3074
Rv3296	Rv2788	Rv3666c	Rv3040c	Rv2918c	Rv3075c
Rv3298c	Rv2789c	Rv3668c	Rv3041c	Rv2919c	Rv3076
Rv3299c	Rv2790c	Rv3670	Rv3042c	Rv2920c	Rv3077
Rv3300c	Rv2791c	Rv3671c	Rv3044	Rv2921c	Rv3079c
Rv3301c	Rv2792c	Rv3672c	Rv3045	Rv2922A	Rv3080c
Rv3303c	Rv2793c	Rv3673c	Rv3047c	Rv2922c	Rv3081
Rv3304	Rv2794c	Rv3674c	Rv3048c	Rv2923c	Rv3082c
Rv3305c	Rv2795c	Rv3675	Rv3049c	Rv2924c	Rv3083
Rv3306c	Rv2796c	Rv3676	Rv3050c	Rv2925c	Rv3084
Rv3307	Rv2797c	Rv3680	Rv3051c	Rv2926c	Rv3085
Rv3308	Rv2799	Rv3682	Rv3052c	Rv2927c	Rv3086
Rv3309c	Rv2800	Rv3683	Rv3055	Rv2928	Rv3087
Rv3310	Rv2801c	Rv3684	Rv3056	Rv2929	Rv3088
Rv3311	Rv2802c	Rv3685c	Rv3057c	Rv2930	Rv3089
Rv3312c	Rv2803	Rv3688c	Rv3058c	Rv2931	Rv3090
Rv3313c	Rv2804c	Rv3691	Rv3059	Rv2932	Rv3091
Rv3314c	Rv2805	Rv3692	Rv3060c	Rv2933	Rv3092c
Rv3315c	Rv2807	Rv3693	Rv3061c	Rv2934	Rv3093c
Rv3317	Rv2809	Rv3694c	Rv3062	Rv2935	Rv3094c
Rv3318	Rv2811	Rv3695	Rv3063	Rv2936	Rv3095
Rv3319	Rv2812	Rv3696c	Rv3066	Rv2938	Rv3096
Rv3320c	Rv2813	Rv3697c	Rv3067	Rv2939	Rv3098c
Rv3322c	Rv2814c	Rv3698	Rv3068c	Rv2940c	Rv3099c
Rv3323c	Rv2815c	Rv3699	Rv3069	Rv2941	Rv3100c
Rv3324c	Rv2817c	Rv3700c	Rv3071	Rv2942	Rv3101c
Rv3328c	Rv2818c	Rv3701c	Rv3072c	Rv2943	Rv3102c
Rv3329	Rv2819c	Rv3704c	Rv3073c	Rv2943.1	Rv3104c
Rv3330	Rv2820c	Rv3706c	Rv3074	Rv2945c	Rv3105c
Rv3332	Rv2821c	Rv3707c	Rv3075c	Rv2948c	Rv3106
Rv3333c	Rv2822c	Rv3708c	Rv3076	Rv2949c	Rv3107c
Rv3334	Rv2823c	Rv3709c	Rv3077	Rv2950c	Rv3108
Rv3336c	Rv2824c	Rv3710	Rv3078	Rv2951c	Rv3109
Rv3338	Rv2825c	Rv3711c	Rv3079c	Rv2952	Rv3110
Rv3339c	Rv2826c	Rv3712	Rv3080c	Rv2953	Rv3111
Rv3340	Rv2827c	Rv3714c	Rv3081	Rv2954c	Rv3112
Rv3341	Rv2828c	Rv3715c	Rv3082c	Rv2955c	Rv3113
Rv3342	Rv2830c	Rv3717	Rv3083	Rv2956	Rv3114
Rv3344c	Rv2831	Rv3718c	Rv3084	Rv2957	Rv3115
Rv3346c	Rv2832c	Rv3719	Rv3085	Rv2958c	Rv3116
Rv3844	Rv2833c	Rv3720	Rv3086	Rv2959c	Rv3118
Rv3348	Rv2834c	Rv3721c	Rv3087	Rv2960c	Rv3122

Rv3351c	Rv2835c	Rv3725	Rv3088	Rv2961	Rv3123
Rv3352c	Rv2836c	Rv3726	Rv3089	Rv2962c	Rv3124
Rv3353c	Rv2837c	Rv3727	Rv3090	Rv2963	Rv3125c
Rv3356c	Rv2838c	Rv3728	Rv3091	Rv2964	Rv3126c
Rv3357	Rv2839c	Rv3729	Rv3092c	Rv2965c	Rv3127
Rv3358	Rv2840c	Rv3730c	Rv3094c	Rv2966c	Rv3129
Rv3360	Rv2841c	Rv3732	Rv3095	Rv2967c	Rv3130c
Rv3361c	Rv2842c	Rv3734c	Rv3096	Rv2968c	Rv3131
Rv3362c	Rv2843	Rv3736	Rv3098c	Rv2969c	Rv3132c
Rv3363c	Rv2844	Rv3740c	Rv3100c	Rv2970c	Rv3133c
Rv3364c	Rv2845c	Rv3741c	Rv3101c	Rv2971	Rv3134c
Rv3366	Rv2846c	Rv3742c	Rv3102c	Rv2972c	Rv3135
Rv3368c	Rv2847c	Rv3743c	Rv3104c	Rv2973c	Rv3136
Rv3370c	Rv2848c	Rv3744	Rv3105c	Rv2974c	Rv3137
Rv3371	Rv2849c	Rv3747	Rv3106	Rv2976c	Rv3138
Rv3372	Rv2850c	Rv3749c	Rv3107c	Rv2977c	Rv3139
Rv3373	Rv2852c	Rv3750c	Rv3108	Rv2978c	Rv3140
Rv3374	Rv2854	Rv3751	Rv3109	Rv2979c	Rv3141
Rv3376	Rv2855	Rv3752c	Rv3111	Rv2980	Rv3143
Rv3377c	Rv2856	Rv3753c	Rv3113	Rv2981c	Rv3144c
Rv3378c	Rv2857c	Rv3754	Rv3114	Rv2982c	Rv3146
Rv3379c	Rv2858c	Rv3755c	Rv3115	Rv2983	Rv3147
Rv3383c	Rv2859c	Rv3756c	Rv3116	Rv2984	Rv3148
Rv3384c	Rv2860c	Rv3758c	Rv3118	Rv2985	Rv3149
Rv3385c	Rv2861c	Rv3759c	Rv3119	Rv2986c	Rv3150
Rv3386	Rv2862c	Rv3760	Rv3120	Rv2987c	Rv3151
Rv3387	Rv2864c	Rv3761c	Rv3121	Rv2988c	Rv3152
Rv3389c	Rv2865	Rv3762c	Rv3122	Rv2989	Rv3153
Rv3390	Rv2867c	Rv3764c	Rv3123	Rv2990c	Rv3155
Rv3391	Rv2868c	Rv3765c	Rv3124	Rv2991	Rv3157
Rv3392c	Rv2869c	Rv3766	Rv3125c	Rv2992c	Rv3158
Rv3393	Rv2870c	Rv3767c	Rv3126c	Rv2993c	Rv3159c
Rv3394c	Rv2871	Rv3769	Rv3127	Rv2994	Rv3160c
Rv3395c	Rv2873	Rv3770.1	Rv3129	Rv2995c	Rv3161c
Rv3396c	Rv2874	Rv3771c	Rv3130c	Rv2996c	Rv3162c
Rv3397c	Rv2877c	Rv3772	Rv3131	Rv2997	Rv3163c
Rv3398c	Rv2878c	Rv3774	Rv3132c	Rv2998	Rv3164c
Rv3400	Rv2879c	Rv3775	Rv3133c	Rv2998.1	Rv3165c
Rv3401	Rv2880c	Rv3776	Rv3135	Rv2999	Rv3166c
Rv3402c	Rv2881c	Rv3777	Rv3136	Rv3000	Rv3167c
Rv3403c	Rv2882c	Rv3778c	Rv3137	Rv3001c	Rv3168
Rv3404c	Rv2883c	Rv3779	Rv3138	Rv3002c	Rv3169
Rv3405c	Rv2884	Rv3780	Rv3139	Rv3003c	Rv3171c
Rv3406	Rv2885c	Rv3781	Rv3140	Rv3006	Rv3172c
Rv3408	Rv2886c	Rv3782	Rv3141	Rv3007c	Rv3173c
Rv3409c	Rv2887	Rv3783	Rv3142c	Rv3008	Rv3174
Rv3410c	Rv2888c	Rv3784	Rv3143	Rv3009c	Rv3175
Rv3411c	Rv2889c	Rv3786c	Rv3144c	Rv3010c	Rv3176c
Rv3413c	Rv2890c	Rv3787c	Rv3146	Rv3011c	Rv3177
Rv3414c	Rv2891	Rv3790	Rv3147	Rv3012c	Rv3178
Rv3415c	Rv2892c	Rv3791	Rv3148	Rv3013	Rv3179

Rv3416	Rv2893	Rv3792	Rv3149	Rv3014c	Rv3181c
Rv3417c	Rv2894c	Rv3793	Rv3150	Rv3015c	Rv3182
Rv3418c	Rv2895c	Rv3794	Rv3151	Rv3016	Rv3185
Rv3419c	Rv2896c	Rv3795	Rv3152	Rv3018c	Rv3187
Rv3420c	Rv2897c	Rv3796	Rv3154	Rv3020c	Rv3188
Rv3422c	Rv2898c	Rv3797	Rv3155	Rv3024c	Rv3189
Rv3423c	Rv2899c	Rv3799c	Rv3156	Rv3025c	Rv3190c
Rv3429	Rv2900c	Rv3800c	Rv3157	Rv3026c	Rv3191c
Rv3430c	Rv2901c	Rv3801c	Rv3158	Rv3027c	Rv3192
Rv3431c	Rv2902c	Rv3802c	Rv3160c	Rv3028c	Rv3193c
Rv3432c	Rv2903c	Rv3803c	Rv3161c	Rv3029c	Rv3194c
Rv3433c	Rv2904c	Rv3804c	Rv3163c	Rv3030	Rv3195
Rv3436c	Rv2905	Rv3805c	Rv3164c	Rv3031	Rv3196
Rv3437	Rv2906c	Rv3808c	Rv3165c	Rv3032	Rv3197
Rv3438	Rv2907c	Rv3809c	Rv3166c	Rv3033	Rv3197.1
Rv3440c	Rv2908c	Rv3811	Rv3167c	Rv3034c	Rv3198c
Rv3441c	Rv2909c	Rv3813c	Rv3168	Rv3035	Rv3199c
Rv3442c	Rv2910c	Rv3814c	Rv3169	Rv3036c	Rv3200c
Rv3443c	Rv2911	Rv3815c	Rv3170	Rv3037c	Rv3201c
Rv3444c	Rv2912c	Rv3817	Rv3171c	Rv3038c	Rv3202c
Rv3445c	Rv2913c	Rv3818	Rv3172c	Rv3039c	Rv3203
Rv3446c	Rv2914c	Rv3822	Rv3173c	Rv3040c	Rv3204
Rv3448	Rv2915c	Rv3823c	Rv3174	Rv3041c	Rv3205c
Rv3449	Rv2916c	Rv3824c	Rv3175	Rv3042c	Rv3206c
Rv3450c	Rv2917	Rv3825c	Rv3176c	Rv3043c	Rv3207c
Rv3452	Rv2918c	Rv3826	Rv3177	Rv3044	Rv3208
Rv3453	Rv2919c	Rv3827c	Rv3179	Rv3045	Rv3208.1
Rv3455c	Rv2920c	Rv3828c	Rv3181c	Rv3046c	Rv3209
Rv3456c	Rv2921c	Rv3829c	Rv3183	Rv3048c	Rv3210c
Rv3457c	Rv2922A	Rv3830c	Rv3184	Rv3049c	Rv3211
Rv3458c	Rv2922c	Rv3834c	Rv3185	Rv3050c	Rv3212
Rv3460c	Rv2923c	Rv3837c	Rv3186	Rv3051c	Rv3213c
Rv3463	Rv2924c	Rv3838c	Rv3187	Rv3052c	Rv3214
Rv3464	Rv2925c	Rv3839	Rv3189	Rv3053c	Rv3215
Rv3466	Rv2926c	Rv3846	Rv3190c	Rv3054c	Rv3216
Rv3468c	Rv2927c	Rv3849	Rv3191c	Rv3055	Rv3217c
Rv3469c	Rv2928	Rv3850	Rv3192	Rv3056	Rv3220c
Rv3470c	Rv2929	Rv3851	Rv3193c	Rv3057c	Rv3221.1
Rv3471c	Rv2930	Rv3852	Rv3194c	Rv3058c	Rv3221c
Rv3472	Rv2931	Rv3853	Rv3195	Rv3059	Rv3223c
Rv3476c	Rv2932	Rv3854c	Rv3196	Rv3060c	Rv3224
Rv3480c	Rv2933	Rv3855	Rv3196.1	Rv3061c	Rv3224.1
Rv3482c	Rv2934	Rv3856c	Rv3197	Rv3062	Rv3225c
Rv3484	Rv2935	Rv3858c	Rv3198c	Rv3063	Rv3226c
Rv3485c	Rv2936	Rv3859c	Rv3200c	Rv3066	Rv3227
Rv3486	Rv2937	Rv3860	Rv3201c	Rv3068c	Rv3228
Rv3487c	Rv2938	Rv3863	Rv3202c	Rv3071	Rv3229c
Rv3488	Rv2939	Rv3864	Rv3203	Rv3072c	Rv3230c
Rv3490	Rv2940c	Rv3865	Rv3204	Rv3073c	Rv3231c
Rv3492c	Rv2941	Rv3866	Rv3205c	Rv3074	Rv3232c
Rv3493c	Rv2942	Rv3868	Rv3206c	Rv3075c	Rv3235

Rv3494c	Rv2943	Rv3869	Rv3207c	Rv3076	Rv3237c
Rv3495c	Rv2943.1	Rv3870	Rv3208	Rv3077	Rv3239c
Rv3496c	Rv2944	Rv3871	Rv3210c	Rv3079c	Rv3240c
Rv3497c	Rv2945c	Rv3874	Rv3211	Rv3080c	Rv3241c
Rv3498c	Rv2946c	Rv3876	Rv3212	Rv3081	Rv3242c
Rv3499c	Rv2947c	Rv3877	Rv3213c	Rv3082c	Rv3243c
Rv3500c	Rv2948c	Rv3879c	Rv3214	Rv3083	Rv3244c
Rv3501c	Rv2949c	Rv3881c	Rv3215	Rv3084	Rv3245c
Rv3502c	Rv2950c	Rv3882c	Rv3218	Rv3085	Rv3246c
Rv3504	Rv2951c	Rv3884c	Rv3220c	Rv3086	Rv3247c
Rv3505	Rv2952	Rv3885c	Rv3221.1	Rv3087	Rv3248c
Rv3506	Rv2953	Rv3886c	Rv3221c	Rv3088	Rv3249c
Rv3509c	Rv2954c	Rv3887c	Rv3222c	Rv3089	Rv3250c
Rv3510c	Rv2955c	Rv3888c	Rv3223c	Rv3090	Rv3253c
Rv3513c	Rv2956	Rv3889c	Rv3224	Rv3091	Rv3254
Rv3515c	Rv2957	Rv3891c	Rv3224.1	Rv3092c	Rv3255c
Rv3516	Rv2958c	Rv3894c	Rv3224.2	Rv3093c	Rv3256c
Rv3517	Rv2959c	Rv3895c	Rv3225c	Rv3094c	Rv3257c
Rv3518c	Rv2960c	Rv3896c	Rv3226c	Rv3095	Rv3259
Rv3519	Rv2961	Rv3897c	Rv3227	Rv3096	Rv3260c
Rv3520c	Rv2962c	Rv3898c	Rv3228	Rv3097c	Rv3261
Rv3521	Rv2963	Rv3899c	Rv3229c	Rv3098c	Rv3262
Rv3522	Rv2964	Rv3900c	Rv3230c	Rv3099c	Rv3263
Rv3523	Rv2966c	Rv3904c	Rv3231c	Rv3100c	Rv3264c
Rv3524	Rv2967c	Rv3907c	Rv3232c	Rv3101c	Rv3265c
Rv3526	Rv2969c	Rv3908	Rv3233c	Rv3102c	Rv3266c
Rv3527	Rv2970c	Rv3909	Rv3234c	Rv3104c	Rv3267
Rv3528c	Rv2971	Rv3910	Rv3235	Rv3105c	Rv3268
Rv3529c	Rv2972c	Rv3911	Rv3236c	Rv3106	Rv3269
Rv3530c	Rv2973c	Rv3912	Rv3237c	Rv3107c	Rv3270
Rv3531c	Rv2974c	Rv3913	Rv3238c	Rv3108	Rv3271c
Rv3532	Rv2975c	Rv3914	Rv3239c	Rv3109	Rv3272
Rv3533c	Rv2976c	Rv3915	Rv3240c	Rv3110	Rv3273
Rv3534c	Rv2977c	Rv3916c	Rv3242c	Rv3111	Rv3274c
Rv3535c	Rv2978c	Rv3918c	Rv3243c	Rv3113	Rv3275c
Rv3536c	Rv2979c	Rv3919c	Rv3244c	Rv3114	Rv3276c
Rv3537	Rv2981c	Rv3922c	Rv3245c	Rv3116	Rv3277
Rv3538	Rv2982c	Rv3923c	Rv3246c	Rv3122	Rv3279c
Rv3539	Rv2983		Rv3247c	Rv3123	Rv3280
Rv3540c	Rv2984		Rv3248c	Rv3124	Rv3282
Rv3541c	Rv2985		Rv3249c	Rv3125c	Rv3283
Rv3542c	Rv2986c		Rv3250c	Rv3127	Rv3284
Rv3543c	Rv2987c		Rv3252c	Rv3129	Rv3285
Rv3545c	Rv2988c		Rv3253c	Rv3130c	Rv3286c
Rv3546	Rv2989		Rv3254	Rv3131	Rv3287c
Rv3547	Rv2990c		Rv3255c	Rv3132c	Rv3288c
Rv3548c	Rv2991		Rv3256c	Rv3133c	Rv3290c
Rv3549c	Rv2992c		Rv3257c	Rv3134c	Rv3291c
Rv3550	Rv2993c		Rv3259	Rv3135	Rv3292
Rv3551	Rv2994		Rv3260c	Rv3136	Rv3293
Rv3552	Rv2995c		Rv3261	Rv3137	Rv3294c

Rv3553	Rv2996c	Rv3262	Rv3138	Rv3295
Rv3554	Rv2997	Rv3263	Rv3139	Rv3296
Rv3555c	Rv2998	Rv3264c	Rv3140	Rv3297
Rv3556c	Rv2998.1	Rv3265c	Rv3141	Rv3299c
Rv3557c	Rv2999	Rv3266c	Rv3143	Rv3301c
Rv3559c	Rv3000	Rv3267	Rv3144c	Rv3302c
Rv3560c	Rv3001c	Rv3268	Rv3146	Rv3303c
Rv3561	Rv3002c	Rv3269	Rv3147	Rv3304
Rv3562	Rv3003c	Rv3270	Rv3148	Rv3305c
Rv3563	Rv3004	Rv3271c	Rv3149	Rv3306c
Rv3567c	Rv3006	Rv3272	Rv3150	Rv3307
Rv3568c	Rv3007c	Rv3273	Rv3151	Rv3308
Rv3569c	Rv3009c	Rv3274c	Rv3152	Rv3309c
Rv3570c	Rv3010c	Rv3275c	Rv3153	Rv3310
Rv3571	Rv3011c	Rv3276c	Rv3154	Rv3311
Rv3573c	Rv3012c	Rv3277	Rv3155	Rv3312c
Rv3575c	Rv3013	Rv3278c	Rv3156	Rv3313c
Rv3576	Rv3014c	Rv3279c	Rv3157	Rv3314c
Rv3579c	Rv3015c	Rv3280	Rv3158	Rv3315c
Rv3580c	Rv3016	Rv3282	Rv3159c	Rv3317
Rv3581c	Rv3023c	Rv3283	Rv3160c	Rv3318
Rv3582c	Rv3024c	Rv3284	Rv3161c	Rv3319
Rv3583c	Rv3025c	Rv3285	Rv3163c	Rv3322c
Rv3584	Rv3026c	Rv3286c	Rv3164c	Rv3323c
Rv3585	Rv3027c	Rv3287c	Rv3165c	Rv3324c
Rv3586	Rv3028c	Rv3288c	Rv3166c	Rv3326
Rv3588c	Rv3029c	Rv3290c	Rv3167c	Rv3327
Rv3589	Rv3030	Rv3291c	Rv3168	Rv3328c
Rv3592	Rv3031	Rv3292	Rv3169	Rv3329
Rv3594	Rv3032	Rv3293	Rv3170	Rv3330
Rv3595c	Rv3033	Rv3294c	Rv3171c	Rv3331
Rv3596c	Rv3034c	Rv3295	Rv3172c	Rv3332
Rv3598c	Rv3035	Rv3296	Rv3173c	Rv3333c
Rv3600c	Rv3037c	Rv3297	Rv3174	Rv3334
Rv3602c	Rv3038c	Rv3299c	Rv3175	Rv3335c
Rv3604c	Rv3039c	Rv3300c	Rv3176c	Rv3336c
Rv3607c	Rv3040c	Rv3301c	Rv3178	Rv3337
Rv3608c	Rv3041c	Rv3302c	Rv3179	Rv3339c
Rv3609c	Rv3042c	Rv3303c	Rv3180c	Rv3341
Rv3610c	Rv3043c	Rv3304	Rv3181c	Rv3342
Rv3615c	Rv3044	Rv3305c	Rv3182	Rv3344c
Rv3616c	Rv3045	Rv3306c	Rv3183	Rv3346c
Rv3617	Rv3048c	Rv3307	Rv3185	Rv3347c
Rv3618	Rv3049c	Rv3308	Rv3187	Rv3348
Rv3620c	Rv3050c	Rv3309c	Rv3188	Rv3349c
Rv3621c	Rv3051c	Rv3311	Rv3189	Rv3351c
Rv3623	Rv3052c	Rv3312c	Rv3190c	Rv3355c
Rv3624c	Rv3053c	Rv3313c	Rv3191c	Rv3356c
Rv3625c	Rv3054c	Rv3314c	Rv3193c	Rv3357
Rv3627c	Rv3055	Rv3318	Rv3194c	Rv3358
Rv3628	Rv3056	Rv3319	Rv3195	Rv3359

Rv3629c	Rv3057c	Rv3321c	Rv3196	Rv3360
Rv3630	Rv3058c	Rv3322c	Rv3196.1	Rv3361c
Rv3631	Rv3059	Rv3323c	Rv3197	Rv3362c
Rv3632	Rv3060c	Rv3324c	Rv3198c	Rv3363c
Rv3633	Rv3061c	Rv3325	Rv3199c	Rv3364c
Rv3634c	Rv3062	Rv3326	Rv3200c	Rv3365c
Rv3635	Rv3063	Rv3327	Rv3201c	Rv3368c
Rv3637	Rv3065	Rv3328c	Rv3202c	Rv3370c
Rv3638	Rv3066	Rv3329	Rv3203	Rv3371
Rv3639c	Rv3068c	Rv3330	Rv3204	Rv3372
Rv3640c	Rv3070	Rv3331	Rv3205c	Rv3373
Rv3641c	Rv3071	Rv3332	Rv3206c	Rv3375
Rv3644c	Rv3072c	Rv3333c	Rv3207c	Rv3377c
Rv3645	Rv3073c	Rv3334	Rv3208.1	Rv3378c
Rv3647c	Rv3074	Rv3339c	Rv3209	Rv3379c
Rv3649	Rv3075c	Rv3341	Rv3210c	Rv3380c
Rv3651	Rv3076	Rv3342	Rv3211	Rv3382c
Rv3655c	Rv3077	Rv3344c	Rv3212	Rv3383c
Rv3657c	Rv3078	Rv3348	Rv3213c	Rv3384c
Rv3658c	Rv3079c	Rv3349c	Rv3214	Rv3385c
Rv3659c	Rv3080c	Rv3350c	Rv3215	Rv3386
Rv3660c	Rv3081	Rv3351c	Rv3216	Rv3387
Rv3661	Rv3082c	Rv3355c	Rv3217c	Rv3389c
Rv3662c	Rv3083	Rv3356c	Rv3218	Rv3390
Rv3663c	Rv3084	Rv3357	Rv3220c	Rv3391
Rv3664c	Rv3085	Rv3359	Rv3221.1	Rv3392c
Rv3665c	Rv3086	Rv3360	Rv3222c	Rv3393
Rv3666c	Rv3087	Rv3361c	Rv3223c	Rv3394c
Rv3667	Rv3088	Rv3362c	Rv3224	Rv3395.1
Rv3669	Rv3089	Rv3363c	Rv3224.1	Rv3395c
Rv3670	Rv3090	Rv3365c	Rv3224.2	Rv3396c
Rv3671c	Rv3091	Rv3368c	Rv3225c	Rv3397c
Rv3672c	Rv3092c	Rv3370c	Rv3226c	Rv3398c
Rv3673c	Rv3093c	Rv3371	Rv3227	Rv3399
Rv3674c	Rv3094c	Rv3372	Rv3228	Rv3400
Rv3676	Rv3095	Rv3373	Rv3229c	Rv3401
Rv3677c	Rv3096	Rv3374	Rv3230c	Rv3402c
Rv3680	Rv3097c	Rv3375	Rv3231c	Rv3403c
Rv3682	Rv3099c	Rv3376	Rv3232c	Rv3404c
Rv3683	Rv3101c	Rv3377c	Rv3233c	Rv3405c
Rv3684	Rv3102c	Rv3378c	Rv3234c	Rv3406
Rv3685c	Rv3104c	Rv3379c	Rv3235	Rv3407
Rv3688c	Rv3105c	Rv3380c	Rv3236c	Rv3409c
Rv3690	Rv3106	Rv3381c	Rv3237c	Rv3410c
Rv3692	Rv3107c	Rv3382c	Rv3238c	Rv3411c
Rv3694c	Rv3108	Rv3383c	Rv3239c	Rv3413c
Rv3696c	Rv3109	Rv3384c	Rv3240c	Rv3414c
Rv3699	Rv3110	Rv3385c	Rv3241c	Rv3415c
Rv3700c	Rv3111	Rv3386	Rv3242c	Rv3416
Rv3701c	Rv3112	Rv3387	Rv3243c	Rv3417c
Rv3702c	Rv3113	Rv3389c	Rv3244c	Rv3418c

Rv3703c	Rv3115	Rv3391	Rv3245c	Rv3419c
Rv3707c	Rv3116	Rv3392c	Rv3246c	Rv3420c
Rv3708c	Rv3118	Rv3393	Rv3247c	Rv3422c
Rv3710	Rv3119	Rv3394c	Rv3248c	Rv3423c
Rv3711c	Rv3120	Rv3395c	Rv3249c	Rv3424c
Rv3712	Rv3121	Rv3396c	Rv3252c	Rv3425
Rv3713	Rv3122	Rv3397c	Rv3253c	Rv3430c
Rv3714c	Rv3123	Rv3398c	Rv3254	Rv3431c
Rv3715c	Rv3124	Rv3399	Rv3255c	Rv3432c
Rv3717	Rv3125c	Rv3400	Rv3256c	Rv3433c
Rv3718c	Rv3126c	Rv3401	Rv3257c	Rv3434c
Rv3719	Rv3127	Rv3403c	Rv3259	Rv3435c
Rv3721c	Rv3129	Rv3405c	Rv3261	Rv3436c
Rv3722c	Rv3130c	Rv3406	Rv3262	Rv3437
Rv3723	Rv3131	Rv3407	Rv3263	Rv3438
Rv3725	Rv3132c	Rv3408	Rv3264c	Rv3439c
Rv3726	Rv3133c	Rv3409c	Rv3265c	Rv3441c
Rv3729	Rv3134c	Rv3410c	Rv3266c	Rv3442c
Rv3730c	Rv3135	Rv3411c	Rv3267	Rv3443c
Rv3731	Rv3136	Rv3412	Rv3268	Rv3444c
Rv3732	Rv3137	Rv3413c	Rv3269	Rv3445c
Rv3733c	Rv3138	Rv3414c	Rv3270	Rv3446c
Rv3734c	Rv3139	Rv3416	Rv3272	Rv3447c
Rv3735	Rv3140	Rv3417c	Rv3273	Rv3448
Rv3736	Rv3141	Rv3418c	Rv3274c	Rv3449
Rv3737	Rv3143	Rv3419c	Rv3275c	Rv3450c
Rv3738c	Rv3146	Rv3420c	Rv3276c	Rv3451
Rv3740c	Rv3147	Rv3422c	Rv3277	Rv3454
Rv3741c	Rv3148	Rv3423.1	Rv3279c	Rv3455c
Rv3742c	Rv3149	Rv3423c	Rv3280	Rv3456c
Rv3743c	Rv3150	Rv3424c	Rv3281	Rv3457c
Rv3744	Rv3151	Rv3425	Rv3282	Rv3458c
Rv3746c	Rv3152	Rv3427c	Rv3285	Rv3460c
Rv3747	Rv3153	Rv3428c	Rv3286c	Rv3462c
Rv3748	Rv3154	Rv3429	Rv3287c	Rv3463
Rv3749c	Rv3155	Rv3430c	Rv3288c	Rv3464
Rv3750c	Rv3157	Rv3431c	Rv3289c	Rv3465
Rv3752c	Rv3158	Rv3432c	Rv3290c	Rv3466
Rv3754	Rv3159c	Rv3433c	Rv3291c	Rv3467
Rv3755c	Rv3160c	Rv3434c	Rv3292	Rv3468c
Rv3756c	Rv3161c	Rv3435c	Rv3293	Rv3469c
Rv3757c	Rv3163c	Rv3436c	Rv3294c	Rv3470c
Rv3758c	Rv3164c	Rv3438	Rv3295	Rv3472
Rv3759c	Rv3165c	Rv3439c	Rv3296	Rv3473c
Rv3760	Rv3166c	Rv3440c	Rv3297	Rv3475
Rv3761c	Rv3167c	Rv3441c	Rv3298c	Rv3476c
Rv3762c	Rv3168	Rv3442c	Rv3299c	Rv3477
Rv3763	Rv3169	Rv3443c	Rv3300c	Rv3478
Rv3764c	Rv3170	Rv3444c	Rv3301c	Rv3479
Rv3765c	Rv3171c	Rv3445c	Rv3302c	Rv3480c
Rv3767c	Rv3172c	Rv3446c	Rv3303c	Rv3481c

Rv3768	Rv3173c	Rv3447c	Rv3304	Rv3482c
Rv3769	Rv3174	Rv3448	Rv3305c	Rv3484
Rv3772	Rv3175	Rv3450c	Rv3306c	Rv3485c
Rv3773c	Rv3176c	Rv3451	Rv3307	Rv3486
Rv3774	Rv3177	Rv3452	Rv3308	Rv3487c
Rv3776	Rv3178	Rv3455c	Rv3309c	Rv3490
Rv3777	Rv3179	Rv3456c	Rv3310	Rv3492c
Rv3778c	Rv3180c	Rv3457c	Rv3311	Rv3493c
Rv3779	Rv3181c	Rv3458c	Rv3312c	Rv3494c
Rv3780	Rv3182	Rv3460c	Rv3313c	Rv3495c
Rv3781	Rv3183	Rv3462c	Rv3314c	Rv3496c
Rv3782	Rv3184	Rv3463	Rv3315c	Rv3497c
Rv3783	Rv3185	Rv3464	Rv3317	Rv3498c
Rv3784	Rv3186	Rv3465	Rv3318	Rv3499c
Rv3785	Rv3187	Rv3466	Rv3319	Rv3501c
Rv3787c	Rv3188	Rv3467	Rv3320c	Rv3502c
Rv3788	Rv3189	Rv3468c	Rv3321c	Rv3504
Rv3789	Rv3190c	Rv3469c	Rv3322c	Rv3505
Rv3790	Rv3191c	Rv3470c	Rv3323c	Rv3506
Rv3791	Rv3192	Rv3471c	Rv3324c	Rv3509c
Rv3792	Rv3193c	Rv3472	Rv3326	Rv3510c
Rv3793	Rv3194c	Rv3473c	Rv3327	Rv3511
Rv3794	Rv3195	Rv3474	Rv3328c	Rv3513c
Rv3796	Rv3196	Rv3475	Rv3329	Rv3515c
Rv3798	Rv3196.1	Rv3476c	Rv3330	Rv3516
Rv1313c	Rv3197	Rv3478	Rv3331	Rv3517
Rv3799c	Rv3197.1	Rv3479	Rv3332	Rv3518c
Rv3800c	Rv3198A	Rv3480c	Rv3333c	Rv3519
Rv3801c	Rv3198c	Rv3482c	Rv3334	Rv3520c
Rv3804c	Rv3199c	Rv3484	Rv3335c	Rv3521
Rv3805c	Rv3200c	Rv3485c	Rv3336c	Rv3522
Rv3806c	Rv3201c	Rv3487c	Rv3337	Rv3523
Rv3808c	Rv3202c	Rv3489	Rv3339c	Rv3524
Rv3809c	Rv3203	Rv3490	Rv3341	Rv3525c
Rv3811	Rv3204	Rv3492c	Rv3342	Rv3526
Rv3813c	Rv3205c	Rv3493c	Rv3343c	Rv3527
Rv3814c	Rv3206c	Rv3494c	Rv3347c	Rv3528c
Rv3815c	Rv3207c	Rv3495c	Rv3349c	Rv3529c
Rv3816c	Rv3208	Rv3496c	Rv3351c	Rv3530c
Rv3817	Rv3208.1	Rv3497c	Rv3354	Rv3531c
Rv3818	Rv3210c	Rv3499c	Rv3356c	Rv3532
Rv3819	Rv3211	Rv3501c	Rv3357	Rv3534c
Rv3820c	Rv3212	Rv3502c	Rv3358	Rv3535c
Rv3822	Rv3213c	Rv3504	Rv3359	Rv3536c
Rv3823c	Rv3214	Rv3505	Rv3362c	Rv3537
Rv3826	Rv3215	Rv3506	Rv3363c	Rv3538
Rv3828c	Rv3216	Rv3509c	Rv3364c	Rv3539
Rv3829c	Rv3217c	Rv3510c	Rv3365c	Rv3540c
Rv3833	Rv3218	Rv3512	Rv3368c	Rv3541c
Rv3834c	Rv3220c	Rv3513c	Rv3369	Rv3542c
Rv3835	Rv3221.1	Rv3515c	Rv3370c	Rv3543c

Rv3837c	Rv3221c	Rv3516	Rv3371	Rv3544c
Rv3838c	Rv3222c	Rv3517	Rv3372	Rv3545c
Rv3839	Rv3223c	Rv3519	Rv3373	Rv3546
Rv3840	Rv3224	Rv3520c	Rv3375	Rv3547
Rv3841	Rv3224.1	Rv3521	Rv3376	Rv3548c
Rv3843c	Rv3224.2	Rv3523	Rv3377c	Rv3549c
Rv3845	Rv3225c	Rv3524	Rv3378c	Rv3550
Rv3846	Rv3226c	Rv3525c	Rv3379c	Rv3551
Rv3847	Rv3227	Rv3526	Rv3380c	Rv3552
Rv3848	Rv3228	Rv3527	Rv3382c	Rv3553
Rv3849	Rv3229c	Rv3528c	Rv3383c	Rv3554
Rv3850	Rv3230c	Rv3529c	Rv3384c	Rv3555c
Rv3851	Rv3231c	Rv3530c	Rv3386	Rv3556c
Rv3852	Rv3232c	Rv3531c	Rv3387	Rv3557c
Rv3853	Rv3233c	Rv3532	Rv3388	Rv3559c
Rv3855	Rv3234c	Rv3534c	Rv3389c	Rv3560c
Rv3856c	Rv3235	Rv3535c	Rv3391	Rv3561
Rv3858c	Rv3236c	Rv3536c	Rv3392c	Rv3562
Rv3859c	Rv3237c	Rv3537	Rv3393	Rv3563
Rv3860	Rv3238c	Rv3538	Rv3394c	Rv3564
Rv3862c	Rv3239c	Rv3540c	Rv3395.1	Rv3565
Rv3863	Rv3240c	Rv3542c	Rv3395c	Rv3566.1
Rv3866	Rv3241c	Rv3543c	Rv3396c	Rv3566c
Rv3867	Rv3242c	Rv3544c	Rv3397c	Rv3567c
Rv3868	Rv3244c	Rv3545c	Rv3398c	Rv3568c
Rv3869	Rv3245c	Rv3546	Rv3399	Rv3569c
Rv3870	Rv3246c	Rv3547	Rv3400	Rv3571
Rv3875	Rv3247c	Rv3548c	Rv3401	Rv3573c
Rv3876	Rv3248c	Rv3549c	Rv3402c	Rv3574
Rv3877	Rv3249c	Rv3550	Rv3403c	Rv3575c
Rv3878	Rv3252c	Rv3551	Rv3404c	Rv3576
Rv3879c	Rv3253c	Rv3552	Rv3405c	Rv3577
Rv3880c	Rv3254	Rv3553	Rv3406	Rv3578
Rv3882c	Rv3255c	Rv3554	Rv3407	Rv3579c
Rv3884c	Rv3256c	Rv3555c	Rv3408	Rv3580c
Rv3885c	Rv3257c	Rv3556c	Rv3409c	Rv3581c
Rv3887c	Rv3258c	Rv3557c	Rv3410c	Rv3582c
Rv3888c	Rv3259	Rv3558	Rv3411c	Rv3583c
Rv3889c	Rv3260c	Rv3559c	Rv3413c	Rv3585
Rv3891c	Rv3261	Rv3560c	Rv3414c	Rv3586
Rv3892c	Rv3262	Rv3561	Rv3415c	Rv3587c
Rv3894c	Rv3263	Rv3562	Rv3416	Rv3588c
Rv3895c	Rv3264c	Rv3563	Rv3417c	Rv3589
Rv3896c	Rv3265c	Rv3564	Rv3418c	Rv3591c
Rv3897c	Rv3267	Rv3565	Rv3419c	Rv3592
Rv3898c	Rv3268	Rv3566.1	Rv3420c	Rv3593
Rv3900c	Rv3269	Rv3566c	Rv3421c	Rv3594
Rv3901c	Rv3270	Rv3567c	Rv3422c	Rv3595c
Rv3902c	Rv3272	Rv3568c	Rv3423c	Rv3596c
Rv3904c	Rv3273	Rv3569c	Rv3424c	Rv3598c
Rv3906c	Rv3274c	Rv3570c	Rv3430c	Rv3600c

Rv3907c	Rv3275c	Rv3571	Rv3431c	Rv3601c
Rv3908	Rv3276c	Rv3572	Rv3432c	Rv3602c
Rv3909	Rv3277	Rv3573c	Rv3433c	Rv3604c
Rv3910	Rv3278c	Rv3574	Rv3434c	Rv3608c
Rv3912	Rv3279c	Rv3575c	Rv3436c	Rv3609c
Rv3913	Rv3280	Rv3576	Rv3437	Rv3610c
Rv3914	Rv3281	Rv3577	Rv3438	Rv3611
Rv3915	Rv3282	Rv3578	Rv3439c	Rv3614c
Rv3916c	Rv3283	Rv3579c	Rv3440c	Rv3623
Rv3917c	Rv3284	Rv3580c	Rv3441c	Rv3624c
Rv3918c	Rv3285	Rv3582c	Rv3442c	Rv3625c
Rv3920c	Rv3286c	Rv3583c	Rv3443c	Rv3626c
Rv3921c	Rv3287c	Rv3584	Rv3444c	Rv3627c
Rv3922c	Rv3288c	Rv3585	Rv3445c	Rv3628
Rv3923c	Rv3289c	Rv3586	Rv3446c	Rv3631
	Rv3290c	Rv3587c	Rv3447c	Rv3633
	Rv3291c	Rv3588c	Rv3448	Rv3634c
	Rv3292	Rv3589	Rv3449	Rv3635
	Rv3293	Rv3591c	Rv3450c	Rv3636
	Rv3294c	Rv3593	Rv3451	Rv3637
	Rv3295	Rv3594	Rv3452	Rv3638
	Rv3296	Rv3596c	Rv3454	Rv3639c
	Rv3297	Rv3598c	Rv3455c	Rv3640c
	Rv3298c	Rv3599c	Rv3456c	Rv3641c
	Rv3299c	Rv3600c	Rv3457c	Rv3644c
	Rv3300c	Rv3602c	Rv3458c	Rv3645
	Rv3301c	Rv3603c	Rv3459c	Rv3646c
	Rv3302c	Rv3604c	Rv3460c	Rv3651
	Rv3303c	Rv3606c	Rv3461c	Rv3652
	Rv3304	Rv3607c	Rv3462c	Rv3653
	Rv3305c	Rv3608c	Rv3463	Rv3654c
	Rv3306c	Rv3609c	Rv3464	Rv3655c
	Rv3307	Rv3610c	Rv3466	Rv3656c
	Rv3308	Rv3611	Rv3467	Rv3657c
	Rv3309c	Rv3612c	Rv3468c	Rv3658c
	Rv3310	Rv3616c	Rv3469c	Rv3659c
	Rv3311	Rv3618	Rv3470c	Rv3660c
	Rv3312c	Rv3623	Rv3471c	Rv3661
	Rv3313c	Rv3624c	Rv3472	Rv3662c
	Rv3314c	Rv3625c	Rv3473c	Rv3663c
	Rv3315c	Rv3626c	Rv3475	Rv3665c
	Rv3317	Rv3627c	Rv3477	Rv3666c
	Rv3318	Rv3628	Rv3478	Rv3667
	Rv3319	Rv3631	Rv3479	Rv3669
	Rv3320c	Rv3633	Rv3480c	Rv3670
	Rv3322c	Rv3634c	Rv3482c	Rv3671c
	Rv3324c	Rv3635	Rv3484	Rv3672c
	Rv3325	Rv3636	Rv3485c	Rv3673c
	Rv3326	Rv3638	Rv3486	Rv3674c
	Rv3327	Rv3639c	Rv3487c	Rv3675
	Rv3328c	Rv3640c	Rv3489	Rv3676

Rv3329	Rv3641c	Rv3490	Rv3677c
Rv3330	Rv3642c	Rv3491	Rv3679
Rv3331	Rv3643	Rv3492c	Rv3680
Rv3332	Rv3644c	Rv3493c	Rv3681c
Rv3333c	Rv3645	Rv3494c	Rv3682
Rv3334	Rv3646c	Rv3495c	Rv3683
Rv3335c	Rv3647c	Rv3496c	Rv3684
Rv3336c	Rv3649	Rv3497c	Rv3685c
Rv3338	Rv3650	Rv3498c	Rv3687c
Rv3339c	Rv3651	Rv3499c	Rv3688c
Rv3341	Rv3653	Rv3501c	Rv3690
Rv3342	Rv3654c	Rv3502c	Rv3692
Rv3344c	Rv3655c	Rv3504	Rv3693
Rv3345c	Rv3657c	Rv3505	Rv3694c
Rv3346c	Rv3658c	Rv3506	Rv3695
Rv3347c	Rv3660c	Rv3509c	Rv3696c
Rv3348	Rv3661	Rv3510c	Rv3698
Rv3349c	Rv3662c	Rv3511	Rv3699
Rv3350c	Rv3663c	Rv3513c	Rv3700c
Rv3351c	Rv3664c	Rv3515c	Rv3701c
Rv3352c	Rv3665c	Rv3516	Rv3702c
Rv3353c	Rv3666c	Rv3517	Rv3703c
Rv3355c	Rv3667	Rv3518c	Rv3704c
Rv3356c	Rv3669	Rv3519	Rv3707c
Rv3357	Rv3670	Rv3520c	Rv3708c
Rv3358	Rv3671c	Rv3521	Rv3709c
Rv3359	Rv3672c	Rv3522	Rv3710
Rv3360	Rv3673c	Rv3523	Rv3711c
Rv3361c	Rv3674c	Rv3525c	Rv3712
Rv3362c	Rv3675	Rv3526	Rv3713
Rv3363c	Rv3676	Rv3527	Rv3714c
Rv3365c	Rv3677c	Rv3528c	Rv3715c
Rv3368c	Rv3678c	Rv3529c	Rv3716c
Rv3369	Rv3680	Rv3530c	Rv3717
Rv3370c	Rv3682	Rv3531c	Rv3719
Rv3371	Rv3683	Rv3532	Rv3720
Rv3372	Rv3684	Rv3533c	Rv3721c
Rv3373	Rv3685c	Rv3534c	Rv3722c
Rv3374	Rv3687c	Rv3535c	Rv3723
Rv3375	Rv3688c	Rv3536c	Rv3724.2
Rv3376	Rv3689	Rv3537	Rv3725
Rv3377c	Rv3690	Rv3538	Rv3726
Rv3378c	Rv3691	Rv3540c	Rv3727
Rv3379c	Rv3692	Rv3542c	Rv3728
Rv3380c	Rv3693	Rv3543c	Rv3729
Rv3381c	Rv3694c	Rv3545c	Rv3730c
Rv3382c	Rv3695	Rv3546	Rv3731
Rv3384c	Rv3696c	Rv3547	Rv3732
Rv3385c	Rv3698	Rv3548c	Rv3733c
Rv3386	Rv3700c	Rv3549c	Rv3734c
Rv3387	Rv3701c	Rv3550	Rv3736

Rv3388	Rv3702c	Rv3551	Rv3737
Rv3389c	Rv3703c	Rv3552	Rv3740c
Rv3390	Rv3704c	Rv3553	Rv3741c
Rv3391	Rv3705c	Rv3554	Rv3743c
Rv3392c	Rv3707c	Rv3555c	Rv3744
Rv3393	Rv3709c	Rv3556c	Rv3746c
Rv3394c	Rv3710	Rv3557c	Rv3748
Rv3395.1	Rv3711c	Rv3558	Rv3749c
Rv3395c	Rv3712	Rv3559c	Rv3750c
Rv3396c	Rv3713	Rv3560c	Rv3751
Rv3397c	Rv3714c	Rv3561	Rv3752c
Rv3398c	Rv3715c	Rv3562	Rv3753c
Rv3399	Rv3716c	Rv3563	Rv3754
Rv3400	Rv3718c	Rv3564	Rv3755c
Rv3401	Rv3719	Rv3565	Rv3756c
Rv3402c	Rv3720	Rv3566.1	Rv3758c
Rv3403c	Rv3721c	Rv3566c	Rv3759c
Rv3404c	Rv3722c	Rv3567c	Rv3760
Rv3405c	Rv3723	Rv3568c	Rv3761c
Rv3406	Rv3725	Rv3569c	Rv3762c
Rv3407	Rv3726	Rv3570c	Rv3763
Rv3408	Rv3727	Rv3571	Rv3764c
Rv3409c	Rv3728	Rv3572	Rv3765c
Rv3410c	Rv3729	Rv3573c	Rv3766
Rv3411c	Rv3730c	Rv3574	Rv3767c
Rv3413c	Rv3731	Rv3575c	Rv3769
Rv3414c	Rv3732	Rv3576	Rv3770.1
Rv3415c	Rv3733c	Rv3577	Rv3770.2
Rv3416	Rv3734c	Rv3578	Rv3771c
Rv3417c	Rv3735	Rv3579c	Rv3772
Rv3418c	Rv3736	Rv3580c	Rv3773c
Rv3419c	Rv3737	Rv3581c	Rv3774
Rv3420c	Rv3738c	Rv3583c	Rv3775
Rv3421c	Rv3740c	Rv3584	Rv3776
Rv3422c	Rv3742c	Rv3585	Rv3777
Rv3423.1	Rv3743c	Rv3586	Rv3778c
Rv3423c	Rv3744	Rv3587c	Rv3779
Rv3424c	Rv3745c	Rv3588c	Rv3780
Rv3425	Rv3746c	Rv3589	Rv3781
Rv3426	Rv3747	Rv3591c	Rv3782
Rv3427c	Rv3749c	Rv3593	Rv3783
Rv3428c	Rv3750c	Rv3594	Rv3784
Rv3429	Rv3751	Rv3595c	Rv3785
Rv3430c	Rv3752c	Rv3596c	Rv3786c
Rv3431c	Rv3753c	Rv3597c	Rv3787c
Rv3432c	Rv3755c	Rv3598c	Rv3788
Rv3433c	Rv3756c	Rv3600c	Rv3790
Rv3434c	Rv3757c	Rv3602c	Rv3791
Rv3435c	Rv3758c	Rv3603c	Rv3792
Rv3436c	Rv3760	Rv3604c	Rv3793
Rv3437	Rv3761c	Rv3605c	Rv3794

Rv3438	Rv3762c	Rv3606c	Rv3795
Rv3439c	Rv3764c	Rv3607c	Rv3796
Rv3440c	Rv3765c	Rv3608c	Rv3797
Rv3441c	Rv3766	Rv3609c	Rv3798
Rv3442c	Rv3767c	Rv3610c	Rv3799c
Rv3443c	Rv3770.2	Rv3611	Rv3800c
Rv3445c	Rv3771c	Rv3613c	Rv3801c
Rv3446c	Rv3772	Rv3614c	Rv3802c
Rv3447c	Rv3773c	Rv3615c	Rv3804c
Rv3448	Rv3774	Rv3616c	Rv3805c
Rv3449	Rv3775	Rv3624c	Rv3807c
Rv3450c	Rv3776	Rv3625c	Rv3808c
Rv3451	Rv3777	Rv3626c	Rv3809c
Rv3453	Rv3778c	Rv3627c	Rv3811
Rv3454	Rv3779	Rv3628	Rv3813c
Rv3455c	Rv3780	Rv3629c	Rv3814c
Rv3456c	Rv3781	Rv3630	Rv3815c
Rv3457c	Rv3782	Rv3631	Rv3816c
Rv3458c	Rv3783	Rv3632	Rv3817
Rv3459c	Rv3784	Rv3633	Rv3818
Rv3460c	Rv3785	Rv3634c	Rv3819
Rv3461c	Rv3786c	Rv3635	Rv3820c
Rv3462c	Rv3787c	Rv3636	Rv3821
Rv3463	Rv3788	Rv3637	Rv3822
Rv3464	Rv3790	Rv3638	Rv3823c
Rv3465	Rv3791	Rv3639c	Rv3824c
Rv3466	Rv3792	Rv3640c	Rv3825c
Rv3467	Rv3793	Rv3641c	Rv3826
Rv3468c	Rv3794	Rv3642c	Rv3827c
Rv3469c	Rv3795	Rv3644c	Rv3828c
Rv3470c	Rv3796	Rv3645	Rv3829c
Rv3471c	Rv3797	Rv3646c	Rv3832c
Rv3472	Rv3798	Rv3647c	Rv3833
Rv3473c	Rv3799c	Rv3648c	Rv3834c
Rv3474	Rv3800c	Rv3649	Rv3835
Rv3475	Rv3801c	Rv3651	Rv3837c
Rv3476c	Rv3802c	Rv3652	Rv3838c
Rv3477	Rv3803c	Rv3653	Rv3839
Rv3478	Rv3804c	Rv3655c	Rv3840
Rv3479	Rv3805c	Rv3657c	Rv3841
Rv3480c	Rv3808c	Rv3658c	Rv3842c
Rv3482c	Rv3809c	Rv3659c	Rv3843c
Rv3483c	Rv3811	Rv3660c	Rv3844
Rv3484	Rv3813c	Rv3661	Rv3845
Rv3485c	Rv3814c	Rv3662c	Rv3846
Rv3486	Rv3815c	Rv3663c	Rv3847
Rv3487c	Rv3816c	Rv3664c	Rv3850
Rv3488	Rv3818	Rv3665c	Rv3851
Rv3489	Rv3819	Rv3666c	Rv3854c
Rv3490	Rv3820c	Rv3667	Rv3855
Rv3492c	Rv3821	Rv3669	Rv3856c

Rv3493c	Rv3822	Rv3670	Rv3857c
Rv3494c	Rv3823c	Rv3671c	Rv3858c
Rv3495c	Rv3824c	Rv3672c	Rv3859c
Rv3496c	Rv3825c	Rv3673c	Rv3860
Rv3497c	Rv3826	Rv3674c	Rv3861
Rv3498c	Rv3827c	Rv3676	Rv3863
Rv3499c	Rv3828c	Rv3677c	Rv3864
Rv3501c	Rv3829c	Rv3678c	Rv3865
Rv3502c	Rv3830c	Rv3679	Rv3866
Rv3504	Rv3833	Rv3680	Rv3867
Rv3505	Rv3834c	Rv3681c	Rv3868
Rv3506	Rv3835	Rv3682	Rv3869
Rv3509c	Rv3836	Rv3683	Rv3870
Rv3510c	Rv3837c	Rv3684	Rv3871
Rv3512	Rv3838c	Rv3685c	Rv3881c
Rv3515c	Rv3839	Rv3687c	Rv3882c
Rv3516	Rv3842c	Rv3688c	Rv3883c
Rv3517	Rv3843c	Rv3689	Rv3884c
Rv3518c	Rv3844	Rv3690	Rv3885c
Rv3519	Rv3845	Rv3692	Rv3886c
Rv3520c	Rv3846	Rv3693	Rv3887c
Rv3521	Rv3848	Rv3694c	Rv3888c
Rv3522	Rv3849	Rv3695	Rv3889c
Rv3523	Rv3850	Rv3696c	Rv3891c
Rv3524	Rv3852	Rv3698	Rv3892c
Rv3526	Rv3853	Rv3699	Rv3894c
Rv3527	Rv3854c	Rv3700c	Rv3895c
Rv3528c	Rv3855	Rv3701c	Rv3896c
Rv3529c	Rv3856c	Rv3702c	Rv3899c
Rv3530c	Rv3857c	Rv3703c	Rv3900c
Rv3531c	Rv3858c	Rv3704c	Rv3902c
Rv3532	Rv3859c	Rv3705c	Rv3903c
Rv3533c	Rv3860	Rv3707c	Rv3904c
Rv3534c	Rv3861	Rv3708c	Rv3906c
Rv3535c	Rv3862c	Rv3709c	Rv3907c
Rv3536c	Rv3863	Rv3710	Rv3908
Rv3537	Rv3864	Rv3711c	Rv3909
Rv3538	Rv3865	Rv3712	Rv3910
Rv3539	Rv3866	Rv3713	Rv3911
Rv3540c	Rv3868	Rv3714c	Rv3912
Rv3542c	Rv3869	Rv3715c	Rv3913
Rv3543c	Rv3870	Rv3716c	Rv3915
Rv3544c	Rv3871	Rv3717	Rv3916c
Rv3545c	Rv3873	Rv3718c	Rv3917c
Rv3546	Rv3874	Rv3719	Rv3918c
Rv3547	Rv3876	Rv3720	Rv3919c
Rv3548c	Rv3879c	Rv3721c	Rv3920c
Rv3549c	Rv3880c	Rv3722c	Rv3921c
Rv3550	Rv3881c	Rv3723	Rv3923c
Rv3551	Rv3882c	Rv3725	Rv3924c
Rv3552	Rv3883c	Rv3726	

Rv3553	Rv3884c	Rv3727
Rv3554	Rv3885c	Rv3728
Rv3555c	Rv3886c	Rv3729
Rv3556c	Rv3887c	Rv3730c
Rv3557c	Rv3888c	Rv3731
Rv3558	Rv3889c	Rv3732
Rv3559c	Rv3892c	Rv3733c
Rv3560c	Rv3894c	Rv3734c
Rv3561	Rv3895c	Rv3735
Rv3562	Rv3896c	Rv3736
Rv3563	Rv3899c	Rv3737
Rv3564	Rv3900c	Rv3740c
Rv3565	Rv3901c	Rv3741c
Rv3566c	Rv3902c	Rv3742c
Rv3567c	Rv3903c	Rv3743c
Rv3568c	Rv3906c	Rv3744
Rv3569c	Rv3907c	Rv3745c
Rv3570c	Rv3908	Rv3746c
Rv3571	Rv3909	Rv3747
Rv3573c	Rv3910	Rv3750c
Rv3574	Rv3911	Rv3751
Rv3575c	Rv3912	Rv3752c
Rv3576	Rv3913	Rv3753c
Rv3577	Rv3914	Rv3754
Rv3578	Rv3915	Rv3755c
Rv3579c	Rv3916c	Rv3756c
Rv3580c	Rv3917c	Rv3757c
Rv3581c	Rv3918c	Rv3758c
Rv3582c	Rv3919c	Rv3760
Rv3583c	Rv3920c	Rv3761c
Rv3584	Rv3921c	Rv3762c
Rv3585	Rv3922c	Rv3764c
Rv3586	Rv3923c	Rv3766
Rv3588c		Rv3767c
Rv3589		Rv3769
Rv3591c		Rv3770.2
Rv3592		Rv3771c
Rv3593		Rv3772
Rv3594		Rv3774
Rv3596c		Rv3775
Rv3597c		Rv3776
Rv3598c		Rv3777
Rv3599c		Rv3778c
Rv3600c		Rv3779
Rv3601c		Rv3780
Rv3602c		Rv3781
Rv3603c		Rv3782
Rv3604c		Rv3783
Rv3606c		Rv3784
Rv3607c		Rv3785
Rv3608c		Rv3786c

Rv3609c
Rv3610c
Rv3611
Rv3612c
Rv3614c
Rv3615c
Rv3616c
Rv3617
Rv3618
Rv3620c
Rv3623
Rv3625c
Rv3626c
Rv3627c
Rv3628
Rv3629c
Rv3630
Rv3631
Rv3632
Rv3633
Rv3634c
Rv3635
Rv3636
Rv3637
Rv3638
Rv3639c
Rv3640c
Rv3641c
Rv3642c
Rv3643
Rv3644c
Rv3645
Rv3646c
Rv3647c
Rv3649
Rv3651
Rv3655c
Rv3656c
Rv3657c
Rv3658c
Rv3659c
Rv3660c
Rv3661
Rv3662c
Rv3663c
Rv3665c
Rv3666c
Rv3667
Rv3669
Rv3670
Rv3671c
Rv3787c
Rv3788
Rv3789
Rv3790
Rv3791
Rv3792
Rv3793
Rv3794
Rv3795
Rv3796
Rv3797
Rv3799c
Rv3800c
Rv3801c
Rv3802c
Rv3804c
Rv3805c
Rv3807c
Rv3808c
Rv3809c
Rv3811
Rv3813c
Rv3814c
Rv3815c
Rv3816c
Rv3817
Rv3818
Rv3819
Rv3820c
Rv3821
Rv3822
Rv3823c
Rv3824c
Rv3825c
Rv3826
Rv3827c
Rv3828c
Rv3829c
Rv3830c
Rv3832c
Rv3833
Rv3834c
Rv3835
Rv3836
Rv3837c
Rv3838c
Rv3839
Rv3840
Rv3841
Rv3842c
Rv3843c

Rv3672c
Rv3673c
Rv3674c
Rv3675
Rv3676
Rv3677c
Rv3678c
Rv3679
Rv3680
Rv3681c
Rv3682
Rv3683
Rv3684
Rv3685c
Rv3687c
Rv3688c
Rv3690
Rv3691
Rv3692
Rv3693
Rv3694c
Rv3695
Rv3696c
Rv3697c
Rv3698
Rv3699
Rv3700c
Rv3701c
Rv3702c
Rv3703c
Rv3704c
Rv3706c
Rv3707c
Rv3708c
Rv3709c
Rv3710
Rv3711c
Rv3712
Rv3713
Rv3714c
Rv3715c
Rv3716c
Rv3718c
Rv3719
Rv3720
Rv3721c
Rv3722c
Rv3723
Rv3724.2
Rv3725
Rv3726
Rv3845
Rv3846
Rv3847
Rv3848
Rv3849
Rv3850
Rv3851
Rv3853
Rv3854c
Rv3855
Rv3856c
Rv3857c
Rv3858c
Rv3859c
Rv3860
Rv3861
Rv3862c
Rv3863
Rv3864
Rv3865
Rv3866
Rv3868
Rv3869
Rv3870
Rv3871
Rv3873
Rv3874
Rv3876
Rv3877
Rv3878
Rv3879c
Rv3881c
Rv3882c
Rv3883c
Rv3884c
Rv3885c
Rv3886c
Rv3889c
Rv3891c
Rv3892c
Rv3894c
Rv3895c
Rv3896c
Rv3899c
Rv3900c
Rv3902c
Rv3903c
Rv3904c
Rv3907c
Rv3908
Rv3909

Rv3727
Rv3728
Rv3729
Rv3730c
Rv3731
Rv3732
Rv3733c
Rv3734c
Rv3735
Rv3736
Rv3737
Rv3738c
Rv3740c
Rv3741c
Rv3742c
Rv3743c
Rv3744
Rv3745c
Rv3746c
Rv3747
Rv3750c
Rv3752c
Rv3753c
Rv3754
Rv3755c
Rv3756c
Rv3758c
Rv3759c
Rv3760
Rv3761c
Rv3762c
Rv3763
Rv3764c
Rv3765c
Rv3766
Rv3767c
Rv3768
Rv3769
Rv3770.1
Rv3770.2
Rv3771c
Rv3772
Rv3773c
Rv3774
Rv3775
Rv3776
Rv3777
Rv3778c
Rv3779
Rv3780
Rv3781
Rv3910
Rv3911
Rv3912
Rv3913
Rv3915
Rv3916c
Rv3917c
Rv3919c
Rv3920c
Rv3921c
Rv3922c
Rv3923c
Rv3924c

Rv3782
Rv3783
Rv3784
Rv3785
Rv3786c
Rv3787c
Rv3788
Rv3789
Rv3790
Rv3791
Rv3792
Rv3793
Rv3794
Rv3795
Rv3796
Rv3797
Rv3798
Rv3799c
Rv3800c
Rv3801c
Rv3802c
Rv3803c
Rv3804c
Rv3805c
Rv3806c
Rv3807c
Rv3808c
Rv3809c
Rv3811
Rv3813c
Rv3814c
Rv3815c
Rv3816c
Rv3818
Rv3819
Rv3820c
Rv3821
Rv3822
Rv3823c
Rv3824c
Rv3825c
Rv3826
Rv3827c
Rv3828c
Rv3829c
Rv3830c
Rv3832c
Rv3834c
Rv3835
Rv3837c
Rv3838c

Rv3839
Rv3840
Rv3841
Rv3842c
Rv3843c
Rv3844
Rv3845
Rv3846
Rv3848
Rv3849
Rv3850
Rv3851
Rv3853
Rv3854c
Rv3855
Rv3856c
Rv3857c
Rv3858c
Rv3859c
Rv3860
Rv3861
Rv3862c
Rv3863
Rv3864
Rv3865
Rv3866
Rv3867
Rv3868
Rv3869
Rv3870
Rv3871
Rv3873
Rv3874
Rv3875
Rv3876
Rv3877
Rv3878
Rv3879c
Rv3880c
Rv3881c
Rv3882c
Rv3883c
Rv3884c
Rv3885c
Rv3886c
Rv3887c
Rv3888c
Rv3889c
Rv3890c
Rv3891c
Rv3892c

Rv3894c
Rv3895c
Rv3896c
Rv3899c
Rv3900c
Rv3902c
Rv3903c
Rv3904c
Rv3906c
Rv3907c
Rv3908
Rv3909
Rv3910
Rv3911
Rv3912
Rv3913
Rv3914
Rv3915
Rv3916c
Rv3917c
Rv3918c
Rv3919c
Rv3920c
Rv3921c
Rv3922c
Rv3923c